A Systems-level Case Study of Conservation Agriculture in the UK

Joe Collins

Harper Adams University

A thesis submitted for the degree of

Doctor of Philosophy

2025

Declaration

I declare that this thesis was composed by myself, that the work contained herein is my own except where explicitly stated otherwise in the text, and that this work has not been submitted for any other degree or professional qualification except as specified.

Acknowledgments

The author would like to acknowledge and thank the following people who have contributed their expertise to the project:

Professor S. Jeffery, **Dr E. Harris**, and **Professor K. Behrendt** (Harper Adams University), for their guidance, knowledge, and experience throughout this process. Without whom, this project would not have been possible.

P. Cawood (Soil First Farming) and **A. Sibbett** (BCW Agriculture), for their professional agronomy services and expert advice throughout the project.

M. Bower, **W. Bower** (W G Bower & Son Ltd.), and **M. Cornes** (Cornes & Co) for their professional agricultural services, managing the field trials, and expert advice throughout the project.

N. Peers and **W. Heywood-Lonsdale** (Shavington and Cloverley Estate Management Ltd) for use of their land for the experimental work, which has made this project possible.

K. Jones (Harper Adams University) for his expertise in gas chromatography.

L. Martinez-Chavez (Harper Adams University) for her entomology expertise, who performed the micro-arthropod identification and analysis in this project.

G. Weston (Harper Adams University) for his support and knowledge with field trials, and general fixing, building, and design of equipment.

JJ. Collins (Earth Rover Program) for his support and expertise with coding.

M. Cousins (Natural England) for her support and expertise in ecology.

P. Collins (Historic England) for his support with processing crop samples.

The author would also like to extend their gratitude to those who have provided invaluable personal support and encouragement:

K. and N. Collins for their general support and guidance.

J. and A. Norris (T G Norris & Son) for their support, knowledge, and encouragement to a young lad interested in agriculture.

The author would like to acknowledge and thank the following organisations who have contributed services and expertise to the project:

- CERC - Harper Adams University
- Laboratories - Harper Adams University
- BCW Agriculture
- Soil First Farming
- Spunhill Ltd.
- SOYL
- Omnia

The author would like to acknowledge and thank the following organisations who have contributed funding to the project:

- Biotechnology and Biological Sciences Research Council (BBSRC)
- Midlands Integrative Bioscience Training Partnership (MIBTP)
- Rabobank UK
- BASE-UK

The author gratefully acknowledges the provision by UKCEH of hydrometeorological and soil data collected by the COSMOS-UK project. COSMOS-UK is supported by the Natural Environment Research Council award number NE/R016429/1 as part of the UK-SCAPE programme delivering National Capability.

Abstract

Conservation Agriculture (CA) is an agricultural system designed to manage agroecosystems for improved and sustained productivity by conserving and enhancing soil quality and biota (FAO, 2014; Page et al., 2020). This thesis presents the results of a three-year case study that evaluated the effects of the transition to CA in comparison to Conventional Agriculture (CON), conducted using a systems-level methodology in Shropshire, UK.

Throughout the experiment, the agronomic plan varied considerably between the experimental treatments, with the CON treatment using significantly higher quantities of fungicide and insecticide active ingredients (kg ha^{-1}), and the CA treatment using significantly higher quantities of herbicide active ingredients (kg ha^{-1}). Despite this, the total quantity of pesticide active ingredients applied did not differ significantly between systems. Regarding nutrient inputs, the CA treatment applied significantly less nitrogen (N) fertiliser (kg ha^{-1}), aided by both crop rotation choices and the use of foliar N. Although crop yield variability was high in both systems, no statistically significant differences were found between the treatments in overall crop yield (t ha^{-1}).

Soil nutrient availability (phosphorus (P), potassium (K), magnesium (Mg), and total N) increased under CA, suggesting improved nutrient cycling and retention. However, CA significantly increased soil bulk density and led to a significant decline in soil microarthropod diversity; however, no significant differences were identified in individual ecotypes or total earthworm abundance between the treatments.

In terms of farm management operations, CA required significantly less machinery operational passes ha^{-1}, machinery operational time ha^{-1}, and fuel usage ha^{-1}, identifying clear operational benefits to farmers from CA adoption in terms of labour and machinery expenditure. This resulted in significantly reduced expenditure on machinery operations and crop applications, whilst not statistically compromising revenue or gross margin compared to CON.

Agronomic risk assessment using the Danish Pesticide Load Index identified significantly higher potential environmental risks in CA. The main driver of this was a significantly higher environmental fate load in the CA treatment, due to higher usage of herbicide active ingredients. No significant treatment differences were observed for the ecotoxicity or human health risks of the pesticide agronomic plans.

The findings of this study demonstrate that the transition period of CA presents both opportunities and challenges for farmers. While it can reduce inputs and oper-

ational costs, it may increase reliance on herbicides and require careful management of soil health to achieve the best outcomes. As a knowledge-intensive and context-specific system, CA demands a high degree of local adaptation. Therefore, future research should focus on multi-disciplinary and multi-stakeholder methodologies, such as Farming Systems Research, to support farmers and agronomists in managing and adapting CA to suit local conditions.

Contents

List of Figures

List of Tables

Chapter 1

General Introduction

1.1 Background and Context

Modern agriculture faces a fundamental challenge: how to meet the growing demand for food, fibre, and fuel while maintaining the natural resource base and ecosystem functions on which agriculture itself depends. Intensification of agricultural systems over the past century has increased productivity dramatically, but often at the cost of environmental degradation, soil health decline (FAO and ITPS, 2015), biodiversity loss (Cardinale et al., 2012), and increased greenhouse gas emissions (Ponce et al., 2022). In response, there has been growing interest in sustainable intensification to achieve higher productivity with reduced environmental impact (Xie et al., 2019).

Conservation Agriculture (CA) has emerged as a widely advocated approach within sustainable intensification frameworks (FAO, 2014; Page et al., 2020). Defined by its three core principles: minimum soil disturbance, permanent soil cover, and crop diversification, CA aims to enhance soil structure and fertility, reduce erosion, improve water retention, and support ecological functions in agroecosystems. While it has been promoted globally, especially in the Global South (Giller et al., 2009, 2015), adoption in temperate regions such as the United Kingdom has been slower and more variable (Basch et al., 2015; Kassam et al., 2009).

This thesis is motivated by the need to evaluate how CA performs in the UK context, not just in terms of individual agronomic outcomes, but as a system. A systems-level perspective is necessary because CA influences and is influenced by complex interactions between agronomic practices, soil processes, climate, biodiversity, economics, and farmer decision-making. Understanding these interactions requires an interdisciplinary, case-study-based approach that integrates ecological, economic, and management data in a real-world scenario.

1.2 The UK Agricultural Context

The UK agricultural sector is currently undergoing significant transformation. Drivers of this change include the transition to post-Brexit agricultural policy (Vigani et al., 2021), the UK's net-zero greenhouse gas emissions target (NFU, 2023; HM Government, 2023), concerns over food security (Prosekov and Ivanova, 2018), and increasing public scrutiny of farming's environmental impacts (Potter, 2009). These changes create both challenges and opportunities for more sustainable systems like CA.

Soil degradation has been identified as a national concern in the UK, with over half of agricultural soils showing signs of deterioration (DEFRA, 2019). Compaction, loss of organic matter, and erosion are among the key issues (Dragović and Vulević, 2021). These problems are often linked to conventional agricultural practices (CON) such as repeated tillage, monoculture cropping, and high reliance on external inputs (Lal, 2015). In this context, CA has the potential to address multiple goals simultaneously: improving soil health (Cárceles Rodríguez et al., 2022), enhancing resilience to climate variability (Michler et al., 2019), reducing input dependency (Parihar et al., 2018; Das et al., 2021), and contributing to ecosystem services (Kassam et al., 2014a).

Yet, empirical evidence for these benefits in the UK, particularly from real-world farm systems, remains limited. Many existing studies are plot-based and short-term, or based solely on the individual principles of CA (Brown et al., 2021; Drinkwater et al., 2016). There is a need for more comprehensive, system-level assessments that consider the performance of CA over time, across multiple dimensions (e.g. soil, yield, biodiversity, economics), and under practical farm conditions that are representative of the practices used by farmers in the UK.

1.3 Systems Thinking in Agricultural Research

Adopting a systems-level approach means recognising that agricultural systems are built from interactions between many components and not just individual systems (Drinkwater et al., 2016). For example, the effect of NT on soil structure may depend on crop rotations, residue management, or climate (Triplett and Dick, 2008). Similarly, economic outcomes of CA adoption are influenced not only by yield and input costs, but also by broader policy, market dynamics, and farmers' risk preferences (Schiere et al., 2004; Francaviglia et al., 2023; Kassam et al., 2014b).

This thesis adopts such an approach by using a multi-year, on-farm case study of CA in the UK. The research design integrates soil, ecological, agronomic, and

economic data to evaluate the system as a whole. The case-study methodology adopts a systems-level design in which crop management decisions are made independently for each treatment and each year by industry experts. This allows management to vary substantially between systems, reflecting the tailored and adaptive approaches typical of real-world commercial farming.

1.4 Thesis Plan, Research Aims, and Hypotheses

The thesis structure is detailed in the following section. The research aims and the hypotheses to be tested are specified for each chapter.

Chapter 2: Literature review

This chapter reviews both historical and current literature on CA, including a brief overview of its origins, the context of its application, and a summary of its core components. The review places particular emphasis on large-scale systematic reviews and meta-analyses, where available, to highlight general trends in the effects of CA across diverse soil types and climatic conditions.

The research aims ($\boldsymbol{A}$) of this chapter are:

- A_1: Assess existing research and literature on the benefits and drawbacks of conservation agriculture systems.
- A_2: Assess the methodologies available for on-farm experimental systems research.
- A_3: Assess the applicability of a single-site system-level methodology for research on Conservation Agriculture.

Chapter 3: Application of Soil Proximal Sensors to Guide the Transition to Conservation Agriculture

This chapter investigates the potential of commercially available soil proximal sensing technologies: specifically gamma-ray spectrometry (GRS) and electrical conductivity (EC) scanning, as precision agriculture tools for characterising field-scale soil texture to support the transition to Conservation Agriculture. As soil texture strongly influences both the outcomes of reduced tillage practices (Rochette et al., 2008; Zhao

et al., 2020; Pannell et al., 2014; Ren et al., 2023) and equipment performance (Baker et al., 2006; Stengel et al., 1984; Agrii, 2021), the ability to map its spatial variability is critical for informed management. Traditional laboratory-based methods for soil texture analysis are costly and time-consuming, limiting their practicality at high resolutions (Rhymes et al., 2023). Therefore, this chapter evaluates the accuracy of EC and GRS in predicting soil texture using spatial correlation analysis and a Random Forest machine learning model. It tests whether these technologies, individually or in combination, can provide sufficiently accurate texture maps to guide agronomic decision-making, and explores the potential benefits of a multi-sensor "soil sensor fusion" approach for improving prediction reliability.

The research aims ($\boldsymbol{A}$) of this chapter are:

- A_1: Assess the accuracy of gamma-ray spectrometry (GRS) and electrical conductivity (EC) scanning in predicting field-scale soil texture in a UK agricultural context.
- A_2: Evaluate the potential of a multi-sensor (GRS + EC) "soil sensor fusion" approach for improving the spatial resolution and reliability of soil texture maps.

This chapter tests the following hypotheses ($\boldsymbol{H}$):

- H_1: Commercially available soil scanning technologies are effective estimators of soil textural variation to aid farmers in the transition to CA.
- H_2: A soil texture prediction model which combines data derived from several soil proximal sensors will exceed the accuracy of a model with data from a single source.

Chapter 3: Soil Health and Function Under Conservation Agriculture

This chapter assesses the performance of CA on soil health metrics and soil function in comparison to conventional agriculture (CON). This is done by monitoring various soil physical, chemical, and biological indicators throughout the three-year experiment and evaluating the performance of CA in comparison to CON.

The research aims ($\boldsymbol{A}$) of this chapter are:

- A_1: Analyse the effects of the transition to CA on the soil chemical environment in comparison to a CON system.

- A_2: Analyse the effects of the transition to CA on the soil physical environment in comparison to a CON system.
- A_3: Analyse the effects of the transition to CA on the soil biological environment in comparison to a CON system.

This chapter tests the following hypotheses (H):

- H_1: CA results in significantly higher diversity and abundance of soil micro arthropods and earthworms compared to CON practices.
- H_2: CA increases soil organic carbon content over time compared to CON.
- H_3: Soil bulk density and compaction are lower under CA, than CON, due to reduced mechanical disturbance.

Chapter 4: Agronomy and Crop Productivity Under Conservation Agriculture

This chapter assesses the agronomic performance of CA in comparison to conventional agriculture (CON). This is done by monitoring the agronomic crop protection regimes devised by industry professionals during the experiment, and evaluating crop performance and productivity.

The research aims (A) of this chapter are:

- A_1: Monitor variability of crop responses during the transition to CA in comparison to CON.
- A_2: Monitor variability of crop inputs during the transition to CA in comparison to CON.

This chapter tests the following hypotheses (H):

- H_1: CA will result in a significant reduction in crop establishment compared to CON.
- H_2: CA will result in significant alterations to the total quantity of pesticide and fertiliser used compared to CON.
- H_3: CA will result in a significantly lower yield than the CON treatment.
- H_4: CA agronomy will result in a reduced risk to the environment and human health compared to CON.

Chapter 5: Soil Greenhouse Gas Emissions Under Conservation Agriculture

This chapter aims to quantify the soil-derived greenhouse gas emissions (GHG) from CA in comparison to CON. This is done by using the static chamber method (Collier et al., 2014; Pumpanen et al., 2004; Clough et al., 2020) in a crop of winter wheat during the second year of the experiment.

The research aims (*A*) of this chapter are:

- Monitor in-field greenhouse gas emissions during the transition to CA in comparison to a CON and evaluate the effectiveness of CA as a methodology to reduce soil-derived GHG emissions.

This chapter tests the following hypotheses (*H*):

- H_1: CA is an effective methodology for reductions of soil CO_2 emissions in comparison to CON.
- H_2: CA is an effective methodology for reductions of soil N_2O emissions in comparison to CON.
- H_3: CA is an effective methodology for reductions of soil CH_4 emissions in comparison to CON.
- H_4: CA reduces the overall Global Warming Potential (GWP) compared to CON.

Chapter 5: Economic Analysis of Conservation Agriculture

This chapter details the economic analysis of the three-year systems-level field experiment. It compares both experimental treatments in terms of economic performance and models future performance of the systems using a Markov Chain Monte Carlo simulation.

The research aims (*A*) of this chapter are:

- Assess the economic performance of CA during the experimental duration in comparison to CON.
- Model the economic performance of both experimental treatment systems in a variety of different scenarios.

This chapter tests the following hypotheses (*H*):

- H_1: CA reduces crop production expenditure in comparison to CON.
- H_2: CA reduces the quantity of machinery operation passes ha^{-1} required.
- H_3: CA has no significant effect on the gross margin of the system compared to conventional practices.

Chapter 2

Literature Review

2.1 Introduction

Soils are fundamental to life on Earth, but anthropogenic pressures on global soil resources are reaching critical limits (FAO and ITPS, 2015). Currently, it is estimated that over 75% of global soils are classed as substantially degraded (Scholes et al., 2018). Soil degradation is estimated to result in an economic loss in the order of 10% of annual global gross product due to loss of biodiversity and ecosystem services, negatively impacting the food security of at least 3.2 billion people globally, and is linked to mass migrations, violence, and armed conflict (Scholes et al., 2018; Kraamwinkel et al., 2021). Without action, it is predicted that by 2050 the combination of climate change and soil degradation will reduce global crop yields in the region of 10%, extending to up to 50% in certain at-risk regions (Scholes et al., 2018). This will affect the world during a period when it is predicted that the global population will increase by two billion over 30 years, from 7.7 billion in 2019 to 9.7 billion in 2050 (United Nations, 2019; Kraamwinkel et al., 2021).

Global agriculture stands to be greatly affected by climate change, as severe weather and global warming will affect ecosystems, which will have a significantly degraded function due to soil degradation. This will lead to a higher incidence of drought due to decreased soil water holding capacity and a higher incidence of flooding due to decreased soil infiltration rate. Significant reductions in food availability and land productivity have been linked with widespread societal vulnerability and socioeconomic instability (Kraamwinkel et al., 2021). Thus, by 2050, it is estimated that land degradation and climate change are likely to force 50 to 700 million people to migrate if no actions are taken to reduce their severity (Scholes et al., 2018).

During the Green Revolution in the 1960s, substantial increases were made to global food production with the introduction of modern cultivars grown with heavy

usage of tillage, synthetic fertilisers and pesticides (Mulvaney et al., 2009). This approach is primarily focused on maximising grain yield with little regard for the longevity of the soil and environmental resources, which is crucial for sustained crop growth (Mulvaney et al., 2009). Cultivated soils cover around 35% of the terrestrial land area of the planet, and contain a large carbon pool which is sensitive to land-use change and agricultural management practices (Betts et al., 2007; Haddaway et al., 2017). Many practices in conventional agriculture (CON), such as tillage, have been strongly linked with substantial degradation of the soil resource base (Farooq and Siddique, 2015; Jeffery and Verheijen, 2020). In England and Wales, the total economic cost of soil degradation is estimated to be £1.2 bn per year, linked to the loss of soil organic matter, erosion and compaction (Graves et al., 2015). Considering the time scale of soil formation, soils are considered a finite non-renewable resource (Gadermaier et al., 2012; Graves et al., 2015). Therefore, it is of imperative importance to implement productive agricultural systems which conserve and enhance soil quality and health (Doran, 2002).

Conservation Agriculture (CA) is proposed as a means of reducing soil degradation associated with food production (FAO, 2014; Page et al., 2020). CA is predicated on no-tillage (NT) management practice with direct drilling of seeds to achieve minimal disturbance of the soil, combined with cover crops and the return of crop residues to the soil. The aim is to disturb the soil and its biological communities as little as possible, while facilitating them to do work that traditionally the plough and agrochemicals would otherwise do (FAO, 2014; Page et al., 2020). Furthermore, the CA practices of residue return and cover crop use work to protect the soil from erosion while concurrently providing substrate for the soil biota during decomposition, while the main crop is growing. This can reduce the need for artificial fertilisers, and higher levels of soil biodiversity can reduce pest and pathogen load, and so reduce the need for spraying pesticides.

Considering there is disagreement in the literature on the efficacy and applicability of CA, this thesis aims to review the literature on the benefits, drawbacks, and adoption of the key principles of CA systems and experimental designs suitable for systems-level analysis of CA.

2.2 Agricultural soil degradation

Tillage is primarily used by farmers to create a fine seedbed suitable for planting seeds, which improves the uniformity of seed germination, manages weeds, aids in the release

of soil nutrients through mineralisation and oxidation, manages crop residues and therefore provides improved conditions for crop establishment and growth (Cannell, 1985; Farooq and Siddique, 2015). Many agricultural systems using very little or no-tillage (NT) have been utilised since ancient times by indigenous cultures, mainly due to the physical toll of tilling a significant area of land by hand or with livestock (Triplett and Dick, 2008). For example, the ancient Egyptians and the Incas in the Andes of South America used a stick to make a hole in the ground and put seeds by hand into an unprepared seedbed (Derpsch, 1998). Early tillage implements, designed to be pulled by people or livestock, did not invert the soil but scratched or scarified the soil surface. In the 17th century, ploughs were invented that partially inverted the soil, thus achieving better control of weeds in crop establishment. However, it was not until the 18th and 19th centuries that plough designs began to morph into the shape of the plough mouldboards still used in agriculture today, which can invert the soil 135°, achieving very efficient burial of weed seeds (Derpsch, 1998). This innovation quickly became popular in Europe as it was very successful at controlling the invasive weed couch grass (*Elymus repens*), which had spread across much of Europe's cropland and was difficult to control with non-inversion tillage tools.

The power requirement for tillage is considerable; thus, when tractors were introduced in the late 1800s, they enabled large-scale, regular tillage to be more viable. This led to many farmers believing that higher instances of tillage resulted in higher yields (Derpsch, 1998). In modern agricultural practice in many countries in the world, conventional tillage is the use of a mould-board plough to invert the soil to a required depth, thus burying the previous season's crop residues. Ploughing is then followed by a variety of other tillage operations to work the furrows down to a suitable seedbed. During the past centuries, tillage has undoubtedly greatly aided the enhancement of food production for a growing population, by improving seedbeds for crop establishment and reducing the burden of weeds, pests and diseases in cropping systems (Triplett and Dick, 2008). However, increases in the use of agricultural tillage have been strongly linked with the declining state of the world's soil resources in recent decades (Lindstrom et al., 2001; Van Oost et al., 2006).

2.3 Tillage Erosion

Tillage is responsible for significant soil erosion via downslope translocation of soil material, causing heavy deposition in lower slope positions and thinning of topsoils in upper-slope positions (FAO, 2019a). Cultivation not only moves soil particles in

the direction of the tillage, but it can also disturb the soil profile and break up soil aggregates into smaller and lighter aggregates, which are more prone to wind and water erosion. Unlike wind and water-based erosion, which are often immediately obvious to the naked eye following extreme weather events, tillage erosion becomes apparent on a much longer timescale, via changes to visual soil properties (Van Oost et al., 2006). The importance and severity of global tillage erosion was only recognised by soil scientists in the 1990s, and to this day remains far less well known compared to wind or water-based erosion (FAO, 2019a).

Typically, soil erosion from arable agricultural land is an order of magnitude higher than under undisturbed native vegetation, and contributes a disproportional impact on global sediment production for its total land area of 33% of the Earth's surface (Van Oost et al., 2009). Using a tillage model and land use databases, Van Oost et al. (2009) estimated that the mean gross tillage erosion rates for a large part of Europe (6.5% of global cropland) were an average of 3.3 t ha^{-1} y^{-1}, corresponding to a sediment flux of 0.35 Pg y^{-1} (shown in Figure 2.1).

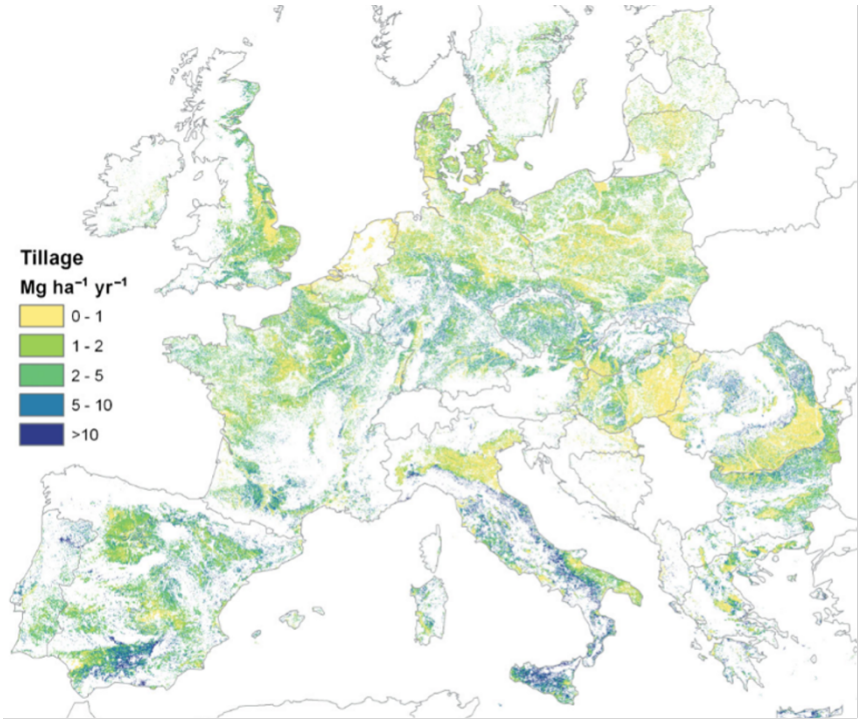

Figure 2.1: Tillage erosion rates calculated for Europe. The values represent the mean gross tillage erosion rate aggregated at 1 km and are approximately half of the erosion rate over the eroded area. Adapted from (Van Oost et al., 2009).

When tillage, wind, and water erosion are combined, it has serious implications for future agricultural productivity. Doetterl et al. (2012) predicted a global soil erosion

rate of 10.5 t ha^{-1} y^{-1} for cropland and 1.7 t ha^{-1} y^{-1} for pastures. This degree of soil erosion also results in significant erosion of soil organic carbon (SOC) from the topsoil, estimated to be 193 kg C ha^{-1} y^{-1} from cropland and 40.4 kg C ha^{-1} y^{-1} from eroding pastures, and results in a global flux of 20.5 ± 10.3 Pg y^{-1} of soil and 403.5 ± 201.8 Tg C y^{-1}. A visual representation of this process is presented in Figure 2.2.

Although erosion does not induce carbon losses from soil to the atmosphere, as the SOC is deposited elsewhere, it does threaten to seriously degrade agricultural soil productivity and resilience over long periods. It is estimated that water erosion alone causes annual fluxes of 23-42 Mt Nitrogen (N) and 14.6-26.4 Mt Phosphorus (P) from agricultural soil (FAO and ITPS, 2015). In comparison to annual fertiliser application, which is *ca.* 112 Tg for N and *ca.* 18 Tg of P. Considering that N and P fertilisers are costly to farmers (Clark, 2022), this highlights the significant annual economic cost for replacing nutrient losses from agricultural soil (FAO and ITPS, 2015). Loss of topsoil results in the gradual reduction in the crop rooting zone as well as the soil water holding capacity, which in turn increases the likelihood of crop failure due to drought and the incidence of flooding due to increases in surface run-off.

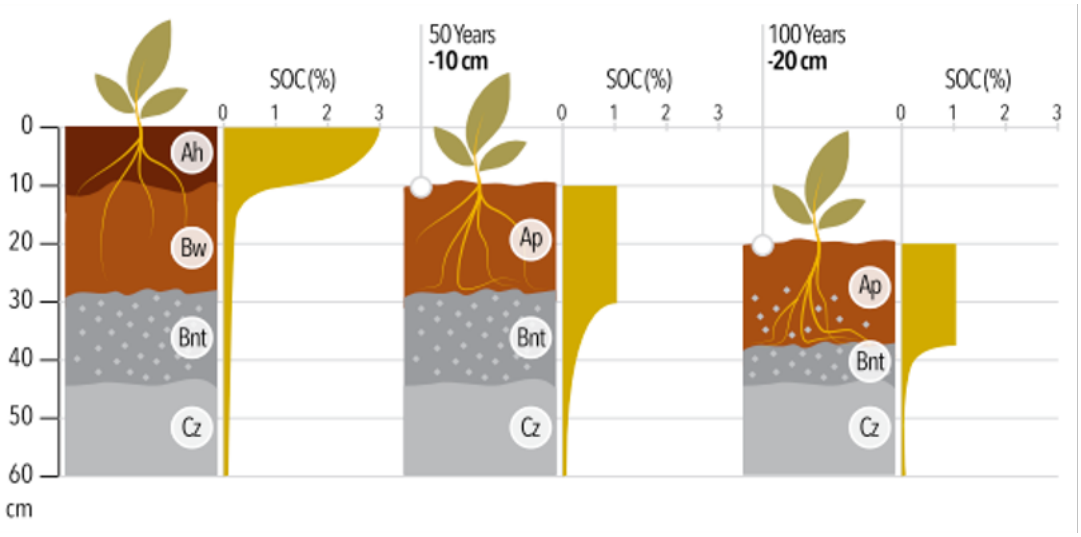

Figure 2.2: The effect of erosion on soil horisonation and the depth function of soil organic carbon. The Ah horizon is the undisturbed SOM-rich layer; the Ap horizon is the ploughed surface horizon. The Bnt horizon is growth-limiting due to high clay and sodium. Adapted from (FAO, 2019a)

2.4 Soil Organic Carbon Loss

Globally, soils contain the largest terrestrial carbon (C) pool sensitive to changes in land use and agricultural management practices, and are therefore of high importance in the global carbon cycle (Haddaway et al., 2017). In only the first meter of soil, the Soil Organic Carbon (SOC) pool stores an estimated 1500 PgC, which equates to more than the atmospheric (roughly 800 PgC) and terrestrial vegetation (500 PgC) carbon cycles combined (FAO and ITPS, 2015; FAO, 2017). SOC is formed by photoautotrophic organisms, mainly plants, synthesising atmospheric CO_2 into organic material. When this organic material dies, soil fauna incorporate it into the soil profile and where it is consumed by heterotrophic microorganisms, resulting in SOC accumulation in a complex biogeochemical mixture of microbial decomposition products and plant residues in various stages of decomposition (FAO, 2017).

The SOC pool has much potential to provide a vital ecosystem service in the future by acting as a C sink by exchanging with the atmospheric C pool and storing as SOC, thus mitigating climate change (Follett, 2001). The loss of SOC is widely regarded as a clear indicator of land degradation, as it affects many physical, chemical, and biological soil processes due to the broad range of soil functions it influences (Reeves, 1997). SOC does not directly influence ecosystem services but is a regularly used proxy for soil organic matter (SOM); however, the traditionally used assumption that soil organic matter contains 58% carbon has been shown to only apply to some soils or only to particular components of soil organic matter (Pribyl, 2010). SOM is a critical attribute to many essential soil ecosystem functions and global warming. SOM encompasses all organic constituents of the soil, less the 2mm in size, including plant and animal residues and soil organisms (FAO, 2017). It is thought of as a key indicator of agricultural productivity and environmental resilience because it is a critical factor in the maintenance of water-holding capacity, stabilisation of soil aggregate structure and turnover of plant available nutrients in all soils (FAO, 2017). SOC has traditionally been used as a proxy for SOM because of the ease of measurement of SOC and the more direct connections between atmospheric C and SOC (FAO and ITPS, 2015).

SOC is naturally removed from the soil through soil autotrophic and heterotrophic respiration, where carbon (C) is released as CO_2 (Turmel et al., 2015). However, it is well reported that tillage significantly accelerates these losses to the atmosphere, especially following land use changes (Kucharik et al., 2001). This is because cultivation breaks up soil aggregates and exposes SOM that was previously shielded within soil

micro-aggregates to microbial decay, releasing C to the atmosphere (Hendrix et al., 1986; Beare et al., 1994; Page et al., 2020). Cultivation also fragments surface crop residues, which increases the rate of microbial decomposition of the organic residues (Beare et al., 1993).

Modern usage of synthetic N fertiliser in cropping systems can positively or negatively affect SOM mineralisation via several direct and indirect pathways. This has led to much debate regarding the sustainability of synthetic N fertilisation (Mahal et al., 2019). Repeated over-usage of synthetic N fertilisers can reduce SOC stocks via accelerating C mineralisation, leading to further soil degradation in over-fertilised soils (Mulvaney et al., 2009). However, some studies suggest that N fertiliser addition increases SOC stocks by enhancing the net primary productivity of production of crop biomass, thus increasing SOM return (Mulvaney et al., 2009). $NH_4{}^+$ application can have an inhibitory effect on microbial activity, thus suppressing C mineralisation (Mahal et al., 2019).

It was estimated by Kucharik et al. (2001) using a dynamic terrestrial ecosystem model with field measurements, that the transition from native prairie lands in Wisconsin (USA) to agricultural land between 1860 and 1950 may have caused the depletion of up to 63% of the original SOC density. This was due to changes to C and N cycling that occur during land use change from undisturbed native environments to, in this case, continuous Maize production, which results in larger amounts of C leaving the system compared to C that is returned.

SOC concentrations can be maintained by either increasing organic matter inputs, or by slowing down SOC decomposition rates or in conjunction (Paustian et al., 1997). Reductions in the quantity of tillage in cropping systems have been regularly cited to have the potential to slow the loss of SOC from agricultural soils, and in some cases, even to build SOC (Derpsch and Friedrich, 2009; Page et al., 2020; Wang et al., 2020; Kumara et al., 2020). This is due to a reduction in soil erosion and therefore losses of topsoil, which is high in SOC, a reduction in soil to residue contact and also decreases the turnover rate of soil macro-aggregates, which increases the physical protection of particulate organic material to the susceptibility of microbial decay (Page et al., 2020).

2.5 History of Reduced Tillage Systems

It was the 'Dust Bowl' in North America during the 1930s that sparked the beginning of the movement towards soil conservation management in agriculture. The disastrous droughts during this period caused widespread economic and ecological damage, thus

driving the shift towards alternative and innovative agricultural concepts (Farooq and Siddique, 2015). Lowering the intensity of tillage was identified as a potential solution to reducing the environmental impact of agriculture and to improve cropping system sustainability (Townsend et al., 2016).

This is characterised by the publication of "Plowman's Folly" by Edward H. Faulkner in 1943, where he linked the vast soil erosion to over-usage of the then universally used and well-regarded tool of the mould-board plough (Faulkner, 1987). This book is widely regarded as a milestone in changes to agricultural tillage practices as he questions the efficacy of ploughing, stating "No one has ever advanced a scientific reason for plowing"; "There is simply no need for plowing in the first instance. And most of the operations that customarily follow the plowing are entirely unnecessary, if the land has not been plowed"; "There is nothing wrong with our soil, except our interference" (Faulkner, 1987). Faulkner also advocated for the addition of 'Green Manure' into the crop rotation to improve the soil's water holding capacity as well as the infiltration rate.

The views of Faulkner were seen as somewhat controversial at the time, as alternatives to ploughing at the time would not allow for adequate weed control. It was described by the Readers Digest as "no book on agricultural subject has ever prompted so much discussion in the United States, at the time it was written". It was met with fierce criticism from both farmers and researchers, with an article published in Nature in 1944 stating "Farmers are cautious men, and are not likely to take very seriously the extravagant claims made by Mr. Faulkner" however the author notes that "some enterprising farmers in Great Britain may try their hand" at non-inversion tillage and green manure cropping (Schofield, 1944). Advancements in seeding machinery technology that allowed seeds to be planted with no tillage were first demonstrated in the USA in 1950 (Harrington, 2008). This enabled commercial agricultural systems predicated on reduced tillage to gain popularity in North American agriculture, where the term was coined as "conservation tillage". One of the earliest uses of this phrase was in 1967 in Illinois to encourage governmental support for various forms of reduced tillage (Allmaras and Dowdy, 1985).

Since then, cropping systems predicated on reduced-tillage (RT) have been made increasingly more viable with the introduction of plant growth regulators (PGRs) developed during World War II (Phillips, 1984; Derpsch, 1998) and effective herbicides to control weeds in the 1960-70's, such as atrazine, paraquat, and glyphosate (Manno, 1996; Giller et al., 2015). This was a significant development, as the use of rotational ploughing had traditionally been used to invert the topsoil, thus burying the weed

seed bank to a depth where the seeds became unviable. The commercial release of Paraquat in 1961 led many agricultural chemical firms to begin intensive RT research in many countries (Derpsch, 1998). Also, during this time, there were significant advances in tractor horsepower and machinery designed with reduced tillage in mind, with the first commercial NT drill introduced by Allis-Chalmers in 1967 (Lindwall and Sonntag, 2010).

Additionally, during this period, there was an increasingly expressed public alarm about the dangers of soil erosion (Allmaras and Dowdy, 1985), resulting in the issue of soil degradation being raised at the World Conservation Strategy in 1980 (IUCN, 1980) and the World Soil Charter in 1982 (FAO, 1982; Kassam et al., 2014b). This was combined with significant increases in fuel prices during the 1970's resulting in many farms becoming interested in systems that utilised less intensive management to reduce production and maintenance costs (Farooq and Siddique, 2015). Reduced tillage systems were preferred by some farmers as the traditional plough-based system was considered by some to be a grossly inefficient use of time and fuel and causes much mechanical degradation to the agricultural machines and implements (Waydelin, 1995; Derpsch, 1998). During this evolving period in agricultural practice, the term "Conservation Agriculture" was first coined in the latter part of the 1990s, which was followed by the 1st World Congress on Conservation Agriculture held in Madrid in 2001 (Giller et al., 2015).

2.6 Definitions of tillage systems

Today, tillage practices, systems and terminology vary considerably globally. Farmers opt for tillage systems which suit their cropping system, budget, weather and soil conditions (Alskaf et al., 2020). For example, in Scandinavia, the term 'conservation tillage' regularly involves some form of reduced tillage, but encompasses many variants from this, e.g., stubble cultivation in autumn followed by harrowing in spring, to no-tillage (NT) systems with no cultivation at all before sowing (Wang et al., 2006). The wide variety of commonly used tillage systems makes tillage system categorisation a complex process, and terminology commonly varies amongst practitioners and researchers (Morris et al., 2010; Alskaf et al., 2020). This is shown by the inconsistency of the literature on the adoption of emerging tillage systems, where there is much variation in practices, cropping systems, and climates. This document uses the tillage system definitions set out by (Townsend et al., 2016), which are presented in Table 2.1 below.

Table 2.1: Description of types of tillage systems. NB: Tillage definitions in the literature vary widely and may differ from those given in this table. Adapted from Townsend et al. (2016).

Tillage systems	Description
Conventional tillage (CON)	CON usually relates to the practice of ploughing, which is performed using a mould-board plough to invert the soil to a required depth, thus burying the previous season's crop residues and weeds. This is then followed by a variety of other tillage operations to work the furrows down to a suitable seedbed. (NB: Some definitions of CON include deep non-inversion tillage.)
Non-inversion tillage; reduced tillage; reduced cultivation; minimum tillage	Tillage practices that do not invert the soil. Some definitions specify maximum cultivation depths (e.g., no greater than 100 mm) and/or a particular percentage cover, usually 30% of crop residues left on the soil surface.
Deep reduced tillage	Non-inversion tillage to a depth greater than 100 mm/150 mm.
Shallow reduced tillage	Non-inversion tillage to a depth of less than 100 mm.
Strip-tillage	Strips (covering less than a third of the soil surface) are tilled and the residue moved onto the untilled strips. Seeds are then drilled on the tilled strips.
Zero-tillage; No-tillage (NT); direct drilling	This is where the seed is drilled into the stubble of the previous crop with only very minor soil disturbance.
Conservation tillage	Reduced tillage combined with at least 30% residue cover, where water erosion predominates, or at least 1120 kg crop residue left on the surface, where wind erosion predominates.
Conservation Agriculture (CA)	No-tillage combined with permanent organic soil cover (either residue or cover crop), and diverse crop rotations.
Rotational ploughing	A system where the land is ploughed at specific points in the rotation, with other tillage practices used in between.
Strategic tillage	A flexible, responsive system where ploughing is used within the rotation in response to specific conditions.
Secondary tillage	This term tends to refer to shallower and finer-scale tillage practices occurring after the main tillage practice.

2.7 Adoption of reduced tillage systems

As already detailed, the journey towards the NT system that exists today began in the USA with the first successful demonstration of NT direct sowing in 1950 (Harrington, 2008). However, it wasn't until the registration of the broad-spectrum bipyridyl herbicide Paraquat in 1962 that the system (then known as 'Chemical Fallow') began to slowly become something of global interest (Lindwall and Sonntag, 2010).

The first NT seeding experiments outside of the USA began in Australia in 1964, where the potential use of bipyridyl herbicides as a replacement for tillage was assessed (Farooq and Siddique, 2015). The Australian landscape is prone to high instances of soil degradation due to very light soils (up to 90% sand in some areas) and extremely dry conditions (< 250mm year^{-1} in some cases), coupled with anthropogenic factors such as land clearance and regular cultivation in agricultural areas (Derpsch, 1998; Derpsch and Friedrich, 2009). These factors combine to make NT cropping appealing to Australian farmers for the moisture-conservation and seeding timeliness benefits of the NT system (Lindwall and Sonntag, 2010). As a result, farmer adoption of NT cropping has been steady and consistent in Australia since its introduction in the 1960s. Now the proportion of farmers using at least some NT is peaking at nearly 90% in many regions of Australia (Figure 2.3) (Llewellyn et al., 2009; Lindwall and Sonntag, 2010) with the proportion of Australian grain crop areas sown using NT or zero-till estimated to be 74% in 2016 (Llewellyn and Ouzman, 2019).

Although Figure 2.3 shows that NT is now to be considered 'conventional practice' in Australian grain production, the figure illustrates the time-scale involved in a shift towards a new agricultural cropping system (Llewellyn and Ouzman, 2019). It also illustrates the variation in the rate of adoption between agro-ecological zones, possibly due to scepticism of the methodology in certain climates and soil types. However, ultimately, it shows the successful application of NT in a country with wide-ranging agro-ecological conditions, with most regions now exceeding 90% NT adoption (Llewellyn and Ouzman, 2019). Although Figure 2.3 does not account for dis-adoption, it is thought that the instance of dis-adoption is less than 5% nationally (Lindwall and Sonntag, 2010).

NT introduction in Australia was quickly followed by several trials across Europe, in Germany in 1966 (Baeumer, 1970), Belgium in 1967 (Cannell and Hawes, 1994), and Italy in 1968 (Farooq and Siddique, 2015). The introduction and development of NT in South America in 1969 was primarily to address issues with extensive soil degradation caused by changing agricultural practices and technology developed from

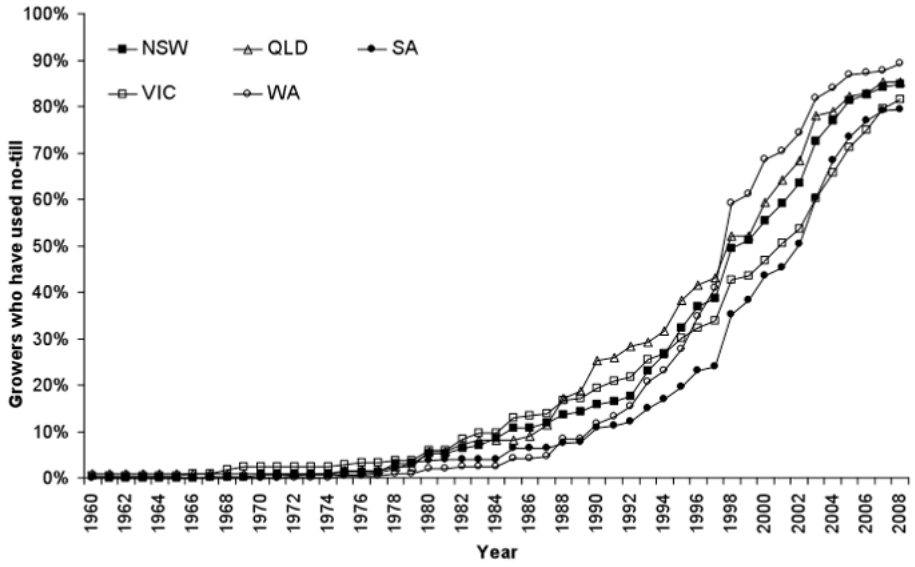

Note: NSW - New South Wales; VIC - Victoria; QLD - Queensland; WA - Western Australia, SA - South Australia

Figure 2.3: Cumulative proportion of Australian crop growers who have used no-tillage (NT) by region. Source: (Llewellyn et al., 2009)

European colonists (Speratti et al., 2015). The use of plough-based establishment had been popular and successful on European soils, and many European experts believed that tillage improves soil fertility. Whereas it is now known that increased tillage intensity can reduce SOC due to increased microbial activity and carbon (C) oxidation (Page et al., 2020).

In the UK, the popularity of RT systems peaked in the 1970's where it is estimated that around 35% of the crops were established under RT; however, this declined to 10% - 25% in the late 1980s due to problems with weeds associated with non-inversion tillage (Alskaf et al., 2020). The use of RT then declined severely in England and Wales due to the ban on straw burning in 1993. Straw burning had been used to reduce crop residue biomass and to control weeds, pests and disease on crop stubble. The ban on this practised resulted in many farmers in the UK opting for plough-based tillage instead of RT because of fears of higher weed, pest and disease burden and the remaining crop residue blocking seed drill coulters and seed placement (Townsend et al., 2016).

Table 2.2: The three principles of Conservation Agriculture with descriptions of the practice.

Principle	Description
No tillage (NT)	NT is defined as the direct planting of crops with a minimum of soil disturbance (Derpsch et al., 2014). NT is generally used synonymously with the terms "direct-seeding" or "direct drilling", which denotes the process of planting crops in previously unprepared soil by opening a narrow slot, trench, or band only of sufficient width and depth to obtain proper seed coverage. No other soil preparation is performed (Derpsch, 1998; Speratti et al., 2015). NT systems are well-reported management tools for preventing soil erosion and conserving soil fertility (Gadermaier et al., 2012).
Soil organic cover	A permanent use of soil organic cover, either by use of crop residue or cover crops. Covering at least 30% of the soil between harvest and seeding (Page et al., 2020).
Crop rotation	Stimulating soil biology using a diversified crop rotation, sequence or association which are specifically tailored to local environments and climatic conditions, with the inclusion of leguminous crops and cover/catch crops (Kassam et al., 2009; Derpsch et al., 2014; Knapp and van der Heijden, 2018).

2.8 Conservation Agriculture

CA is an agricultural system designed to manage agro-ecosystems for improved and sustained productivity by conserving and enhancing soil quality and biota (FAO, 2014; Page et al., 2020). It is being increasingly promoted as a farming system that can contribute to sustainable crop production intensification (Pretty, 2008; Kassam et al., 2014b) and is claimed to mitigate or revert many negative effects of conventional crop production practice, such as SOM decline (Page et al., 2020), soil erosion, and greenhouse gas (GHG) emissions. CA consists of three crop management principles, shown below in Table 2.2:

Although the terms NT or direct seeding are sometimes referred to as CA, this is not strictly correct. CA is not a single technology, but a production system predicated on the three main technologies described above. The first and second principles are interdependent on one another, as a permanent soil cover is not possible whilst the use of tillage is optional. Many farmers have and continue to implement various combinations of the CA principles (Giller et al., 2015). However, it is commonly deemed that it is only accurate to claim that a system is CA when all three principles are meticulously applied in practice (Derpsch et al., 2014; Giller et al., 2015). The term Conservation Agriculture has been widely encouraged and promoted as it encourages farmers to think of their farm as a holistic production system and not just focus on the tillage component (FAO, 2014; Speratti et al., 2015). The three Conservation Agriculture principles are commonly used with various companion practices such as Integrated Pest Management (IPM) or Integrated Weed Management (IWM), which

can be incorporated into the Conservation Agriculture system on a site-specific basis, as shown in Figure 2.4 (Farooq and Siddique, 2015; Page et al., 2020).

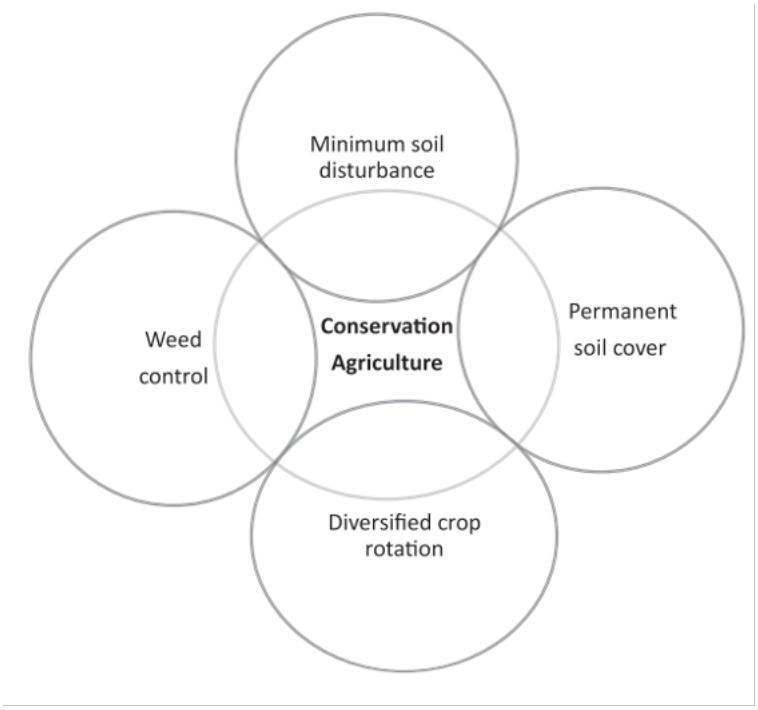

Figure 2.4: The principles of Conservation Agriculture, with an addition of Integrated Weed Management. Adapted from: (Farooq and Siddique, 2015).

Adequate weed control is a key pillar to successful CA systems due to the lack of inversion tillage, as there can be a build-up of problematic weeds in the topsoil. Therefore, weed control in CA systems is performed with a combination of adaptive and appropriate crop rotations, adapted and aggressive cover crop species inclusion in the rotation, and application of herbicides (Derpsch et al., 2014). CA is a system designed to be a means of crop production that has soil and water enhancement as its foremost priority. It is regularly cited to improve rainfed crop productivity in dry climates due to moisture conservation; therefore, it may be an important climate change adaptation strategy for regions of the world which are prone to drought (Pittelkow et al., 2015).

2.8.1 Adoption

CA systems are now practised globally in varying agricultural ecologies and climates. The spread of the application of CA systems has been significant. In 1973, the global area of farmland farmed under CA principles was only 2.8 million hectares (ha). However, since then total land area of CA has risen to 106 M ha in 2008/09, and then to

180 M ha in 2015/16, constituting an increase of 69% since 2008 (Kassam et al., 2009, 2019). Although it has been introduced and promoted in many countries globally, widespread adoption has only occurred in certain regions (Speratti et al., 2015). A range of factors have influenced the rate and extent of CA adoption in various global regions, such as climate, soil type, average holding size, and topographic conditions, to name a few. To date, the regions which have witnessed widespread adoption of CA have been Australia (Llewellyn and Ouzman, 2019), North America, and South America (Speratti et al., 2015). However, it is worth noting that objective measurement of CA adoption is challenging to quantify, as none of the underlying principles are systematically captured globally, especially when it comes to the combination of all three CA principles together (Giller et al., 2015). Often, there is confusion between terminology, where NT adoption is counted as CA adoption. Currently, Europe is far behind other regions in uptake of CA, with only the African continent having a lower relative uptake (1 million ha) than Europe, compared to Europe's 1.36 million ha (Basch et al., 2015). Within Europe, Finland, Spain, Portugal, Switzerland and the UK have the highest rates of CA adoption in terms of relative land cover.

2.8.2 Support and Criticism

CA has received strong and widespread international support in recent years, including the Food and Agriculture Organisation (FAO) (FAO, 2014). However, the widespread adoption of CA is strongly debated, in particular its crop yield potential, its applicability in different farming systems, and the economic benefits of the system (Giller et al., 2015). A meta-analysis by Pittelkow et al. (2015) using observations from 610 studies to assess the individual pillars of CA found that overall NT reduced yields; however, this response was found to be variable and highly subject to the conditions in which it was implemented. In some cases, it has the potential to produce higher yields. This study also noted that they found that when all the principles of CA were implemented, the negative impacts were significantly reduced in comparison to CON. This highlights the importance of the combination of all three of the CA principles together for successful evaluation of the CA system, and that true evaluation of the system cannot be achieved by isolating individual principles, as there is evidence to suggest that there is an interaction effect between the principles. There are commonly confounding practices compared in the literature, where some principles are adhered to, and others are not.

As a result of this, the application and benefits of CA in different agro-ecologies are a polarising subject in the scientific community, especially when it is promoted for

application in small-scale, resource-poor farms in Sub-Saharan Africa and South Asia. The 2013 Nebraska Declaration on CA was held as an attempt to find a consensus amongst scientists about the CA system applicability; however, it was subsequently criticised by some for constraining scientific debate (Andersson et al., 2014; Giller et al., 2015). Therefore, the following sections break down the individual principles in more detail and evaluate them individually and as a combination.

2.9 No-tillage

Modern No-Tillage (NT) uses specifically designed seeding equipment with discs (low disturbance) or narrow tines/coulters (higher disturbance) that are designed to open a narrow slot into the soil and plant seeds at a required depth (Derpsch et al., 2014). This section focuses on some of the known effects of transitioning to NT systems.

2.9.1 Crop Yield

The response of CA on crop yield can vary depending on a range of site-specific factors (climate, soil types, etc.) and crop management factors, for example, if it is combined with crop residue retention and diversified crop rotation (Corbeels et al., 2014). In general, NT yields are typically found to be higher in moderate- to well-drained soils, but slightly lower on poorly drained soils compared to CON (Triplett and Dick, 2008). There is also evidence to suggest that root growth may be limited in some NT systems in comparison to CON systems (Pietola, 2005).

A meta-analysis by Corbeels et al. (2014) comparing CA practices to CON-based practices in sub-Saharan Africa found that NT reduced crop yield in comparison to CON when it was not combined with crop residue retention and crop rotation diversification. However, in contrast to this, they found that when crop residues were not exported from the field, NT crop yield was higher in comparison to CON systems. When they compared the effects of crop rotation on yield, there was no significant difference between the yields of the two systems.

A global meta-analysis by Shakoor et al. (2021) using 50 peer-reviewed publications found no significant difference between the average crop yield of NT systems in comparison to CON crops. Additionally, a global meta-analysis by Pittelkow et al. (2015) used 5463 paired yield observations from 610 studies comparing NT with CON from 48 crops and 63 countries. They found that there were no statistical differences between NT and CON yields for oilseed, cotton, and legume crops. However, they

found yield penalties for NT in some cereal crops in comparison to CON; wheat (-2.6%), rice (+7.5%), and maize (-7.6%). They found that all crop yields declined in the transitional years from tillage to NT over the first two years, except for oilseed and cotton crops. However, from years 3 – 10, they found NT yield was not significantly different from the CON yield, apart from maize and wheat grown in humid climates. When they considered N addition, they found a 12% yield decline without N fertiliser addition and a 4% decline with inorganic N addition.

The meta-regression analysis by (Van den Putte et al., 2010) included 47 European studies (563 observations) and compared crop yields under CON, RT and NT techniques. They found that on average, overall yield reductions for NT by 6.05% in comparison to CON, and that soil type was a significant factor in the magnitude of reduction, with NT performing better in clay soils.

2.9.2 Soil Organic Carbon

It is widely considered that tillage is a factor in losses of SOC from agricultural soils due to reductions in soil structural stability, redistributions of SOM within the soil profile, and a decrease in soil aggregate size resulting in losses of SOC as CO_2 (Hendrix et al., 1986; Kucharik et al., 2001). Reviews of NT and SOC regularly conclude that NT causes stratification of SOC in the upper 5 or 10 cm depth (Blanco-Canqui and Ruis, 2018), whereas the accumulation of SOC lower down the soil profile is a matter of debate amongst researchers (Gadermaier et al., 2012). However, a meta-analysis by Govaerts et al. (2009) synthesised the knowledge and data of C and N cycling in agriculture, summarising the influence of tillage, residue management, and crop rotation on SOC stocks. The meta-analysis found inconclusive results, where 7 of the 78 cases examined found that SOC concentrations were higher in CON in comparison to NT; in 31 cases, there was no significant difference found, and in only 40 of the cases examined did they find a significant improvement in SOC stocks under NT in comparison to CON. In contrast, a meta-analysis of NT from South Asian countries by Kumara et al. (2020) using a total of 670 paired observations from 147 studies representing 67 crops found that the C sequestration potential of systems predicated on NT was higher (26.83 Mg ha^{-1}) in comparison to CON systems (24.5 Mg ha^{-1}). The authors found that soil type, irrigation, and inclusion of the other CA principles were the main drivers for the magnitude change of C sequestration, specifically the inclusion of legume crops in the crop rotation.

2.9.3 Soil Physical Properties

Soil compaction is a concern amongst farmers, as this can cause issues with crop establishment and growth, and as a result is thought to be a significant barrier to adopting NT (Logsdon and Karlen, 2004). Others argue that soil in NT systems is not a concern as dynamic processes such as wetting-drying, freeze-thawing, and crop rooting can help to alleviate any compaction caused by the lack of tillage (Blanco-Canqui and Ruis, 2018).

Soil bulk density and penetration resistance can be used as a measure of soil compaction and, therefore, are both commonly used as an appropriate indicator of the physical condition of the soil (Cooper et al., 2020). Pidgeon and Soane (1977) compared the soil properties of NT and plough-based tillage systems over seven years in the UK. They found significantly higher soil bulk density in NT systems; however, they found that there were no increases in NT bulk density after the third year, as the soil reached an equilibrium density for the current management practices. In contrast, Blanco-Canqui and Ruis (2018) summarised 62 studies conducted focusing on soil bulk density under NT and CON systems. They found that NT had no effects on soil bulk density in 26 of the 62 studies, increased bulk density in 24 of the 62 studies and reduced it in 12 studies relative to the CON treatment. The magnitude of the change from 0-50 cm soil depth was by 0.6% to 42% in about 39% of studies, while it reduced bulk density by 0.6% to 11% in about 19% of studies. The authors noted that most of these changes to bulk density were attributed to changes in the top 0-10 cm of soil and that the bulk density of NT soils may be influenced by the duration under NT management.

2.9.4 Crop Nutrition

Distribution and the cycling and availability of nutrients to crops are regularly influenced by soil tillage management (Doran, 1987). In general, the distribution of many soil nutrients in NT systems in comparison to tillage systems is similar to the stratification of SOC under NT systems, where there is a concentration in the soil surface layer and little or no change at lower depths (Gadermaier et al., 2012). This is particularly common with Phosphorus (P) and Potassium (K), which are relatively immobile in the soil and are partially fixed in slowly available or unavailable forms (Triplett and Dick, 2008).

Due to this stratification effect, NT generally results in accumulation of greater amounts of P and K in the upper topsoil layer (Gómez-Rey et al., 2012). However,

changes in SOM accumulation on the soil surface in NT systems can alter the nature and rate of P and K fixation and exchange in these zones. Karathanasis and Wells (1990) studied the soil K status occurring as a result of shifting management practice from CON to NT. They found large increases of up to three times the exchangeable and soluble K in most upper soil surface horizons managed using NT compared to conventionally managed land. The authors also found that these increases in K correlated well with SOM accumulation during the study period.

Doran (1987) studied the distribution of potentially mineralisable nitrogen (PMN) in long-term tillage comparisons at various sites in the USA. The author found that PMN levels of NT soils were 37% higher than those compared to conventionally cultivated soils. Highest levels of PMN in NT soils were found in the top 0 – 7.5 cm soil horizon, and in the ploughed soils, this was found to be lower from 7.5 – 15 cm in the soil. The PMN were primarily associated with the distributions of microbial biomass and total N.

Fertiliser is usually applied via broadcast spreader or via the seed drill spouts at drilling. In tillage systems, this fertiliser can be worked into the soil to a required depth before planting, whilst with NT systems, these applied nutrients remain banded in the topsoil or on the soil surface. This can result in greater amounts of nutrition in NT systems as a consequence of minimised soil disturbance, thereby reducing crop residue decomposition, and resulting in accumulation of crop residues and fertiliser in the top soil (Gómez-Rey et al., 2012). Cereal yields are lower in NT systems at lower rates of N fertiliser in comparison to plough-based tillage.

2.9.5 Soil Biological Properties

Soil microbial communities are important regulators of SOM dynamics and nutrient availability in the soil, and as such, microbial biomass is considered a good indicator of soil fertility (Gadermaier et al., 2012). It is thought that the transition to NT cropping systems may temporarily reduce soil fertility by reducing total plant available N through increases in N immobilisation in the soil due to higher inputs of organic residues (Doran, 1987). However, there is evidence to suggest that over a long-term crop rotation, NT may improve N availability and reduce N losses from leaching, by increasing labile N pool and soil N retention in the uppermost layers of the soil (Gómez-Rey et al., 2012).

Doran (1987) studied the distribution of soil microbial biomass in long-term tillage comparisons at various sites in the USA. The author found that microbial biomass averaged 54% higher in NT soils in comparison to the surface of ploughed soils. The

greatest levels of microbial biomass were found in the 0 – 7.5 cm soil depth in NT; however, in the tillage system, this was greatest at the 7.5 -15 cm depth. The study found that the differences in microbial biomass distribution at different depths were closely associated with the corresponding levels of SOC and N, water content, and water-soluble C as influenced by the differences in tillage management.

2.9.6 Greenhouse Gas Emissions

Anthropogenic emissions of Greenhouse Gases (GHG) are attributed to increasing the global temperature by $\sim 0.89°C$ in the 20th century. (IPCC, 2013; Mei et al., 2018). The atmosphere is comprised of nitrogen (N_2) (78%) and oxygen (O_2) (21%) (IPCC, 2013). When solar radiation reaches the atmosphere, around two-thirds of it will penetrate the atmosphere and be absorbed by the earth's surface, and in turn is then emitted back out in the form of infrared rays towards the atmosphere, some of which is reabsorbed (Signor and Cerri, 2013). This process is known as the greenhouse effect. The atmospheric GHG's in order of abundance are: Water vapour (H_2O), Carbon Dioxide (CO_2), Methane (CH_4), Nitrous Oxide (N_2O), Ozone (O_3), Chlorofluorocarbons (CFC's), Hydrofluorocarbon (HFC's), and Fluorocarbons. Although H_2O is the most abundant in the atmosphere, its concentrations are not affected by anthropogenic activities, and as such CO_2, CH_4, and N_2O are considered to be the most damaging GHGs (Signor and Cerri, 2013). It is estimated that since 1750, atmospheric concentrations of CO_2, CH_4, and N_2O increased by 148%, 260%, and 123%, respectively, to levels that are unprecedented in the past 800,000 years (IPCC, 2013). This has been attributed to increasing global temperature in the 20th century and has sparked global concern and dthe evelopment of climate change mitigation strategies.

Much of the focus of climate change mitigation has been on CO_2 reduction strategies. However, in recent years, there has been a focus on climate change mitigation via reduction in non-CO_2 greenhouse gases. One of the main focuses for GHG reduction globally has been mitigating nitrous oxide (N_2O) emissions. Atmospheric concentrations of N_2O are now estimated to be over 19% higher than pre-industrial atmospheric concentration (Montzka et al., 2011).

Rises in atmospheric concentrations of N_2O are particularly damaging to the climate as it has been found to have a high Global Warming Potential (GWP) to CO_2 and CH_4 and have a significant contribution to ozone depletion (Mei et al., 2018). The GWP is the internationally agreed method published by the Intergovernmental Panel on Climate Change (IPCC), which converts all GHGs to CO_2 equivalents

(Wang et al., 2021). It is defined as an index based upon radiative properties that can be used to estimate both direct and indirect effects of emissions of different gases upon the climate system in a relative sense (Muralikrishna and Manickam, 2017). It is the characteristic of each gas and is assigned as a function of its lifetime in the atmosphere and rated to CO_2 as it is the most abundant GHG (Signor and Cerri, 2013).

The main N_2O sink is via photolysis and oxidation reactions in the stratosphere, and it is estimated to have an atmospheric lifespan of 131 ± 10 years (Prather et al., 2012). This is a long atmospheric lifespan in comparison to CH_4 (9.1 ± 0.9) (Prather et al., 2012), thus highlighting the importance of the task of mitigating N_2O emissions from agricultural soils in the future.

NT is widely considered to be an effective method for combating the effects of climate change due to evidence on SOC sequestration in some research (Blanco-Canqui and Ruis, 2018). However, the effects of NT on GHG emissions are highly debated, and research findings vary greatly amongst the literature (Shakoor et al., 2021). It is commonly thought that tillage disturbs the soil profile and thus stimulates the microbial decomposition of SOM, resulting in the losses of C and N in the forms of CO_2 and N_2O (Turmel et al., 2015). This process is reduced in NT systems due to improvements to soil aggregation and a reduction in soil temperature as a result of the lack of tillage, thus leading to improved C storage (Page et al., 2020; Shakoor et al., 2021).

Typically, NT systems are found to have higher microbial biomass in the top soil in comparison to CON systems (Wang et al., 2006). The microbial community structure also changes; typically, there are more denitrifiers, aerobic microorganisms, and facultative anaerobes found in NT with fewer nitrifiers and aerobic conditions (Wang et al., 2006). When crop residue is left on the soil surface in NT systems is a source of N and C substrate for the soil biology, which can result in higher heterotrophic respiration from stimulation of soil biological activity, leading to increases in GHG fluxes from soils. This process is also affected by fertiliser application. In tillage systems, fertiliser can be incorporated into the soil profile; however, in NT it is surface applied, which in combination with surface crop residues can result in stimulation of the denitrification process resulting in increased N_2O emissions (Hu et al., 2019).

A meta-analysis by Shakoor et al. (2021) found that NT increased CO_2 by 7.1%, N_2O emissions by 12%, and CH_4 emissions by 20.8% in comparison to CON systems. However, the analysis also calculated the GWP, which is used to calculate the CO_2

equivalent emissions for all GHGs. This GWP analysis found that NT significantly reduced the GWP in comparison to CON by 7.5

2.10 Crop Residue Management

Crop residues are defined as crop biomass remaining on the soil's surface after harvest (Page et al., 2020). Global agricultural production generates around four billion metric tonnes of crop residue per year, representing more than half of the world's agricultural phytomass (Smil, 1999; Lal, 2005). Management of crop residues varies greatly depending on the climatic conditions and farming system. In general, crop residue is either buried into the soil profile with tillage, burnt in situ or exported from the field and is used or sold as biofuel or livestock feed and bedding (Turmel et al., 2015). Due to global agricultural soil degradation and declining SOC concentrations, many farmers are now being advised to increase the quantity of organic matter being applied to their soils, as this is known to have multiple benefits to many ecosystem services such as erosion control, enhanced nutrient cycling, and soil C sequestration (Chen et al., 2013; Turmel et al., 2015). As well as many agronomic benefits, such as SOM content, soil physical properties, water use efficiency (WUE), soil structural stability, and reducing soil bulk density (Turmel et al., 2015; Lu, 2020). For most farmers, the most readily accessible and inexpensive form of organic matter is crop residue. However, this regularly results in farmers facing a 'trade-off' when managing crop residue, having to balance the economic benefit of sale or use of these crop residues with the long-term benefits to their soils.

The quantity of crop residue buried below the soil surface varies considerably depending on the type of tillage, machinery usage and soil conditions. With advancements in modern agricultural machinery in recent years, there have been advancements in the tractor horsepower, implement size and operation speed and machinery design, which generally reduces the quantity of crop residue left on the soil surface. However, the retention of crop residue on the soil surface is thought to enhance and maintain physical, chemical, and biological properties in agricultural soils via multiple mechanisms (Turmel et al., 2015).

2.10.1 Soil Organic Carbon

Crop residues are the precursors of the labile and stabilised SOM pool, its decomposition in the soil is the initial formation stage that results in nutrient release driving improved microbial communities and plant growth, and in the longer-term results in

repeated cycling of C through the microbial biomass and the formation of recalcitrant stable SOM known as humus (Collins et al., 1997; Govaerts et al., 2009). Therefore, crop residue addition is very important for increasing and/or maintaining SOC concentrations in agricultural soils. However, the effect and speed of change may be controlled by soil type, climate and soil management factors (Turmel et al., 2015).

A study by Blanco-Canqui and Lal (2007) assessed long-term (10 year) impacts of three levels (0, 8, 16 t ha^{-1} dry matter (DM)) of wheat straw applied annually on SOC concentration and soil physical properties (0–50 cm depth) under zero tillage on a Crosby silt loam in central Ohio. They found that between 0-10 cm total amount of SOC was 16.0 t ha^{-1} in the treatment with no addition of straw, 25.3 t ha^{-1} in the treatment with 8 t ha^{-1} straw added, and 33.5 t ha^{-1} of SOC in the treatment with 16 t ha^{-1} straw added. Although below the 10 cm depth, they found no significant differences between the SOC pool concentrations of the treatments. They noted that, around 33% of the total C addition during the 10 years was sequestered to SOC and hypothesised the remaining quantity of C was lost via CO_2 and CH_4 emissions.

2.10.2 Soil Physical Properties

Crop residues protect the soil surface from solar radiation and erosion from wind or water, as well as acting as a buffer to excessive surface sealing, crusting, and compaction whilst reducing the dispersion of soil aggregates (Blanco-Canqui and Lal, 2009). The effectiveness of this is thought to be a function of percentage soil cover, rainfall intensity, soil type, and wind velocity (Ruan et al., 2001).

The presence of crop residues and growing crops in the field can have an effective reduction in soil erosion. This is due to increases in soil cover reducing the wind speed at the surface of the soil, thus reducing the flux of soil particles (Blanco-Canqui and Lal, 2009). The presence of crop residue on the soil surface helps to reduce the velocity of surface water movement, which reduces the risks of water erosion. The effect of vegetation cover on soil loss is highlighted in Figure 2.5.

Surface crop residue addition can cause problems with herbicide efficacy; therefore, CA systems may require weed control plans to be modified in comparison to tillage-based cropping systems (Fryrear and Skidmore, 1985). Surface crop residues can also be effective at reducing evaporation losses from soils, conserving soil moisture, which can be a highly beneficial agronomic practice in climates and soil types prone to drought (Fryrear and Skidmore, 1985). The study mentioned in the previous section by Blanco-Canqui and Lal (2007) assessing long-term impacts of three levels (0, 8, 16 t ha^{-1} DM) of annual wheat straw application under NT found that that the majority

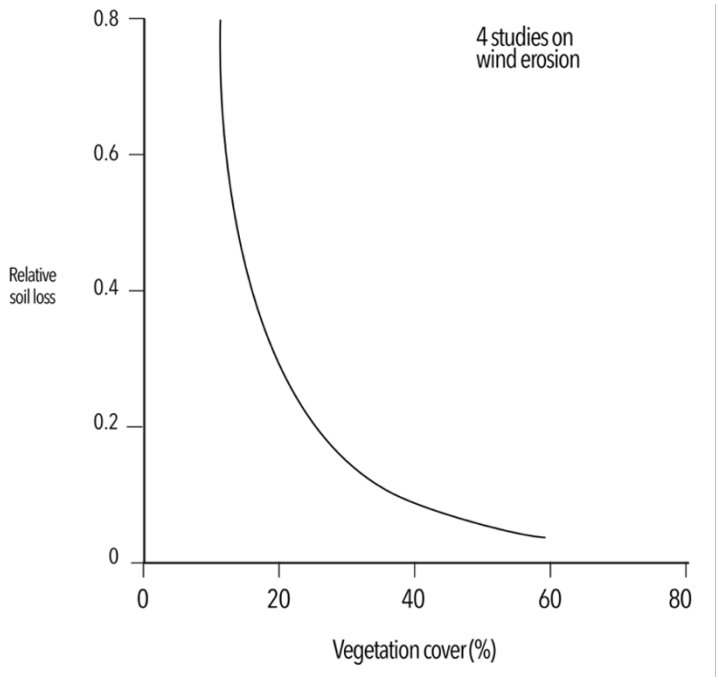

Figure 2.5: Graphical summary of four studies on the relationship between relative soil loss by wind erosion and percent vegetation cover by wheat. Adapted from; (FAO, 2019a)

of the changes to soil physical properties due to crop residue addition were found in the upper 5 cm of the soil, where crop residues decreased bulk density by 40–50%, aggregate density by 30–40%, and particle density by 10–15%, and increased tensile strength of aggregates by up to 14 times compared to soil without crop residues. They also found that the quantity of surface crop residue addition can affect the soil temperature (Figure 2.6), which can reduce evapotranspiration losses as well as influence total GHG fluxes from the soil.

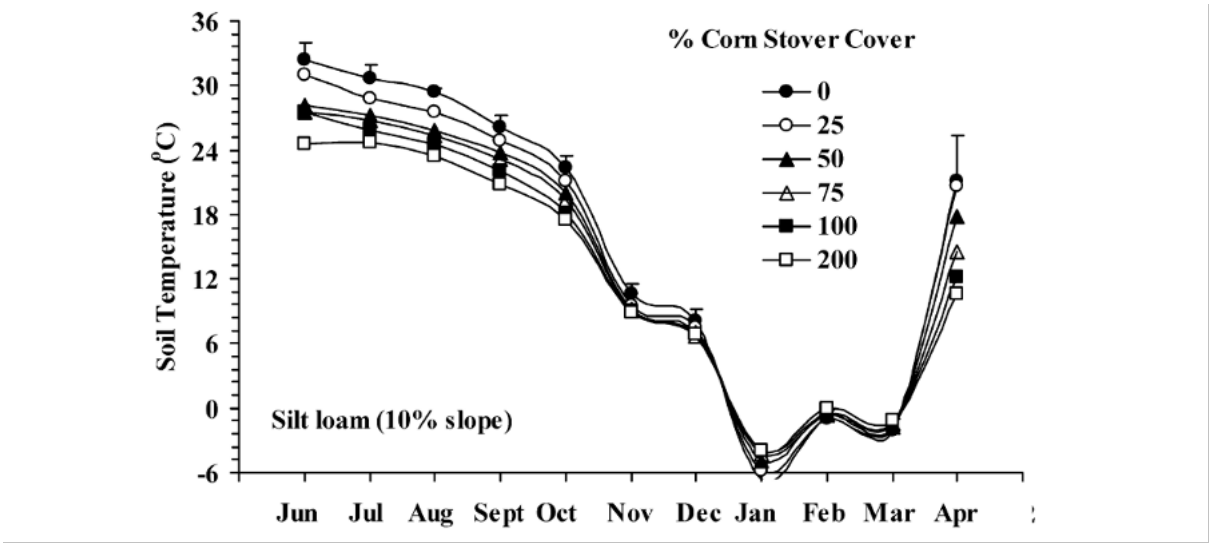

Figure 2.6: Response of soil temperature to varying rates of crop residue soil cover in a NT corn. The error bars represent the LSD values of the mean. Adapted from (Blanco-Canqui and Lal, 2009)

2.10.3 Greenhouse Gas Emissions

The main direct sources of global N_2O emissions are from agricultural practice, manufacturing processes, and burning biomass (Reay et al., 2012). Indirect emissions are predominantly attributed to anthropogenic manipulation of the Nitrogen (N) cycle, via usage of fossil fuels resulting in NO_x deposition, inorganic/organic N-fertiliser application resulting in leaching and runoff, and cultivation of N-fixing crops (Reay et al., 2012). These processes can promote increased availability of mineralised N and thus the likelihood of occurrence of microbially mediated nitrification or denitrification resulting in N_2O emissions (Montzka et al., 2011). Nitrification is the aerobic microbial oxidation of ammonium (NH_4^+) to nitrate (NO_3^-), emitting N_2O as a by-product of the reaction (Hergoualc'h et al., 2019). Nitrifier denitrification is the reduction of nitrite (NO_2^-) to nitrogen monoxide (NO), followed by the reduction to N_2O, and finally reduced down to dinitrogen (N2) (Wang et al., 2021). Denitrification is a two-step anaerobic process whereby NO_3^- is converted to N_2O and then into inert N_2 (Wang et al., 2021). N_2O is the gaseous intermediate in the denitrification reaction and the by-product of nitrification that is emitted from soil microbiology into the atmosphere (Hergoualc'h et al., 2019). The principal N transformations leading to the emission of N_2O in soils are shown in Figure 2.7. It is generally thought that denitrification is the main source of N_2O in soils, as denitrification N_2O yield potential is much higher (1–100%) than nitrification (0.1–1%) (Hu et al., 2019). There are

a number of regulatory factors that control the rate of these processes, such as soil N concentration, fertiliser application, moisture, temperature, and land management techniques (Signor and Cerri, 2013).

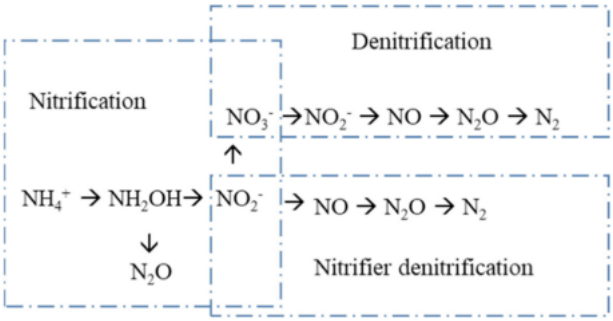

Figure 2.7: Principal N transformations leading to the emission of N_2O in soils. Source: (Wang et al., 2021)

N_2O emissions are of particular concern in agricultural soils, which are estimated to contribute about two-thirds of total anthropogenic emissions (Van Der Weerden et al., 2012; Mei et al., 2018). With an increasing population globally and the consequent demand for increases in food production, N_2O emissions will likely continue to rise in the coming decades without significant changes to our agricultural systems. Considering the high GWP and lifespan of N_2O and the significant emissions from agriculture, the development of future emission-reduction strategies should have agricultural practice at the heart of the strategy. Currently, there is much interest in methodologies to reduce agricultural soils N_2O emissions; however, accurate estimation, prediction, and mitigation have proved to be challenging for researchers and practitioners.

The rapid increase in NO_x from fossil fuel burning due to industrialisation in the past century was also coupled with the rapid intensification of agricultural practice. These practices have resulted in large increases in N_2O and NH_4 emissions, to the extent that anthropogenic reactive nitrogen (Nr) emissions have increased between three to five times in the past 100 years (Reay et al., 2012). Intensification of agricultural practice is responsible for a significant disturbance to the global N cycle, with the usage of Nr as fertilisers, manures and widespread growth of N-fixing crops (Reay et al., 2012). As agricultural practices continue to intensify globally, N_2O emissions are presently increasing at a rate of 0.25% per year (Wang et al., 2021). The rising N_2O from agriculture are presented in Figure 2.8.

Due to declining soil organic matter levels, many farmers are now being advised to retain crop residues in the field. This practice not only reduces greenhouse gas

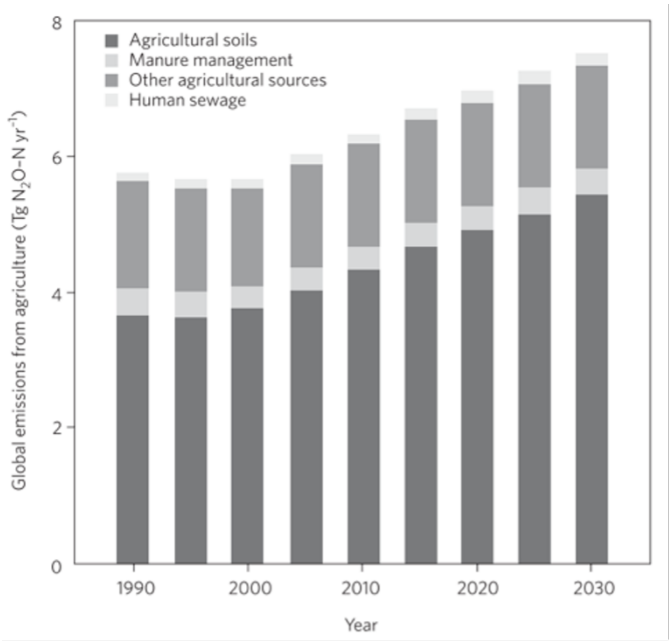

Figure 2.8: Global N_2O emissions and estimated values from agriculture between 1990 and 2030. Source: (Reay et al., 2012; USEPA, 2012)

emissions associated with burning but also returns organic material to the soil, supporting key ecosystem services such as erosion control, improved nutrient cycling, and carbon sequestration (Chen et al., 2013). In addition to these environmental benefits, crop residue retention offers several agronomic advantages, including enhanced soil organic matter content, improved soil physical properties, increased water use efficiency (WUE), greater soil structural stability, and reduced soil bulk density (Lu, 2020).

However, these ecosystem service improvements from crop residue addition can be offset by substantial soil N_2O emissions (Garcia-Ruiz and Baggs, 2007; Chen et al., 2013). Crop residue decomposition can have multiple effects on soil mitigation and production of N_2O emissions. This is because, as plants decompose, the organic material is subject to microbial N mineralisation and nitrification. Depending on the N content of the crop residues, this may release large amounts of labile N and thus reduce the C:N ratio of the soil (Garcia-Ruiz and Baggs, 2007; Chen et al., 2013). Crop residues also add C substrate back to the soil, which can result in N immobilisation in the soil, as this addition stimulates microbial N assimilation. This results in heterotrophic microorganisms and autotrophic nitrifiers rapidly assimilating NH_4^+, which reduces future N_2O production as the labile N pool is reduced (Chen et al., 2013).

The chemical composition and the quantity of crop residue additions play an important role in determining the availability of NH_4^+ and NO_3^- in the soil and therefore control the nitrification and denitrification processes, and thus the total magnitude of the N_2O emissions (Aulakh et al., 1991). A meta-analysis by Hu et al. (2019) found that N_2O emissions are increased when high and low quantities of biomass are added to the soil, but not significantly affected when medium quantities are added. This is suggested by the authors to be related to the C:N ratio and the lignin:N ratio of the biomass. When high amounts of C and N are applied to the soil, this promotes heterotrophic microbial respiration, which depletes soil O_2 concentrations (Gomes et al., 2009). These anaerobic soil conditions promote denitrification and thus N_2O production. For example, a study by Garcia-Ruiz and Baggs (2007) found that soils with the addition of legume crop residues can have N_2O emissions of close to three times that of a non-amended soil. The magnitude of these soil GHG fluxes is a result of crop residue addition but also heavily influenced by the rate and type of fertiliser, crop type, soil temperature and soil moisture (Skiba et al., 1996).

2.11 Crop Rotation

Crop rotation is the practice of growing a series of crops sequentially over time on the same land (Yates, 1954). It has been a widely adopted crop management practice for many years to mitigate weed, insect, and pathogen pressure, as well as to increase plant diversity in agricultural cropping systems (Zhao et al., 2020). However, the variation and complexity in crop rotations vary vastly across the world in modern agriculture. Since the introduction of modern herbicides and synthetic fertilisers in previous decades, some cropping systems are now dramatically simplified and predicated on mono-culture cash crop production, relying heavily on pesticides to control problems with crop weeds, pests and pathogens in the place of rotational cropping.

Due to the rise in understanding about global soil degradation in recent years, cover cropping is becoming a more common practice in global agriculture. These are planted as longer-term over-winter cover crops or can be planted as fast-growing species as a catch-crop in between harvest and drilling of cash crops. There are many cited benefits to cover crop inclusion in a crop rotation, including: reducing soil erosion, improving soil fertility, sequestering SOC, improvements to soil structure and water stable aggregation, and improvements to in-field biodiversity (Govaerts et al., 2009).

2.11.1 Crop Yield

During the coming years, it is predicted that land use intensity may have to increase to meet growing demands for food and bioenergy, and therefore, longer crop rotations may not be as economically viable (Bennett et al., 2012; Vera et al., 2022). As land use intensity increases to meet rising demand for food and bioenergy, farmers may face stronger economic pressure to prioritise high-yielding, high-profit crops in shorter rotations, reducing the appeal of longer rotations that tie up land in less profitable uses. However, there is much evidence to suggest that monoculture or un-complex crop rotations are prone to yield decline in comparison to complex or longer crop rotations (Bennett et al., 2012). Many biotic and abiotic factors are linked to this crop rotation yield decline. Biotic factors include plant pathogens, mycorrhizal pathogens, crop allelopathy, or crop auto-toxicity. Abiotic factors include land management practices and soil nutrient availability (Bennett et al., 2012).

A meta-analysis by (Zhao et al., 2020) using 45 studies with 214 comparisons from China to examine the effects of crop rotation on yield, found that in comparison to monoculture crop production, crop rotation increased crop yields by 20% on average. They noted that the strength of the effects of crop rotation on yield was strongly linked to the total rainfall of the area. In southwestern China, yield benefit was found to be +38% improved yield in complex crop rotations; however, in areas with moderate annual rainfall (400−550 mm), the yield benefit was smaller and less pronounced (+10%). They also found that the yield response of crop rotation heavily depended on soil texture and previously cultivated crops. Greater yield benefits were seen in soils with medium-coarse texture, lower total N (≤ 1.2 g kg^{-1}), and with intermediate levels of initial soil organic carbon (7–10 g kg^{-1}). However, they also found that the yield benefits of crop rotation were more pronounced in CON systems in comparison to NT systems.

2.11.2 Soil Organic Carbon

CA practices are regularly cited to have the potential to sequester more SOC because of improvements to the water-holding capacity of the soil, which results in the ability to grow catch-crops in between the harvest and drilling of cash crops. The improvements to water retention increase the chance for plant establishment and growth during this period, when soil moisture can be at its most depleted. Cover crops can increase SOC sequestration by increasing the input of plant residues and providing organic matter cover, preventing soil erosion.

A meta-analysis by West and Post (2002) using a global database of 67 long-term agricultural experiments, consisting of 276 paired treatments, compared potential soil C sequestration rates for different crops in response to decreasing tillage intensity or enhancing rotation complexity. They found that enhancing the rotation complexity has the potential to sequester an average 20 $\pm$ 12 g C m^{-2} yr^{-1} in many cropping systems. The study also estimates the time in which sequestration can occur; for this, they estimated that following the implementation of complex rotations, SOC may reach a new equilibrium in 40−60 years.

2.12 Combined Principles

2.12.1 Crop Yield

In recent years, widespread uptake of NT has taken place globally over an estimated 125 million ha, which is equivalent to 9% of global cropping area. However, the degree in which this is combined with the other principles of CA is highly variable and is difficult to quantify accurately (Pittelkow et al., 2015; Giller et al., 2015).

As already detailed in Section 2.9 on NT, the practice implemented by itself is highly variable when compared to crop yield under CON. Despite individual studies claiming yield benefits of CA ranging from 20 – 120% in Latin America, Africa and Asia (Kassam et al., 2009; Rockström et al., 2009), there are many cases where no yield responses are found. The meta-analysis by Pittelkow et al. (2015) found significant yield reductions (-9.9% when NT was implemented on its own. However, when combined with crop residue retention and diversified crop rotations, the yield decline is minimised (-2.5%) in comparison to CON. When two of the CA principles were combined, they found yield declines of −5.2% for NT and crop residue retention and -6.2% when NT was combined with crop rotation. The authors state that the results from the analysis suggest that for the best results of CA cropping systems that NT should be the last principle to be implemented into a system already employing crop residue retention and crop rotation. Whereas typically, it has been the first principle that is implemented in many cropping systems globally. The results from the meta-regression analysis by Van den Putte et al. (2010) also concur with these findings. This study found that, on average, NT resulted in a crop yield decline of 8.5%. However, the yield decline is more pronounced in systems with less diverse crop rotations, where only cereals are present (12%) in comparison to a diverse rotation (6.2%).

Pittelkow et al. (2015) highlights the need for a nuanced view when assessing CA practice, as yield responses to crops and agro-ecologies differ greatly from CA implementation (Giller et al., 2015). The paper found significant yield enhancements for NT (7.3%) under rainfed agriculture in dry climates when the other two CA principles are also implemented. However, when NT is applied alone in these climatic conditions, it resulted in yield reductions of −11.9%. When this was compared to humid climates, it was found that NT results in yield declines regardless of the application of any other CA principles. It was hypothesised that the yield response to climatic conditions is based upon improved water infiltration and greater soil moisture conservation that are associated with NT systems. Thus, CA has the potential to provide the most agronomic benefit in regions where crops are prone to drought.

2.12.2 Soil Organic Carbon

The magnitude of the effects of CA on SOC compared to CON systems varies considerably in the literature. This is influenced by many factors, including soil type, crop management, climate, baseline SOC content, duration of CA implementation, and soil sample depth and methodology (Page et al., 2020). Most of the studies available concentrate on NT and residue retention in comparison to CON and residue removal. There are a small number of studies that factor in the inclusion of crop rotation diversification and the effects of cover crops. When just NT and crop residue retention are monitored the narrative review by Page et al. (2020) found that values of the magnitude change in SOC ranged from -0.15 Mg ha^{-1} year^{-1} in areas such as the midwestern USA to $+0.93$ Mg ha^{-1} year^{-1} in tropical Brazil. When all CA management principles were conducted together, it was often found that this leads to greater SOC concentrations compared to NT and residue retention practices.

The meta-analysis of NT from South Asian countries by (Kumara et al., 2020) using a total of 670 paired observations from 147 studies representing 67 crops found that the C sequestration potential of systems predicated on NT was higher ($+2.33$ Mg ha^{-1}) in comparison to CON systems. When the other CA principals were evaluated, this was found to have the potential to sequester more C than NT alone. They found NT + crop rotation treatments increased C sequestration by 2.85 Mg ha^{-1} in comparison to CON + crop rotation and found that NT + crop residue addition increased C sequestration by 1.29 Mg ha^{-1} compared to the CON + crop residue treatments. However, when all principles were applied, this resulted in the largest difference between the systems (4.6 Mg ha^{-1}). They also found significant effects of soil type on C sequestration potential, finding that clay-based soils had the potential

to sequester significantly more C than sand or silt loams. They also found that duration of practice was a significant factor in the magnitude of C sequestration potential, which they hypothesise to be because of improvements to soil quality over time in CA systems.

2.12.3 Economic Performance

Many economic benefits of CA systems have been well reported; these include; reduced expenditure and improved profitability (FAO, 2014, 2001; Syngenta, 2024), lower energy requirements (Parihar et al., 2018; Das et al., 2021), lower water usage (Kumara et al., 2020; Das et al., 2021), reduce expenditure (Kumara et al., 2020; Lorenzetti and Fiorini, 2024; Kumara et al., 2020), reduce machinery operation times and improve timeliness of machinery operations (Kassam et al., 2014a; Morris et al., 2010), and improve system gross profit margin (Lorenzetti and Fiorini, 2024). However, when considering the farm-level economic variables and factors of CA adoption, it is imperative to consider not only the short-term financial effects of agronomic and machinery changes, but also the implications for the wider farm management. These include the risks and uncertainty that accompany new methodologies, financial constraints to enable systems change, the availability and knowledge base of the labour force, and time-related factors, such as interest rates and subsidy payments (Pannell et al., 2014). It is also worth noting that there is not a large body of literature assessing the economics of CA, and that most of those published highlight that the economics of CA are highly heterogeneous between regions and individual farms within a region and therefore need to be considered on a case-by-case basis. This heterogeneity is also present within individual farms, where soil textures can vary considerably, potentially leading to partial adoption of CA or its application only in specific soil types or cropping systems (Pannell et al., 2014). Therefore, economic analyses of CA systems are best conducted at a local scale to account for these site-specific variations.

A meta-analysis by Kumara et al. (2020) analysed the system economics of 67 crops grown in South Asian countries under NT, RT and CA practices. They found significant cost of production reductions under NT and RT systems in comparison to CON systems in all the selected crops analysed; however, they did not differentiate between systems inclusion of other CA principles (crop rotation and residue management) in the economic analysis. They found the cost of production to be significantly less in NT and RT rice (-22%), legumes (-20%), wheat (-14%), and other crops (-10%).

Table 2.3: Cost comparison of conventional (CON) practice and Conservation Agriculture (CA) in US dollars ha^{-1}. Adapted from (Farooq and Siddique, 2015).

	CON (USD ha^{-1})	CA (USD ha^{-1})	Cost Saving (%)
Fuel	75	25	66.67
Depreciation	115	65	43.47
Maintenance	22	10	54.55
Pesticides	35	45	-28.57
Total Costs	247	145	41.30

2.12.4 Barriers to Adoption

As the previous sections of this report have touched upon, there are many agronomic, social, and practical considerations for the adoption of CA systems. It is a challenging transition for farmers to implement all three CA principles, as it requires a holistic change at the individual farm level, where broad advice does not suit site-specific conditions. The common barriers to its adoption are: knowledge of how to manage the system for the best outcome, many social factors (tradition, prejudice etc.), availability and cost of specialist machinery, the opportunity cost of crop residues for feed rather than mulch, lack of supporting policy in certain countries, lack of suitable herbicides to control weeds in the place of tillage, and constraints on the availability of land, labour and capital at key times of year (Derpsch and Friedrich, 2009; Pannell et al., 2014). One of the most significant factors affecting the lack of uptake of CA is the well-reported yield decline in the transition period from CON to CA. Although there is evidence to suggest that CA systems are more profitable, most of the benefit is a result of cost savings and not from production increases (Farooq and Siddique, 2015). Despite this, transitional yield declines can severely discourage poorer farmers who may be focused on short-term goals, and thus is considered a key limiting factor in the uptake of CA (Pittelkow et al., 2015).

A study by Llewellyn and Ouzman (2019) analysed data collected from two Australian national surveys of cereal growers, a country where there has been wide uptake of CA. They found that most farmers believed that NT systems with stubble retention would result in increased incidence of weed, pest and disease problems as well as raising crop input costs. Despite this, more than half of the farmers believed that NT wheat yield would become more reliable, and over 70% in the northern region of Australia. Pittelkow et al. (2015) notes that for successful implementation of CA in the dry climates that would agronomically benefit the most from the system (sub-Saharan Africa and South Asia), it is important that it is adjusted to local conditions involving

multi-stakeholders that consider equipment availability, local market opportunities, and farmers' production objectives.

2.12.5 Equipment for Conservation Agriculture

One of the key practical management decisions for farmers in the UK who are considering the transition to CA is the choice of seed drill. Drills designed to function in tilled soil do not perform well in undisturbed soils, which are usually coupled with surface crop residue. Therefore, specialist equipment is required (Triplett and Dick, 2008). There has been a plethora of NT-based drills emerging on the market in the UK in recent years with a range of designs, widths, and costs (Examples shown in Figure 2.9 and 2.10 below). Matching the type of seed drill to the soil conditions is key to successful crop establishment (Baker et al., 2006). As the prices of these drills range from £20,000 to in the region of £120,000 (Mowbray and Clarke, 2019), this decision is usually considered with great care by farmers.

Figure 2.9: A Sky Agriculture EasyDrill HD. Source: Author's own

Figure 2.10: A Horsch CO3. Source: Author's own

One of the main problems encountered by farmers when using NT seed drills is the closure of the "seed slot"" (the area of the soil which is moved by the seed drill coulter to plant the seed in to). This is of particular importance in clay soil types, where the effect of the drill passing through the soil can smear the uncultivated soil, leaving the planted seed exposed and a localised area of compaction within the seed slot (Baker et al., 2006). This can lead to problems with slugs and water running down the channels created by the seed drill (Clarke, 2015). The main difference in NT seed drill design is that of the openers, the only components of an NT drill that break the soil surface. There are many different types and variations of openers

available to farmers. However, the two main categories are tine-based or disc-based openers, examples of which are displayed in Figures 2.11 and 2.12 below. Both tine and disc-based approaches have different mechanical variations which alter the shape of the slots they create in the soil and their interaction with seed placement and seedling emergence and growth (Baker et al., 2006). The openers are also coupled with a trailing implement which is designed to close the seed slot, which can work on a variety of principles from rolling, pressing, or deflecting disturbed soil back over the planted seed (Baker et al., 2006). The study by Choudhary (1979) found varying responses for a range of NT openers to the establishment of wheat seedlings at different soil moisture contents.

In general, most openers with mechanical components (e.g. disc-based openers) have some limitations in wet and sticky soils (Baker et al., 2006). However, disc-based drills create much less soil disturbance and can drill directly into larger cover crop stands, as the discs cut through the biomass on the soil surface, which can accumulate between the openers and the carrier frame in the tine-based systems. However, one problem that can be encountered whilst drilling into crop residues with disc-based drills is the process of pushing crop residue down into the seeding slot, colloquially known by farmers as "hair pinning", which can reduce crop establishment (Triplett and Dick, 2008; Baker et al., 2006).

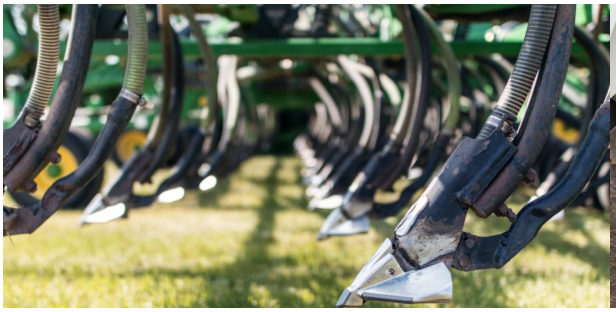

Figure 2.11: An example of a tine opener. Source: Swire (2017)

Figure 2.12: An example of a disc opener. Source: Oliver (2017)

Another consideration for farmers is the horsepower needed to operate the drill; tine-based drills require significantly less weight to operate effectively as the tines pull into the ground, creating downforce whilst in operation. In comparison, disc-based systems require weight on the drill carrier frame to achieve the same downforce, therefore typically requiring larger tractors with higher horsepower. The study by Baker et al. (2006) showed that a disc-based drill required four times as much downforce to penetrate the soil as a tine-based alternative. However, required 50% less draught

force to pull the drill through the soil. These points emphasise the importance of NT drill opener choice dependent on soil conditions and the existing farming system.

Many farmers who have been practising CA for many years in the UK advocate for a two-drill approach to farm management. In this scenario, it allows the farmer to choose the type of drill best suited to the soil and crop residue conditions of the moment. A key barrier to this approach is the initial costs of the NT drills; in many cases, farmers cannot economically justify having two NT-specific drills on the farm. As an alternative to this, there is a growing movement of farmers purchasing second-hand drills and retrofitting low-disturbance openers to them to create low-cost NT drills (Mowbray, 2020).

2.12.6 Regenerative Agriculture

Regenerative Agriculture (RA) is an emerging approach to land management that aims to restore and enhance the resilience of agroecosystems by improving soil health, biodiversity, and ecosystem services (Rhodes, 2017; White, 2020). While it shares several foundational principles with CA, including minimal soil disturbance and permanent soil cover, RA differs in its broader ecological goals and more holistic system-level focus. A range of claims have been made about the potential for RA to enhance the sustainability of food production, including the possibility that RA can be a part of a climate change mitigation strategy, although despite widespread interest, no legal or regulatory definition exists nor has a widely accepted definition emerged in common usage. (Newton et al., 2020; Schreefel et al., 2020).

The RA movement began in the 1980s when the term was used by the US-based Rodale Institute. Robert Rodale, the then president and chief executive officer of the institute, described RA as "one that, at increasing levels of productivity, increases our land and soil biological production base. It has a high level of built-in economic and biological stability. It has minimal to no impact on the environment beyond the farm or field boundaries. It produces foodstuffs free from biocides. It provides for the productive contribution of increasingly large numbers of people during a transition to minimal reliance on non-renewable resources" (Giller et al., 2021). This was expanded on by Harwood (1983), the Director of Rodale Research Centre, who gave a 10-point summary of the 'Regenerative Agriculture Philosophy':

1. Agriculture should produce highly nutritional food, free from biocides, at high yields.

2. Agriculture should increase rather than decrease soil productivity, by increasing the depth, fertility and physical characteristics of the upper soil layers.

3. Nutrient-flow systems, which fully integrate soil flora and fauna into the pattern of are more efficient and less destructive of the environment, and ensure better crop nutrition. Such systems accomplish a new upward flow of nutrients in the soil profile, reducing or eliminating adverse environmental impact. Such a process is, by definition, a soil genesis process.

4. Crop production should be based on biological interactions for stability, eliminating the need for synthetic biocides.

5. Substances which disrupt the biological structuring of the farming system (such as present-day synthetic fertilisers) should not be used.

6. Regenerative agriculture requires, in its biological structuring, an intimate relationship between the manager/participants of the system and the system itself.

7. Integrated systems, which are largely self-reliant in nitrogen through biological nitrogen fixation, should be utilised.

8. Animals in agriculture should be fed and housed in such a manner as to preclude the use of hormones and the prophylactic use of antibiotics, which are then present in human food.

9. Agricultural production should generate increased levels of employment.

10. A Regenerative Agriculture requires national-level planning but a high degree of local and regional self-reliance to close nutrient-flow loops.

Although there was limited press and academic coverage of RA from the 1980s, since 2010 the term has seen a huge growth in usage from producers, retailers, researchers, and consumers, as well as politicians and the mainstream media (Newton et al., 2020) (See Figure 2.13). Despite widespread interest in RA, no legal, scientific, or regulatory definition of the term exists, nor has a widely accepted definition emerged in common usage (Schreefel et al., 2020; Newton et al., 2020; Giller et al., 2021). The study by Newton et al. (2020) reviewed 229 journal articles and 25 practitioner websites to characterise the term RA. They found many definitions and descriptions of RA in use in the scientific and practitioner publications, and they also found some publications which did not put forward a definition of RA, and when

contacted, expressed reluctance to define the term. They found that for those who could define the term, the definitions were based predominantly upon "processes" (e.g. use of cover crops, mob grazing, etc.) and "outcomes" (e.g. increase soil organic carbon, increase biodiversity, etc.) based approaches. The authors note that both "process" and "outcome" based approaches leave ambiguity on the actual definition of RA. For example, process-based definitions may imply that users are open-minded about the possible outcomes of these processes, and similarly, outcome-based definitions may imply that users are open-minded about the processes that may lead to those outcomes (Newton et al., 2020).

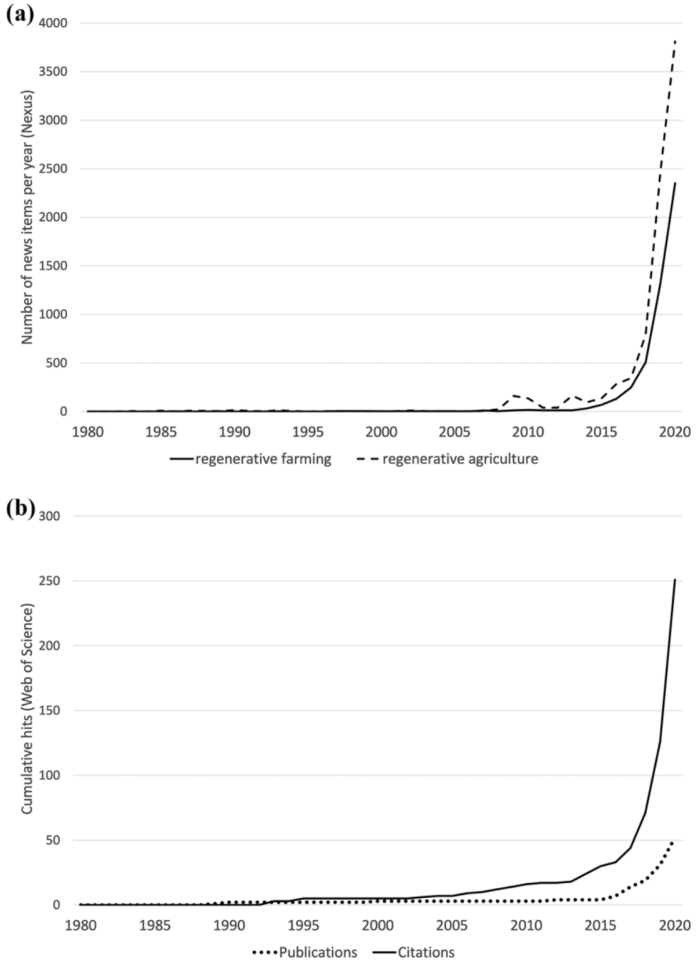

Figure 2.13: **A:** Occurrence of Regenerative Agriculture or Regenerative Farming in news items. **B:** Academic peer-reviewed publications on Regenerative Agriculture or Regenerative Farming. Adapted from: Giller et al. (2021)

Similar to CA, practical advice about RA is usually disseminated using a set of principles; however, currently there is no consensus in the agricultural industry literature on those principles, but generally they contain the CA principles with some

additions (Landers et al., 2021). This is highlighted by the comparison between Figure 2.14 and Figure 2.15, where Syngenta Group (2025) define six principles of RA, and Wood (2023) defines five principles, however the only "Minimise soil disturbance", "Maintain living roots", "Maximise cropping diversity", and "Integrate livestock" are shared between both sets of principles. Wood (2023) uses "Keep the soil covered" and an additional principle of "Context of the farm operation", whilst Syngenta Group (2025) opt for "Precision application of biological and chemical inputs". This principle, suggested by Syngenta Group (2025), highlights the risks of having a poorly defined technology, which can then be used for marketing purposes. Syngenta Group manufactures agrochemicals, thus has an economic interest in additions to the principles of RA, which incorporate agrochemical usage. As (Landers et al., 2021) states, failure to define RA will likely, at times, be harmful to society when sustainable food systems are urgently needed.

Whilst there is an urgent need for a clear scientific definition of RA, there is some consensus that it broadly features the principles of CA, with, typically, the addition of livestock grazing. The rise of RA is a great opportunity for the agricultural industry as it already has gained support from industry and consumers (Giller et al., 2021). It is not a direct threat to CA, as it embodies the CA principles; therefore, it should be seen as the evolution of CA to a broader scope and a more meaningful contribution to sustainability (Landers et al., 2021), although the lack of a universally accepted definition or certification system remains a challenge for wider adoption and policy integration.

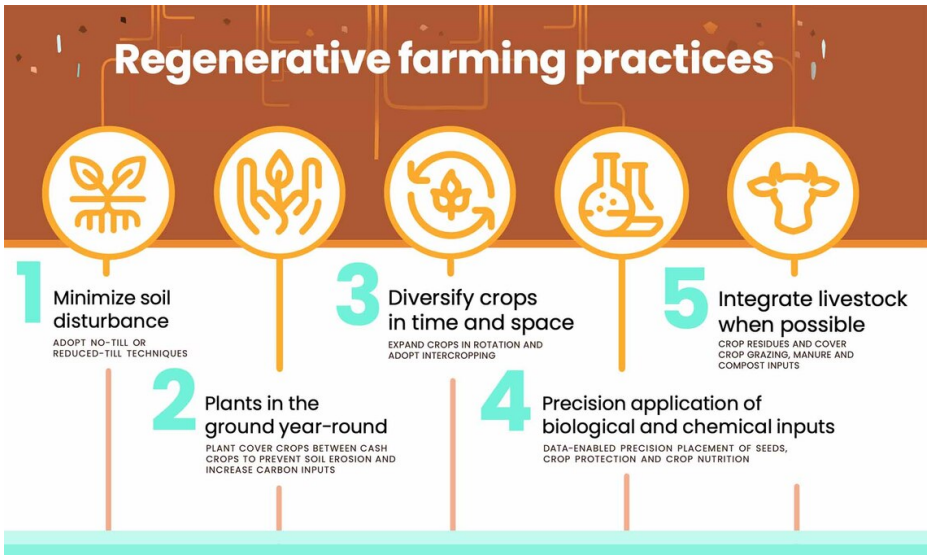

Figure 2.14: The principles of Regenerative Agriculture defined by: Syngenta Group (2025)

Figure 2.15: The principles of Regenerative Agriculture defined by: Wood (2023)

2.13 Conservation Agriculture Experimentation

Experiments designed to evaluate CA are often criticised by proponents of the CA system that necessary aspects of the system were omitted from the experiment and that the results therefore do not represent 'true' CA that would be practised commercially (Giller et al., 2009). This can either be in the form of an experimental design where principals are removed to isolate the effects of a singular principal, or in the case of systems experiments, where it becomes difficult to isolate the variables and evaluate responses (Derpsch et al., 2014). Additionally, this is exacerbated by the highly heterogeneous results from CA experimentation between regions and individual farms. For greater consensus on the effects of CA systems, there is a need

for more experimentation on the subject and a greater variety of methodologies to evaluate the practice.

2.13.1 On-Farm Experiments

On-farm experiments (OFE) are experiments conducted at a commercial scale on commercial farms, and in most cases, in collaboration with farmers (Roques et al., 2022). Traditionally, applied agricultural research has been conducted in research centres and university-owned farms, with the findings then disseminated to farmers by the researchers and knowledge exchange organisations (Mutsaers, 1997; Cho et al., 2021). Research conducted on existing commercial farms, however, can allow for improved knowledge transfer from academia to industry, as the research is conducted is often more commercially relevant to the farmer in terms of environment, location, and management practices (Cho et al., 2021; Roques et al., 2022). This type of on-farm research is generally adapted to fit in with the existing agricultural system being implemented on the farm, and as a result, has the potential to deliver more adoptable and sustainable solutions for farmers. This is unlike traditional agronomic experimentation, where the various crop production variables are tightly controlled and assigned to small and highly representative areas (Pringle et al., 2004a). OFE offers some advantages over the traditional small plot approach as it not only greatly improves the relevance of the results, due to the field-scale area and farm-scale machinery used, but it also allows for spatial variable analysis of in-field characteristics that is relevant to commercial application (Roques et al., 2022).

Over the past two decades, there has been increased interest and use of OFE conducted by farmers in partnership with researchers due to demonstrated improvements to land and agronomic productivity and advancements in technology (Kyveryga, 2019; Cho et al., 2021). For example, recommendations and results derived from small-scale research experiments conducted by researchers in small plots are often disregarded by farmers due to the difference between the scale and their own scale of operation (Jin et al., 2021). OFE can help to address this problem by demonstrating new technology and methodology in agriculture at a systems level. However, this type of research carries greater risks of failure compared to traditional experiments due to a variety of scenarios, e.g. errors in trial establishment, data collection, or farmer withdrawal from the experiment (Roques et al., 2022). It also comes with different methodologies to traditional agronomic research strategies, for example, systems experiments require much larger experimental areas to accommodate farm-scale equipment (Drinkwater et al., 2016). There are also many confounding factors in systems research because the

entire system, including the treatments, is the unit of study; therefore, it frequently requires different experimental and statistical analyses in comparison to traditional research (Drinkwater et al., 2016). In general, in factorial field experiments, a "Control" plot is included, which does not receive a treatment. In systems experiments, however, this is not representative of commercial agricultural systems, where the option to not farm the land is not financially viable. Many studies opt for the use of a reference system to compare with the experimental systems, which is generally the "conventional" management practice used in that area in commercial farming (Drinkwater et al., 2016).

The use of precision farming technologies in the agricultural industry has sparked interest in on-farm research from farmers and researchers alike because of the ease of collecting low-cost production data (Griffin et al., 2006). Although some farmers regularly conduct rudimentary analysis, such as treatment yield averages from predefined management areas on their farms, many still do not take this approach, opting for incremental changes to their management practices over time. This traditional decision-making process is a complex one that is based on many factors and not primarily based purely on agronomic results (Pringle et al., 2004b). For example, many farms are family businesses and therefore, there is often pressure to take risk-averse business decisions and opt for the management practices that are tried and tested. This results in the uptake of new technologies being slower in the agricultural industry in comparison to other industries. On-farm experimentation may hold the key to improving the rate of technology and methodologies in the agricultural industry by involving direct communication between farmers and researchers, which can support and improve research relevance and enhance the adoption rate of new technologies in the industry (Kyveryga, 2019). The interest and usage of on-farm research has increased greatly during the last twenty years in developed countries. This is related to the wider uptake of precision farming technologies such as Global Positioning Systems (GPS), yield sensors and variable-rate applicators (VRA), which have made collecting data over remote and large areas more possible at low cost.

2.13.2 Experimental Design

Although the rise of new precision agriculture technologies has made the collection of on-farm data an easier process, the main problem with site-specific field-scale (SSFS) data is the occurrence of large spatial variance, which reduces the use of the classical statistical approaches to agronomic experimentation (Griffin, 2006). However, Pringle

et al. (2004a) note that in contrast to traditional experimentation, SSFS experimentation should not attempt to reduce or ignore the spatial and temporal variation of agronomic data, as this is the very reason for this type of research methodology. This can result in large amounts of data that would usually not be available in more traditional agronomic experimental designs to become useful to farmers and researchers. The authors also note that it is important when designing OFE that the design should not disrupt the farmer's normal cropping management operations. Therefore, designs of OFE experiments need to have flexibility, simplicity, and economic risk reduction as the main objectives of the design (Pringle et al., 2004a).

2.13.3 Data Collection in On-Farm Research

In agronomic experimental designs, the method of how treatments are allocated to plots is either by random or systematic allocation. Randomisation is seen as vitally important by many as: (i) it neutralises environmental variation; and (ii) the standard estimation of variance is valid only when applied to a random sample. Therefore, in most cases, randomisation, blocking, and replication are essential to minimise external variation in OFE over large spatial areas. However, the basic intrinsic features of cropping systems, which include agronomic and mechanical considerations, should be taken into account when designing OFE experiments, and therefore, in some cases, compromises on statistical power have to be made (Alesso et al., 2019). Simple designs such as completely randomised and randomised complete block designs (RCBD) are very popular choices in OFE; however, occasionally systematic, non-randomised arrangements of treatments are used (Piepho et al., 2011). This is usually when more complex statistical methodologies are being utilised, such as spatial analysis (Kyveryga et al., 2018). Pringle et al. (2004a) evaluate field-scale experimental designs and discuss the choice of randomisation and systematic treatment allocations. They state that the choice of randomised or systematic treatment allocations is affected by whether the goal of the experiment is a comparison of crop responses or estimation of crop responses. Panten et al. (2010) elaborates on this and states that "The main aim of whole-of-block on-farm trials is to estimate treatment effects spatially for the whole area. Therefore, systematic as opposed to randomised treatment application is preferred."

OFE can be grouped based on the primary objective of the experiment: (i) experiments that aim to quantify crop responses, and (ii) experiments that are designed to explore the spatial variability of crop responses within fields Pringle et al. (2004b); Alesso et al. (2019). Georeferenced data is therefore not required for OFEs aiming

to just quantify the effect of a treatment compared to a control treatment. However, if the aim is to spatially map the response patterns over a large area, then it is of imperative importance that the spatially referenced data is collected (Alesso et al., 2019).

2.13.4 Randomised complete block design

The most common methodology to OFE is the randomised complete block design (RCBD), which utilises field length strips or tramlines as the plots (Piepho et al., 2011; Cho et al., 2021). This type of design allows for Analysis of variance (ANOVA) to test the statistical significance of the treatment. This is shown below in Figure 2.16.

This type of RCBD, although simple, is difficult for farmers to implement in their businesses as it requires planning, treatment randomisation can cause operational problems in crop management, and for the data to be analysed it requires each experimental unit to be harvested individually and the yield recorded, which can significantly slow down farm operations during very busy periods for the farm business (Cho et al., 2021). In recent years, this has been aided by the availability and increase in use of yield monitors in modern combine harvesters.

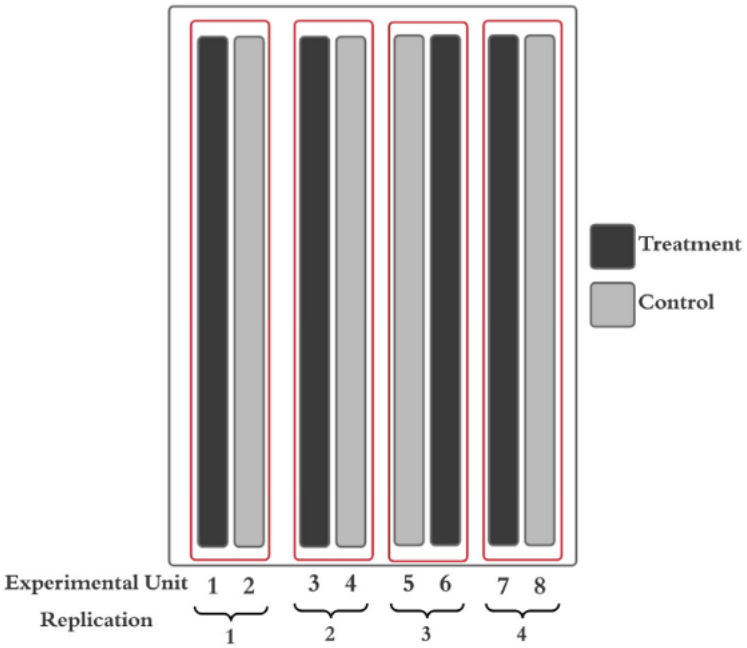

Figure 2.16: Randomised complete block design for field scale experiments. There is one treatment and one control plot allocated per block, replicated four times. Source: (Cho et al., 2021)

2.13.5 Split Plot Design

A split-plot design is another commonly used experimental design for OFE trials. Unlike an RCBD, the split-plot design has two treatments and experimental units that differ in size (Kyveryga et al., 2018). Split-plot design allows for smaller and fewer experimental units. The sub-plots embedded in the design can be used to test the hypothesis and are effective at identifying underlying mechanistic differences across the systems (Drinkwater et al., 2016). However, this type of design is complicated for machinery operators as it utilises multiple treatment factors and randomisation. This is a time-consuming design for OFE, as it involves harvesting multiple plots individually, which can slow down harvest operations on farms. An example of the split plot design is shown below in Figure 2.17.

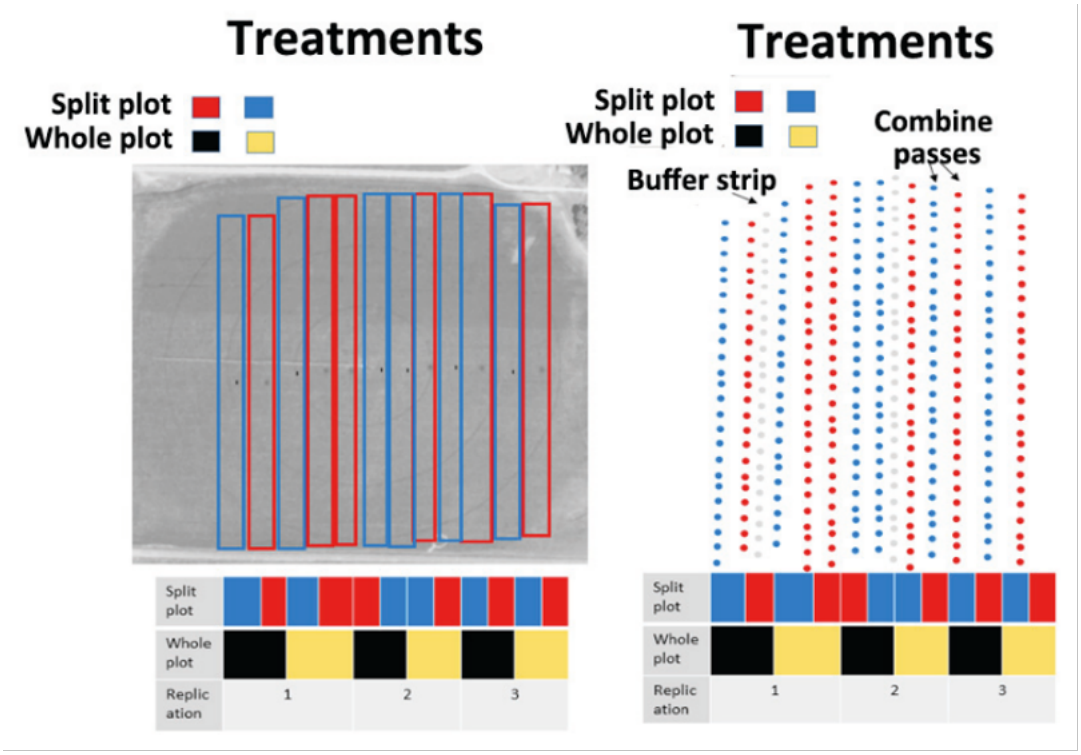

Figure 2.17: The split-plot design detailed by Kyveryga et al. (2018). Whole plots are denoted by black and yellow, split plots are denoted by red and blue.

2.13.6 Systematic strip design

The systematic strip design or adjacent strip comparison method is a simple and low-cost methodology for evaluating treatment comparisons on a large commercial scale (Doerge and Gardner, 2015). Due to the simplicity and ease of establishment

of this design, it is one of the most common types of agronomic experimental design (Pringle et al., 2004a). This method utilises parallel alternating strips across a whole field, with varying strip widths depending on the farming system. Commonly, the width of the strip is dictated by machinery operational widths; however, this method is occasionally adapted in a 'split planter' design where two halves of a seed drill are used for different seed varieties (Doerge and Gardner, 2015; Alesso et al., 2019). When the farmer drills the field, the result is alternating strips of differing varieties, allowing for comparison between the two treatments.

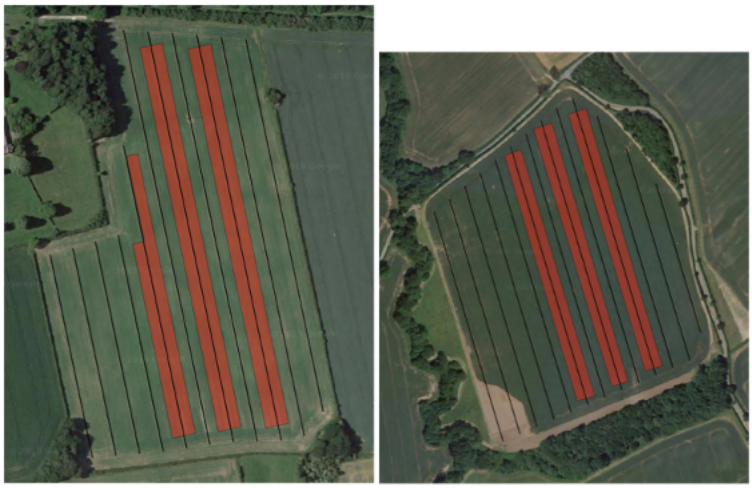

Figure 2.18: The systematic strip design used by Roques et al. (2022). The black lines are the tramlines for machinery operations, and the red shaded area is the width of the tramline plots

2.14 Conclusion

There is much evidence to suggest that CA practice may be beneficial for not only farm economics but also many different soil quality parameters, including SOC sequestration, improving SOM, soil structure, water holding capacity and aggregate stability in agricultural soils over time. There is evidence to suggest that even though NT has been found to result in yield declines in comparison to CON, the severity of the yield suppression is reduced by the inclusion of crop residue retention and crop rotation in the cropping system, and the duration of the NT system.

Currently, CA adoption in the UK is lagging behind much of the rest of the world (Basch et al., 2015), despite much promotion from research and development bodies. There are many causes for hesitancy in the adoption of CA, including evidence of yield

declines, increased weed and pest incidence, and lack of knowledge of the systems. This is coupled with complications in comparing and evaluating the effects of CA in scientific literature, due to variation in climatic and soil type conditions, lack of standardisation of research methodologies, as well as variation in the application and terminology of all CA principles for effective comparisons (Derpsch et al., 2014).

To improve understanding, scientific consensus and commercial adoption of CA practices in the UK, there is a need for more systems-level experimentation over a wider variety of conditions, which assess the combination of NT, crop residue return, and diverse crop rotations and their interactions on UK farms. It is also recommended that to mitigate yield reductions when adopting CA practices, farmers implement crop residue retention and crop rotation diversification into their cropping system before implementing NT, as well as growing crops which have been shown to suffer less from NT yield decline in their specific region in the transitional years.

Chapter 3

General methodologies

3.1 Introduction

This chapter provides an overview of the general techniques employed to collect, analyse, and interpret the data collected in this study. This mainly details the general experimental design and general management of the main field experiment, data collection methodologies, and the statistical approach to evaluating the effects of the experimental treatments.

3.2 Experimental site

3.2.1 Location and Climate

The study was conducted at Shavington and Cloverley Estate, Calverhall, Whitchurch, UK (Lat 52.915, Lon −2.606). The area has a humid temperate oceanic climate, with a mean annual air temperature from the past 20 years of 9.82°, the coldest month being January with a mean temperature of 1.15°, and the hottest month being July with a mean temperature of 21.13°. During the previous 20 years, the mean precipitation was 682.53 mm, with the mean number of days receiving ≥ 1 mm of rain being 131.6 per year (Met Office, 2023). Historic mean climate data (1946 - 2024) is shown in Figure 3.2.

The experiment began in 2022 and was conducted over two fields, which are situated adjacently (Figure 3.1), and are 3.7 ha and 5.7 ha in area. The main soil type of the site is a sandy clay loam, which is classified by the National Soil Resources Institute as a slowly permeable, seasonally wet, slightly acid but base-rich loamy and clayey soils (SoilScape 18) (Hallett et al., 2017). The topsoil A horizon is approximately 25 cm deep, with a B horizon extending from approximately 25 cm to 60 cm

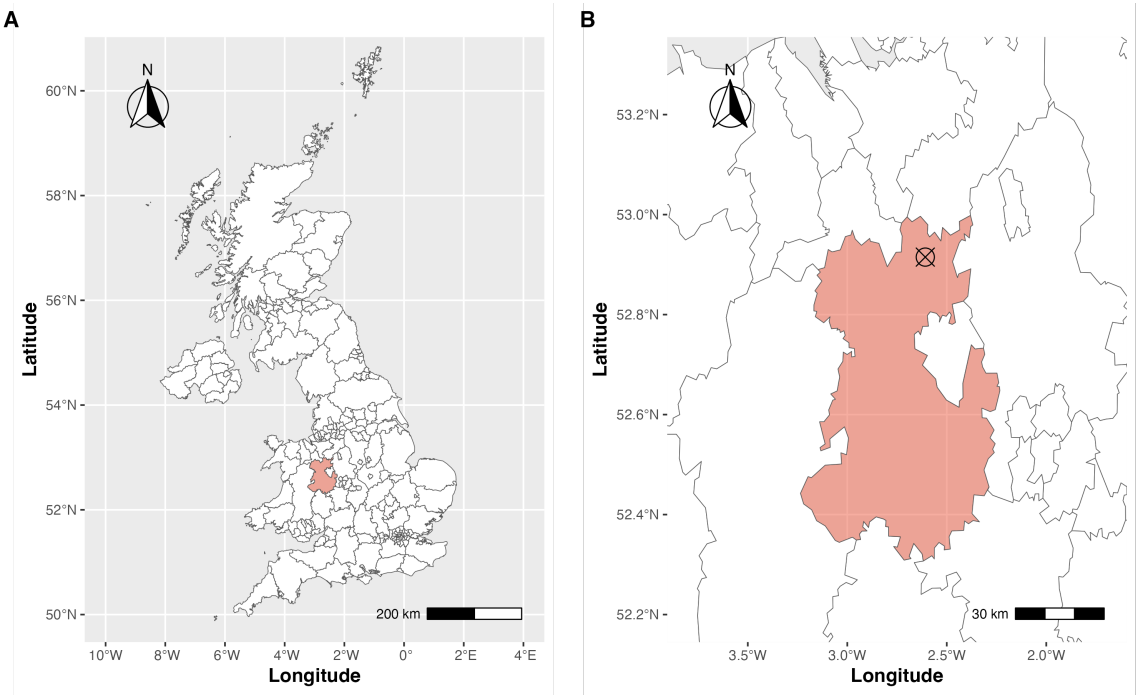

Figure 3.1: Figure indicates the location of the experiment in the west of England (**A**), on Whitegates Estate located in north Shropshire (**B**).

deep (Figure 3.5). The site is drained with 100 mm diameter clay piping at a depth of 1.2 m. Unfortunately, no field drainage maps are available as the system has been adapted on multiple occasions over the years since its installation.

Daily temperature and precipitation data were obtained from a local weather station located 20 km from the experimental site at Lat 52.794, Lon -2.663, 72 metres above sea level (Met Office, 2023; Meteostat, 2024). Sunshine data taken from an automatic Kipp & Zonen sensor. The weather data is presented below in Figure 3.2; however, the effects on the experiment are discussed in each of the following chapters.

3.2.2 Previous Cropping

There is limited data available about the previous cropping on the experimental site; however, it included a mixed rotation of grass leys and some arable cropping grown conventionally, utilising pesticides and tillage. In recent years, the site has been used to grow forage maize.

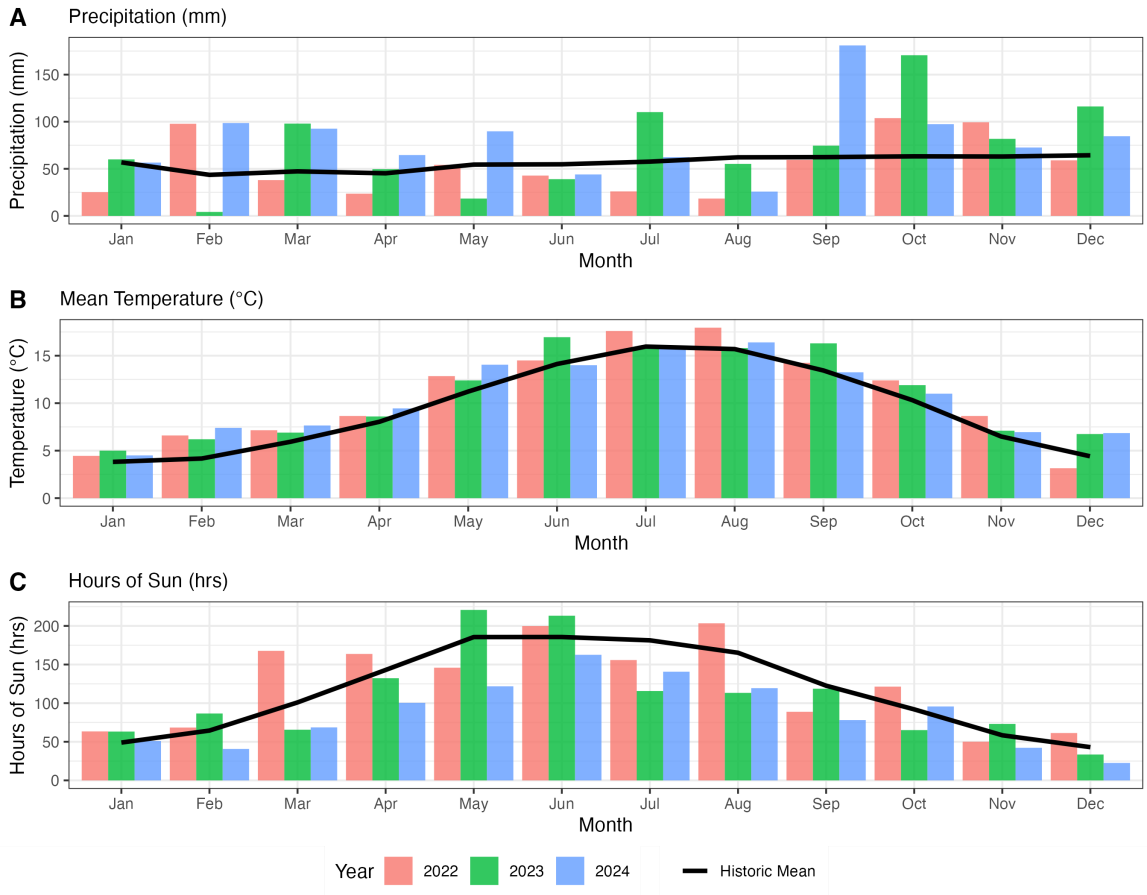

Figure 3.2: Climatic data for the experimental years and the mean historic data (1946 - 2024) for **A:** Mean precipitation (mm), **B:** Mean temperature (°C), **C:** Mean hours of sun (hrs). Data source: Met Office (2023); Meteostat (2024).

3.3 Baseline soil sampling

Baseline soil sampling was conducted on 02/02/2022, with one pooled sample and one undisturbed sample collected from the north, south, east, and west of each field. The pooled sample was composed of soil taken from five locations at a depth of 0–10 cm, which were mixed in a bucket before subsampling for chemical analysis. The undisturbed sample was taken from a randomly selected location within the field and used to determine dry bulk density. Soil samples were sent to NRM Laboratories Ltd., Bracknell, UK (division of Cawood Scientific Ltd.), who are largest commercial laboratory for agronomic soil analysis in the UK. The laboratories hold ISO/IEC accreditation (ISO/IEC 2017) from UKAS (Staines upon Thames, UK). Samples were sent for standardised soil agronomic analysis as recommended by UK nutrient management guidelines (AHDB, 2017). Measurements included soil pH and soil indices P

(Olsen P method (Olsen, 1954)), Mg and K (NRM, 2021a). The baseline soil sample results are summarised in Table 3.1.

Table 3.1: Soil properties from the baseline sampling.

Position	Phosphorus (mg l^{-1})	Potassium (mg l^{-1})	Magnesium (mg l^{-1})	pH	Bulk density (g cm^{-3})	SOC (%)	N (%)
Field 1 NORTH	20.2	130.1	61.6	6.55	1.29	1.821	0.1656
Field 1 EAST	25.2	123.25	68.65	6.1	1.15	1.651	0.1623
Field 1 SOUTH	20.2	113.6	68.3	6.21	1.5	1.694	0.161
Field 1 WEST	23.4	134.15	64.8	6.44	1.28	1.678	0.1637
Field 1 CENTRE	19.2	123.65	65.7	6.28	1.23	1.655	0.1641
Field 2 NORTH	17.6	127.3	68.35	6.33	1.17	1.435	0.1371
Field 2 SOUTH	13.4	132.55	51.85	6.06	1.47	1.705	0.1688
Field 2 EAST	14.8	121.25	50.05	6.38	1.14	1.525	0.1373
Field 2 WEST	13.8	130.5	54.3	6.2	1.14	1.849	0.1764
Field 2 CENTRE	21.8	151.85	47.95	6.09	1.13	1.594	0.1474

3.4 Sampling Point Generation

Before the experiment started, an electrical conductivity (EC) scan was performed on 24/03/2022 to determine the variation in soil properties across the trial site. This was performed using a trailed scanner operating at 24 m widths. The scan was performed by running the scanner 12 m from the tramlines, recording data at one-second intervals. The EC scanner records at one-second intervals and produces data points recorded in Siemens m^{-1} across the field site at 24-metre widths. Further details of the EC scanning methodology can be found in Section 5.1.1.

Ordinary kriging was then performed using R (version 4.3.0) (R Core Team, 2023) to interpolate the variation in soil EC across the whole field. Ordinary kriging is a widely used spatial interpolation method. It serves to estimate a value at a point of a region for which a variogram is known, using data in the neighbourhood of the estimation location (Wackernagel, 2003; Vasques et al., 2020; Heil and Schmidhalter, 2012). The zonal maps of soil EC produced by the kriging interpolation process were then used to divide the field into soil sampling zones where differences in soil properties are hypothesised to correspond with variation in the EC results. To achieve a representative spread of samples taken across the whole site, the results of the EC kriging were then simplified using a smoothing function in QGIS (version 3.22.11) (QGIS Association, 2024) into 10 soil zones across both fields. These were defined to encompass all experimental units in the field.

Using QGIS, the treatment plots were then used to generate random sampling points with soil zone and experimental unit as factors. The programme generates

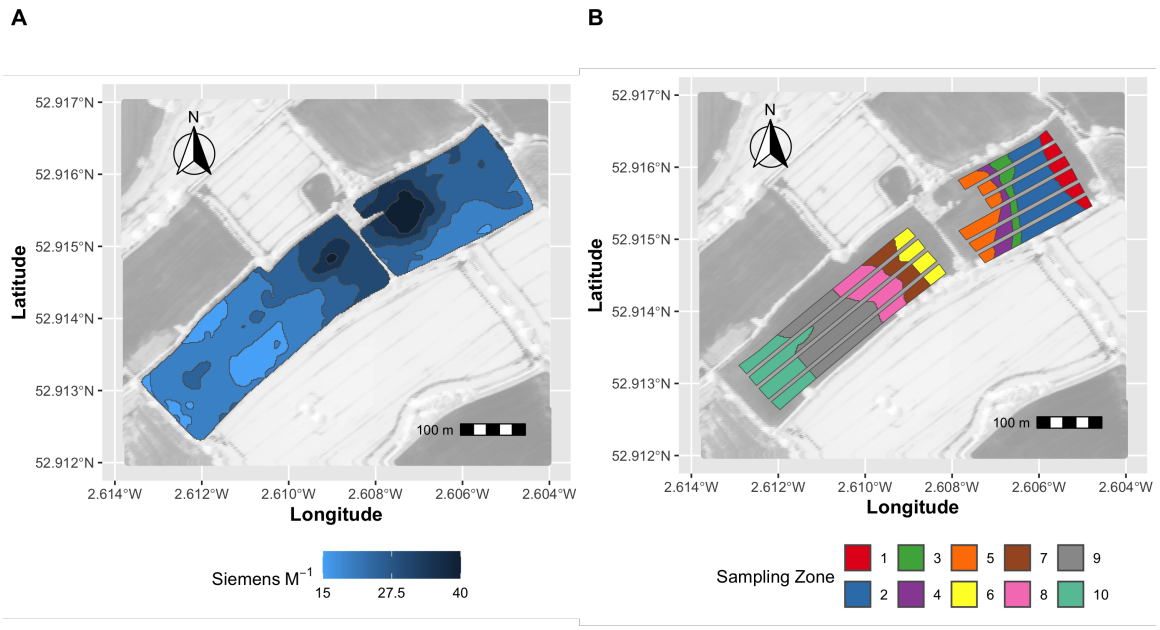

Figure 3.3: **A:** An interpolated map of the electrical conductivity scanning on 24/03/2022. **B:** A plot of the sampling zones and randomly generated sampling points. Sampling zones are indicated with coloured areas, whilst the sampling points are indicated with black points.

three sampling points per area, with a 10-meter buffer from other points generated. The experimental unit areas were reduced by 3m to reduce the effect of the neighbouring treatment. 150 sampling points were generated randomly throughout the trial site using treatment and soil zone as factors. This resulted in each treatment being sampled at 15 points distributed evenly between the five soil zones of that treatment. Points were identified using a Garmin eTrex22 with a predicted accuracy of 3m (Garmin, 2022).

This sampling strategy was designed to provide a representative, unbiased, and spatially independent set of data points, improving the reliability and generalisability of conclusions drawn from the study. Agricultural fields often show substantial spatial heterogeneity in soil physical and chemical properties, such as texture, moisture, organic matter, and nutrient content (Nyengere et al., 2023). These underlying differences can strongly influence key soil processes, including greenhouse gas fluxes, nutrient cycling, and crop performance.

By performing an electrical conductivity (EC) scan before sampling, zones of contrasting soil properties were identified, enabling a stratified sampling approach.

Randomising the selection of sampling points within these zones minimised the risk of sampling bias, for example, by unintentionally over-representing areas of certain soil conditions. This increases the likelihood that the resulting dataset accurately captures the variability within the system, providing a more robust basis for comparing treatment effects and ensuring that observed differences are not simply due to localised soil conditions.

Randomisation also helps to avoid systematic errors that might arise from operator decisions or field patterns, and improves the statistical validity of subsequent analyses by ensuring independence of samples. Furthermore, applying minimum distance buffers between points and reducing sampling areas near plot edges reduced the risk of spatial autocorrelation or treatment contamination from neighbouring plots.

3.5 Experimental design

The experiment consists of a systems-level comparison of Conservation Agriculture (CA) and Conventional Agriculture (CON) crop production systems with 10 plots and five replicates using a systematic plot design. Plots were 24 m wide and varied in length due to the field shape. The experimental design is presented in Figure 3.4 and a photo of the experimental site is presented in Figure 3.5.

All machinery operations were conducted by local agricultural contractors. All grain haulage, storage, and drying were conducted by agricultural contractors. The two systems were managed independently by qualified agronomists, one specialising in commercial agronomy and the other specialising in conservation/regenerative agronomy. The agronomic plan was devised by the agronomists independently for each system, from regular field observations during the season, as is common practice in a commercial setting. The agronomists were asked to adhere to the following principles for each system:

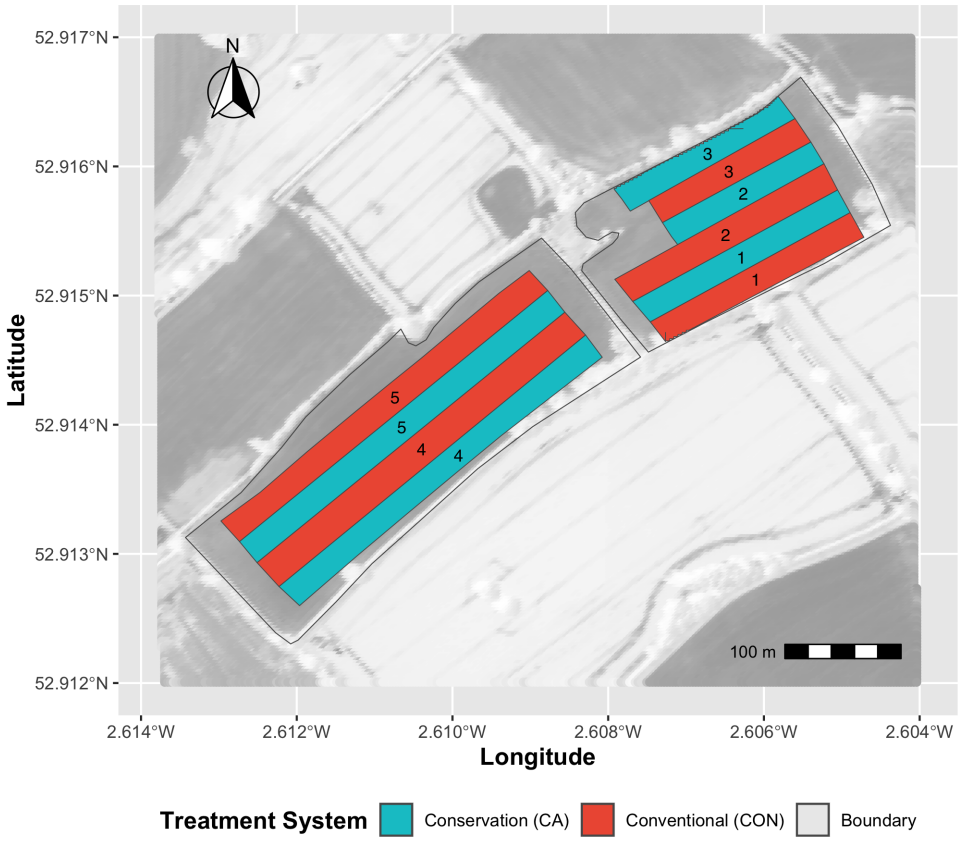

Figure 3.4: Experimental design - Light blue denotes the Conservation Agriculture (CA) treatment, and red shaded areas denote the conventional agriculture (CON) treatment. Numbered labels refer to the block number.

Conventional Agriculture (CON):

1. Tillage: Ploughing and cultivation to be performed ahead of crop establishment when judged necessary by the agronomist, using conventional methods.

2. Residue management: Cereal straw to be baled and removed from the field following harvest; oilseed rape residues were also removed or lightly incorporated.

3. Cover crops: No cover crops to be sown at any point during the rotation. The fields are to fallow between cash crops.

4. Pest and disease control: Standard agrochemical practices are to be followed, including the use of insecticides, fungicides, and herbicides according to commercial recommendations and seasonal pest pressure.

5. Crop rotation: A typical rotation should be followed for the region, primarily focusing on maximising profitability.

Conservation Agriculture (CA):

1. Tillage: No tillage to be used at any stage. All crops to be established using a low-disturbance direct drill (e.g., John Deere 750A or equivalent).

2. Residue management: All straw and crop residues to be chopped and evenly redistributed over the soil surface at harvest to maintain continuous ground cover.

3. Cover crops and companion crops: Where possible, diverse cover crop mixes should be sown in the autumn or spring during fallow periods between cash crops.

4. Pest and disease control: Herbicide and fungicide applications to be used according to commercial recommendations, depending on weed and disease pressure. Insecticides are not to be used.

5. Crop rotation: The rotation should include both cereal and broadleaf crops, with deliberate diversification.

Figure 3.5: **A:** A drone photograph of the trial taken in July 2024. Source: Andrew Watson. **B:** A photo from the experimental site showing the soil profile. The A horizon is featured from the soil surface to approximately 25 cm, the B horizon is from approximately 25 cm to 60 cm.

3.6 Crop Rotations

During the first three years of the experiment, both systems used the same crop rotation. This was to allow for direct comparisons between treatments. This decision was contrary to one of the key principles of agricultural systems research, where the entire decision-making process for crop management should have been performed by the agronomists. This would allow the crop rotation to be tailored to the system in which it is being implemented. This would be the preferred option, as it would be a more accurate representation of industry practice, where crop rotations would be altered during the transition to CA to allow for cover cropping and a wider diversity of crops. The systems-level research approach of using different cropping systems would have been preferable if there were more years' worth of data available during this study period, as trends over time could have been analysed. The rotation used was spring beans (*Vicia faba*) in 2022, winter wheat (*Triticum aestivum*) in 2023, and oilseed rape (*Brassica napus*) in 2024. The oilseed rape crop in the CA treatment was drilled with a companion crop of berseem clover (*Trifolium alexandrinum*) and buckwheat (*Fagopyrum esculentum*); however, this crop failed over the winter of 2023; therefore, spring barley (*Hordeum vulgare*) was planted in the spring of 2024. The crop rotation is detailed in Figure 3.6.

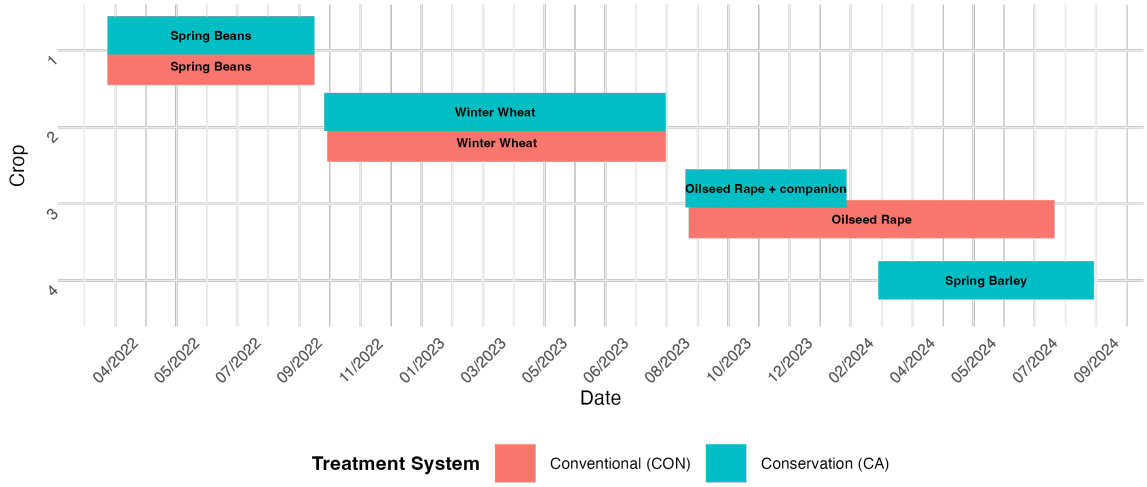

Figure 3.6: The crop rotation for both experimental treatments during the experimental duration.

3.7 Management Operations

3.7.1 Year 1

The CON plots were established on 19/03/2022 with a John Deere 6250R (250 HP) with a six furrow Kverneland plough to a depth of 20 cm (Figure 3.7). They were then drilled with spring beans (var. Lynx) on 24/03/2022 with HORSCH Pronto 3 DC (HORSCH Maschinen GmbH, Schwandorf, Germany) at a seed rate of 300 kg ha^{-1}. The CA treatment was drilled on 28/03/2022 with a SAME (SDF Group, Treviglio, Italy) Iron 165.7 tractor (163 HP) and a John Deere 750a direct drill at 330 kg ha^{-1} (Figure 3.8). All spraying was done using a Bateman RB35 self-propelled sprayer. The crop was harvested on 03/10/2022 with a tracked CLAAS Lexion 760 (CLAAS KGaA mbH, Harsewinkel, Germany) combine harvester equipped with a CLAAS Vario 930 header. Each experimental plot was harvested individually, the grain transferred to a trailer, and the individual plot yield quantified using a weigh bridge. The cutter bar height was 20 cm from the soil surface, and the straw for both treatments was chopped and spread back to the soil using the combine harvester. The complete list of operations performed during this cropping year is summarised in Table 3.2.

Figure 3.7: John Deere 6250R (250HP) with a six furrow Kverneland plough establishing the CON treatment on 19/03/2022. Source: Author's own

Figure 3.8: A SAME Iron 165.7 tractor (163 HP) equipped with a John Deere 750a drilling spring beans (var. Lynx) on 28/03/2022 Source: Author's own

3.7.2 Year 2

Winter wheat (*Triticum aestivum* var. Extase) was drilled in the CON treatment on 16/10/2022 using a HORSCH Pronto 3 DC (HORSCH Maschinen GmbH, Schwan-

Table 3.2: Machinery operations in 2022 for the crop of spring beans for both treatments, detailing machinery, equipment, and horsepower (HP) used for all field operations

Date	Crop	Treatment	Area (ha)	Operation	Machine	HP	Implement	Width (m)
22/01/2022	Spring beans	CON	5.14	Spraying	Bateman RB35	225	Self propelled sprayer	24
19/03/2022	Spring beans	CON	5.14	Cultivation	John Deere 6250R	250	6 furrow Kverneland plough	3
21/03/2022	Spring beans	CON	5.14	Fertiliser	John Deere 6R 215	237	Fert speader	24
24/03/2022	Spring beans	CON	5.14	Drilling	John Deere 6R 215	237	HORSCH Pronto 3 DC	4
29/03/2022	Spring beans	CON	5.14	Drilling	John Deere 6250R	250	POTTINGER 3M COMBI DRILL	4
29/03/2022	Spring beans	CON	5.14	Rolling	John Deere 6R 215	237	NA	12
31/03/2022	Spring beans	CON	5.14	Spraying	Bateman RB35	225	Self propelled sprayer	24
15/05/2022	Spring beans	CON	5.14	Spraying	Bateman RB35	225	Self propelled sprayer	24
08/06/2022	Spring beans	CON	5.14	Spraying	Bateman RB35	225	Self propelled sprayer	24
29/06/2022	Spring beans	CON	5.14	Spraying	Bateman RB35	225	Self propelled sprayer	24
22/08/2022	Spring beans	CON	5.14	Spraying	Bateman RB35	225	Self propelled sprayer	24
03/10/2022	Spring beans	CON	5.14	Harvest	CLAAS Lexion 750	429	CLAAS V900 header	9.2
03/10/2022	Spring beans	CON	5.14	Tractor + Trailer	John Deere 6250R	250	18t trailer	NA
22/01/2022	Spring beans	CA	3.25	Spraying	Bateman RB35	225	Self propelled sprayer	24
21/03/2022	Spring beans	CA	3.25	Fertiliser	John Deere 6R 215	237	Fert Spreader	24
28/03/2022	Spring beans	CA	3.25	Drilling	SAME Iron 165.7	163	John Deere 750a	4
31/03/2022	Spring beans	CA	3.25	Spraying	Bateman RB35	225	Self propelled sprayer	24
30/06/2022	Spring beans	CA	3.25	Spraying	Bateman RB35	225	Self propelled sprayer	24
22/08/2022	Spring beans	CA	3.25	Spraying	Bateman RB35	225	Self propelled sprayer	24
03/10/2022	Spring beans	CA	3.25	Harvest	CLAAS Lexion 750	429	CLAAS V900 header	9.2
03/10/2022	Spring beans	CA	3.25	Tractor + Trailer	John Deere 6250R	250	18t trailer	NA

dorf, Germany) at a seed rate of 220 kg ha^{-1} at a seed depth of 3 - 4 cm. Before drilling, the CON treatment was cultivated using a VÄDERSTAD TopDown 3000 cultivator (Vaderstad Ltd, Väderstad, Sweden) to a depth of 15 cm (3.9). The CA treatment were drilled on 12/10/2022 with a SAME Iron (SDF Group, Treviglio, Italy) 165.7 tractor (163 HP) and a John Deere 750a direct drill (Deere & Company, Moline, Illinois, United States) at 200 kg ha^{-1} at a seed depth of 3 - 4 cm, with no prior cultivation. The wheat crop was harvested on 20/08/2023 with a tracked CLAAS Lexion 760 (CLAAS KGaA mbH, Harsewinkel, Germany) combine harvester equipped with a CLAAS Vario 930 header (3.10). Each experimental plot was harvested individually, and the grain was transferred to a trailer and weighed using a weighbridge. The cutter bar height was approximately 20 cm from the ground, with the straw residue baled and removed for sale in the CON treatment and chopped and spread back to the soil surface in the CA treatment.

3.7.3 Year 3

Oilseed rape (*Brassica napus*) for the 2024 season was drilled in the CA treatment on 28/08/2023 using a SAME Iron 165.7 tractor (SDF Group®, Treviglio, Italy; 163 HP) and a John Deere 750a direct drill (Deere & Company®, Moline, Illinois, United States) at a working width of 4 m. The CON treatment was first cultivated on 29/08/2023 using a John Deere 8370R tractor (370 HP) with a VÄDERSTAD TopDown (Vaderstad Ltd®, Väderstad, Sweden) cultivator, followed by drilling oilseed rape (*Brassica napus*) with a John Deere 6R 215 tractor (237 HP) and a HORSCH

Figure 3.9: A photo of the CON treatment being cultivated using a VÄDERSTAD TopDown 3000 cultivator on 16/10/2022. Source: Author's own

Figure 3.10: A tracked CLAAS Lexion 760 with a CLAAS Vario 930 header harvesting the experiment on 20/08/2023. Source: Author's own

Table 3.3: Machinery operations in 2022/3 for the crop of winter wheat, detailing machinery, equipment, and horsepower (HP) used for all field operations

Date	Crop	Treatment	Area (ha)	Operation	Machine	HP	Implement	Width (m)
13/10/2022	Winter wheat	CON	5.14	Cultivation	John Deere 8370R	370	Vaderstad TopDown	4
14/10/2022	Winter wheat	CON	5.14	Drilling	John Deere 6R 215	237	HORSCH Pronto 3 DC	4
20/10/2022	Winter wheat	CON	5.14	Spraying	Bateman RB35	225	Self propelled sprayer	24
27/10/2022	Winter wheat	CON	5.14	Spraying	Bateman RB35	225	Self propelled sprayer	24
13/02/2023	Winter wheat	CON	5.14	Fertiliser	John Deere 6R 215	237	NA	24
23/03/2023	Winter wheat	CON	5.14	Spraying	Bateman RB35	225	Self propelled sprayer	24
07/04/2023	Winter wheat	CON	5.14	Fertiliser	Bateman RB35	225	Self propelled sprayer	24
16/04/2023	Winter wheat	CON	5.14	Spraying	Bateman RB35	225	Self propelled sprayer	24
11/05/2023	Winter wheat	CON	5.14	Spraying	Bateman RB35	225	Self propelled sprayer	24
15/05/2023	Winter wheat	CON	5.14	Fertiliser	Bateman RB35	225	Self propelled sprayer	24
05/06/2023	Winter wheat	CON	5.14	Spraying	Bateman RB35	225	Self propelled sprayer	24
20/08/2023	Winter wheat	CON	5.14	Harvest	CLAAS Lexion 750	429	CLAAS V900 header	9.2
20/08/2023	Winter wheat	CON	5.14	Tractor + Trailer	John Deere 6250R	250	18t trailer	NA
12/10/2022	Winter wheat	CA	3.25	Drilling	SAME Iron 165.7	163	John Deere 750a	4
20/10/2022	Winter wheat	CA	3.25	Spraying	Bateman RB35	225	Self propelled sprayer	24
13/02/2023	Winter wheat	CA	3.25	Fertiliser	Bateman RB35	225	Self propelled sprayer	24
27/03/2023	Winter wheat	CA	3.25	Fertiliser	Bateman RB35	225	Self propelled sprayer	24
12/04/2023	Winter wheat	CA	3.25	Spraying	Bateman RB35	225	Self propelled sprayer	24
20/05/2023	Winter wheat	CA	3.25	Spraying	Bateman RB35	225	Self propelled sprayer	24
15/06/2023	Winter wheat	CA	3.25	Spraying	Bateman RB35	225	Self propelled sprayer	24
20/08/2023	Winter wheat	CA	3.25	Harvest	CLAAS Lexion 750	429	CLAAS V900 header	9.2
20/08/2023	Winter wheat	CA	3.25	Tractor + Trailer	John Deere 6250R	250	18t trailer	NA

Pronto 3 DC (HORSCH Maschinen GmbH, Schwandorf, Germany) at the same working width. Multiple pesticide applications were conducted throughout the season for both treatments, with a Bateman RB35 (Bateman Sprayers®, UK; 225 HP) self-propelled sprayer (24 m boom) and quad biked with a mounted 12 m pellet applicator for slug pellet applications. Oilseed rape was harvested on 09/08/2024 using a CLAAS Lexion 750 (CLAAS KGaA mbH®, Harsewinkel, Germany; 429 HP) combine harvester equipped with a CLAAS V900 9.2 m header. Grain was transferred using a John Deere 6250R (250 HP) tractor and an 18-tonne trailer.

Spring barley (*Hordeum vulgare*) for the 2024 season was grown only in the CA treatment. It was managed with a series of pesticide applications beginning on 03/02/2024, primarily using the Bateman RB35 sprayer, with additional slug pellet applications applied via quad bike. The crop was harvested on 15/09/2024 using the same CLAAS Lexion 750 combine and 9.2 m V900 header. Grain transport was carried out with the John Deere 6250R tractor and 18-tonne trailer.

Table 3.4: Machinery operations in 2023/4 for the crops of oilseed rape and spring barley, detailing machinery, equipment, and horsepower (HP) used for all field operations

Date	Crop	Treatment	Area (ha)	Operation	Machine	HP	Implement	Width (m)
29/08/2023	Oilseed Rape	CON	5.14	Cultivation	John Deere 8370R	370	Vaderstad TopDown	4
29/08/2023	Oilseed Rape	CON	5.14	Drilling	John Deere 6R 215	237	HORSCH Pronto 3 DC	4
31/08/2023	Oilseed Rape	CON	5.14	Spraying	Bateman RB35	225	Self propelled sprayer	24
04/09/2023	Oilseed Rape	CON	5.14	Spraying	Bateman RB35	225	Self propelled sprayer	24
20/09/2023	Oilseed Rape	CON	5.14	Spraying	Bateman RB35	225	Self propelled sprayer	24
29/10/2023	Oilseed Rape	CON	5.14	Spraying	Bateman RB35	225	Self propelled sprayer	24
03/02/2024	Oilseed Rape	CON	5.14	Spraying	Bateman RB35	225	Self propelled sprayer	24
03/02/2024	Oilseed Rape	CON	5.14	Spraying	Bateman RB35	225	Self propelled sprayer	24
01/04/2024	Oilseed Rape	CON	5.14	Spraying	Bateman RB35	225	Self propelled sprayer	24
22/03/2024	Oilseed Rape	CON	5.14	Spraying	Bateman RB35	225	Self propelled sprayer	24
21/04/2024	Oilseed Rape	CON	5.14	Spraying	Bateman RB35	225	Self propelled sprayer	24
03/07/2024	Oilseed Rape	CON	5.14	Spraying	Bateman RB35	225	Self propelled sprayer	24
09/08/2024	Oilseed Rape	CON	5.14	Harvest	CLAAS Lexion 750	429	CLAAS V900 header	9.2
09/08/2024	Oilseed Rape	CON	5.14	Tractor + Trailer	John Deere 6250R	250	18t trailer	NA
28/08/2023	Oilseed Rape	CA	3.25	Drilling	SAME Iron 165.7	163	John Deere 750a	4
15/09/2023	Oilseed Rape	CA	3.25	Spraying	Quad	30	Slug pellet applicator	12
03/02/2024	Spring Barley	CA	3.25	Spraying	Bateman RB35	225	Self propelled sprayer	24
18/04/2024	Spring Barley	CA	3.25	Spraying	Bateman RB35	225	Self propelled sprayer	24
10/05/2024	Spring Barley	CA	3.25	Spraying	Bateman RB35	225	Self propelled sprayer	24
18/04/2024	Spring Barley	CA	3.25	Spraying	Bateman RB35	225	Self propelled sprayer	24
08/05/2024	Spring Barley	CA	3.25	Spraying	Quad	30	Slug pellet applicator	12
16/05/2024	Spring Barley	CA	3.25	Spraying	Bateman RB35	225	Self propelled sprayer	24
15/09/2024	Spring Barley	CA	3.25	Harvest	CLAAS Lexion 750	429	CLAAS V900 header	9.2
15/09/2024	Spring Barley	CA	3.25	Tractor + Trailer	John Deere 6250R	250	18t trailer	NA

3.8 Pesticide application

The following section details all of the applications of pesticides applied throughout the experiment. All products used during the experimental duration were recorded, alongside the timing and application rates. In this study, herbicides and crop desiccants are distinguished differently, despite being the same active ingredients, as they were used for different agronomic purposes. The application rates were normalised using the following equation 3.1:

$$\text{Normalized Rate (kg ha}^{-1}) = \begin{cases} R \cdot \frac{w}{100} \cdot \delta, & \text{if formulation is w/w\% and } \delta = \begin{cases} 1, & \text{if unit is kg} \\ 0.001, & \text{if unit is g} \end{cases} \\ R \cdot \frac{v}{100}, & \text{if formulation is w/v\% and unit is l} \\ \frac{R \cdot g}{1000}, & \text{if formulation is g/l and unit is l} \end{cases} \tag{3.1}$$

Where R is the application rate in units per hectare, w is the percentage of active ingredient by weight (w/w %), v is the percentage of active ingredient by volume (w/v %), g is the concentration of active ingredient in grams per litre (g/l), and δ is the conversion factor (1 if the unit is kg, 0.001 if the unit is g).

3.8.1 Year 1

The experimental site (i.e. both treatments) was sprayed off using a systemic broad-spectrum herbicide (Glyphosate 360 g/l) on 22/01/2022 at a rate of 2.13 l ha^{-1} with addition of a water conditioner drift retardant (Intracrop Sprayforce DRT) at 0.53 l ha^{-1}. Following the planting of the spring bean crops in both treatments on 31/03/2022, both agronomists used a pre-emergence herbicide of Clomazone (360 g/l) at 0.2 l ha^{-1}, combined with Imazamox (16.7 g/l) and Pendimethalin (250 g/l) at 3.37 l ha^{-1}. On 15/05/2022 (Growth Stage (GS) 15 (Zadoks et al., 1974)), an insecticide (Lambda-cyhalothrin 50 g/l) was applied to the CON treatment at a rate of 0.15 l ha^{-1}. This was followed on 08/06/2022 (GS 64) by a fungicide application of Azoxystrobin (250 g/l) and Tebuconazole (430 g/l) at a rate of 0.48 l ha^{-1}, which was then repeated on 29/06/2022 (GS 69). The CA treatment used a single application of fungicide on 30/06/2022, which consisted of a combination of Boscalid (26.7% w/w) and Pyraclostrobin (6.7% w/w) at a rate of 0.65 l ha^{-1}. Both treatments were desiccated on 22/08/2022 using Glyphosate (490 g/l) at 2.9 l ha^{-1}, with addition of a pod sealant (Intracrop Senate) at 1 l ha^{-1}.

3.8.2 Year 2

For the winter wheat crop, the CON treatment was applied with a pre-emergence herbicide on 09/10/2022 of Diflufenican (500 g/l) at 0.15 l ha^{-1} in combination with Flufenacet (500 g/l) at 0.24 l ha^{-1}. The CA treatment was applied with a post-emergence herbicide at GS 12 on 11/10/2022, consisting of Flufenacet (60 g/l) and Pendimethalin (300 g/l) at 3.44 l ha^{-1} in combination with Diflufenican (500 g/l) at 0.22 l ha^{-1}. On 08/11/2022 (GS 13), a follow-up herbicide application was applied in the CON treatment of Florasulam (50 g/l) at 0.07 l ha^{-1} combined with an insecticide Lambda-cyhalothrin (50 g/l) at 0.1 l ha^{-1}. In the spring, at growth stage 30, a plant growth regulator (PGR) mix was applied on 23/03/2023 (GS 30) in the CON treatment consisting of Chlormequat (750 g/l) and Trinexapac-ethyl (250 g/l) at rates of 0.96 l ha^{-1} and 0.05 l ha^{-1} respectively. The timing of this fungicide application was

Table 3.5: Fertiliser applications and timings for the first experimental year for both treatments. The application date is shown by date and crop growth stage (Zadoks et al., 1974), the normalised rate ha^{-1} was calculated using Equation 3.1. All product names are registered trademarks ®.

Date	Growth Stage	Crop	Treatment	Category	Product	Active Ingredient	Normalized Rate (Kg Ha^{-1})
2022-01-22	-10	Spring beans	CON	Herbicide	Gallup XL	Glyphosate (360 g/l)	0.77
2022-03-31	-1	Spring beans	CON	Herbicide	Mohawk CS	Clomazone (360 g/l)	0.07
2022-03-31	-1	Spring beans	CON	Herbicide	Nirvana	Imazamox (16.7 g/l)	0.06
2022-03-31	-1	Spring beans	CON	Herbicide	Nirvana	Pendimethalin (250 g/l)	0.84
2022-05-15	14	Spring beans	CON	Insecticide	Clayton Sparta	Lambda-cyhalothrin (50 g/l)	0.01
2022-06-08	64	Spring beans	CON	Fungicide	Azofin Plus	Azoxystrobin (250 g/l)	0.12
2022-06-08	64	Spring beans	CON	Fungicide	Toledo	Tebuconazole (430 g/l)	0.21
2022-06-29	69	Spring beans	CON	Fungicide	Azofin Plus	Azoxystrobin (250 g/l)	0.12
2022-06-29	69	Spring beans	CON	Fungicide	Clayton Ohio	Tebuconazole (430 g/l)	0.21
2022-08-22	98	Spring beans	CON	Desiccant	Gallup Hi-Aktiv	Glyphosate (490 g/l)	1.42
2022-01-22	-10	Spring beans	CA	Herbicide	Gallup XL	Glyphosate (360 g/l)	0.77
2022-03-31	-1	Spring beans	CA	Herbicide	Mohawk CS	Clomazone (360 g/l)	0.07
2022-03-31	-1	Spring beans	CA	Herbicide	Nirvana	Imazamox (16.7 g/l)	0.06
2022-03-31	-1	Spring beans	CA	Herbicide	Nirvana	Pendimethalin (250 g/l)	0.84
2022-06-30	67	Spring beans	CA	Fungicide	Signum	Boscalid (26.7% w/w)	0.18
2022-06-30	67	Spring beans	CA	Fungicide	Signum	Pyraclostrobin (6.7% w/w)	0.04
2022-08-22	98	Spring beans	CA	Desiccant	Gallup Hi-Aktiv	Glyphosate (490 g/l)	1.42

at T0 (Timing 0), targeting the early tillering growth stage of cereal crops. Typically, in winter wheat crop management in the UK this is followed throughout the season with fungicide applications T1 (stem elongation GS 31-32), T2 (flag leaf fully emerged GS 39), and T3 (anthesis GS 59-69). From here on, this section refers to the timings using the T number to highlight the key fungicide application timings.

At T1, a fungicide application of Bixafen(65 g/l), Fluopyram (65 g/l), Folpet (500 g/l), and Prothioconazole (130 g/l) at a rate of 1.14 l ha^{-1} was applied to the CA treatment on 12/04/2023 (GS 31). This was combined with a PGR of Chlormequat (750 g/l) at a rate of 1.14 l ha^{-1}. In comparison, the CON treatment used Fluxapyroxad (75 g/l) at 0.5 l ha^{-1}, Folpet (500 g/l) at 0.96 l ha^{-1}, Mefentrifluconazole (97 g/l) at 1 l ha^{-1}, and Pyraclostrobin (150 g/l) at 0.5 l ha^{-1} at T1 on 16/04/2023. This was combined with a PGR of Chlormequat (750 g/l) at 0.96 l ha^{-1}, and Trinexapac-ethyl (250 g/l) at 0.14 l ha^{-1}. A herbicide mix was applied in the CA treatment consisting of Florasulam (20% w/w) and Tribenuron-methyl (60% w/w) at 22.93 l ha^{-1} on 22/04/2023.

At T2, on 11/05/2023, the CON treatment was sprayed with a fungicide mix of Fenpicoxamid (50 g/l) at 1.4 l ha^{-1}, Fluxapyroxad (75 g/l) at 0.7 l ha^{-1}, Folpet (500 g/l) at 0.96 l ha^{-1}, and Pyraclostrobin (150 g/l) at 0.7 l ha^{-1}. As well as PGR mix of Chlormequat (305 g/l) and 2-chloroethylphosphonic acid (155 g/l) at a rate of 0.4 l ha^{-1}. For the CA treatment T2, Fluxapyroxad (47.5 g/l) and Mefentrifluconazole(100

g/l) were used at rate of 0.8 l ha^{-1}, in combination with Folpet (500 g/l) at 1.14 l ha^{-1} applied on 20/05/2023.

At T3, on 05/06/2023, a fungicide mix of Prothioconazole (125 g/l) and Tebuconazole (125g/l) was used on the CON treatment at a rate of 0.75 l ha^{-1}. Whilst the CA treatment was applied with Fluxapyroxad (47.5 g/l) and Mefentrifluconazole(100 g/l) at a rate of 0.34 l ha^{-1} on 15/06/2023. No pre-harvest desiccant was used in either experimental treatment.

Table 3.6: Fertiliser applications and timings for the second experimental year for both treatments. The application date is shown by date and crop growth stage (Zadoks et al., 1974), the normalised rate ha^{-1} was calculated using Equation 3.1. All product names are registered trademarks ®.

Date	Growth Stage	Crop	Treatment	Category	Product	Active Ingredient	Normalized Rate (Kg Ha^{-1})
2022-10-09	-1	Winter wheat	CON	Herbicide	Sempra XL	Diflufenican (500 g/l)	0.07
2022-10-09	-1	Winter wheat	CON	Herbicide	System 50	Flufenacet (500 g/l)	0.12
2022-11-08	13	Winter wheat	CON	Herbicide	Lector	Florasulam (50 g/l)	0.00
2022-11-08	13	Winter wheat	CON	Insecticide	Clayton Sparta	Lambda-cyhalothrin (50 g/l)	0.00
2023-03-23	30	Winter wheat	CON	PGR	Belcocel 750	Chlormequat (750 g/l)	0.72
2023-03-23	30	Winter wheat	CON	PGR	Moddus	Trinexapac-ethyl (250 g/l)	0.01
2023-04-16	33	Winter wheat	CON	Fungicide	Syrex	Fluxapyroxad (75 g/l); (7.3 w/w%)	0.04
2023-04-16	33	Winter wheat	CON	Fungicide	Arizona	Folpet (500 g/l)	0.48
2023-04-16	33	Winter wheat	CON	Fungicide	Myresa	Mefentrifluconazole (97 g/l)	0.10
2023-04-16	33	Winter wheat	CON	Fungicide	Syrex	Pyraclostrobin (150 g/l) (14.6 w/w%)	0.07
2023-04-16	33	Winter wheat	CON	Herbicide	Ally Max SX	Metsulfuron-methyl (14.3 %w/w) 143 g/kg	0.00
2023-04-16	33	Winter wheat	CON	Herbicide	Ally Max SX	Tribenuron-methyl (14.3 % w/w); 143 g/kg	0.00
2023-04-16	33	Winter wheat	CON	PGR	Belcocel 750	Chlormequat (750 g/l) (65.2 w/w%)	0.72
2023-04-16	33	Winter wheat	CON	PGR	Moddus	Trinexapac-ethyl (250 g/l)	0.04
2023-05-11	39	Winter wheat	CON	Fungicide	Aquino	Fenpicoxamid (50 g/l)	0.07
2023-05-11	39	Winter wheat	CON	Fungicide	Syrex	Fluxapyroxad (75 g/l); (7.3 w/w%)	0.05
2023-05-11	39	Winter wheat	CON	Fungicide	Arizona	Folpet (500 g/l - 39%w/w)	0.48
2023-05-11	39	Winter wheat	CON	Fungicide	Syrex	Pyraclostrobin (150 g/l) (14.6 w/w%)	0.10
2023-05-11	39	Winter wheat	CON	PGR	Chlormephon	2-chloroethylphosphonic acid (155 g/l);	0.06
2023-05-11	39	Winter wheat	CON	PGR	Chlormephon	Chlormequat (305 g/l)	0.12
2023-06-05	61	Winter wheat	CON	Fungicide	Prosaro	Prothioconazole (125 g/l);	0.09
2023-06-05	61	Winter wheat	CON	Fungicide	Prosaro	Tebuconazole (125g/l)	0.09
2022-10-11	12	Winter wheat	CA	Herbicide	Prefect	Diflufenican (500 g/l)	0.11
2022-10-11	12	Winter wheat	CA	Herbicide	Crystal	Flufenacet(60 g/l)	0.21
2022-10-11	12	Winter wheat	CA	Herbicide	Crystal	Pendimethalin (300 g/l);	1.03
2023-04-12	31	Winter wheat	CA	Fungicide	Ascra Xpro	Bixafen(65 g/l)	0.07
2023-04-12	31	Winter wheat	CA	Fungicide	Ascra Xpro	Fluopyram (65 g/l);	0.07
2023-04-12	31	Winter wheat	CA	Fungicide	Mirror	Folpet (500 g/l)	0.57
2023-04-12	31	Winter wheat	CA	Fungicide	Ascra Xpro	Prothioconazole (130 g/l);	0.15
2023-04-12	31	Winter wheat	CA	PGR	3C Chlormequat 750	Chlormequat (750 g/l)	0.86
2023-04-22	32	Winter wheat	CA	Herbicide	Paramount Max	Florasulam (20% w/w)	0.00
2023-04-22	32	Winter wheat	CA	Herbicide	Paramount Max	Tribenuron-methyl (60 % w/w);	0.01
2023-05-20	39	Winter wheat	CA	Fungicide	Mivyto XE	Fluxapyroxad (47.5 g/l);	0.04
2023-05-20	39	Winter wheat	CA	Fungicide	Arizona	Folpet (500 g/l)	0.57
2023-05-20	39	Winter wheat	CA	Fungicide	Mivyto XE	Mefentrifluconazole(100 g/l)	0.08
2023-06-15	61	Winter wheat	CA	Fungicide	Mivyto XE	Fluxapyroxad (47.5 g/l);	0.02
2023-06-15	61	Winter wheat	CA	Fungicide	Mivyto XE	Mefentrifluconazole(100 g/l)	0.03

3.8.3 Year 3

Before the emergence of the oilseed rape crop, a pre-emergence herbicide (Clomazone (360 g/l)) was applied to the CON treatment on 01/09/2023 at a rate of 1.04 l ha^{-1}. An insecticide (Lambda-cyhalothrin (50 g/l)) was also included, which was applied

at a rate of 0.15 l ha^{-1}. This was followed by a molluscicide application of ferric phosphate (2.11 % w/w), in pellet form at a rate of 5 kg ha^{-1}. The CA treatment also had a molluscicide treatment of ferric phosphate (2.42 % w/w) at a rate of 6.95 kg ha^{-1}. On 20/09/2023, the CON treatment was applied with another insecticide, lambda-cyhalothrin (50 g/l) at 0.15 l ha^{-1} and another molluscicide application of ferric phosphate at 4 kg ha^{-1}. At GS 11, a post-emergence herbicide (Propaquizafop (100 g/l)) was applied at a rate of 0.5 l ha^{-1}, combined with an insecticide lambda-cyhalothrin (50 g/l) at 0.1 l ha^{-1}. This was followed by a molluscicide application at GS 12 on 02/10/2023 of ferric phosphate at 3 kg ha^{-1}. At GS 16 (29/10/2023), the CON treatment was applied with a herbicide mix of Halauxifen-methyl and Picloram at 0.4 l ha^{-1} and 0.5 l ha^{-1} respectively, and a fungicide of Prothioconazole at 0.45 l ha^{-1}. This was followed by an application of ferric phosphate at 4 kg ha^{-1}.

In 2024, the CON treatment was applied with a fungicide at GS 51 (22/03/2024) of Prothioconazole (250 g/l) at 0.4 l ha^{-1}, and a fungicide and herbicide mix at GS 64 (21/04/2024) of Azoxystrobin (250 g/l) and Prothioconazole (250 g/l) at 0.5 l ha^{-1}. The crop was dessicated with Glyphosate (360 g/l) at GS 86 (03/07/2024) at a rate of 3.84 l ha^{-1}.

The spring barley crop in the CA treatment was applied with a pre-emergence herbicide at GS -1 of Chlorotoluron (250 g/l), Diflufenican (40 g/l), and Pendimethalin (300 g/l) at a rate of 2 l ha^{-1}, and Glyphosate (360 g/l) at a rate of 1.5 l ha^{-1}. This was followed by an post-emergence application of herbicide at GS 13 on 16/05/2024 of Fluroxypyr (200 g/l) at a rate of 0.46 l ha^{-1} and a molluscicide application of Ferric Phosphate (2.11 % w/w) on 08/05/2024 at a rate of 4 kg ha^{-1}.

All pesticide application data were summarised to total application of each key category (herbicides, fungicides, dessicants, insecticides, molluscicides, and PGRs) applied per year and was tested for normality and homogeneity of variances using the methodology previously outlined in Section 3.10. No statistical analysis of this data was applied due to a limited sample size.

Table 3.7: Agro-chemical applications and timings for the third experimental year for both treatments. The application date is shown by date and crop growth stage (Zadoks et al., 1974), the normalised rate ha^{-1} was calculated using Equation 3.1. All product names are registered trademarks ®.

Date	Growth Stage	Crop	Treatment	Category	Product	Active Ingredient	Normalized Rate (Kg Ha^{-1})
2023-09-01	-5	Oilseed Rape	CON	Herbicide	Mohawk CS	Clomazone (360 g/l)	0.37
2023-09-01	-5	Oilseed Rape	CON	Insecticide	Clayton Sparta	Lambda-cyhalothrin (50 g/l)	0.01
2023-09-01	-5	Oilseed Rape	CON	Molluscicide	Epitaph	Ferric Phosphate (2.11 % w/w)	0.11
2023-09-04	-1	Oilseed Rape	CON	Herbicide	Mohawk CS	Clomazone (360 g/l)	0.09
2023-09-04	-1	Oilseed Rape	CON	Molluscicide	Epitaph	Ferric Phosphate (2.11 % w/w)	0.08
2023-09-20	11	Oilseed Rape	CON	Insecticide	Clayton Sparta	Lambda-cyhalothrin (50 g/l)	0.01
2023-09-20	11	Oilseed Rape	CON	Molluscicide	Epitaph	Ferric Phosphate (2.11 % w/w)	0.08
2023-10-02	11	Oilseed Rape	CON	Herbicide	Falcon	Propaquizafop (100 g/l)	0.05
2023-10-02	11	Oilseed Rape	CON	Insecticide	Clayton Sparta	Lambda-cyhalothrin (50 g/l)	0.01
2023-10-02	12	Oilseed Rape	CON	Molluscicide	Epitaph	Ferric Phosphate (2.11 % w/w)	0.06
2023-10-29	16	Oilseed Rape	CON	Fungicide	Ecana	Prothioconazole (250 g/l)	0.11
2023-10-29	16	Oilseed Rape	CON	Herbicide	Belkar	Halauxifen-methyl (10 g/l)	0.00
2023-10-29	16	Oilseed Rape	CON	Herbicide	Belkar	Picloram (48 g/l)	0.02
2023-10-29	14	Oilseed Rape	CON	Molluscicide	Epitaph	Ferric Phosphate (2.11 % w/w)	0.08
2024-03-22	51	Oilseed Rape	CON	Fungicide	Ecana	Prothioconazole (250 g/l)	0.10
2024-04-21	64	Oilseed Rape	CON	Fungicide	Azofin Plus	Azoxystrobin (250 g/l)	0.12
2024-04-21	64	Oilseed Rape	CON	Herbicide	Ecana	Prothioconazole (250 g/l)	0.12
2024-07-03	86	Oilseed Rape	CON	Desiccant	Motif	Glyphosate (360 g/l)	1.38
2023-09-15	10	Oilseed Rape	CA	Molluscicide	Sigon	Ferric Phosphate (2.42 % w/w)	0.17
2024-04-18	-1	Spring Barley	CA	Herbicide	Tower	Chlorotoluron (250 g/l);	0.50
2024-04-18	-1	Spring Barley	CA	Herbicide	Tower	Diflufenican (40 g/l)	0.08
2024-04-18	-1	Spring Barley	CA	Herbicide	Ovation	Glyphosate (360 g/l)	0.54
2024-04-18	-1	Spring Barley	CA	Herbicide	Tower	Pendimethalin (300 g/l);	0.60
2024-05-08	12	Spring Barley	CA	Molluscicide	Sluxx HP	Ferric Phosphate (2.11 % w/w)	0.08
2024-05-16	13	Spring Barley	CA	Herbicide	Hurler	Fluroxypyr (200 g/l)	0.09

3.9 Fertiliser application

3.9.1 Year 1

The following section details all of the applications of fertilisers applied throughout the experiment. Before drilling of the first crops of the experiment, both treatments had Polysulphate solid fertiliser (14 % w/w potassium oxide (K_2O), 17 % w/w calcium oxide (CaO), 48 % w/w sulphur trioxide (SO_3), and 6 % w/w magnesium oxide (MgO) applied at 250 kg ha^{-1}. This was followed at GS 14 in the CON treatment by a foliar application of boron (B) as disodium octaborate (7.72 % w/w), magnesium sulphate $MgSO_4$ 7.2 % (4.32 % w/w Mg), manganese (Mn) as manganese sulphate $MnSO_4$+H_2O (5.15 % w/w), and molybdenum (Mo) as sodium molybdate Na_2MoO_4 (0.05 % w/w) at a rate of 1.72 l ha^{-1}. This was accompanied with a phosphite-based biostimulant containing phosphorus tetroxide (P_2O_4) (28 % w/w) as dipotassium phosphite (50-75 % w/w), and potassium oxide (K_2O (23 % w/w) as monopotassium phosphite (50-75 % w/w) at a rate of 0.96 l ha^{-1}. This application was then repeated again in the CON treatment at GS 64 at the rate of 1.72 ha^{-1}. The nutrient appli-

cations for each treatment during the first year of the experiment are shown below in Table 3.8.

Table 3.8: Fertiliser applications and timings for the first experimental year for both treatments. The application date is shown by date and crop growth stage (Zadoks et al., 1974), the normalised rate ha^{-1} was calculated using Equation 3.1. All product names are registered trademarks ®.

Date	Growth Stage	Crop	Treatment	Product	Chemical Element	Normalized Rate (Kg Ha^{-1})
2022-03-21	-5	Spring beans	CON	Polysulphate	K	35.00
2022-03-21	-5	Spring beans	CON	Polysulphate	Ca	42.50
2022-03-21	-5	Spring beans	CON	Polysulphate	S	120.00
2022-03-21	-5	Spring beans	CON	Polysulphate	Mg	15.00
2022-05-15	14	Spring beans	CON	Intracrop Maxim PPE	B	0.13
2022-05-15	14	Spring beans	CON	IntraCrop Odessy	K	0.58
2022-05-15	14	Spring beans	CON	Intracrop Maxim PPE	Mg	0.07
2022-05-15	14	Spring beans	CON	Intracrop Maxim PPE	Mn	0.09
2022-05-15	14	Spring beans	CON	Intracrop Maxim PPE	Mo	0.00
2022-05-15	14	Spring beans	CON	IntraCrop Odessy	K	0.58
2022-05-15	14	Spring beans	CON	Intracrop Maxim PPE	S	0.37
2022-05-15	14	Spring beans	CON	Intracrop Maxim PPE	Zn	0.00
2022-06-08	64	Spring beans	CON	Intracrop Maxim PPE	B	0.13
2022-06-08	64	Spring beans	CON	IntraCrop Odessy	K	0.58
2022-06-08	64	Spring beans	CON	Intracrop Maxim PPE	Mg	0.07
2022-06-08	64	Spring beans	CON	Intracrop Maxim PPE	Mn	0.09
2022-06-08	64	Spring beans	CON	Intracrop Maxim PPE	Mo	0.00
2022-06-08	64	Spring beans	CON	IntraCrop Odessy	K	0.58
2022-06-08	64	Spring beans	CON	Intracrop Maxim PPE	S	0.15
2022-06-08	64	Spring beans	CON	Intracrop Maxim PPE	Zn	0.00
2022-03-21	-5	Spring beans	CA	Polysulphate	K	35.00
2022-03-21	-5	Spring beans	CA	Polysulphate	Ca	42.50
2022-03-21	-5	Spring beans	CA	Polysulphate	S	120.00
2022-03-21	-5	Spring beans	CA	Polysulphate	Mg	15.00

3.9.2 Year 2

During the second experimental year, both treatments received a base fertiliser application of urea (46 N % w/w) with a urease inhibitor (80 kg N ha^{-1}) on 13-02-2023. However, after this application, the fertiliser plan varied for each treatment. The total nitrogen (N) applied for the CON system totalled 185 kg N ha^{-1}, in comparison to 133 kg N ha^{-1} in the CA treatment. The CON treatment received three splits of N based fertiliser throughout the growing season; the first dose of urea (46 N % w/w) of 13/02/2023, a second dose of liquid fertiliser (80 kg N ha^{-1} + 23.5 kg SO_3 ha^{-1}) on 07-04-2023, and a final dose of liquid fertiliser (80 kg N ha^{-1} + 23.5 kg SO_3 ha^{-1}) on 2023-05-15. This was complemented with several foliar micronutrient applications. At the T0 (Growth Stage (GS) 20 (Zadoks et al., 1974)) fungicide timing a micronutrient foliar spray (54.72 g N ha^{-1}, 41.28 g S ha^{-1}, 2.33 g Mg ha^{-1}, 30.24 g

Zn ha^{-1}, 132 g Mn ha^{-1}), and a biostimulant of MTU (1-(2-methoxyethyl)-3-(1,2,3-thiadiazol-5yl)urea) and pidolic acid was applied alongside a plant growth regulator (PGR) of Chlormequat (750 g/l) and Trinexapac-ethyl (250 g/l) combined. At the T1 fungicide timing (GS 32) a micronutrient foliar spray (54.72 g N ha^{-1}, 41.28 g S ha^{-1}, 2.33 g Mg ha^{-1}, 30.24 g Zn ha^{-1}, 132 g Mn ha^{-1}) was also applied, as well as another application of plant growth regulator (PGR) of Chlormequat (750 g/l) and trinexapac-ethyl (250 g/l) combined. At T2 (GS 39) a specific Mg (76.76 g ha^{-1}) and S (155.93 g ha^{-1}) water soluble fertiliser was applied, alongside a liquid fertiliser and biostimulant (268.66 g N ha^{-1}, 134.33 g P ha^{-1}, 134.33 g K ha^{-1}, 61.16 g Mg ha^{-1}), and a PGR of 2-chloroethylphosphonic acid (155 g/l) and Chlormequat (305 g/l). At the final T3 (GS 61) timing, a Mg (76.76 g ha^{-1}) and S (155.93 g ha^{-1}) water-soluble fertiliser was applied. The complete fertiliser application for the CON treatment is detailed in Table 3.9.

The CA treatment used a base fertiliser application of urea (46 N % w/w) with a urease inhibitor (80 kg N ha^{-1}) on 13/02/2023, followed liquid fertiliser (54.26 kg N ha^{-1} + 15.93 kg SO_3 ha^{-1}) on 27/04/2023. Subsequently, foliar N was applied in four doses along with a combination of liquid micronutrients and biostimulants: micronutrient foliar fertiliser (70.2 g P ha^{-1}, 23.6 g K ha^{-1}, 464 g S ha^{-1}, 40 g Mg ha^{-1}, 302.2 g Mn ha^{-1}, 3.8 g Zn ha^{-1}) was first applied on 27/03/2023, alongside a soluble mix of humic and fulvic acids (< 10 g l^{-1}). At the T1 fungicide timing (GS 31) a foliar macro and micronutrient fertiliser (73.4 g N ha^{-1}, 121.58 g Mg ha^{-1}, 4.58 g Zn ha^{-1}, 50.46 g ha^{-1}, 137.64 g B ha^{-1}, 64 g Mn ha^{-1}) was also included. This was followed at T1.5 (GS 32) by the first dose of foliar N (5250 g N ha^{-1}) in addition to foliar Mg (30.28 g ha^{-1}) and S (15.36 g S ha^{-1}). This fertiliser application was then repeated at T2 (GS 39) and T3 (GS 61) with the addition of sulphate of potash (1462.17 g ha^{-1}, 516.06 g S ha^{-1}). The complete fertiliser application data for both the CA and CON experimental treatments for the second year of the experiment are detailed in Table 3.9.

3.9.3 Year 3

During the final experimental year of the project, on 02/10/2023 (GS 11), the CON treatment was applied with a mix of magnesium oxide (0.35 % w/v), nitrogen (14 % w/v), phosphorus pentoxide (7 % w/v), and potassium oxide (7 % w/v) at a rate of 1 l ha^{-1}. This was followed at GS 21 by nitrogen (N 32 % w/v) and sulphur trioxide (SO_3 % w/v) at a rate of 125 l ha^{-1}. Both treatments were applied with a P and K solid fertiliser, which consisted of P (24 % w/w) in the form of phosphorus

pentoxide (P_2O_5) and K (24 % w/w) in the form of potassium oxide (K_2O). The CON treatment then was applied with two applications of liquid nitrogen (N 32 % w/v) and sulphur trioxide (SO_3 % w/v) at GS 30 and GS 50, at a rate of 200 and 250 l ha^{-1} respectively. This was followed at GS 51 by an application of magnesium oxide (0.35 % w/v), nitrogen (14 % w/v), phosphorus pentoxide (7 % w/v), and potassium oxide (7 % w/v) at a rate of 3 l ha^{-1}, and boron (150 g/l) at a rate of 1.91 l ha^{-1}. The final fertiliser application from the CON treatment in the oilseed rape crop occurred on 21/04/2024 (GS 64), which was magnesium oxide (MgO 16 % w/w) and sulphur trioxide (SO_3 % w/w).

After the failed oilseed rape crop, the CA treatment began the spring barley crop in 2024 with two applications of urea (46% w/w N) with a urease inhibitor (BASF Limus®) at a rate of 180 kg ha^{-1} at GS 13 and at GS 30. This was co-applied with an application of a bio-stimulant of Mn (10 %), SO_3 (18 %), and N (2 %) at a rate of 2.29 l ha^{-1}. This was combined with another biostimulant containing MgO (43 g/l) and P_2O_5 (63 g/l) at a rate of 1.15 l ha^{-1}. The nutrient applications for each treatment during the third year of the experiment are shown in Table 3.10.

All fertiliser data were summarised to total application of each chemical element applied per year and were tested for normality and homogeneity of variances using the methodology previously outlined in Section 3.10. No statistical analysis of this data was applied due to a limited sample size.

Table 3.9: Fertiliser applications and timings for the second experimental year for both treatments. The application date is shown by date and crop growth stage (Zadoks et al., 1974), the normalised rate ha^{-1} was calculated using Equation 3.1. All product names are registered trademarks ®.

Date	Growth Stage	Crop	Treatment	Product	Chemical Element	Normalized Rate (Kg Ha^{-1})
2023-02-14	20	Winter wheat	CON	Urea - Limus coated	N	57.50
2023-03-23	30	Winter wheat	CON	Intracrop Status	NA	0.00
2023-03-23	30	Winter wheat	CON	Intracrop Status	NA	0.06
2023-03-23	30	Winter wheat	CON	Intracrop Cearum	S	0.03
2023-03-24	31	Winter wheat	CON	Intracrop Cearum	Cu	0.01
2023-03-25	32	Winter wheat	CON	Intracrop Cearum	Mn	0.09
2023-03-26	33	Winter wheat	CON	Intracrop Cearum	Zn	0.02
2023-04-07	31	Winter wheat	CON	Chafer N32 +9.4 SO3	N	80.00
2023-04-07	31	Winter wheat	CON	Chafer N32 +9.4 SO3	S	23.50
2023-04-16	33	Winter wheat	CON	Intracrop Cearum	Cu	0.01
2023-04-16	33	Winter wheat	CON	Intracrop Cearum	Mn	0.09
2023-04-16	33	Winter wheat	CON	Intracrop Cearum	S	0.03
2023-04-16	33	Winter wheat	CON	Intracrop Cearum	Zn	0.02
2023-05-11	39	Winter wheat	CON	Epsotop	Mg	0.46
2023-05-11	39	Winter wheat	CON	Epsotop	S	0.62
2023-05-11	39	Winter wheat	CON	ProGrAm	Mg	0.01
2023-05-11	39	Winter wheat	CON	ProGrAm	N	0.27
2023-05-11	39	Winter wheat	CON	ProGrAm	P	0.13
2023-05-11	39	Winter wheat	CON	ProGrAm	K	0.13
2023-05-15	40	Winter wheat	CON	Chafer N32 +9.4 SO3	N	48.00
2023-05-15	40	Winter wheat	CON	Chafer N32 +9.4 SO3	S	14.10
2023-06-05	61	Winter wheat	CON	Epsotop	Mg	0.46
2023-06-05	61	Winter wheat	CON	Epsotop	S	0.62
2023-02-14	20	Winter wheat	CA	Urea - Limus coated	N	57.50
2023-03-27	24	Winter wheat	CA	AMIX BioMan	Mg	0.04
2023-03-27	24	Winter wheat	CA	Maxi-Phi Fast Root	Mn	0.02
2023-03-27	24	Winter wheat	CA	AMIX BioMan	Mn	0.30
2023-03-27	24	Winter wheat	CA	Maxi-Phi Fast Root	P	0.70
2023-03-27	24	Winter wheat	CA	Maxi-Phi Fast Root	K	0.24
2023-03-27	24	Winter wheat	CA	AMIX BioMan	S	0.46
2023-03-27	24	Winter wheat	CA	Maxi-Phi Fast Root	Zn	0.04
2023-04-07	31	Winter wheat	CA	Chafer N32 +9.4 SO3	N	80.00
2023-04-07	31	Winter wheat	CA	Chafer N32 +9.4 SO3	S	23.50
2023-04-12	31	Winter wheat	CA	Stoker	B	0.14
2023-04-12	31	Winter wheat	CA	Stoker	Mg	0.12
2023-04-12	31	Winter wheat	CA	Stoker	Mn	0.05
2023-04-12	31	Winter wheat	CA	Stoker	Mo	0.00
2023-04-12	31	Winter wheat	CA	Stoker	N	0.07
2023-04-12	31	Winter wheat	CA	Stoker	S	0.34
2023-04-12	31	Winter wheat	CA	Stoker	Zn	0.00
2023-04-22	32	Winter wheat	CA	Maxi-Phi Hi-Mag	Mg	0.15
2023-04-22	32	Winter wheat	CA	Poly N Plus	N	4.80
2023-04-22	32	Winter wheat	CA	Poly N Plus	S	0.90
2023-04-22	32	Winter wheat	CA	Maxi-Phi Hi-Mag	S	0.30
2023-05-20	39	Winter wheat	CA	YaraTera KRISTA SOP	K	1.46
2023-05-20	39	Winter wheat	CA	Maxi-Phi Hi-Mag	Mg	0.15
2023-05-20	39	Winter wheat	CA	Poly N Plus	N	4.80
2023-05-20	39	Winter wheat	CA	Poly N Plus	S	0.90
2023-05-20	39	Winter wheat	CA	YaraTera KRISTA SOP	S	1.29
2023-05-20	39	Winter wheat	CA	Maxi-Phi Hi-Mag	S	0.30
2023-06-15	61	Winter wheat	CA	YaraTera KRISTA SOP	K	1.46
2023-06-15	61	Winter wheat	CA	Maxi-Phi Hi-Mag	Mg	0.15
2023-06-15	61	Winter wheat	CA	Poly N Plus	N	4.84
2023-06-15	61	Winter wheat	CA	Poly N Plus	S	0.91
2023-06-15	61	Winter wheat	CA	YaraTera KRISTA SOP	S	1.29
2023-06-15	61	Winter wheat	CA	Maxi-Phi Hi-Mag	S	0.30

Table 3.10: Fertiliser applications and timings for the third experimental year for both treatments. The application date is shown by date and crop growth stage (Zadoks et al., 1974), the normalised rate ha^{-1} was calculated using Equation 3.1. All product names are registered trademarks ®.

Date	Growth Stage	Crop	Treatment	Product	Chemical Element	Normalized Rate (Kg Ha^{-1})
2023-10-02	11	Oilseed Rape	CON	ProGrAm	Mg	0.00
2023-10-02	11	Oilseed Rape	CON	ProGrAm	N	0.14
2023-10-02	11	Oilseed Rape	CON	ProGrAm	P	0.07
2023-10-02	11	Oilseed Rape	CON	ProGrAm	K	0.07
2024-02-03	21	Oilseed Rape	CON	Chafer N32 +9.4 SO3	N	40.00
2024-02-03	21	Oilseed Rape	CON	Chafer N32 +9.4 SO3	S	11.75
2024-02-03	21	Oilseed Rape	CON	0-24-24-5	P	82.80
2024-02-03	21	Oilseed Rape	CON	0-24-24-5	K	82.80
2024-02-03	21	Oilseed Rape	CON	0-24-24-5	S	17.25
2024-02-03	30	Oilseed Rape	CON	Chafer N32 +9.4 SO3	N	64.00
2024-02-03	30	Oilseed Rape	CON	Chafer N32 +9.4 SO3	S	18.80
2024-02-03	50	Oilseed Rape	CON	Chafer N32 +9.4 SO3	N	80.00
2024-02-03	50	Oilseed Rape	CON	Chafer N32 +9.4 SO3	S	23.50
2024-03-22	51	Oilseed Rape	CON	ProGrAm	Mg	0.01
2024-03-22	51	Oilseed Rape	CON	ProGrAm	N	0.42
2024-03-22	51	Oilseed Rape	CON	ProGrAm	P	0.21
2024-03-22	51	Oilseed Rape	CON	ProGrAm	K	0.21
2024-03-22	51	Oilseed Rape	CON	Proleaf Boron 15	B	0.29
2024-04-21	64	Oilseed Rape	CON	Epsotop	Mg	0.46
2024-04-21	64	Oilseed Rape	CON	Epsotop	S	0.62
2024-02-03	-10	Spring Barley	CA	0-24-24-5	P	82.80
2024-02-03	-10	Spring Barley	CA	0-24-24-5	K	82.80
2024-02-03	-10	Spring Barley	CA	0-24-24-5	S	17.25
2024-04-18	13	Spring Barley	CA	Urea - Limus coated	N	82.80
2024-04-18	30	Spring Barley	CA	Urea - Limus coated	N	46.00
2024-05-16	13	Spring Barley	CA	EvoPlex Mn	Mn	0.23
2024-05-16	13	Spring Barley	CA	EvoPlex Mn	S	0.41
2024-05-16	13	Spring Barley	CA	EvoPlex Mn	N	0.05
2024-05-16	13	Spring Barley	CA	Maxi-Phi Activate MP	Mg	0.05
2024-05-16	13	Spring Barley	CA	Maxi-Phi Activate MP	P	0.07

3.10 Statistical analysis

3.10.1 Power Analysis

In a large field experiment, such as the one being used in this study, it is important to plan the sampling design to maximise statistical power, within the constraints of labour and time frame available. Therefore, multiple power analysis simulations were performed using the `Pwr` package (Champely et al., 2020) in R (R Core Team, 2023) (version 4.3.0) to determine the most efficient sampling design possible to test the hypotheses. Effect sizes (Cohen's d) were taken from previous literature for a variety of variables, which were planned to be monitored during the duration of the crop rotation. This was done to calculate the quantity of observations required to test the hypothesis with a satisfactory level of statistical power (α). With α being defined as the probability of correctly rejecting the null hypothesis for a fixed effect size and fixed sample size.

Cohen's d was calculated using the following formula:

$$d = \frac{\bar{x}_1 - \bar{x}_2}{s_{\text{pooled}}} \tag{3.2}$$

Where $\bar{x}_1$ and $\bar{x}_2$ are the sample means of the two groups being compared, and s_{pooled} is the pooled standard deviation, calculated as:

$$s_{\text{pooled}} = \sqrt{\frac{(n_1 - 1)s_1^2 + (n_2 - 1)s_2^2}{n_1 + n_2 - 2}} \tag{3.3}$$

Where $n1$ and $n2$ represent the sample sizes of the two groups, while s_1^2 and s_2^2 denote the variances of the respective groups. The numerator ($\bar{x}_1$ - $\bar{x}_2$) captures the mean difference between the groups, while the denominator (s_{pooled}) standardises this difference by accounting for the variability within both groups. A larger value of d indicates a greater separation between the group means relative to their variability, with commonly accepted thresholds for interpreting the magnitude of the effect (small - $d = 0.2$, medium - $d = 0.5$, large - $d = 0.8$. This metric is particularly useful for comparing the magnitude of effects across studies or when the units of measurement differ between variables (Cohen, 2013).

3.10.2 Data distribution assessment

Data normality assessment for all data collected in this study was analysed using the Shapiro-Wilk Test from the base R `stats` package (R Core Team, 2023), and the

Anderson-Darling normality test from the `MVN` package (Korkmaz et al., 2014) in R version 4.3.0. Results were visualised using histograms and qqplots generated using the `ggplot2` package (Wickham, 2016). The Shapiro-Wilk tests were formulated using the following equation:

$$W = \frac{\left(\sum_{i=1}^{n} a_i x_{(i)}\right)^2}{\sum_{i=1}^{n}(x_i - \bar{x})^2} \tag{3.4}$$

Where:

- W is the Shapiro-Wilk test statistic.
- a_i are constants that depend on the sample size and are pre-determined from the expected order statistics of a normal distribution.
- $x_{(i)}$ are the ordered sample values, where $x_{(1)} \leq x_{(2)} \leq \cdots \leq x_{(n)}$.
- $\bar{x}$ is the sample mean.
- n is the sample size (the number of observations).

The null hypothesis (H_0) for the Shapiro-Wilks tests used for this study were that the data followed a normal distribution:

$$H_0 : \text{The data is normally distributed.}$$

The alternative hypothesis (H_1) was that the data does not follow a normal distribution:

$$H_1 : \text{The data is not normally distributed.}$$

The test statistic W was compared to a computed p-value. If the p-value was less than the recommended significance level (i.e., $\alpha = 0.05$), the null hypothesis was rejected, indicating that the data does not follow a normal distribution.

3.10.3 Homoscedasticity Assessment

To assess for the homoscedasticity, the Bartlett's Test was used to test for homogeneity of variances across different groups for all data collected in this study. This was performed using Bartlett's Test from the `stats` package in R version 4.3.0 (R Core Team, 2023). The Bartlett's Test equation is presented below in Equation 3.5.

$$\chi^2 = \frac{(N-k)}{(k-1)} \ln\left(\prod_{i=1}^{k} s_i^2\right) - \sum_{i=1}^{k} \frac{(N_i - 1)\ln(s_i^2)}{2} \tag{3.5}$$

Where:

- χ^2: The test statistic used in Bartlett's test. This value follows a chi-squared distribution under the null hypothesis of equal variances across the groups.
- N: The total number of observations across all groups.
- k: The number of groups being compared for equality of variances.
- s_i^2: The sample variance of the i-th group. Each group is assumed to have a normal distribution.
- N_i: The number of observations in the i-th group.
- $\prod_{i=1}^{k} s_i^2$: The product of the variances of all k groups. The natural logarithm of this product is taken as part of the formula.

The test compares the observed variances across groups to the expected variances under the null hypothesis.

$$H_0 : \text{The variances are equal across all groups.}$$

The alternative hypothesis (H_1) is that the data does not follow a normal distribution:

$$H_1 : \text{At least one group has a different variance.}$$

If the p-value was less than the recommended significance level (0.05), the H_0 was rejected, indicating that the variances are not homogeneous. If the p-value was greater than the significance level, this results in a failure to reject H_0, suggesting that there was no significant difference in variances across the groups.

3.10.4 Data Overdispersion Assessment

A large quantity of the data collected in this project was count data or count-like non-integer data (due to averaging, scaling, or aggregation), which is commonly overdispersed (Ver Hoef and Boveng, 2007). The presence or not of overdispersion in the dataset determines the appropriate statistical methodology. Overdispersal was tested using the following equation:

$$\text{Dispersion Statistic} = \frac{\text{Residual Deviance}}{\text{Residual Degrees of Freedom}} \tag{3.6}$$

The overdispersion test is based on the ratio of the residual deviance to the residual degrees of freedom in a Poisson regression model.

- **Residual Deviance** (D): This measures how well the model fits the data by comparing the likelihood of the fitted model to the likelihood of a saturated model (which perfectly fits the data). The formula for residual deviance is:

  $$D = -2 \cdot (\log L_{\text{model}} - \log L_{\text{saturated}})$$

  where L_{model} is the likelihood of the model and $L_{\text{saturated}}$ is the likelihood of the saturated model.

- **Residual Degrees of Freedom** (df_{residual}): This represents the number of observations minus the number of estimated parameters in the model. The formula is:

  $$df_{\text{residual}} = n - p$$

  where n is the number of observations and p is the number of parameters in the model.

- **Dispersion Statistic**: The dispersion statistic is calculated as the ratio of residual deviance to residual degrees of freedom:

  $$\text{Dispersion Statistic} = \frac{D}{df_{\text{residual}}}$$

  If the dispersion statistic is greater than 1, it suggests overdispersion. This means the variance in the data is larger than expected under the Poisson model. A value close to 1 indicates a good fit with no significant overdispersion.

The presence of over-dispersion was also tested for using Fisher's index of dispersion, as the previous dispersion equation mainly evaluates the basic variance-to-mean ratio, and if the variance is close to the mean, it might not indicate overdispersion. The Fisher index provides a measure of how much the variance deviates from what would be expected in a distribution. It is particularly sensitive to skewness and outliers in the data. Therefore, it can highlight overdispersion even when the dispersion statistic suggests no presence of overdispersion. The Fisher Index for dispersion was calculated using the following equation:

$$FisherIndex = \frac{1}{n-1}\sum_{i=1}^{n}\left(\frac{x_i - \bar{x}}{\bar{x}}\right)^2 \tag{3.7}$$

Where:

- n is the number of observations in the dataset.
- x_i represents the individual data points in the dataset.
- $\bar{x}$ is the mean of the dataset, calculated as:

$$\bar{x} = \frac{1}{n}\sum_{i=1}^{n} x_i$$

- The term $\frac{x_i - \bar{x}}{\bar{x}}$ represents the normalized deviation of each observation from the mean, scaled by the mean value.
- The squared deviations, $\left(\frac{x_i - \bar{x}}{\bar{x}}\right)^2$, measure the relative magnitude of each deviation.
- The sum of squared deviations is then averaged by dividing by $(n-1)$ to account for the degrees of freedom.

3.10.5 Statistical model fitting

3.10.5.1 Linear Mixed-effects Models

Dependent variables that met Gaussian assumptions were analysed using a linear mixed-effects model (LMM) using the `lme4` package (Bates et al., 2015) in R Version 4.3.1 (R Core Team, 2023). The basic model formula was:

$$y_i = \beta_0 + \beta_1 \cdot \text{treatment}_i + u_{\text{block}_i} + u_{\text{crop}_i} + u_{\text{year}_i} + \epsilon_i \tag{3.8}$$

Where:

- The β_0 term represents the overall intercept of the model.
- The β_1 term estimates the fixed effect of the treatment factor, which indicates the impact of treatment on the response variable.
- The random effects (u_{block_i}, u_{crop_i}, and u_{year_i}) account for the variability in the response variable that is associated with the hierarchical structure of the data (block, crop, and year). These random intercepts allow for individual deviations within each of these factors.

- The residual error term ϵ_i accounts for the unexplained variation in the response variable that is not captured by the fixed and random effects.

Linear mixed-effects models were fitted using the Restricted Maximum Likelihood (REML) method to account for both fixed and random effects in the data (Corbeil and Searle, 1976). The analysis was performed using the `lmer` function from the `lme4` package in R (version 4.3.0) (Bates et al., 2015). REML was chosen to provide unbiased estimates of variance components by maximising the likelihood of the residuals after accounting for the fixed effects. Model diagnostics, including residual plots and checks for normality and homoscedasticity, were conducted to ensure model validity.

3.10.5.2 Generalised Linear Models

If the overdispersion assessment identified significant overdispersion in the data, a generalised linear model (GLM) with a quasi-Poisson family with a log-link function was applied (Ver Hoef and Boveng, 2007). This was performed in the `stats` package in base `R` with the following model syntax:

$$y = \beta_0 + \beta_1 \cdot \text{treatment} + \beta_2 \cdot \text{year} + \beta_3 \cdot \text{block} + \epsilon \tag{3.9}$$

Where:

- y: The response variable, modelled as a function of fixed effects.
- β_0: The intercept term, representing the baseline response when all predictor variables are at their reference levels.
- $\beta_1 \cdot$treatment: The fixed effect of the `treatment` variable, capturing its influence on the response.
- $\beta_2 \cdot$year: The fixed effect of the `year` variable, accounting for temporal variation in the response.
- $\beta_3 \cdot$block: The fixed effect of the `block` variable, controlling for spatial variation within experimental blocks.
- ϵ: The error term, assumed to follow a quasi-Poisson distribution to account for overdispersion in the response variable.

- The model is fitted using the quasi-Poisson family with a log link function, allowing for flexible dispersion estimation beyond standard Poisson assumptions. This choice was informed by prior assessment of dispersion magnitude in the dataset.

3.10.5.3 Generalised Linear Mixed-effects Models

Dependent variables that did not meet Gaussian assumptions, but were not overdispersed, were analysed using generalised linear mixed-effects models using the `glmer` function from the `lme4` package in R (Version 4.3.0). The basic model formula is detailed in Equation 3.10:

$$y = \beta_0 + \beta_1 \cdot \text{treatment} + u_{\text{block}} + u_{\text{crop}} + u_{\text{year}} \tag{3.10}$$

Where:

- y: The response variable, which is modelled based on a linear combination of predictors and random effects.
- β_0: The intercept term, representing the baseline value when all predictor variables are at their reference levels.
- $\beta_1 \cdot \text{treatment}$: The fixed effect of the `treatment` variable, which quantifies the influence of different treatment levels on the response.
- u_{block}, u_{crop}, and u_{year}: The random effects corresponding to the grouping factors `block`, `crop`, and `year`. These random effects account for the variability in the response variable due to differences within each of these groups. Models were tested with all random effects and checked for the singularity issue. If model singularity was present, the specific random effects were removed from the model.
- The model is fitted using a suitable model family and link function depending on the distribution and overdispersion magnitude of the response variable. This was dependent on the results of the distribution assessments previously detailed in this chapter.

The generalised linear mixed model (GLMM) was fitted using maximum likelihood estimation with Laplace approximation. Maximum likelihood estimation uses an iterative approach to determine estimates for population parameter values that

maximise the likelihood that the sample data came from a population with these parameter values (Ng and Cribbie, 2017). This method was chosen due to the hierarchical structure of the data, with random effects for block, crop, and year. Any deviation from these stated model formulas is noted in each method's section. The results from the models are presented using the estimate (β), standard error (SE), test statistic (Z), and the p-value. All post-hoc analyses for both the generalised linear mixed-effect models and the linear mixed-effect models were performed using the `emmeans` package on R (Version 4.3.0) (Lenth, 2023) using pairwise comparisons to compute estimated marginal means for specified factors.

3.10.6 Model Diagnostics

For both the linear mixed models (LMM), generalised linear models (GLM), and generalised linear mixed-effects models (GLMM) used in this study, several diagnostic plots were generated to evaluate the assumptions underlying the models and to identify potential issues such as influential data points or model misfit. The following plots were generated to check the fit and assumptions of the model:

- **Residuals vs. Fitted Values Plot**: This plot helps detect patterns in the residuals and assess whether the GLM provides an adequate fit (Dodge, 2008). The plot was checked for heteroscedasticity or patterns that would suggest model misfit.

- **Q-Q Plot of Residuals**: The Q-Q plot of residuals was used to visually inspect whether the residuals of the model deviate from normality (Marden, 2004). Significant deviations would suggest that the model may not be appropriate for the data.

- **Cook's Distance Plot**: Cook's distance (Cook, 1977) was calculated to identify influential observations that could disproportionately affect model estimates. A threshold of $\frac{4}{n}$ (where n is the number of observations) was used to highlight potentially influential points.

The results from these diagnostic plots were examined to identify any potential violations of model assumptions, such as non-linearity, non-normality, or influential data points. Where issues were identified, further investigations were conducted, and potential remedies were considered (e.g., transformations or removal of outliers) to improve the model fit.

After reviewing the diagnostic plots, adjustments were made where necessary, including refining the model specification or addressing influential data points. In cases where significant departures from model assumptions were found, alternative approaches were explored. The model was re-evaluated through these diagnostic plots until a satisfactory fit was achieved. Following the methodology of Zuur and Ieno (2016), this study presents the model diagnostics of all models employed during this study in the supporting appendices for each chapter (A, B, C, D).

Chapter 4

Application of Soil Proximal Sensors to Guide the Transition to Conservation Agriculture

4.1 Introduction

Before and during the transition to Conservation Agriculture (CA), it is important for farmers to understand the soil texture across the land that they farm, to facilitate planning for future management decisions and outcomes. This is because the soil textural class will alter the effect of CA on soil physical properties and subsequent crop growth (Rochette et al., 2008; Zhao et al., 2020; Pannell et al., 2014; Ren et al., 2023). The meta-analysis by Blanco-Canqui and Ruis (2018) showed that soil textural class significantly altered the magnitude of the effect of no-tillage (NT) on a range of soil physical properties. Among the most responsive to changes in tillage systems were found to be medium-textured soils, where soil bulk density, penetration resistance, and wet aggregate stability were all altered by NT. They hypothesise that this could be because the higher organic matter in NT systems interacts more favourably with medium-textured soils, such as loams, where the balance of sand, silt, and clay allows organic matter to enhance aggregation and pore structure effectively. In contrast, in sandy soils, low water-holding capacity and limited cohesion reduce the impact of added organic matter, while in clay-rich soils, the dominance of fine particles and strong shrink-swell behaviour can overshadow the structural benefits provided by organic matter.

Soil textural class also influences machinery and equipment requirements; for example, disc-based direct drills may struggle to close the seeding slot in heavy clay soils (Agrii, 2021; Baker et al., 2006). To understand soil textural variation on their

farms, most farmers rely on historical knowledge, with some opting to use conventional soil testing from commercial laboratories. Conventional soil textural analysis by the pipette method (Bieganowski and Ryżak, 2011) is the most accurate method of soil textural classification. However, it is a laborious process and thus it is an expensive analysis for farmers to utilise in the resolution required to accurately map soil textural spatial variation (Rhymes et al., 2023). Therefore, there is very little high-resolution data on soil textural spatial variability in agricultural land in the UK.

Currently, there are several methodologies for scanning soil texture at a high spatial resolution using proximal sensors. Most commonly, these commercial soil property mapping products involve the use of electrical conductivity (EC), visible and near-infrared spectroscopy (Vis–NIR) or gamma-ray spectroscopy (GRS), which are paired with global navigation satellite systems (GNSS) positioning for mapping landscape features (Rhymes et al., 2023). All of these technologies have been promoted heavily to farmers in recent years and have become popular due to the interest in adopting precision agricultural principles such as variable rate product application, which requires spatial knowledge of soil and crop properties. Soil scanning has also been preferred to the traditional grid sampling method by farmers because it is faster, simpler, and less expensive (Grisso et al., 2009).

Soil electrical conductivity (EC) scanning has become one of the most frequently used methodologies to characterise in-field variability for precision agriculture (Corwin and Lesch, 2003). EC is the ability of a material to conduct an electrical current, which is influenced largely by the proportion of clay in a soil combined with the quantity of moisture between soil particles (Grisso et al., 2009). As a result, EC can be used to spatially estimate changes in soil texture, due to differences in soil moisture content in soils with varying quantities of sand, silt and clay particles, which hold on to moisture in different ways. However, EC is also influenced by various other soil properties, including drainage conditions, salinity, soil organic matter, and subsoil characteristics.

Gamma quant-emitting radionuclides naturally occur in all soils (Reinhardt and Herrmann, 2019; Pätzold et al., 2020). Gamma-ray spectrometry (GRS) scanning records these radionuclides emitted from the soil from the decay of Caesium-137, Uranium-238, Thorium-232, and Potassium-40 (Reinhardt and Herrmann, 2019; Pätzold et al., 2020). Approximately 90 % of the gamma radiation that can be measured above ground originates from the top 30 cm of the soil (Pätzold et al., 2020). Thus, it has potential for use in agricultural soil science, where most of the focus for farmers and researchers is on the A horizon of the soil. This data can be used to map field-scale

variation of the gamma-spectra, which can be correlated with soil mineralogy or texture (Pätzold et al., 2020). GRS has been shown in previous studies to perform well at single sites where the calibration model can be trained on the soil type of the single site (Mahmood et al., 2013), or at sites with similar geo-pedological conditions (Pätzold et al., 2020). In some of these cases, it is possible to link soil properties and GRS data using linear correlations (Mahmood et al., 2013). However, in sites where there is high soil property variation, methodologies based on machine learning are superior as this can enable calibration of site-independent texture prediction models, overcoming interferences from different parent materials (Pätzold et al., 2020). This chapter section compares EC and GRS scanning data for mapping soil texture variation using a Random Forest Machine Learning Algorithm to assess the accuracy of the model predictors, and discusses the use of both EC and GRS as a farmer decision-making tool for field-scale agronomic decisions.

4.1.1 Research Aims and Hypotheses

The research aims (A) of this chapter are:

- A_1: Assess the accuracy of gamma-ray spectrometry (GRS) and electrical conductivity (EC) scanning in predicting field-scale soil texture in a UK agricultural context.
- A_2: Evaluate the potential of a multi-sensor (GRS + EC) "soil sensor fusion" approach for improving the spatial resolution and reliability of soil texture maps.

This section addresses the tests of the following hypotheses (H):

- H_1: Commercially available soil scanning technologies are effective estimators of soil textural variation to aid farmers in the transition to CA.
- H_2: A soil texture prediction model which combines data derived from several soil proximal sensors will exceed the accuracy of a model with data from a single source.

4.2 Materials and Methods

4.2.1 Soil Texture

A subset of 50 of the 150 randomly generated sampling points described in Chapter 3 was taken using a random number generator, to include 5 sampling points for each

experimental plot. This ensures a representative spread of data points from across the experimental site. The sampling points are presented in Figure 4.1.

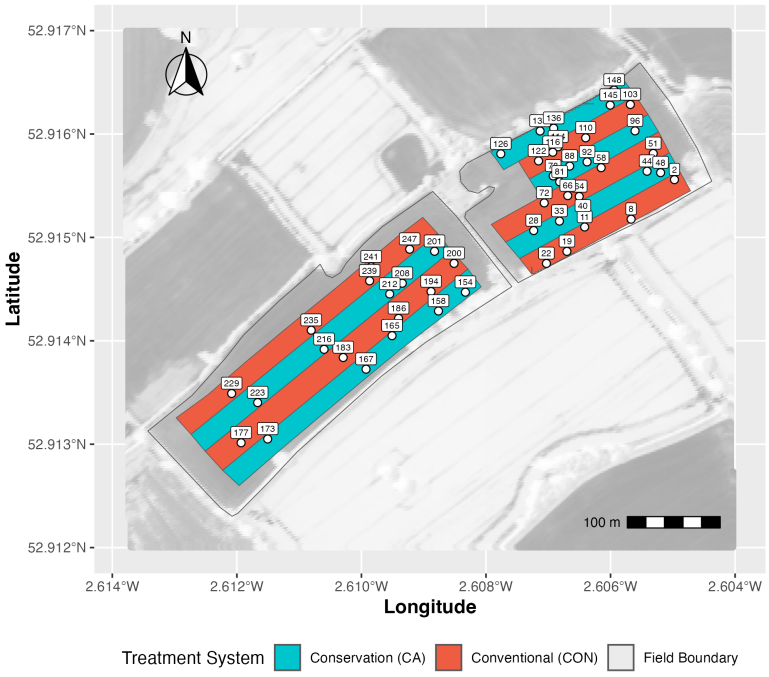

Figure 4.1: Soil sampling points during the experimental duration. The CA treatment is shown in blue and CON in red.

Soil texture samples were then collected on 09/10/2022 to a depth of 20 cm, dried, disaggregated and analysed using the laser diffraction method (NRM, 2021b). Laser-diffraction analysis (LDA) is a rapid automated method achieving highly resolved frequency distributions of particle sizes (Taubner et al., 2009). This method consists of suspending the soil sample in water and passing this through a flow cell, positioned in the path of a laser beam. The passing of soil particles through the flow cell causes the laser to be diffracted. The magnitude of diffraction is directly related to the size of the soil particle. Thus, it is possible to predict the size and relative population of particles in a sample (NRM, 2021b). The laser diffraction method has been shown to have a highly significant linear correlation with the traditionally used pipette method for each of the particle-size fractions from clay to coarse silt (Taubner et al., 2009). Although, the methodology is not as accurate as the pipette method, and it is recommended to calibrate the laser diffraction method with the pipette method (Taubner et al., 2009), it was decided that in this study it was appropriate to use the laser diffraction method as it is a greatly faster process and the main aim

is to assess spatial variation in soil texture of the site and not to accurately quantify it.

The individual percentages of sand, silt, and clay were combined and plotted in a soil textural triangle using the `soiltexture` package (Moeys et al., 2024) in `R` (R Core Team, 2023). The classification of the soil texture was based on these values, adapted from Avery (2006):

Table 4.1: Soil Textural Classification for England and Wales. Adapted from: Avery (2006).

Texture Class	**Sand (%)**	**Silt (%)**	**Clay (%)**
Sand	85–100	0–15	0–10
Loamy Sand	70–85	0–30	0–15
Sandy Loam	43–85	0–50	0–20
Loam	23–52	28–50	7–27
Silt Loam	0–20	50–88	0–27
Silt	0–20	88–100	0–12
Sandy Clay Loam	45–80	0–28	20–35
Clay Loam	20–45	15–53	27–40
Silty Clay Loam	0–20	40–73	27–40
Sandy Clay	45–65	0–20	35–55
Silty Clay	0–20	40–60	40–60
Clay	0–45	0–40	40–100

4.2.2 Interpolation

To estimate spatially distributed values at unsampled locations, the spatial correlation between the individual soil separate samples at different locations was modelled using variograms. This was performed to quantify the semi-variance against the distance between data points. The models fitted to the variogram were automatically generated using the `automap` package in `R` (Hiemstra et al., 2009). All soil separates were modelled using a Matern semi-variogram model with varying values for the nugget, sill, and range, which were all automatically computed. The semi-variograms were then used to perform Ordinary Kriging using `automap` and `gstat` (Pebesma, 2004) and plotted using `ggplot2` (Wickham, 2016). The statistics from the interpolated models are detailed in Appendix A.16. The interpolated datasets for sand, silt, and clay were used to calculate the interpolated soil textural class throughout the experimental site.

4.2.3 Soil Proximal Sensing

An electrical conductivity (EC) scan and a gamma-ray spectrometry (GRS) scan were conducted on 24/03/2022 and 18/10/2022, respectively. The EC scan was performed

using a trailed scanner, and the GRS scan was performed mounted on an all-terrain vehicle. Both scanners were set up to operate at 24 m widths at 12 m distance from the tramlines, recording data at one-second intervals. The EC scanner produced data points recorded in Siemens m^{-1} across the field site. The GRS data were measured in Electron Volts (eV) and then transformed to soil texture fraction percentages using an algorithm produced by the SoilOptix®Intelligence System (597112 Hwy 59, Tavistock, Ontario N0B 2R0 Canada). The sensor measures gamma radiation emitted from the decay of Caesium-137, Uranium-238, Thorium-232, and Potassium-40 emitted from 20 - 30 cm depth (Enesi et al., 2024; Pätzold et al., 2020; Harmer, 2024). A proprietary, multivariate calibration algorithm was used to estimate soil properties, which was calibrated by measured samples taken from field locations recommended by the software, which were dependent on the range of sensor values (Enesi et al., 2024). Harmer (2024) stated that "Sample quantity per field is based on field size, stemming from a ratio of one sample per 3 ha: where a minimum of three samples are required for fields less than 10 ha."

4.2.4 Analysis

To assess which scanning technology was a more accurate predictor of soil texture, a Random Forest machine learning model and spatial correlation models were implemented. The Random Forest machine learning algorithm was selected due to its robustness in handling non-linear relationships and its suitability for feature importance assessment (Breiman, 2001; Wehrle and Pätzold, 2024). First, a spatial grid of 10 m points was generated for the extent of the experimental site, and mean values from the nearest EC and GRS point were assigned to the grid point using the `st_nearest_feature` function in the `sf R` package (Pebesma et al., 2024). An 80% subset of soil texture values derived from the sampled points was used as the response variable to train the model, with EC and GRS used as predictor variables. The remaining 20% of the data was used to test the model's performance. Random data division was performed to create the training and test datasets using the `createDataPartition` function from the `caret` package (Kuhn et al., 2023). The random forest model was applied using the `randomForest` package (Breiman et al., 2024) in `R` (R Core Team, 2023). To balance model accuracy and computational efficiency, the model was configured with 10,000 trees, and to assess the importance of the predictors was assessed to assess the relative contribution of each predictor to soil texture prediction.

Before the spatial correlation analysis, the data for the sampled soil texture values, EC, and GRS datasets were interpolated across the experimental site using inverse distance weighting (IDW) using the `gstat` package (Pebesma, 2004) and converted to raster images. The raster images were then correlated with the `stats` package in base `R` (R Core Team, 2023). The spatial correlation analysis was performed using a Pearson correlation coefficient between predicted and sampled values. Accuracy of the prediction was assessed using the prediction Mean Absolute Error (MAE), Mean Square Error (MSE), and the Root Mean Squared Error ($RMSE$).

4.3 Results

4.3.1 Soil Texture

The soil texture for the site is mainly a sandy loam with patches of sandy clay loam according to the Soil Survey of England and Wales (Natural England, 2008) (Figure 4.2 **A**). However, the GRS scanning predicted that the experimental site was predominantly a sandy silt loam and silty clay loam (Figure 4.2 **B**).

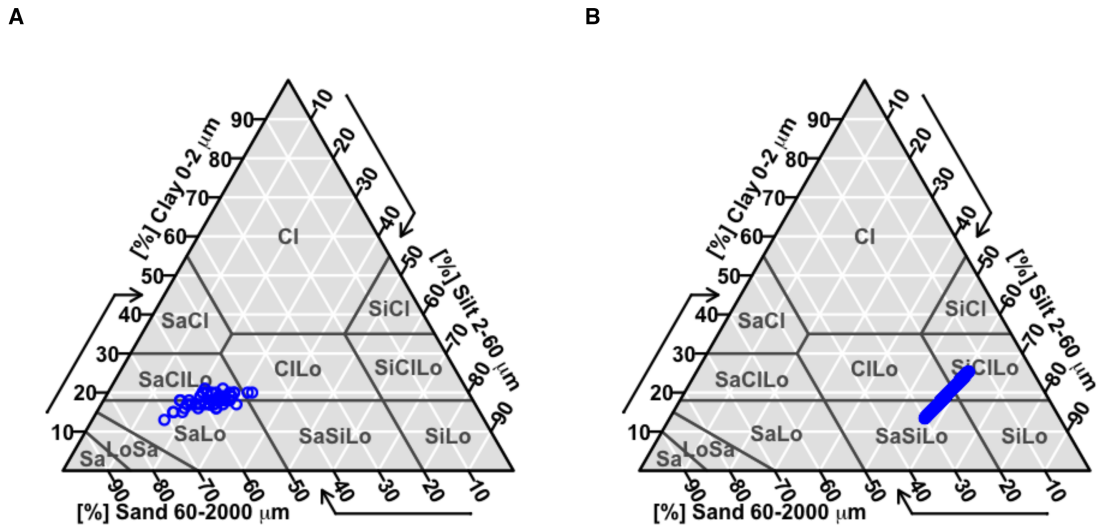

Figure 4.2: **A** - The results from the textural analysis of 50 samples throughout the experimental site plotted on a soil textural triangle using the Soil Textural Classification of England and Wales. **B** - The commercially produced results from the textural variation prediction from the GRS scanning plotted on a soil textural triangle using the Soil Textural Classification of England and Wales.

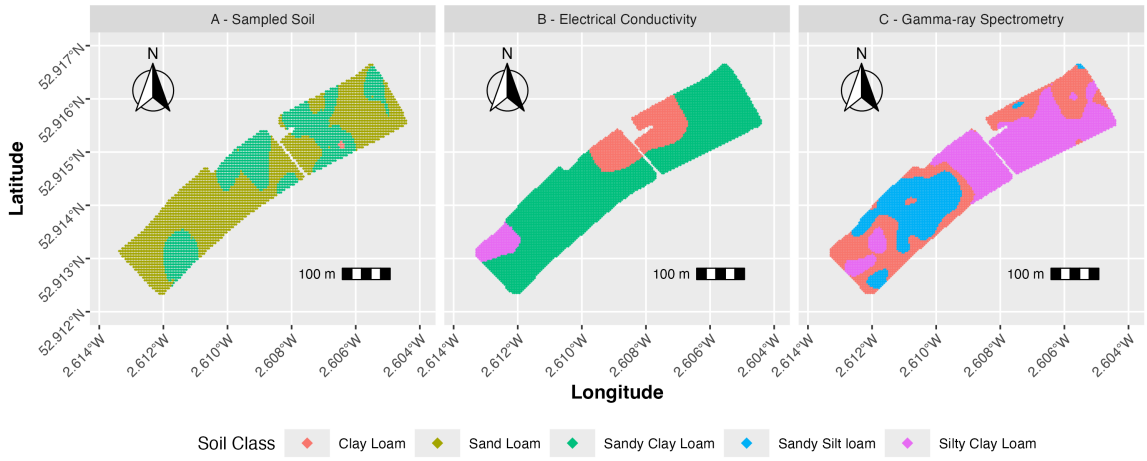

Figure 4.3: **A** - The results from the textural analysis of 50 samples interpolated using ordinary kriging and plotted spatially in the experimental site. The commercial textural prediction from the EC (**B**) and GRS (**C**) scanning is plotted spatially in the experimental site.

4.3.2 Spatial correlation analysis

Correlation and error analysis of the Inverse Distance Weighting (IDW) interpolation found the clay content of the soil was predicted well ($RMSE$ = 3.09) by the GRS scanning (M = 20.19, SE = 0.03, CI = 0.06) in comparison to the sampled data (M = 17.96, SE = 0.24, CI = 0.49). However GRS predicted the contents of sand (M = 21.05, SE = 0.04, CI = 0.08, $RMSE$ = 38.1) and silt (M = 58.75, SE = 0.01, CI = 0.02, $RMSE$ = 35.75) poorly in comparison to the sampled data (sand: M = 58.46, SE = 0.68, CI = 1.36, silt: M = 23.58, SE = 0.54, CI = 1.08).

The prediction correlations for clay content were similar for both EC (r = 0.3) and GRS (r = 0.39), showing a mildly positive correlation between the predicted value and the sampled values. The lower MAE (2.56) and $RMSE$ (3.09) indicate that GRS predictions for clay were moderately more accurate in this experiment. GRS predicted sand content also had a moderate positive correlation with the sampled values (r = 0.49), albeit with high error margins (MAE = 38, $RMSE$ = 38.1). The EC predicted sand content, however, had a negative correlation (r = -0.33, MAE = 38, $RMSE$ = 38.1) with the sampled values, meaning that the EC scan was a poor predictor of sand particle content. Additionally, EC silt content prediction was found to have a weak positive correlation with the sampled values (r = 0.3, MAE = 2.65, $RMSE$ =

3.35). Although the error of the prediction was low, it was still a poor indicator of soil silt particle content. GRS scanning had an improved correlation with the sampled silt particle content ($r = 0.46$); however, the prediction also had higher error values ($MAE = 35.7$, $RMSE = 35.75$) in comparison to the EC prediction. Overall, GRS performed better than EC for the prediction of soil clay particle content in terms of correlation and accuracy. It was also a better linear predictor with the sampled silt content, but it is not as accurate in terms of prediction errors in comparison to EC. GRS had an improved correlation to EC; however had much higher prediction error. Overall, both scanning techniques were poor predictors of sand particle content. The results of the error and correlation analysis for GRS and EC, compared to sampled values shown below in Figure 4.2 and the prediction error of the GRS scanning is shown in Table 4.2.

Table 4.2: Pearson Correlation Coefficient analysis values (r) for the Inverse Distance Weighting (IDW) interpolation of soil textural prediction from Electro-conductivity scanning (EC) and gamma-ray spectrometry scanning (GRS). Prediction accuracy is characterised by the Mean Absolute Error (MAE), Mean Square Error (MSE), and the Root Mean Squared Error ($RMSE$).

Soil Texture	Scanning Prediction	Correlation (r)	MAE	MSE	$RMSE$
Clay	EC	0.3	7.37	58.48	7.65
Clay	GRS	0.394	2.56	9.56	3.09
Sand	EC	-0.33	33.77	1155.12	33.99
Sand	GRS	0.49	38	1451.81	38.1
Silt	EC	0.3	2.65	11.22	3.35
Silt	GRS	0.46	35.7	1278.22	35.75

4.3.3 Machine learning analysis

The Random Forest model predictions are presented in Figure 4.4 compared to the physical sample prediction and the commercial GRS prediction. The model with both GRS and EC included as predictor variables had moderate accuracy at predicting soil texture within the experimental site, with an accuracy of 0.86 (95 % CI : (0.1841, 0.901), No info rate = 0.57, $p = 0.65$). The model p-value indicates that the model does not predict soil texture significantly differently than random chance, and is only performing marginally better than random chance. High model accuracy confidence intervals suggest that there is uncertainty around the overall accuracy estimate. The No-Information Rate (NIR) also suggests that there was not enough soil texture data

to train the model sufficiently, as this suggests that if the model were to predict solely the most common class, the predicted accuracy would still be 57 %. There was shown to be a moderate level of agreement between the two predictor variables (GRS + EC), which is evidenced by the κ value of 0.22.

The Random Forest model with only GRS included as a predictor variable was less accurate at predicting soil texture within the experimental site than the model with GRS and EC predictor variables. The overall model accuracy was 0.43 and a 95% CI of 0.1 - 0.82, indicating a lot of uncertainty in the model's true model accuracy. The model p-value of 0.8734 and NIR 57.14% indicate that the model's accuracy is not a significant improvement over predicting the most frequent class. The confusion matrix for both model outputs is shown below in Figure 4.3. Neither model assessed in this study was shown to be satisfactorily accurate due to high uncertainty, κ and p values. However, higher accuracy in the model with GRS and EC included illustrates the importance of the inclusion of multiple predictor variables. The full confusion statistics for the model are detailed below in Table 4.3.

The Random Forest variable importance analysis (Table 4.4) revealed distinct patterns in the predictive relevance of soil electrical conductivity (EC) and gamma-ray spectrometry (GRS) predictors for the classification of soil textural classes (clay, sand, and silt). For clay, GRS predictors such as GRS clay predictor, GRS sand predictor, and GRS silt predictor demonstrated the highest Mean Decrease Accuracy (MDA), with values of 27.08, 26.45, and 25.26, respectively. This shows the strength of GRS as a model variable for the prediction of soil clay particle content. Conversely, the EC predictors contributed less to the clay content classification, with the deep EC data showing a slightly negative MDA of -2.03; however, the shallow EC data was a moderately strong prediction variable with an MDA of 23.86. Full predictor importance data from the model is detailed in Table 4.4 below.

Table 4.3: This table presents confusion statistics for the prediction of soil textural classes using different predictor models. The accuracy, Kappa statistic, and the range for accuracy (lower and upper bounds) are provided for the combined model (GRS + EC) and the individual GRS model. Additionally, the accuracy based on null models and associated p-values from hypothesis tests (Accuracy p-value and McNemar's p-value) is included. Values marked as NA indicate that the McNemar test was not applicable for the comparison.

Predictor	**Model**	**Accuracy**	**Kappa** (κ)	**Accuracy (Lower)**	**Accuracy (Upper)**	**Accuracy (Null)**	**Accuracy** (***PValue***)	**Mcnemar** (***PValue***)
GRS + EC	Textural Class	0.86	0.72	0.42	1.0	0.57	0.12	NA
GRS	Textural Class	0.57	0.22	0.18	0.9	0.57	0.65	NA

Table 4.4: Random Forest machine learning algorithm predictor importance for the electrical conductivity (EC) and the gamma-ray spectrometry (GRS) scanning soil texture prediction model. Mean Decrease Accuracy measures how much accuracy a random forest model loses when a variable is permuted, or its values are changed to random values. Mean Decrease Gini is a measure of how important a variable is in a Random Forest model by quantifying its contribution to the model output.

Predictor	**Model**	**Mean Decrease Accuracy (MDA)**	**Mean Decrease Gini (MDG)**
EC Shallow	Clay	23.86	5.45
EC Deep	Clay	-2.03	5.53
GRS Clay	Clay	27.08	3.47
GRS Sand	Clay	26.45	3.44
GRS Silt	Clay	25.26	3.40
EC Shallow	Sand	-10.83	4.50
EC Deep	Sand	17.56	6.38
GRS Clay	Sand	-17.99	3.39
GRS Sand	Sand	-16.63	3.62
GRS Silt	Sand	-17.13	3.35
EC Shallow	Silt	36.26	5.64
EC Deep	Silt	33.69	5.51
GRS Clay	Silt	10.93	4.07
GRS Sand	Silt	10.69	4.10
GRS Silt	Silt	10.95	4.06

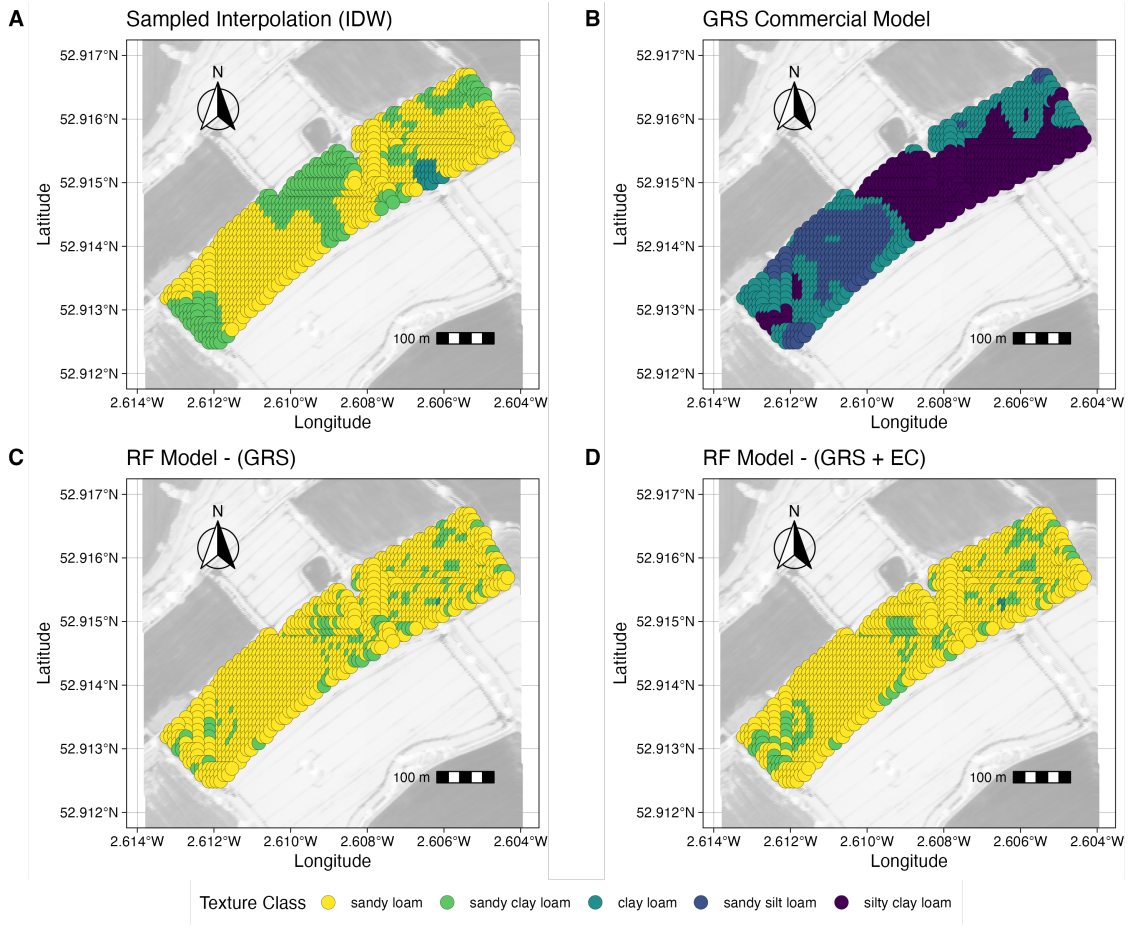

Figure 4.4: **A**: Interpolated prediction of soil textural variation in the experimental site. The interpolation was performed using Inverse Distance Weighting (IDW). **B**: The commercial produced model of soil texture variation from GRS scanning. **C**: The Random Forest (RF) model of soil textural variation using GRS data as a predictor. **D:** The random forest (RF) model of soil textural variation using GRS and EC data as predictors. Colours indicate soil textural classification using the Soil Textural Classification of England and Wales, adapted from Avery (2006).

4.4 Discussion

Understanding the spatial variability of soil texture is essential for tailoring management practices during the transition to CA. This study aimed to assess the utility of two commercially available soil proximal sensing technologies: gamma-ray spectrometry (GRS) and electrical conductivity (EC), for predicting soil texture at the field scale. The discussion that follows interprets the results of spatial correlation and machine learning analyses, evaluates the relative performance of EC and GRS scanning in estimating sand, silt, and clay content, and considers the implications of these findings for the adoption of precision agriculture practices. In doing so, it critically examines the extent to which these technologies can provide reliable, high-resolution soil texture maps to inform agronomic decision-making and highlights the limitations of current sensor-based approaches. The potential benefits of combining sensor outputs in a multi-sensor "soil sensor fusion" framework are also explored.

This section addresses the tests of the following hypotheses (H):

- H_1: Commercially available soil scanning technologies are effective estimators of soil textural variation to aid farmers in the transition to CA.
- H_2: A soil texture prediction model which combines data derived from several soil proximal sensors will exceed the accuracy of a model with data from a single source.

The results of the correlation and error analysis presented in this study (Table 4.2) indicate that both commercially available soil proximal sensing services—electroconductivity (EC) and gamma-ray spectrometry (GRS)—predicted soil texture poorly overall when compared to sampled field data. Prediction accuracy varied considerably between soil texture components.

The site was predominantly sandy loam and sandy clay loam (Natural England, 2008); however, GRS scanning classified it as silty clay loam. This discrepancy suggests that GRS scanning may be less effective at detecting sand particles. For clay content, GRS scanning performed moderately well, with a root mean squared error (RMSE) of 3.09 and a moderate positive correlation ($r = 0.39$) with sampled values. In contrast, EC showed lower accuracy for clay (RMSE = 7.65, $r = 0.3$). For sand, both methods performed poorly. GRS had a moderate positive correlation ($r = 0.49$) with sampled sand content, but high prediction errors (RMSE = 38.1). EC scanning showed a negative correlation (r = -0.33), indicating an inverse and unreliable relationship, although with slightly lower error (RMSE = 33.99). For silt content, the

results were mixed. GRS scanning showed a stronger correlation with sampled values ($r = 0.46$), but the associated RMSE was high (35.75), suggesting large deviations from actual values. EC scanning, while showing a weaker correlation ($r = 0.3$), had much lower prediction errors (RMSE = 3.35), indicating better absolute accuracy. Overall, GRS scanning tended to capture spatial trends in clay and sand content more effectively (as shown by higher correlation coefficients), but EC scanning produced lower prediction errors for silt. Both methods were inadequate for accurate sand prediction and should be interpreted with caution.

It has been suggested that machine learning methods may outperform linear regression approaches for calibrating models on soil data; this is because machine learning algorithms are capable of determining complex and non-linear relationships (Wehrle and Pätzold, 2024). Therefore, this study employed a Random Forest (RF) machine learning algorithm to assess which scanning technology was a more accurate predictor of soil texture in the experimental site. The results of the RF model highlight the different predictive power of EC and GRS variables in the classification of soil texture. When assessing model predictor variable importance, there are two key outputs to a RF model: Mean Decrease Accuracy (MDA) and Mean Decrease Gini (MDG). MDA quantifies how much the accuracy of the model decreases when a particular feature is permuted, which disrupts its ability to contribute to the model prediction. This helps in understanding which features have the most influence on the model's predictions. Whereas, MDG is a quantification method of a variable's importance in a Random Forest model. It quantifies how much a variable decreases impurity as classification is performed. Therefore, the higher the MDG score, the more important the variable is to the model. In this study, model parameter importance was assessed using both metrics for the random forest model with both GRS and EC included as model predictors.

For clay content prediction, GRS predictors consistently demonstrated high MDA values, with the GRS clay predictor (27.08), GRS sand predictor (26.45), and GRS silt predictor (25.26) being the most influential variables. This indicates that GRS-based variables are particularly well-suited for identifying clay particle content. Whereas EC predictors resulted in mixed accuracy for clay classification. The deep EC data exhibited a slightly negative MDA of -2.03, indicating that it did not contribute positively to model accuracy for clay content. On the other hand, the shallow EC data exhibited a moderately strong predictive capacity, with an MDA of 23.86. However, the deep EC variable emerged as the most important predictor of sand content with

an MDA of 17.56, indicating its relevance in detecting coarse-textured soils. Conversely, the GRS-based predictors exhibited negative MDAs, suggesting that GRS scanning methodologies may be inadequate or even misleading when applied to sand content prediction. For silt content classification, both shallow and deep EC predictors demonstrated the highest variable importance, with MDAs of 36.26 and 33.69, respectively. Additionally, MDG values were generally lower than MDA values but followed a similar trend, reinforcing the relative dominance of GRS predictors for clay classification and EC predictors for silt and sand. These findings suggest that the combination of both GRS and EC predictors could enhance the overall model accuracy.

Although GRS and EC have both been shown to be able to predict soil texture variation with some accuracy in some cases (Mahmood et al., 2013; Heil and Schmidhalter, 2012), demonstrating the potential of both technologies. Much of the success or failure of prediction accuracy is attributed to the model that the scanning data is used in, and the covariate parameter of that model. Accurate models of soil textural variation underpin the very idea of precision agriculture, as this is the tool for identifying areas of farm land which require different management (e.g variable rate nutrient application and seeding). However, investment in this technology is only worthwhile for farmers if the underlying soil mapping is accurate and sufficiently precise enough to support effective spatially variable management application rates (Rhymes et al., 2023). Unfortunately, the widespread application of these technologies within an agricultural setting is complex, as the correlation between soil textural properties and the directly measured variables (soil electrical conductivity, gamma ray emission, etc.) varies greatly between sites, soil types and management practices.

The GRS data in particular was found to have high prediction error for sand ($RMSE = 38.1$) and silt ($RMSE = 35.75$) concentration in particular when compared to the samples analysed by laser diffraction. The high error in this prediction of soil texture is possibly due to insufficient representative calibration data; the scan was calibrated against three samples ha^{-1}. However, the results of this chapter demonstrated that five samples ha^{-1}, combined with another predictor variable, were not sufficient to train an accurate machine learning model to predict the spatial soil textural accurately in one site. Rhymes et al. (2023) highlighted concerns regarding the lack of commercial regulations to ensure accurate data is provided by soil mapping agribusinesses. They compared this to commercial soil testing laboratories, which offer more accurate services and require mandatory ISO accreditation (ISO/IEC, 2019).

They recommend that businesses that provide soil scanning also be required to provide independent accuracy estimates for analysis, which will help the farmer or end user to critically assess the accuracy of the services provided. They also recommend that future commercial services should include a multi-proximal sensor approach, as a combination of these technologies has been shown to have the potential to significantly improve prediction accuracy (Ji et al., 2019; Vasques et al., 2020; Rhymes et al., 2023). The effects of "soil sensor fusion" were shown in this small machine learning model in this chapter, where EC and GRS were both found to be important for the model in different ways; GRS improved the model's contribution to the homogeneity of the nodes and leaves in the random forest, whereas EC improved the accuracy of the model. Both variables showed promise for accurate modelling of clay (GRS), silt and sand (EC) in combination. However, each scan in isolation did not predict soil texture with sufficient accuracy that it would likely be useful for a farmer to make evidence-based decisions on the implementation of precision agriculture operations.

Hypothesis H_1 was only partially supported by the results. While both GRS and EC scanning technologies showed some capacity to predict soil texture, their effectiveness was highly variable depending on the soil property in question. GRS performed moderately well in predicting clay content but failed to accurately estimate sand and silt, with high RMSE values and poor correlation with sampled data. Conversely, EC scanning performed relatively better in predicting sand and silt content but had inconsistent results for clay. Random Forest modelling highlighted that GRS predictors were more important for clay classification, while EC predictors contributed more to accurate predictions of sand and silt. These findings indicate that neither scanning technology alone provided reliable soil texture maps, and prediction accuracy was likely limited by the low density of calibration samples and site-specific variability.

Hypothesis H_2 was supported by the results of this study, as the findings suggest that the combination of both GRS and EC predictors could enhance the overall model accuracy. The study supports the idea that a multi-sensor "soil sensor fusion" approach may enhance predictive power, but also emphasises that, in their current form, these commercial scanning tools lack the accuracy required for informed precision agriculture decision-making at the field scale.

4.5 Conclusion

The study assessed the potential of commercial scanning technologies, Gamma-Ray Spectrometry (GRS) and Electrical Conductivity (EC) to predict soil texture. The

hypothesis was only partially supported. GRS performed moderately well for predicting clay content, while EC was more accurate for sand and silt. However, prediction errors remained high, particularly for sand, and the low density of calibration samples likely limited model performance. Random Forest modelling showed that both technologies contributed complementary information, supporting a multi-sensor "soil sensor fusion" approach. Nonetheless, neither scanning method, in isolation or combination, delivered the precision necessary for robust application in precision agriculture. Furthermore, the adoption of sensor technologies in agriculture should be accompanied by robust validation protocols and greater calibration sample density to ensure the reliability of their outputs for on-farm decision making. In the short term, farmers should continue to use physical sampling for soil texture analysis, as this study has shown that there is poor accuracy for two commonly used commercially available soil proximal sensors for soil textural prediction.

Chapter 5

Soil Health and Function Under Conservation Agriculture

5.1 Introduction

Soil health underpins the productivity and resilience of agricultural systems, acting as a critical interface between environmental processes and crop performance. Conservation Agriculture (CA) has been increasingly promoted as a systems-based approach to enhance long-term soil function by minimising disturbance, maintaining organic cover, and promoting crop diversity (Kassam et al., 2014b). However, the outcomes of CA are often context-dependent, particularly during the transition from conventional (CON) practices. This chapter characterises the main effects of the transition to CA on the soil biological, physical, and chemical characteristics, and compares this with conventional agriculture (CON).

5.1.1 Soil Physics in Conservation Agriculture

This section seeks to assess the effects of the transition to CA on soil physical properties. During the initial transitional years to CA, many farmers and academic studies reported rises in soil bulk density in CA systems (Soane et al., 2012; Pidgeon and Soane, 1977; Li et al., 2020a). This is to be expected in the absence of mechanical tillage; however, as the system develops over time, the bulk density of the soil typically decreases as the effect of soil biology begins to naturally alter the physical structure (Blanco-Canqui and Ruis, 2018; Mondal et al., 2019). Other common results from the application of CA include improvements to soil mechanical strength, aggregate stability, and improvements to vertical macro-porosity (Soane et al., 2012). This is evidenced by Li et al. (2007), who presents data from a 15-year experiment in China, comparing the long-term effects of no-tillage (NT) and residue cover with CON in

a winter wheat (*Triticum aestivum L.*) monoculture. They found that long-term residue removal in combination with CON resulted in poor cropping productivity and soil structure. The NT system with residue retention had 1.5% reduction in bulk density and 3.2 % greater capillary porosity.

5.1.2 Soil chemistry in Conservation Agriculture

Soil nutrient availability is a fundamental contributing principle of a productive cropping system, especially nitrogen availability at key crop growth stages (AHDB, 2023b; Dordas, 2015). Typically, CON systems have been designed to supply the growing crop with available nutrients during the cropping season via synthetic fertiliser applications (AHDB, 2023b). However, as already detailed in this chapter, the soil physical and biological conditions alter significantly in CA in comparison to CON systems. For example, many studies have detected significant alteration of soil organic matter pools and the stratification throughout the soil profile, which in turn can influence microbial biomass and community structure (Wacker et al., 2022). Such changes in microbial biomass can result in alteration of plant nutrient availability and the distribution of available nutrients in the soil profile (Page et al., 2020; Badagliacca et al., 2021; Wacker et al., 2022).

Much of the change in nutrient availability in the two systems can be attributed to greater plant residue retention in CA systems, as the residues contain nutrients which result in higher quantities of soil nutrient stores, and the lack of tillage, which breaks down organic material and incorporates it into the soil resulting in faster microbial decomposition and mineralisation of plant nutrients. Hence, typically there is found to be differences in total, organic, and inorganic N fractions with CA and CON systems (Mukherjee et al., 2024). This was found by Li et al. (2007) where, after 15 years of NT and residue retention, the total N and P were 27.9% and 25.6% higher, respectively, than the CON treatment, where residue removal had taken place. This result was also found by Badagliacca et al. (2021), who found 20% higher extractable N in the CA system than the CON after 23 years of application of both systems. However, during the early stages of the transition to CA, the combination of tillage, residue incorporation, N fertilisation, and the higher soil temperatures associated with CON systems may cause higher N availability in the short term in CON systems (Mukherjee et al., 2024). Conversely, in the early stages of the transition to CA, it is not uncommon for the total soil N to increase, but the quantity of plant available N to decrease (Page et al., 2020). This is due to a combination of slower rates of N mineralisation and N immobilisation in response to higher quantities of C being

added with crop residues. These factors combine to reduce available N supply in the short term, although over longer durations, as the total N and C content increase, the C:N ratio reaches an equilibrium, thus resulting in improvements to N supply (Page et al., 2020; Wang et al., 2006).

The absence of mechanical mixing of the soil and crop residues in CA systems can result in stratification of immobile nutrients in the upper soil layers (Dang et al., 2018; Page et al., 2020). In most cases, this is of agronomic benefit as this results in higher nutrient availability in the rhizosphere. However, this is sometimes considered a problem in arid cropping regions, as the surface of the soil dries to the extent that plants cannot access the stored nutrients, leading to interest in strategic tillage in CA systems in certain regions to mix the nutrients to deeper areas of the soil profile (Dang et al., 2018; Çelik et al., 2019; Lawrence et al., 2023). The study by Wacker et al. (2022), who studies organic matter stratification patterns to 50 cm depth in two Danish farms, found the C:N ratio in the top 5cm of soil was 1.86 in the CA treatment and 1.04 in the CON treatment. However, in this study, they also found significant differences in the C:N stratification at lower soil depths, for example, at 20 - 30 cm, the C:N ratio in the CA treatment was 1.61 compared to 1.06 in the CON treatment.

When other nutrients are considered, Lv et al. (2023) used a global meta-analysis to analyse the effects of conservation tillage systems on the stratification of soil nutrients. They found that compared to the CON agriculture control treatment that a variety of combinations of conservation tillage and residue retention increased availability of N, P, and K in the topsoil.

5.1.3 Soil Biology in Conservation Agriculture

Agricultural intensification during the green revolution is often shown to have had strong negative impacts on soil biota (Henneron et al., 2015; Postma-Blaauw et al., 2010). Typically, during agricultural intensification, the soil ecosystem regulatory functions of soil biodiversity are gradually replaced by regulation through chemical and mechanical inputs (Giller et al., 1997). However, tillage and cropping system intensity have a complex interaction with the soil biological environment. The diversity, activity, and abundance of the soil biota are all affected by the degree of tillage, agrochemical inputs, and the type and quantity of crop residues returned to the soil (Kladivko, 2001).

Soil biology itself plays an integral role in the overall health and function of a soil. For example, macrofauna, such as earthworms, are key to soil structural formation.

They mix organic material throughout the soil profile, whilst forming large soil pores which aid in improvements to crop root development, soil aeration, and water infiltration and storage (Kladivko, 2001). In comparison, soil microorganisms are important for soil organic matter decomposition and nutrient cycling (Henneron et al., 2015), although each species of soil organism affects the soil in a different manner.

Typically, soil organisms are divided between soil microflora (bacteria, fungi, and algae), and soil fauna, which is in turn divided into three separate categories: **A:** Microfauna, typically small organisms which dwell in the water-filled pore space of the soil (e.g. protozoa and nematodes). **B:** Mesofauna, which typically have an average size of 0.2 mm and live in air-filled pore space of soil and litter (e.g. micro arthropods and springtails). **C:** Macrofauna, which are larger than 2 mm and have the ability to burrow through the soil (e.g. termites, earthworms, and large arthropods) (Kladivko, 2001).

Soil organic matter is an integral driver of many soil functions and processes, as the organic material provides substrate to the soil biota, as well as contributing to nutrient cycling, water retention and soil structural genesis and maintenance (Palm et al., 2014). As discussed previously in this chapter (Section 5.1.1), there is debate amongst the scientific community regarding the magnitude of soil organic matter accumulation in CA systems (Gadermaier et al., 2012). However, typically, any improvements to soil organic matter accumulation are generally confined to upper levels of the topsoil and are not identified further down the soil profile (Blanco-Canqui and Ruis, 2018).

Soils under RT agricultural systems, such as CA or NT, are generally found to have higher microbial biomass in the topsoil compared to CON systems (Wang et al., 2006; Doran, 1987; Muhammad et al., 2021; Li et al., 2018). This is often attributed to a combination of factors commonly associated with CA systems, including increased soil organic matter, reduced physical disturbance, and greater crop diversity (Palm et al., 2014). These changes typically lead to increased abundance, diversity, and stratification of soil biota. In turn, the feedback between soil organisms and soil processes can enhance soil physical properties such as structure and aggregate stability (Li et al., 2018).

Due to the important role soil biology plays within the soil ecosystem, future research must aim to quantify the effects of transitions to different agricultural systems on the soil. In recent years, there has been a significant advancement in the standardisation of protocols for sampling, extraction and determination of soil invertebrates in particular, which has resulted in improved ease of monitoring changes to

soil biodiversity (Gardi et al., 2009). One of the principal difficulties when monitoring soil biodiversity relates to the taxonomic classification of soil invertebrates, which requires skill and in-depth knowledge of taxonomic classifications at the species level (Parisi et al., 2005). As a result, there has been increased usage of soil biodiversity indices, based on a broader taxonomic resolution, key species, or morphological characteristics, which are used to quantify and compare the diversity within ecological communities. These indices offer a standardised way to assess biodiversity, making it easier to analyse patterns and/or monitor changes over time. This reduces the need for specialist knowledge when determining taxonomic classifications (Gardi et al., 2009; Parisi et al., 2005).

This chapter compares several soil biodiversity indices to compare the differences in soil biological diversity between the experimental treatments. These are: The "Qualità Biologica del Suolo" (Biological quality of the soil), which is usually abbreviated to the QBS-ar index Parisi et al. (2005). This index is based upon a simple concept: the higher the soil quality, the higher the number of micro arthropod groups well adapted to soil habitats (Parisi et al., 2005). It uses morphological characteristics and assigns higher scores to organisms that exhibit greater adaptation to the belowground soil environment, which will reflect habitat quality and stability. It does not require a species-level diagnosis, meaning it is a fast method that does not require specialist skills in taxonomic identification. Thus, it is typically used for large experiments with many samples.

Although the QBS-ar index has been designed to be user-friendly to non-experts in taxonomy, there are still significant limitations for farmers in terms of the practicality of using both of these indices to assess their own land. One of the key reasons for this is that the organisms required for both indices require extraction using a Berlese-Tüllgren extractor and are analysed under a stereomicroscope. This equipment is specialist and therefore the methodologies are not particularly accessible to the average farmer. Therefore, this chapter also assesses one EMI based on earthworms, as these are one of the most frequently used bioindicators to evaluate soil quality. They are easy to sample, require no specialist equipment, and the eco-types are distinguishable to non-experts. In this chapter, a new earthworm abundance index based on the QBS index system is used, known as QBS-e (Fusaro et al., 2018).

The eco-morphological indexes introduced above are compared to the Shannon Diversity Index (Shannon, 1948). This is a widely used and well-established index in soil ecology for quantifying biodiversity within a community, accounting for both

species richness (the total number of species present) and species evenness (the distribution of individuals across these species) (Van Leeuwen et al., 2015). A higher Shannon biodiversity index indicates greater diversity, including both a large number of species and a more even distribution of individuals within the species. It is generally considered that higher levels of biodiversity are indicative of healthier soils or ecosystems (Lehman et al., 2015a; Rose et al., 2016).

As the adoption of CA globally continues to increase, there is currently a lack of understanding in the scientific literature on the effects of CA systems on soil fauna communities. Many studies are available evaluating the individual principles of CA (Li et al., 2020b; Muhammad et al., 2021; Venter et al., 2016), however, more systemic approaches are needed to consider all CA principles as a whole at the cropping system level for a fuller understanding of the effects of the system on soil biota (Dulaurent et al., 2023; Henneron et al., 2015; Denier et al., 2022).

5.1.4 Research Aims and Hypotheses

The research aims (A) of this chapter are:

- A_1: Analyse the effects of the transition to CA on the soil chemical environment in comparison to a CON system.
- A_2: Analyse the effects of the transition to CA on the soil physical environment in comparison to a CON system.
- A_3: Analyse the effects of the transition to CA on the soil biological environment in comparison to a CON system.

This chapter tests the following hypotheses (H):

- H_1: CA results in significantly higher diversity and abundance of soil micro arthropods and earthworms compared to CON practices.
- H_2: CA increases soil organic carbon content over time compared to CON.
- H_3: Soil bulk density and compaction are lower under CA, than CON, due to reduced mechanical disturbance.

5.2 Materials and Methods

5.2.1 Soil Sampling and Preparation

The standard sampling consisted of 50 samples from the experimental site (25 samples per treatment) taken at randomly generated points following the methodology outlined in Chapter 3. The sampling points are presented in Table 5.1 and in Figure 5.1. However, the quantity of samples collected from each plot depended on the type of analysis. Thus, the following sections detailing the specific soil sample analysis also detail the quantity of samples taken.

Samples were prepared and dried following the standard operating procedure for soil samples for chemical and physical analyses FAO (2019b). Samples were dried in foil trays at 35 ± 5 °C in a soil drying room at Harper Adams University, Shropshire, UK. The drying process was assisted by breaking up the soil's large aggregates. The dried samples were then disaggregated using a ceramic mortar and pestle in a well-ventilated area and passed through a 2 mm stainless steel sieve, removing large stones and plant material.

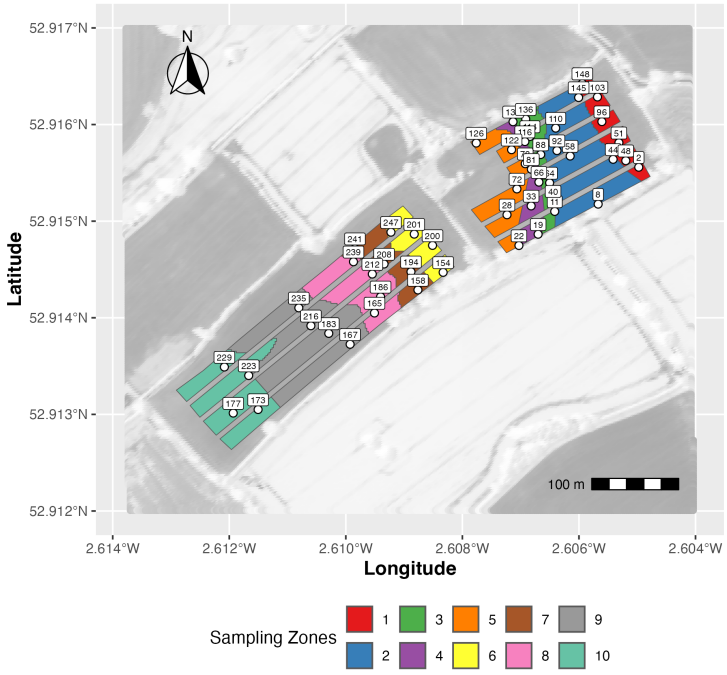

Figure 5.1: Soil sampling points during the experimental duration ($n = 25$). The sampling zones, generated using the methodology outlined in Chapter 3, are also presented.

Table 5.1: Randomly generated soil sampling point coordinates with experimental treatment and soil zone classification

Longitude	Latitude	Sample	Plot	Treatment	Soil Zone
-2.60497394	52.91555848	2	1	Conservation	1
-2.60567013	52.9151764	8	1	Conservation	2
-2.60641565	52.91510095	11	1	Conservation	3
-2.60670045	52.91486498	19	1	Conservation	4
-2.60702974	52.91474819	22	1	Conservation	5
-2.60723424	52.91506616	28	2	Conservation	5
-2.60682046	52.91515785	33	2	Conservation	4
-2.60644411	52.91520737	40	2	Conservation	3
-2.60541382	52.91564033	44	2	Conservation	2
-2.60519641	52.91562634	48	2	Conservation	1
-2.60531422	52.91581217	51	3	Conservation	1
-2.60615086	52.91567413	58	3	Conservation	2
-2.60650305	52.91539601	64	3	Conservation	3
-2.60668698	52.91540406	66	3	Conservation	4
-2.60706456	52.91533377	72	3	Conservation	5
-2.60692161	52.91559476	78	4	Conservation	5
-2.60681713	52.91553725	81	4	Conservation	4
-2.60665621	52.91568972	88	4	Conservation	3
-2.6063768	52.9157305	92	4	Conservation	2
-2.60560688	52.91603044	96	4	Conservation	1
-2.60568222	52.91628565	103	5	Conservation	1
-2.6063992	52.91596317	110	5	Conservation	2
-2.60684083	52.91587669	114	5	Conservation	3
-2.60692782	52.91582384	116	5	Conservation	4
-2.60715622	52.91573972	122	5	Conservation	5
-2.60776209	52.91580854	126	6	Conservation	5
-2.60713123	52.91602907	135	6	Conservation	4
-2.60691328	52.91605611	136	6	Conservation	3
-2.60600544	52.91627966	145	6	Conservation	2
-2.60594246	52.91642491	148	6	Conservation	1
-2.60833057	52.91447029	154	7	Conservation	1
-2.60876278	52.91428819	158	7	Conservation	2
-2.60950852	52.9140496	165	7	Conservation	3
-2.60992644	52.9137257	167	7	Conservation	4
-2.61150515	52.91305053	173	7	Conservation	5
-2.61193212	52.91301373	177	8	Conservation	5
-2.61029275	52.91383847	183	8	Conservation	4
-2.60940362	52.91421718	186	8	Conservation	3
-2.60888236	52.91447639	194	8	Conservation	2
-2.60851254	52.91474912	200	8	Conservation	1
-2.60882623	52.91486601	201	9	Conservation	1
-2.60934382	52.9145568	208	9	Conservation	2
-2.609546	52.91445272	212	9	Conservation	3
-2.61059953	52.91391754	216	9	Conservation	4
-2.61166641	52.91340229	223	9	Conservation	5
-2.61208396	52.91349043	229	10	Conservation	5
-2.61080668	52.91410248	235	10	Conservation	4
-2.60986895	52.91457981	239	10	Conservation	3
-2.60984365	52.91471595	241	10	Conservation	2
-2.60922597	52.91488609	247	10	Conservation	1

5.2.2 Dry Bulk Density

Soil dry bulk density is the ratio of the dry mass to the bulk volume of soil particles plus pore spaces in a sample (Blake, 1965). To calculate the quantity of observations (n) required in this experiment to test the hypothesis, the effect sizes (Cohen's d) were taken from Brown et al. (2021) who examined the effects of reduced tillage on

soil carbon and dry bulk density from three medium-term experiments in sites with contrasting soil and climatic characteristics in the UK. The effect size and Cohen's d were calculated following the methodology outlined in Chapter 3, and the power plotted as a function of effect size and observation number.

Fifty soil cores were taken for dry bulk density analysis on 09/10/2021, 23/08/2023 and 21/08/2024 to a depth of 5 cm following the methodology of Soto Gómez et al. (2020). The Eijkelkamp sample ring kit model C53 was used, which consists of a steel ring with a sharpened edge, with a height of 5.1 mm, an outside diameter of 53 mm, and an internal volume of 100 cm^3 (Eijkelkamp Soil & Water, 2019). The steel ring is placed into a ring holder and inserted into the soil to the required depth. The ring holder is then removed from the soil, and the ring is removed from the holder with the undisturbed soil sample inside. The samples were placed into foil trays and dried to a constant weight at 105 °C. The samples were cooled in a desiccator and then weighed to determine the true dry bulk density using the following equation:

$$\rho b = \frac{(m2 - m1)}{V} \tag{5.1}$$

Where ρb is the dry bulk density of the soil (g cm^{-3}), $m1$ is the mass of the foil tray (g), $m2$ is the mass of the foil tray with the soil after drying (g), and V is the volume of the steel ring used for the sample extraction (g cm^{-3}).

5.2.3 Organic Matter and Total Carbon

Soil samples were taken from the field using an auger on 09/10/2021, 23/08/2023 and 21/08/2024 to a depth of 20 cm. Five samples per plot were taken, resulting in 25 samples per treatment. The samples were placed into bags and transported to the lab, where they were dried and prepared as per the methodology detailed in section 5.2.1. Soil organic matter content was determined using the Loss on Ignition (LOI) methodology detailed by Soto Gómez et al. (2020). Firstly, 10 g of the 2 mm sieved soil was placed into crucibles and dried at 105 °C until the sub-samples were a constant weight. Then, the initial mass was recorded and the samples placed into a muffle furnace at 450 °C for 4 hours and cooled in a desiccator and re-weighed. The percentage of soil organic matter within the sample was then calculated with this equation:

$$\%SOM = \frac{(m_{DS} - m_{BS})}{m_{DS} - m_C} \times 100 \tag{5.2}$$

Where m_{DS} is the mass of the dry soil and the crucible (g), m_{BS} is the mass of the burnt soil and the crucible (g), and m_C is the mass of the crucible (g).

The total carbon (C) concentration was analysed using the Dumas dry combustion method (FAO, 2019c), which determines the content of all forms of C in the soil by burning samples at a high temperature (between 900 and 1000 °C or 1400 and 1600 °C) in an atmosphere of pure oxygen (FAO, 2019c; Soto Gómez et al., 2020). 1.5 g of sieved and dried soil was ground using a pestle and mortar and placed into a foil wrap and inserted into an element analyser (LECO FP-528), which was calibrated before use with known C standards. Replicated blanks were also analysed to determine the baseline according to the equipment procedure.

5.2.4 Penetration Resistance

Dry bulk density is usually considered to be the most accurate field measurement of soil structure as it is directly related to soil porosity, as it expresses the relationship between the soil mass and the volume it occupies (Hernanz et al., 2000). However, dry bulk density sampling is labour-intensive and can be an especially slow process if dry bulk density at multiple depths is required, as this requires taking deep soil cores. Soil penetration resistance measures a soil's resistance to deformation or compaction, which can be influenced by soil strength numerous factors, including soil texture, compaction, structure, moisture content, dry bulk density, vegetation, and agricultural history (Kumi et al., 2023). Soil penetration resistance in field conditions is measured with cone penetrometers. A cone penetrometer consists of a steel cone mounted on a steel rod, which is pushed vertically into the ground (Hernanz et al., 2000).

An Eijkelkamp GPS-enabled penetrologger (Eijkelkamp Soil & Water, 2024) was used to record at 20 sample points per plot on 10/05/2024. The sample locations were randomly generated using the methodology outlined in Section 3.4. The penetrologger was equipped with a 2 cm diameter cone with a 60° slope inserted at a rate of 2 cm s^{-1}. Data normality and heterogeneity of variances were analysed using the methodology outlined in Section 3.10. The penetration resistance data were analysed using a generalised linear mixed-effects model following the model formula detailed in Section 3.10 using the depth of the measurement as a random model effect. An inverse link function was chosen as the penetration resistance data was continuous, and negatively skewed as shown in Appendix A.2. The mean penetration resistance was then calculated for 5 cm increments, and separate generalised linear mixed effects models were then run for each 5 cm increment from 0 - 80 cm depths.

5.2.5 Soil Chemical Analysis

Soil samples were sent to NRM Laboratories Ltd., Bracknell, UK (division of Cawood Scientific Ltd.). The laboratories hold ISO/IEC accreditation (ISO/IEC 2017). Samples were sent for standardised soil agronomic analysis as recommended by UK nutrient management guidelines (AHDB, 2017). Measurements included soil pH and soil indices P (Olsen P method (Olsen, 1954)), Mg and K (NRM, 2021a). Treatment differences were modelled using generalised linear mixed-effects models using the model formula outlined in Equation 3.8 in Section 3.10.5.3.

5.2.6 Earthworm Abundance

Earthworm abundance and ecotype sampling occurred on 04/03/2022, 26/04/2023, and 13/05/2024 at random points in each plot following the methodology previously outlined in Section 5.2.1. The hand-sorting technique was used following the method of Soto Gómez et al. (2020). A 50 cm x 50 cm x 25 cm block was excavated from the soil and placed upon a plastic tray, where it was sorted by hand. Earthworms were then transferred to sealed plastic jars with a damp paper towel at the bottom. All jars were labelled and moved from the field to the laboratory in a cool box.

In the laboratory, earthworms were washed and classified into ecotypes. Although these are not functional groups, their habitats differ; therefore, they have different effects on the ecosystem (Burton et al., 2024). After 24 hours, the total mass of earthworms was then weighed and recorded, and the abundance of each ecotype was recorded. These were then assigned an eco-morphological score (EMI). The EMI method used was the QBS-e index, which is based on scoring each systematic group's adaptation level in the soil, as per the methodology of (Fusaro et al., 2018).

Earthworm abundance was checked for normality and homogeneity of variances using the methodology outlined in Section 3.10. Overdispersion was assessed using the methodology outlined in Section 3.10.4. The data were not normally distributed, were not overdispersed, and had a positive skew. Therefore, to assess the effect of the treatment on the response variable, a generalised linear mixed effects model (GLMM) was fitted using a Gamma distribution with a log link function in the `R` package `lme4` (Bates et al., 2015). The model was specified with the experimental treatment as the fixed effect. The effects of Crop and Block were assessed and accounted for little of the variation within the model; therefore, these were not included due to singularity. Model convergence issues were identified; therefore, the models were fitted using a bound optimisation by quadratic approximation (BOBYQA) model optimiser using

the `bobyqa` control function (Powell, 2009) in `lme4` (Bates et al., 2015). In addition, diagnostic plots were generated to visually assess the fit of the model, verify model assumptions, and identify potential issues, such as overdispersion or non-linearity. Pairwise comparisons between the treatment levels, if applicable, were performed using `emmeans` to assess the magnitude of differences between treatment groups.

Table 5.2: EcoMorphological (EMI) scores attributed to each ecological category and age. Source: Fusaro et al. (2018); Paoletti et al. (2013).

Ecological category	**Age**	**EMI score**
Hydrophilic (HYD)	Immature (Im)	1
Hydrophilic (HYD)	Adult (Ad)	1
Coprophagic (COP)	Immature (Im)	2
Coprophagic (COP)	Adult (Ad)	2
Epigeic (EPI)	Immature (Im)	2.5
Endogeic (END)	Immature (Im)	2.5
Epigeic (EPI)	Adult (Ad)	3
Endogeic (END)	Adult (Ad)	3.2
Anecic/Deep-burrower (ANE)	Immature (Im)	10
Anecic/Deep-burrower (ANE)	Adult (Ad)	14.4

5.2.7 Micro-arthropod Abundance

Undisturbed soil cores with a diameter of 10 cm were taken on 09/10/2022, 23/08/2023 and 15/08/2024, to a depth of 10 cm from randomly generated points within the field site (n = 25) shown in Figure 5.1. The samples were bagged and transported to the laboratory, where they were placed into a Berlese-Tüllgren extractor within 24 hours after sampling. The extractor consisted of an incandescent lamp (60 W) situated 30 cm above the soil sample, a sieve (2 mm mesh) where the soil samples are placed above a stainless-steel funnel. The samples were left in the extractor for 14 days, and the micro arthropods were collected in a solution of 70% industrial methylated spirits. The extracted specimens were observed under a stereomicroscope at low magnification in the preservative liquid, and the biological forms (morphotypes) were characterised and assigned an eco-morphological score (EMI). The EMI method used was the QBS-ar index, which is based on scoring each systematic group's adaptation level in the soil, as per the methodology of (Parisi et al., 2005).

Table 5.3: Eco-morphological index (EMI) scores used to assess soil microarthropod abundance. Adapted from Parisi et al. (2005).

Group	**EMI Score**
Protura	20
Diplura	20
Collembola	1–20
Microcoryphia	10
Zygentomata	10
Dermaptera	1
Orthoptera	1–20
Embioptera	10
Blattaria	5
Psocoptera	1
Hemiptera	1–10
Thysanoptera	1
Coleoptera	1–20
Hymenoptera	1–5
Diptera (larvae)	10
Other holometabolous insects (larvae)	10
Other holometabolous insects (adults)	1
Acari	20
Araneae	1–5
Opiliones	10
Palpigradi	20
Pseudoscorpiones	20
Isopoda	10
Chilopoda	10–20
Diplopoda	10–20
Pauropoda	20
Symphyla	20

For the extracted and characterised soil micro arthropod morphotypes, the Shannon Diversity Index was also applied as a measure to characterise the diversity of species within the morphotype communities as per the well-established methodology (Shannon, 1948). The methodology is based upon communication theory where the Shannon Function H' is a measure of uncertainty, corresponding to the entropy concept defined by:

$$H' = -\sum_{i=1}^{S} p_i \log(p_i)) \tag{5.3}$$

Where H' is the Shannon-Wiener Index, S is the total number of species, p_i is the proportion of individuals belonging to species i.e., $p_i = \frac{n_i}{N}$, where n_i is the number of individuals of species and N is the total number of individuals. The Shannon Index was generated using the vegan package in `R` (Oksanen et al., 2024).

Data normality and heterogeneity of variances were analysed using the methodology outlined in Chapter 3.10, and analysed using the generalised linear model formula outlined previously (3.10). No transformations performed before modelling as is rec-

ommended for count data (O'Hara and Kotze, 2010). A quasi-Poisson distribution was chosen as there was a high amount of overdispersion in the data, which was tested using the methodology outlined previously in Section 3.10. As a quasi-Poisson model family was used, random effects could not be modelled; therefore, the experimental year and block were included as fixed effects.

The data calculated using the Shannon Index was analysed using the `lmerTest` `R` package (Kuznetsova et al., 2017), with Treatment and Year as fixed effects with an interaction term and the experimental block included as a random effect to account for potential spatial correlation. A linear mixed-effects model was chosen for this dataset as it met the normality assumptions of the model criteria and was not over-dispersed. The model syntax followed the linear mixed effect model outlined previously in Section 3.10, with the exception of the experimental block being modelled as a random effect to take into account spatial variation. Further multivariate analysis was conducted using principal component analysis (PCA) using the `ggbiplot` package (Vu et al., 2024). This was performed to evaluate the change in the eco-morphological community structure of individual treatments over the experimental duration. PCA multivariate analysis was also performed for the different taxonomic groupings within and between treatments. PCA was performed separately for each year of the experiment, where individual variables were centred and scaled.

5.3 Results

5.3.1 Dry Bulk Density

The power analysis of the data from Brown et al. (2021) found an d value of 0.8 for detecting changes in dry bulk density between the tillage treatment at the 4 cm depth, a d value of 0.58 at 9 cm depth, and a d value of 0.63 at 27 cm depth. At a d value of 0.8, it was found that sufficient power ($\alpha = 0.05$) is achieved with $n = 120$. However, for statistically testing the hypothesis that CA alters the dry bulk density at depths lower down the soil profile, it was found that an observation size of $n = 160$ would be sufficient for a simulated d value of 0.6. This is shown below in Figure 5.2, which is a simulation of the required sample sizes for reliable detection of soil dry bulk density differences in agricultural tillage systems using a range of d values ranging from 0.1 - 1.

Analysis of the soil dry bulk density identified that the CA treatment had a significantly higher dry bulk density than the CON treatment for the experimental duration (β = -0.05, SE = 0.02, Z = -3.45, p = 0.002). The baseline soil dry bulk

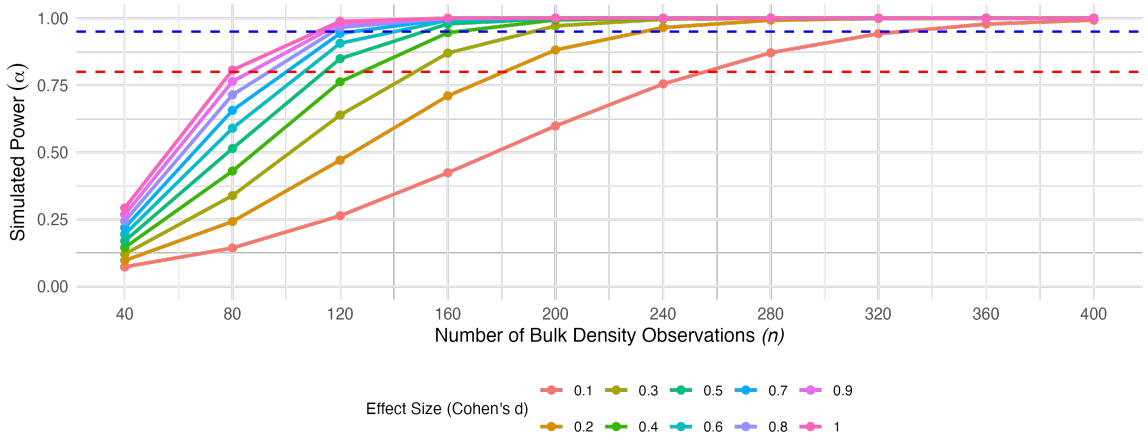

Figure 5.2: Power (α) curve for detecting differences in soil dry bulk density across various effect sizes and sample sizes. The curve illustrates the relationship between the number of observations (x-axis) and statistical power (y-axis) for different effect sizes (Cohen's d).

density for the experimental site was 1.25 g cm^{-3}, which increased in both the CA treatment (1.39 g cm^{-3}) and the CON treatment (1.29 g cm^{-3}) during the first year of the experiment. Following the second year of the experiment, the dry bulk density had risen again to 1.37 g cm^{-3} in the CON treatment and also risen to 1.41 g cm^{-3} in the CA treatment. The final year of the experiment followed the same trend as previous years, with the dry bulk density rising in both treatments to 1.44 g cm^{-3} in the CON treatment and to 1.53 g cm^{-3} in the CA treatment. Statistical analysis identified no significant differences between the CON (β = -0.09, SE = 0.07, Z = -1.33, p = 0.38) or CA treatments and the baseline values (β = -0.14, SE = 0.07, Z = -2.14, p = 0.08). The results from the soil dry bulk density analysis are presented below in Figure 5.3. Distributions and model diagnostics are presented in Appendix A.1.

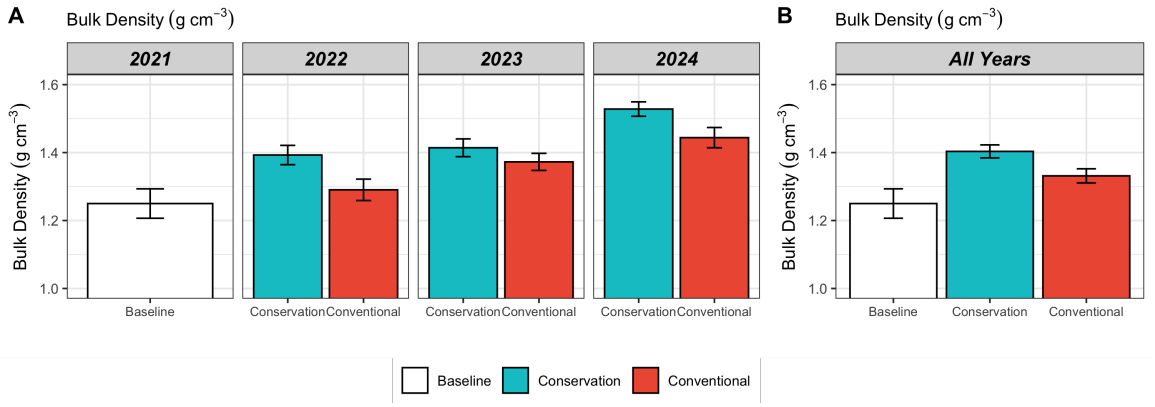

Figure 5.3: Mean soil dry bulk density (g cm^{-3}) for the baseline measurements and each treatment presented by year (**A** $n = 25$) and by treatment for the total experimental duration (**B**: $n = 2$). Error bars indicate the standard error of the mean. **Note:** Y-axis truncated to highlight treatment differences.

5.3.2 Penetration Resistance

Overall, the CON treatment was found to have a significantly higher penetration resistance from 0 - 80 cm in depth in comparison to the CA treatment ($\beta = 0.039$, $SE = 0.015$, $Z = 2.5$, $p = 0.013$). When the 5 cm depth increments were analysed, it was found to be no significant difference between the two treatments in the first 10 cm of the top soil; however, from 10 - 45 cm, the CON treatment was found to have a significantly higher penetration resistance in comparison to the CA treatment. There were no significant differences found from 45 - 50 cm; however, from 50 - 70 cm, the CA treatment had a significantly higher penetration resistance in comparison to the CON treatment. No significant differences were then found further down the soil profile. The penetration resistance for both treatments is presented in Figure 5.4.

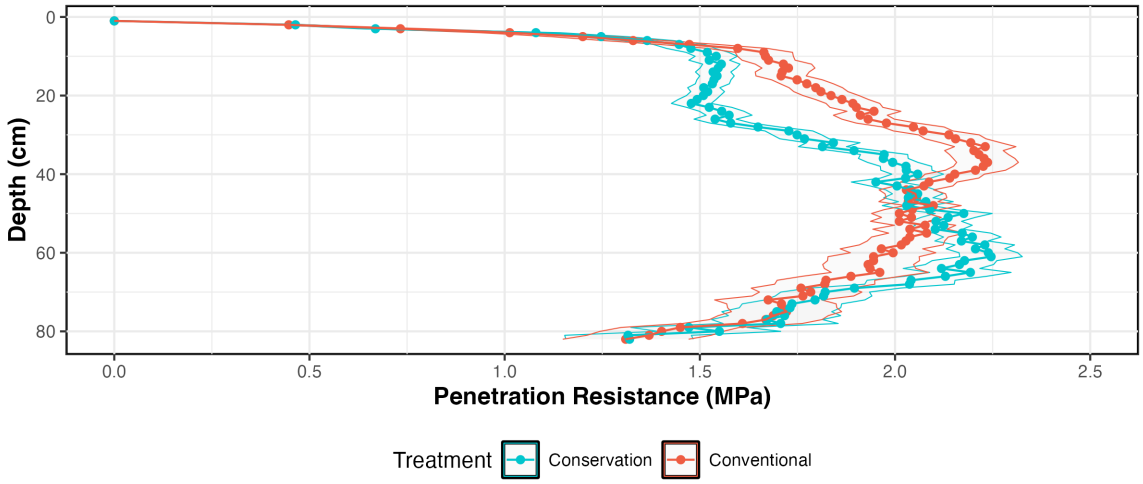

Figure 5.4: The results from the penetration resistance sampling measured in megapascals (MPa). The CA treatment is shown in blue, and the CON treatment in red (n=100). The ribbon indicates the standard error of the mean.

5.3.3 Soil Chemical Analysis

Total Carbon

Analysis of soil total carbon identified weak evidence of an increase in soil total carbon in the CA treatment compared to the CON treatment for the experimental duration (β = -0.04, SE = 0.02, Z = -2.33, p = 0.051). The mean baseline soil total carbon was 1.66%, which was found to fall slightly in the first year of the experiment to 1.52% in the CON treatment and to 1.62% in the CA treatment. In the second year of the experiment, the mean soil total carbon increased in both treatments from the previous year, to 1.6% in the CON treatment and to 1.64% in the CA treatment. Samples were collected for the final year of the experiment, but due to time constraints, have not been included in these results and analysis. The mean soil total carbon in the CON treatment was not found to have statistically changed from the baseline value (β = 0.07, SE = 0.1, Z = 0.64, p = 0.8), which was similar for the CA treatment (β = 0.02, SE = 0.1, Z = 0.2, p = 0.97). The results from the soil total carbon analysis are presented below in Figure 5.5. Distributions and model diagnostics are presented in Appendix A.3.

Phosphorus

Analysis of soil available Phosphorus (P) identified a significant increase in soil available P (mg l^{-1}) in the CA treatment throughout the experiment compared to the

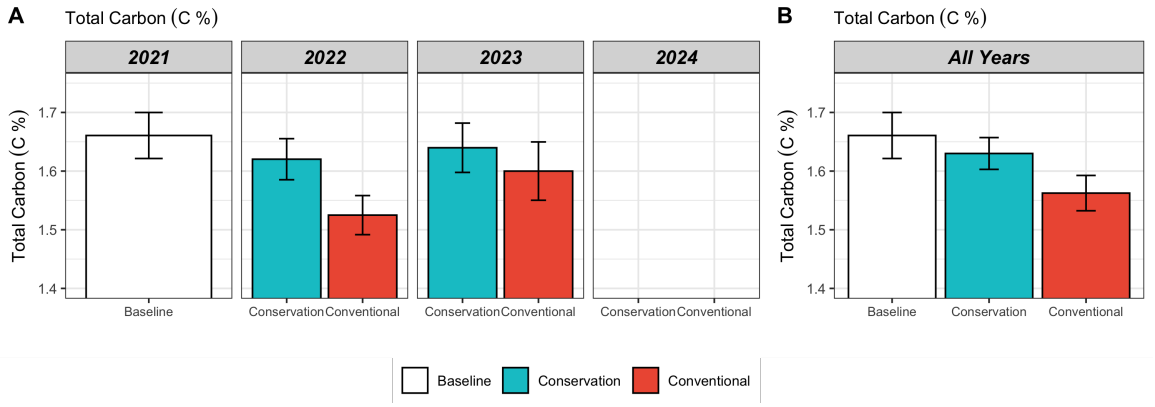

Figure 5.5: Mean soil total carbon (%) for the baseline measurements (n = 10) and each treatment presented by year (**A** n = 25) and by treatment for the total experimental duration (**B** n = 2). Error bars indicate the standard error of the mean. **Note:** Y-axis truncated to highlight treatment differences.

CON treatment (β = -0.23, SE = 0.03, Z = -6.67, $p < .0001$). The baseline mean available P was 19 mg l^{-1}, this reduced in both treatments during the first year of the experiment, to 12.8 mg l^{-1} in the CON treatment, and to 15.8 mg l^{-1} in the CA treatment. During the second year of the experiment, the available P rose in both treatments from the previous year to 14.2 mg l^{-1} in the CON treatment and to 18.3 mg l^{-1} in the CA treatment. During the final year of the experiment, the trend continued in both treatments, where the soil available P rose to 17.3 mg l^{-1} in the CON treatment and to 22.2 mg l^{-1} in the CA treatment, the first mean available P results above the baseline mean result. The mean soil available P in the CON treatment was not found to have statistically changed from the baseline value (β = 0.26, SE = 0.25, Z = 1.07, p = 0.53), or for the CA treatment (β = 0.04, SE = 0.25, Z = 0.15, p = 0.98). The results from the soil total carbon analysis are presented below in Figure 5.6. Distributions and model diagnostics are presented in Appendix A.5.

Potassium

Analysis of soil available Potassium (K) identified a significant increase in soil available K (K mg l^{-1}) in the CA treatment throughout the experiment compared to the CON treatment (β = -0.46, SE = 0.04, Z = -11.78, $p < .0001$). The baseline mean available K was 129 mg l^{-1}, which reduced in the CON treatment during the first year of the experiment to 97.8 mg l^{-1}; however increased in the CA treatment to 185 mg l^{-1}. There was a similar result in the second year of the experiment, where the soil K availability in the CON treatment reduced to 81.3 mg l^{-1}, and the CA treatments'

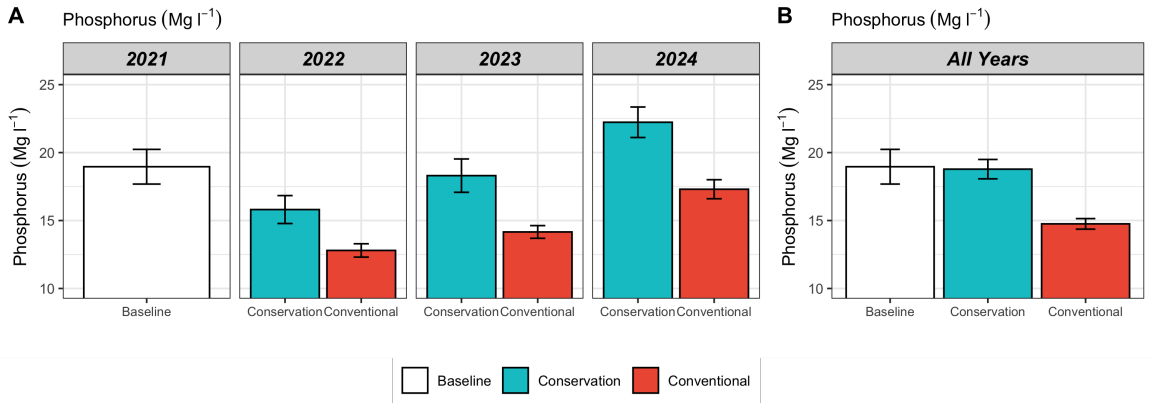

Figure 5.6: Mean soil available Phosphorus (P mg l^{-1}) for the baseline measurements ($n = 10$) and each treatment presented by year (**A** $n = 25$) and by treatment for the total experimental duration (**B** $n = 3$). Error bars indicate the standard error of the mean. **Note:** Y-axis truncated to highlight treatment differences.

mean available K content also reduced from the previous year to 142 mg l^{-1}. During the final year of the experiment, both treatments had increases in the mean available K to 135 mg l^{-1} in the CON treatment, and to 168 mg l^{-1} in the CA treatment. The mean soil available K in the CON treatment was not found to have statistically changed from the baseline value (β = 0.24, SE = 0.27, Z = 0.87, p = 0.66), or for the CA treatment (β = -0.23, SE = 0.27, Z = -0.83, p = 0.69). The results from the soil available K analysis are presented below in Figure 5.7. Distributions and model diagnostics are presented in Appendix A.6.

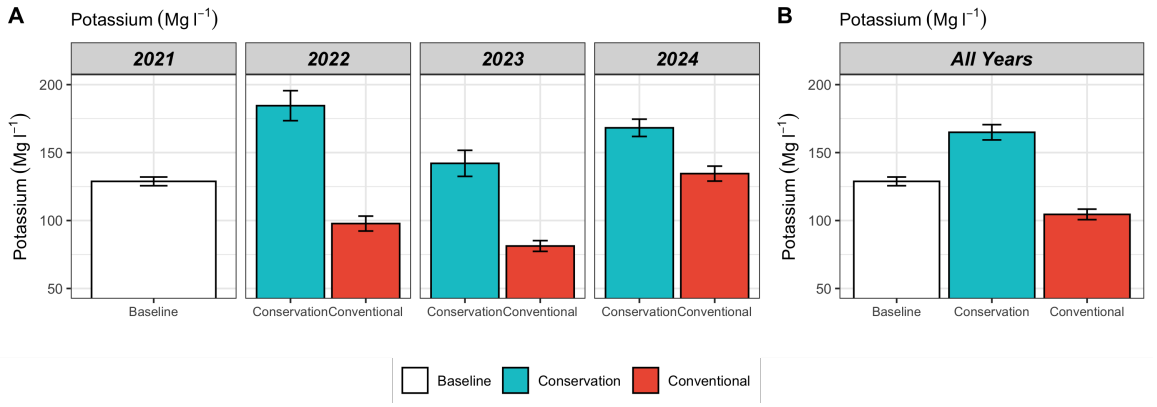

Figure 5.7: Mean soil available Potassium (K mg l^{-1}) for the baseline measurements ($n = 10$) and each treatment presented by year (**A** $n = 25$) and by treatment for the total experimental duration (**B** $n = 3$). Error bars indicate the standard error of the mean. **Note:** Y-axis truncated to highlight treatment differences.

Magnesium

Analysis of soil available Magnesium (Mg) identified a significant increase in soil available K (K mg l^{-1}) in the CA treatment throughout the experiment compared to the CON treatment (β = -0.46, SE = 0.04, Z = -11.78, $p < .0001$). The baseline available Mg mean was 60.2 mg l^{-1}, which rose in both treatments after the first year of the experiment to 72.6 mg l^{-1} in the CON treatment and to 79.5 mg l^{-1} in the CA treatment. There were similar results identified in the second year of the experiment, where the CON treatment had a mean available Mg of 73.3 mg l^{-1} and the CON treatment had a mean of 77.3 mg l^{-1}. In the final year of the experiment, there were increases in mean available Mg identified in both treatments, 75.6 mg l^{-1} in the CON treatment, and 81.6 mg l^{-1} in the CA treatment. The mean soil available Mg in the CON treatment was not found to have statistically changed from the baseline value (β = -0.2, SE = 0.14, Z = -1.48, p = 0.3), or for the CA treatment (β = -0.27, SE = 0.14, Z = -1.98, p = 0.12). The results from the soil available Mg analysis are presented below in Figure 5.8. Distributions and model diagnostics are presented in Appendix A.7.

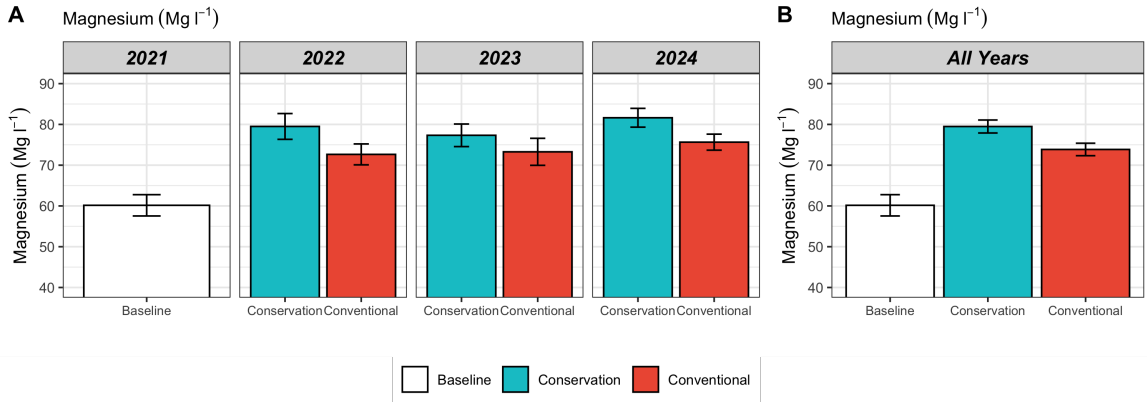

Figure 5.8: Mean soil available Magnesium (mg l^{-1}) for the baseline measurements (n = 10) and each treatment presented by year (**A** n = 25) and by treatment for the total experimental duration (**B** n = 3). Error bars indicate the standard error of the mean. **Note:** Y-axis truncated to highlight treatment differences.

Total Nitrogen

Analysis of soil total Nitrogen (N) identified a significant increase in soil total N (%) in the CA treatment throughout the experiment compared to the CON treatment (β = -0.05, SE = 0.02, Z = -2.86, p = 0.01). The mean baseline total N for the experimental site was 15.8%, which was found to reduce in both treatments during

the first year of the experiment to 14.2% in the CON treatment, and to 15% in the CA treatment. During the second year of the experiment, there were mild increases in the mean total N in the CON treatment to 14.9%, whilst the mean total N in the CA treatment remained relatively unchanged from the previous year at 15.5%. Samples were collected for the final year of the experiment, but due to time constraints, have not been included in these results and analysis. The mean soil total N in the CON treatment was not found to have statistically changed from the baseline value ($\beta = 0.09$, $SE = 0.1$, $Z = 0.9$, $p = 0.64$), and for the CA treatment ($\beta = 0.04$, $SE = 0.1$, $Z = 0.4$, $p = 0.9$). The results from the soil total N analysis are presented below in Figure 5.9. Distributions and model diagnostics are presented in Appendix A.

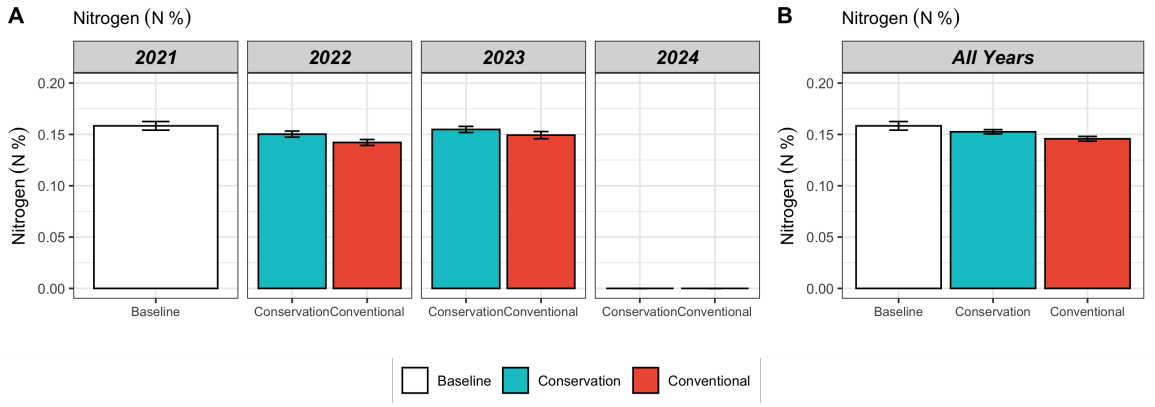

Figure 5.9: Mean soil available Nitrogen (N mg l^{-1}) for the baseline measurements ($n = 10$) and each treatment presented by year (**A** $n = 25$) and by treatment for the total experimental duration (**B** $n = 2$). Error bars indicate the standard error of the mean. **Note:** Y-axis truncated to highlight treatment differences.

pH

Analysis of soil pH identified a significant decrease in soil pH in the CA treatment throughout the experiment compared to the CON treatment ($\beta = 0.03$, $SE = 0.01$, $Z = 3.7$, $p < 0.001$). The mean baseline pH was 6.26. In the CA treatment, this reduced gradually throughout the experiment from 6.19 in 2022, 6.00 in 2023, and finally to 5.89 in the final year of the experiment, 2024. In contrast, the CON treatment was found to have an increased pH of 6.39 in 2022 in comparison to the baseline measurement. From 2022, this gradually declined, following a similar trend to the CA treatment, to 6.25 in 2023 and to 5.93 in 2024. When statistically analysed, neither CA ($\beta = 0.04$, $SE = 0.04$, $Z = 0.89$, $p = 0.64$) or CON ($\beta = 0.01$, $SE = 0.04$, $Z = 0.29$, $p = 0.95$)were found to be significantly different to the baseline

measurement. The results from the soil total N analysis are presented below in Figure 5.10. Distributions and model diagnostics are presented in Appendix A.

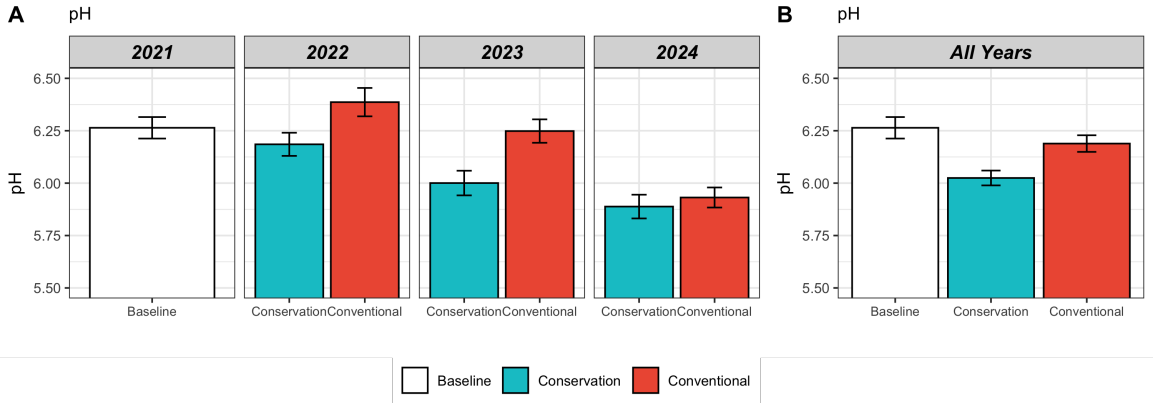

Figure 5.10: Mean soil pH for the baseline measurements ($n = 10$) and each treatment presented by year (**A** $n = 25$) and by treatment for the total experimental duration (**B** $n = 3$). Error bars indicate the standard error of the mean. **Note:** Y-axis truncated to highlight treatment differences.

5.3.4 Earthworm Abundance

5.3.4.1 Juvenile Earthworms

There were no significant differences detected in the abundance of epigeic earthworms in both experimental treatments during this study ($\beta = 0.24$, $SE = 0.3$, $Z = 0.82$, $p = 0.41$). During the first year of the experiment, the extrapolated mean of juvenile earthworms m^{-2} for the CA treatment was 240, compared to the CON treatment, which had a lower abundance of 169 juvenile earthworms m^{-2}. During the second year of the experiment, a low abundance of juvenile earthworms was identified in both treatments, with both treatments having the same mean quantity of juvenile earthworms; 37.2 m^{-2}. However, during the final year of the experiment, the mean abundance rose in both treatments to 128 m^{-2} in the CA treatment and to 90.9 m^{-2} in the CON treatment. Mean abundance of juvenile earthworms is shown in Figure 5.11 by year (**A**) and for the duration of the experiment (**B**). Model diagnostics are presented in Figure A.18.

5.3.4.2 Epigeic Earthworms

There were no significant differences detected in the abundance of epigeic earthworms in both experimental treatments during this study ($\beta = 0.1$, $SE = 0.27$, $Z = 0.4$, $p = 0.69$). In the first year of the experiment, the CA treatment had an extrapolated mean

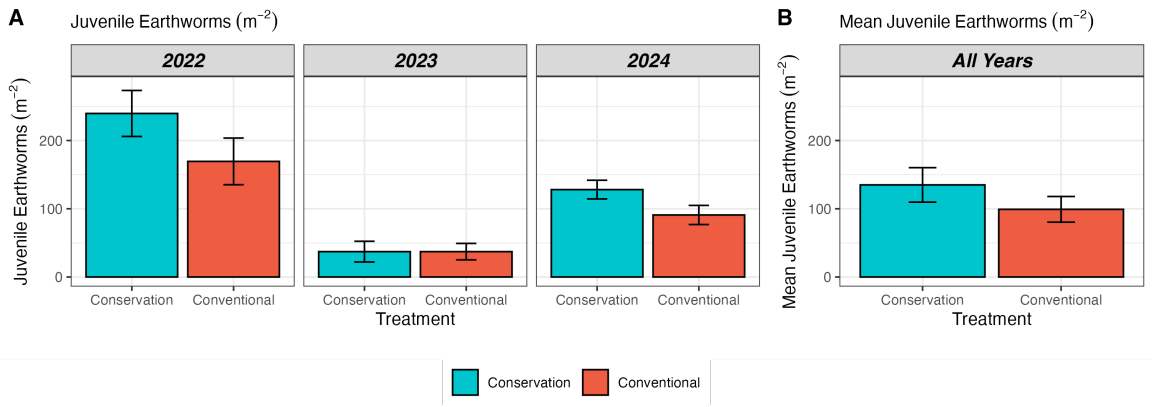

Figure 5.11: Extrapolated mean abundance of juvenile earthworms (m^{-2}) for each treatment presented by year (**A**, $n = 5$) and by treatment for the total experimental duration (**B**, $n = 3$). Error bars indicate the standard error of the mean.

abundance of 66.1 Epigeic earthworms m^{-2}, and the CON treatment had a mean of 49.6 m^{-2}. In the second year, mean abundance for both treatments was similar, with a mean of 70.2 m^{-2} in the CA treatment and 57.9 m^{-2} in the CON treatment. During the final year of the experiment, both treatments had similar mean abundance of 70.2 m^{-2} in the CA treatment and 78.5 m^{-2} in the CON treatment. Mean abundance of Epigeic earthworms is shown in Figure 5.12 by year (**A**) and for the duration of the experiment (**B**). Model diagnostics are presented in Figure A.19.

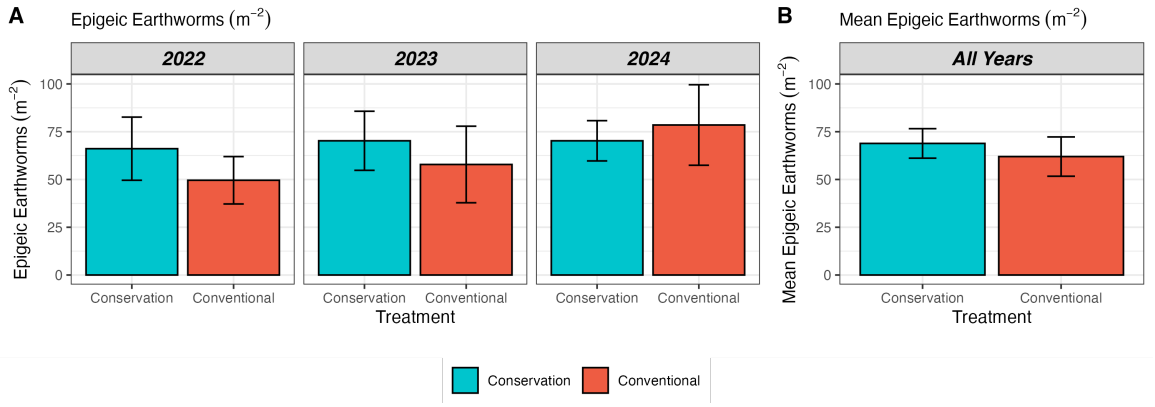

Figure 5.12: Extrapolated mean abundance of juvenile earthworms (m^{-2}) for each treatment presented by year (**A**, $n = 5$) and by treatment for the total experimental duration (**B**, $n = 3$). Error bars indicate the standard error of the mean.

5.3.4.3 Endogeic Earthworms

There were no significant differences detected in the abundance of Endogeic earthworms in both experimental treatments during this study ($\beta = 0.02$, $SE = 0.42$, $Z = 0.04$, $p = 0.97$). During the first year of the experiment, the CA treatment had a higher mean abundance of Endogeic earthworms (90.9 m^{-2}), compared to the CON treatment (41.3 m^{-2}). However, during the second year of the experiment, the inverse was observed, where the mean abundance of Endogeic earthworms in the CON treatment was 74.4 m^{-2} compared to 16.5 m^{-2} in the CA treatment. The final year of the experiment had the highest mean abundance of endogenic earthworms during the experiment for both treatments, 124 m^{-2} in the CA treatment and 112 m^{-2} in the CON treatment. Mean abundance of Endogeic earthworms is shown in Figure 5.13 by year (**A**) and for the duration of the experiment (**B**). Model diagnostics are presented in Figure A.20.

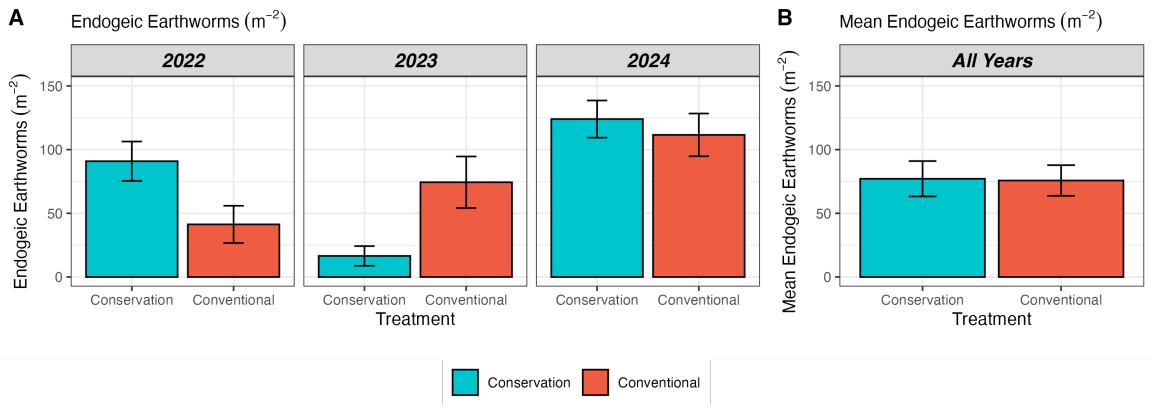

Figure 5.13: Extrapolated mean abundance of juvenile earthworms (m^{-2}) for each treatment presented by year (**A**, $n = 5$) and by treatment for the total experimental duration (**B**, $n = 3$). Error bars indicate the standard error of the mean.

5.3.4.4 Anecic Earthworms

There were no significant differences in the mean abundance of Anecic earthworms identified in this study ($\beta = 0.41$, $SE = 0.46$, $Z = 0.9$, $p = 0.37$). In the first year of the experiment, the CA treatment had a higher extrapolated mean abundance of Anecic earthworms (37.2 m^{-2}) compared to the CON treatment (12.4 m^{-2}), however in the second year the difference in mean abundance between the treatments was reduced (Conservation = 20.7 m^{-2}, CON = 16.5 m^{-2}). In the final year of the experiment, the CON treatment had a mean abundance of 37.2 m^{-2} and the CA treatment had

a mean abundance of 33.1 m^{-2}. Mean abundance of Anecic earthworms is shown in Figure 5.14 by year (**A**) and for the duration of the experiment (**B**). Model diagnostics are presented in Figure A.21.

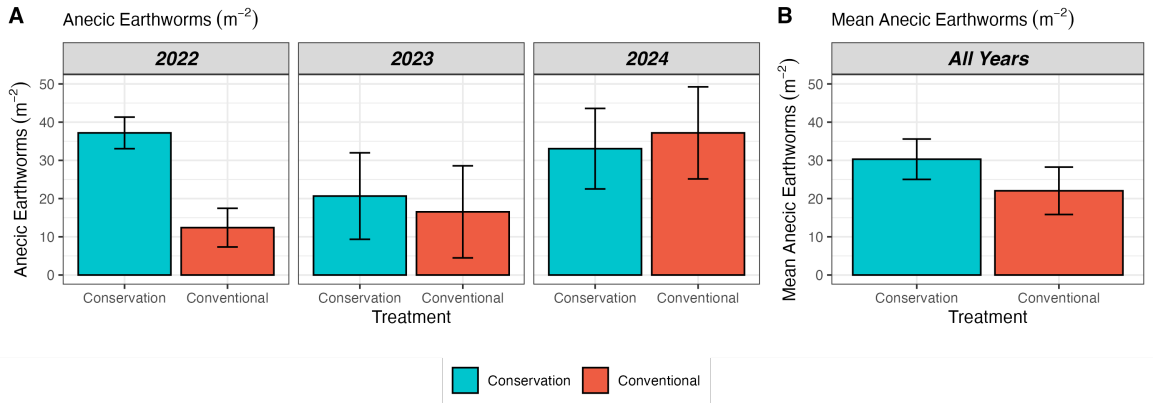

Figure 5.14: Extrapolated mean abundance of juvenile earthworms (m^{-2}) for each treatment presented by year (**A**, $n = 5$) and by treatment for the total experimental duration (**B**, $n = 3$). Error bars indicate the standard error of the mean.

5.3.4.5 Total Earthworms

There was no statistical difference in mean total earthworm abundance identified in this study ($\beta = 0.11$, $SE = 0.13$, $Z = 0.9$, $p = 0.36$). During the first year of the experiment, the CA treatment had a mean total earthworm abundance of 434 m^{-2}, compared to the CON treatment, which had 272 m^{-2}. In the second year, the mean abundance of earthworms declined in both treatments to 145 m^{-2} in the CA treatment and to 186 m^{-2} in the CON treatment. In the final year of the experiment, the CA treatment had a mean of 355 total earthworms m^{-2} and the CON treatment had 318 m^{-2}. Mean abundance of Epigeic earthworms is shown in Figure 5.15 by year (**A**) and for the duration of the experiment (**B**). Model diagnostics are presented in Figure A.22.

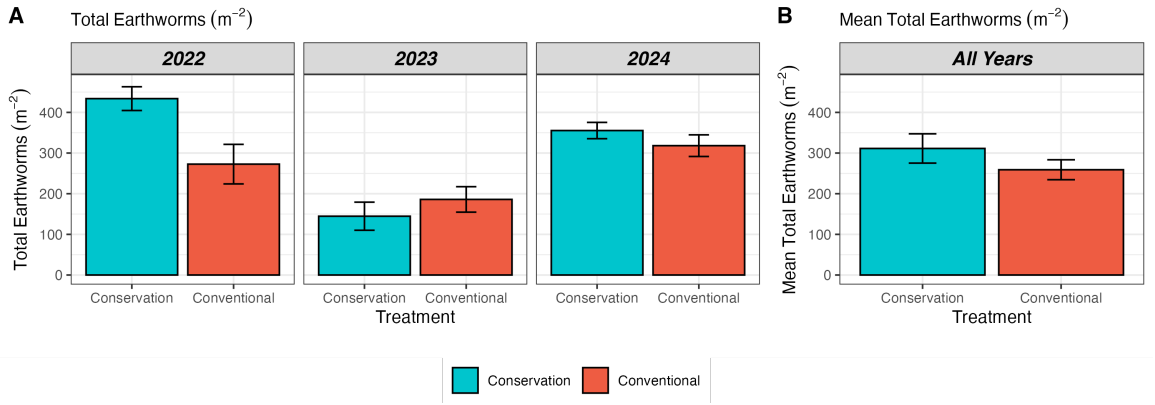

Figure 5.15: Extrapolated mean abundance of juvenile earthworms (m^{-2}) for each treatment presented by year (**A**, $n = 5$) and by treatment for the total experimental duration (**B**, $n = 3$). Error bars indicate the standard error of the mean.

5.3.5 Micro-Arthropod Abundance

5.3.5.1 Chelicerata

Analysis using a GLM identified no statistical differences in the mean abundance of the taxonomic group Chelicerata in this experiment ($\beta = 0.11$, $SE = 0.13$, $Z = 0.9$, $p = 0.36$). The extrapolated mean of abundance of Chelicerata in the CA treatment was 18184 m^{-2} in the first year of the experiment, compared to a higher extrapolated mean abundance of 21752 m^{-2} in the CON treatment. During the second year of the experiment, mean abundance was much lower in both treatments, 3080 m^{-2} in the CA treatment and 2272 m^{-2} in the CON treatment. This was similar in the final year of the experiment, where the CA treatment had a mean of 4064 m^{-2} compared to 3560 m^{-2} in the CON treatment 3560 m^{-2}. Mean abundance of Chelicerata is shown in Figure 5.16 by year (**A**) and for the duration of the experiment (**B**). Model diagnostics are presented in Figure A.23.

5.3.5.2 Crustacea

There were very low numbers of Crustacea in all years between both treatments, and as a result, no statistical analysis was possible. The only incidence of Crustacea abundance was identified in the first year of the experiment in the CA treatment (4 m^{-2}), and in the second year of the experiment in the CON treatment (72 m^{-2}). Mean abundance of Crustacea is shown in Figure 5.16 by year (**A**) and for the duration of the experiment (**B**).

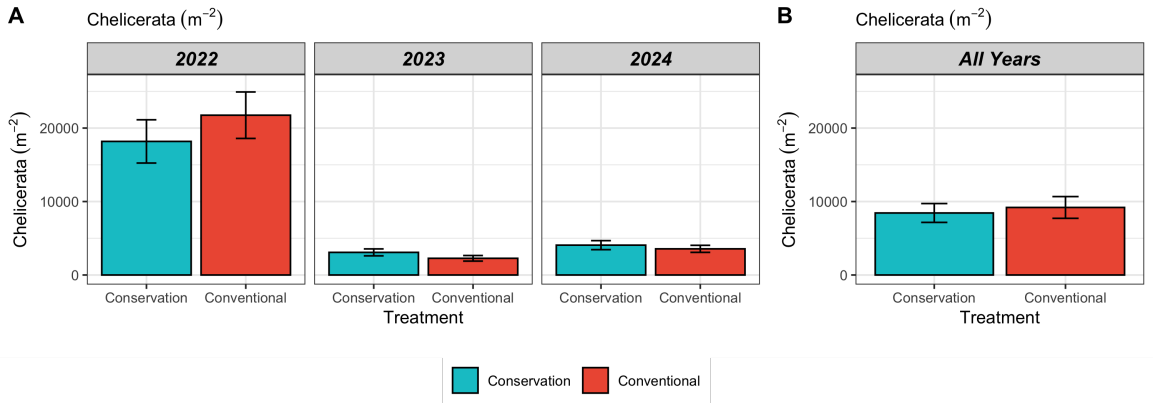

Figure 5.16: Extrapolated mean abundance of Chelicerata (m^{-2}) for each treatment presented by year (**A**, $n = 5$) and by treatment for the total experimental duration (**B**, $n = 3$). Error bars indicate the standard error of the mean.

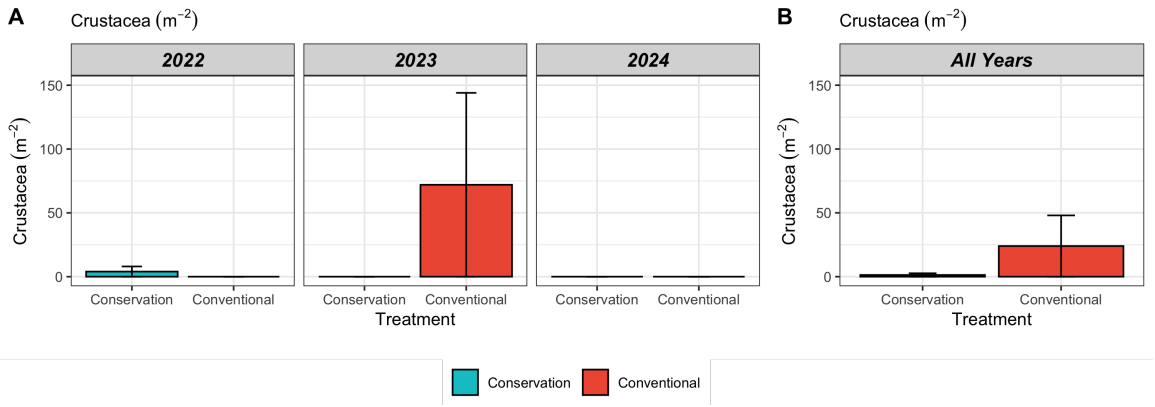

Figure 5.17: Extrapolated mean abundance of Crustacea (m^{-2}) for each treatment presented by year (**A**, $n = 5$) and by treatment for the total experimental duration (**B**, $n = 3$). Error bars indicate the standard error of the mean.

5.3.5.3 Myriapoda

Statistical analysis using a GLM identified a significant increase in Myriapoda extrapolated mean abundance in the CON treatment in comparison to the CON treatment (β = -0.51, $SE = 0.25$, Z = -2.01, $p = 0.04$). During the first year of the experiment, both treatments had similar mean abundance of 120 m^{-2} in the CA treatment, and 112 m^{-2} in the CON treatment. The second year saw a higher extrapolated mean abundance in the CON treatment of 232 m^{-2} and a reduction of abundance in the CA treatment to 92 m^{-2}. A similar trend was observed in the final year, where again, the CON treatment had a higher mean abundance of Myriapoda of 180 m^{-2} compared to 104 m^{-2} in the CA treatment. Mean abundance of Myriapoda is shown in Figure 5.18 by year (**A**) and for the duration of the experiment (**B**). Model diagnostics are

presented in Appendix A.25.

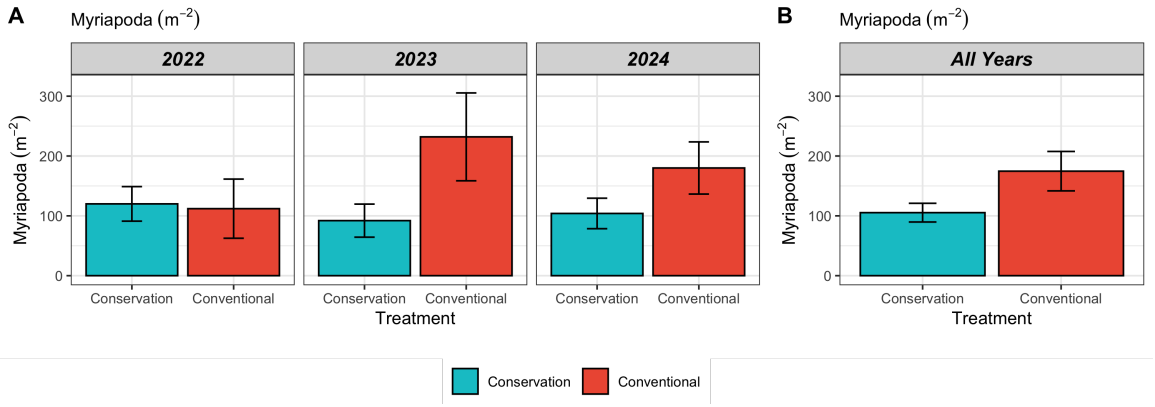

Figure 5.18: Extrapolated mean abundance of Myriapoda (m^{-2}) for each treatment presented by year (**A**, $n = 5$) and by treatment for the total experimental duration (**B**, $n = 3$). Error bars indicate the standard error of the mean.

5.3.5.4 Hexapoda

There were no statistical differences in Hexapoda mean abundance between the two treatments identified in this study ($\beta = 0.13$, $SE = 0.1$, $Z = 1.35$, $p = 0.18$). Both treatments had similar extrapolated mean abundance in the first year of experimentation (Conservation = 44836 m^{-2}, CON = 41308 m^{-2}), and in the second year of the experiment (Conservation = 6840 m^{-2}, CON = 7144 m^{-2}) where the mean abundance for both treatments declined from the first year. In the final year of the experiment, the CA treatment had a higher mean abundance (22976 m^{-2}) than the CON treatment (17264 m^{-2}). Mean abundance of Myriapoda is shown in Figure 5.19 by year (**A**) and for the duration of the experiment (**B**). Model diagnostics are presented in Appendix A.24.

Principal components analysis (PCA) was performed to assess the differences in soil micro arthropod taxonomic communities between conservation and CON agriculture treatments over three years (2022–2024). During the experiment, the proportion of the variance explained by the first two principal components gradually increases, from 60.4% in 2022, 62.4 % in 2023, and 87 % in 2024. The full breakdown of PCA dimensions and the percentage of explained is shown in the PCA scree plots in Figure A.17. In 2022 and 2023, the variance in the PCA was explained in four dimensions, and 2024, this was reduced to three dimensions. While there is substantial overlap between the treatments, indicating similarities in the community composition, there is a slight increase in differentiation between the treatments over the experimental

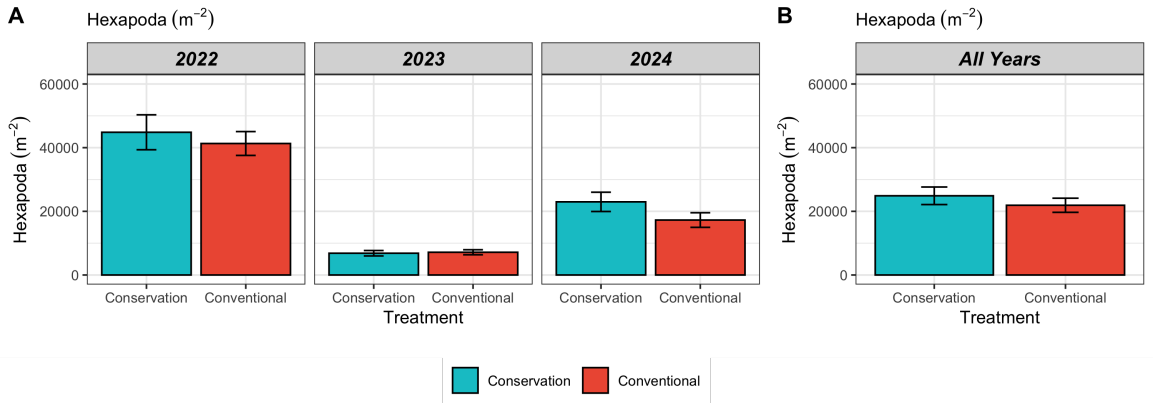

Figure 5.19: Extrapolated mean abundance of Hexapoda (m^{-2}) for each treatment presented by year (**A**, $n = 5$) and by treatment for the total experimental duration (**B**, $n = 3$). Error bars indicate the standard error of the mean.

duration. This is evidenced in the increasing variance explained by PC1 and PC2 throughout the course of the experiment. The CA treatment exhibits more variability compared to the CON treatment, as shown by the wider spread of points and the larger confidence ellipses, particularly in 2024.

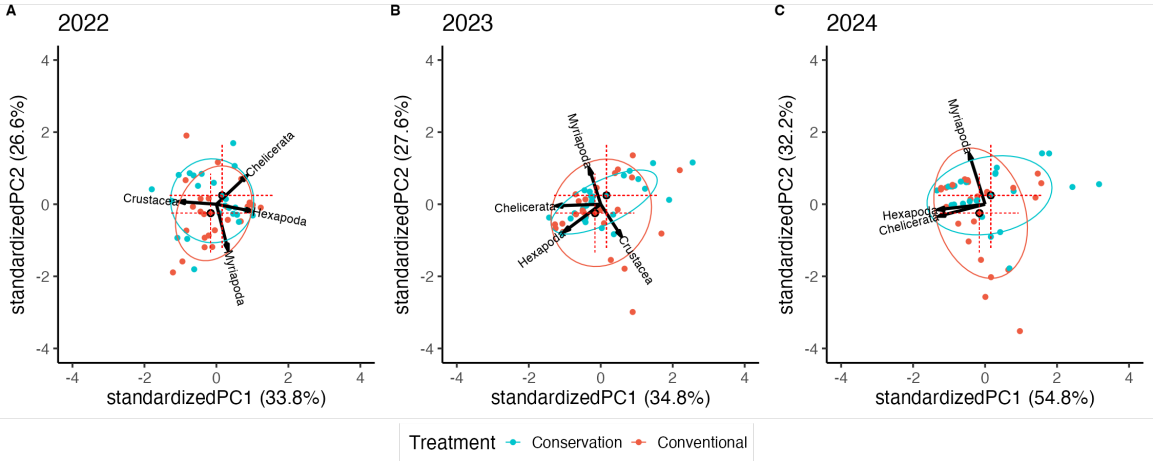

Figure 5.20: Principal Component Analysis (PCA) for soil organisms based on measures of four taxonomic groupings. Ellipses show the 95% confidence intervals for each treatment. Treatment mean eigenvalues are shown with error bars (±1 standard deviation in red). The standardised Principal Component 1 (PC1) is displayed on the x-axis, and PC2 on the y-axis. Both PC's are displayed with the proportion of the total variation in the data that is explained by each component. Analyses are shown separately for 2022 (**A**), 2023 (**B**), and 2024 (**C**).

5.3.6 Soil Biodiversity Indexes

5.3.6.1 QBS-e eco-morphological score

Statistical analysis using a quasi-Poisson Generalised Linear Model identified no significant differences in the QBS-e eco-morphological score between the experimental treatments ($\beta = 0.18$, $SE = 0.17$, $Z = 1.06$, $p = 0.29$). In the first year of the experiment, the CA treatment had a higher mean QBS-e score of 1025, compared to 460 in the CON treatment. However, during the second year of the experiment, the CON treatment had a higher mean QBS-e score of 650, and the CA treatment had a score of 561. Both treatments had higher mean QBS-e scores in the final year of the experiment, 1083 in the CA treatment and 1128 in the CON treatment. Mean QBS-e score is shown in Figure 5.21 by year (**A**) and for the duration of the experiment (**B**). Model diagnostics are presented in Appendix A.26.

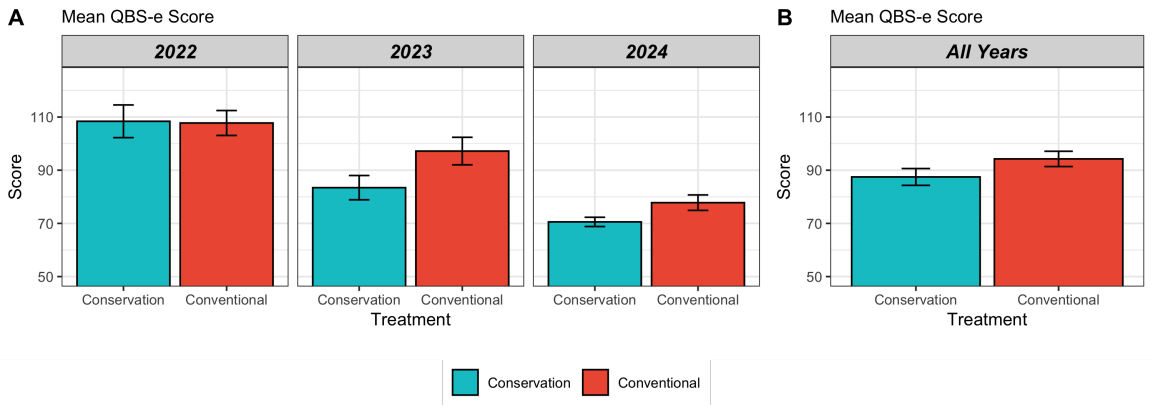

Figure 5.21: Mean QBS-e score for each treatment presented by year (**A**, $n = 5$) and by treatment for the total experimental duration (**B**, $n = 3$). Error bars indicate the standard error of the mean. **Note:** Y-axis truncated to highlight treatment differences.

5.3.6.2 QBS-ar eco-morphological score

Statistical analysis using a quasi-Poisson generalised linear model identified a marginal, but non-significant increase in the mean QBS-ar in the CON treatment compared to the CA treatment in this study (β = -0.07, SE = 0.04, Z = -1.89, p = 0.059). Both treatments had a similar mean QBS-ar score in the first year of the experiment (108); however, in the second year, the CON treatment was found to have a higher mean QBS-ar score of 97.2 compared to 83.4 in the CA treatment. This was also seen in the final year of the experiment, where the CON treatment had a higher mean of 77.8 in comparison to 70.6 in the CA treatment. Mean QBS-ar score is shown in Figure 5.22 by year (**A**) and for the duration of the experiment (**B**). Model diagnostics are presented in Appendix A.27.

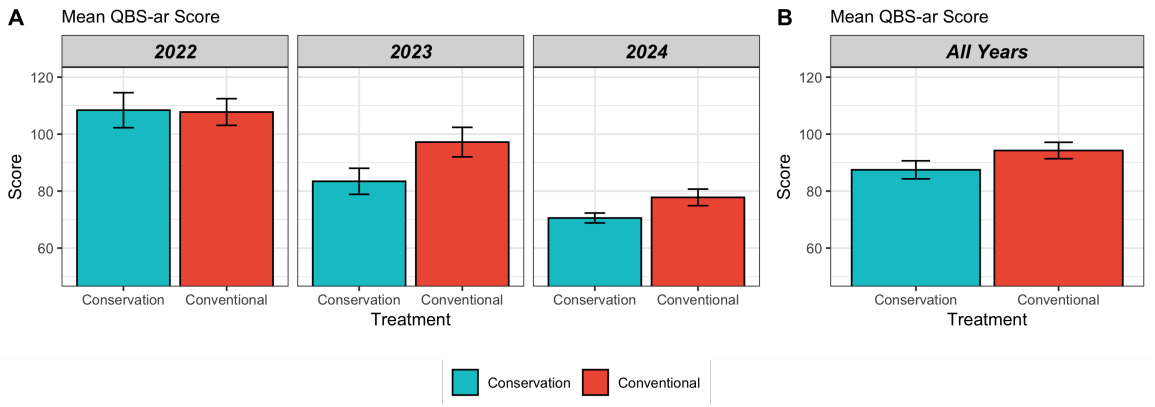

Figure 5.22: Mean total QBS-ar score for each treatment presented by year (**A**, $n = 25$) and by treatment for the total experimental duration (**B**, $n = 3$). Error bars indicate the standard error of the mean. **Note:** Y-axis truncated to highlight treatment differences.

5.3.6.3 Shannon Diversity Index

Statistical analysis using a linear mixed-effects model identified a significant increase in the mean Shannon Biodiversity Index in the CON treatment competitively to the CA treatment (β = -0.08, SE = 0.03, Z = -2.62, p = 0.01). The CON treatment was found to have a higher mean Shannon Biodiversity Index in all experimental years. During the first year of the experiment, the CA treatment had a mean of 1.21, compared to an increased mean of 1.28 in the CON treatment. During the second experimental year, both treatments had higher mean indexes of 1.4 in the CA treatment and 1.53 in the CON treatment. This trend continued in the final year of the experiment, where the CA treatment had a lower mean Shannon Biodiversity Index of 1.35, compared to 1.4 in the CON treatment. Mean Shannon Biodiversity Index scores are shown in Figure A.15 by year (**A**) and for the duration of the experiment (**B**). Model diagnostics are presented in Appendix A.28.

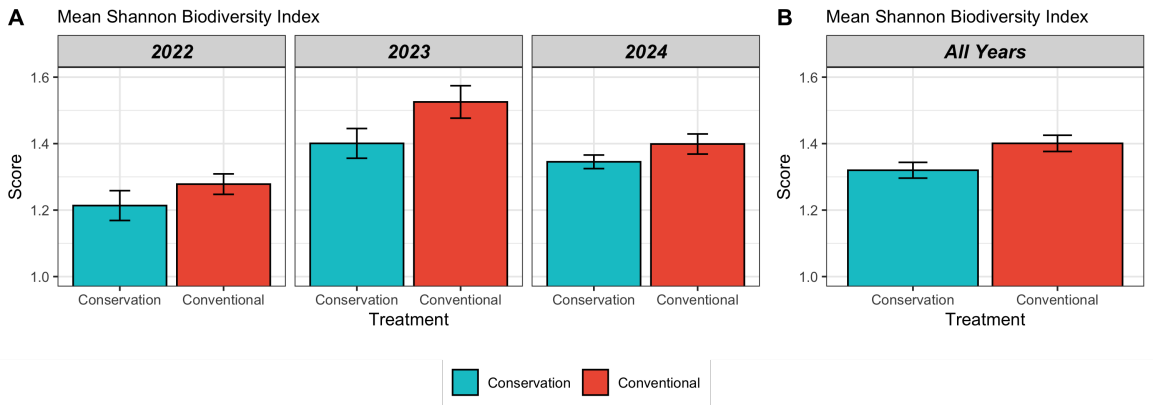

Figure 5.23: Mean Shannon Biodiversity Index for each treatment presented by year (**A**, $n = 25$) and by treatment for the total experimental duration (**B**, $n = 3$). Error bars indicate the standard error of the mean. **Note:** Y-axis truncated to highlight treatment differences.

5.4 Discussion

This chapter examined the effects of CA practices on soil health and function, with a focus on biological, chemical, and physical indicators of soil quality. The transition to CA is often promoted as a means to enhance long-term soil function and resilience, yet its outcomes can vary depending on site conditions, soil type, and management history. Through a multi-year comparison of CA and CON systems, this study assessed key soil health metrics—including organic matter content, biological activity, and physical structure—to determine whether CA delivered measurable improvements. This discussion interprets those findings in light of existing literature, evaluates the consistency of responses across indicators and years, and considers the implications for the wider adoption of CA in temperate arable systems. Limitations of the study and areas for future research are also addressed.

5.4.1 Soil Biology

This section addresses the test of the following hypothesis (H):

- H_1: CA results in significantly higher diversity and abundance of soil micro arthropods and earthworms compared to CON practices.

Intensive agriculture strongly affects the soil ecosystem diversity in many cases (Giller et al., 1997; Postma-Blaauw et al., 2010). Although this chapter mainly focuses on evaluating the effect of CA on the soil mesofauna and macrofauna, it was

shown by Postma-Blaauw et al. (2010) that the taxonomic groups with larger body size are the most negatively affected by intensive agriculture in comparison to smaller organisms. This is mainly due to the disruption of the soil structure and changes to the soil moisture and temperature associated with tillage (Kladivko, 2001). Although the negative effects of tillage are usually more pronounced in larger-bodied organisms, it is worth noting that there are usually negative impacts on total microbial biomass detected in agricultural systems which utilise more tillage (Kladivko, 2001); unfortunately, this chapter does not analyse microfauna abundance.

Although there is information available about soil biological abundance and diversity in established CA systems, there is little research on the effects of the transition to CA on soil biological communities (Christel et al., 2021). For example, Henneron et al. (2015) compared the long-term effects of CA, organic farming, and CON on major soil organisms. They found that both CA and organic systems increased the abundance and biomass of all soil organisms, except predatory nematodes. Overall, they found that CA showed a higher overall improvement than organic farming, increasing the abundance of phytophagous and rhizophagous arthropods, anecic earthworms, bacteria, and fungi. They suggest that in their study, the combination of long-term NT and cover cropping in the CA system had greater beneficial effects on soil biota in comparison to the CON and organic systems. This conclusion is widely accepted in the literature; however, the response of soil biota in CA systems is thought to vary greatly depending on the age of the system and the quality and biomass production of cover crops (Dulaurent et al., 2023).

There was no significant difference detected in individual ecotypes or total earthworm abundance in this study between the two experimental treatments. Earthworms are one of the most important soil macrofaunal groups, which play a major role in agricultural ecosystems. Previous research has shown that the principles of CA are generally beneficial to earthworm abundance in agricultural ecosystems (Baldivieso-Freitas et al., 2018; Soane et al., 2012; Pelosi et al., 2009). The study by Pelosi et al. (2009) found that Anecic and Epigeic earthworm abundance was 3.2 - 7.2 times higher in a CA system compared to CON and organic systems, respectively. This was also the case for total Anecic and Epigeic earthworm biomass, which were 3.4 - 12.5 times higher in the CA system. However, they also found that Endogeic earthworms were significantly less numerous in some years of the study in the CA system compared to the CON and organic treatments. Endogeic species are thought to be more favoured in agricultural systems which utilise tillage, as this results in the incorporation of organic matter throughout the top soil (Baldivieso-Freitas et al., 2018; Pelosi et al.,

2009). The abundance of earthworms in previous research studies is highly variable depending on the year and timing of sampling (Pelosi et al., 2009). However, in this study, earthworm samples were taken on progressively later dates each year due to logistical constraints, and the sampling did not have a high quantity of replicates ($n = 5$); therefore, it could also be concluded that this study did not have the statistical power to identify treatment differences. Future research could perform sampling several times per year, and over a longer duration, to identify treatment effects.

Statistical analysis of soil micro-arthropod taxonomic groups found no significant differences in the abundance of Chelicerata or Hexapoda groups in this study. An abundance of micro-arthropods from the Crustacea taxonomic group was not possible to statistically analyse due to low abundance throughout the experiment. However, statistical analysis identified a significant increase in Myriapoda mean abundance in the CON treatment in comparison to the CA treatment. The Myriapoda taxonomic group includes Pauropoda and Symphyla; it is considered to be one of the least abundant groups of soil arthropods, and is considered to have been poorly studied regarding the research on other soil micro-arthropod taxonomic groups (Bedano et al., 2006). Typically, Symphylans and Pauropods are characteristic of undisturbed habitats, mainly grassland, where the soil is high in organic matter and has high porosity (Curry and Momen, 1988; Davis and Sutton, 1978; Bedano et al., 2006). Pauropoda are highly susceptible to desiccation from extreme temperatures and are considered to be a group of soil animals most susceptible to harm from agrochemicals (Lagerlöf and Scheller, 1989). Therefore, it could be hypothesised that Pauropoda would be more likely to be more abundant in CA than in CON systems. However, in this study, the inverse was identified, with a significant increase in Myriapoda in the CON treatment. As Bedano et al. (2006) states, the effect of tillage systems on Symphylan and Pauropod populations has not been investigated thoroughly; therefore, there is little literature on the subject. In their study on soil micro-arthropod abundance in different tillage systems, Bedano et al. (2006) found that CON management decreased the abundance of Pauropoda; however, it increased the abundance of Symphyla. More analysis of individual micro-arthropods is required in this study to identify which class within the subphylum Myriapoda is the key driver of the significant increase in total Myriapoda abundance.

Although the PCA found substantial overlap in soil biota diversity and abundance between the two treatments. There was found to be an increased explanation of the variance in the first principal component from 10.1% in 2022 to 16.3% in 2024. This would indicate that the differences in soil micro-fauna community structure

are becoming more pronounced between the treatments. However, this is still a low percentage of the total variance explained by the treatments; therefore, we can hypothesise that although CON and CA create contrasting soil physical environments, soil fauna may take longer to adapt to those changing conditions during the transition to CA.

When statistical analysis of the soil biodiversity indices was undertaken, there were found to be no statistical differences in QBS-e scores were found between the two experimental treatments. However, there was found to be weak, non-significant ($p = 0.059$) evidence of an increase in the QBS-ar index in the CON treatment in comparison to the CA treatment. QBS-e was hypothesised to be an EMI where statistically significant differences were likely, as larger biota are more affected by tillage systems in comparison to smaller biota (Postma-Blaauw et al., 2010; Dulaurent et al., 2023). However, this was not found to be the case in this study, where there was a significantly higher Shannon biodiversity index in the CON treatment. This result suggests that the presence of a lack of tillage is not the only factor which is a strong driver of soil biodiversity, for example, in this case, both treatments utilised different pesticide and fertiliser programmes throughout the experiment, which could have a strong influence on soil biodiversity and abundance (Lehman et al., 2015b). However, as previously mentioned, low numbers of replicates in the earthworm sampling in comparison to the soil micro-arthropod sampling could be influencing the statistical power of the study and therefore increasing the likelihood of a Type II error. Increasing the sample size and including other covariates, such as soil moisture and temperature, may be appropriate methodologies to improve the ability to detect significant treatment effects across years in this study.

Hypothesis H_1 was not supported by the results. No significant differences were detected between CA and CON in the overall abundance or diversity of soil micro-arthropods or earthworms. While literature typically reports increased abundance of larger soil fauna under CA, particularly in long-term systems, this study found no significant treatment effect, possibly due to low replication, short study duration, and inter-annual variability. Notably, the abundance of Myriapoda was unexpectedly higher in the CON treatment, contradicting expectations based on their typical habitat preferences. In addition, the biodiversity indices QBS-e and QBS-ar showed no consistent pattern in favour of CA; QBS-ar and Shannon index values were significantly higher under CON. These results suggest that soil biotic responses to CA may require longer timeframes to become evident and may also be influenced by other management factors such as pesticide and fertiliser use.

5.4.2 Soil Chemistry

This section addresses the test of the following hypothesis (H):

- H_2: CA increases soil total carbon content over time compared to CON.

There was weak evidence (β = -0.04, SE = 0.02, Z = -2.33, p = 0.051) for an increase in soil total C was identified in the CA treatment in this study in comparison to the CON treatment; however, there was no significant increase identified from the baseline samples. Both treatments were found to have slightly lower total C than the baseline in this study. Therefore, the significant effect of the experimental treatment should be presented with caution, as this study does not show evidence of C sequestration in CA; rather, it shows a significant difference in the rate of C loss from the soil in each treatment. A slower rate of C decomposition would be hypothesised in CA, as tillage is shown to rapidly accelerate the process of C loss due to the breaking of soil aggregates, which exposes soil organic matter to microbial decay (Hendrix et al., 1986; Beare et al., 1994).

This study identified significant increases in available P, K, Mg, and total N in the CA treatment compared to CON. As previously discussed in the introduction to this chapter, common changes to the soil's physical and biological properties under CA typically result in significant differences in nutrient availability in comparison to conventionally managed cropping systems. This is commonly reported in the previous literature in regards to N, where the total N can increase due to reduced rates of N decomposition and reductions in N leaching (Shelton et al., 2017; Soane et al., 2012). However, plant available N is commonly not found to increase as rapidly as total N during the transition to CA, again, which is due to slower rates of N mineralisation and great C inputs to the system (Page et al., 2020). As this study does not test for N availability, no conclusions can be made about the crop productivity potential of the systems, as it could be possible that the CA treatment has significantly higher total N but lower plant-available N. However, it could be hypothesised that during the years following the adoption of CA, the abundance of soil microorganisms will have significantly increased, improving the rate of N mineralisation, resulting in the reduction of N fertiliser requirements (Dordas, 2015; Wang et al., 2006; Soane et al., 2012). This study could have been improved by studying the availability of N throughout the experiment to identify if the significant rise in total N in the CA treatment could result in agronomic benefit.

This study also observed a marginal, but non-significant increase in soil total C content, which can affect plant nutrient availability due to both changes to the quantity of nutrients available and their distribution in the soil profile (Page et al., 2020). Although this trend approached statistical significance ($p = 0.051$), neither treatment showed a significant change from the baseline value when considered independently. These findings suggest a potential benefit of CA practices for SOC improvements, yet these results are inconclusive and require a larger dataset to draw conclusions. It remains unclear if these early trends reflect long-term SOC trends or short-term fluctuations.

This study identified a significant overall decline in soil pH under the CA treatment compared to the CON treatment over the three-year experimental period. While both treatments exhibited a gradual acidification trend from 2022 to 2024, the decline was more pronounced in the CA plots. Despite this trend, statistical comparisons to the baseline pH revealed no significant change within either treatment across the study period. The consistently lower pH observed in the CA treatment may reflect cumulative impacts of changes in nutrient cycling due to residue retention or NT. This is commonly observed in previous literature, as increased SOC at the surface of the profile in CA systems is commonly associated with greater acidity relative to CON systems due to the accumulation of plant residues and organic acids at the soil surface (Page et al., 2020; Limousin and Tessier, 2007; Sithole and Magwaza, 2019). Although these pH shifts were not statistically significant relative to baseline, the overall pattern requires further monitoring, particularly as continued acidification under CA could influence nutrient availability and microbial activity over time (Goulding, 2016).

Hypothesis H_2 was only partially supported by the results. Although a marginal, but non-significant increase in total soil C was observed in the CA treatment relative to the CON treatment, neither treatment showed an increase compared to baseline levels. Instead, both treatments exhibited slight declines in total C over the study period. This suggests that while CA may slow the rate of soil C loss, possibly due to reduced soil disturbance and slower organic matter decomposition, it does not lead to measurable soil C sequestration within the time frame of this study. These findings align with existing literature, which reports that increases in soil organic C under CA typically require longer periods to become evident. Caution should therefore be exercised in interpreting the treatment effect as evidence of C accumulation.

5.4.3 Soil Physics

This section addresses the test of the following hypothesis (H):

- H_3: Soil bulk density and compaction are lower under CA due to reduced mechanical disturbance.

Both treatments in this study resulted in an increased soil dry bulk density in comparison to the baseline data. This was attributed to higher than average rainfall throughout the experimental duration, where in this three-year study, there have been multiple incidences of higher than average rainfall, particularly in 2023 and 2024, where some parts of the UK received more than a third more rainfall than the historic average (Met Office, 2025). Raindrop impact is considered a main factor increasing topsoil bulk density, as the raindrops detach particles and soil aggregates, modifying the soil surface structure, thus causing compaction (Todisco et al., 2022). The CA treatment was found to have significantly increased the soil bulk density in comparison to the CON treatment. This result is in line with previous literature, where the bulk density in CA has risen in the early years of the transition to the system (Soane et al., 2012).

Hypothesis H_3 was not supported by the results. Contrary to expectations, soil bulk density was significantly higher under CA compared to CON. This outcome is attributed in part to above-average rainfall during the study period, which likely contributed to surface compaction through raindrop impact. The findings are consistent with previous studies reporting increased bulk density during the early years of transition to CA.

5.5 Conclusion

This chapter evaluated the effects of CA compared to CON for soil biology, soil chemistry, and soil physics. The hypotheses tested were partially or not supported by the data, highlighting the complexity of soil system responses and the challenges associated with detecting meaningful treatment effects within short-term experimental timescales.

In terms of soil biology, the results did not support the hypothesis that CA increases the diversity and abundance of soil fauna. No significant differences were observed in total earthworm or soil micro-arthropod abundance between treatments. Contrary to expectations, Myriapoda abundance and the Shannon index were significantly higher under CON. These findings suggest that short-term transitions to CA may not produce immediate benefits for soil biological communities, and that other management practices such as pesticide and fertiliser regimes may confound

treatment effects. Low replication and limited temporal sampling may have resulted in treatment impacts not being detected.

Regarding soil chemistry, only partial support was found for the hypothesis that CA increases SOC. While there was weak non-significant evidence of total C increases in the CA treatment compared to the CON treatment, neither treatment showed gains relative to baseline levels, suggesting a slower rate of C loss under CA rather than active sequestration. Notably, the CA treatment exhibited significantly higher concentrations of total N, P, K, and Mg, aligning with expectations based on reduced nutrient leaching and increased organic matter inputs. However, without corresponding data on plant-available N or microbial activity, it is difficult to infer agronomic benefit or nutrient cycling efficiency.

In terms of soil physics, the hypothesis that CA reduces soil compaction was not supported. Soil bulk density increased in both treatments over time, but was significantly higher under CA. This is consistent with literature on the early stages of CA transition, and was likely exacerbated by above-average rainfall during the study period, which can increase surface compaction through raindrop impact. These findings emphasise that improved soil structure under CA may only emerge over longer timescales and under stable climatic conditions.

Overall, this study suggests that while CA holds promise for improving soil properties and ecosystem functioning, the benefits may take longer to materialise and are influenced by multiple interacting factors, including climate variability and management intensity. Future research should prioritise longer-term monitoring with increased replication, finer temporal resolution, and integrated measurements of biological, chemical, and physical soil parameters.

Chapter 6

Agronomy and Crop Productivity Under Conservation Agriculture

6.1 Introduction

The major challenge of feeding a growing global population, with an increasing dietary preference for resource-intensive food, is a significant consideration for the future and prosperity of humanity (Foley et al., 2011; Pittelkow et al., 2015). The evaluation of agricultural cropping systems needs to consider environmental effects to reduce future environmental impacts, as well as agricultural output, to produce enough food to feed a growing population. There is evidence to suggest that Conservation Agriculture (CA) may be successfully implemented in a variety of contexts with no or only minor reductions in yield (Pittelkow et al., 2015; Kassam et al., 2022), thereby potentially achieving the aim of maintaining food security while reducing environmental impacts.

The adherence to the three principles of CA is not the only factor which dictates the success of the system; productivity and sustainability are also dependent on several tailored agronomic management strategies that optimise system performance. The transition from CON to CA usually requires different management strategies to be implemented for control of weeds, pests, and diseases, as well as overall crop nutrition strategy (Derrouch et al., 2020; Kassam et al., 2022; Farooq and Siddique, 2015; Page et al., 2020). This chapter aims to evaluate the key differences in the agronomic approach to management of a CA system in the UK, and analyse the key differences in crop growth and productivity.

6.1.1 Crop Management

One of the key changes with the agronomic management of CA systems is weed management. This is due to the absence of tillage, which means that typically there are

changes to weed expression, including seed bank status, distribution, dispersal mechanisms, diversification, growing patterns and competition trends within CA systems (Bajwa, 2014). CON systems can use rotational ploughing to bury weed seeds to a depth that restricts germination, so tillage can create a "stale seed bed". This is a technique where surface cultivation is used to encourage germination of weeds before crop drilling, which can be sprayed off with a non-selective herbicide (Riemens et al., 2007). Typically, any system which utilises no-tillage (NT) will exhibit a distinct weed ecology and weed management in comparison to CON systems (Bajwa, 2014; Triplett and Dick, 2008). Previously agronomically unimportant and non-dominant weeds in a CON system can become more problematic and dominant in NT systems; their germination and dormancy characteristics are different when there is no mechanical inversion of the soil (Soane et al., 2012). In general, populations of dicotyledonous weeds in NT systems are similar to tillage-based systems, or in some cases, reduced. This is because many dicotyledonous agricultural weeds produce seeds with a long dormancy period, resulting in improved adaptation to inversion tillage-based systems, where repeated ploughing can result in them being brought back to depths where they can germinate (Morris et al., 2010). However, grass weed populations are usually greatly increased in NT systems (Soane et al., 2012; Morris et al., 2010). In colder climates, perennial grass weeds can exert significant pressure, whereas in warmer climates, which prevent or reduce perennial grass growth, problems can occur from annual grass weeds (Soane et al., 2012; Morris et al., 2010).

Another factor that influences the weed burden in CA systems is the surface crop residue. Crop residues have been shown to suppress the emergence of some weed species (Nikolić et al., 2021; Morris et al., 2010). However, crop residues have been shown to reduce herbicide efficacy (Flower et al., 2021; Bajwa, 2014), with negative effects on weed control. Both these factors need to be considered by farmers and agronomists when managing weeds in a CA system as the magnitude of these effects is dependent on the quantity (Nikolić et al., 2021), type (Flower et al., 2021), and spread uniformity of the crop residue (Flower et al., 2022), as well as the weed population and species present in the system (Morris et al., 2010).

The combination of surface crop residues and CA systems can also cause issues with crop establishment due to pest damage (Richard et al., 1995; Earl and Spoor, 1994). Slugs are a significant problem, as they thrive in the low-disturbance, residue-rich environments characteristic of no-till fields (Morris et al., 2010; Douglas and Tooker, 2012). Slugs can be a significant pest of many field crops, reducing crop establishment by a sizeable degree. Many CA farmers use multiple applications of

molluscicides, which are effective at reducing slug populations. However, these applications can cause water course pollution, dependent on the active ingredient of the molluscicide (Douglas and Tooker, 2012). Soil managed with CA can also contain improved habitats for natural enemy populations for slugs such as Carabid Beetles (Howlett, 2012). Therefore, this approach has the potential to improve the contribution of predators to improve slug control in comparison to CON systems (Douglas and Tooker, 2012).

6.1.2 Pesticide usage

Commercial, large-scale CA relies on the availability of herbicides suitable for control of a wide range of dicotyledonous and monocotyledonous weed species (Soane et al., 2012). As previously discussed in Section 2.5, the introduction of the broad-spectrum herbicide Paraquat and, more recently, Glyphosate in 1971, made weed management in NT systems easier. Currently, many commercial CA systems utilise a combination of broad-spectrum herbicides and selective herbicides during crop growth to manage weeds before and during the growing season (Soane et al., 2012). As such, a significant threat to the success of CA adoption is the concern of increasing weed resistance to herbicide groups (Soane et al., 2012; Morris et al., 2010; Hull et al., 2014). Herbicide resistance has been identified in several species of grass weeds across multiple countries. *Alopecurus myosuroides* (black-grass) is the major herbicide-resistant weed problem and is estimated to occur on virtually all of the 20,000+ farms in 35 countries where herbicides are applied regularly, including in the UK (Hull et al., 2014). In addition, herbicide resistance has been detected in wild oats (*Avena fatua*), and Italian ryegrass (*Lolium perenne L.*) to commonly used herbicides atrazine, simazine and glyphosate for numerous weed species on no-till farms in the USA (Triplett and Dick, 2008). This has led to speculation that CA may not be an appropriate course of action for long-term agricultural weed management (Morris et al., 2010).

Widespread dependence on regular applications of herbicides in CA has raised concern regarding the fate of applied herbicides and the environmental consequences (Soane et al., 2012). There are mixed reports on the application rates of herbicides in CA systems, with some literature reporting that herbicide application rates are similar for CA and CON systems (Bajwa, 2014), some report significantly higher herbicide usage in CA (Zentner et al., 1991), and other reporting significantly higher usage of pre-emergence herbicides in CA, with no significant differences in post-emergence usage (Dong et al., 2024; Morris et al., 2010; FAO, 2001). Whereas, some studies suggest that although initial usage of herbicides is increased in CA, this declines over

time to a level equal to that of CON systems (FAO, 2001). There is concern that some herbicides that are primarily used in CA have substantial persistence in soil that has the potential to cause harm to microorganisms in the rhizosphere, as well as contamination of groundwater (Bajwa, 2014).

6.1.3 Research Aims and Hypotheses

This chapter aims to investigate the main effects of the transition to CA on crop establishment, growth, and yield, and assess pesticide usage and risk in CA agronomic management using the systems-level experimental site, detailed in Chapter 3.

The research aims (*A*) of this chapter are:

- A_1: Monitor variability of crop responses during the transition to CA in comparison to CON.
- A_2: Monitor variability of crop inputs during the transition to CA in comparison to CON.

This chapter tests the following hypotheses (*H*):

- H_1: CA will result in a significant reduction in crop establishment compared to CON.
- H_2: CA will result in significant alterations to the total quantity of pesticide and fertiliser used compared to CON.
- H_3: CA will result in a significantly lower yield than the CON treatment.
- H_4: CA agronomy will result in a reduced risk to the environment and human health compared to CON.

6.2 Materials and Methods

The experimental site location, experimental design, and management are detailed in Chapter 3. This section details the monitoring methodology for crop establishment and productivity and the analysis methodology for the crop input data.

6.2.1 Crop application analysis

The total pesticide (active ingredient kg ha^{-1} $year^{-1}$) and fertiliser (chemical element kg ha^{-1} $year^{-1}$) data were assessed for normality and homogeneity of variances using the methodology outlined in Section 3.10. Data distributions are presented in Appendix B.3. All data were non-normally distributed; therefore, a generalised linear mixed effects model with a Gamma link log function was used to analyse the effects of the experimental treatments (Ng and Cribbie, 2017), using the experimental year as random model effects following the methodology outlined in Section 3.10. The crop was removed as a random effect in the model as issues with model singularity were identified. Model diagnostics are presented in Appendix B.4. The model was implemented using the package `lme4` in `R` (Bates et al., 2015; R Core Team, 2023).

6.2.2 Crop Establishment and Biomass

Crop establishment was assessed by counting plants using a 33 cm^2 quadrat in the first year of the experiment, which was then subsequently changed to a 1 m^2 quadrat for the remaining experimental years. During crop senescence, crop biomass was assessed using the methodology of Franks and Goings (1997). All crop vegetation was cut to the soil surface, bagged, and transported to the laboratory. All non-crop biomass was then removed from the sample, and the total fresh mass of crop biomass was weighed using an analytical balance. The fresh samples were then dried at 60 °C for 24 hours, and re-weighed to determine the moisture content of the biomass and the crop dry-matter biomass per the sampled area. The crop samples per the sampled area were then extrapolated to kg/biomass ha^{-1} using the following equation (6.1):

$$Biomass \text{ ha}^{-1} = Biomass \text{ m}^{-2} \times 10,000 \tag{6.1}$$

Where applicable, yield components (tillers, shoots, ears, pods *etc.*) were quantified for each sample. They were then processed using a HALDRUP LT-21 laboratory thresher (HALDRUP, 2024) to separate the straw and grain. Once the grain yield per sample had been analysed, the harvest index was calculated using the following equation (6.2):

$$\text{Harvest Index} = \frac{\text{Harvestable Biomass}}{\text{Total Biomass}} \tag{6.2}$$

All crop establishment variables were evaluated for distribution normality and homogeneity of variances using the methodology outlined in Section 3.10. The results of this evaluation are shown in Appendix B. The majority of the crop establishment data was not normally distributed. Therefore, all variables were analysed using a generalised linear mixed effects model following the methodology outlined in Section 3.10, and plotted using the `ggplot2` package (Wickham, 2016). Treatment was included as a fixed effect, with the experimental block, crop, and year all included as random effects. Most data was positively skewed. Therefore, a Gamma log link was applied as the model family to account for this (Ng and Cribbie, 2017).

To assess the performance of the treatments with national averages, the percentage of target plant populations achieved for each crop in the UK was quantified. The target plant populations used in this analysis were;

- 50 plants m^{-1} for spring beans (PGRO, 2024),
- 260 plants m^{-1} for winter wheat (Sylvester-Bradley et al., 2015).
- 30 plants m^{-1} for oilseed rape (Berry et al., 2015).
- 305 plants m^{-1} for spring barley (AHDB Cereals & Oilseeds, 2018).

6.2.3 Normalised Difference Vegetation Index

Ortho-rectified, surface reflectance-corrected raster imagery for the experimental site was sourced from Planet Labs PBC (Planet Labs PBC, 2024) services throughout the experiment. The data had a 3 m resolution and contained four spectral bands (Blue: 455–515 nm, Green: 500–590 nm, Red: 590–670 nm, Near-Infrared (NIR): 780–860 nm). Each image was trimmed to the extent of each experimental plot using the `sf R` package (Pebesma et al., 2024), and the Normalised Difference Vegetation Index (NDVI) was calculated using the following equation, and plotted using `ggplot2`:

$$\text{NDVI} = \frac{NIR - Red}{NIR + Red} \tag{6.3}$$

Where *NIR* represents the reflectance of near-infrared light, and *Red* represents the reflectance of red light. This equation produced the NDVI values for each pixel of the dataset between -1 and 1. Low values in this index range suggest sparse crop cover, and conversely, high values indicate dense, healthy crops.

To reduce short-term fluctuations in NDVI values caused by variations in image quality and atmospheric conditions, a moving average smoothing technique was applied. The 5-point centred moving average was computed separately for each treatment group to highlight temporal trends while retaining meaningful seasonal variations. NDVI data were grouped by treatment and arranged chronologically. A moving average was calculated using the `rollmean()` function from the `zoo` package in `R` (Zeileis, A and Grothendieck, G, 2005) using the following equation:

$$\text{NDVI}_{\text{smoothed},i} = \frac{1}{k} \sum_{j=i-\frac{k-1}{2}}^{i+\frac{k-1}{2}} \text{NDVI}_j \tag{6.4}$$

where $k = 5$ is the window size, and i represents each time point. The function was applied with `align = "center"` to ensure that the smoothed value at each time point incorporated data from both preceding and following observations, minimising phase shifts. For dates at the beginning and end of the dataset where fewer than five observations were available within the window, missing values (`NA`) were assigned to maintain data integrity. To indicate variability, the standard error (SE) was also smoothed using the same 5-point moving average using the following equation:

$$\text{SE}_{\text{smoothed},i} = \frac{1}{k} \sum_{j=i-\frac{k-1}{2}}^{i+\frac{k-1}{2}} \text{SE}_j \tag{6.5}$$

This ensured that the error ribbon in the visualisation reflected a representative measure of uncertainty while preventing artificially inflated variability in sparsely sampled periods.

Smoothed NDVI values were plotted over time with the original raw data points overlaid for reference. A ribbon representing the smoothed standard error was included to illustrate variability in NDVI estimates across sampling dates. Data was tested for normality and homogeneity of variances using the methodology in Section 3.10. The data had a non-normal distribution. Therefore, a generalised linear mixed effect model was implemented using the mean NDVI as the response variable and the experimental treatment as a fixed effect using the `lme4` package in `R` (Bates et al., 2015) with no transformations applied before modelling.

6.2.4 Crop Yield

To calculate the quantity of yield sampling points required in this experiment, the effect sizes (Cohen's d) were taken from the 6000 paired yield observations from

the global meta-analysis from Pittelkow et al. (2015) and the power was plotted as a function of effect size and observation number. Effect size and Cohen's d were calculated following the methodology outlined in Section 3.

The mechanical harvest of the crops was done using a CLAAS Lexion 750 combine harvester with a CLAAS V900 header (9.14 m). Data was recorded using a weigh bridge to assess the mass of grain harvested from individual experimental units, taking into account the total mass of the tractor and trailer combination by weighing with a full load and then subsequently weighing when the trailer had been tipped. Data normality was assessed as per the methodology detailed in Section 3.10.

In addition to the mechanical harvest, hand harvesting was done using a 1 m^2 quadrat to assess spatial yield variation throughout the site for each treatment. Sampling points were generated using the methodology outlined in chapter 3, with 150 sampling points used in the first cropping year ($n = 75$). This was then reduced to 100 samples ($n = 50$) in subsequent years, due to time constraints. Grain and straw samples were cut approximately 5 cm from the soil surface, bagged, and transported to the laboratory. They were then processed using a HALDRUP LT-21 laboratory thresher (HALDRUP, 2024) to separate the straw and grain. Grain samples were individually weighed to assess crop yield m^{-1} and analysed using a DICKEY-john GAC™ 2700-UGMA (DICKEY-john, 2024) to quantify the moisture content and specific weight of the individual samples. If required, the samples were dried to the recommended moisture contents for storage (AHDB, 2023a).

The crop yield data were tested for normality and homogeneity of variances using the methodology in Section 3.10. The data had a normal distribution, which is detailed in Appendix B.3. Therefore, it was statistically assessed using Gaussian family linear mixed effects models as per the method in Section 3.10. To assess the performance of each treatment with national averages, the percentage achieved of the UK average yield was assessed by using national average crop yield data from 2017 to 2020, obtained from the AHDB (AHDB Cereals & Oilseeds, 2021).

To statistically assess crop yield t ha^{-1} and the percentage achieved compared to the UK average yield for each treatment during the experiment, Gaussian family linear mixed effects models were used, following the methodology outlined in Section 3.10. The treatment was included as a fixed effect, with the experimental block, crop, and year all included in the model as random effects.

To estimate spatially distributed crop yield at unsampled locations, the spatial correlation between the individual hand-harvest yield samples was modelled using variograms. This was done to quantify the semi-variance against the distance between

data points. The models fitted to the variogram were automatically generated using the `automap` package in `R` (Hiemstra et al., 2009). All crop yields were modelled using automatically fitted semi-variogram models with varying values for the nugget, sill, and range. The semi-variograms were then used to perform Ordinary Kriging using `automap` and `gstat` (Pebesma, 2004), and plotted using `ggplot2` (Wickham, 2016). The statistics from the interpolated models are detailed in Appendix B.15. The interpolated datasets for each treatment's crop yield were used to calculate the predicted yield for each treatment throughout the experimental site. These treatment yield datasets were then subtracted from each other to produce spatial yield difference maps to assess spatial yield variation between the experimental treatments.

6.2.5 Pesticide Risk Assessment

To assess the environmental and health risks of the agronomic approaches to the experimental treatments in this study, the chemical identity, physicochemical, human health and ecotoxicological data for all pesticide active ingredients was acquired from the Pesticide Properties Database (PPDB) (Lewis et al., 2016). A custom `R`-based web scraper was developed to extract data for specific pesticide active ingredients from the PPDB. The web scraper was implemented using the `rvest` package in `R`, which facilitates parsing and extracting data from HTML content. For each active ingredient, the scraper accessed the corresponding pesticide report page on the PPDB and extracted the pesticide properties of interest for analysis (e.g degradation half-life in soil (DT_{50}), acute toxicity (LD_{50}), and pesticide physicochemical properties). The web scraper was executed for all active ingredients used in the experiment. Extracted data were validated by comparing a subset of results with manual extractions from the PPDB. This process ensured the accuracy and reliability of the acquired data, which were subsequently used for calculating pesticide risk assessment indexes.

6.2.5.1 Danish Pesticide Load Indicator

To evaluate the environmental impact of pesticide applications in this study, the Danish Pesticide Load Index (PLI) was used (Kudsk et al., 2018; Lewis et al., 2021). The PLI outlined by Kudsk et al. (2018) is a composite indicator designed to assess the potential environmental and human health risks associated with pesticide applications. The index comprises three sub-indicators: Human Health Load, Environmental Fate Load, and Ecotoxicology Load. These sub-indicators are calculated separately and

summed to obtain the total PLI score. In this study, the approach used here incorporates the application rate to account for potential exposure risks between the experimental treatments.

Human Health Load

The Human Health Load evaluates operator exposure risk based on hazard classifications (H-phrases), as per EU Classification, Labelling and Packaging (CLP) Regulation No. 1907/2006 (European Commission, 2008). The human health indicator focuses largely on operator exposure and is determined by assigning a score between 10 and 100 for the risk phrases for each pesticide active substance. Each H-phrase score was assigned as follows:

- 10 points = Low hazard (e.g., skin irritant, H302)
- 50 points = Moderate hazard (e.g., toxic if inhaled, H331)
- 100 points = High hazard (e.g., fatal if swallowed, H300; carcinogenic, H350)

The Human Health PLI sub-indicator was calculated as follows:

$$PLI_{HH} = \frac{\sum \text{H-phrase scores}}{300} \tag{6.6}$$

Where:

- PLI_{HH} is the Human Health PLI sub indicator.
- $\sum$ H-phrase scores is the sum of the H-phrase scores
- The total score is converted to pesticide load points by dividing the score by 300. The value 300 was used to ensure that the contribution of PLHH to the overall PL was close to 1/3 in the reference year, following the methodology of (Kudsk et al., 2018).

Environmental Fate Load

The Environmental Fate sub-indicator (PLI_{FATE}) assesses pesticide persistence and mobility using three key parameters: the soil degradation half-life (days) (DT_{50}), the SCI-GROW index (which is an indicator of mobility and leaching risk (USEPA, 2016)), and bioaccumulation using the bio-concentration factor (USEPA, 2015). Each factor is normalised by dividing it by a respective reference value for each pesticide.

In this study, the UK reference pesticides were acquired from Lewis et al. (2021) and the PL_{FATE} was calculated as follows:

$$PLI_{FATE} = \frac{DT_{50}}{DT_{50}^{ref}} + \frac{\text{SCI-GROW}}{\text{SCI-GROW}^{ref}} + \frac{\text{BCF}}{\text{BCF}^{ref}} \tag{6.7}$$

Where:

- PLI_{FATE} is the Environmental Fate Load.
- DT_{50} is the soil degradation half-life (in days).
- SCI-GROW is the indicator of mobility and leaching risk.
- BCF is the bio-concentration factor.
- DT_{50}^{ref}, SCI-GROW^{ref}, and BCF^{ref} are the reference values used for normalization.

Ecotoxicology Load

The Ecotoxicology Load quantifies pesticide toxicity to non-target organisms. It is calculated using the $LC/LD/EC_{50}$ values for mammals, birds, fish, daphnia, algae, aquatic plants, earthworms and bees following the methodology of Kudsk et al. (2018). The calculation of the Ecotoxicology Load is calculated in a similar way to the PLI_{FATE}; however, instead of the maximum values, the lowest values are used (i.e. greatest toxicity), and an inverse relationship is used to devise the loading points. In this study, the UK reference pesticides were acquired from Lewis et al. (2021) and the PLI_{FATE} was calculated as follows:

$$\text{Normalized Toxicity} = \frac{1}{\left(\frac{\text{Active Substance Value}}{\text{Reference Minimum Value}}\right)} \tag{6.8}$$

The "Pesticide Loading Points" for each measure are then determined by multiplying this value by a weighting factor. The weighting value varies from parameter to parameter, allowing weighting for issues or policy concerns, such as loss of pollinators or groundwater contamination, to be given greater relative significance within the sub-indicators. The weighting factors used in this study are outlined by Lewis et al. (2021), who applied the Danish PLI to arable agriculture in the UK. They are as follows:

- Mammals = 1

- Birds = 1
- Fish = 30
- Daphnia = 30
- Algae = 3
- Aquatic plants = 3
- Earthworms = 2
- Honey bees = 100

The weighting factors were then used to calculate the Ecotoxicology Load indicator (PL_{ECO}) using the following equation:

$$PLI_{ECO} = \sum (\text{Normalized Toxicity} \times \text{Weighting Factor}) \tag{6.9}$$

Where:

- PLI_{ECO} is the total Ecotoxicology sub-indicator PLI.

Total PLI

To ensure comparability across different pesticide impact categories, all pesticide load indicator components were scaled between 0 and 1 using min-max normalisation. Min-max normalisation was performed as follows:

$$X_{\text{scaled}} = \frac{X - \min(X)}{\max(X) - \min(X)} \tag{6.10}$$

where:

- X_{scaled} is the normalized value,
- X is the original value of the indicator,
- $\min(X)$ and $\max(X)$ are the minimum and maximum observed values for each indicator across all pesticides.

This transformation preserves the relative differences between pesticides while ensuring that all indicators are expressed on a common scale ranging from 0 to 1, where 0 represents the lowest observed impact and 1 represents the highest observed impact. The scaled values were then used in subsequent calculations of the total Pesticide Load Indicator (PLI), incorporating pesticide application rates.

The total Pesticide Load Index (PLI) is calculated as the sum of the three sub-indicators:

$$PLI = PLI_{HH} + PLI_{FATE} + PLI_{ECO} \tag{6.11}$$

Where:

- PLI is the total Pesticide Load indicator score.
- PLI_{HH} is the total Human Health sub-indicator PLI.
- PLI_{FATE} is the total Environmental Fate sub-indicator PLI.
- PLI_{ECO} is the total Ecotoxicology sub-indicator PLI.

Since exposure risk also depends on the quantity of the pesticide applied, the final application rate-adjusted PLI is computed as:

$$PLI_{adj} = PLI \times R \tag{6.12}$$

Where:

- PLI_{adj} is the Pesticide Load Indicator score adjusted for the application rate.
- PLI is the total Danish Pesticide Load indicator score.
- R is the application rate of the pesticide (kg ha^{-1}).

6.2.5.2 Statistical analysis

The PLI and all PLI sub-indicator data (PL_{HH}, PL_{FATE}, PL_{ECO}) were assessed for normality and homogeneity of variances using the methodology outlined in Section 3.10. Data distributions are presented in Appendix B.3. All data were non-normally distributed, with a positive skew; therefore, a generalised linear mixed effects model with a Gamma link log function was used to analyse the effects of the experimental treatments (Ng and Cribbie, 2017). The model was fitted using the experimental year as random model effects following the methodology outlined in Section 3.10. Model diagnostics are presented in Appendix B.4.

6.3 Results

6.3.1 Crop Establishment

The CON treatment achieved a higher mean percentage of the target plant population (84%) than the CA treatment (66%) for the duration of the experiment; however, this was not found to be a statistically significant difference ($\beta = 3.14$, $SE = 3.27$, $Z = 0.96$, $p = 0.34$). During the first year of the experiment in the crop of spring beans, the CON treatment achieved a mean plant population of 36.4 plants m^{-2}, falling below the target plant population of 50 plants m^{-2}. This was similar in the CA treatment, which achieved a plant population of 37.7 plants m^{-2}. Despite the lower plant population, the CON treatment had a higher mean amount of spring bean shoots, 6.0 shoots m^{-2}, compared to the CA treatment, which had a mean of 5.6 shoots m^{-2}. In the second year of the experiment, the CA treatment had a mean winter wheat plant population of 283.4 plants m^{-2}, which was 109% of the target plant population of 260 plants m^{-2}. The CON treatment had a lower plant population of 245.4 plants m^{-2}, thus achieving 94.4% of the target plant population. The CA treatment also had a higher mean quantity of shoots/tillers m^{-2} in this crop, 750.8 shoots m^{-2}, compared to the CON treatment, which had a mean shoot quantity of 666.4 m^{-2}. In the final year of the experiment, the CON treatment had an oilseed rape mean plant population of 17 plants m^{-2}, which was 85% of the target plant population of 20 plants m^{-2}. Conversely, the CA treatments oilseed rape crop failed, the following spring barley crop achieved 243 plants m^{-2}, which was 81.1% of the 300 plants m^{-2} target plant population.

The CA treatment had a significantly higher percentage of seed loss than the CON treatment ($\beta = 0.03$, $SE = 0.06$, $Z = 0.51$, $p = 0.001$). The CA treatment had a mean loss of 49.7% for all years of the experiment, and the CON treatment had a reduced mean seed loss of 45.6%. In the first year of the experiment, the CA treatment had a mean loss of 37.7% of the beans planted, and the CON treatment had a mean loss of 34.5%. During the second year of the experiment, the CON treatment had a higher mean loss (36.3%) of wheat seeds than the CA treatment (22%). The final year of the experiment saw the complete loss of the CA treatments' oilseed rape crop (100%). However, while the CON treatments crop survived, there were higher losses of the seeds planted than in previous years (66%). The spring barley grown to replace the failed oilseed rape crop in the CA treatment had a mean loss of 39.1% of the seeds planted. The mean seed loss for each crop (**C**) and by treatment (**D**) is shown below in Figure 6.1.

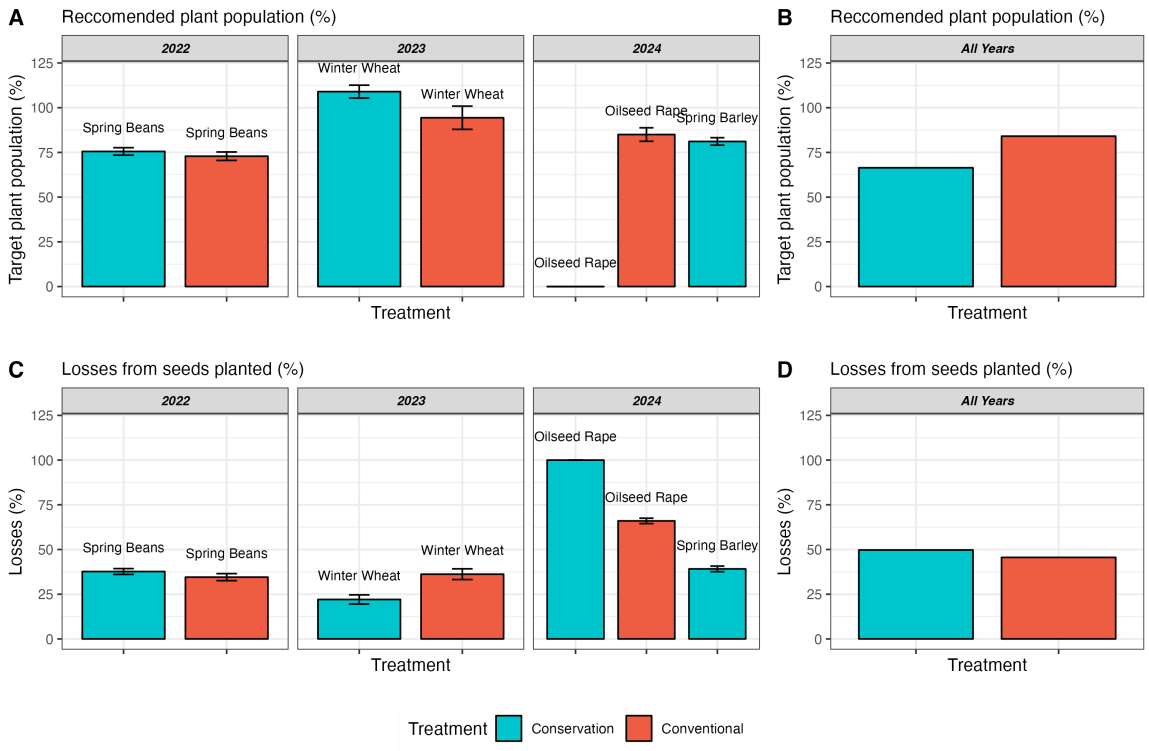

Figure 6.1: The mean plant population achieved in each treatment expressed as a percentage (%) of the national recommended plant population for that crop (**A**, n = 25) and the full experimental duration (**B**, n = 3). The mean losses (%) of seeds from the seeds planted for that crop (**C**, n = 25) and the full experimental duration (**D**, n = 3).

6.3.2 Normalised Difference Vegetation Index

The output of the evaluation of the data normality and homogeneity of variances is detailed in Appendix B. There was no statistically significant difference in mean NDVI during the spring bean crops (β = 0.01, SE = 0.06, Z = 0.09, p = 0.93), the winter wheat crop (β = 0.04, SE = 0.03, Z = 1.22, p = 0.22), or the final year of the experiment between the oilseed rape and spring barley crops (β = -0.02, SE = 0.02, Z = -0.84, p = 0.4). The smoothed mean NDVI throughout the experimental duration is shown in Figure 6.2.

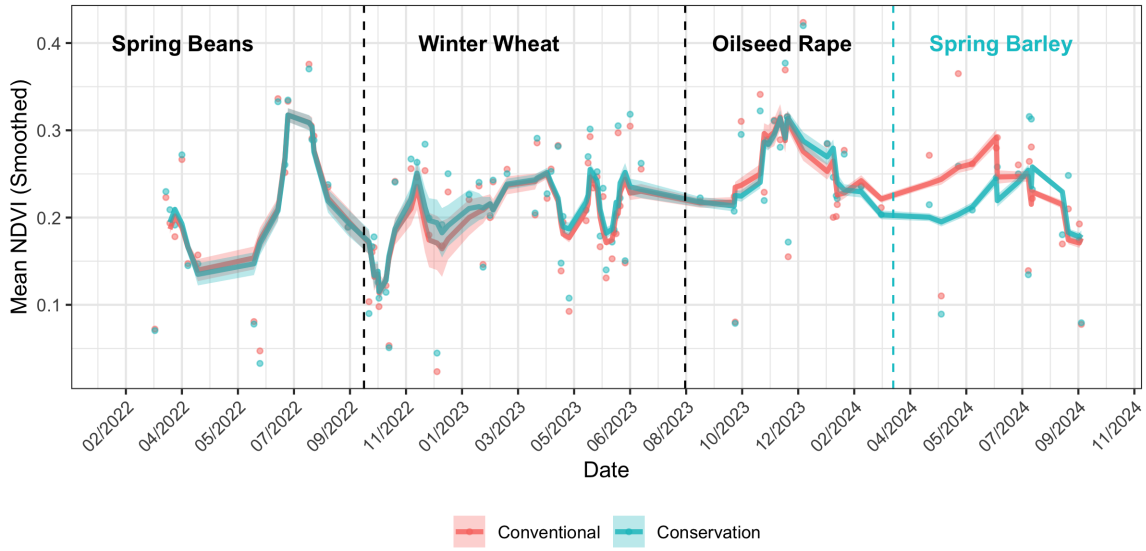

Figure 6.2: Temporal trends in Normalised Difference Vegetation Index (NDVI) for CA and CON treatments ($n = 5$). Solid lines represent the 5-point moving average of NDVI values over time, smoothing short-term fluctuations. Shaded ribbons indicate the smoothed standard error (SE) around the mean NDVI. Faded points show the original, unsmoothed NDVI measurements for reference.

6.3.3 Crop Applications

6.3.3.1 Pesticides

There were no significant differences identified in total pesticide active ingredient application between the two treatments for the experimental duration (β = -0.02, SE = 0.01, Z = -1.03, p = 0.3). For the three-year experiment, the CON treatment applied 10.1 kg ha^{-1} of pesticide active ingredient, compared to the CA treatment, which applied 9.3 kg ha^{-1}. When this was analysed by year, the total quantity of agrochemical active ingredient used in the production of the spring bean crop was 13% higher in the CON treatment (3.82 kg ha^{-1}) than the CA treatment (3.38 kg ha^{-1}). However, the quantity of agrochemicals used in the second year of the experiment was 10% higher in the CA treatment (3.85 kg ha^{-1}) than in the CON (3.47 kg ha^{-1}). In the final year of the experiment, the CA treatment used 2.07 kg ha^{-1} of agrochemical in comparison to the CON treatment, which used 2.83 kg ha^{-1}, a 37% increase. All pesticide mass applications by year and treatment are shown in Figure 6.3.

The CA treatment applied significantly more herbicide active ingredient per year than the CON treatment ($\beta = 0.87$, $SE = 0.39$, $Z = 2.3$, $p = 0.03$). Throughout the experiment, the CA treatment used 6.34 kg ha^{-1} of herbicide active ingredient, which

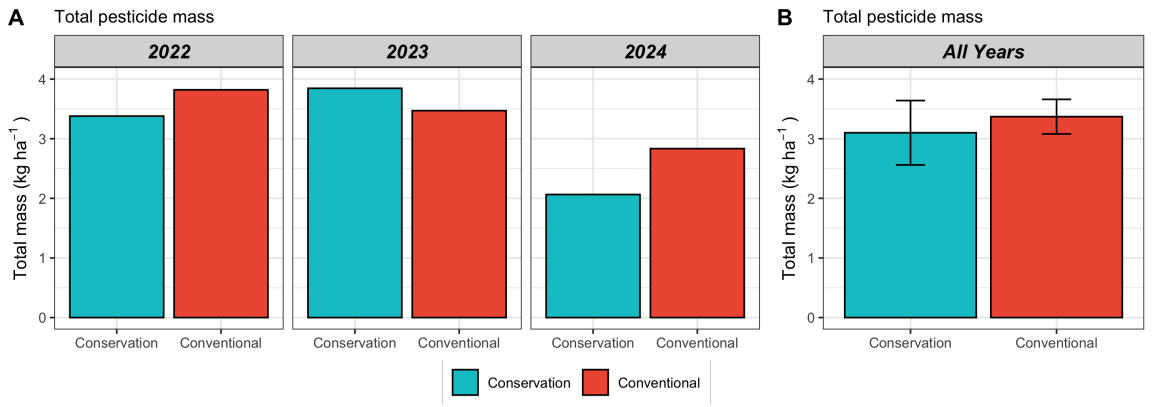

Figure 6.3: Total pesticide application throughout the experiment (active ingredient kg ha^{-1} treatment^{-1}).

was a 36% increase on the usage of the CON treatment, which applied 4.04 kg ha^{-1}. During the first year of the experiment, both treatments used the same quantity of herbicide active ingredients (3.6 kg ha^{-1}), however during the second year, the total herbicide application in the CA treatment (1.37 kg ha^{-1}) was 85% higher than the CON treatment (0.21 kg ha^{-1}). During the final year, there was again higher usage (63%) of herbicide active ingredients in the CA treatment (1.81 kg ha^{-1}) compared to the CON treatment (0.67 kg ha^{-1}). All herbicide applications by year and treatment are shown in Figure 6.4.

The CON treatment applied significantly more fungicide active ingredient per year than the CA treatment (β = -0.19, SE = 0.07, Z = -2.8, p = 0.004). During the first year of the experiment, fungicide usage in the CON treatment (0.65 kg ha^{-1}) was 195% higher than the CA treatment (0.22 kg ha^{-1}). During the second year, the quantity of fungicide active ingredient application was similar across both treatments (CON - 1.58 kg ha^{-1}, CA - 1.61 kg ha^{-1}). In the final year of the experiment, the CA treatment did not use any fungicide active ingredients, and the CON treatment used 0.34 kg ha^{-1} of fungicide. All fungicide applications by year and treatment are shown in Figure 6.4.

The CA treatment applied no insecticides throughout the experiment, whilst the CON treatment applied 0.1 kg ha^{-1} of insecticide during the spring bean crop in the first year, 0.005 kg ha^{-1} during Year 2, and 0.225 kg ha^{-1} in the final year of the experiment. All insecticide applications by year and treatment are shown in Figure 6.4.

There was only PGR usage in 2023 in both treatments, where the PGR active ingredient application rate was 94% higher in the CON treatment (1.67 kg ha^{-1})

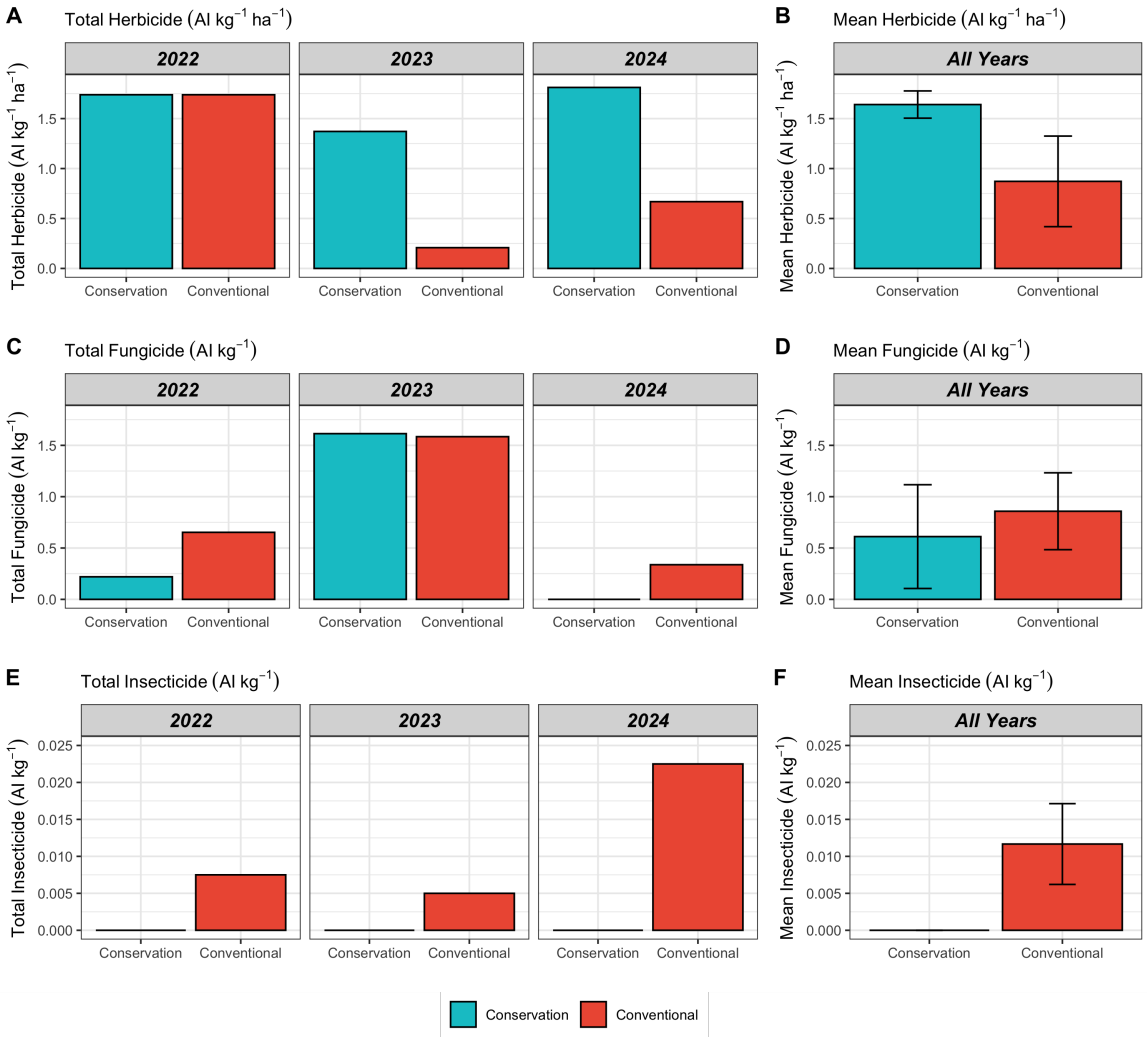

Figure 6.4: The total application of active ingredient (AI kg ha^{-1} treatment^{-1}) by each year of the experiment for; Herbicides (**A**), Fungicides (**C**), and Insecticides (**E**), and the mean application of active ingredient (AI kg ha^{-1} treatment^{-1}) for the experimental duration for; Herbicides (**B**), Fungicides (**D**), and Insecticides (**F**).

compared to the CA treatment (0.86 kg ha^{-1}). However, no statistical differences were detected overall in PGR usage between the treatments ($\beta = 0.12$, $SE = 0.08$, $Z = 1.5$, $p = 0.13$). All PGR applications by year and treatment are shown in Figure 6.5.

During the final year of the experiment, molluscicides were used in both treatments, with the CON treatment (0.42 kg ha^{-1}) using 68% more molluscicide active ingredient than the CA treatment (0.25 kg ha^{-1}). All molluscicide applications by year and treatment are shown in Figure 6.5.

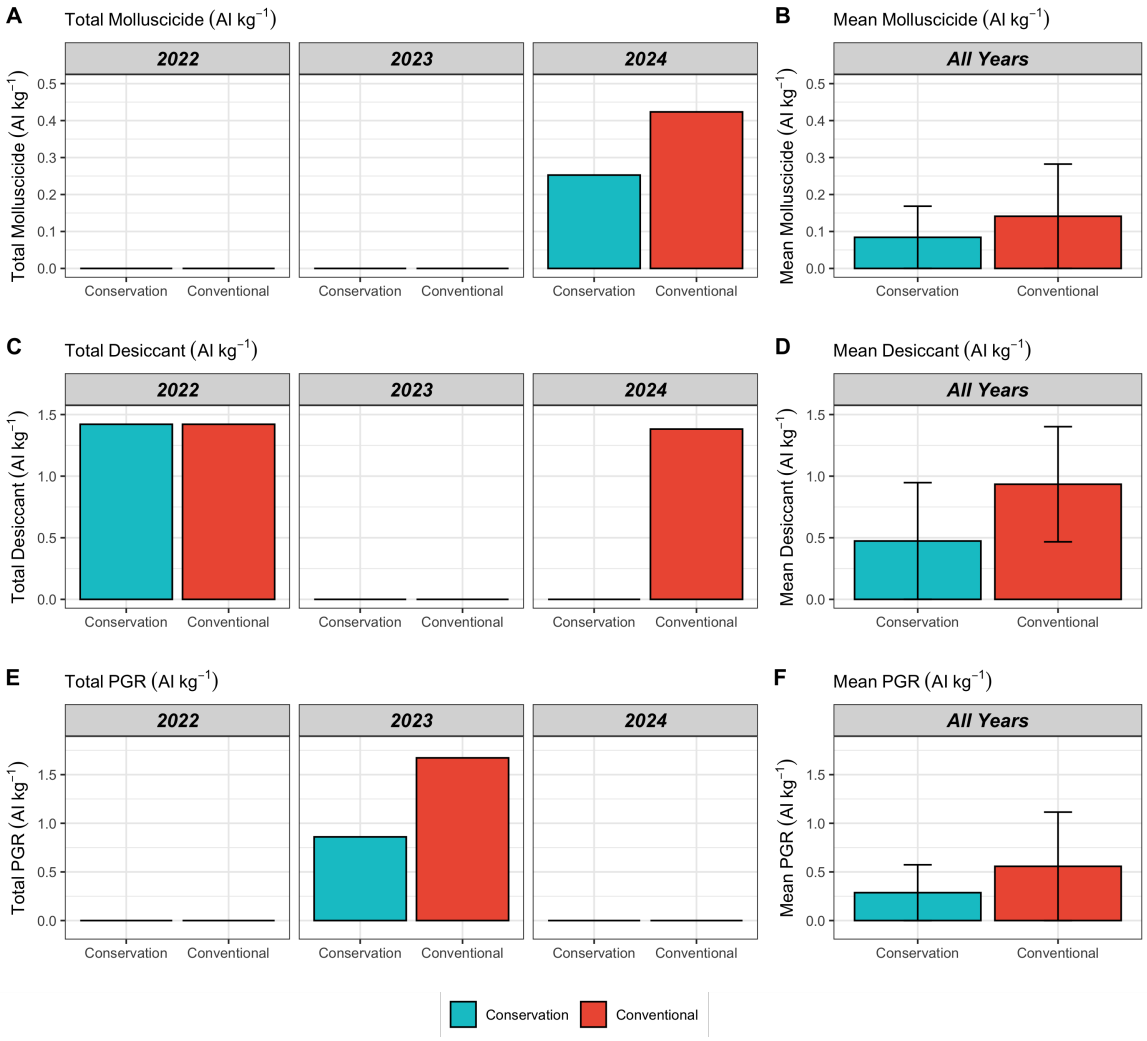

Figure 6.5: The total application of active ingredient (AI kg ha^{-1} treatment^{-1}) by each year of the experiment for; Molluscicides (**A**), Desiccants (**C**), and Plant Growth Regulators (PGRs) (**E**), and the mean application of active ingredient (AI kg ha^{-1} treatment^{-1}) for the experimental duration for; Molluscicides (**B**), Desiccants (**D**), and Plant Growth Regulators (PGRs) (**F**).

6.3.3.2 Fertiliser

The CON treatment applied significantly more fertiliser (kg ha^{-1} year^{-1}) than the CA treatment (β = -0.17, SE = 0.06, Z = -3.04, p = 0.003). During the first year of the experiment, both treatments applied very similar quantities of fertiliser (CON = 215.9 kg ha^{-1}, CA = 212.5 kg ha^{-1}). During the second year of the experiment, the CON treatment applied 226 kg ha^{-1} of fertiliser compared to 187.5 kg ha^{-1} in the CA treatment. The final year saw the highest quantities of fertiliser being applied, where the CON treatment applied 423.4 kg ha^{-1} of fertiliser compared to 312.5 kg

ha^{-1} in the CA treatment. All fertiliser mass applications by chemical element are shown in Figure 6.6.

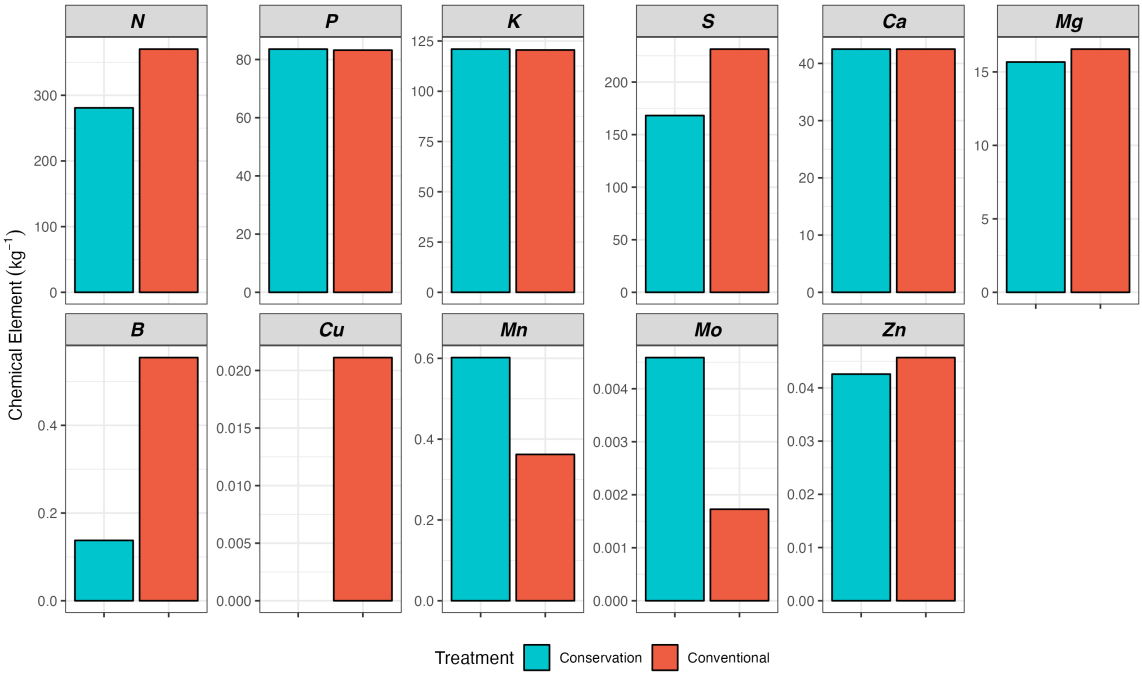

Figure 6.6: Total plant nutrient application throughout the experiment (chemical element kg ha^{-1} treatment^{-1}).

There was significantly higher N usage in the CON treatment (N kg ha^{-1} year^{-1}) than the CA treatment (β = -0.19, SE = 0.07, Z = -2.77, p = 0.006). There were no applications of N in the first year of the experiment, as both treatments grew spring beans. During the crop of winter wheat, the CON treatment applied 186 kg ha^{-1} of N and the CA treatment applied 152 kg ha^{-1}, a 22 % increase. During the final year of the experiment, the CON treatment received 185 kg ha^{-1} of N for the crop of oilseed rape and the CA treatment received 129 kg ha^{-1} in the crop of spring barley. This was an increase in N application in the CON treatment of 43%. For the duration of the experiment (3 years), the CA treatment was applied with 281 kg ha^{-1} of N and the CON treatment was applied with 370 kg ha^{-1}; a 32 % increase of N usage in the CON treatment. Total N applications for each experimental year are presented in Figure 6.7.

The first year of the experiment saw a blanket application of 36 kg ha^{-1} K, in solid form, across both treatment This was followed by smaller foliar applications of 3.16 kg ha^{-1} in the CA treatment and 0.13 kg ha^{-1} in the CON treatment in the second year. During the final year, both treatments received the same quantity of K

(83 kg ha^{-1}). There were no applications of P in the first year of the experiment and very low levels of application during the second year (CA = 0.7 kg ha^{-1}, CON = 0.13 kg ha^{-1}). In the final year of the experiment, both treatments received 83 kg ha^{-1} of P. In total, across the experimental duration, both treatments received the same amount of P (83 kg ha^{-1}) and K (121 kg ha^{-1}). There were no significant differences in the quantity of P (β = 0.13, SE = 0.09, Z = 1.52, p = 0.13), or K (β = 0.38, SE = 0.29, Z = 1.32, p = 0.19). Total K and P applications for each experimental year are presented in Figure 6.7.

There were no significant differences detected in the quantity of S applied to both treatments (β = -0.5, SE = 0.28, Z = -1.8, p = 0.07). However, throughout the experiment, the CON treatment applied 231.3 kg ha^{-1} compared to 168.2 kg ha^{-1}. During the first year of the experiment both treatments received the same application rate of polysulphate (120 S kg ha^{-1}), and there was also similar application rates of S in the second year of cropping (CON = 38.9 kg ha^{-1}, CA = 30.5 kg ha^{-1}). However, in the final year of the experiment, the CON treatment received 71.9 kg ha^{-1} of S compared to 17.6 kg ha^{-1} in the CA treatment. Total S applications for each experimental year are presented in Figure 6.7.

Throughout the experiment, both treatments received applications of micronutrients. Both treatments received similar quantities of Ca (42.5 kg ha^{-1}), Mg (CON = 16.5 kg ha^{-1}, CA = 15.6 kg ha^{-1}), and Zn (0.04 kg ha^{-1}). However, the CON treatment applied 300% more B (0.56 kg ha^{-1}) than the CA treatment (0.14 kg ha^{-1}) (β = -0.13, SE = 0.07, Z = -1.67, p = 0.09). The full macro and micro nutrient application data for the duration of the experiment are detailed in Tables 3.8, 3.9, and 3.10 and Figures 6.7 and 6.8.

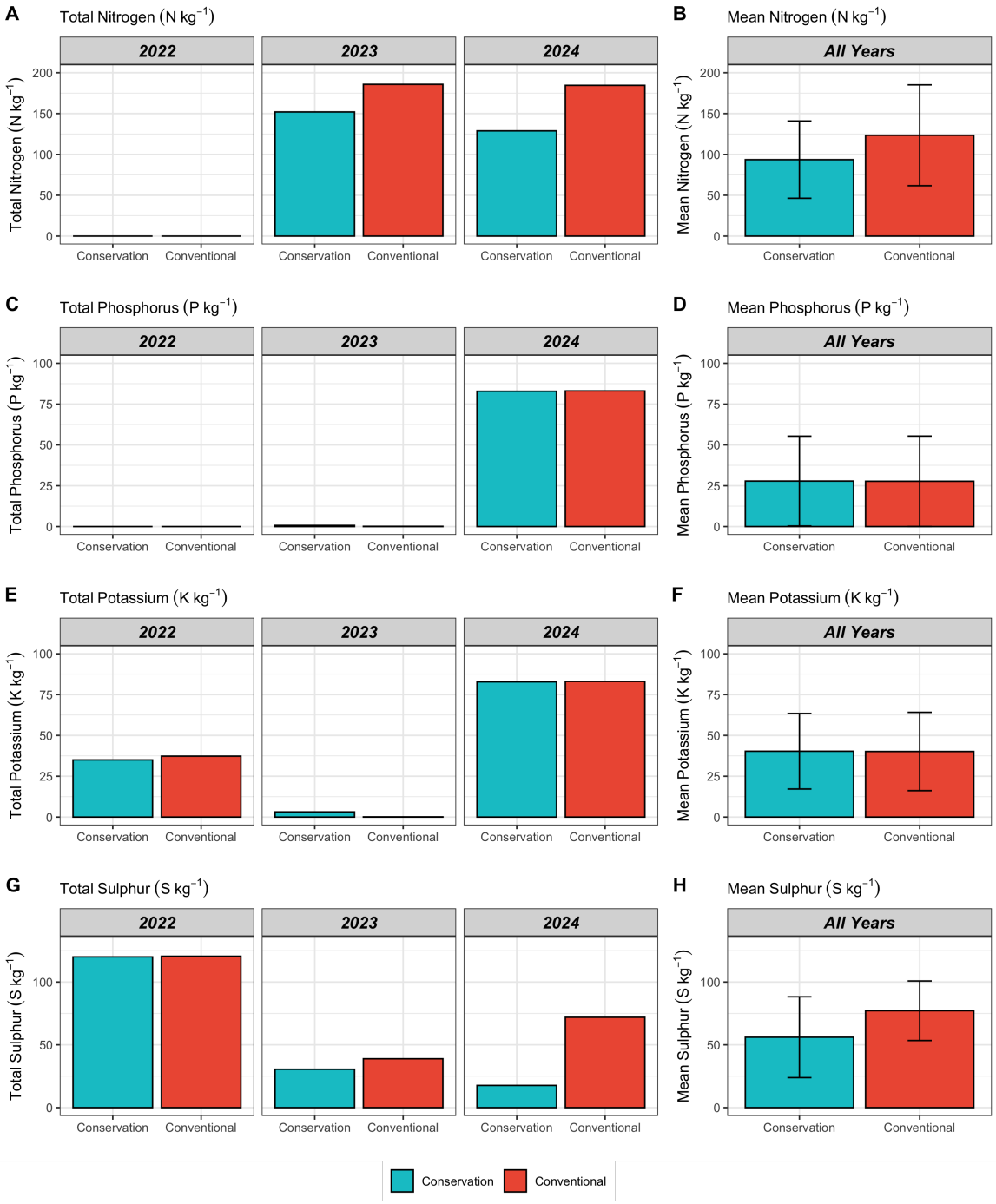

Figure 6.7: The total application of fertiliser chemical element (kg ha^{-1} treatment^{-1}) by each year of the experiment for; Nitrogen (**A**), Phosphorus (**C**), Potassium (**E**), and Sulphur **G**, and the mean application of fertiliser chemical element (kg ha^{-1} treatment^{-1}) for the experimental duration for; Nitrogen (**B**), Phosphorus (**D**), Potassium (**F**), and Sulphur **H**.

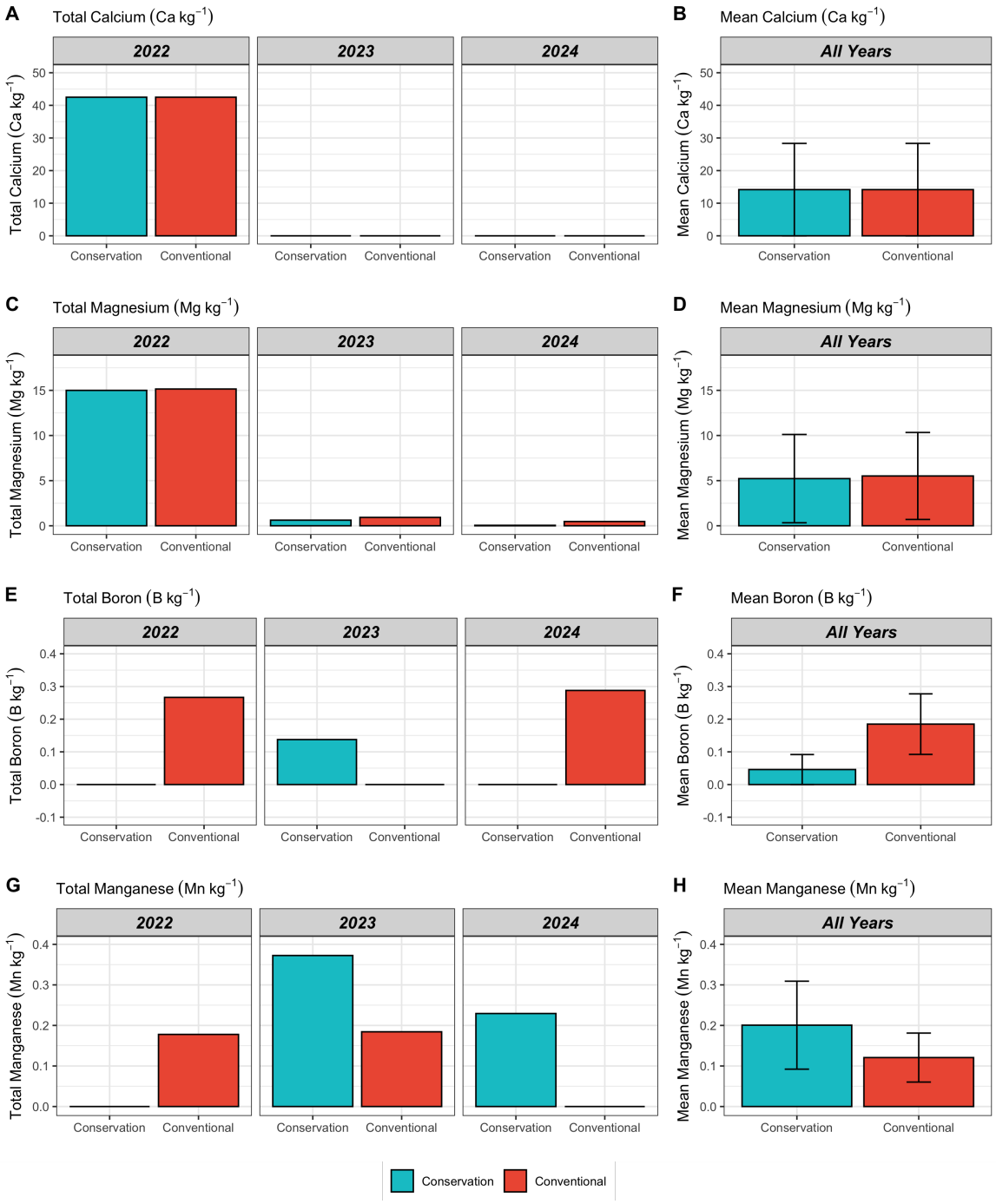

Figure 6.8: The total application of fertiliser chemical element (kg ha^{-1} treatment^{-1}) by each year of the experiment for; Calcium (**A**), Magnesium (**C**), Boron (**E**), and Manganese **G**, and the mean application of fertiliser chemical element (kg ha^{-1} treatment^{-1}) for the experimental duration for; Calcium (**B**), Magnesium (**D**), Boron (**F**), and Manganese (**H**).

6.3.4 Pesticide Load Indicator

6.3.4.1 Ecotoxicology

The analysis of the ecotoxicology pesticide load sub-indicator found no significant difference in the PLI_{ECO} for both treatments during the experimental duration ($\beta = 0.01$, $SE = 0.01$, $Z = 0.96$, $p = 0.33$). Despite the lack of a statistical difference, there were higher PLI_{ECO} values in the CON treatment during all experimental years. During the first year of the experiment, the CON treatment had a PLI_{ECO} score of 0.28, compared to the CA treatment's PLI_{ECO} score of 0.16. There was a less pronounced difference in the PLI_{ECO} score in 2023, where the CON treatment had an increased PLI_{ECO} of 0.68, compared to the CA treatment, which had a PLI_{ECO} of 0.67. The CA treatment had a reduced PLI_{ECO} score in 2024 of 0.32; however, the CON treatment had an increased PLI_{ECO} of 0.41. For the entire experimental duration, the CON had a higher mean PLI_{ECO} of 0.46, compared to 0.38 in the CA treatment. The total PLI_{ECO} score for the experimental duration and for each year of the experiment is presented below in Figure 6.9.

The pesticide group that contributed the most to the PLI_{ECO} in the CON treatment was insecticides, which contributed 91% to the PLI_{ECO}. In the CA treatment, the largest contribution was from herbicides, accounting for 87% of the PLI_{ECO}. In comparison, herbicide usage only accounted for 3% of the PLI_{ECO} in the CON treatment. Fungicides were a minor contributor to both the CON and CA treatments, accounting for 4% and 8% of the PLI_{ECO}, respectively. The contribution proportions for different pesticide groups to PLI_{ECO} are presented in Figure 6.13.

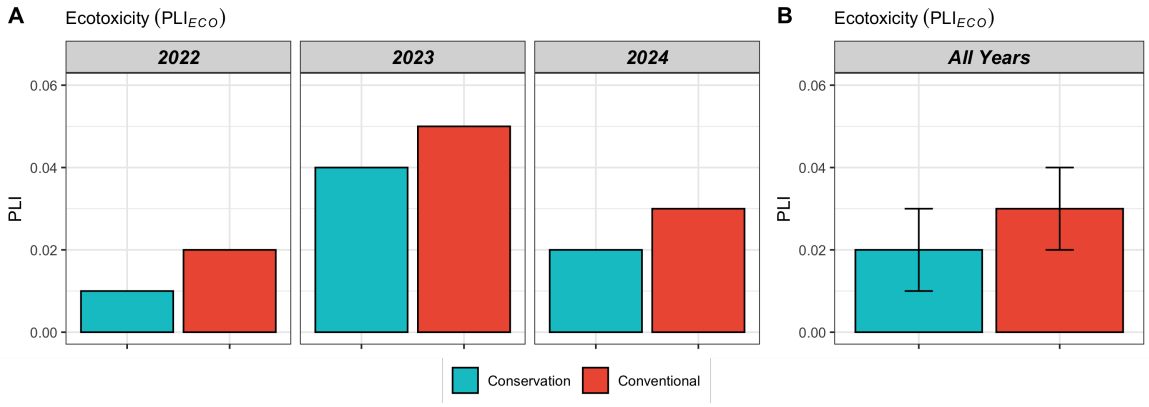

Figure 6.9: **A:**The mean ecotoxicology pesticide load indicator for all experimental years (PLI_{ECO} year^{-1} treatment^{-1}) and; **B:** the mean PLI_{ECO} for the entire experimental period.

6.3.4.2 Environmental Fate

Analysis of the environmental fate pesticide load sub-indicator found a significant increase in the PLI_{FATE} for the CA treatment compared to the CON treatment during the experimental duration (β = 2.3, SE = 0.49, Z = -4, p = 0.0001). There were similar PLI_{FATE} scores for both treatments during 2022 (CA = 0.89, CON = 0.9); however, the following years of the experiment exhibited large differences in the PLI_{FATE} score. In 2023, the CA treatment had a PLI_{FATE} score of 1.16 compared to the far lower score of 0.13 in the CON treatment. This was similar in 2024, where the CA treatment had a far higher PLI_{FATE} score of 0.64, compared to the CON treatment's score of 0.08. The mean PLI_{FATE} score for the CA treatment was 0.9 (SE = 0.15) and 0.37 for the CON treatment (SE = 0.27). The total PLI_{FATE} score for the experimental and each year of the experiment is presented below in Figure 6.10.

The pesticide groups that contributed the most to PLI_{FATE} in the CON treatment were insecticides (64%), herbicides (24%), and fungicides (10%). The largest groups to contribute to the CA treatments PLI_{FATE} value were: herbicides (82%) and fungicides (17%). The contribution proportions for different pesticide groups to PLI_{FATE} are presented in Figure 6.13.

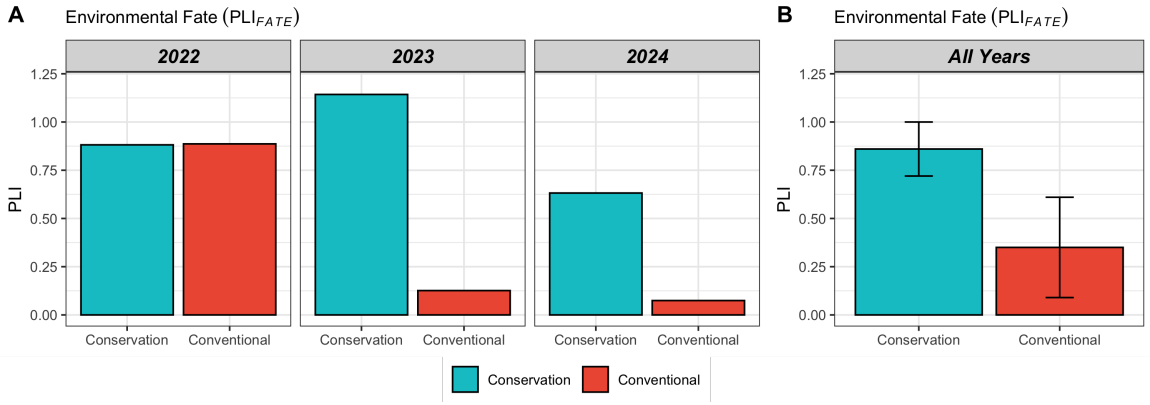

Figure 6.10: **A:**The mean environmental fate pesticide load indicator for all experimental years (PLI_{FATE} year^{-1} treatment^{-1}) and; **B:** the mean PLI_{FATE} for the entire experimental period.

6.3.4.3 Human Health

Analysis of the human health pesticide load sub-indicator found no significant difference in the PLI_{HH} for both treatments during the experimental duration (β = 0.03,

$SE = 0.02$, $Z = 1.05$, $p = 0.29$). There were similar PLI_{HH} scores for both treatments in 2022 (CA = 0.42, CON = 0.53) and 2023 (CA = 1.34, CON = 1.21). However, in 2024, the CON treatment had a higher PLI_{HH} score of 0.39, compared to the score of 0.3 in the CA treatment. The total PLI_{FATE} score for the experimental duration and each year of the experiment is presented below in Figure 6.11.

The pesticide group that contributed the most to the PLI_{HH} for both treatments was fungicides. In the CA treatment, this accounted for 60% of the PLI_{HH}, and in the CON treatment, this accounted for 44%. The second largest contribution by pesticide group was 30% from herbicides in the CA treatment, and 29% from insecticides in the CON treatment. Herbicides contributed to 15% of the PLI_{HH} in the CON treatment. The contribution proportions for different pesticide groups to PLI_{HH} are presented in Figure 6.13.

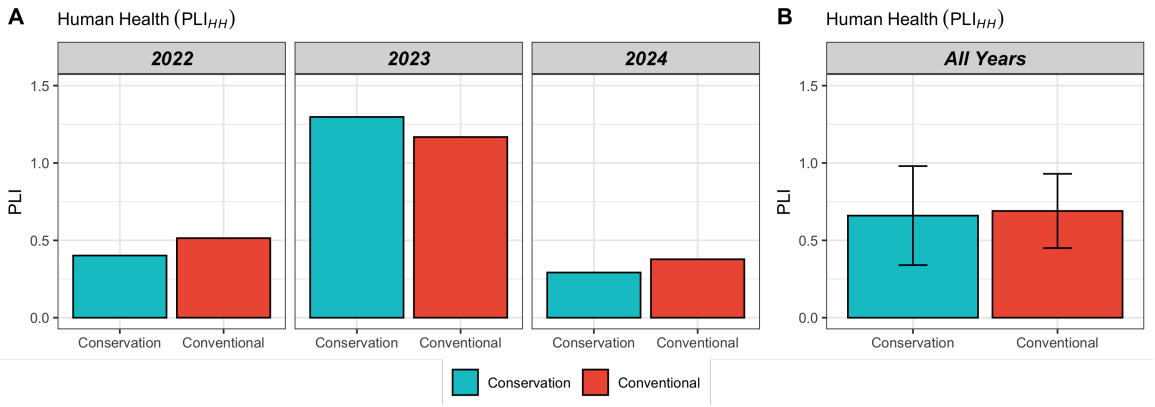

Figure 6.11: **A:**The mean human health pesticide load indicator for all experimental years (PLI_{HH} year^{-1} treatment^{-1}) and; **B:** the mean PLI_{HH} for the entire experimental period.

6.3.4.4 Total Pesticide Load Indicator

Analysis of the total Pesticide Load Indicator (PLI) identified a significant increase in the CA treatment PLI, compared to the CON system during the experimental duration (β = -0.09, SE = 0.04, Z = -2.24, p = 0.02). The mean PLI of the CA treatment was 1.57 (SE = 0.47) and the mean of the CON treatment was 1.08 (SE = 0.3). There were similar PLI scores for both treatments in 2022; the CA treatment had a PLI of 1.29, and the CON treatment had a PLI of 1.42. However, in 2023, the largest difference in the PLI between the treatments was exhibited, with the CA treatment having a far higher PLI value of 2.48, compared to a PLI value of 1.34 in the CON treatment. A similar trend was observed in 2024, both treatments had lower

PLI values; however, the CA treatment had a PLI of 0.95 and the CON treatment a PLI of 0.48. The total PLI score for the experimental duration and each year of the experiment is presented below in Figure 6.12.

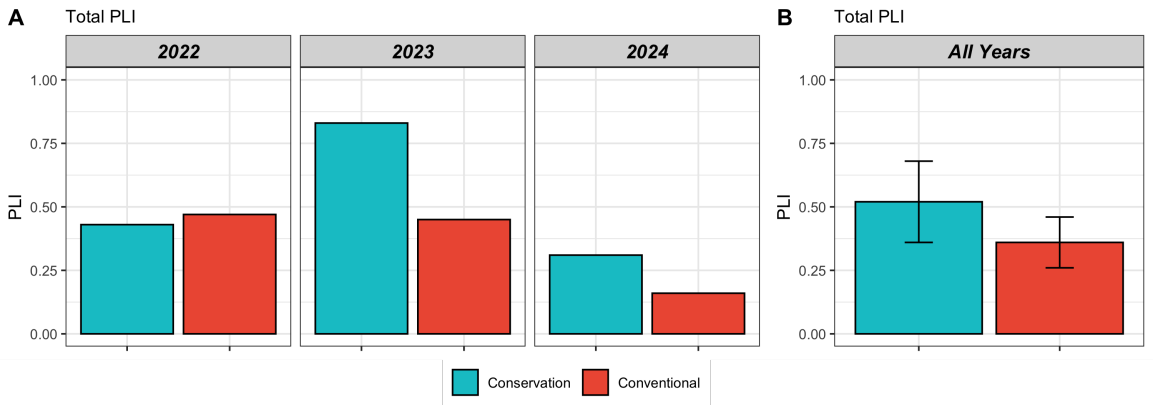

Figure 6.12: **A:**The mean pesticide load indicator for all experimental years (PLI year^{-1} treatment^{-1}) and; **B:** the mean PLI for the entire experimental period.

The largest contributor pesticide group to the total PLI in the CA treatment was found to be herbicides, which contributed to 58% of the total PLI. However, in the CON treatment, the largest contributor to the PLI was insecticides, which accounted for 57% of the PLI. The CA treatment did not use any insecticides during the experiment; therefore had no contribution from insecticide active ingredients. The second highest contributor to the PLI was fungicides, which accounted for 37% of the PLI, compared to the CON treatment, where fungicides contributed more (22%) to PLI than herbicides (15%). The contribution proportions for different pesticide groups to PLI are presented in Figure 6.13.

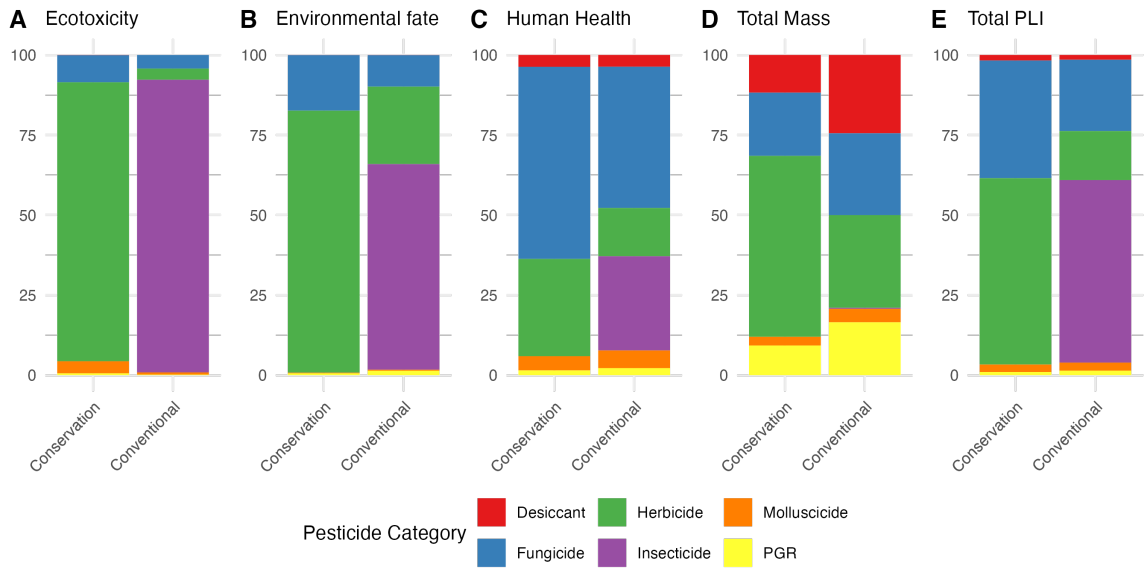

Figure 6.13: The proportional contributions of pesticides for the crop rotation to the **A:** The Ecotoxicology Pesticide Load Indicator (PLI_{ECO}), **B:** The Environmental Fate Pesticide Load Indicator (PLI_{FATE}), **C:** The Human Health Pesticide Load Indicator (PLI_{HH}), **D:** The total mass of pesticides applied (kg ha^{-1}), and **E:** The total Pesticide Load Indicator (PLI). Data source: Lewis et al. (2016).

6.3.5 Crop Yield

The results from the power analysis from the 6000 paired yield observations from the global meta-analysis from Pittelkow et al. (2015) found that the expected effect size for detection of crop yield differences was low ($d = 0.02$). Figure 6.14 suggests that, to achieve a simulated power (α) of 80 % +, over 1000 observations (n) would be required, at a d value of 0.14. Figure 6.14 is a simulation of the required sample sizes for reliable detection of yield differences in agricultural tillage systems using a range of d values ranging from 0.04 - 0.14.

During the first year of the experiment, the CON treatment had a mean yield of 6.03 t ha^{-1} and the CA treatment had a lower mean yield of 5.31 t ha^{-1}. Both treatments yielded higher than the national average yield of 3.5 t ha^{-1}, the CON treatment yield exceeded the national average by 172.3% and the CA treatment by 148.8%. In second year of the experiment, the CON treatment had a higher mean yield of 10.9 t ha^{-1} achieving 121.1% of the national average yield for winter wheat (9 t ha^{-1}), and the CA treatment yielded 9.3 t ha^{-1}, 103.8% of the national average. During the final year of the experiment, the CON treatments crop of oilseed rape had a mean yield of 2.1 t ha^{-1}, and therefore only achieved 63.5% of the national average oilseed rape yield (3.4 t ha^{-1}). In comparison, the CA treatment oilseed rape crop

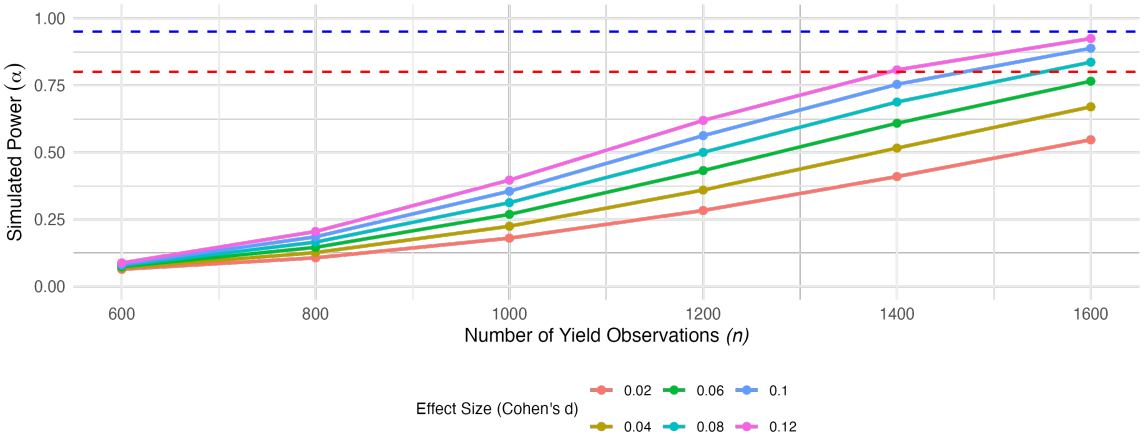

Figure 6.14: Power curve for detecting differences in crop yield across various effect sizes and sample sizes. The curve illustrates the relationship between the number of observations (x-axis) and statistical power (y-axis) for different effect sizes (Cohen's d).

failed; therefore, spring barley was planted instead. This crop had a mean yield of 5.3 t ha^{-1}, and only achieved 84.4% of the national average spring barley yield of 6.3 t ha^{-1}.

No statistically significant differences were observed in the percentage achieved of the UK average yield between the CON and CA treatment (β = -17.8, SE = 11.1, Z = -1.6, p = 0.12). The pairwise comparison indicated that the percentage achieved of the UK national average crop yield during the experiment was on average 104% (SE = 2.7) for the CA treatment, and 122% (SE = 8.71, 95% CI : 19.32% to 225%) for the CON treatment. There was substantial uncertainty in this model output, which is indicated by a high SE in both treatments. Most of the variability in the achieved crop yield percentage can be attributed to random spatial and temporal differences, as indicated by the high variance of the random effects (Block: V = 207.5, SD = 14.41, Crop: V = 651.1, SD = 25.52, Year: V = 1381, SD = 37.16). The sum of the random effect variances (207.5 + 651.1 + 1381.0 = 2239.6) was much larger than the residual variance (515.6). This indicates that the random effect grouping factors explain a significant portion of the total variability in yield percentages. Model diagnostics are presented in Appendix B.

When the yield difference maps were assessed, there was high spatial variability in crop yield between the two treatments in the first year of the project. There were large areas of the smaller field which were estimated to have a higher crop yield in the CON treatments, whereas the inverse was detected in the larger field, where the

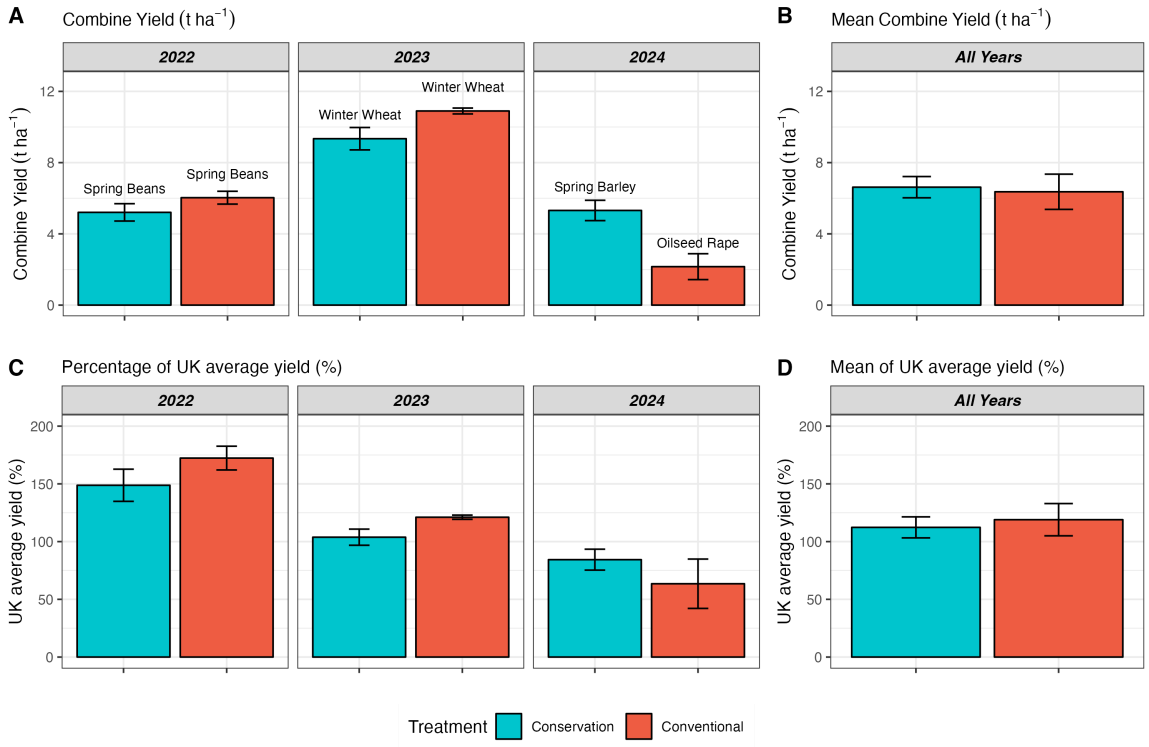

Figure 6.15: **A:** The mean yield of each experimental treatment (t ha^{-1} year^{-1}) (n = 5). **B:** The mean yield of each experimental treatment (t ha^{-1}) (n = 3). **C:** The percentage of the national average for the previous five years (%) (n = 5). **D:** The mean percentage of the national average for the previous five years (%) (n = 3). National average crop yield data from 2017 to 2020 were obtained from the AHDB (AHDB Cereals & Oilseeds, 2021). Error bars signify standard error.

CA treatment was estimated to have a higher crop yield in a larger proportion of the field. This trend was not identified in 2023 in the winter wheat crop. Here, the yield difference map identified less spatial variability between the two treatments, as the majority of both fields were estimated to have a similar or higher yield in the CON treatments. The spatial crop yield difference between both treatments is shown in Figure 6.16.

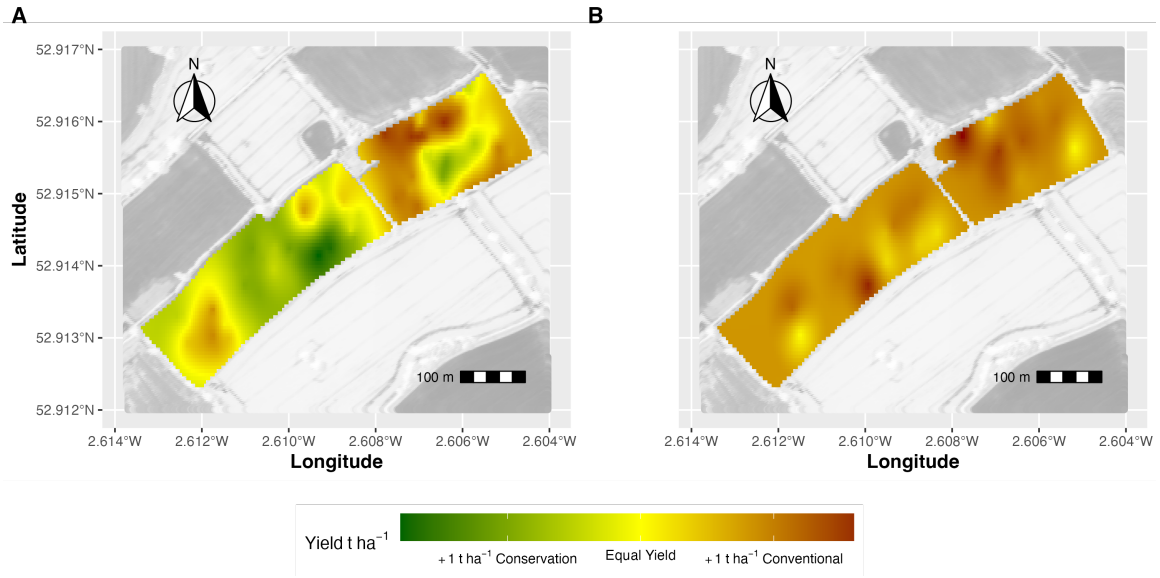

Figure 6.16: A figure containing: **A:** A yield difference map for the crop of spring beans in 2022. **B:** A yield difference map for the crop of winter wheat in 2023. Green indicates a prediction of higher yield in the CA treatment, red indicates a higher predicted yield in the CON treatment. Semi-variogram statistics are detailed in Appendix B.15

6.4 Discussion

This discussion section interprets the agronomic results of the three-year field experiment previously outlined in this chapter. The analysis focused on crop establishment, nutrient and pesticide input use, environmental risk, and crop yield. Each hypothesis is discussed in turn, regarding both the study findings and broader literature. The practical implications of CA are discussed, including the operational challenges experienced during crop establishment and the complexities of managing inputs in an NT system. Where relevant, the limitations of the experimental design are acknowledged to provide context for the interpretation of results.

6.4.1 Crop Establishment and Growth

This section addresses the tests of the following hypotheses (H):

- H_1: CA will result in a significant reduction in crop establishment compared to the CON system.

One of the most notable differences in the agronomic management during this study was the failure of the oilseed rape crop in 2024. The poor establishment of

the oilseed rape crop is shown in Figures 6.17 and 6.18, both of which were taken on the same day and show oilseed rape seedling emergence in the CON treatment and no seedling emergence in the CA treatment. This was attributed to poor crop establishment due to sub-optimal seed to soil contact, due to difficult weather and soil conditions. As a result, the CA plot had to be re-drilled later in the season to avoid a complete loss of crop data. While this ensured continued crop cover and management continuity, it introduced a confounding factor in the interpretation of agronomic and soil biological responses in 2024. Therefore, caution should be exercised when interpreting the results, and they should not be directly compared to earlier years without considering this limitation.

Figure 6.17: An example photo of the oilseed rape establishment in the CON treatment. Source: Author's own

Figure 6.18: An example photo of the oilseed rape establishment in the CA treatment. Source: Author's own

As discussed previously in Section 6.1, drilling operations are a key concept to successful crop establishment in CA. This result highlights some of the operational difficulties farmers can experience when implementing NT systems. This is because tillage is typically used in agriculture to create a seedbed that promotes uniform and efficient crop establishment (Triplett and Dick, 2008). In CA, tillage cannot be used to create preferable soil conditions for crop establishment; therefore, drill opener type and timeliness of drilling are key factors to successful crop establishment. In this study, a John Deere 750a direct drill was used for all crop planting operations in the CA treatment. The 750a is a disc-based opener drill, utilising a 460mm diameter single disk with 7-degree bevelled edge (John Deere, 2024). During the drilling operations of the oilseed rape crop in the CA treatment, the soil conditions were wet, and the drill struggled to close the seeding slot following planting, resulting in poor establishment. If it were logistically possible, a tine-based NT drill would have

been the most preferable option in this scenario (Baker et al., 2006). In general, it has been shown that machinery work rates are much improved under non-inversion tillage systems offering greater flexibility and timeliness for weather-dependent operations (Morris et al., 2010). However, the presence of surface crop residues in CA systems can also reduce solar radiation to the soil surface, and reduce the rate of soil evaporation, which can result in wetter and colder soils, which can delay the sowing of crops in wet and cold conditions (Soane et al., 2012). The results in this study emphasise the benefit for farmers in the UK who are practising CA to have access to disc and tine-based opener drills. This can greatly improve the flexibility and success of crop establishment, as in some cases, challenging drilling conditions cannot be totally avoided even with improvements to work rate efficiency that are associated with NT systems.

The CA treatment used a higher seed rate in this study, which is a common and recommended methodology for farmers practising CA in the UK to account for higher losses within the system (DEFRA, 2024; Allison, 2023). This was found to be the case in this study, where the CA treatment had significantly higher seed losses in comparison to the CON treatment. However, this result was heavily influenced by the complete loss (100%) of the CA treatment's oilseed rape crop in 2024. For the other crops in the CA rotation, losses were in the region of 20-30% of the planted seeds, which were similar to the CON treatment. This illustrates the importance of the initial stages of management to achieve a good crop establishment in CA, as once the crop is established, losses are then similar to the CON systems. During 2023, the CA treatment was drilled at a lower seed rate than the CA treatment, but also had higher seed losses throughout the growing season. This resulted in a sub-optimal plant population of 94% of the recommended plants m^{-2} according to Sylvester-Bradley et al. (2015). This is compared to the CA treatment, which was drilled at a higher seed rate (220 kg ha^{-1}), and achieved a plant population of 109% of the recommended plants m^{-2}. Although visually, there were some differences in crop colours observable during 2022 and 2023 when the same crops were being grown in both treatments, there were no statistical differences detected in the NDVI throughout the experiment for the experimental treatments. One hypothesis for this not being detectable in the data is the quality of the satellite imagery that was used in this study, which was not of the resolution needed to quantify small differences in the NDVI of the same crops. This is evidenced by this dataset, where the only observable differences in the mean NDVI were in 2024, when different crops were being grown in each treatment; despite this, no significant differences in treatment mean NDVI were identified.

Hypothesis H_1 was partially supported by the results. The CA treatment experienced significantly greater challenges in crop establishment, most notably the complete failure of the oilseed rape crop in 2024 due to poor seed-to-soil contact under wet conditions. This outcome illustrates the vulnerability of NT systems to adverse drilling conditions and highlights the importance of appropriate equipment and timing. However, for other crops in the CA rotation, seed losses were comparable to the CON treatment (20-30%), and plant population targets were largely met. While higher seed rates were used in the CA treatment, as is standard practice to offset expected establishment losses, these adjustments were only partially effective. No statistically significant differences in NDVI were detected between treatments across the study, though this may reflect limitations in satellite image resolution rather than an absence of agronomic differences. Overall, the results support the hypothesis that CA can reduce establishment success, especially under suboptimal conditions. However, this also shows that with appropriate management, establishment can be similar to CON systems for some crops.

6.4.2 Crop Nutrition

This section addresses the tests of the following hypotheses (H):

- H_2: CA will result in significant alterations to the total quantity of pesticide and fertiliser used compared to CON Agriculture.

Nutrient management in CA has received little attention in research, despite its key importance to a range of crop health metrics (Dordas, 2015). This has led to calls for more research on the topic, and proposals for nutrient management to be included as the fourth principle of CA by some (Dordas, 2015). The combination of all of the management practices associated with CA (tillage, residue retention, and crop rotation) is a key driver of changes in nutrient availability and distribution in the soil. This is evidenced by the results presented in Section 5.3, where there were significant increases in P, K, Mg availability and soil total N content after just three years of CA. Whilst during this period, the CA treatment applied significantly less fertiliser chemical elements (kg ha^{-1}), compared to the CON treatment. There was also a significant reduction in N fertiliser application in the CA treatment throughout the experiment.

Despite not being a core principle of CA, many farmers and agronomists practising CA are also trying to reduce their crop inputs with the goal to reduce costs and to

create a more resilient soil system, which requires less synthetic nutrient applications (Impey, 2022b). This is a topic of debate amongst farmers and researchers, as some CA practitioners state that during the transition phase of CA, it is important to raise the N fertiliser application rates to account for increased rates of N immobilisation in CA, as previously discussed in Section 5.1 (Oyeogbe, 2021; Soane et al., 2012; Ehlers and Claupein, 1994). N immobilisation is one of the major limitations to CA systems during the transition to the system, due to the increase in organic matter being returned to the soil and the absence of tillage, which can accelerate the breakdown of organic matter and therefore hasten the mineralisation of plant nutrients (Page et al., 2020). After this initial period of increased N usage to compensate for lower N availability, there may be opportunities for farmers to reduce overall N rates, as there is a body of evidence to suggest that the total N can increase in CA over time in comparison to CON systems (Mukherjee et al., 2024; Page et al., 2020; Wang et al., 2006). The increase in soil organic carbon, which is associated with CA, has the potential to reduce N leaching; when this is combined with a higher total N content, it could result in higher N use efficiency. Therefore, established CA systems could require lower N fertiliser rates for a similar productivity of CON (Soane et al., 2012).

In this study, the CA treatment used significantly less N fertiliser throughout the experimental duration. This is partially attributed to the different crop rotations used in this study, where, in the final year, the CA treatment grew spring barley and the CON treatment grew oilseed rape. Both crops require different N fertiliser plans, for example, the recommended N fertiliser rate for spring barley for animal feed is 110 kg ha^{-1} at a soil N supply index of 2 (AHDB, 2017). In comparison, the recommended N fertiliser rate for a winter-sown oilseed rape crop is 190 kg ha^{-1} at a soil N supply index of 2. Another reason for the reduced N application rate in the CA treatment was the choice of fertilisers used in the winter wheat crops during the second year of the experiment. Here, the CA treatment used foliar N, as opposed to the usage of soil-applied N in the CON treatment. Foliar fertilisation provides more rapid utilisation of the applied fertiliser as well as improvements to nutrient usage efficiency compared to soil-applied equivalent fertilisers (Fageria et al., 2009). In the UK, foliar applied N is typically applied by farmers targeting economic premiums from increasing grain protein for milling purposes (Woolfolk et al., 2002). However, in some cases, farmers are opting to use foliar N earlier in the season to try to improve N use efficiency, reduce costs, and reduce total N applied to their crops (Gillbard, 2024). No organic fertiliser was applied during this study due to logistical reasons with availability and application. Both agronomists tried to supplement their synthetic fertiliser plans

with organic fertilisers throughout the experiment; however, this did not prove to be possible. This was disappointing, as many farmers practising CA in the UK aim to reduce synthetic N input in favour of organic fertilisers, which have been shown to contribute to a more efficient soil available N under long-term CA systems (Oyeogbe, 2021).

Hypothesis H_2 was supported by the results. The CA treatment resulted in a significant reduction in the total quantity of fertiliser applied, particularly N, compared to the CON system. This reduction was influenced both by management choices—such as the use of foliar N in place of soil-applied fertilisers—and by the differing crop rotations, with lower-N-demand crops grown in the CA system. Despite lower fertiliser inputs, soil nutrient availability (P, K, Mg, and total N) increased under CA over the three years, indicating improved nutrient cycling and retention. These findings are consistent with the literature suggesting that CA systems can, over time, reduce dependency on synthetic fertilisers due to improved soil structure, increased organic matter inputs, and reduced nutrient leaching. Although no organic fertilisers were used in this study, the results highlight the potential for CA to achieve more nutrient-efficient crop production with lower synthetic input use.

6.4.3 Pesticide Usage

This section addresses the tests of the following hypotheses (H):

- H_2: CA will result in significant alterations to the total quantity of pesticide and fertiliser used compared to CON.
- H_4: CA agronomy will result in a reduced risk to the environment and human health compared to CON.

In this study, there were no statistical differences identified in total pesticide application between the treatments, although the CON treatment did apply a higher quantity of pesticide active ingredients than the CA treatment. When this was broken down by pesticide category, the CON treatment used significantly higher quantities of fungicide and insecticide active ingredients per hectare throughout the experiment than the CA treatment. Conversely, the CA treatment used significantly higher quantities of herbicide active ingredients per hectare. There was limited data on the usage of crop desiccants, molluscicides, and PGR usage in this study due to only three years' worth of data, as these inputs are not typically used in all crops. Therefore, robust conclusions on treatment effects were not possible. In addition, differences in

the total usage of fungicides (and to some extent, herbicides) are also dependent on the crop being grown; therefore, conclusions about pesticide usage need to be made with caution in this study, due to different crops being grown. In addition, both experimental treatments were managed by different agronomists, and therefore, they may have different opinions and recommendations for certain scenarios based on their assessments and preferences. For example, in this systems-level study, significantly higher herbicide usage may be an agronomic decision to opt for a risk-averse approach to weed management, rather than a response to higher weed populations observed in that treatment.

There are mixed results in the literature which discuss herbicide usage in CA in relation to CON practice (Bajwa, 2014; Dong et al., 2024; Morris et al., 2010). Several studies show that there is generally a higher use of pre-emergence herbicides in CA agronomy (Dong et al., 2024; Morris et al., 2010; FAO, 2001). However, this was not the case in this experiment, where the larger increases in the herbicide active ingredient rates in the CA treatment compared to the CON treatment in 2023 and 2024 were applied post-emergence (1.37 kg ha^{-1}) and pre-emergence (1.81 kg ha^{-1}), respectively. Due to no data being collected on weed abundance in this study, it was not possible to conclude whether there were distinct differences in weed type and abundance within the experimental treatments. Although much literature points to higher weed abundance and changes to weed populations in CA systems due to the lack of mechanical weed management (Triplett and Dick, 2008; Soane et al., 2012), it cannot be concluded that higher herbicide usage in this study was a result of a higher weed burden in the CA treatment. One explanation for higher herbicide usage is the presence of surface residues in the CA treatment, which have been shown to reduce the efficacy of some herbicide active ingredients (Nikolić et al., 2021; Flower et al., 2021, 2022).

Both experimental treatments were managed with distinct differences in the chemical approach to agronomy with respect to the chemistry used, the application rates of pesticide active ingredients, and the application timings. Therefore, this study also assessed the environmental and health risks of the agronomic approaches to the experimental treatments. This was achieved by obtaining the chemical identity, physicochemical, human health and ecotoxicological data for all pesticide active ingredients from the Pesticide Properties Database (PPDB), an online resource, hosted by the University of Hertfordshire (Lewis et al., 2016) using the methodology outlined in Section 6.2.5. The pesticide properties data were then used to calculate the Danish Pesticide Load Indicator (PLI), outlined by Kudsk et al. (2018); Lewis et al.

(2021). The PLI does not try to account for damage to the environment but aims to reflect the relative environmental pressure that occurs due to the differing hazardous nature of the pesticides used and the variability in quantities applied (Lewis et al., 2021). The indicator is comprised of three sub-indicators that aim to measure the potential pressure on human health (PLI_{HH}), environmental fate (PLI_{FATE}), and ecotoxicity (PLI_{ECO}). This indicator is designed to be used at a national level to determine appropriate taxation of certain pesticides and to enable monitoring of usage trends and environmental load over time. In this study, we used the PLI to assess the environmental load of the experimental treatment agronomic decisions at a local level. These results can be used as a general guide to estimate the potential pesticide environmental load in CA systems, compared to CON. However, caution is advised with extrapolating the data to wider systems, as the agronomic plans used in this study are tailored to a local level, and as previously mentioned in this section, were devised by different agronomists. Therefore, at a national scale, we would hypothesise variability in the treatment pesticide load, due to local conditions and individual agronomists' opinions and assessments.

Overall, there was found to be a significantly higher PLI in the CA treatment than in the CON treatment. Despite the CON treatment having a mildly higher non-significant increases in PLI_{ECO}, PLI_{HH}, and total mass of pesticide active ingredients applied (kg ha^{-1}), the main driver to the total PLI score, was derived from a significant increase in the PLI_{FATE} in the CA treatment. Herbicides contributed 58% to the total PLI in the CA treatment, compared to the CON treatment, where herbicide usage only accounted for 15% of the total PLI. As the study by Bajwa (2014) discusses, herbicide active ingredients have substantial persistence in the soil, which can have implications for groundwater pollution and harmful effects to soil microorganisms. Therefore, higher usage of herbicides in the CA treatment in this study was a key driver of higher PLI_{FATE} and the total PLI values. This result highlights the importance for farmers and agronomists managing CA systems who want to reduce the environmental risk of their crop management to take into account not only product toxicity, but also environmental persistence. It also highlights the importance for farmers and agronomists to use an Integrated Weed Management (IWM) approach to CA, combining a variety of principles to control weed populations and not to rely solely on a chemical approach (Farooq and Siddique, 2015; Bajwa, 2014).

Hypothesis H_2 was supported by the results. While total pesticide application rates (kg ha^{-1} of active ingredients) did not differ significantly between treatments, there were notable significant differences in the composition and crop management

programme. The CON treatment applied significantly higher quantities of fungicides and insecticides, while the CA treatment applied significantly more herbicides. This aligns with existing literature suggesting increased herbicide reliance in CA systems due to the absence of mechanical weed control. However, due to differences in crop rotations and agronomists managing each system, these findings should be interpreted with caution.

Hypothesis H_4 was not supported by the results of this study. Environmental risk, assessed using the Danish PLI, was significantly higher in the CA treatment, primarily due to elevated PLI_{FATE} scores associated with herbicide persistence. These results underscore the importance of integrating non-chemical weed control strategies within CA systems to avoid potential negative environmental trade-offs and demonstrate that reduced pesticide quantities do not necessarily equate to reduced environmental risk.

6.4.4 Crop Yield

This section addresses the tests of the following hypotheses (H):

- H_3: CA will result in a significantly lower yield than the CON treatment.

There is currently mixed evidence on the effects of CA on crop yields (Pittelkow et al., 2015; Rockström et al., 2009; Corbeels et al., 2014; Shakoor et al., 2021; Van den Putte et al., 2010). Crop yield responses are highly dependent on a range of crop, climate, soil, and management factors. For example, Pittelkow et al. (2015) found that the response to crop yield in CA was highly dependent on crop choice. Yield declines were observed in wheat (-2.6%), rice (7.5%), and maize (-7.6%); however, no yield differences were detected in oilseed, cotton, and legume crops. Whereas, the meta-regression analysis by Van den Putte et al. (2010) found that the soil type was a significant factor in the crop yield response to CA. Typically, there is consensus that yield declines in the initial years of the transition to CA are likely, which reduce over time, and the magnitude of the observed yield declines can be minimised by implementation of all three principles of CA and not just NT (Pittelkow et al., 2015; Van den Putte et al., 2010).

Fear of reduced yields under CA is seen as a primary constraint to the uptake of the system in Europe (Morris et al., 2010). Despite the likelihood of lower yields in the initial years of CA, this has not stopped many farmers from adopting the system, citing reductions in expenditure which balance the loss of yield. However, one of the

key barriers to large-scale adoption of CA is the view that crop yields are more variable than a CON system, as any lack of yield reliability will strongly influence farmer acceptability of NT-based systems (Soane et al., 2012). This is of particular concern in a wet climate like the UK, as already discussed in this chapter, crop establishment can be more variable in CA in some cases (Cannell et al., 1986). For example, it has been shown that in northern and western Europe crop yields in NT systems are lower than those after ploughing in wet seasons, while there may be little or no difference in dry seasons (Alakukku et al., 2009; Riley et al., 2017; Soane et al., 2012). This has also been shown in the UK, where the study by Cannell et al. (1986) found that winter wheat yields for drained and undrained ploughed treatments were more variable in NT systems. The NT treatment established poorly in a wet autumn, resulting in poor yields, whereas there was no difference detected in crop establishment or yield for the tillage-based treatments. These results concur with the findings in this study, where during a wet-autumn crop establishment in the CA treatment resulted in a failed crop, compared to the CON treatment, which established an, albeit sparsely populated, crop of oilseed rape. However, both treatments in this study exhibited large yield variability when compared to the national average; the CON treatment yield ranged from 172% to 63% of the national average. Whereas the CA treatment yielded from 148% to 84% of the national average, this figure discounts the failed crop of oilseed rape in the final year of the experiment. These results highlight that once established, CA has similar variability in crop yield. Despite identifying higher yields in the CON treatment in the first and second years of this experiment, no statistical differences in crop yield between the experimental treatments were identified.

The results of the yield power analysis performed in this study found that the expected effect size for the detection of crop yield differences was low ($d = 0.02$). This suggests that detecting statistically significant differences in yield would require a very large sample size to achieve sufficient power. This indicates that the average yield differences between the agricultural systems analysed in this dataset are negligible relative to the variability within the data. Such a large quantity of samples was not possible within the constraints of this study, due to the experimental design. This study uses only five true replicates and therefore for some variables, such as crop yield, it poses limitations for detecting statistical differences even if they exist within the experiment (e.i, a Type II error). In this study, the percentage difference from the national crop yield for the experimental treatments was analysed for statistical differences. As we failed to reject the null hypothesis that the experimental treatments

did not affect crop yield, there remains a possibility of a Type II error, meaning that a true effect may exist but was not detected due to limited statistical power.

The assessment of yield difference maps revealed notable spatial and temporal dynamics in the performance of the CON and CA treatments across the study fields. In the first year, substantial spatial variability was observed, with contrasting patterns between the two fields. The smaller field exhibited higher estimated yields under the CON treatment across large areas, whereas in the larger field, the CA treatment appeared to outperform CON management over a greater proportion of the area. This suggests that the relative benefits of the two management systems may be field-specific, possibly influenced by underlying biophysical heterogeneity such as soil type, topography, or historical management, which may interact differently with the treatments.

Interestingly, this field-specific trend was not maintained in the second year during the winter wheat crop. The yield difference maps from Year 2 showed reduced spatial variability, with most areas in both fields showing either similar yields or a slight advantage under CON management. This shift could reflect several factors, including seasonal climatic conditions, crop-specific responses to the treatment management, or the cumulative effects of the treatments over time.

Overall, these findings highlight the importance of considering both spatial and temporal factors when evaluating the performance of CA. The results suggest that CA and CON practices do not have uniform effects in space or time, and that management decisions should account for site-specific characteristics. Future research should aim to identify the drivers of spatial crop performance in CA.

Hypothesis H_3 was not supported by the results. Although the CA treatment experienced a complete crop failure in one year due to poor establishment under wet conditions, there were no statistically significant differences in crop yield between the CA and CON treatments across the study period. Yield variability was high in both systems, and the CA treatment showed comparable yield ranges to the CON system, excluding the failed oilseed rape crop. Power analysis revealed a very low expected effect size ($d = 0.02$), indicating that a much larger sample size would be needed to detect meaningful differences. As such, the lack of statistical significance may be due to insufficient replication (Type II error) rather than the absence of a real treatment effect. These findings are consistent with broader literature, which suggests yield declines may occur in the early years of CA adoption, particularly under wet conditions, but that yield outcomes are highly context-dependent and may converge with CON yields over time.

6.5 Conclusion

This chapter has evaluated the agronomic outcomes of adopting CA compared to CON over three years, addressing hypotheses related to crop establishment, input usage, environmental impact, and yield.

CA presented significant challenges for crop establishment, particularly under adverse weather conditions. The failure of the oilseed rape crop in 2024 highlighted the vulnerability of NT systems to wet soil conditions and the importance of appropriate equipment and timing. However, for other crops, establishment losses in CA were comparable to the CON system, indicating that with appropriate management, reliable establishment is achievable. Thus, Hypothesis H_1 was partially supported.

Regarding nutrient inputs, the CA treatment applied significantly less N fertiliser, aided by both crop rotation choices and the use of foliar N. Despite these reductions, soil nutrient availability (P, K, Mg, and total N) increased under CA, suggesting improved nutrient cycling and retention. These results support Hypothesis H_2 for fertiliser use, demonstrating that CA can achieve more nutrient-efficient production with lower synthetic inputs.

For pesticides, total quantities applied did not differ significantly between systems, but the CA treatment relied more heavily on herbicides, while the CON system used more fungicides and insecticides. The environmental risk, measured using the Danish Pesticide Load Indicator, was significantly higher under CA, driven by herbicide persistence (PLI_{FATE}). This finding underscores the importance of integrated weed management strategies in CA systems. Therefore, Hypothesis H_2 was only partially supported for pesticide use: while overall inputs may not increase, their environmental impact may be greater under CA if not managed carefully.

Finally, although crop yield variability was high in both systems, no statistically significant differences were found between treatments. A complete crop failure in the CA treatment in one year did not result in a significant overall treatment effect, likely due to the low statistical power of the study (only five replicates). Power analysis indicated that very large sample sizes would be needed to detect differences of the magnitude observed. Hypothesis H_3 was not supported, though the findings align with literature suggesting that yield outcomes under CA vary by context and may improve over time.

In summary, the results indicate that CA can reduce input use and maintain comparable yields under certain conditions, but poses challenges in crop establishment and may increase environmental pesticide risks without careful management. These

findings highlight the importance of the continued development of site-specific agronomic strategies to support the successful implementation of CA in the UK context.

Chapter 7

Soil Greenhouse Gas Emissions in Conservation Agriculture

7.1 Introduction

Human activities are driving climate change, principally through emissions of greenhouse gases (GHG). Global surface temperature in 2011–2020 reached 1.1°C above temperature averages from 1850–1900 (IPCC, 2023). Urgent action is required, at unprecedented scales and across all sectors, to meet the target of no more than 1.5 °C of warming above pre-industrial levels, set out by the IPCC (Allen et al., 2022).

Net GHG emissions have increased since 2010 across all major sectors, with 22% of total GHG emissions (13 Gt $CO_2{-}eq$) attributed to the Agriculture, Forestry and Other Land Use (AFOLU) sector (IPCC, 2023). The global agricultural industry faces major challenges due to changing climates, whilst simultaneously being a significant contributor to climate change itself (Guidoboni et al., 2023). Without action, it is predicted that by 2050 the combination of climate change and soil degradation will reduce global crop yields by approximately 10%, extending to up to 50% in at-risk regions (Scholes et al., 2018). Therefore, there is a need for agriculture to adapt to climate change whilst maintaining food security and minimising impacts to the environment, such as reducing GHG emissions and sequestering CO_2 in the soil (Follett, 2001). In recent years, there has been a growing number of calls to redesign the global food system (Giller et al., 2021).

Conservation Agriculture (CA) is proposed as an alternative to conventional agriculture (CON). It claims to improve production sustainability by conserving and enhancing soil health and the associated biota (FAO, 2014; Page et al., 2020). It therefore has the potential to mitigate the negative effects of traditional crop production, such as soil organic matter depletion, soil erosion, and GHG emissions (Page

et al., 2020).

CA consists of three crop management principles: 1) No tillage: defined as the direct planting of crops with a minimum of soil disturbance (Derpsch et al., 2014). 2) Permanent soil organic cover: defined as the use of crop residues or cover crops on the soil surface during the crop rotation, covering at least 30% of the soil between harvest and seeding (Page et al., 2020). 3) Diversified crop rotation: defined as the process of using a diversified complex crop rotation, sequence or association which are specifically tailored to local environments and climatic conditions, with the inclusion of leguminous crops and cover crops (Kassam et al., 2019; Derpsch and Friedrich, 2009; Knapp and van der Heijden, 2018).

Soil management practices are known to affect soil GHG fluxes, including carbon dioxide (CO_2), methane (CH_4) and nitrous oxide (N_2O) (Dendooven et al., 2012b). In the UK, agriculture is a major source of GHG emissions, accounting for 1.7% of total CO_2 emissions, 69% of total N_2O emissions, and 48% of all CH_4 emissions in 2020 (DEFRA, 2022). Reducing these emissions is a major challenge for the sector and is a key goal of the National Farmers Union (NFU) in the UK, which is aiming for a net-zero agricultural sector by 2040 (NFU, 2023). This is also the goal set by the Department for Environment, Food and Rural Affairs (DEFRA), which is aiming to reduce net GHG emissions from the agriculture sector as much as possible to aid meeting the goal of the UK government of a net-zero emission economy by 2050 (HM Government, 2023). For this to be achieved, it is necessary for researchers to accurately estimate potential GHG emissions from any proposed changes to crop management and tillage practices to be able to advise farmers on the most effective methodologies under different environmental and soil conditions.

Reduced tillage is considered an effective technique for mitigating agricultural contributions to climate change, especially when considering reducing soil degradation and energy usage in crop production, while potentially increasing C sequestration. However, the effects of reduced tillage on GHG emissions are still controversial (Shakoor et al., 2021). Previous research reports increases (Shakoor et al., 2021; Valujeva et al., 2022), decreases (Abdalla et al., 2016; Sainju, 2016; Zhang et al., 2010), and no changes (Dendooven et al., 2012b; Tellez-Rio et al., 2015) in GHG emissions in comparison to CON.

The retention of crop residues as soil cover can support many agronomic and ecosystem service improvements, such as erosion control (Fryrear and Skidmore, 1985), enhanced nutrient cycling (Turmel et al., 2015), and soil C sequestration (Blanco-Canqui and Lal, 2007; Chen et al., 2013). However, the effects of crop

residue return on GHG emissions can also be variable, with previous research reporting increased emissions in treatments where crop residues are retained compared to treatments where residues are removed (Zhang et al., 2016). A meta-analysis by Hu et al. (2019) found that N_2O emissions are significantly increased when high and low quantities of biomass are added to the soil, but not significantly affected when medium quantities are added. This is suggested by the authors to be related to the C:N ratio and the lignin:N ratio of the biomass; when high amounts of C and N are applied to the soil this promotes heterotrophic microbial respiration which depletes soil O_2 concentrations, thus promoting denitrification and N_2O production (Gomes et al., 2009). For example, a study by Garcia-Ruiz and Baggs (2007) found that soils with the addition of legume crop residues can have N_2O emissions of close to three times that of a non-amended soil.

Crop sequence and crop type can also be important drivers of net GHG flux from agricultural cropping systems, which is mainly thought to be driven by differences in N availability and root biomass (Abdalla et al., 2016). The meta-analysis by Shakoor et al. (2021) found that crop species showed significant positive and negative effects on GHG fluxes, depending on the individual crop species. They found that non-legume crops increased global warming potential (GWP) in comparison to legume crops because non-legume crops required a high amount of N fertiliser to sustain crop production, which stimulates increased N_2O emissions. In addition, the global meta-analysis by Sainju (2016) reported that GHG flux was 168 - 215% lower with perennial than annual cropping systems, but 41 to 46% greater with crop rotation than mono-cropping.

There are many studies investigating the effects of specific components of CA practice on GHG fluxes. However, the effects of the simultaneous application of these components via typical management on net GHG flux are less well studied. Many previous studies are based on the reductive approach of evaluating soil GHG flux from CA, where a single variable is changed. However, this approach is uninformative for real-world scenarios where farmers must adopt all the principles of a given cropping system to achieve the best performance. This is illustrated by the results from the meta-analysis by Pittelkow et al. (2015) who show that adoption of no till in isolation significantly reduces crop yield. They also reported that, when CA principles are unanimously applied, the magnitude of yield decline is minimised and concluded that all three principles must be adhered to for the best outcomes. Therefore, there is a need for more "systems-level" studies evaluating CA in realistic commercial settings to assess the differences in GHG flux between CA and CON.

7.1.1 Research Aims and Hypotheses

The objective of this research chapter is to evaluate the greenhouse gas (GHG) emissions in winter wheat (*Triticum aestivum* var. *Extase*) managed using a CA compared to a CON with a systems-level design. The aim is to evaluate the effectiveness of implementing CA for in-field GHG flux reduction in the UK agricultural sector. To do so, this paper will test the hypothesis that crop production utilising the CA principles.

The research aims (*A*) of this chapter are:

- Monitor in-field greenhouse gas emissions during the transition to CA in comparison to a CON and evaluate the effectiveness of CA as a methodology to reduce soil-derived GHG emissions.

This chapter tests the following hypotheses (*H*):

- H_1: CA is an effective methodology for reductions of soil CO_2 emissions in comparison to CON.
- H_2: CA is an effective methodology for reductions of soil N_2O emissions in comparison to CON.
- H_3: CA is an effective methodology for reductions of soil CH_4 emissions in comparison to CON.
- H_4: CA reduces the overall Global Warming Potential (GWP) compared to CON.

7.2 Materials and Methods

The experiment was carried out at the field experiment detailed in Section 3, during 2023. A subset of 10 of the 150 randomly generated sampling points described in Chapter 3 were taken using a random number generator, to include 1 sampling point for each experimental plot. The positions of the randomly generated sampling points are shown below in Figure 7.1.

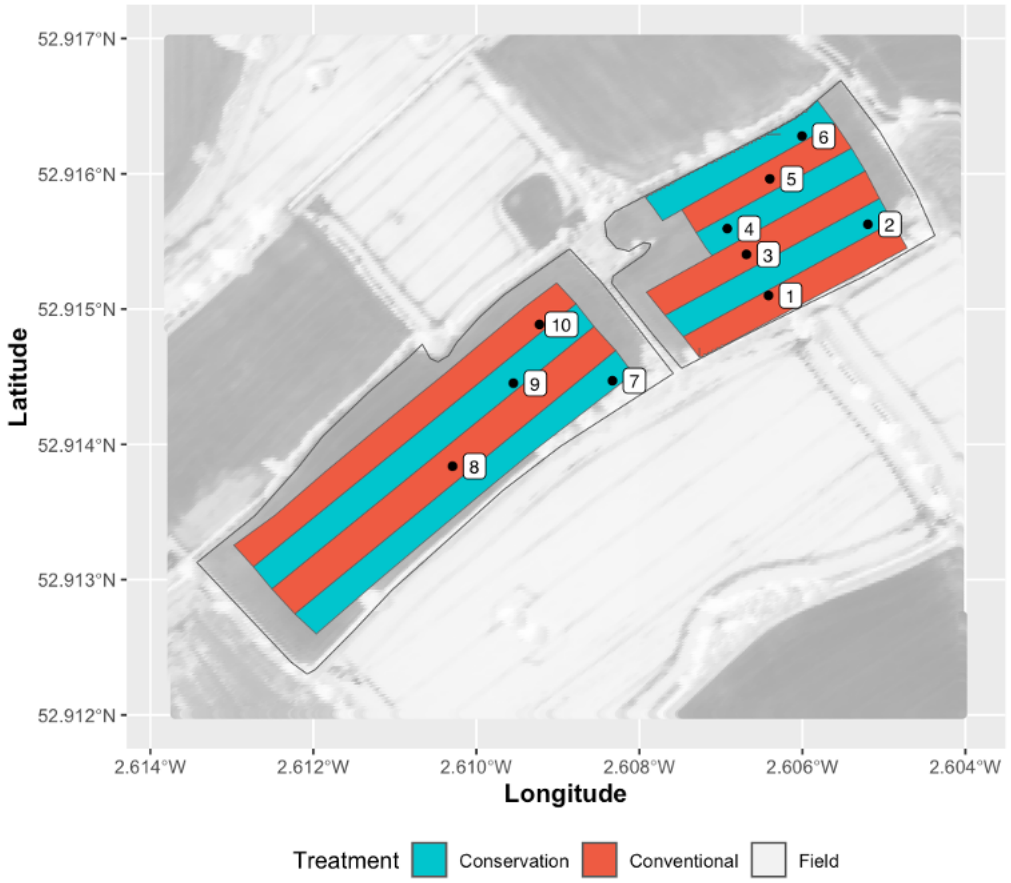

Figure 7.1: Experimental design - Sampling points are indicated by the black points with the corresponding sample number labelled.

7.2.1 Greenhouse Gas Sampling

The sampling for GHG emission analysis was performed twice weekly, where possible, from 10/03/2023 to 28/07/2023. Samples were manually taken from 10 static flux chambers, with one chamber base allocated per plot. Chambers consisted of a cylindrical galvanised steel chamber (400 mm diameter x 300 mm height) with the top of the chamber completely sealed. They were equipped with an internal fan at the top, which was also fitted with a rubber butyl gas septa to allow for the extraction of gas samples. Chambers were hermetically sealed on top of stainless-steel bases (diameter 399 mm x height 150 mm) which were inserted into the soil to a depth of 75 mm. The chamber bases were inserted seven days before the first sample was collected to allow time for the gas flux from the soil disturbance caused by insertion of the chamber bases to subside. The chamber and base contained rubber seals on the inside of the chamber and the outside of the base to create an airtight seal.

Figure 7.2: The static chamber base, which remained in the soil for the duration of the sampling period. Source: Author's own

Figure 7.3: The static chamber top, which was placed onto the chamber base during individual samples. Source: Author's own

The sampling order of all chambers was randomised every sampling date, with samples collected between 15:00 and 17:00 each sample day when possible. Before sampling, the internal fan was turned on for two minutes. All chambers were sampled 60 minutes after closing. Samples were extracted using a 60 ml polypropylene syringe and transferred to pre-evacuated 20 ml crimp top vials, venting excess gas to ensure samples were stored at atmospheric pressure. An additional three vials were filled with atmospheric samples at equal times between soil flux samples, to allow for correction of sampled gases for the atmospheric gas concentrations during the sampling period. The samples were stored at room temperature and analysed as soon as possible after collection.

7.2.2 Greenhouse Gas Flux Analysis

The concentration of GHGs was determined by gas chromatography using an Agilent 7890A gas chromatograph fitted with a Hewlett-Packard automated head-space sampler, and an Electron Capture Detector (ECD). Methane (CH_4) and carbon dioxide (CO_2) were detected using a Flame Ionisation Detector (FID), fitted with a methaniser (350°C), and nitrous oxide (N_2O) via an Electron Capture Detector (ECD; 300°C). Daily fluxes were measured in parts per million (ppm) and were converted to mg CO_2−C hr^{-1} m^{-2}, mg CH_4−C hr^{-1} m^{-2} and mg N_2O−C hr^{-1} m^{-2} using the following equation (7.1):

$$mg\ x{-}Xhr^{-1}m^{-2} = \frac{\frac{ppm}{h}\ \times VH\ \times U}{T \times R} \tag{7.1}$$

Where:

- $x{-}X$ is the daily flux.
- VH is the total head-space volume (l).
- u is the atomic weight.
- T is the mean day temperature (K).
- R is the gas constant (0.0821 atm L^{-1} mol K^{-1}).

Values were converted to cumulative fluxes, assuming linearity of flux rate between each measurement day.

7.2.3 Environmental Data Collection

The chambers were fitted with an internal thermometer and hygrometer to monitor internal temperature and humidity. Daily temperature and precipitation data were obtained from a weather station located 20 km from the experimental site at Lat. 52.794, Lon. -2.663, 72 metres above sea level (Met Office, 2023). Soil temperature and volumetric soil moisture content were acquired from `https://cosmos.ceh.ac.uk/` for a site 17 km from the experimental site (Lat. 53.0264, Lon. -2.7005, 78 metres above sea level) collected as part of the COSMOS-UK project (Cooper et al., 2021).

7.2.4 Global Warming Potential

Global warming potential was calculated for all cumulative fluxes for the entire sampling period using the global warming potential values reported in the IPCC Sixth Assessment Report ($CO_2 = 1$, $CH_4 = 27.2$, $N_2O = 273$; (IPCC, 2023)). The equations for calculating the GWP CO_2 equivalents are presented below in Equations 7.2, 7.3, and 7.4.

$$CO_2{-}e\ m^{-2}day^{-1} = CO_2\ m^{-2}day^{-1} \times 1 \tag{7.2}$$

$$CO_2{-}e\ m^{-2}day^{-1} = CH_4\ m^{-2}day^{-1} \times 27.2 \tag{7.3}$$

$$CO_2{-}e\ m^{-2}day^{-1} = N_2O\ m^{-2}day^{-1} \times 273 \tag{7.4}$$

Yield-scaled GWP was calculated by dividing the CO_2 equivalent emissions by the crop yield (harvested at 14.5% moisture) and expressed in units of kg $CO_2{-}e$ eq. kg^{-1} following the methodology of O'Neill et al. (2021). A detailed methodology of the crop growth and yield can be viewed in Chapter B.

7.2.5 Statistical Analysis

Statistical analysis was done using `R` version 5.1 (R Core Team, 2023). The `lme4` package (Bates et al., 2015) was used to employ linear mixed-effect models to compare CO_2, N_2O, and CH_4 emissions in the experimental treatment systems. The basic model formula was:

$$\log(y_i) = \beta_0 + \beta_1 \cdot \text{Treatment}_i + u_{\text{block}_i} + u_{\text{batch.date}_i} + \epsilon_i \tag{7.5}$$

Where:

- β_0 is the overall intercept of the model.
- β_1 is the fixed effect of the treatment factor, estimating the effect of treatment on log-transformed GHG emissions.
- u_{block_i} is the random intercept for block, accounting for variability between experimental blocks.
- $u_{\text{batch.date}_i}$ is the random intercept for batch date, accounting for variability associated with sampling or measurement dates.
- ϵ_i is the residual error, representing unexplained variation in the response.

The model was fitted using REML (restricted maximum likelihood estimation), a modification of maximum likelihood estimation that is more precise for mixed-effects modelling (Baayen et al., 2008). Crop yield for both treatments was compared using a generalised linear model using the `glm` function within the stats package (R Core Team, 2023) using the total crop yield as the response vector and the treatment as the linear predictor of the response variable. Yield-scaled Global Warming Potential (GWP) was also compared using a generalised linear model, with the yield-scaled GWP as the response variable and the treatment as the linear predictor.

7.3 Results

7.3.1 Environmental Conditions

The mean daily temperature during the study period ranged from 0°C on 08/03/2023 to 21.3°C on 24/06/2023 (Figure 7.4). Total rainfall during the study period was 222 mm, with a mean of 1.73 mm per day (Figure 7.4). The highest daily rainfall was on 09/03/2023, which recorded 12.57 mm. The mean relative humidity for the study period was 75.7%, ranging from 54.1% to 93%. The climate data for the study period is presented below in Figure 7.4 and the comparison with historic averages is presented in Figure 3.2.

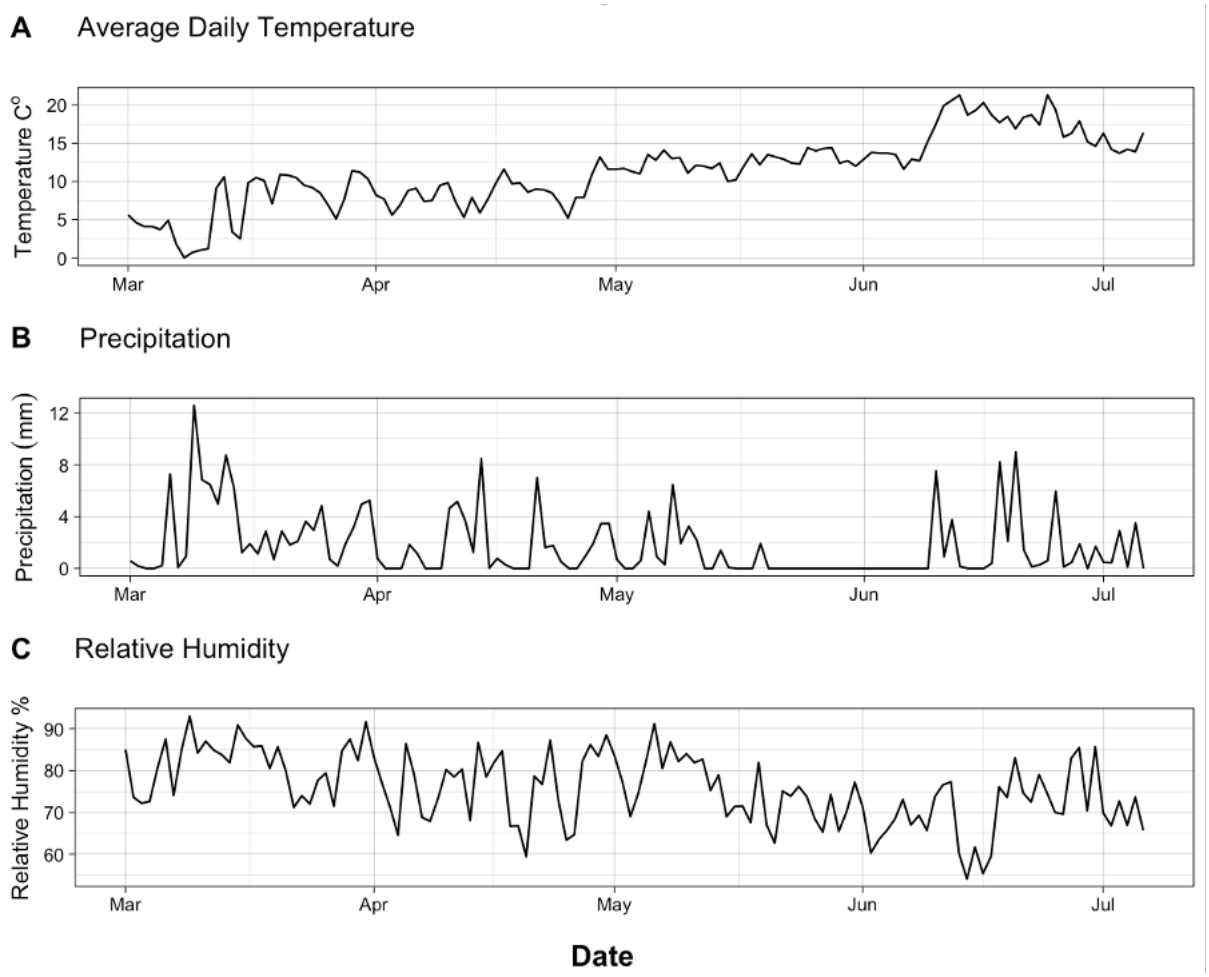

Figure 7.4: Daily mean temperature (°C) (**A**), Daily precipitation (mm) (**B**), Daily Relative humidity (%) (**C**).

7.3.2 Soil Data

Soil samples ranged from 48% - 65% sand content, 16% - 21% clay content and 19% - 32% silt content, classified either as a clay loam, sandy loam or sandy clay loam (Figure 4.2). Soil organic matter ranged from 3.05% - 4.17%, with a bulk density from 1.14 g cm^{-3} – 1.58 g cm^{-3} (5.3), and a pH from 5.78 - 6.72. Soil available phosphorus ranged from 9.6 mg l^{-1} - 17.2 mg l^{-1} (Figure 5.6), and available potassium from 79.75 mg l^{-1} - 234.85 mg l^{-1} (Figure 5.7). Soil temperature during the sampling period ranged from 3.7 °C on 11/03/2023 to a maximum temperature of 19.6 °C on 19/06/2023 (Figure 7.5). Volumetric soil moisture ranged from the minimum of 6.8% on 09/06/2023 to a maximum of 32.4% on 15/04/2023 (Figure 7.5).

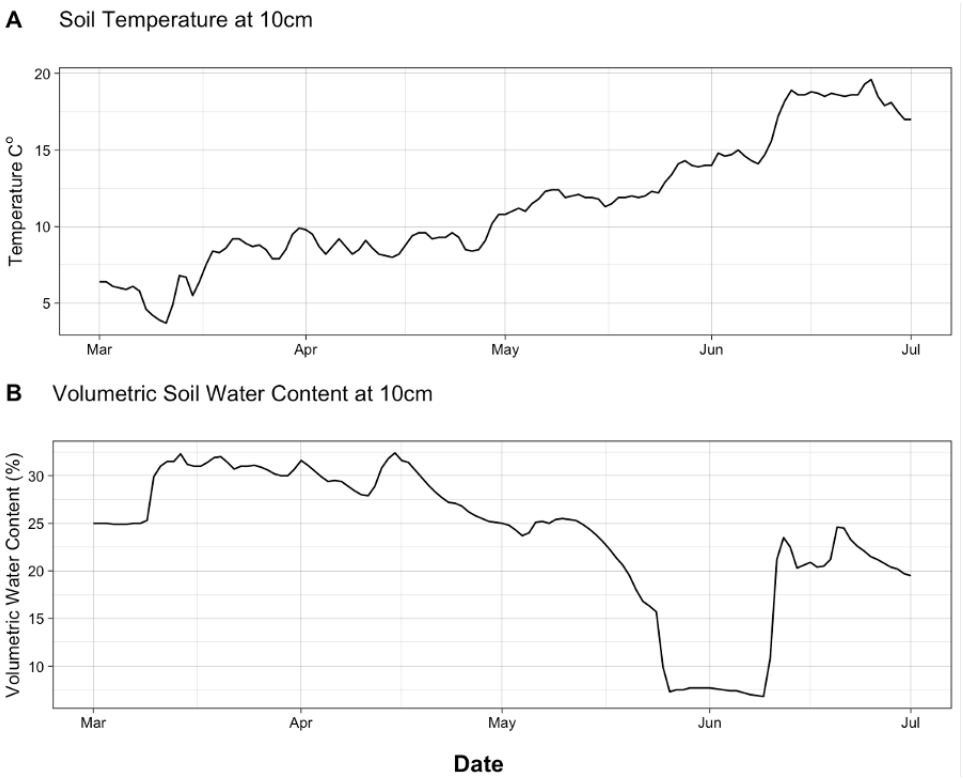

Figure 7.5: Soil temperature (°C) (**A**) and Volumetric Soil Moisture (**B**). Data collected from (Cooper et al., 2021)

7.3.3 Carbon Dioxide Flux

The mean daily CO_2 flux ranged from 0.04 g CO_2−C m^{-2} day^{-1} to 29.22 g CO_2−C m^{-2} day^{-1} in the CON treatment and 0.06 g CO_2−C m^{-2} day^{-1} to 30.41 g CO_2−C m^{-2} day^{-1} in the CA treatment (Figure 7.6). The lowest mean daily CO_2 flux detected

in both treatments occurred on 07/04/2023, and the greatest mean daily CO_2 flux was detected on 17/05/2023 in both treatments. The mean daily CO_2 flux detected for the whole sampling period was 14.70 g CO_2−C m^{-2} day^{-1} in the CON treatment and 15.43 g CO_2−C m^{-2} day^{-1} in the CA treatment. Cumulatively, the CON treatment emitted 264.7 g CO_2−C m^{-2} day^{-1} during the sampling period, compared to the CA treatment which emitted 277.9 g CO_2−C m^{-2} day^{-1} in total during the sampling period (Figure 7.7).

The CA treatment did not significantly affect soil CO_2 emissions in comparison to the CON treatment (β = 0.02, SE = 0.06, Z = 0.05, p = 0.96). Additionally, CO_2 emissions were not affected by N fertiliser addition (β = -0.001, SE = 0.02, Z = -1.27, p = 0.2), or volumetric soil moisture content (β = 0.08, SE = 0.05, Z = 1.7, p = 0.1). However, soil CO_2 emissions were significantly affected by mean daily soil temperature (β = 0.68, SE = 1.67, Z = 4.1, $p < 0.001$).

7.3.4 Nitrous Oxide Flux

The mean daily N_2O flux ranged from -0.25 mg N_2O−N m^{-2} day^{-1} to 2.88 mg N_2O−N m^{-2} day^{-1} in the CON treatment and -0.16 mg N_2O−N m^{-2} day^{-1} to 2.32 mg N_2O−N m^{-2} day^{-1} in the CA treatment (Figure 7.6). The lowest mean flux occurred on 03/04/2023 for both treatments, where the mean flux was found to be negative for both the CON (-0.25 mg N_2O−N m^{-2} day^{-1}) and the CA (-0.16 mg N_2O−N m^{-2} day^{-1}) treatments. The greatest N_2O flux was on 16/04/2023 for both treatments, 2.88 mg N_2O−N m^{-2} day^{-1} in the CON treatment and 2.32 mg N_2O−N m^{-2} day^{-1} in the CA treatment. The mean daily N_2O flux detected for the whole sampling period was 0.51 mg N_2O−N m^{-2} day^{-1} in the CON treatment and 0.31 mg N_2O−N m^{-2} day^{-1} in the CA treatment. The total cumulative flux for the CON treatment was 9.27 mg N_2O−N m^{-2} day^{-1} and in the CA treatment it was 5.59 mg N_2O−N m^{-2} day^{-1} for the entire sampling period (Figure 7.7).

The CA treatment significantly reduced N_2O emissions when compared to the CON treatment (β = -0.56, SE = 0.12, Z = -5.55, $p < 0.001$). When other variables were considered, soil N_2O emissions were not significantly effected by soil temperature (β = -0.1, SE = 0.15, Z = -0.75, p = 0.46) or volumetric soil moisture (β = 0.02, SE = 0.04, Z = 0.58, p = 0.56). However N_2O emissions were significantly effected by N fertiliser addition (β = 0.01, SE = 0.003, Z = 5.09, $p < 0.001$).

7.3.5 Methane Flux

The mean daily flux in the CON treatment ranged from -0.68 – 0.15 mg CH_4−C m^{-2} day^{-1} and ranged from -0.59 – 0.05 mg CH_4−C m^{-2} day^{-1} in the CA treatment (Figure 7.6). The greatest flux in the CON treatment occurred on 10/03/2023 and on 22/03/2023 for the CA treatment. The lowest CH_4 flux in the CA treatment occurred on 07/04/2023 and on 03/04/2023 in the CON treatment. The mean flux for the sampling period was -0.14 and -0.17 mg CH_4−C m^{-2} day^{-1} for the CON and CA treatments, respectively. The total cumulative flux during the sampling period for the CON treatment was -2.48 mg CH_4−C m^{-2}, and -3.04 mg CH_4−C m^{-2} for the CA treatment (Figure 7.7).

CH_4 flux was not significantly affected by the treatment ($\beta = 5.56 \times 10^{-5}$, $SE = 1.11 \times 10^{-3}$, $Z = 0.05$, $p = 0.96$). When other variables were considered, CH_4 flux was not significantly affected by N fertiliser addition (β = -0.004, $SE = 0.005$, Z = -0.69, $p = 0.49$), soil temperature ($\beta = 0.14$, $SE = 0.13$, $Z = 1.16$, $p = 0.29$), or volumetric soil moisture content ($\beta = 0.0006$, $SE = 0.03$, $Z = 0.02$, $p = 0.98$).

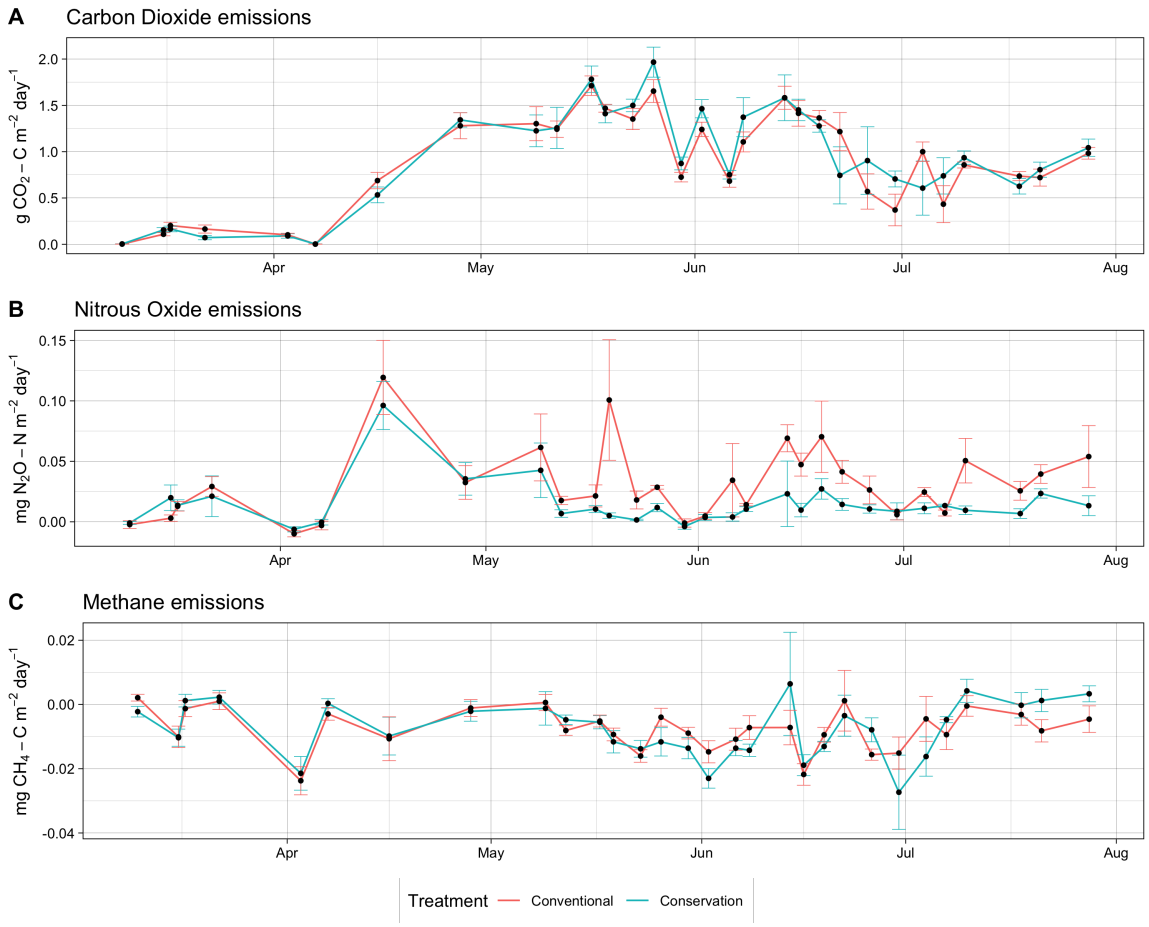

Figure 7.6: Daily GHG flux for CO_2 (**A**), N_2O (**B**), and CH_4 (**C**). Lines signify the mean ($n = 5$) and error bars show the standard error of the mean.

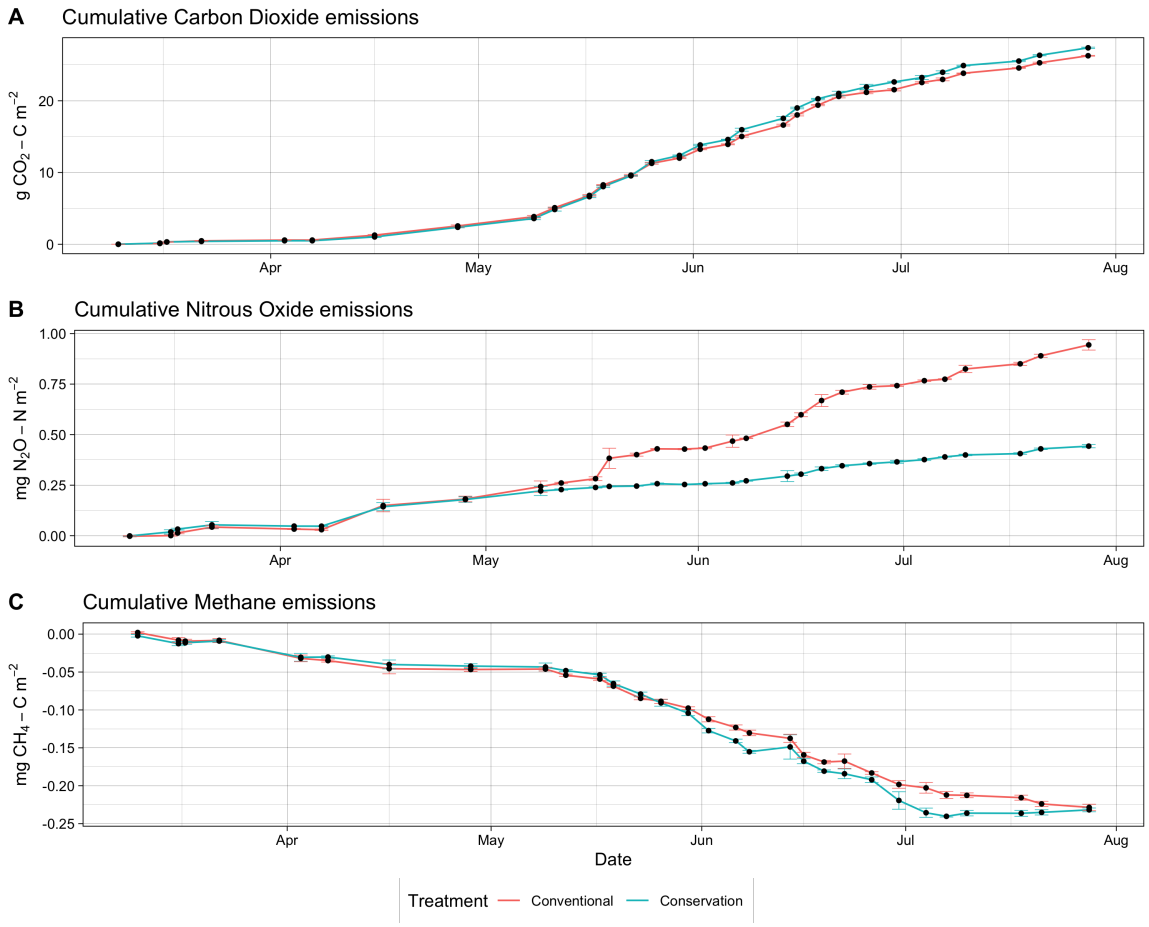

Figure 7.7: Cumulative daily GHG flux for CO_2 (**A**), N_2O (**B**), and CH_4 (**C**). Lines signify the mean ($n = 5$) and error bars show the standard error of the mean.

7.3.6 Global Warming Potential

CO_2 emissions were the largest contributor to global warming in the CON treatment (264.77 g CO_2−e m^{-2} day^{-1}) and the CA treatment (277.9 g CO_2−C m^{-2} day^{-1}) during the experimental period (Figure 7.8). In comparison, the GWP of N_2O emissions was much lower than CO_2. The N_2O flux from the CON treatment emitted 2.53 g CO_2−e m^{-2} day^{-1} (CO_2−equivalent) and 1.53 g CO_2−e m^{-2} day^{-1} in the CA treatment. Both treatments had negative methane fluxes of CH_4, which in the CON treatment reduced the GWP by -0.06 g CO_2−e m^{-2} day^{-1} and the CA treatment by -0.08 g CO_2−e m^{-2} day^{-1}.

Overall, the GWP was not significantly affected by the treatment (β = 25.55, SE = 29.15, Z = 0.88, p = 0.38), N fertiliser addition (β = -0.77, SE = 0.74, Z = -1.04, p = 0.3), or soil volumetric moisture content ((β = 17.71, SE = 18.89, Z = 0.94, p = 0.36). However, it was significantly affected by soil temperature (β = 177.6, SE = 69, Z = 2.57, p = 0.02). The CO_2−equivalent emissions of the three gases in terms of their GWPs, over a 100-year time horizon (IPCC, 2023), are shown in Figure 7.8.

Crop yield in the CON treatment ranged from 10.47 t ha^{-1} to 11.49 t ha^{-1}, with a mean of 10.96 t ha^{-1} (Figure 6.15 **B**). The crop yield in the CA treatment ranged from 7.08 t ha^{-1} to 10.78 t ha^{-1}, with a mean of 9.4 t ha^{-1}. The CA treatment produced a significantly lower yield (p = 0.044) in comparison to the CON treatment.

CO_2 emissions were the largest contributor to the yield-scaled GWP in both treatments (Figure 7.8 B). The CA treatment produced more CO_2 flux per unit of yield (295.64 kg CO_2−e ha^{-1} t^{-1} yield) in comparison to the CON treatment (241.58 kg CO_2−e ha^{-1} t^{-1} yield). However, the CON treatment produced more N_2O flux per unit of yield (2.31 kg CO_2−e ha^{-1} t^{-1} yield) in comparison to the CA treatment (1.62 kg CO_2−e ha^{-1} t^{-1} yield). In addition, the CA treatment oxidised more CH_4 per unit of yield (-7.78 kg CO_2−e ha^{-1} t^{-1} yield) in comparison to the CON treatment (-7.38 kg CO_2−e ha^{-1} t^{-1} yield). Overall, the CA treatment produced 289.48 kg CO_2−e ha^{-1} t^{-1} yield in comparison to the CON treatment which emitted 236.51 CO_2−e ha^{-1} t^{-1} yield. The yield-scaled GWP was significantly higher in the CA treatment ($\beta = 1.48 \times 10^5$, $SE = 3.19 \times 10^4$, Z = 4.65, $p < 0.001$) when compared with the CON treatment.

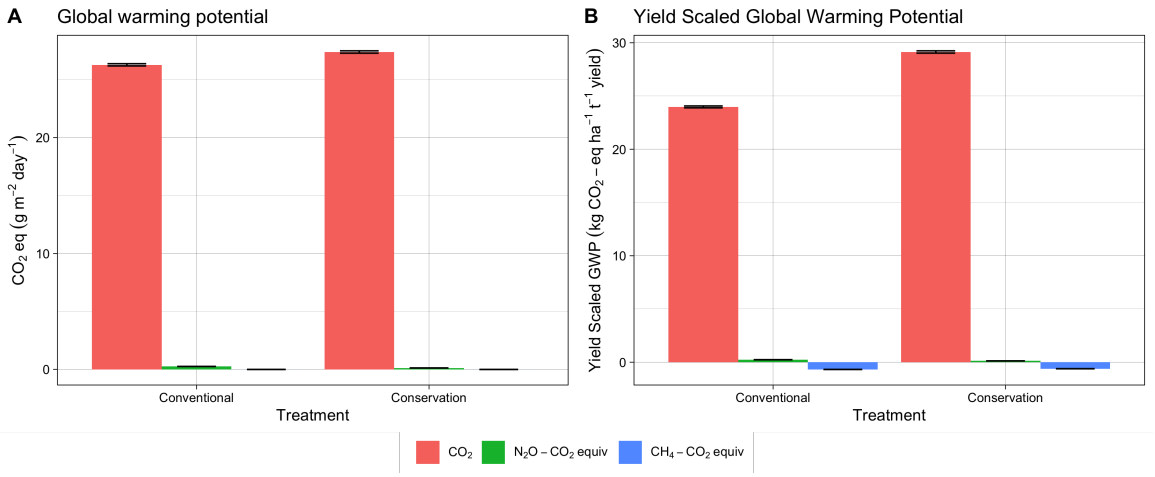

Figure 7.8: **A:** Cumulative emissions of as CO_2-equivalents for the sampling period based on the GWP of soil GHG fluxes. **B:** Yield-scaled Global Warming Potential (GWP) as CO_2-equivalents. GWP values calculated using the values reported in the IPCC Sixth Assessment Report (IPCC, 2023). Columns show means ($n = 5$), error bars show standard errors.

7.4 Discussion

This discussion section interprets the results of the in-field soil GHG flux experiment detailed in this chapter. The analysis focused on the effects of the CA and CON on soil CO_2, N_2O, and CH_4, as well as other factors that drive these fluxes. The soil GHG fluxes are also presented in relation to the crop yield of the experimental treatment as yield-scaled Global Warming Potential (GWP). The implications of treatment differences are discussed. The hypotheses to be addressed are as follows:

- H_1: CA is an effective methodology for reductions of soil CO_2 emissions in comparison to CON.
- H_2: CA is an effective methodology for reductions of soil N_2O emissions in comparison to CON.
- H_3: CA is an effective methodology for reductions of soil CH_4 emissions in comparison to CON.
- H_4: CA reduces the overall GWP compared to CON.

The hypotheses are discussed with reference to both the study findings and broader literature. The limitations of the experimental design are acknowledged to provide context for the interpretation of results.

7.4.1 Carbon Dioxide Flux in Conservation Agriculture

The CA treatment did not significantly affect soil CO_2 emissions in comparison to the CON treatment ($\beta = 0.02$, $SE = 0.06$, $Z = 0.05$, $p = 0.96$). Therefore, this study rejects the hypothesis H_1, as in this context CA was not found to reduce soil CO_2 emissions in comparison to the CON treatment. Additionally, CO_2 emissions were not affected by N fertiliser addition (β = -0.001, $SE = 0.02$, Z = -1.27, $p = 0.2$), or volumetric soil moisture content ($\beta = 0.08$, $SE = 0.05$, $Z = 1.7$, $p = 0.1$).

The most significant predictor of CO_2 emissions was soil temperature ($\beta = 0.68$, $SE = 1.67$, $Z = 4.1$, $p < 0.001$). This result is consistent with previous literature, where soil temperature has been found to be a major driver of net GHG emissions. Increases in soil temperature promote decomposition of soil organic C due to increases in microbial activity and increased gas solubility, promoting greater loss of GHGs to the atmosphere (Cosentino et al., 2013; Zhang et al., 2020). The review by Blanco-Canqui and Ruis (2018) found that no-tillage (NT) reduced the soil temperature in 12 of 18 studies reviewed, which was suggested to be due to an insulating effect and a reduction of evaporation because of the presence of surface crop residues. However, the findings by Blanco-Canqui and Ruis (2018) suggest that the rate of change that NT systems alter the soil physical environment is dependent on the duration of NT implementation. Therefore, to fully assess the effects of CA on GHG emissions, 10 years of data or more is recommended to detect the consistent effects of CA (Cusser et al., 2020; Valujeva et al., 2022). This was found by the meta-analysis by van Kessel et al. (2013) who reported that yield-scaled N_2O was increased significantly when NT was implemented <10 years, however, decreased significantly after >10 years of implementation.

Another limitation of this study was that it did not study the effects of CA on soil organic carbon (SOC) sequestration. Sequestration of SOC is an effective methodology for reducing the net GWP from agriculture. However, even though earlier reviews indicated that CA has improved potential to sequester C into the soil due to the reduction in tillage (Kassam et al., 2009; Dendooven et al., 2012b), it is now recognised that the magnitude of SOC sequestration is more variable than previously thought (Palm et al., 2014; Abdalla et al., 2016). Reviews of CA and SOC sequestration regularly conclude that it causes stratification of SOC in the upper 5 or 10 cm depth (Blanco-Canqui and Ruis, 2018), whereas the accumulation of SOC lower down the soil profile is a matter of debate amongst researchers (Gadermaier et al., 2012). This is because, in some studies, tillage is reported to have been a net sink of CO_2 by distributing SOC to lower soil horizons where it decomposes more

slowly (Abdalla et al., 2016). In addition, increased SOC can lead to increased GHG emissions, thus negating any benefit from improvements to C sequestration (Li et al., 2005). This highlights that it is important for studies reporting GHG emissions to also factor in C sequestration to the net GWP of the tillage system to understand the full C balance. For example, Dendooven et al. (2012b) reported that the GHG emissions were similar for both CA and CON treatments. However, when they considered the SOC content in the 0 - 60 cm layer, it was significantly higher in CA (117.7 t C ha^{-1}) than in CON treatment (69.7 t C ha^{-1}). When this was considered, combining the direct and indirect GHG emissions, they found that the contribution of CA to the GWP was significantly lower compared to that of the CON treatment.

7.4.2 Nitrous Oxide Flux in Conservation Agriculture

CA significantly reduced total N_2O fluxes compared to the CON in this experiment (β = -0.56, SE = 0.12, Z = -5.55, $p < 0.001$). N_2O fluxes were similar in this experiment across sampling points, except for 17/05/2023, where there was a spike in N_2O emissions in the CON treatment following N fertiliser application. Therefore, the data collected in this study supports the hypothesis H_2 as in this case, CA was demonstrated to be an effective methodology for reductions of soil N_2O emissions in comparison to CON. These results align with previous literature where several authors have reported lower N_2O emissions in well-established NT systems (>10 years of NT implementation) (van Kessel et al., 2013). However, some previous literature reports no observed changes in N_2O emissions in CA with emissions from CON treatments. For example, Dusenbury et al. (2008) and Tellez-Rio et al. (2015) both found that NT did not significantly affect N_2O emissions in comparison to CON. This illustrates the variability of soil-derived N_2O emissions, which are strongly linked with crop management, soil type, climate, and a variety of factors. For example, Rochette (2008) found that NT generally increased N_2O emissions in poorly aerated soils but had no effect in soils with good to medium aeration. This could be the case in this experiment, where the sandy clay loam soil type is well drained with field drains and thus large N_2O fluxes are unlikely as waterlogged conditions are generally avoided.

N fertiliser addition was found to be a significant driver of N_2O flux in this experiment. This result is consistent with previous studies where emissions of N_2O from agricultural soils are largely associated with N fertiliser application and organic N-based fertilisers (Cosentino et al., 2013; Rees et al., 2013). Fertiliser applications promote increased availability of mineralised N and thus the likelihood of occurrence of microbially mediated nitrifier denitrification or denitrification resulting in N_2O

emissions (Montzka et al., 2011), and thus may be influenced by the adoption of CA practices aimed at reducing nutrient inputs (Palm et al., 2014). In this experiment, the total N applied for the CON system totalled 185 kg N ha^{-1}, in comparison to the CA treatment, which totalled 133 kg N ha^{-1}, with 21 kg ha^{-1} being applied in foliar N form in four different applications. This was done to reduce losses of N via leaching and reduce the incidence of fungal crop diseases within the crop, which N fertiliser is linked with (Maywald et al., 2023). This experiment found that in the early stages of CA adoption, N fertiliser is a larger driver of N_2O emissions than the CA system. This highlights that reducing N fertilisation rates by improving Nitrogen Use Efficiency (NUE) should be a focus of future methodologies for reducing in-field GHG emissions in UK crop production. Agronomic management that can reduce N fertiliser usage and improve N use efficiency without influencing crop yields has the potential to reduce net GWP whilst maintaining current agricultural productivity (Sainju et al., 2014).

Additionally, it could be hypothesised that the effects of CA on N_2O emissions would be more pronounced where there have been more significant changes to soil properties, particularly to soil structure, which then has consequences for water and gas exchange dynamics (Tellez-Rio et al., 2015). Therefore, it could be that the N_2O emissions reported in this study after two years of implementation of a CA system are not representative of an established CA system. Where it would be hypothesised that larger differences in the soil physical and chemical properties would have occurred over time, influencing N_2O emissions (Cusser et al., 2020).

7.4.3 Methane Flux in Conservation Agriculture

CH_4 flux was not significantly affected by the treatment ($\beta = 5.56 \times 10^{-5}$, $SE = 1.11 \times 10^{-3}$, $Z = 0.05$, $p = 0.96$). Therefore does not support the hypothesis H_2 as CA was not shown to be an effective methodology for reductions of soil CH_4 emissions in comparison to CON crop production. The observed CH_4 fluxes were consistently negative across both CON and CA treatments, indicating that the soils acted as a net sink for atmospheric methane during the sampling period. The mean daily fluxes were slightly more negative in the CA treatment (-0.17 mg CH_4-C m^{-2} day^{-1}) compared to the CON treatment (-0.14 mg CH_4-C m^{-2} day^{-1}), and the total cumulative flux was similarly greater in the CA treatment (-3.04 vs. -2.48 mg CH_4-C m^{-2}). Although these differences are modest, they suggest that the CA management may slightly enhance methane uptake compared to the CON system. Importantly, while the CA system showed a slightly greater methane sink strength, the magnitude of differences

between treatments was small, and no statistical difference was observed. Therefore, further data and replication would be necessary to robustly test the hypothesis. When other variables were considered, CH_4 flux was not significantly affected by N fertiliser addition (β = -0.004, SE = 0.005, Z = -0.69, p = 0.49), soil temperature (β = 0.14, SE = 0.13, Z = 1.16, p = 0.29), or volumetric soil moisture content (β = 0.0006, SE = 0.03, Z = 0.02, p = 0.98).

7.4.4 The Global Warming Potential of Conservation Agriculture

Overall, the GWP was not significantly affected by the treatment (β = 25.55, SE = 29.15, Z = 0.88, p = 0.38), therefore this study fails to support the hypothesis H_4: CA reduces the overall Global Warming Potential (GWP) compared to CON. When the contributing components of GWP were analysed, it was identified that CO_2 emissions were the largest contributor to GWP in both treatments. This concurs with the findings of Dendooven et al. (2012b) who showed the cumulative GHG emissions over two years were similar for both CA and CON production of maize (*Z. mays L.*) in the central highlands of Mexico. However, this result was not consistent with the results of a meta-analysis by Shakoor et al. (2021) who found that NT increased CO_2 by 7.1%, N_2O emissions by 12%, and CH_4 emissions by 20.8% in comparison to CON tillage systems. However, their net GWP analysis found that NT significantly reduced the GWP in comparison to CON by 7.5%. The significant drivers of reduced GWP in NT were found to be soil physicochemical properties, crop types, climate zones, N application rate and water management compared to CON.

One limitation of this experiment was that it did not consider the indirect emissions (fuel, fertiliser, and pesticides) from the treatment systems to fully assess the GWP of both treatments. In CA systems, it is commonly found that there is a reduction in use of machinery and in crop inputs in comparison to CON systems (Kassam et al., 2009). For example, a seven-year energy audit of a CA system in India by Parihar et al. (2018) reported 49.7 - 51.5% less energy used for land preparation and 16.8 - 22.9% less energy used for irrigation compared to the CON treatment. This can result in reductions in indirect GHG emissions in comparison to CON agriculture due to a lowering in fuel usage, synthetic input application and machinery usage, which combine to reduce the overall GWP of CA systems (Ponce et al., 2022).

When the yield-scaled GWP was analysed, it was found that the yield-scaled GWP was significantly higher in the CA treatment ($\beta = 1.48 \times 10^5$, $SE = 3.19 \times 10^4$, Z = 4.65, $p < 0.001$) when compared with the CON treatment. This was due to the CA

treatment yielding significantly less than the CON treatment in this experiment. This could be linked with the reported yield decline in NT systems in the first $1-2$ years of adoption reported by Pittelkow et al. (2015). As this experiment was conducted in the second year of transition to CA, it could be hypothesised that yield decline was likely in comparison to the CON treatment. The meta-analysis by Pittelkow et al. (2015) also states that the magnitude of the yield decline diminishes from years $3-10$ post-adoption on NT practices; therefore, as this experiment continues, there may be less observable yield declines in the CA treatment and the yield-scaled GWP to reduce in the CA treatment as production increases. The reduction in crop yield could also be hypothesised to be linked to considerably less N fertiliser usage in the CA treatment. Increased N fertiliser addition has a strong non-linear relationship with increased cereal yields, where there is found to be a very strong response of grain yield to N fertiliser addition up to an economic threshold which varies depending on the cultivar (Hawkesford, 2014). Currently in the UK, farmers can legally apply between 0 – 280 kg N ha^{-1} to a wheat crop depending on the soil type and soil mineral N supply (AHDB, 2023b), with the average N application being under 200 kg ha^{-1} (Hawkesford, 2014). Therefore, it could be hypothesised that the 133 kg N ha^{-1} applied in the CA treatment was unlikely to match the grain yield of the CON treatment, which received 185 kg N ha^{-1}.

7.5 Conclusion

This chapter evaluated the effects of CA on GHG emissions in a winter wheat crop during the second year of transition from CON management. The findings showed that, while CA significantly reduced soil N_2O emissions compared to the CON system, there were no significant differences in CO_2 or CH_4 fluxes between treatments. Importantly, the overall GWP was not significantly reduced under CA, and when scaled per unit of crop yield, the CA system had a significantly higher GWP due to reduced grain yields in this early transition phase.

These results suggest that CA has the potential to lower direct soil-derived N_2O emissions, but that benefits for overall GHG mitigation and climate outcomes are contingent on maintaining or improving crop productivity and considering indirect emissions and soil C sequestration. The study highlights that the short-term effects of adopting CA may not immediately deliver GHG mitigation benefits, aligning with previous findings that long-term implementation (beyond 5–10 years) is often necessary to achieve stable improvements in soil properties and productivity.

In summary, while CA demonstrates promise as a climate-smart management approach, its effectiveness in reducing net GHG emissions will depend on context-specific management, duration of adoption, and integration with practices that sustain yields and improve nitrogen use efficiency. However, there is a need for more research to be performed across multiple soil and climate types, and crop species, as all are known to be significant drivers in GHG emissions (Abdalla et al., 2016; Shakoor et al., 2021). Future research should focus on long-term monitoring of both direct and indirect GHG emissions, changes in soil C stocks, and yield performance to provide a comprehensive assessment of CA's potential for climate change mitigation in UK arable systems, as the effects of CA on soil physicochemical properties take time to change and thus may influence GHG emissions over time (van Kessel et al., 2013; Cusser et al., 2020).

Agriculture is a key industry in the focus of future climate change mitigation, and currently, policymakers are identifying support mechanisms that could be provided to farmers to reduce GHG emissions whilst maximising agricultural production. However, before the introduction of any support mechanisms, it is necessary to understand which management practices reduce GHG emissions in specific soil and climatic conditions (Valujeva et al., 2022). Thus, there is a need for more research on CA management components as well as systems-level studies which combine those components, which focus on the effects of CA on net GHG emissions and net GWP.

Chapter 8

Economic Analysis of Conservation Agriculture

8.1 Introduction

Farmers in the UK and abroad have been encouraged to adopt Conservation Agriculture (CA) practices in recent years, with much support and promotion from large organisations such as the Food and Agriculture Organisation (FAO, 2014). Many of the promotional materials disseminate the associated environmental benefits that can be achieved through CA adoption; however, many of these materials also claim that CA can help farmers to reduce expenditure and improve the profitability of their businesses (FAO, 2014, 2001; Syngenta, 2024). These claims have been substantiated by research, where CA has been shown in some cases to lower energy requirements (Parihar et al., 2018; Das et al., 2021), lower water usage (Kumara et al., 2020; Das et al., 2021), reduce expenditure (Kumara et al., 2020; Lorenzetti and Fiorini, 2024; Kumara et al., 2020), reduce machinery operation times and improve timeliness of machinery operations (Kassam et al., 2014a; Morris et al., 2010), and improve system gross profit margin (Lorenzetti and Fiorini, 2024). However, there is not a large body of research to draw substantial conclusions about many of the economic effects of the implementation of CA. The results of the research that has been published about CA economics are highly heterogeneous, and therefore it is recommended that the effects of CA on farm economics be considered on a case-by-case basis (Pannell et al., 2014). That said, it is widely considered that in most cases there are economic benefits to farmers to adopt CA (Pannell et al., 2014; Farooq and Siddique, 2015; Wang et al., 2006).

Despite evidence suggesting that, in many cases, CA can be more profitable than conventional practices (CON) (Wang et al., 2006), some farmers are still hesitant to

adopt it. One suggested reason for this is that when the benefits and costs associated with CA are modelled at the on-site and off-site levels, it is found that most benefit to CA adoption is seen at the off-site level, where there is net-gain to society and the environment in the form of improvements to surface hydrology, reductions in water sediment loads, and carbon sequestration (Knowler and Bradshaw, 2007; FAO, 2001). However, much of the costs associated with CA adoption are at the farm-level, in relation to changing farm practices and the initial costs of changing farm machinery (Knowler and Bradshaw, 2007; FAO, 2001). For example, Mueller et al. (1985) found that total production costs of CA were initially up to 18% higher than a CON system; however, over time resulted in lower long-term production costs due to savings in machinery and fertiliser costs.

These initial short-term costings and risks of lower yields are disincentives for farmers to transition to a system, even when there is scientific evidence to suggest improvements to long-term profitability under CA systems (Mueller et al., 1985; Pittelkow et al., 2015). Other economic disincentives of CA at the farm level include the loss of crop residues as a revenue stream or as livestock feed or bedding. This is a serious consideration for farmers in the UK, where in recent years the competition for cereal straw from bioenergy and agricultural markets has resulted in limited availability of cereal straw and has led to higher prices for crop residues (Townsend et al., 2018). Loss of this revenue stream during the CA transition could be a strong disincentive for farmers to change their systems (Pannell et al., 2014).

One of the key drivers of long-term improvements to profitability in CA is the reduction of expenditure. The major factor which influences reduced expenditure in CA is no-tillage (NT), in comparison to CON systems, which incurs a great cost financially in terms of machinery, fuel, and labour (Das et al., 2021). The results of the meta-analysis by Kumara et al. (2020) using a total of 670 paired observations from 147 studies representing 67 crops of South Asian countries, found that the cost of production in all the selected crops was significantly lower under CA. They also found that the net returns under CA compared to CON were significantly increased for wheat, legumes and other crop categories. However, during this study, they also found crop yield was significantly improved in CA, which is not always the case in the literature on the subject of crop yields in CA (Pittelkow et al., 2015; Pittelkow et al., 2015; Van den Putte et al., 2010).

As the effects of climate change become more severe in the future, this may also influence the economics of CA with respect to CON. This is because CA is widely thought to be more resilient to extreme weather conditions compared to CON systems

due to a reduced vulnerability to effects of drought (Madejón et al., 2023; Thierfelder and Wall, 2010; Kumara et al., 2020), reduce soil erosion (Du et al., 2022), and lesser extremes of soil temperatures (Kassam et al., 2009; Blanco-Canqui and Lal, 2007).

The economic outcomes of CA are thought to be highly specific to an individual farm business, as the economic performance is highly influenced by the region, soil texture, farm size, and the existing business model and economic resources. This is coupled with a range of variables which are based upon the individual farmer, e.g. their attitude to business risk, and their interest and knowledge about CA (Pannell et al., 2014; Knowler and Bradshaw, 2007). Therefore, a better understanding of the economics would more extensively aid in guiding and advising farmers on the transition to CA, and specifically, to help them adapt their system to local conditions (Pannell et al., 2014).

8.1.1 Research Aims and Hypotheses

This chapter aims to identify the key differences in the on-farm expenditure and revenue during the transition to a CA system using the experiment outlined in Chapter 3.

The research aims (A) of this chapter are:

- Assess the economic performance of CA during the experimental duration in comparison to CON.
- Model the economic performance of both experimental treatment systems in a variety of different scenarios.

The hypothesis to be tested is as follows:

- H_1: CA reduces crop production expenditure in comparison to CON.
- H_2: CA reduces the quantity of machinery operation passes ha^{-1} required.
- H_3: CA has no significant effect on the gross margin of the system compared to CON.

8.2 Methods

The experimental design and agronomic management discussed in this chapter are detailed in Chapter 3. The site is based in Shropshire in the West Midlands of the UK, and situated in an area of traditionally mixed arable and livestock farms. Some of the main agricultural enterprises throughout the region are dairy, beef, and sheep production. Additionally, there are several anaerobic digesters located locally; therefore, competition and price for crop residues are relatively high, proportionate to mainly arable crop-producing areas of the UK. The following section outlines the methodology for the collection and analysis of the economic data relating to experimental treatment management throughout the course of the project. All data analysis was performed in `R` (version 4.3.0) (R Core Team, 2023).

8.2.1 Revenue

Crop yield was calculated using the methodology previously outlined in Chapter 6, and the revenue for all agricultural produce sold was used in the analysis. The spring beans were sold at a price of £300 t^{-1}, the winter wheat crop at £190 t^{-1}, the oilseed rape at £403 t^{-1}, and the spring barley at £160 t^{-1}. The winter wheat straw sold in 2023 was sold for a price of £54 t^{-1}.

The total revenue per hectare (TR_{ha}) is calculated as:

$$TR_{ha} = (Y_g \times P_g) + (Y_s \times P_s) \tag{8.1}$$

where:

- TR_{ha}: Total revenue ha^{-1}.
- Y_g: Grain yield per hectare (t ha^{-1}).
- P_g: Price per tonne of grain (£ t^{-1}).
- Y_s: Straw yield per hectare (t ha^{-1}).
- P_s: Price per tonne of straw (£ t^{-1}).

8.2.2 Expenditure

All product and fertiliser expenditure data were sourced from the invoices from suppliers. All machinery operations data was sourced from the National Association of Agricultural Contractors Contracting Prices Survey 2022 (NAAC, 2022). In this database, the contracting prices are based on a fuel cost of "red" (untaxed) diesel at £1.00 per litre. All grain drying and handling expense data were sourced from the invoices.

The total expenditure per hectare (TE_{ha}) was calculated as:

$$TE_{ha} = E_a + E_o + (Y_g \times (C_d + C_h)) \tag{8.2}$$

Where:

- TE_{ha}: Total expenditure per hectare (£ ha^{-1}).
- E_a: Expenditure on agri-chemical application per hectare (£ ha^{-1}).
- E_o: Expenditure on machinery operations per hectare (£ ha^{-1}).
- Y_g: Grain yield per hectare (t ha^{-1}).
- C_d: Drying cost per tonne of grain (£ t^{-1}).
- C_h: Handling cost per tonne of grain (£ t^{-1}).

This equation calculates the total cost of production per hectare, combining three main components:

1. Fixed costs associated with applying inputs (E_a) and operating machinery (E_o).
2. Variable costs related to grain yield, including drying (C_d) and handling (C_h), which are proportional to the quantity of grain produced (Y_g).

8.2.3 Gross Margin

The gross margin per hectare (GM_{ha}) was calculated as:

$$GM_{ha} = TR_{ha} - TE_{ha} \tag{8.3}$$

- GM_{ha}: Gross margin per hectare (£ ha^{-1}).
- TR_{ha}: Total revenue per hectare (£ ha^{-1}).
- TE_{ha}: Total expenditure per hectare (£ ha^{-1}).

8.2.4 Net Profit Margin

The net profit margin was calculated for each treatment year^{-1} and the entire experimental period. Expressed as a percentage, it measures the proportion of total revenue that remains as profit after deducting total expenditures and indicates the profitability of production relative to revenue. A positive net profit margin signifies profitability, while a negative margin indicates that costs exceed revenue. The net profit margin per hectare (NPM_{ha}) was calculated as:

$$NPM_{ha} = \frac{(TR_{ha} - TE_{ha})}{TR_{ha}} \times 100 \tag{8.4}$$

Where:

- NPM_{ha}: Net profit margin per hectare (%).
- TR_{ha}: Total revenue per hectare (£ ha^{-1}).
- TE_{ha}: Total expenditure per hectare (£ ha^{-1}).

Due to the presence of strong outliers in the data for revenue, the net profit margin was winsorized by capping its values at the 5th and 95th percentiles following a methodology by Cornaggia (2013), ensuring that extreme values do not disproportionately affect the analysis while preserving the overall distribution of the data.

$$NPM_{ha}^{winsorized} = \begin{cases} \text{5th percentile}, & \text{if } NPM_{ha} < \text{5th percentile} \\ \text{95th percentile}, & \text{if } NPM_{ha} > \text{95th percentile} \\ NPM_{ha}, & \text{otherwise} \end{cases}$$

8.2.5 Theoretical Field Capacity Calculation

The Theoretical Field Capacity (TFC) in hectares per hour was calculated following the methodology outlined by Hanna (2016). The TFC is the rate at which an agricultural machine can perform its primary function in perfect conditions with no stoppages. This equation is detailed below:

$$TFC = \frac{\text{width}_m \times \text{speed}_{kmh^{-1}}}{10} \tag{8.5}$$

Where:

- width_m is the working width of the machine in meters,
- $\text{speed}_{kmh^{-1}}$ is the operating speed in kilometres per hour,
- Dividing by 10 accounts for the conversion from square meters to hectares.

8.2.6 Time Required per Hectare

The theoretical time required to manage each treatment ha^{-1} was calculated as:

$$\text{Time per ha} = \frac{1}{TFC} = \frac{10}{\text{width}_m \times \text{speed}_{kmh^{-1}}} \tag{8.6}$$

Where:

- width_m is the working width of the machine in meters,
- $\text{speed}_{kmh^{-1}}$ is the operating speed in kilometres per hour,
- TFC is the Theoretical Field Capacity.

This equation expresses the time (in hours) required to complete one hectare of field operations.

8.2.7 Theoretical Fuel Consumption Calculation

The theoretical fuel consumption for each agricultural operation was estimated using fuel consumption values obtained from the *AGRIBALYSE* database (Colomb et al., 2014). The database provides fuel consumption in kg ha^{-1} for various field operations. To convert these values into litres ha^{-1}, the following conversion factor was applied:

$$\text{Diesel Consumption (L ha}^{-1}) = \frac{\text{Diesel Consumption (kg ha}^{-1})}{\rho} \tag{8.7}$$

Where:

- $\rho = 0.835$ kg L^{-1} is the density of diesel.

8.2.8 Statistical Analysis

Economic data was assessed for normality and homogeneity of variances using the methodology outlined in section 3.10. Total revenue, total expenditure, operational expenditure, application expenditure, and gross margin were statistically analysed using generalised linear mixed effects models following the methodology detailed in section 3.10, using block, year, and crop as random effects within the model formula. Distributions were analysed, positively skewed data were analysed using a generalised linear mixed effects model with a Gamma log link applied, and negatively skewed data were modelled with a Gamma inverse link function using the package `lme4` in `R` (version 4.3.0) (R Core Team, 2023).

To interpret the results of any model generated using the Gamma inverse link, the response scale, estimated marginal means and pairwise contrasts were calculated using the `emmeans` package in R. Since the Gamma model with an inverse link function reports results on the inverse scale, back-transformation was applied to obtain interpretable values using the `regrid()` function to force contrasts onto the response scale. Therefore Gamma model with an inverse link function contrasts are displayed in the response scale in this study.

8.2.9 Markov Chain Monte Carlo Simulation

To estimate future performance of the experimental treatments in different scenarios, a series of Markov Chain Monte Carlo (MCMC) simulations (Amorim et al., 2024) were performed using `R` (R Core Team, 2023) for key economic variables. The individual simulations are detailed in the sections below. The simulation algorithms were performed to simulate 6 years' worth of crop and economic data for both experimental treatments. Each treatment was simulated 1000 times for the following crop rotations:

Conventional (CON)

- Winter Wheat (*Triticum aestivum*)
- Winter Barley (*Hordeum vulgare*)
- Oilseed Rape (*Brassica napus*)
- Winter Wheat (*Triticum aestivum*)
- Winter Barley (*Hordeum vulgare*)
- Oilseed Rape (*Brassica napus*)

Conservation (CA)

- Winter Beans (*Vicia faba*)
- Winter Wheat (*Triticum aestivum*)
- Spring Barley (*Hordeum vulgare*)
- Oilseed Rape (*Brassica napus*)
- Feed Peas (*Pisum sativum*)
- Winter Wheat (*Triticum aestivum*)

8.2.9.1 Yield Simulation

A global dataset for crop production under CON and NT systems was obtained from Su et al. (2021). The dataset contains 4403 paired yield observations collected between 1980 and 2017 for eight major staple crops in 50 countries. The data was filtered using the `R` package `dplyr` for all studies that utilise a crop rotation with at least three crops involved, and studies that utilised soil cover in the NT system. These were selected based on the CA principles defined by FAO (2014). This resulted in a database of 669 paired observations from 23 countries and 10 crop species. The location of the studies is shown in Figure 8.1.

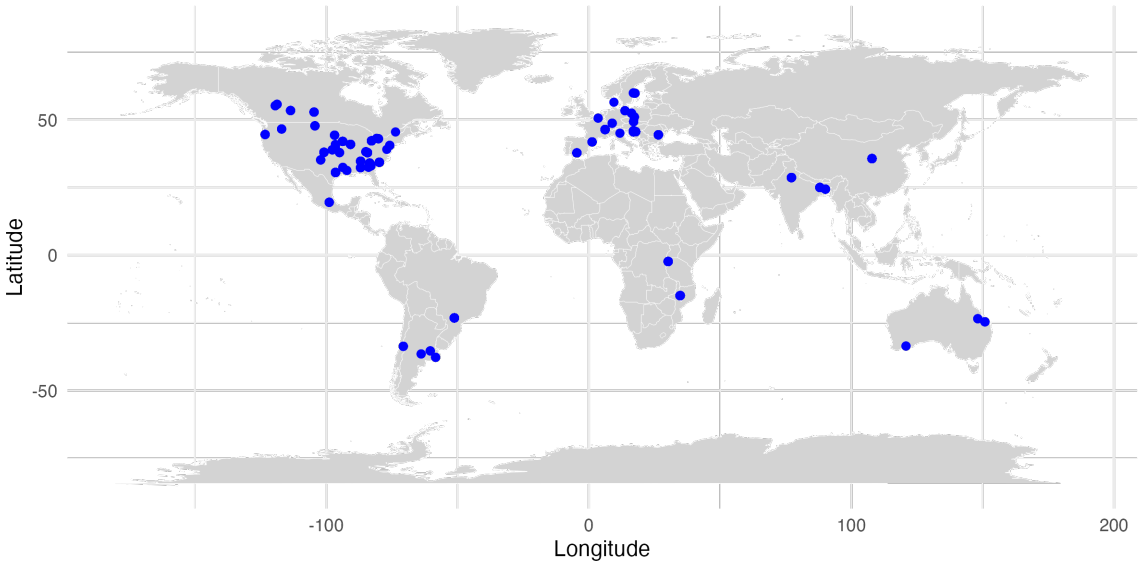

Figure 8.1: The locations of the 669 paired yield observations from studies which utilise the CA principles defined by FAO (2014). Data sourced from the dataset by Su et al. (2021).

The crop yield data were extracted from the filtered Su et al. (2021) database, and the correlation between the duration of the CA system implementation and the relative yield change in comparison to the CON treatment was calculated using a Pearson correlation coefficient using the `stats R` package. The results from this analysis are presented below in Figure 8.2.

In addition, mean yield data for a range of commonly grown crops in the UK were extracted from AHDB (2022). This database is a summary of 11,584 CON combinable crop enterprise performance results for the 2017 to 2021 harvest years. The results are presented by AHDB (2022) in three performance groups: top 25%, middle 50% and bottom 25%, which are based upon full economic net margin. The

mean UK yield was obtained from the middle 50%, and the standard deviation used was obtained by subtracting the top 25% yield from the bottom 25% yield.

A MCMC simulation was employed to predict the potential variation in crop yields over multiple years under different agricultural systems. The simulation was based on a stochastic growth model, where crop yield in each year was influenced by two key parameters:

- **Drift**: A deterministic trend in yield change over time, representing the *systematic effect* of factors like farming practices and environmental changes.
- **Volatility**: A random, normally distributed variability around the drift, capturing *uncertainty* due to factors such as weather fluctuations and soil conditions.

The following steps were implemented to simulate the yield trends for each crop rotation under the CON and CA systems:

1. **Initial Yield Variation**: For each simulation run, the initial yield for the first year was randomly adjusted based on a normal distribution, with a mean equal to the observed average yield for the crop system and a standard deviation determined by the estimated volatility. The initial crop yield for the CON system was obtained from the middle 50% crop yield in the UK from the AHDB (2022). A linear mixed-effects model was used to calculate the initial yield in the CA, relative to the CON system. The intercept coefficient of the linear model was extracted and used as the initial yield, and the slope coefficient was used for the yield change rate. The CON yield was maintained at a constant value for the entire simulation duration.
2. **Yearly Yield Growth**: Starting from the first-year yield, the crop yield for each subsequent year was calculated as follows:

$$Y_t = Y_{t-1} \times (1 + drift + \mathcal{N}(0, volatility)) \tag{8.8}$$

where:

- Y_t is the yield for year t,
- Y_{t-1} is the yield from the previous year,
- $drift$ represents the deterministic change in yield from one year to the next,

- *volatility* introduces stochastic fluctuation around the drift, simulated from a normal distribution $\mathcal{N}(0, volatility)$.

3. **Simulations**: This process was repeated for a total of 1000 simulation runs to capture a wide range of possible future yield trajectories for both experimental treatments.

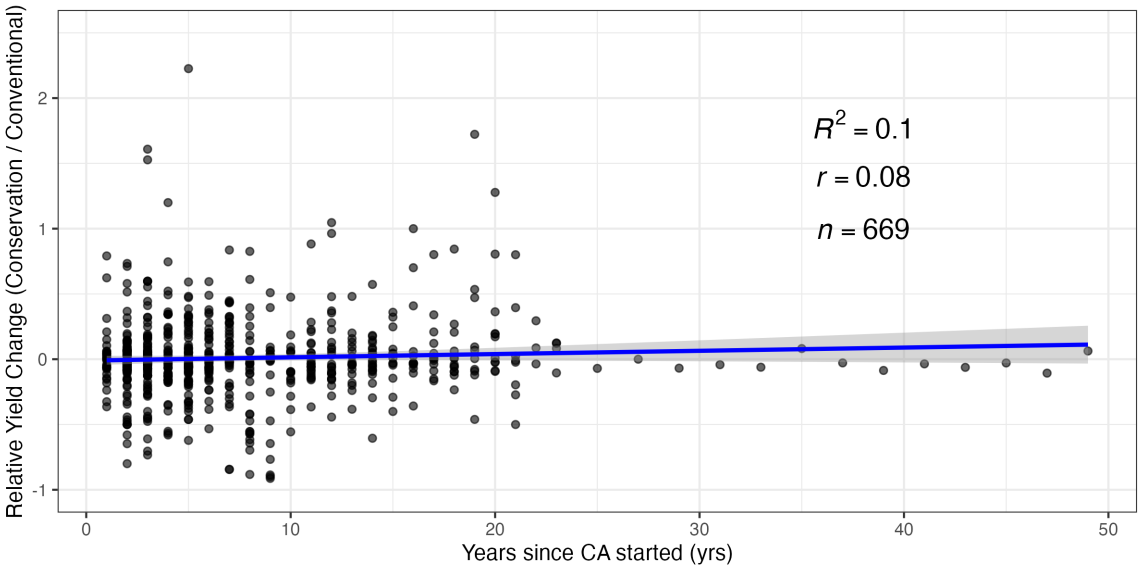

Figure 8.2: The relative yield change data defined as $\frac{\text{Yield}_{NT} - \text{Yield}_{CON}}{\text{Yield}_{CON}}$ from the 669 paired yield observations year^{-1} from the study by Su et al. (2021).

Table 8.1: Mean yield data for a range of commonly grown crops in the UK extracted from AHDB (2022). This database is a summary of 11,584 conventional combinable crop enterprise performance results for the 2017 to 2021 harvest years presented in three performance groups: top 25%, middle 50% and bottom 25%, which are based upon full economic net margin.

	Top 25%	**Middle 50%**	**Bottom 25%**	*SD*
Spring Barley	7	6.3	5.4	1.6
Winter Barley	8.5	7.6	6.7	1.8
Spring Beans	4.5	3.7	2.8	1.7
Winter Beans	4.3	3.6	2.8	1.5
Linseed	2.3	1.6	1.1	1.2
Spring Oats	6.7	5.5	4.8	1.9
Winter Oats	7.4	7	6	1.4
Winter Oilseed Rape	4.2	3.4	2.7	1.5
Feed Peas	4.3	3.1	2.9	1.4
Spring Wheat	6.7	5.8	4.9	1.8
Winter Wheat	9.9	8.9	8	1.9

8.2.9.2 Revenue Simulation

A MCMC simulation was employed to model the potential variation in crop sale prices over time. This approach was selected to capture the inherent uncertainty in agricultural markets, driven by factors such as supply and demand fluctuations, economic conditions, and policy changes. The simulation was based on a stochastic price evolution model (Amorim et al., 2024), incorporating both deterministic and random components:

- **Drift**: A systematic trend in price change over time, representing long-term economic and market trends. In this study, the price drift for the simulation of both treatments was set to 3.5%, corresponding with the current UK consumer price inflation rate at the time of writing (Office for National Statistics, 2025).
- **Volatility**: A stochastic variation component capturing short-term price fluctuations due to unpredictable market factors.

The simulation process for each crop was structured as follows:

1. **Initial Price Variation**: The starting price in the first year was randomly adjusted using a normal distribution:

$$P_1 = P_{\text{initial}} \times (1 + \mathcal{N}(0, \text{volatility})) \tag{8.9}$$

   where:

   - P_1 is the initial simulated price,
   - P_{initial} is the observed historical price for the crop,
   - $\mathcal{N}(0, \text{volatility})$ represents a random adjustment based on market uncertainty.

2. **Yearly Price Evolution**: For each subsequent year, price evolution was modelled using a multiplicative process:

$$P_t = P_{t-1} \times (1 + \text{drift} + \mathcal{N}(0, \text{volatility})) \tag{8.10}$$

   where:

   - P_t is the price for year t,

- P_{t-1} is the price from the previous year,
- **drift** represents the long-term trend in price change,
- **volatility** introduces random fluctuations simulated from a normal distribution.

3. **Simulations**: The process was repeated for 1000 independent simulation runs over a time horizon of 6 years, generating a range of potential price trajectories for each crop.

8.2.9.3 Expenditure Simulation

The trend of agricultural expenditure over a six-year crop rotation period was simulated using a MCMC algorithm. The simulation incorporated both inflation and market volatility; the inflation rate was set to 3.5% annually, and the volatility was set to 5%. The simulation was performed for 6 years and performed 1000 simulation runs. The methodology is outlined as follows:

- **Initial Expenditure:** Which represents the expenditure at the start of the simulation.
- **Inflation:** An annual inflation rate, inflation, is applied to simulate the gradual increase in expenditure over time. In this study, an annual inflation rate of 2% is assumed.
- **Volatility:** The model incorporates random market fluctuations, which are simulated as a random normal variable with a mean of 0 and a standard deviation of volatility. This volatility captures the unpredictable market dynamics that affect agricultural expenditure. In this study, a volatility of 2% (volatility = 0.02) is used.
- **Simulation Years:** The function simulates the expenditure trend over a period of 6 years.
- **Simulation Runs:** 1000 independent simulation runs to generate a distribution of possible expenditure trajectories.

The model for expenditure growth is defined recursively. At each time step, the expenditure at year `t` is calculated as:

$$Expenditure_t = Expenditure_{t-1} \times (1 + inflation + \mathcal{N}(0, volatility)) \quad (8.11)$$

Where:

- $Expenditure_t$ is the expenditure at time t.
- $Expenditure_{t-1}$ is the expenditure at the previous time step $(t-1)$.
- $inflation$ represents the deterministic inflation rate affecting expenditure.
- $\mathcal{N}(0, volatility)$ is a normally distributed random variable with a mean of 0 and a standard deviation of volatility, accounting for stochastic fluctuations. This process simulates both the expected annual increase due to inflation and the random fluctuations.
- *volatility* represents the level of uncertainty or variability in the expenditure growth rate.

8.2.9.4 Climate-driven Yield Shock Simulation

To incorporate climate shocks into the simulation, a probability of occurrence is assigned, increasing over time for both CON and CA systems. The probability of a climate shock in any given year follows a linear sequence from 5% in year one to 20% in Year 6. The severity of yield reduction due to a climate shock is determined using a random uniform distribution:

- Conventional agriculture (CON): Yield reduction ranges between 10% and 30%.
- Conservation agriculture (CA): Yield reduction ranges between 5% and 15%.

These distributions reflect the assumption that CA enhances resilience to climate shocks, leading to reduced yield losses compared to CON (Madejón et al., 2023; Thierfelder and Wall, 2010; Kumara et al., 2020; Du et al., 2022; Kassam et al., 2009; Blanco-Canqui and Lal, 2007; Teng et al., 2024). For example, Teng et al. (2024) found that climate warming increased wheat yield in CA by 9.3% in comparison to CON.

Climate shocks are applied at the individual observation level as follows:

1. A climate shock indicator is generated based on a probabilistic comparison.

2. A shock factor is computed to adjust the yield based on the severity of the shock.

3. Yield is modified according to the presence or absence of a shock.

4. Revenue is recalculated by multiplying the adjusted yield by the crop price.

The simulation applies the following equation to determine the shocked yield (Equation 8.12), revenue (Equation 8.13), and gross margin (Equation 8.14):

$$Y_{shocked} = Y \times (1 - S)^I \tag{8.12}$$

$$R_{shocked} = Y_{shocked} \times P \tag{8.13}$$

$$GM_{shocked} = R_{shocked} \times E_{sim} \tag{8.14}$$

where:

- $Y_{shocked}$ is the shocked yield,
- Y is the original yield,
- S is the severity factor (sampled from a uniform distribution),
- I is a binary indicator (1 if a shock occurs, 0 otherwise),
- $R_{shocked}$ is the shocked revenue, and
- P is the crop price.
- $GM_{shocked}$ is the climate-driven shocked gross margin.
- E_{sim} is the simulated expenditure.

The implementation ensures that shocks are applied separately for CON and CA while maintaining consistency within each simulation scenario.

8.2.9.5 Sensitivity Analysis

Pearson Correlation Coefficients between simulated gross margin and crop price, crop yield, and the severity factor of the climate shock were computed for each experimental treatment using the `cor` function from the `stats` package in `R` (version 4.3.0) (R Core Team, 2023). To analyse system sensitivity to variation in key simulation inputs (yield, price, and the severity factor of the climate shock), a differential effect measure was implemented based on selected quantiles of each treatment's simulated gross margin. For crop yield and crop price, the 75th percentile of the gross margin was compared for observations above the median to the 25th percentile for those below the median. This interquartile range captures the spread in gross margin responses associated with higher versus lower values of the variable. The sensitivity effect for a generic variable X on the simulated gross margin is defined as:

$$S_X = Q_{0.75}\Big(GM \mid X > Q_{0.5}(X)\Big) - Q_{0.25}\Big(GM \mid X < Q_{0.5}(X)\Big) \tag{8.15}$$

Where:

- $\mathbf{S_X}$: The sensitivity effect of the variable X on the gross margin outcome .
- $\mathbf{Q_{0.5}(X)}$: The median (50th percentile) of the variable X.
- $\mathbf{Q_{0.75}\Big(GM \mid X > Q_{0.5}(X)\Big)}$: The 75th percentile of simulated gross margin calculated over observations where X exceeds its median.
- $\mathbf{Q_{0.25}\Big(GM \mid X < Q_{0.5}(X)\Big)}$: The 25th percentile of the simulated gross margin calculated over observations where X is below its median.

For the severity factor of the climate shock, data visualisation found that many of the values were 1 (no shock applied); therefore, a different sensitivity analysis quantile model was implemented. The difference between the 95th percentile of the gross margin for observations with a severity factor of the climate shock at or above the median and the 75th percentile for those below the median. This adjustment is intended to capture the sensitivity of gross margin to extreme deviations in the severity factor of the climate shock, particularly highlighting the influence of adverse shocks.

8.3 Results

8.3.1 Expenditure

Expenditure data was assessed for normality and homogeneity of variances using the methodology outlined in section 3.10, and normality visualisation is displayed in Appendix D. There was significantly higher expenditure on crop applications in the CON treatment ($\beta = 0.124$, $SE = 0.009$, $Z = 13.08$, $p = <.0001$) for the experimental period. During the first year of the experiment, the CON treatment spent £547.65 ha^{-1}, and the CA treatment spent £508.28 ha^{-1}, an 8% increase in crop application expenditure. During 2023, the CON treatment also had an increased expenditure (19%) in crop application expenditure (£827 ha^{-1}) in comparison to the CA treatment (£695 ha^{-1}). This trend was also identified in the final year of the experiment, however, with a lower magnitude change (6.6%) with the CON treatment spending £790 ha^{-1} on crop application expenditure, and the CA treatment spending £742 ha^{-1}. Crop application expenditure is presented in Figure 8.3 for each year of the experiment (8.3 **A**), and the mean of the experimental duration (8.3 **B**).

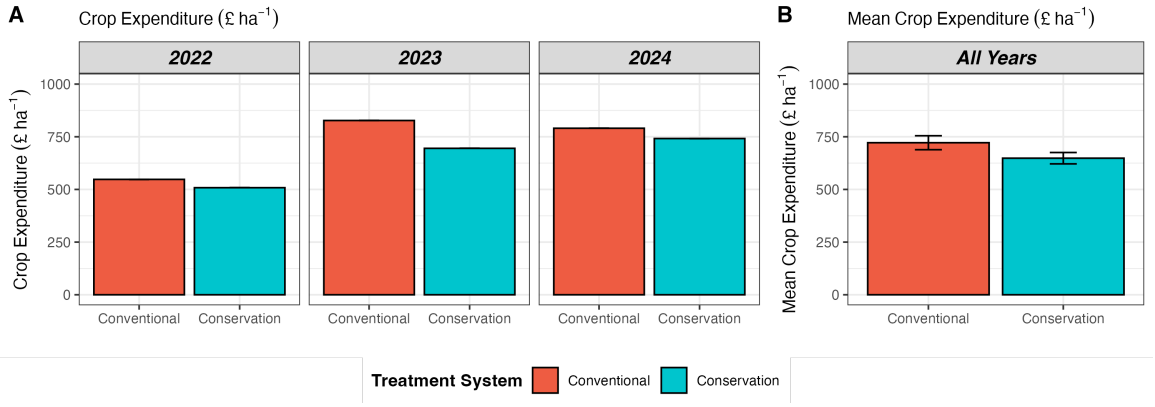

Figure 8.3: **A:** Crop application expenditure (£ ha^{-1} year^{-1}), **B:** Mean crop application expenditure (£ ha^{-1}) for the experimental duration ($n = 3$). Error bars signify standard error.

There was also significantly higher operational expenditure in the CON treatment ($\beta = 0.419$, $SE = 0.021$, $Z = 19.98$, $p = <.0001$) for the experimental period. The CON treatment spent £466 ha^{-1} on machinery operations in the crop of spring beans in comparison to the CA treatment, which spent £272 ha^{-1}, a 71% difference in operational expenditure. During 2023, there was a 37% increase in the operational expenditure in CON treatment (£396.8 ha^{-1}), compared to the CA treatment operational expenditure of £288.6 ha^{-1}. There was also a similar percentage difference in

operational expenditure in the final year of the experiment, with the CON treatment operational expenditure 41.1% higher (£414.4 ha^{-1}) than the CA treatment (£293.6 ha^{-1}). Machinery operational expenditure is presented in Figure 8.4 for each year of the experiment (8.4 **A**), and the mean of the experimental duration (8.4 **B**).

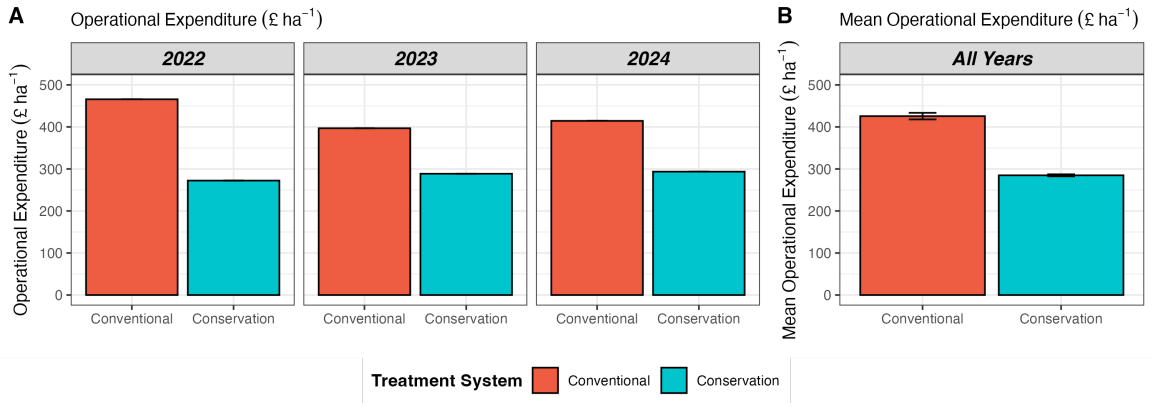

Figure 8.4: **A:** Machinery operation expenditure (£ ha^{-1} year^{-1}), **B:** Mean machinery operation expenditure (£ ha^{-1}) for the experimental duration (n = 3). Error bars signify standard error.

There were no significant differences detected in grain expenditure ($\beta = 0.13$, $SE = 0.166$, $Z = 0{,}79$, $p = 0.43$). Whilst there were no significant differences detected, grain management expenditure varied between the two treatments due to crop yield and crop moisture content variation, coupled with variation in grain drying and storage costs. Both treatments had similar grain expenditure in 2022 (CON = £36.4 ha^{-1}, CA = £31.4 ha^{-1}). During 2023, there was higher grain expenditure for both treatments as winter wheat produces a larger gross yield ha^{-1} than spring beans, therefore the grain in expenditure for the CON treatment was £186 ha^{-1}, and £160 ha^{-1} for the CA treatment due to a lower crop yield. In 2024, the CON treatment's grain expenditure was £13 ha^{-1} for the crop of oilseed rape, and the grain expenditure for CA was £59 ha^{-1} on the spring barley crop. Grain management expenditure is presented in Figure 8.5 for each year of the experiment (8.5 **A**), and the mean of the experimental duration (8.5 **B**).

There was significantly higher gross expenditure in the CON treatment ($\beta = 0.233$, $SE = 0.006$, $Z = 35.9$, $p = <.0001$) for the experimental period. For the 2022 cropping season, the CON treatment spent £1050 ha^{-1} and the CA treatment spent 29.2% less at £812 ha^{-1}. This trend continued in 2023 where the CA treatment total expenditure (£1143 ha^{-1}) was 23.5% lower than the CON treatment (£1410 ha^{-1}), and in 2024 where the CA treatment gross expenditure (£1094 ha^{-1}) was 11.3% lower

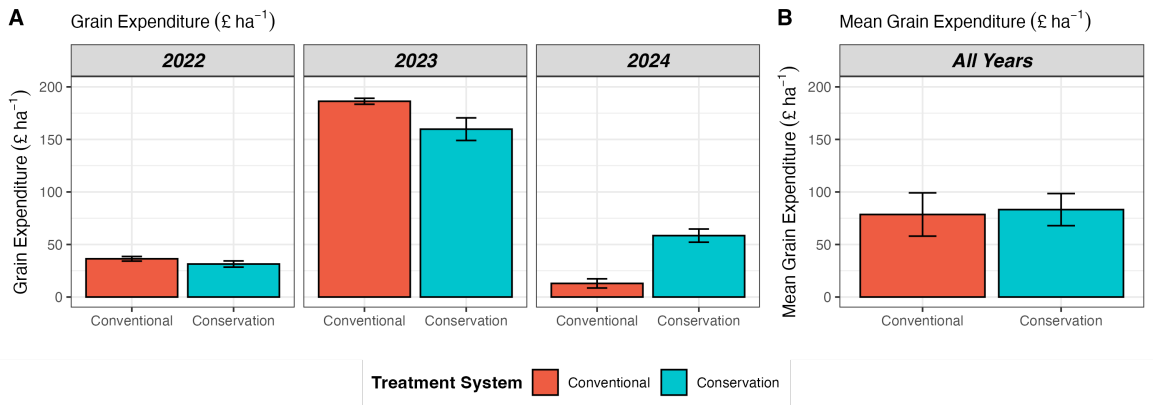

Figure 8.5: **A:** Grain management expenditure (£ ha^{-1} year^{-1}), **B:** Mean grain management expenditure (£ ha^{-1}) for the experimental duration ($n = 3$). Error bars signify standard error.

than the CON treatment (£1218 ha^{-1}). Gross expenditure is presented in Figures 8.6 and 8.7 for each year of the experiment (8.6 **A**), and the mean of the experimental duration (8.6 **B**).

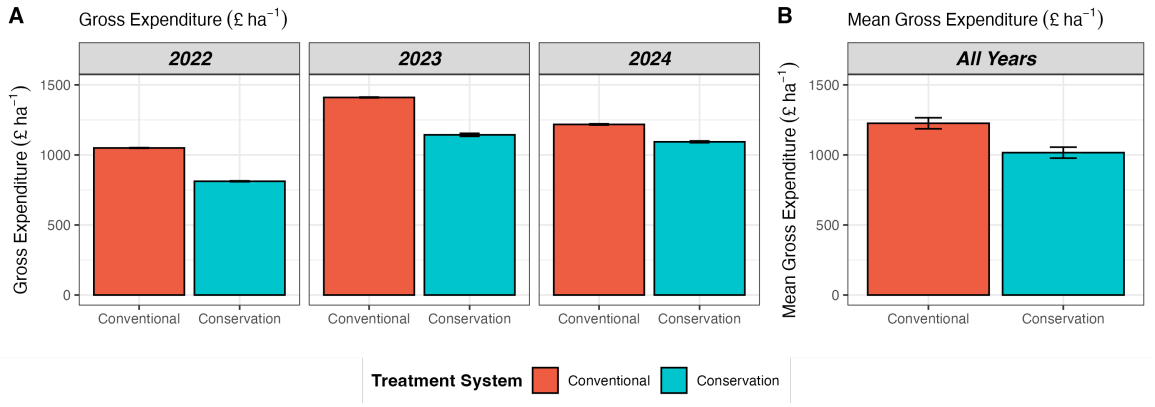

Figure 8.6: **A:** Gross expenditure (£ ha^{-1} year^{-1}), **B:** Mean gross expenditure (£ ha^{-1}) for the experimental duration ($n = 3$). Error bars signify standard error.

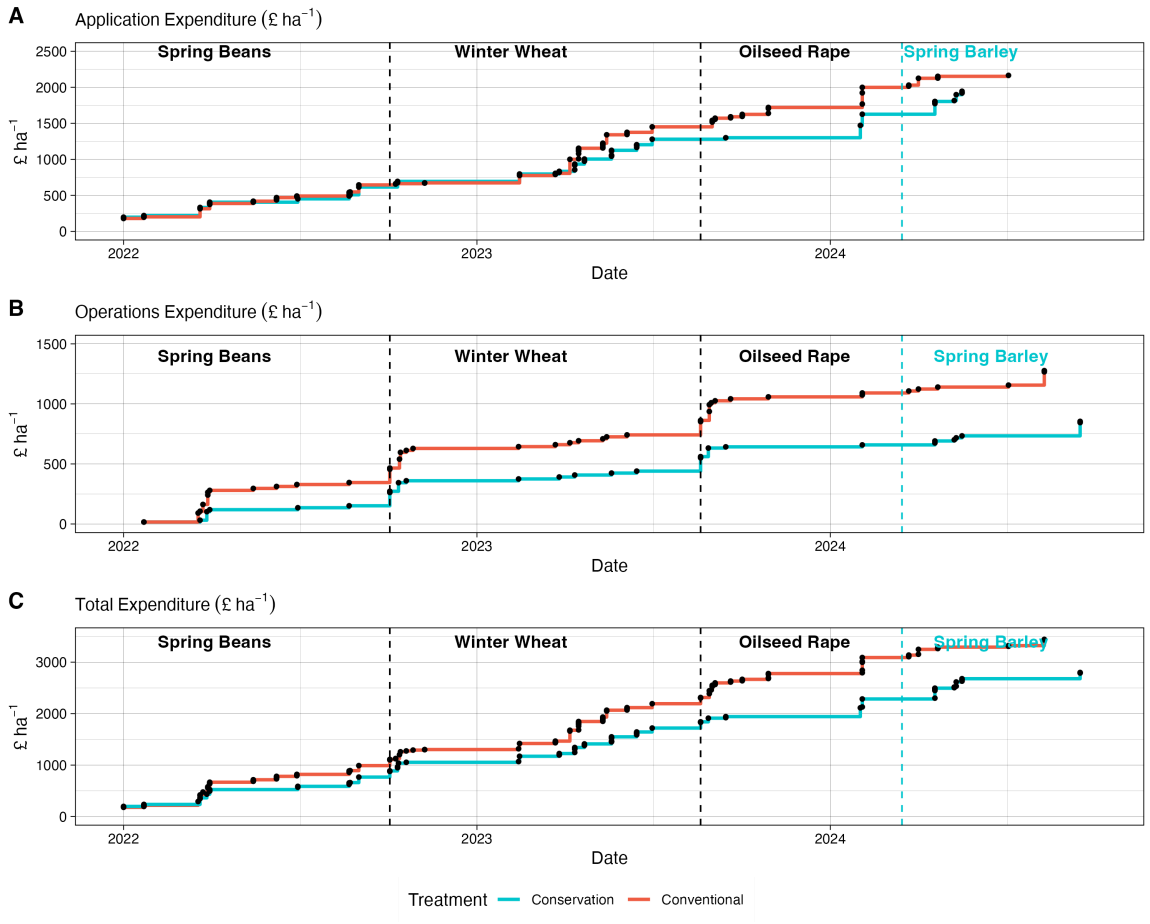

Figure 8.7: A figure containing: **A:** Application expenditure (£ ha^{-1} year^{-1}), **B:** Operations Expenditure (£ ha^{-1} year^{-1}), **C:** Total expenditure (£ ha^{-1} year^{-1}).

Proportional Expenditure

The largest proportion of crop application expenditure (£ ha^{-1}) for each treatment was on fertilisers, with the CON treatment spending a higher proportion of application expenditure (46%), compared to the CA treatment, which spent 42% of application expenditure on fertilisers. The second-highest proportional expenditure for both treatments was on seed. Here, the CA treatment spent a higher proportion of application expenditure (29%) in comparison to the CON treatment (18%). The next highest proportion of application expenditure for both treatments was then on herbicides and fungicides. Here, the CA treatment spent 15% on herbicides and 14% on fungicides, in comparison to the CON treatment, which spent 17% on herbicides and 11% on fungicides.

The largest proportion of machinery operations expenditure (£ ha^{-1}) for the CA treatment was on the harvest (38% of operational expenditure). However, in the CON

treatment, the highest proportional spend on machinery operations was on crop spraying (28%), with the harvest of the crops accounting for 26% of the total machinery operational spend. Crop spraying was the second-highest proportional spend in the CA treatment, accounting for 27% of the total expenditure on machinery operations. Cultivation was a significant expenditure for the CON treatment, accounting for 19% of the total machinery operational expenditure. The proportion of crop application expenditure is presented below in Figure 8.8 A, and the proportion of machinery operations expenditure is presented below in Figure 8.8 B.

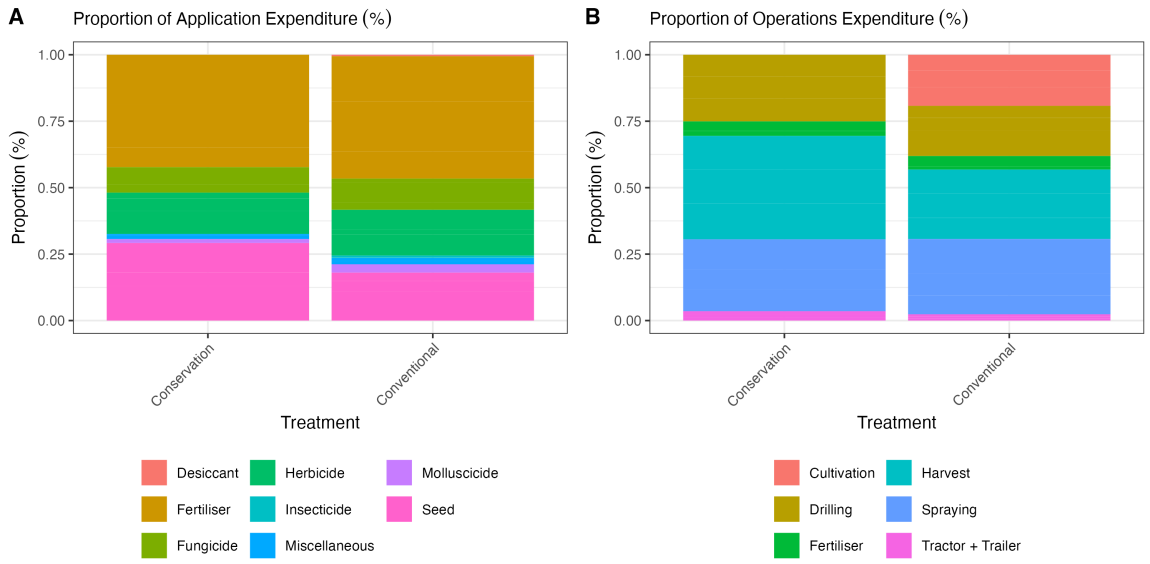

Figure 8.8: A summary of the proportion of expenditure of **A:** crop applications, and **B:** machinery operations.

8.3.2 Operations

Data on the number of operational passes ha^{-1}, theoretical machinery operational time ha^{-1}, and theoretical diesel consumption (l ha^{-1} year^{-1}) was assessed for normality and homogeneity of variances using the methodology outlined in section 3.10 and normality visualisation is displayed in Appendix D. When the number of operational passes ha^{-1} was modelled with the generalised linear mixed effect model, there was a significant reduction in the number of operational passes ha^{-1} needed in the CA treatment identified in comparison to the CON treatment ($\beta = 0.43$, $SE = 0.001$, $Z = 38.32$, $p = <.0001$). The CON treatment required 13 individual machinery passes ha^{-1} during 2022, in comparison to the CA treatment, which required 8 machinery passes ha^{-1}. This was very similar in 2023, where the CON treatment required 13

individual machinery passes ha^{-1} during 2022, in comparison to the CA treatment, which required 9 machinery passes ha^{-1}. In 2024, the CON treatment required 14 individual machinery passes ha^{-1}, and the CA treatment which required 10 machinery passes ha^{-1}. The number of machinery passes ha^{-1} is presented in Figure 8.9 for each year of the experiment (8.9 **A**), and the mean of the experimental duration (8.9 **B**).

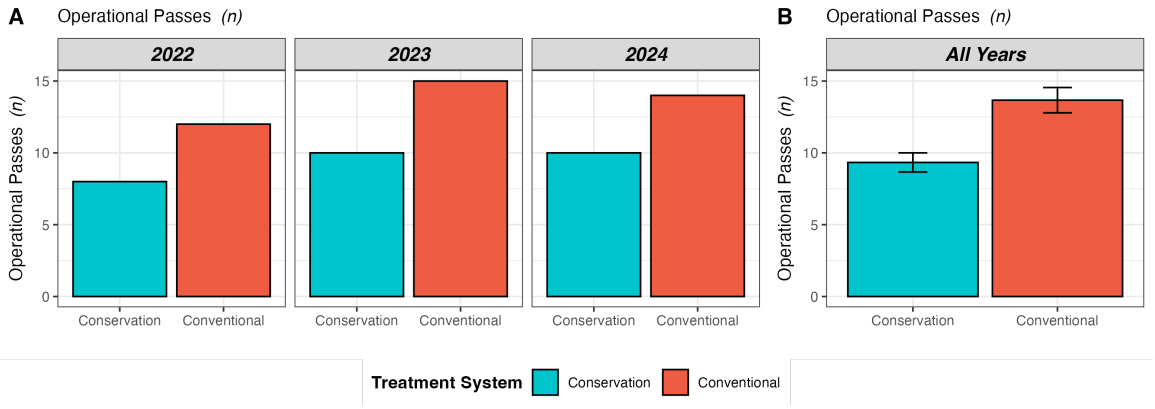

Figure 8.9: **A:** The number of machinery passes (ha^{-1} year^{-1}) for each year of the experiment, **B:** The mean number of machinery passes (ha^{-1}) for the experimental duration ($n = 3$). Error bars signify standard error.

When the theoretical machinery operation time was considered, the CON treatment needed significantly more machinery operational time ha^{-1} to manage than the CA treatment ($\beta = 0.82$, $SE = 0.1$, $Z = 8.2$, $p = <.0001$). In 2022, the theoretical machinery operation time ha^{-1} was 0.7 hours ha^{-1} in the CA treatment and 1.54 hours ha^{-1} in the CON treatment. This trend continued in 2023, where the theoretical machinery operation time ha^{-1} was 0.98 hours ha^{-1} in the CA treatment and 1.61 hours ha^{-1} in the CON treatment. In 2025, there were again similar results, with the CON treatment theoretically requiring 1.47 hours ha^{-1} to manage, in comparison to the CA treatment, which theoretically required 1.1 hours ha^{-1}. The theoretical machinery operation time ha^{-1} for both experimental treatments is presented in Figure 8.10 for each year of the experiment (8.10 **A**), and the mean of the experimental duration (8.10 **B**).

CA was found to significantly reduce theoretical diesel consumption (l ha^{-1} year^{-1}) in this study in comparison to the CON treatment ($\beta =$ -0.01, $SE = 0.004$, $Z =$ -2.32, $p = 0.03$). During 2022, the CA treatments' theoretical diesel consumption was 70.5 l ha^{-1}, compared to the 121.7 l ha^{-1} used in the CON treatment. In 2023, the diesel consumption in both treatments was higher, 80.6 l ha^{-1} in the CA treatment, and 128

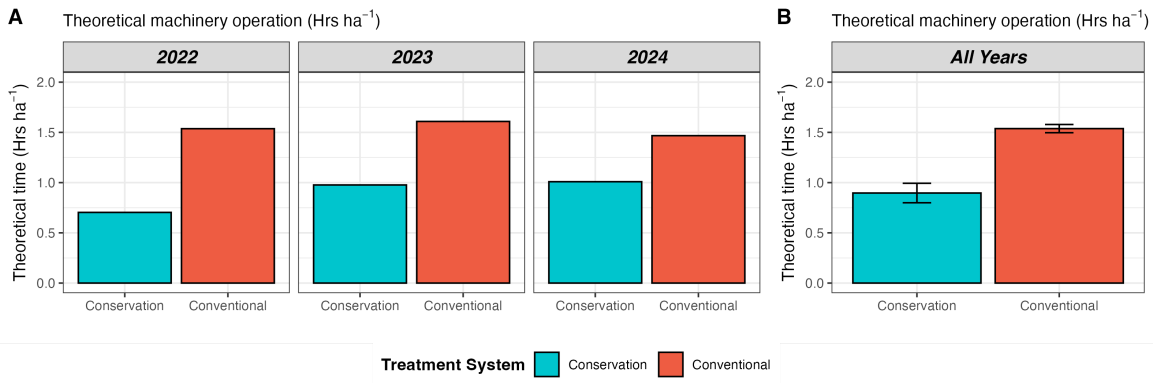

Figure 8.10: **A:** The theoretical number of machinery hours needed to manage the system ha^{-1} year^{-1} for each year of the experiment, **B:** The theoretical mean number of machinery hours needed to manage the system ha^{-1} year^{-1} for the experimental duration ($n = 3$). Error bars signify standard error.

l ha^{-1} in the CON treatment. During the final year of the experiment, a similar trend in the theoretical diesel consumption was observed, with the CA treatment using 68.5 l ha^{-1}, compared to the CON treatment, which theoretically used 109.7 l ha^{-1}. The theoretical machinery diesel consumption l ha^{-1} for both experimental treatments is presented in Figure 8.11 for each year of the experiment (8.11 **A**), and the mean of the experimental duration (8.11 **B**).

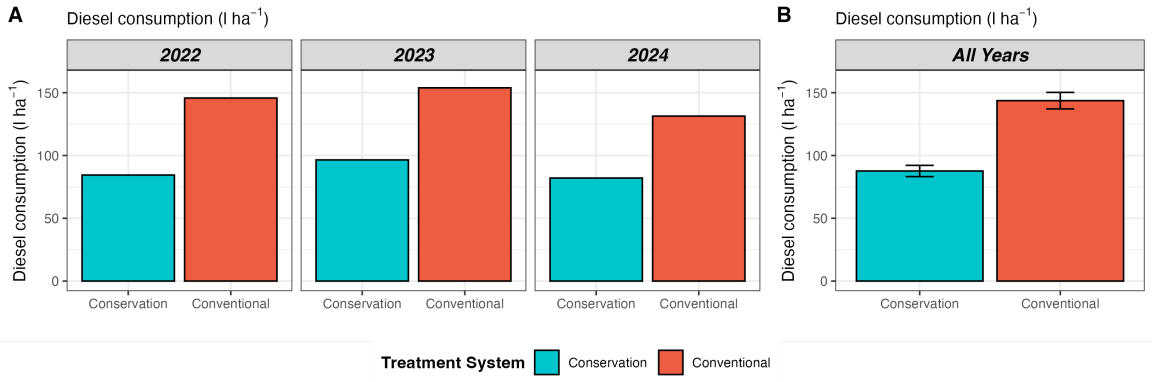

Figure 8.11: **A:** The theoretical fuel consumption of the treatment operations (litres ha^{-1}) for each year of the experiment, **B:** The theoretical mean fuel consumption of the treatment operations (litres ha^{-1}) for the experimental duration ($n = 3$). Error bars signify standard error. Fuel consumption data for individual operations was sourced from the `AGRIBALYSE` database (Colomb et al., 2014).

8.3.3 Revenue

Crop revenue data (£ ha^{-1}) was assessed for normality and homogeneity of variances using the methodology outlined in section 3.10, and normality visualisation is displayed in Appendix D. The generalised linear mixed effects model used to assess the difference in system revenue (£ ha^{-1}) found no statistical differences between the CA and CON treatments ($\beta = 150$, $SE = 154$, $Z = 0.97$, $p = 0.33$). Although there was no statistical difference found between system revenues, the CON treatment produced a higher mean revenue in all years of the experiment. In 2022, the CON treatments mean revenue was £1820 ha^{-1} in comparison to £1571 ha^{-1} in the CA treatment. In 2023, the CON mean revenue was £2261 ha^{-1}, and £1786 ha^{-1} in the CA treatment. The CON treatment total revenue was supplemented by an additional straw revenue of £178 ha^{-1}. In 2024, the mean total revenue was similar for both treatments, with the CON treatment having a marginally higher mean revenue of £872 ha^{-1}, compared to £850 ha^{-1} in the CA treatment. The total grain, straw, and gross revenue (£ ha^{-1}) for both experimental treatments is presented below in Figures 8.12, 8.13, and 8.14.

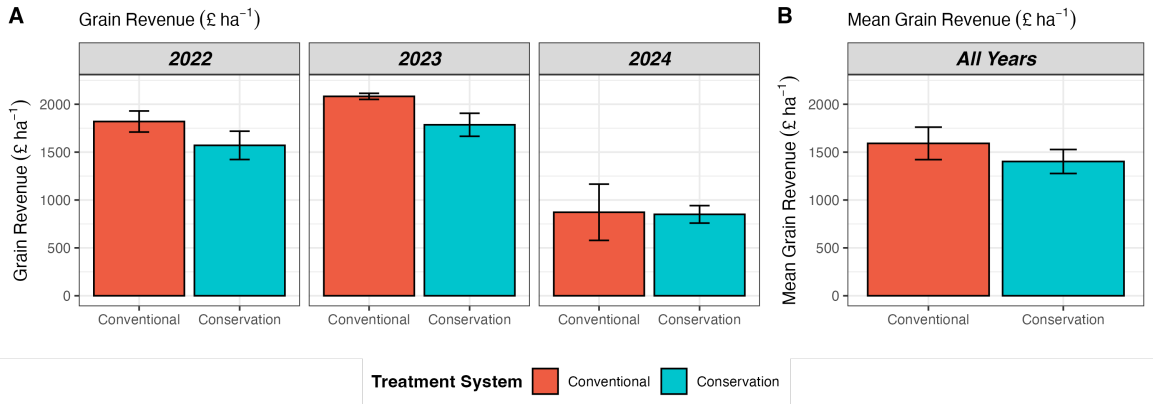

Figure 8.12: **A:** Grain revenue (£ ha^{-1} year^{-1}), **B:** Mean grain revenue (£ ha^{-1}) for the experimental duration ($n = 3$). Error bars signify standard error.

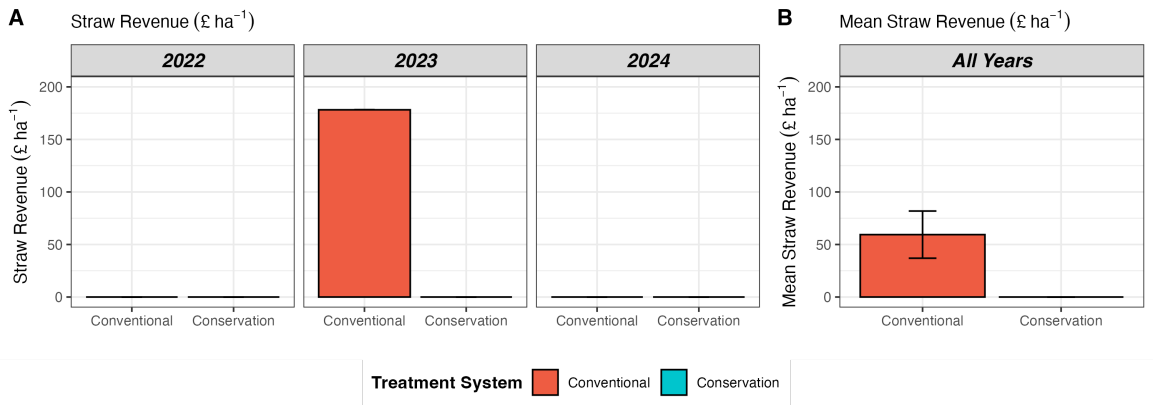

Figure 8.13: **A:** Straw revenue (£ ha^{-1} year^{-1}), **B:** Mean straw revenue (£ ha^{-1}) for the experimental duration (n = 3). Error bars signify standard error.

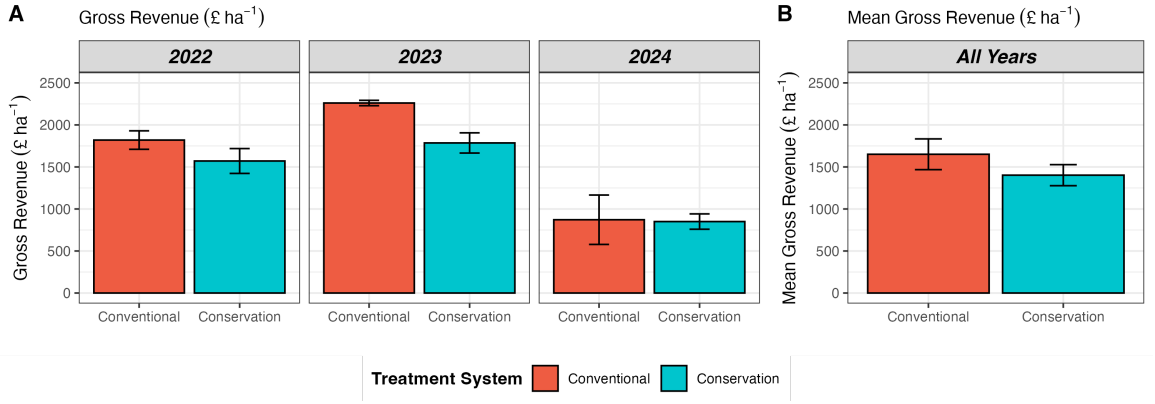

Figure 8.14: **A:** Gross revenue (£ ha^{-1} year^{-1}), **B:** Mean gross revenue (£ ha^{-1}) for the experimental duration (n = 3). Error bars signify standard error.

8.3.4 Net Profit Margin

For the CON treatment (n = 15), the mean net profit margin was 7.52% (SD = 61.54%, SE = 15.89%). In comparison, the CA treatment (n = 15) had a mean net profit margin of 15.04% (SD = 40.86%, SE = 10.55%). However, the generalised linear mixed effects model used to assess the difference in net profit margin (%) found no statistical differences between the CA and CON treatments (β = -66.4, SE = 209, Z = -0.32, p = 0.75). In the CON treatment, the net profit margin was high and positive in 2022, with a mean of 41.5% (SD = 7.84, SE = 3.51; 95%), and slightly lower in 2023 at 37.6% (SD = 1.68, SE = 0.75). However, in 2024, the mean net profit margin for the CON treatment dropped markedly to –56.5% (SD = 74.2, SE = 33.2). Similarly, the CA treatment exhibited a high positive net profit margin in 2022, with a mean of 44.8% (SD = 10.1, SE = 4.50), and a modest decline in 2023

to 34.8% (SD = 9.84, SE = 4.40). In contrast, the CA treatment also showed a negative net profit margin in 2024, with a mean of –34.5% (SD = 31.4, SE = 14.0). The data on the gross margin for each experimental treatment year^{-1} is presented below in Figure 8.15 **A**, and the total gross margin treatment^{-1} is presented in Figure 8.15 **B**.

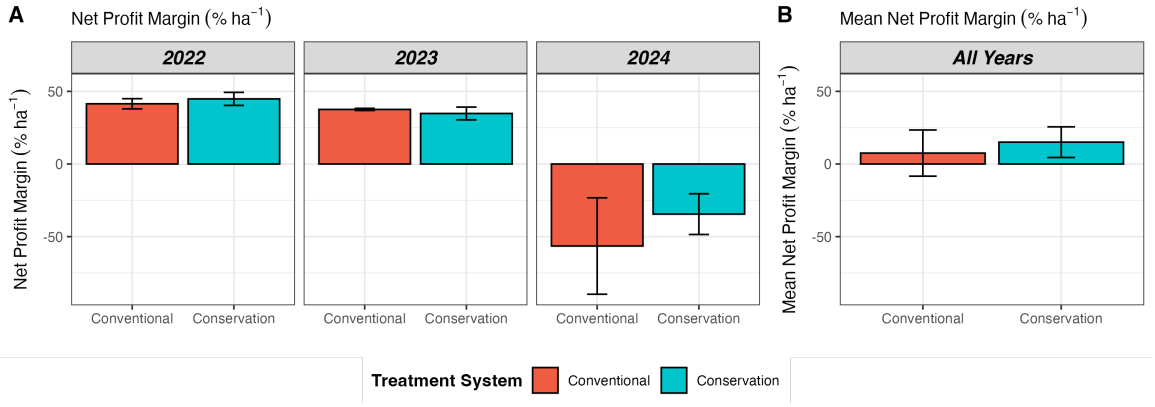

Figure 8.15: **A:** System net profit margin (% year^{-1}) (n = 5) **B:** Mean system net profit margin (% year^{-1}) for the experimental duration (n = 3). Error bars signify standard error.

8.3.5 Gross Margin

Data on the gross margin (£ ha^{-1}) was assessed for normality and homogeneity of variances using the methodology outlined in Chapter 3, and normality visualisation is displayed in Appendix D. The mean gross margin of £428.8 ha^{-1} year^{-1} (SD = 675.8, SE = 174.5) for the CON treatment (n = 15) for the experimental duration was slightly higher than the CA treatment (n = 15) mean gross margin of £385 ha^{-1} year^{-1} (SD = 521.5, SE = 134.7). However, the generalised linear mixed effects model used to assess the difference in system gross margin (£ ha^{-1}) found no statistical differences between the CA and CON treatments (β = 27.5, SE = 268, Z = 0.1, p = 0.92).

During 2022, the gross margin for both treatments for the crop of spring beans was similar, £770 ha^{-1} for the CON treatment (n = 5) and £758.8 ha^{-1} for the CA treatment (n = 5). However, during the winter wheat crop in 2023, larger differences in the gross margins of the experimental treatments were observed. Here, the CA treatment (n = 5) recorded a gross margin of £642.1 ha^{-1}, compared to the CON treatment (n = 5) which had a gross margin of £850.3 ha^{-1}. During the cropping year of 2024, both experimental treatments recorded negative gross margins, the CA

treatment (n = 5) had a gross margin of £-243.42 ha^{-1} and the CON treatment (n = 5) had a lower gross margin of £-345.78 ha^{-1}. The data on the gross margin for each experimental treatment year^{-1} is presented in Figure 8.16 **A**, and the total gross margin treatment^{-1} is presented in Figure 8.16 **B**.

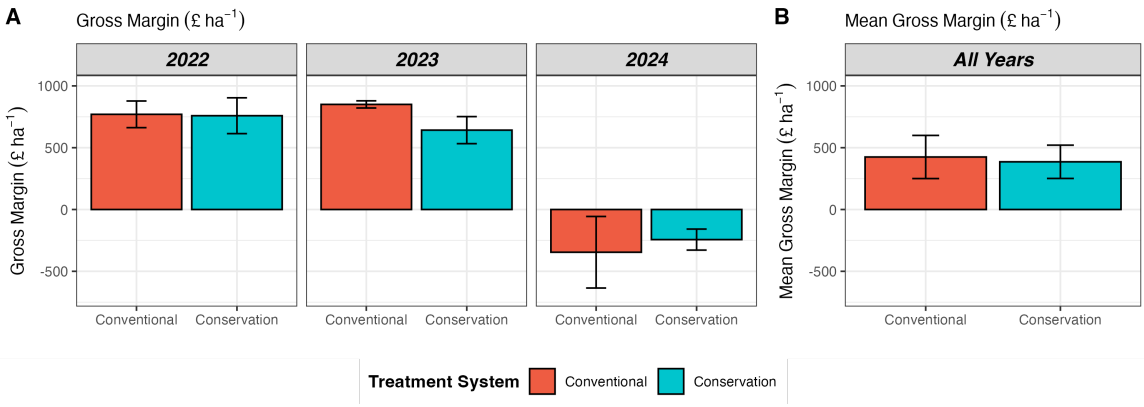

Figure 8.16: **A:** System gross margin (£ ha^{-1}) for each year of the experiment (n = 5) **B:** Mean system gross margin (£ ha^{-1}) for the experimental duration (n = 3). Error bars signify standard error.

8.3.6 Markov Chain Monte Carlo Simulation

8.3.6.1 Yield simulation

The results of the MCMC algorithm deployed to simulate crop yield indicate that winter wheat is projected to be the highest-yielding crop in both treatments across the simulation period. The CA treatment simulation estimated a mean yield of 8.91 t ha^{-1} (SD = 0.27, SE = 0.008) in year one, rising to 9.08 t ha^{-1} (SD = 0.65, SE = 0.02) in year 6, a 1.9% increase in yield. The CON treatment had a mean yield of 8.9 t ha^{-1} (SD = 0.26, SE = 0.005) and a similar yield (+ 0.2%) of 8.91 t ha^{-1} (SD = 0.66, SE = 0.01) in year 6. Both treatments were predicted to have similar yield variability throughout the simulated experimental period. Winter barley was predicted to be the second-highest-yielding crop in the simulation. The CA treatment had a mean yield of 7.58 t ha^{-1} (SD = 0.23, SE = 0.007) in the first year, which was predicted to rise by 1.9% by year six to a mean yield of 7.73 t ha^{-1} (SD = 0.58, SE = 0.018). The CON treatment was predicted to yield a mean of 7.6 t ha^{-1} (SD = 0.22, SE = 0.004) in the first year of the simulation, rising slightly by 0.1% to 7.61 t ha^{-1} (SD = 0.56, SE = 0.01) by year six. The spring barley crop in the CA treatment followed a similar simulated distribution, however, with a reduced yield in

comparison to the winter barley simulated crop yield. The lowest-yielding crops were oilseed rape, feed peas, and winter beans. The mean oilseed rape yield was 3.4 t ha^{-1} ($SD = 0.1$, $SE = 0.003$) in year one of the CA simulation, rising by 1.9% to 3.46 t ha^{-1} ($SD = 0.24$, $SE = 0.007$) in year six. The CON mean yield was 3.39 t ha^{-1} ($SD = 0.1$, $SE = 0.002$) with a mild increase in yield (+ 0.08%) in year six of 3.4 t ha^{-1} ($SD = 0.25$, $SE = 0.006$). The feed peas crop in the CA treatment had a mean yield of 3.12 t ha^{-1} ($SD = 0.09$, $SE = 0.002$), rising by 2.34% to 3.19 t ha^{-1} ($SD = 0.24$, $SE = 0.007$) in year six.

The climate-driven yield shock simulation reduced mean crop yield in the CON treatment by 0.22 t ha^{-1} (-2.48%), compared to a mean yield reduction of 0.09 t ha^{-1} (-1.02%) in the CA treatment. The simulated winter barley mean yield was reduced by 0.19 t ha^{-1} (-2.53%) in the CON treatment, and 0.08 t ha^{-1} (-1.01%) in the CA treatment. Oilseed rape mean yield was reduced by 0.09 t ha^{-1} (-2.52%) in the CON treatment and by 0.03 t ha^{-1} (-0.96%) in the CA treatment. In the CA treatment, the mean reduction in yield were 0.06 t ha^{-1} (-1%) in the spring barley yield, 0.04 t ha^{-1} (-1%) in the winter beans, and 0.03 t ha^{-1} (-1.08%) in the feed peas. Data for the simulated yield with the simulated climate-driven yield reductions is presented in Figure 8.17 below.

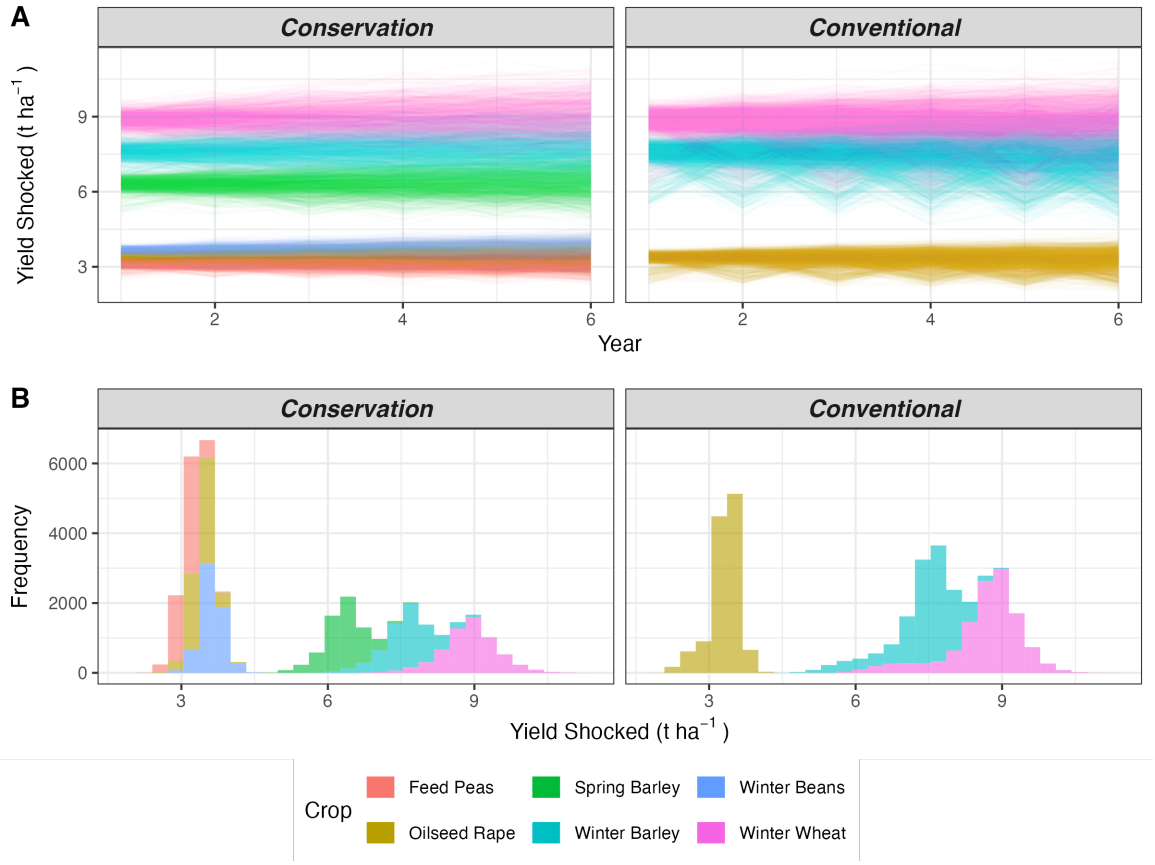

Figure 8.17: **A:** The simulated crop yield (t ha^{-1}) with induced climate-driven yield shocks introduced for the six year period for each experimental treatment. **B:** Histograms of the simulated simulated crop yield (t ha^{-1}) with induced climate-driven yield shocks introduced for each experimental treatment. Data sourced from Su et al. (2021) and AHDB (2022).

8.3.6.2 Revenue simulation

The results from the MCMC simulation of revenue projections across different crops indicate that winter wheat is projected to generate the highest revenue in both the CA and CON treatments over the 6-year period.

In the CA treatment, the mean revenue for winter wheat in year one was estimated at £1,722 ha^{-1} ($SD = 183$, $SE = 5.80$), which is expected to rise by 20.5% to £2,074 ha^{-1} ($SD = 561$, $SE = 17.7$) by year six. Similarly, the CON treatment estimated a mean revenue for winter wheat of £1,699 ha^{-1} ($SD = 192$, $SE = 4.30$) in year one, which is expected to increase by 15.7% to £1,966 ha^{-1} ($SD = 534$, $SE = 11.9$) by year six. Both treatments show similar trends in revenue increase, with CA showing a slightly higher rate of growth.

In contrast, winter barley, the second-highest yielding crop, was projected to gen-

erate an average revenue of £1,082 ha^{-1} ($SD = 119$, $SE = 3.75$) in the first year for CA, with a steady increase of 20.3% by year six, reaching £1,302 ha^{-1} ($SD = 351$, $SE = 11.1$). In the CON treatment, the mean revenue for winter barley was £1,078 ha^{-1} ($SD = 123$, $SE = 2.74$) in year one, which is expected to increase by 16.1% to £1,252 ha^{-1} ($SD = 335$, $SE = 7.49$) by year six. The CA treatment shows greater revenue variability compared to the CON treatment, reflecting the higher unpredictability of winter barley yields.

For oilseed rape, the CA treatment estimates a mean revenue of £1,102 ha^{-1} ($SD = 119$, $SE = 3.77$) in year one, with a 20.0% increase to £1,322 ha^{-1} ($SD = 341$, $SE = 10.8$) by year six. The CON treatment projects a slightly lower revenue of £1,095 ha^{-1} ($SD = 127$, $SE = 2.84$) in the first year, which increases by 15.3% to £1,263 ha^{-1} ($SD = 345$, $SE = 7.72$) by year six. Revenue projections for oilseed rape are fairly stable across both treatments, with CA showing a more notable upward trend over the years.

Feed peas show similar trends in both treatments, with the CA treatment having a mean revenue of £653 ha^{-1} ($SD = 70.9$, $SE = 2.24$) in year one, which increases gradually by 17.1% to £764 ha^{-1} ($SD = 205$, $SE = 6.49$) by year six. The CON treatment shows a similar pattern, with a mean revenue of £670 ha^{-1} ($SD = 75.4$, $SE = 2.85$) in year one, rising by 18.3% to £792 ha^{-1} ($SD = 213$, $SE = 7.80$) by year six. However, feed peas display greater variability in revenue compared to other crops, particularly in the CA treatment.

Spring barley was predicted to be a relatively high-revenue crop, particularly under the CA treatment. The mean revenue in year one was £894 ha^{-1} ($SD = 99.3$, $SE = 3.14$), with a steady increase of 20.2% to £1,074 ha^{-1} ($SD = 278$, $SE = 8.78$) by year six. In the CON treatment, spring barley starts at a mean revenue of £894 ha^{-1} ($SD = 99.3$, $SE = 3.14$) in year one, which increases by 14.4% to £1,074 ha^{-1} ($SD = 278$, $SE = 8.78$) by year six. Revenue for spring barley is relatively stable, with minimal fluctuations in the CON treatment, while the CA treatment shows a more significant increase over time.

Winter beans show moderate revenue projections. In the CA treatment, the mean revenue starts at £647 ha^{-1} ($SD = 68.7$, $SE = 2.17$) in year one, and increases by 20.3% to £778 ha^{-1} ($SD = 194$, $SE = 6.15$) by year six. In the CON treatment, the mean revenue starts at £647 ha^{-1} ($SD = 68.7$, $SE = 2.17$) in year one, increasing slightly by 18.7% to £765 ha^{-1} ($SD = 194$, $SE = 6.49$) by year six. Winter beans exhibit relatively consistent revenue over time, with more modest changes compared to other crops.

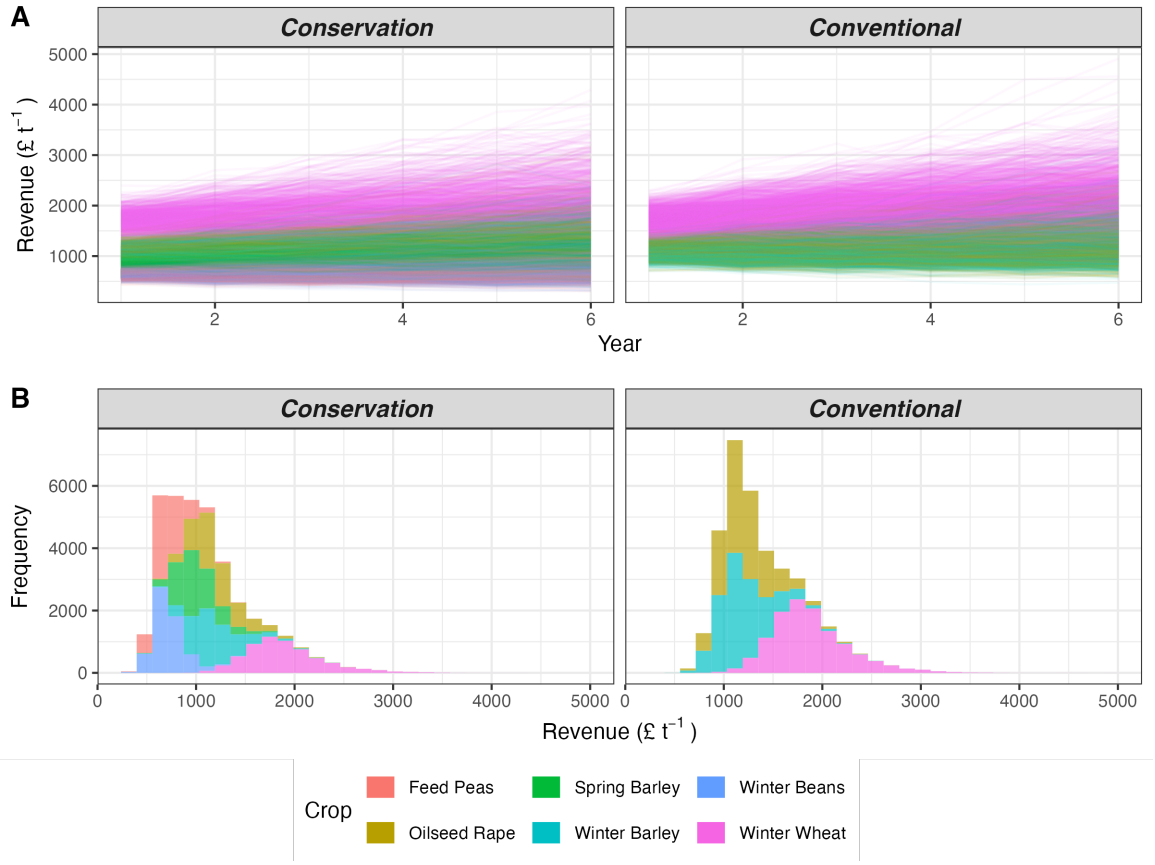

Figure 8.18: **A:** The simulated crop revenue (£ ha^{-1}) for the six year period for each experimental treatment. **B:** Histograms of the simulated crop revenue (£ ha^{-1}) for each experimental treatment. Data sourced from Su et al. (2021) and AHDB (2022).

8.3.6.3 Expenditure simulation

The MCMC simulation results for crop expenditure indicate that winter wheat consistently incurs the highest costs across both CA and CON treatments over the six-year period.

In the CA treatment, the mean expenditure for winter wheat in year one was estimated at £1,018 ha^{-1} (SD = 52.0, SE = 1.65), increasing by 19.2% to £1,214 ha^{-1} (SD = 140, SE = 4.42) by year six. The CON treatment, however, had higher expenditure levels, starting at £1,272 ha^{-1} (SD = 63.6, SE = 1.42) in year one and rising by 18.7% to £1,510 ha^{-1} (SD = 174, SE = 3.88) in year six. The expenditure difference between treatments remains consistent over time, with the CON system requiring approximately 20-25% higher costs compared to CA.

For winter barley, the CA treatment started with an expenditure of £849 ha^{-1} (SD = 43.0, SE = 1.36) in year one, rising to £1,002 ha^{-1} (SD = 121, SE = 3.84)

by year six, reflecting an 18.0% increase. The CON treatment had a higher initial expenditure at £1,058 ha^{-1} ($SD = 52.8$, $SE = 1.18$), which grew by 19.3% to £1,262 ha^{-1} ($SD = 151$, $SE = 3.39$) by year six. These results indicate that expenditure growth trends are similar between treatments, but costs in the CON system remain consistently higher.

Oilseed rape followed a similar pattern, with the CA treatment incurring £952 ha^{-1} ($SD = 46.6$, $SE = 1.47$) in year one, increasing by 19.0% to £1,133 ha^{-1} ($SD = 133$, $SE = 4.20$) by year six. The CON treatment exhibited a significantly higher expenditure profile, starting at £1,190 ha^{-1} ($SD = 61.0$, $SE = 1.36$) in year one and increasing by 18.8% to £1,414 ha^{-1} ($SD = 173$, $SE = 3.87$) by year six. The CON treatment incurred 20-25% higher costs than CA throughout the simulation.

For spring barley, the CA treatment estimated an initial expenditure of £866 ha^{-1} ($SD = 43.0$, $SE = 1.36$) in year one, increasing by 18.8% to £1,029 ha^{-1} ($SD = 123$, $SE = 3.90$) by year six. No expenditure data were available for spring barley in the CON treatment.

Winter beans showed relatively lower expenditure compared to other crops. The CA treatment started at £743 ha^{-1} ($SD = 37.5$, $SE = 1.18$) in year one and increased by 19.1% to £885 ha^{-1} ($SD = 107$, $SE = 3.38$) in year six. No data were available for winter beans in the CON treatment.

Finally, feed peas exhibited the lowest expenditure among all crops, with the CA treatment starting at £800 ha^{-1} ($SD = 40.6$, $SE = 1.28$) in year one and increasing by 18.6% to £949 ha^{-1} ($SD = 112$, $SE = 3.54$) in year six. Again, no expenditure data were available for the CON treatment.

Overall, the results highlight that CON systems consistently exhibit higher expenditure than CA systems across all crops, with differences ranging from 15-25%. Additionally, winter wheat and oilseed rape incur the highest expenditures, while feed peas and winter beans are the least costly to cultivate in both treatments.

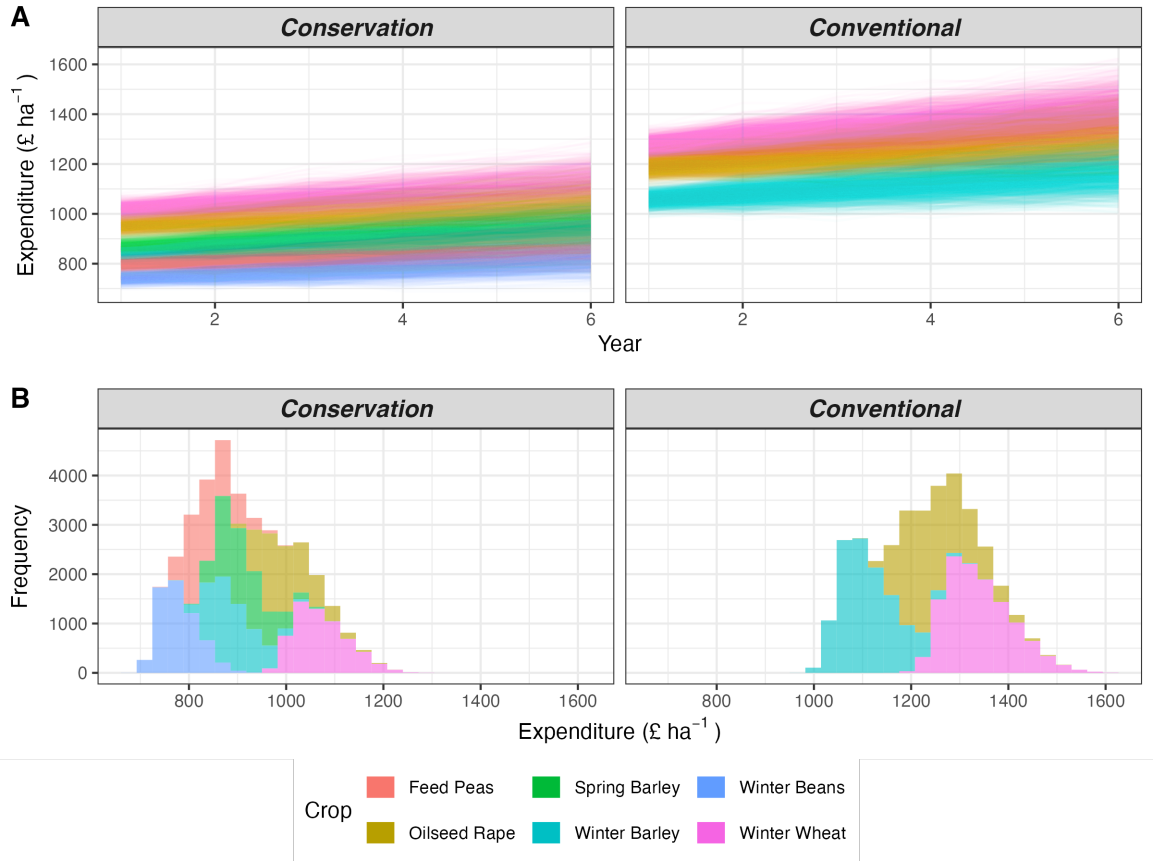

Figure 8.19: **A:** The simulated crop expenditure (£ ha^{-1}) for the six year period for each experimental treatment. **B:** Histograms of the simulated crop expenditure (£ ha^{-1}) for each experimental treatment. Data sourced from Su et al. (2021) and AHDB (2022).

Gross Margin simulation

The results of the MCMC simulations for gross margin indicate that winter wheat is projected to be the most profitable crop across both treatments throughout the simulation period. In the CA treatment, the mean gross margin was estimated at £695 ha^{-1} ($SD = 191$, $SE = 6.03$) in year one, increasing to £810 ha^{-1} ($SD = 518$, $SE = 16.4$) by year six, representing a 16.5% rise. The CON treatment had a lower starting mean gross margin of £425 ha^{-1} ($SD = 203$, $SE = 4.53$) in year one, increasing by 5.2% to £447 ha^{-1} ($SD = 547$, $SE = 12.2$) in year six. Winter barley was projected to have the second-highest gross margin within the CA treatment, with a mean of £236 ha^{-1} ($SD = 127$, $SE = 4.01$) in year one, rising by 24.2% to £293 ha^{-1} ($SD = 361$, $SE = 11.4$) by year six. However, in the CON treatment, winter barley gross margin was lower, starting at £16.3 ha^{-1} ($SD = 139$, $SE = 3.10$) and

declining to -£23.3 ha^{-1} ($SD = 360$, $SE = 8.06$) by year six.

Oilseed rape exhibited contrasting profitability trends between treatments. In the CA treatment, the gross margin increased from £143 ha^{-1} ($SD = 128$, $SE = 4.04$) in year one to £188 ha^{-1} ($SD = 370$, $SE = 11.7$) in year six. Conversely, the CON treatment showed a negative gross margin for oilseed rape throughout the simulation, starting at -£90.5 ha^{-1} ($SD = 138$, $SE = 3.08$) in year one and declining further to -£154 ha^{-1} ($SD = 376$, $SE = 8.40$) in year six. Similarly, winter beans and feed peas had consistently negative gross margins in both treatments, with more pronounced losses over time. In the CA treatment, winter beans started at -£99.9 ha^{-1} ($SD = 77.1$, $SE = 2.44$) and declined to -£114 ha^{-1} ($SD = 214$, $SE = 6.78$) by year six. Feed peas showed a greater reduction, from -£153 ha^{-1} ($SD = 80.5$, $SE = 2.55$) to -£188 ha^{-1} ($SD = 221$, $SE = 7.00$).

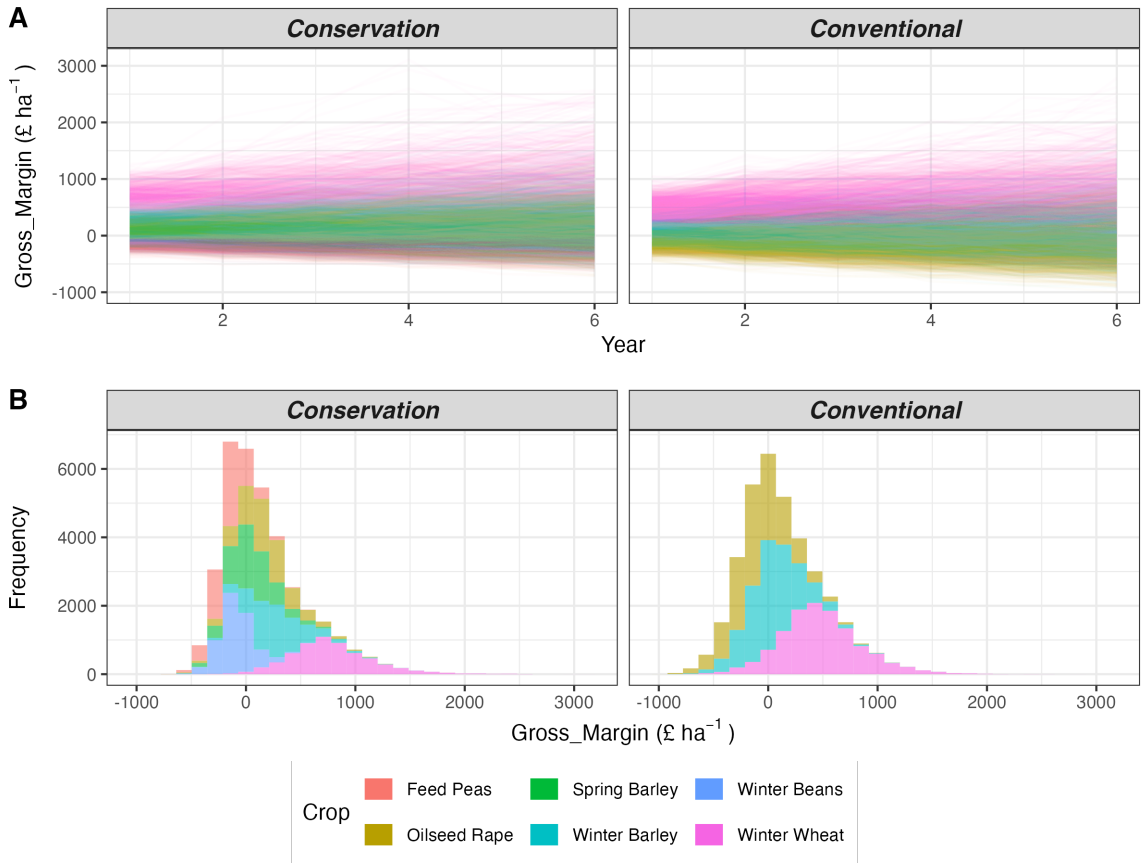

Figure 8.20: **A:** The simulated gross margin (£ ha^{-1}) for the six year period for each experimental treatment. **B:** Histograms of the simulated gross margin (£ ha^{-1}) for each experimental treatment. Data sourced from Su et al. (2021) and AHDB (2022).

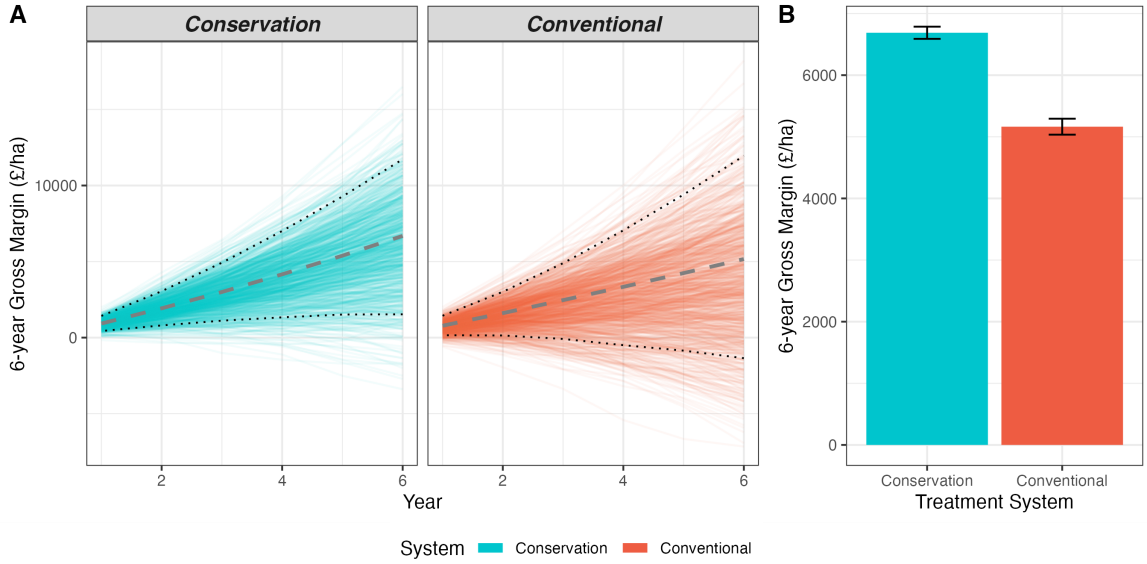

Figure 8.21: **A:** The simulated gross margin (£ ha^{-1}) for the six year period for each experimental treatment. The dashed line signifies the mean simulated cumulative gross margin and the dotted lines represent the 90% confidence interval bounds for the cumulative gross margin **B:** A bar plot of the mean simulated gross margin (£ ha^{-1}) for each experimental treatment. Error bars signify the standard error of the mean. Data sourced from Su et al. (2021) and AHDB (2022).

Sensitivity Analysis

The Pearson correlation coefficient analysis identified the strongest correlated variable with the simulated gross margin was crop yield for both treatments. The CA treatment gross margin was more strongly correlated with crop yield ($\rho = 0.66$) in comparison to the CON treatment ($\rho = 0.52$). The price of the crop commodity (£ t^{-1}) was mildly positively correlated with gross margin for the CA treatment ($\rho = 0.28$), however in the CON treatment this was not the case with a ρ of 0.06, indicating no linear correlation with the simulated gross margin (£ ha^{-1}). When the correlation of the severity factor of the simulated climate shock and the simulated gross margin was assessed, it found that the correlation was stronger in the CON treatment ($\rho = 0.25$), than in the CA treatment. The results of the Pearson correlation coefficient analysis is shown below in Table 8.2 and presented in Figure 8.22.

The sensitivity analysis using the differential effect measure method quantified how variations in key inputs influenced gross margin outcomes under each management system. In the CA system, the sensitivity metrics were £804 ha^{-1} for Yield, £682 ha^{-1} for Price, and £716 ha^{-1} for the Climate Shock Severity Factor. In comparison, the CON system exhibited very similar sensitivity to Yield (£805 ha^{-1}) but a lower

Table 8.2: Pearson correlation coefficients between gross margin and key variables (Yield, Price, and Climate Shock Factor) by system. The pairwise correlations computed separately for each cropping system.

System	Yield (ρ)	Price (ρ)	Climate Shock Severity Factor (ρ)
Conservation	0.66	0.28	0.10
Conventional	0.52	0.06	0.25

sensitivity to Price (£622 ha^{-1}) and a higher sensitivity to the Climate Shock Severity Factor (£807 ha^{-1}). The sensitivity analysis using the differential effect measure method is presented below in Figure 8.22.

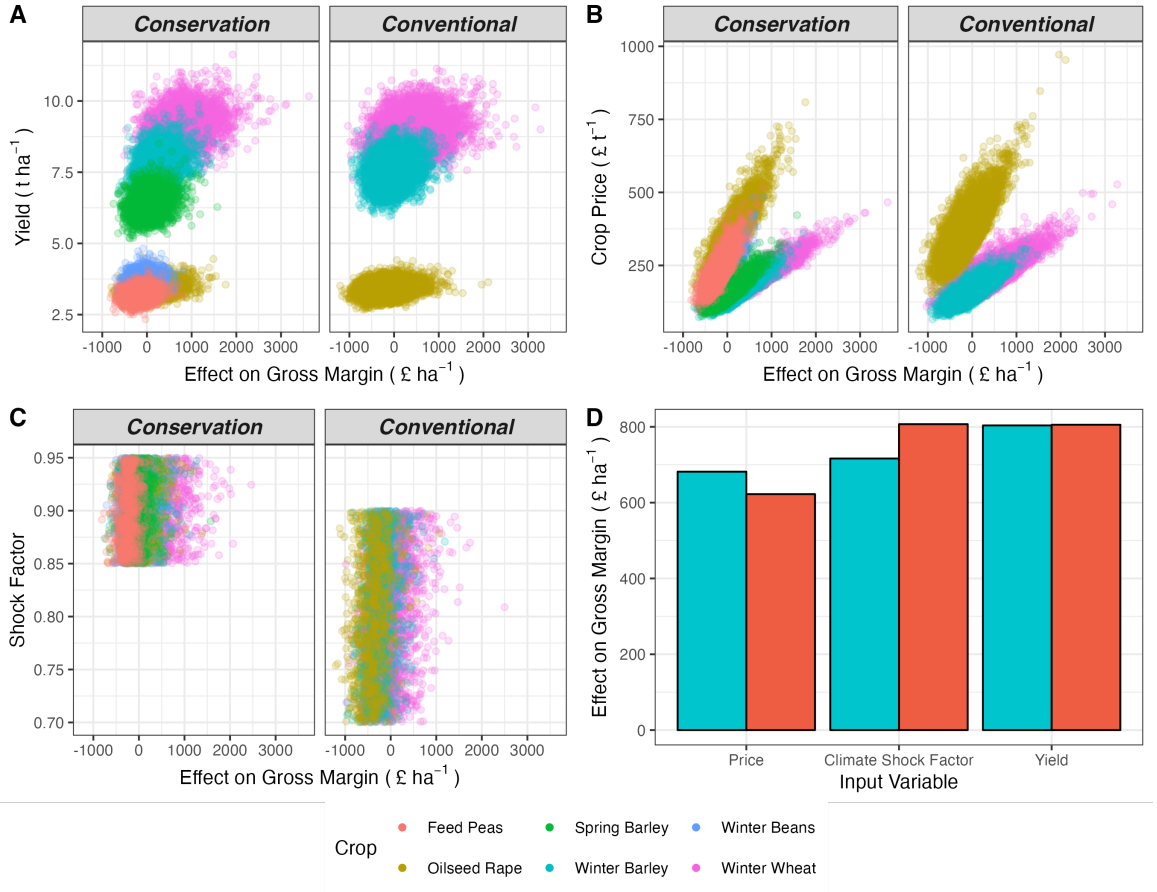

Figure 8.22: The Pearson correlation coefficients (ρ) between crop yield (t ha^{-1}) (**A**), price (£ t^{-1}) (**B**), and the severity factor of the climate shock (**D**) to the simulated gross margin (£ ha^{-1}). Raw data sourced from Su et al. (2021) and AHDB (2022).

8.4 Discussion

This discussion section explores the key economic outcomes of the study, focusing on expenditure, revenue, gross margin, and risk under CA compared to CON. The findings are evaluated against the stated hypotheses, with reference to relevant literature and the broader context of agricultural decision-making. Attention is given to the practical and agronomic implications for farmers, including considerations of transition costs, management complexity, and vulnerability to external shocks such as market fluctuations and climate variability. This section aims to situate the study's results within current research and highlight their relevance for both practice and policy.

8.4.1 Expenditure

This section addresses the tests of the following hypotheses (H):

- H_1: CA reduces crop production expenditure in comparison to CON.
- H_2: CA reduces the quantity of machinery operation passes ha^{-1} required in comparison to CON.

Throughout this study, there was significantly higher expenditure in the CON treatment. Therefore, these results support the hypothesis H_1: CA reduces crop production expenditure in comparison to CON. This result concurs with previous studies, where CA is also found to reduce expenditure (Kumara et al., 2020; Lorenzetti and Fiorini, 2024). Typically, this is attributed to reductions in operational expenditure, due to no use of tillage in CA, which is an expensive operation for farmers, accounting for 19% of the total operational expenditure in the CON treatment in this study. However, in this study, a reduction in crop expenditure as well as operational expenditure was identified. This was attributed to the differing approaches to the agronomy of the treatments, where the CA treatment used significantly less fertiliser than the CON treatment (Figure 6.6). Reduction of inputs is a goal that many farmers practising CA are trying to achieve to create a more resilient soil system and to reduce expenditure (Impey, 2022a). However, as previously discussed in Chapter 6, reduction of inputs, especially fertilisers, in the early stages of the transition to CA can be a complicated balance to reduce inputs without significantly reducing productivity and revenue.

The reduction in operational expenditure observed in this study was linked to the NT approach of the CA treatment and the reduction of the number of machinery passes ha^{-1} to manage the crop in all years. This study highlights the potential of CA to reduce the amount of theoretical diesel consumption ha^{-1}. The price volatility of fuel has been of serious concern for farmers in the UK in recent years, following numerous global issues which have affected the supply and demand of fuel (Clark, 2022). For example, the average price for on-farm red (un-taxed) diesel in 2021 was £65.64 l^{-1}; however, following the Russian invasion of Ukraine in 2022, the average price of red diesel rose to £104.27 in the UK (Clark, 2022; AHDB, 2025). This study also identified significantly less machinery operational time required ha^{-1} to manage the CA treatment. This result is in line with previous research and understanding on the subject (Kassam et al., 2014a; Morris et al., 2010), and will be of appeal to certain

farmers who are looking to reduce the amount of time spent operating machinery on their farms and reduce expenditure on labour.

This study uses standardised costings for all machinery operations performed by agricultural contractors, which include fuel costs, labour, insurance, depreciation, and other costs relating to machinery ownership (NAAC, 2022). Therefore, the initial costings of farmers making the transition to CA may be very different in reality to these figures, as this may require the purchase of new machinery and changes to farm management operations. This study only evaluates the economic comparisons of crop management between the experimental treatments, and therefore cannot conclude the initial startup cost to the farmer to begin the transition to CA. This is an important consideration for future research, as some previous research suggests that the initial expenditure needed to begin the transition to CA can be significant (Knowler and Bradshaw, 2007; FAO, 2001). The initial costs of the transition are a barrier to adoption for many farmers who do not have the financial capital to invest in new machinery, and who are adverse to the financial risks of undertaking changes to their cropping system (Kassam et al., 2014b). This has led to calls for governmental financial support for farmers undertaking the transition to CA to lessen the financial risk of the change (Kassam et al., 2014b; McNairn and Mitchell, 1992). Financial support can take a variety of forms, such as tax credits on equipment, machine rentals, cost-sharing programmes and direct subsidies (Knowler and Bradshaw, 2007). Without financial support for the transition, Pannell et al. (2014) recommends that CA is implemented in large, well-resourced farms which can afford longer time horizons to account for the initial costs of the transition (Lorenzetti and Fiorini, 2024).

8.4.2 Revenue

The analysis of crop revenue (£ ha^{-1}) over the experimental period revealed no statistically significant differences between the CA and CON systems, as indicated by the generalised linear mixed effects model ($\beta = 150$, $SE = 154$, $Z = 0.97$, $p = 0.33$). Despite this, the descriptive data showed a consistent trend of higher mean revenues under the CON treatment across all years. This pattern was most pronounced in 2023, where the CON system generated £2261 ha^{-1} compared to £1786 ha^{-1} under CA, a difference of £475 ha^{-1}. In 2022, the gap was smaller (£1820 vs. £1571 ha^{-1}), and by 2024, revenues between the two systems converged (£872 vs. £850 ha^{-1}), suggesting potential year-to-year variability influencing economic outcomes.

One notable contributor to the higher CON revenue was the inclusion of straw sales, adding £178 ha^{-1} in 2023. This highlights the importance of considering not

only grain yield but also by-product revenues when evaluating the economic performance of different agricultural systems. The straw market can provide a meaningful revenue stream in systems where straw is baled and sold rather than incorporated or retained for soil cover, as is often the case in CA.

The absence of statistical significance may reflect high within-treatment variability or limited replication, reducing the power to detect treatment effects. Furthermore, the relatively small absolute differences in some years (e.g., 2024) suggest that over the long term, system-level revenues might be more similar than initially apparent, particularly when external factors such as weather, market prices, and input costs fluctuate.

8.4.3 Gross Margin

This section addresses the test of the following hypothesis (H):

- H_3: CA has no significant effect on the gross margin of the system compared to CON.

The gross margin results indicate that the mean gross margin over the experimental period was slightly higher for the CON treatment (£428.8 ha^{-1} $year^{-1}$) compared to the CA treatment (£385 ha^{-1} $year^{-1}$). However, statistical analysis using a generalised linear mixed effects model found no significant difference between the two treatments ($p = 0.92$), suggesting that neither system consistently outperforms the other in terms of gross margin under the given experimental conditions. Therefore, the results from this study support the hypothesis H_3: CA has no significant effect on the gross margin of the system compared to CON.

While the overall gross margins between treatments did not significantly differ, notable variations were observed in specific cropping years. In 2022, both treatments performed similarly during the spring bean crop, with gross margins of £770 ha^{-1} for the CON treatment and £758.8 ha^{-1} for the CA treatment. This similarity indicates that spring beans may yield comparable economic returns regardless of the management system employed, which concurs with the results from the global meta-analysis by Pittelkow et al. (2015) where they find that NT yields of legumes are not affected by the tillage system in use. In contrast, more pronounced differences were evident during the winter wheat crop of 2023, where the CON treatment achieved a higher gross margin (£850.3 ha^{-1}) compared to the CA treatment (£642.1 ha^{-1}). This result highlights that the CON system may have an advantage under specific

crop management scenarios, possibly related to the higher N fertiliser usage during the cropping year and the increased yield of the wheat crop in the CON treatment (Figure 6.15). In 2024, both treatments recorded negative gross margins, with the CA treatment returning a loss of £243.42 ha^{-1} and the CON treatment a loss of £345.78 ha^{-1}. The negative returns for both systems suggest that external factors, such as market prices or the unfavourable climatic conditions experienced in the autumn (Figure 3.2), may have outweighed the economic benefits of either management system. This result underscores the vulnerability of both systems to adverse external conditions, highlighting the importance of risk management strategies and diversification for farmers.

Overall, the lack of statistically significant differences between treatments suggests that both CA and CON practices can achieve comparable gross margins over time. However, variability between cropping years points to the influence of specific crop responses and external factors on profitability. These findings emphasise the need for adaptive management and continuous monitoring to optimise economic outcomes under variable conditions.

8.4.4 Markov Chain Monte Carlo Simulation

The MCMC simulation approach employed in this study enabled the assessment of price and climate risk under different scenarios, generating different cost scenarios, and enabling a better understanding of the risks, rather than relying on single estimates or simple averages (Amorim et al., 2024). This provides insights into the stability and predictability of crop profitability under varying economic conditions. The methodology integrates climate shocks into the simulation model by incorporating both probability and severity components. The approach accounts for the increasing likelihood of climate shocks over time and the differential impact of these shocks on CON and CA systems. By dynamically modifying yield and revenue, the model enables an analysis of the economic consequences of climate variability under different agricultural management strategies.

In summary, the MCMC simulation suggests that winter wheat and spring barley are the highest-yielding crops, with winter wheat showing the most pronounced revenue increase in the CA treatment. Oilseed rape and feed peas show relatively stable revenue projections, with slight increases in CA. Winter barley, winter beans, and oilseed rape all show varying degrees of stability and slight fluctuations in revenue across the simulation years. Both treatments exhibit differences in revenue variability, with the CA treatment showing higher variability across most crops. These results

indicate that while both systems are similarly responsive to changes in yield, the CON system appears to be more affected by extreme shock events, whereas the CA system shows a slightly greater sensitivity to price variations. This information can be used to inform risk management and decision-making strategies by highlighting which factors most influence gross margin outcomes under each treatment.

The simulation results indicate that winter wheat consistently emerges as the most profitable crop across both CA and CON treatments, with the CA treatment showing a more pronounced gross margin increase (16.5%) compared to the CON treatment (5.2%) over the six years. Winter barley also performs well under CA practices, with a notable increase of 24.2% in gross margin, while its profitability declines under CON management, reaching negative values by year six. Oilseed rape exhibits contrasting trends, with CA practices showing modest gross margin improvements, whereas CON practices result in persistent negative margins. Winter beans and feed peas consistently yield negative gross margins regardless of treatment, with losses intensifying over time, suggesting these crops may be economically unviable within the agricultural, market, and climatic contexts modelled in this study.

Overall, gross margin predictions indicate that CA generally supports higher profitability and demonstrates resilience to economic variability. The results suggest that crop selection is crucial to maintaining economic viability, as some crops are more suited to the transition to CA, as yield reductions are less common (Pittelkow et al., 2015). These insights can guide decision-making strategies for farmers and agronomists aimed at balancing profitability and risk during the transition to CA, particularly in the context of economic uncertainty, a changing climate, and potential market fluctuations.

8.5 Conclusion

This study highlights the complexity of economic decision-making in agricultural systems, demonstrating that while CA can reduce operational and input expenditures, it did not outperform CON practices in terms of gross margin during this study period. Although the overall difference between treatments was not statistically significant, the analysis revealed that the choice of cropping system has important implications for economic resilience and profitability.

The use of MCMC simulations allowed for the incorporation of risk and variability, reflecting real-world uncertainties in price and climate conditions for future prediction

of the entirety of a predicted crop rotation. This approach underscores the importance of balancing profitability with risk management, particularly when adopting CA practices. The findings suggest that while CA systems offer potential economic advantages through reduced expenditure and increased resilience to some external pressures, however, in some scenarios, they also introduce variability and may not consistently achieve higher gross margins. Future research should focus on evaluating the long-term economic impacts of CA beyond the experimental time frame and exploring strategies to mitigate the initial transition costs that pose barriers to adoption.

Chapter 9

General Discussion

9.1 Introduction

Conservation Agriculture (CA) is an agricultural system designed to manage agroecosystems for improved and sustained productivity by conserving and enhancing soil quality and biota (FAO, 2014; Page et al., 2020). Despite widespread promotion and adoption in various regions globally, the effectiveness and sustainability of CA remain topics of ongoing debate and investigation (Giller et al., 2015). This study presents the results of a systems-level case study evaluating CA in the UK. A series of results is presented to evaluate the effects of CA on the soil physical, chemical and biological environment, the differences in the general agronomic approach to crop production and protection and the risk that associated agrochemicals pose to the environment, soil greenhouse gas emissions, and economic analysis of CA compared to Conventional Agriculture (CON). This chapter synthesises the findings of this research, discusses their implications, and discusses how the results align with the existing body of research.

9.2 Research Limitations

This study presents a systems-level case study of CA in the UK. A systems-level approach offers significant benefits, as it captures the complex interactions between different components of the agricultural system, including soil management, crop performance, economic factors, and environmental outcomes (Drinkwater et al., 2016; Darnhofer et al., 2012; Byerlee et al., 1982). By employing this methodology, the study can assess not only direct economic impacts but also indirect effects, such as changes in soil health and agronomic management. In addition, many previous studies collect economic data from small plot trials, which are less representative of commercial

field conditions and may be more prone to produce misleading results (Madarász et al., 2025; Drinkwater et al., 2016; Byerlee et al., 1982). The methodology used in this study collects economic data at the field scale, which is more representative of commercial conditions.

However, the systems-level methodology also presents certain drawbacks. One key limitation is the increased complexity associated with integrating diverse data sources and accounting for multiple interacting variables, leading to challenges in data interpretation. Furthermore, systems-level analyses are often context-specific, meaning that findings may not be easily generalizable to other regions or farming systems without additional data and contextual adjustments (Darnhofer et al., 2012; Stefanova et al., 2023). Despite these challenges, the systems-level approach remains a valuable, and complements existing reductionist traditional research, as it enables a more comprehensive understanding of how the CA system functions as a whole and how it is applied in a commercial setting, instead of being reduced to its constituents (Drinkwater et al., 2016). Future research could expand on this study to assess the regional differences in the approach and response to CA throughout different regions of the UK.

One considerable limitation to the analysis of the agronomic approaches for the treatments used in this study is that different agronomists managed both experimental treatments. The agronomists may have different opinions and recommendations for certain scenarios based on their assessments, personal preferences, and knowledge of local conditions. Therefore, the crop nutrition and protection strategies used in this study are highly tailored to local conditions and may not be truly representative of the wider UK, where different soil types, crop rotations, and climatic conditions will affect the agronomic decisions made. To draw valid conclusions on the agronomic approaches used in CA practices in the UK, a larger dataset would be required that encompasses cropping data from across the UK. In addition, this study did not use any cover crops because of logistical difficulties with agricultural contractors. However, their use could be an effective methodology for farmers to minimise the risk of yield penalties during the transition to CA (Pittelkow et al., 2015; Van den Putte et al., 2010) via improvements to soil structure (Blanco-Canqui and Ruis, 2020; Wilson et al., 1982).

9.3 Summary and discussion of key findings

9.3.1 Chapter 4: Application of Soil Proximal Sensors to Guide the Transition to Conservation Agriculture

Summary of results

1. Neither GRS nor EC scanning alone provides reliable field-scale soil texture predictions for informing precision agriculture decisions.

2. Soil sensor fusion (combining multiple sensor types) is a promising approach, but current commercial implementations are not yet robust enough.

Discussion of results

This chapter investigated the potential of two widely used commercial sensors, gamma-ray spectrometry (GRS) and electrical conductivity (EC), to generate high-resolution soil texture maps that could inform agronomic decision-making at the field scale and aid in the planning and application of the transition to CA. The results provide important insights, but also highlight critical limitations in current sensor performance and implementation.

The rationale for the use of soil proximal sensors for soil mapping is that they facilitate the collection of larger amounts of spatial data using cheaper, simpler, and less laborious techniques than conventional soil sampling and laboratory analysis (Viscarra Rossel et al., 2011; Schmidinger et al., 2024). However, a key finding of this study was that neither GRS nor EC scanning provided sufficiently accurate predictions of soil texture to replace or substantially supplement physical soil sampling (Figure 4.3). GRS was moderately effective in estimating clay content, while EC predictors showed relative strength in estimating sand and silt fractions. However, the Random Forest machine learning model revealed that both technologies contributed complementary, non-redundant information, with variable importance scores showing that each sensor added predictive value depending on the soil property. These results suggest that multi-sensor approaches, often referred to as "soil sensor fusion," hold promise for improving the accuracy of soil texture prediction. This aligns with previous recommendations in the literature advocating for the integration of multiple sensor data streams to better capture the complex, site-specific relationships that drive soil variability (Ji et al., 2019; Vasques et al., 2020; Rhymes et al., 2023; Kok et al., 2024).

However, the study also exposed significant limitations in the current commercial application of these technologies. Prediction errors, particularly for sand and silt content, were high (Table 4.2), and model performance was likely constrained by the relatively low density of calibration samples. This raises concerns about the reliability of sensor-derived maps provided to farmers and questions the robustness of decision-making based solely on these outputs. Notably, the analysis revealed that even when combining EC and GRS data, the models did not achieve the level of precision necessary for confident implementation of precision agriculture practices, such as variable-rate seeding or nutrient management, where inaccuracies can translate into financial loss or agronomic risk to farmers. This is most likely due to the small training and test datasets in this study. Therefore, future research could focus on scaling this methodology up to larger study areas with a more comprehensive dataset.

While CA promises improvements in agricultural resilience and ecological conditions, its successful implementation depends on an accurate understanding of site-specific soil conditions to tailor management to those areas. Soil maps that fail to deliver reliable spatial information risk undermining this transition by misinforming management decisions. For example, Rhymes et al. (2023) found that the commercial soil mapping services inaccurately predicted soil pH, P, K and Mg on grasslands in the UK, and therefore these methods were not appropriate for calculating variable lime and organic/inorganic fertilisers application rates, which could lead to negative environmental and/or economic implications for farmers. Moreover, the findings reinforce that technological solutions must be accompanied by robust validation frameworks and agronomic support to farmers to ensure they meet the practical needs of farming systems (Rhymes et al., 2023). In the broader context of sustainable agriculture, the study underscores the need for continued research and development in soil proximal sensing methodologies, including improving calibration protocols (Rhymes et al., 2023), enhancing machine learning models (Pätzold et al., 2020), remote sensing (Schmidinger et al., 2024), and standardising commercial services (Rhymes et al., 2023). Overall, this chapter's findings illustrate the potential but also the current limitations of precision agriculture technologies in supporting sustainable farming transitions.

9.3.2 Chapter 5: Soil Health and Function Under Conservation Agriculture

Summary of results

1. CA resulted in a significantly increased soil bulk density compared to the CON treatment.

2. Weak evidence (β = -0.04, SE = 0.02, Z = -2.33, p = 0.051) of an increase in total SOC was observed in the CA treatment compared to CON.

3. CA resulted in significantly higher soil nutrient availability compared to the CON treatment.

4. CA resulted in a significant reduction in soil microarthropod biodiversity in comparison to the CON treatment.

Discussion of results

This study tested the hypothesis that CA would reduce soil bulk density compared to CON, due to the reduction of mechanical disturbance and the expected enhancement of soil structure over time through improved biological activity. However, the results did not support this hypothesis, as both treatments exhibited an increase in bulk density over the three years, with CA showing a significantly higher bulk density than CON (Figure 5.2).

This outcome aligns with previous studies reporting that the initial transition to CA can lead to short-term increases in bulk density, particularly in the surface layers (Soane et al., 2012; Pidgeon and Soane, 1977; Li et al., 2020a). However, this is not found in all studies, for example, the review by Blanco-Canqui and Ruis (2018) found that NT increased bulk density in 39% of the studies assessed and increased penetration resistance in 50% of the studies. They found that changes in soil bulk density were moderately negatively correlated with NT duration, suggesting that bulk density under NT can be initially higher compared with CON, but as the implementation duration of NT increases, differences in bulk density between NT and CON diminish.

In the absence of tillage, natural consolidation processes occur, such as rainfall (Todisco et al., 2022) and anthropogenic, such as repeated traffic with heavy equipment. Blanco-Canqui and Ruis (2018) suggests that soils under NT can be more susceptible to compaction in the first few years after the transition to NT compared to soil managed using CON. The magnitude of these differences decreases with time,

possibly as soil organic C accumulates and the biological activity associated with CA systems—particularly the formation of biopores by earthworms begins to reduce soil bulk density (Yvan et al., 2012), but such improvements typically require long-term system establishment (Mondal et al., 2019). For example, Pidgeon and Soane (1977) found NT system increases in soil bulk density for the first three years; however, after that, no increases in bulk density were identified.

An additional factor influencing the observed increases in bulk density was the above-average rainfall experienced during the experimental period (Figure 3.2). High rainfall intensifies surface compaction through raindrop impact, especially when combined with reduced soil cover or insufficient residue retention (Todisco et al., 2022). This highlights the importance of considering climatic variability when interpreting short-term soil physical responses to management changes.

Penetration resistance data provided a more nuanced picture, with CA exhibiting lower resistance in the upper to mid soil layers (10 - 45 cm) but higher resistance at greater depths (50 - 70 cm) compared to CON (Figure 5.4). This result is similar to the study by Mondal et al. (2019), who found that even though CA and CON had similar bulk density, the CA treatment had lower penetration resistance values in the upper soil layers owing to 14% higher water content. These results suggest that while CA may begin to improve subsoil conditions over time, surface consolidation and legacy effects from prior management can still dominate the early years of transition.

Physical soil conditions are a particular consideration for those planning on moving to CA, as it may pose challenges for crop establishment, root penetration, and water infiltration during the initial transition years (Logsdon and Karlen, 2004; Blanco-Canqui and Ruis, 2018). Farmers should carefully consider soil type and implement complementary practices where possible (Li et al., 2020a). It has generally been shown that NT management is more difficult on heavy soils (Baker et al., 2006; Blanco-Canqui and Ruis, 2018; Morrison Jr. et al., 1990) and so this is a potential limiting factor in the uptake of CA in areas with heavy soils.

Whilst implementing all three of the principles of CA is important to minimise the risk of yield penalties (Pittelkow et al., 2015; Van den Putte et al., 2010), as well as soil structural issues, long term use of NT may result in an overall decline in the functionality of agricultural soils due to stratification of plant nutrients, or herbicide resistant weed problems (Çelik et al., 2019; Lawrence et al., 2023). Here, the application of strategic tillage may be a suitable management option to improve physical soil conditions for crop growth, air and water movement, as shown by Çelik et al. (2019) and Lawrence et al. (2023).

Additionally, farmers will want to carefully consider the type of seed drill they are using. This study discusses the benefits and drawbacks of disc and tine-based NT drills, and emphasises the benefits for farmers in the UK who are practising CA to have access to disc and tine-based opener drills. This can greatly improve the flexibility and success of crop establishment, as in some cases, challenging drilling conditions cannot be avoided even with improvements to work rate efficiency that are associated with NT systems.

Overall, the findings indicate that improvements in soil physical properties under CA are unlikely to emerge rapidly and may initially present as neutral or even negative trends. This underscores the need for long-term assessment to capture the temporal dynamics of physical recovery under CA and to distinguish between short-term transitional effects and the longer-term benefits often reported in the literature.

This study tested the hypothesis that CA increases SOC over time compared to CON systems. While SOC is often cited as a key indicator of soil health and a central benefit of CA adoption, the results of this study provide only partial support for this hypothesis. Across the study period, weak evidence (β = -0.04, SE = 0.02, Z = -2.33, p = 0.051) of an increase in total SOC was observed in the CA treatment compared to CON; however, neither treatment showed an increase relative to the baseline values (Figure 5.5). Both systems exhibited slight declines in SOC over the three years. This suggests that while CA may slow the rate of C loss, it did not lead to measurable C sequestration within the time frame of the experiment. This finding aligns with previous research indicating that SOC accumulation under CA typically requires long-term commitment, often exceeding a decade, before substantial changes are detectable. The reduced soil disturbance in CA slows the decomposition of organic matter by protecting aggregates, yet the system may initially be characterised by an imbalance between organic matter inputs and mineralisation rates.

The study found significant increases in total N, P, K, and Mg under CA compared to CON. These results are consistent with results from previous literature, where NT and residue retention have been found to enhance nutrient pools by decreasing leaching losses and improving nutrient retention in the surface layers (Li et al., 2007). Additionally, previous studies have shown that, during early years of CA adoption, total N may increase while available N can decrease due to slower mineralisation rates and microbial immobilisation driven by high C inputs (Mukherjee et al., 2024). As this study did not assess plant-available N or microbial activity, it remains unclear whether the observed nutrient increases translate into agronomic benefits or improved nutrient

cycling efficiency. Overall, the findings provide partial support for the hypothesis that CA improves soil chemical properties, particularly by enhancing total nutrient pools.

This study set out to test the hypothesis that CA would increase the diversity and abundance of soil meso and macrofauna, particularly earthworms and microarthropods, compared to CON practices. While the literature often highlights the potential for CA to benefit soil biodiversity by reducing disturbance, increasing organic matter inputs, and promoting a beneficial soil habitat, the findings from this study show that these expected benefits may take time. Across the three years of experimentation, no significant differences were detected between CA and CON systems in the abundance of total earthworms, their ecological categories (epigeic, endogeic, anecic), or juvenile stages. This contrasts with several long-term studies reporting higher earthworm biomass and activity under NT or RT systems (Baldivieso-Freitas et al., 2018; Soane et al., 2012; Pelosi et al., 2009). Notably, previous research has shown that endogeic earthworms may sometimes favour tilled systems due to the incorporation of organic matter deeper in the soil, whereas anecic and epigeic earthworms typically benefit from surface residues and undisturbed conditions (Baldivieso-Freitas et al., 2018; Pelosi et al., 2009). The absence of treatment differences in this study may reflect several factors: short experimental duration, low replication, seasonal variability, or the influence of other management practices such as pesticide and fertiliser regimes.

For soil microarthropods, similar patterns were observed. While groups such as Chelicerata and Hexapoda showed no significant differences between treatments, the Myriapoda group was unexpectedly more abundant under CON management. Myriapoda (e.g., Pauropoda, Symphyla) are characteristic of undisturbed habitats, and are therefore often sensitive to disturbance (Curry and Momen, 1988; Davis and Sutton, 1978; Bedano et al., 2006). This result was surprising and suggests a need for more detailed investigation into within-group dynamics and species-level responses.

Analyses using soil biodiversity indices (QBS-e, QBS-ar) and the Shannon Diversity Index highlight the complex and sometimes counterintuitive patterns observed in this study. Shannon index biodiversity index values were significantly higher under CON, contradicting the hypothesis that CA would have higher biological quality and diversity during the experiment. These findings suggest that tillage may not be the sole driver of soil biological responses in this system; other interacting factors, such as chemical inputs, crop rotations, crop health, or the soil physical environment, likely play substantial roles (Lehman et al., 2015b).

Principal components analysis (PCA) revealed gradual changes in community structure between CA and CON throughout the study period, with variance explained by the first two principal components increasing from approximately 60% to 87% across years. This trend suggests the possibility of emerging treatment effects on soil biotic communities, but also highlights that soil biodiversity may respond slowly and require long-term monitoring to detect robust patterns.

Overall, the results did not support the initial hypothesis that CA would result in significantly higher diversity and abundance of soil microarthropods and earthworms in comparison to CON practices. While CA is frequently championed for its potential to rebuild soil biotic communities and enhance ecological function, this study reinforces findings from other research that these benefits may require long-term commitment and favourable management conditions (Henneron et al., 2015). The observed lack of change or unexpected results underscore the importance of considering context-specific variables and avoiding assumptions of universal CA benefits. As Kassam et al. (2022) states; the three interlinked CA principles constitute the ecological foundation upon which sustainable agriculture can be built with complementary good agricultural practices. Future research would benefit from longer time horizons, larger sample sizes, and integrated assessments of microbial, faunal, and functional diversity, alongside agronomic and environmental variables such as moisture, temperature, and input regimes.

9.3.3 Chapter 6: Agronomy and Crop Productivity Under Conservation Agriculture

Summary of results

1. No statistically significant differences were observed in the percentage achieved of the UK average yield between the CON and CA treatments.

2. No significant differences were identified in total pesticide mass applied between the CA treatment and the CON treatment. However, the CA treatment applied significantly more herbicides, and the CON treatment applied significantly more fungicides and insecticides.

3. CA resulted in significantly reduced N fertiliser application; however, no significant differences were detected in P or K applications.

4. The pesticide applications in the CA were found to have significantly higher potential environmental risks in comparison to the CON treatment when assessed with the Danish Pesticide Load Index. The main driver of this was a significantly higher environmental fate load in the CA treatment in comparison to the CON treatment. No significant treatment differences were observed for the ecotoxicity or human health risks of the pesticide agronomic plans.

Discussion of results

This chapter provides an integrated assessment of CA compared to CON over three years in a UK field context, evaluating agronomic performance, input use, environmental risks, and crop yields. One of the insights from this study is the operational vulnerability of CA systems at times, particularly under wet and variable UK weather conditions. The poor establishment and ultimate failure of the oilseed rape under CA in the third year of the experiment is a challenge widely reported (Allison, 2023). While CA offers long-term soil health and sustainability benefits, its success is dependent on appropriate machinery, timing, and field conditions. This reinforces the view that CA is not a simple blueprint solution but rather an adaptive management system requiring flexibility in agricultural practice (AHDB, 2024). Farmers can be aided in CA management by access to different types of seed drills and a readiness to adjust practices in response to local weather and soil conditions.

There is a common perception that CA systems are less reliant on agrochemicals than the CON system (Kassam et al., 2009). However, the lack of significant differences in total pesticide mass usage between CA and the CON system in this study suggests that CA is not inherently more or less reliant on agrochemicals compared to CON. The usage rate and types of chemistry of pesticides are likely to be related to the changing agro-ecological conditions as the systems develop, as well as the cultural influences of the farmer or agronomist. Therefore, future research should prioritise longer studies which encompass a wider dataset of industry practices.

The increased use of herbicides in CA systems raises concerns regarding environmental risks (Dong et al., 2024; Morris et al., 2010; FAO, 2001). The increased use of herbicides could be expected to have significantly higher potential risks to the environment, as demonstrated by the Danish Pesticide Load Index (Figure 6.12). Farmers and agronomists interested in reducing inputs of agrochemicals in CA in the UK have mainly focused on fertiliser and insecticides (Impey, 2022b). However, as the results of this study demonstrate, more consideration should be given to identifying and quantifying trade-offs associated with reductions in the mass of herbicide applied and

crop productivity (Nazarko et al., 2005). This should also be prioritised to enable maximising the potential benefits of CA on biodiversity, as well as prolonging the efficacy of herbicides by restricting the development of herbicide-resistant strains (Varah et al., 2024). Considering the diversity of weed problems in CA systems, no single method of weed control (cultural, mechanical or chemical) typically will provide the desired level of weed control (Singh et al., 2015). Farmers and agronomists should aim to utilise integrated weed management (IWM) strategies (Swanton and Weise, 1991; Varah et al., 2024; Farooq and Siddique, 2015; Singh et al., 2015; Riemens et al., 2022) to reduce herbicide dependency in CA. IWM encompasses a wide variety of weed management strategies, some of which are already commonplace within CA, such as a diversified crop rotation (Singh et al., 2015; Nazarko et al., 2005), increasing crop density (Singh et al., 2015; Nazarko et al., 2005), and use of cover crops (Singh et al., 2015; Nazarko et al., 2005; Fernando and Shrestha, 2023). However, it is important that farmers and agronomists adapt their weed management approach in CA to the local level, which could include identification of the site-specific economic threshold for weeds, improvements to herbicide application timeliness, mechanical weed control, planting dates, and cultivar selection (Nazarko et al., 2005; Singh et al., 2015; Derrouch et al., 2020). A detailed framework for the planning and design of holistic IWM strategies is presented by Riemens et al. (2022), which consists of five pillars: diverse cropping systems, cultivar choice and establishment, field and soil management, direct control, and monitoring and evaluation (Figure 9.1). This framework aims to manage and regulate the weed community over the whole cropping system, instead of a single season-single crop-single year. They stress that the appropriate IWM approach should be tailored to the local level, through a participatory approach including all stakeholders, to tailor the approach based upon the local cropping system and the macro-ecology of the weed communities.

Despite clear differences in agronomic management and crop inputs, no statistically significant differences in crop yields were observed between CA and CON treatments over the study period (Figure 6.15). While this aligns with meta-analytic evidence that yield gaps often close over time, particularly when all three CA principles are implemented (Pittelkow et al., 2015; Su et al., 2021), it also reflects limitations of experimental scale and statistical power in this study. The small sample size ($n = 5$) likely constrained the ability to detect treatment effects, even when agronomically meaningful differences existed. This echoes a wider challenge in agricultural systems research, where complex interactions between weather, soil, management, and biolog-

ical processes generate high variability that can mask underlying trends in short-term trials.

Figure 9.1: The Integrated Weed Management (IWM) Framework by Riemens et al. (2022) for the planning and design of holistic IWM strategies that require combinations of individual management tools appropriately selected from each of the five pillars of IWM: Diverse cropping systems, cultivar choice and establishment, field and soil management, direct control and the cross-cutting pillar monitoring and evaluation.

9.3.4 Chapter 7: Soil Greenhouse Gas Emissions in Conservation Agriculture

Summary of results

1. CA significantly reduced soil-derived N_2O emissions compared to the CON treatment; however, no differences were detected for CO_2 or CH_4 emissions.

2. CA did not significantly affect the Global Warming Potential (GWP); however,

when GWP was considered with crop yield, CA was found to increase the yield-scaled GWP significantly.

Discussion of results

There is a growing awareness of the importance of managing soil GHG emissions in the UK, with an effort for the agricultural industry to become net-zero by 2040 (NFU, 2023; HM Government, 2023). Agriculture is one of the only National Communication Sectors (BEIS, 2023), along with Land Use, Land Use Change and Forestry (LULUCF), that can sequester C and so has the potential to offset emissions from the other sectors (Follett, 2001; Page et al., 2020). However, it is currently a major contributor to GHG emissions, with key GHGs such as N_2O largely being produced in and emitted from the soil (IPCC, 2023; DEFRA, 2022). Previous literature has shown that the effects of the individual principles of CA on GHG emissions produced heterogeneous results in comparison to conventional practices (Shakoor et al., 2021; Valujeva et al., 2022; Abdalla et al., 2016; Dendooven et al., 2012a; Sainju, 2016). This highlights the influence of other factors, other than the farming system, which are also key drivers of GHG emissions. For example, Rochette et al. (2008) found that implementation of NT in a loam soil resulted in similar N_2O emissions in NT and mouldboard ploughed treatments; however, in a heavy clay soil, the N_2O emissions in the NT treatment were more than double that of the ploughed treatment. This result illustrates the influence of soil texture on GHG emissions and how soil texture interacts with the cropping system to produce different physical, chemical, and biological conditions in the soil, which affect GHG flux. Therefore, there is a need for more research on the effects of CA on soil GHG emissions across multiple soil and climate types, and crop species, as all are known to be significant drivers in GHG emissions (Abdalla et al., 2016; Shakoor et al., 2021).

One limitation of this study was that the soil GHG flux data were acquired during one cropping season and not for the entirety of the experiment. The CON system received some sort of cultivation for all crops planted, which is known to accelerate SOM microbial decay, releasing C to the atmosphere (Hendrix et al., 1986; Beare et al., 1994; Page et al., 2020). The CON system also received significantly more N fertiliser throughout the experiment, which has been shown in this study and others to be the major driver of N_2O emissions (Cosentino et al., 2013; Rees et al., 2013). It could be hypothesised that the long-term effects of both tillage and higher N fertilisation would stimulate higher GHG emissions throughout the crop rotation. However, the short-term nature of the GHG sampling period in this study was not sufficient to test

that hypothesis. Another significant limitation of the short-term sampling period used in this study was that the long-term effects of SOC sequestration were not taken into account in the analysis. The SOC data presented in Section 5.3 identify some weak evidence ($p = 0.051$) for an increase in the CA treatment compared to the CON treatment. Although neither treatments were found to be significantly different from the baseline measurements, this shows a difference in the rate of SOC loss between the two treatments. This highlights that the CON treatment has reduced the SOC stock significantly in comparison to the CA treatment, either in the form of direct soil CO_2 emissions, or in the form of crop biomass exported from the field. An improvement to this study would be to extend the GHG sampling period over a longer duration, factor in the SOC stock into the GWP calculations. Future research should also take into account the indirect GHG emissions of crop biomass exported from the field, and the indirect emissions from machinery operations and crop protection products used via Life Cycle Assessment (LCA). This is an important consideration in research on the GWP of CA, as it has been shown in this study and previous research that CA results in lower usage of machinery, fuel, and some pesticides (Kassam et al., 2009; Parihar et al., 2018; Ponce et al., 2022; Nalewaja, 2003; Morris et al., 2010).

9.3.5 Chapter 8: Economic Analysis of Conservation Agriculture

Summary of results

1. CA was shown to significantly reduce expenditure on machinery operations and crop applications compared to the CON treatment, whilst not reducing revenue.

2. CA required significantly less operational passes ha^{-1}, significantly less machinery operational time, and significantly less fuel usage, compared to the CON treatment.

3. There were no statistical differences identified in the gross margin or net profit margin for both the CA and CON treatments.

Discussion of results

One of the most promising aspects of CA identified in this study is the reduction in operational costs, fuel usage, and machinery time without significantly compromising revenue. This makes CA an economically viable option to farmers, particularly in scenarios where labour or machinery availability is a limiting factor for the specific

farm business. In this study, CA significantly reduced the amount of time and number of operational passes needed ha^{-1}, which will save farmers time and allow them to focus on other parts of their businesses. For example, some estimates put the labour requirements of CA in the region of 50 - 60% lower than CON practices (FAO, 2001). On large mechanised farms, this equates to small savings for farmers as typically labour only accounts for around 10% of the total expenditure ha^{-1} (FAO, 2001). Despite this, there is a trend towards increased off-farm work or farm business diversification on farms in the UK, which will make even the relatively small labour savings under CA attractive to some farmers (FAO, 2001).

In addition, CA reduced the economic risk for farmers, due to the significantly lower fuel and N fertiliser usage. Both the fuel and fertiliser markets have been increasingly volatile in recent years (Clark, 2022; AHDB, 2025); therefore, reducing inputs of both reduces the economic risks associated with volatile market prices for farm businesses. However, while CA can reduce input and operational costs, it does not guarantee improvements in gross or net profit margins as shown in this study.

One limitation of the economic analysis of the treatments used in this study is that, as discussed previously in this chapter, the results are highly specific to the local area. To extrapolate the conclusions to wider areas of the UK, wider data collection would be required to capture regional variation in agronomic approach, soil types, crop rotations, climatic conditions, and local markets. This is particularly important as the productivity of CA has been shown to produce highly heterogeneous results dependent on the agro-ecological conditions (Pittelkow et al., 2015; Rockström et al., 2009; Corbeels et al., 2014; Shakoor et al., 2021; Van den Putte et al., 2010). For example, Zentner et al. (1991) found that CA required lower expenditure than CON for fuel, labour, machine repair and machine overhead costs; however, these savings on expenditure were completely offset by significantly increased herbicide costs.

In this study, all operational expenditure data is standardised from the national recommended prices for each agricultural machinery operation (NAAC, 2022). Further research could simulate different ownership scenarios for machinery operations, as the majority of farmers in the UK would not use contractors for the entirety of the cropping operations. This would factor in the initial costs of the transition to CA, as investment in new machinery will significantly affect the economic outlook for farmers during those initial transition years. One important aspect not addressed in the current analysis is the use of Net Present Value (NPV) to assess the long-term financial viability of CA. NPV is a valuable tool for quantifying the present value of future cash flows, accounting for the time value of money (Lalani et al.,

2017). Including NPV analysis in future research would allow for a more comprehensive assessment of the economic sustainability of CA and better inform farmers about the potential long-term benefits and costs associated with transition investments. Another improvement to this study could have been to run the study for a longer duration of time, as economic calculations can be significantly influenced by the yearly variability of the weather during the study period, possibly leading to erroneous conclusions (Madarász et al., 2025). This is of particular note in this study, where there was far higher rainfall than average recorded on several occasions throughout the study (Chapter 3) (Met Office, 2024). This highlights the importance of conducting long-term studies on CA.

9.3.6 General Discussion

The findings of this study demonstrate that CA presents both opportunities and challenges for farmers. By recognising both the benefits and limitations of CA, farmers and agronomists can make informed decisions about integrating these practices into their farming systems. Overall, CA was shown to have no significant effect on the percentage achieved of the UK average yield compared to the CON (Figure 6.15), with a significant reduction in N fertiliser usage (Figure 5.9). In economic terms, CA significantly reduced expenditure, fuel usage, and machinery operational time compared to CON, whilst returning a similar gross margin across the three-year experiment duration. Typically, the transition to CA is championed by farmers who are aiming to improve soil health and resilience on their farm and reduce the environmental impacts of their agricultural practices. However, this study also identified a significant reduction in soil biodiversity in the CA treatment in comparison to the CON treatment. The potential benefits of CA to soil biological health are well documented in the literature (Palm et al., 2014; Li et al., 2018; Page et al., 2020; Oliveira et al., 2024). Therefore, this highlights that farmers and agronomists need to allow the system to develop over time before they can expect to see improvements to soil health (Impey, 2022a; Mondal et al., 2019; Cárceles Rodríguez et al., 2022; Montgomery, 2021). The results presented in this study are in line with the five-year study of NT in the UK by Cooper et al. (2020), who found that NT did not significantly alter the soil's biological, chemical, or physical condition relative to conventional ploughing establishment. However, they found that NT returned a 13% higher net profit margin during the experimental period due to savings in operational efficiency and crop yields.

9.4 Further Research

This study has provided important insights into the agronomic, environmental, and economic implications of CA under UK conditions. However, several knowledge gaps and limitations were identified for future research and are discussed in the following section.

Longer-term studies are needed to assess the cumulative effects of CA on soil health, GHG emissions, and farm economics. Soil biological indicators, in particular, may require many years to show significant change following the transition to CA (Chernov and Zhelezova, 2020). For example, Henneron et al. (2015) found that CA increased the abundance and biomass of all soil organisms, except predatory nematodes, after 14 years of CA. Therefore, it could be hypothesised that this study duration was not long enough to identify significant changes in the abundance of soil organisms. Thus, long-term experiments which capture inter-annual variability in weather, cropping systems, and management adaptations would provide more robust evidence on the resilience and sustainability of CA practices over time. Long-term field-scale studies of CA are also beneficial as they generate evidence to farmers that CA can be productive and profitable, aiding in increased uptake of CA in local communities (Kassam et al., 2022).

This study also observed a significant increase in pesticide environmental load under CA. This may not be representative of all applications of CA in the UK due to differences in agronomic practice. Therefore, further investigation should be undertaken on a wider scale in the UK, on different farms and cropping systems. In addition, further research into integrated weed management (IWM) strategies for CA is critical (Figure 9.1). Future work should aim to design and evaluate holistic IWM approaches that combine cultural, mechanical, and chemical weed control methods tailored to local conditions in CA. This could involve participatory research with farmers, agronomists, and other stakeholders to develop solutions that are both effective and practical at the farm scale (Kassam et al., 2022).

Regional studies are needed to assess how CA performs across diverse UK agroecological zones, soil types, and farm systems. The context-specific nature of CA means that findings from one site cannot be simply extrapolated to others. A network of regional case studies or on-farm trials would help build a more complete picture of the opportunities, risks, and adaptations needed for successful CA adoption nationwide.

The economic analysis of CA would benefit from incorporating Net Present Value (NPV) calculations and scenario analyses to capture the long-term financial implica-

tions and investment risks associated with the transition. Simulating different machinery ownership models (e.g., contractor use, machinery sharing, or ownership) and the capital investment necessary would provide farmers with more realistic estimates of the financial pathways during and after the transition to CA.

This study could be improved by expanding the assessment of environmental impacts through Life Cycle Assessment (LCA). This would enable a more comprehensive evaluation of the indirect emissions and resource use associated with CA, including inputs like fuel, fertiliser, pesticides, and machinery manufacture and maintenance.

Finally, future research should embrace a Farming Systems Research (FSR) approach, working closely with farmers to identify the key barriers to adoption, the knowledge gaps in practice, and the economic or management challenges that they face (Kassam et al., 2022). Understanding the social and cultural parts of CA adoption is as important as agronomic or environmental data for enabling wider uptake.

In summary, future research should prioritise:

1. Long-term and regionally distributed trials.
2. Integration of cover crops.
3. Development of practical IWM solutions.
4. Advanced economic modelling.
5. LCA-based environmental accounting.
6. Participatory, systems-level research with farmers and stakeholders.

Addressing these research needs will be essential to support evidence-based recommendations for CA adoption and its potential role in transitioning UK agriculture towards more sustainable and resilient systems.

9.5 Conclusion

This study demonstrates that the transition period of CA has the potential to be economically similar for farmers in comparison to CON. This result is in line with many previous studies which report similar findings (Zentner et al., 1991; Kumara et al., 2020; Lorenzetti and Fiorini, 2024). Yet the question arises: If CA is economically viable and reduces some economic risk by reductions of inputs and machinery requirements, why is adoption not higher in the UK? CA is knowledge-intensive and a

complex system to learn and implement, requiring more planning than tillage-based systems (Kassam et al., 2009; Vankeerberghen and Stassart, 2016). It cannot be reduced to a simple standard technology and requires a higher degree of localised tailoring to achieve the full potential of the system. Future research needs to be oriented towards solving farmers' problems that inhibit productivity and collecting economic data to aid farmers who are keen to transition their farms into CA. Any environmental benefits from the system cannot be expected to lead masses of farmers, apart from a committed innovator, to adopt CA (Madarász et al., 2025). Therefore, future research needs to draw on multi-disciplinary research, such as Farming Systems Research, to work with all of the stakeholders to collect the economic decision-making data to help farmers and agronomists manage the transition successfully.

Appendix A

Soil Data and Code

A.1 Code availability

The code to produce the data analysis in this chapter can be be viewed and cloned from the following Git repositories:

Soil Biology Code:
`https://github.com/jwollins/soil_biology`
Soil Physics Code:
`https://github.com/jwollins/soil_physics`
Soil Chemistry Code:
`https://github.com/jwollins/soil_chemistry`

A.2 Data availability

The data to produce this chapter will be made available on request from the author. Please contact:

jcollins@harper-adams.ac.uk

A.3 Data Distributions

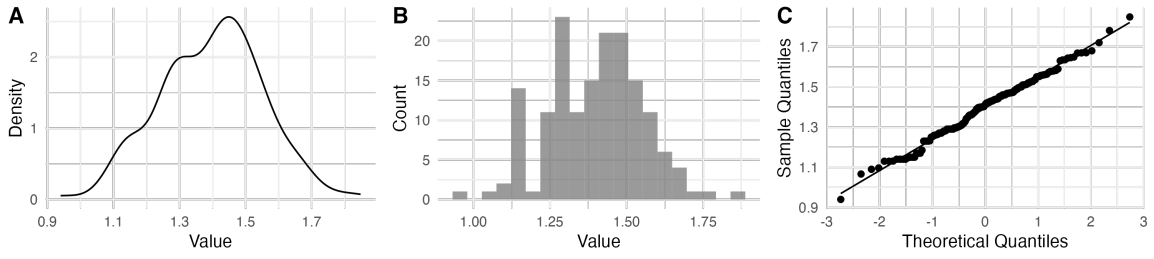

Figure A.1: Joint plot displaying the distribution and normality of soil bulk destiny data (g cm^{-3}). **(A)** Density plot showing the probability density function. **(B)** Histogram to illustrate the frequency distribution across value bins. **(C)** Q-Q plot comparing sample quantiles against theoretical quantiles to assess normality.

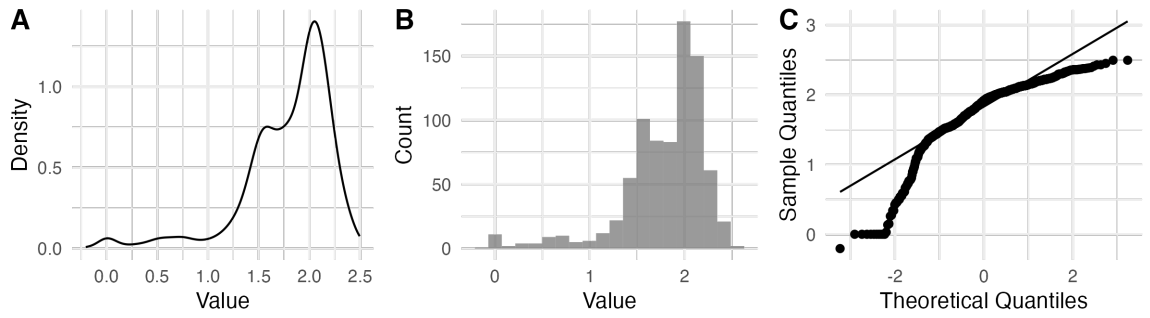

Figure A.2: Joint plot displaying the distribution and normality of the penetration resistance data (MPa). **(A)** Density plot showing the probability density function. **(B)** Histogram to illustrate the frequency distribution across value bins. **(C)** Q-Q plot comparing sample quantiles against theoretical quantiles to assess normality.

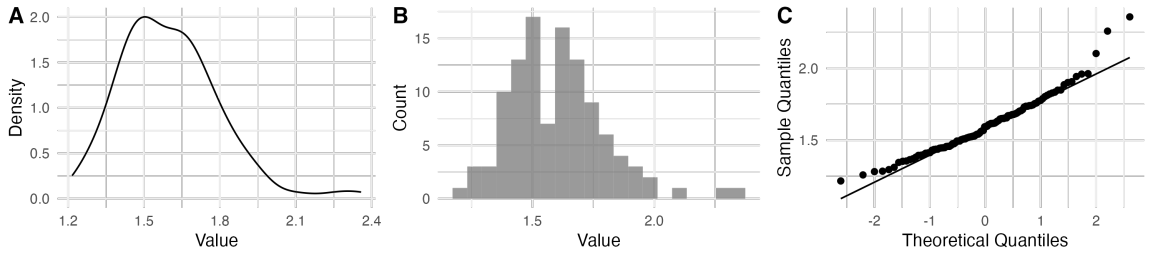

Figure A.3: Joint plot displaying the distribution and normality of soil total carbon content data (%). **(A)** Density plot showing the probability density function. **(B)** Histogram to illustrate the frequency distribution across value bins. **(C)** Q-Q plot comparing sample quantiles against theoretical quantiles to assess normality.

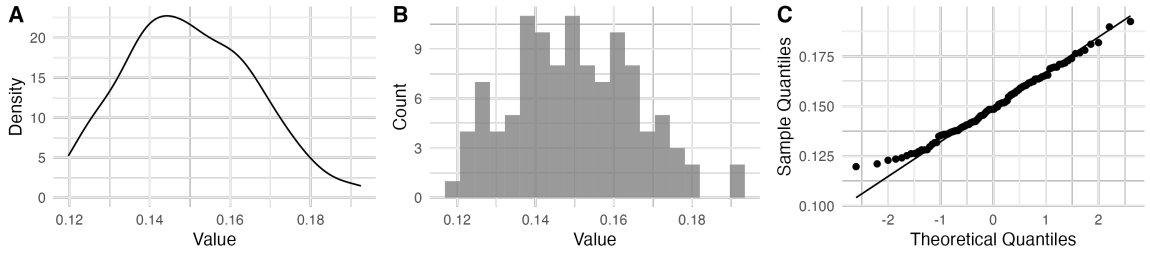

Figure A.4: Joint plot displaying the distribution and normality of soil total nitrogen content data (%). **(A)** Density plot showing the probability density function. **(B)** Histogram to illustrate the frequency distribution across value bins. **(C)** Q-Q plot comparing sample quantiles against theoretical quantiles to assess normality.

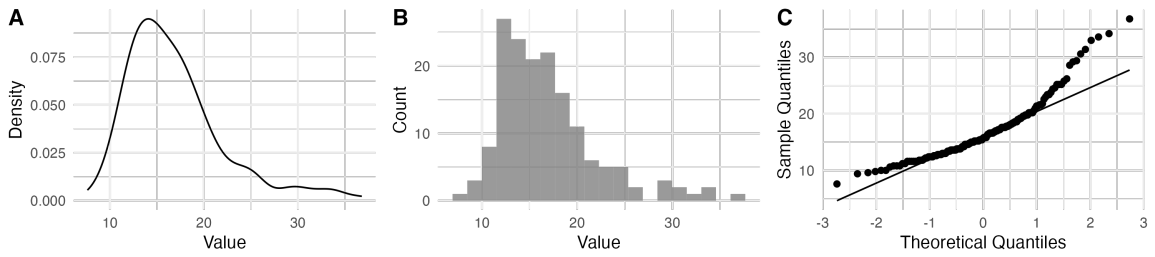

Figure A.5: Joint plot displaying the distribution and normality of soil available Phosphorus (Mg l^{-1}). **(A)** Density plot showing the probability density function. **(B)** Histogram to illustrate the frequency distribution across value bins. **(C)** Q-Q plot comparing sample quantiles against theoretical quantiles to assess normality.

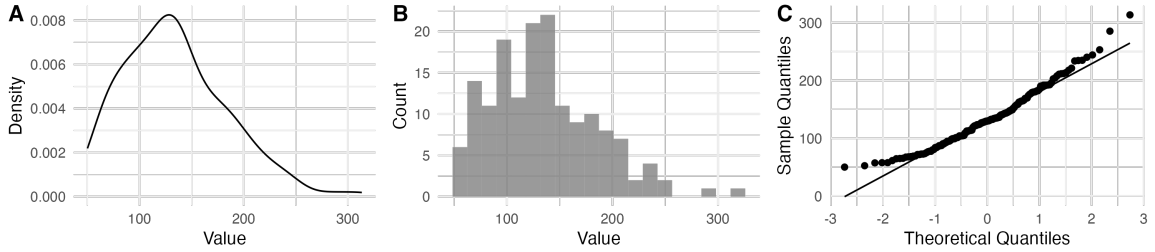

Figure A.6: Joint plot displaying the distribution and normality of soil available Potassium (Mg l^{-1}). **(A)** Density plot showing the probability density function. **(B)** Histogram to illustrate the frequency distribution across value bins. **(C)** Q-Q plot comparing sample quantiles against theoretical quantiles to assess normality.

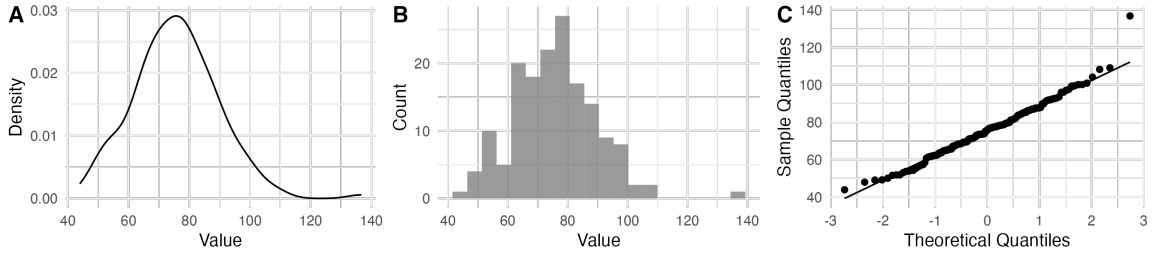

Figure A.7: Joint plot displaying the distribution and normality of soil available Magnesium (Mg l^{-1}). **(A)** Density plot showing the probability density function. **(B)** Histogram to illustrate the frequency distribution across value bins. **(C)** Q-Q plot comparing sample quantiles against theoretical quantiles to assess normality.

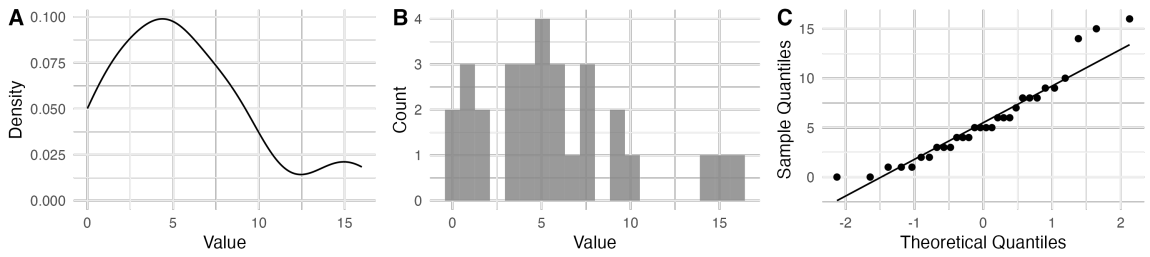

Figure A.8: Joint plot displaying the distribution and normality of juvenile earthworm abundance (m^{-2}). **(A)** Density plot showing the probability density function. **(B)** Histogram to illustrate the frequency distribution across value bins. **(C)** Q-Q plot comparing sample quantiles against theoretical quantiles to assess normality.

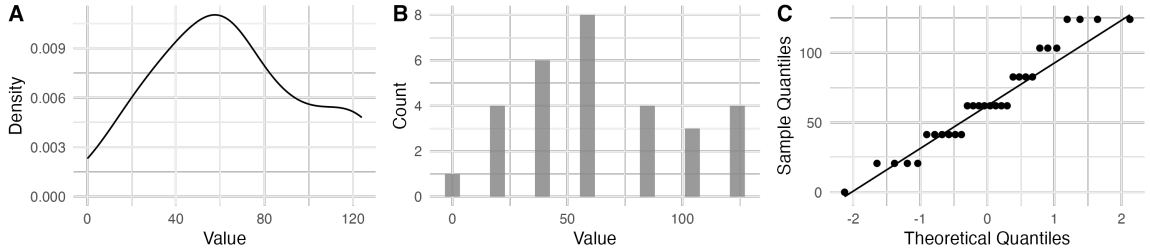

Figure A.9: Joint plot displaying the distribution and normality of Epigeic earthworm abundance (m^{-2}). **(A)** Density plot showing the probability density function. **(B)** Histogram to illustrate the frequency distribution across value bins. **(C)** Q-Q plot comparing sample quantiles against theoretical quantiles to assess normality.

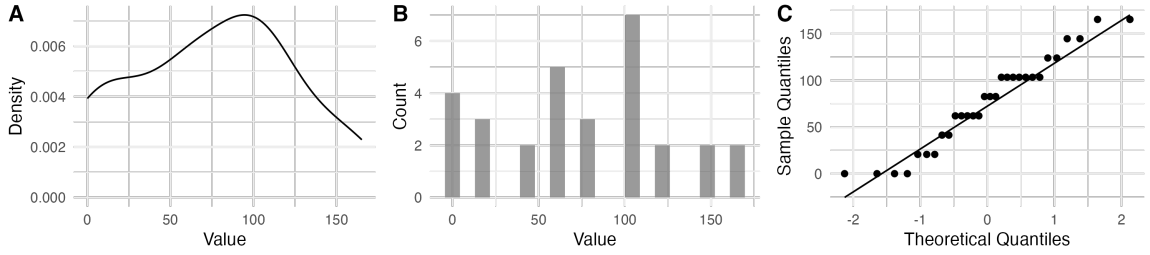

Figure A.10: Joint plot displaying the distribution and normality of Endogeic earthworm abundance (m^{-2}). **(A)** Density plot showing the probability density function. **(B)** Histogram to illustrate the frequency distribution across value bins. **(C)** Q-Q plot comparing sample quantiles against theoretical quantiles to assess normality.

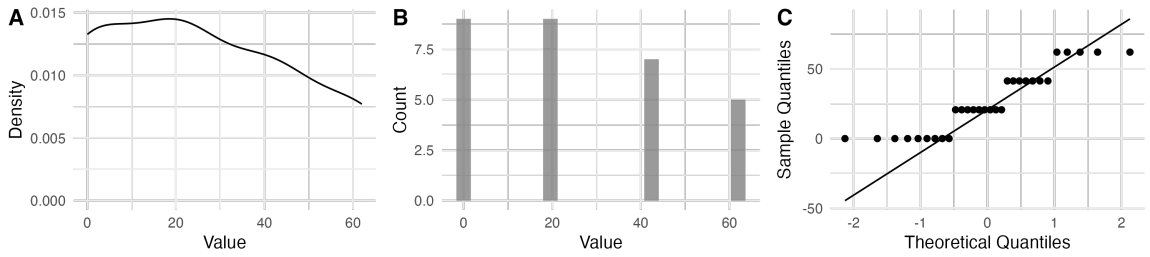

Figure A.11: Joint plot displaying the distribution and normality of Anecic earthworm abundance (m^{-2}). **(A)** Density plot showing the probability density function. **(B)** Histogram to illustrate the frequency distribution across value bins. **(C)** Q-Q plot comparing sample quantiles against theoretical quantiles to assess normality.

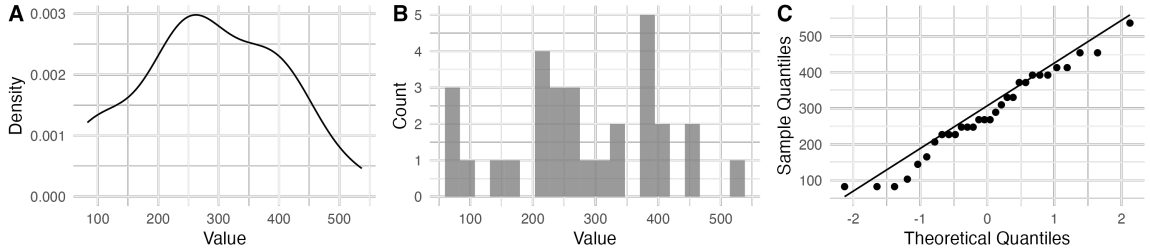

Figure A.12: Joint plot displaying the distribution and normality of total earthworm abundance (m^{-2}). **(A)** Density plot showing the probability density function. **(B)** Histogram to illustrate the frequency distribution across value bins. **(C)** Q-Q plot comparing sample quantiles against theoretical quantiles to assess normality.

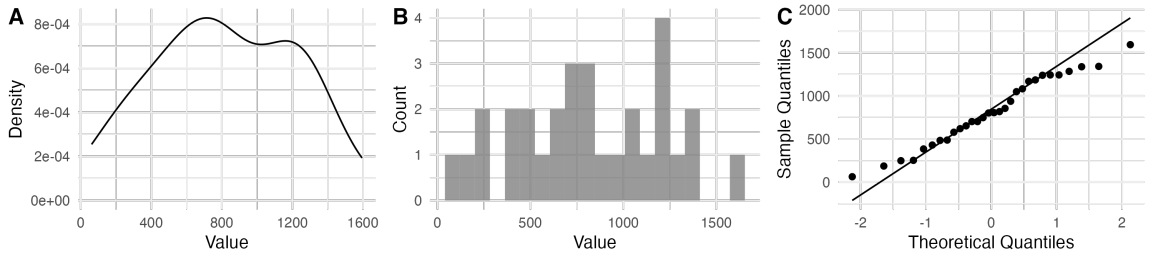

Figure A.13: Joint plot displaying the distribution and normality of QBS-e morphological Index Score. **(A)** Density plot showing the probability density function. **(B)** Histogram to illustrate the frequency distribution across value bins. **(C)** Q-Q plot comparing sample quantiles against theoretical quantiles to assess normality.

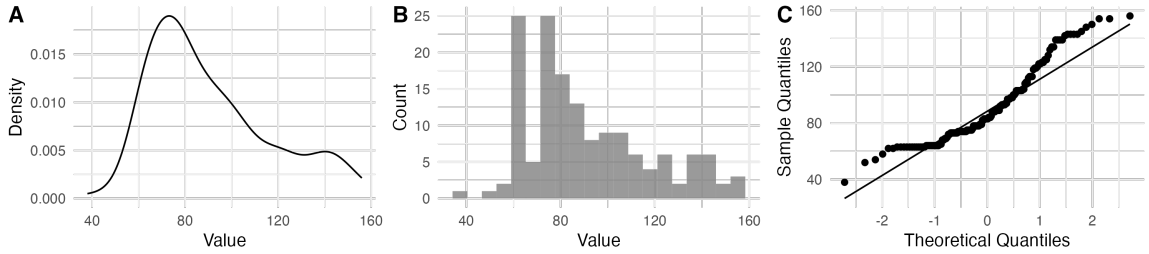

Figure A.14: Joint plot displaying the distribution and normality of QBS-ar morphological Index Score. **(A)** Density plot showing the probability density function. **(B)** Histogram to illustrate the frequency distribution across value bins. **(C)** Q-Q plot comparing sample quantiles against theoretical quantiles to assess normality.

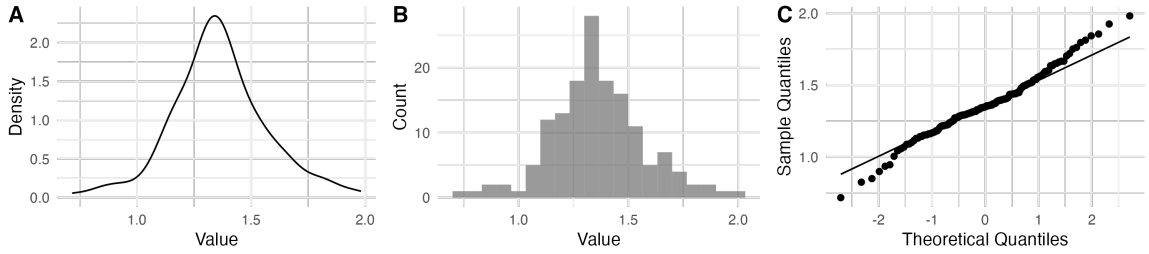

Figure A.15: Joint plot displaying the distribution and normality of Shannon Biodiversity Index Score. **(A)** Density plot showing the probability density function. **(B)** Histogram to illustrate the frequency distribution across value bins. **(C)** Q-Q plot comparing sample quantiles against theoretical quantiles to assess normality.

A.4 Model diagnostics

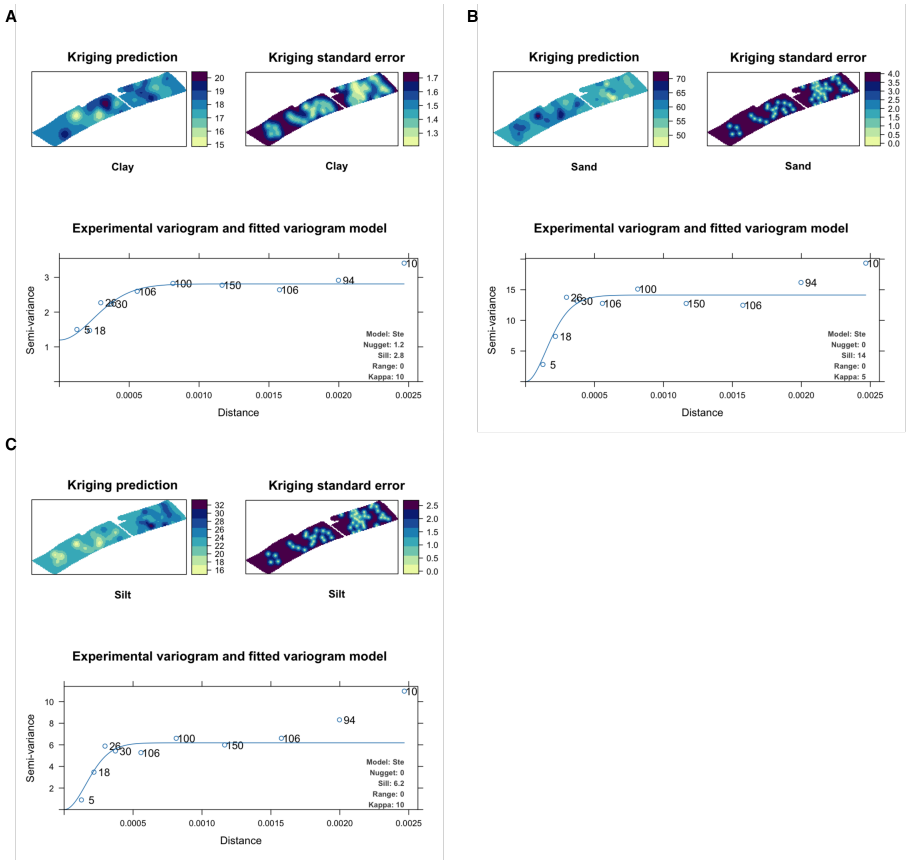

Figure A.16: Plot of soil textural interpolation variograms. (**A**) Ordinary kriging statistical plot for clay soil particle percentage interpolation throughout the experiment site. (**B**) Ordinary kriging statistical plot for sand soil particle percentage interpolation throughout the experiment site. (**C**) Ordinary kriging statistical plot for silt soil particle percentage interpolation throughout the experiment site. The kriging prediction is featured in the top left of the individual plots, the kriging spatial standard error is shown in the top right corner, and the experimental variogram for the prediction model is shown in the centre of the plot. The model parameters used for each model prediction are featured within the variogram plot.

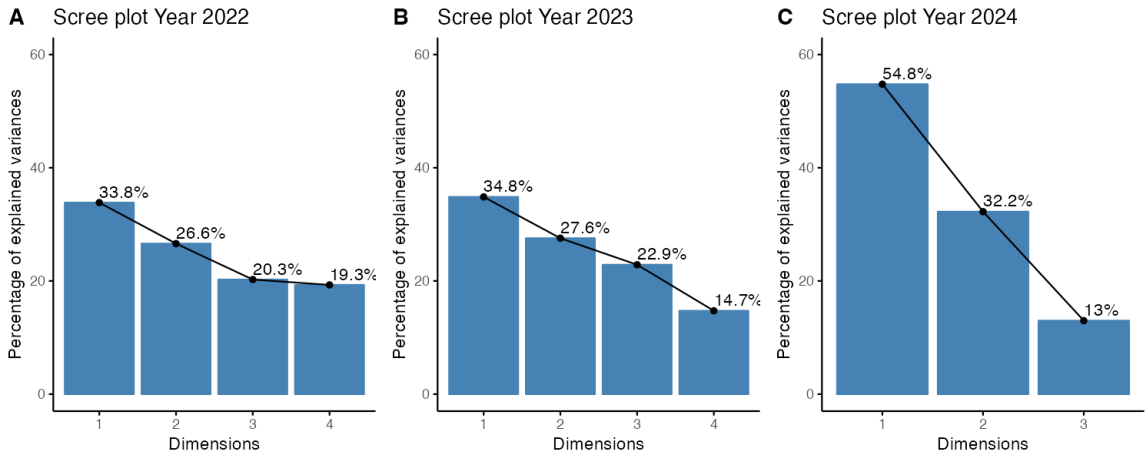

Figure A.17: Combined scree plots for Principal Component Analysis (PCA) of soil micro arthropod taxonomic group abundance. Each scree plot illustrates the percentage of variance explained by each principal component (PC) for the dataset. Analyses are shown separately for 2022 (**A**), 2023 (**B**), and 2024 (**C**).

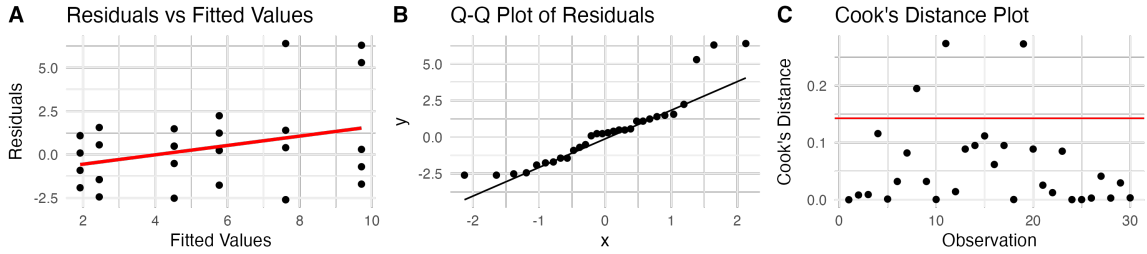

Figure A.18: Diagnostic plots for the generalised linear mixed model assessing juvenile earthworm abundance (m^{-2}). **A:** Residuals vs. Fitted Values. **B:** Q-Q plot. **C:** Cook's distance plot.

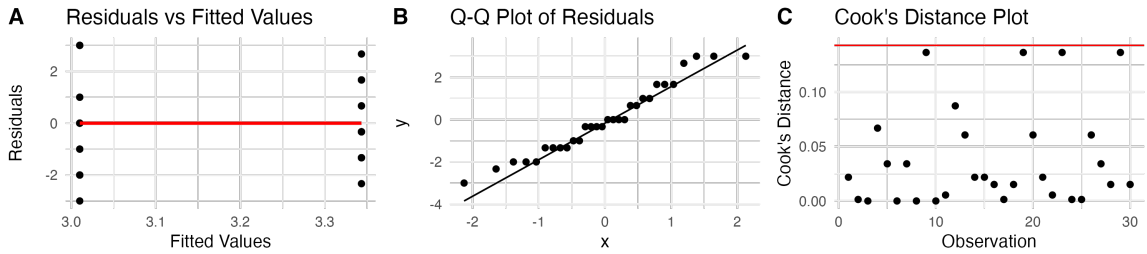

Figure A.19: Diagnostic plots for the generalised linear mixed model assessing Epigeic earthworm abundance (m^{-2}). **A:** Residuals vs. Fitted Values. **B:** Q-Q plot. **C:** Cook's distance plot.

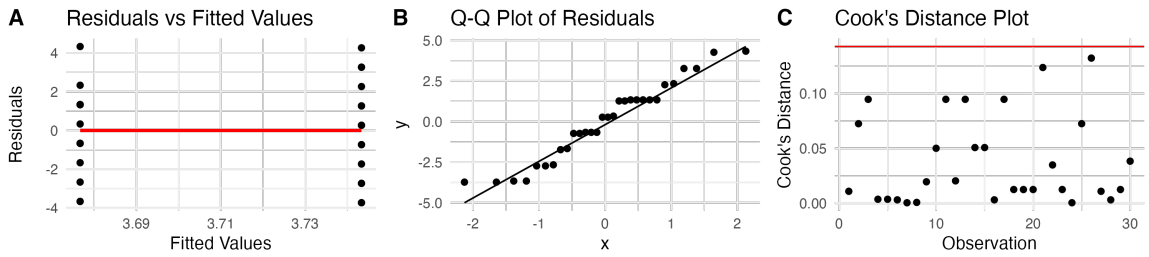

Figure A.20: Diagnostic plots for the generalised linear mixed model assessing Endogeic earthworm abundance (m^{-2}). **A:** Residuals vs. Fitted Values. **B:** Q-Q plot. **C:** Cook's distance plot.

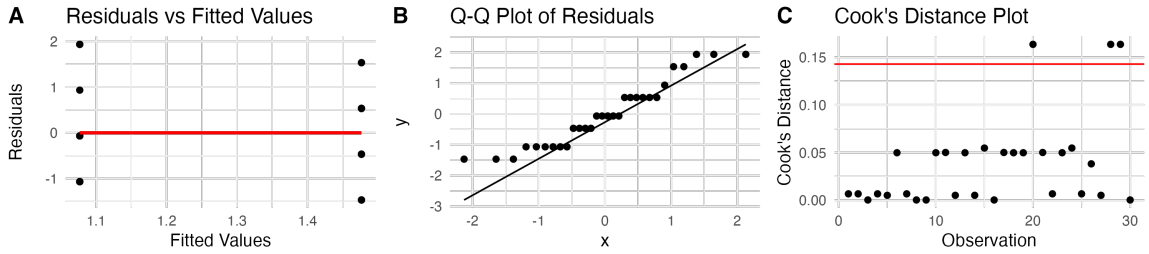

Figure A.21: Diagnostic plots for the generalised linear mixed model assessing Anecic earthworm abundance (m^{-2}). **A:** Residuals vs. Fitted Values. **B:** Q-Q plot. **C:** Cook's distance plot.

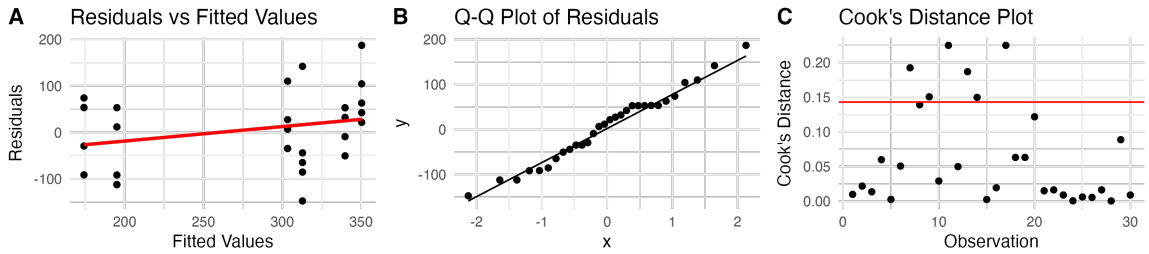

Figure A.22: Diagnostic plots for the generalised linear mixed model assessing total earthworm abundance (m^{-2}). **A:** Residuals vs. Fitted Values. **B:** Q-Q plot. **C:** Cook's distance plot.

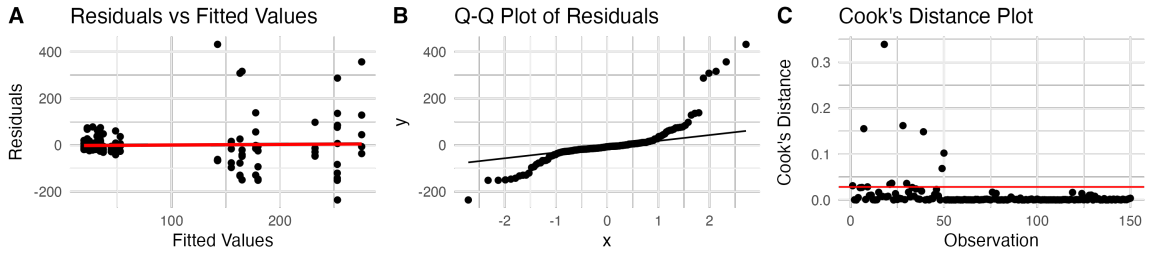

Figure A.23: Diagnostic plots for the generalised linear mixed model assessing total Chelicerata abundance (m^{-2}). **A:** Residuals vs. Fitted Values. **B:** Q-Q plot. **C:** Cook's distance plot.

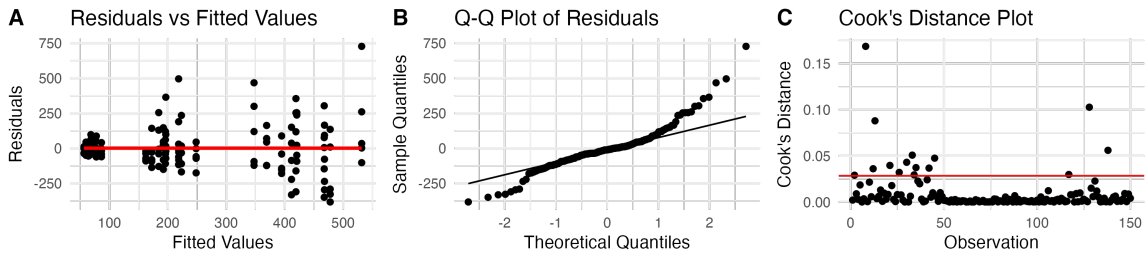

Figure A.24: Diagnostic plots for the generalised linear mixed model assessing total Hexapoda abundance (m^{-2}). **A:** Residuals vs. Fitted Values. **B:** Q-Q plot. **C:** Cook's distance plot.

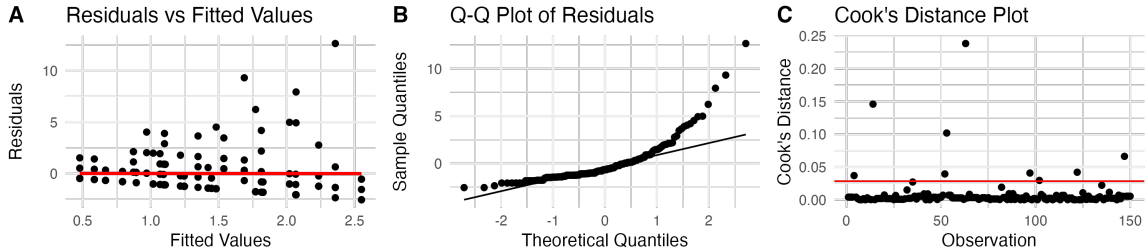

Figure A.25: Diagnostic plots for the generalised linear mixed model assessing total Myriapoda abundance (m^{-2}). **A:** Residuals vs. Fitted Values. **B:** Q-Q plot. **C:** Cook's distance plot.

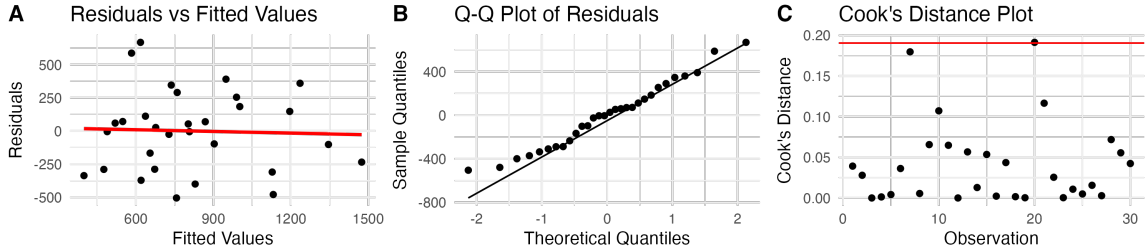

Figure A.26: Diagnostic plots for the generalised linear mixed model assessing total QBS-e score. **A:** Residuals vs. Fitted Values. **B:** Q-Q plot. **C:** Cook's distance plot.

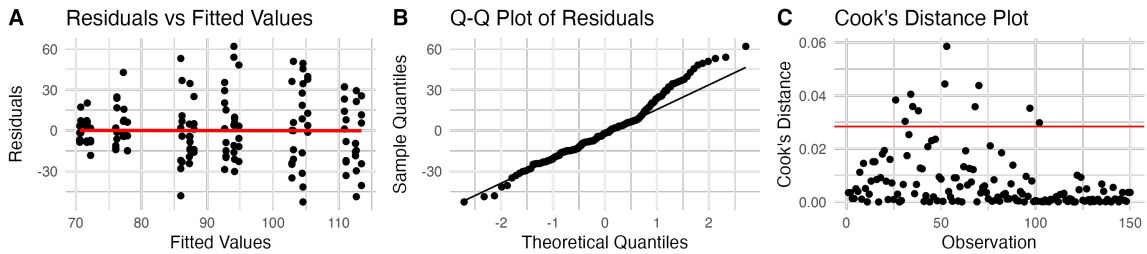

Figure A.27: Diagnostic plots for the generalised linear mixed model assessing total QBS-ar score. **A:** Residuals vs. Fitted Values. **B:** Q-Q plot. **C:** Cook's distance plot.

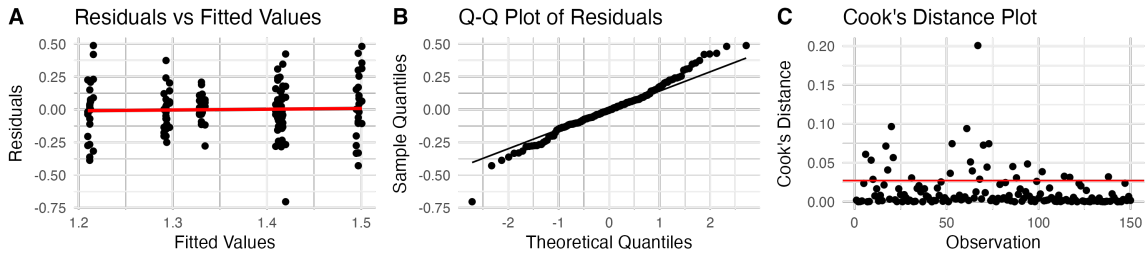

Figure A.28: Diagnostic plots for the generalised linear mixed model assessing Shannon Biodiversity Index. **A:** Residuals vs. Fitted Values. **B:** Q-Q plot. **C:** Cook's distance plot.

Appendix B

Agronomy Data and Code

B.1 Code availability

The code to produce the data analysis in this chapter can be viewed and cloned from the following Git repositories:

General Agronomy Code:
`https://github.com/jwollins/agronomy`
Pesticide Data Web Scraper:
`https://github.com/jwollins/pesticide_info_web_scraper`

B.2 Data availability

The data to produce this chapter will be made available on request from the author. Please contact:

jcollins@harper-adams.ac.uk

B.3 Data Distributions

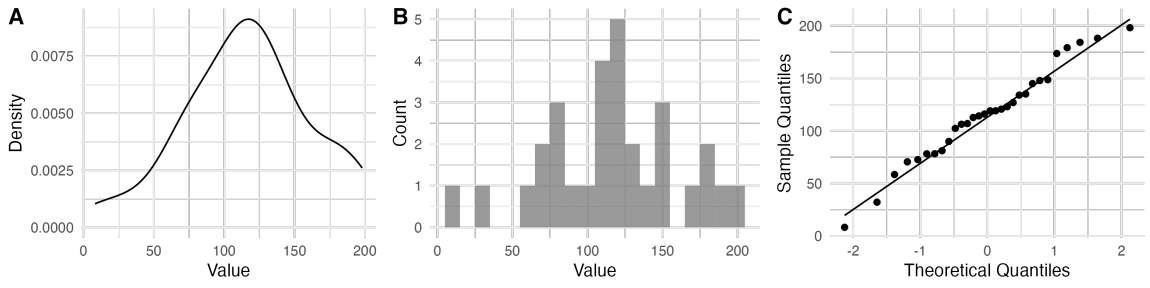

Figure B.1: Joint plot displaying the distribution and normality of the percentage of the UK crop yield average (%). **(A)** Density plot showing the probability density function. **(B)** Histogram to illustrate the frequency distribution across value bins. **(C)** Q-Q plot comparing sample quantiles against theoretical quantiles to assess normality.

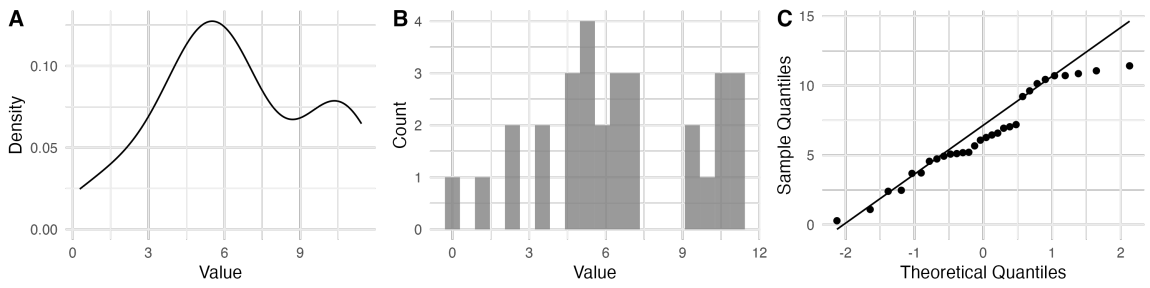

Figure B.2: Joint plot displaying the distribution and normality of the crop yield (t ha^{-1}). **(A)** Density plot showing the probability density function. **(B)** Histogram to illustrate the frequency distribution across value bins. **(C)** Q-Q plot comparing sample quantiles against theoretical quantiles to assess normality.

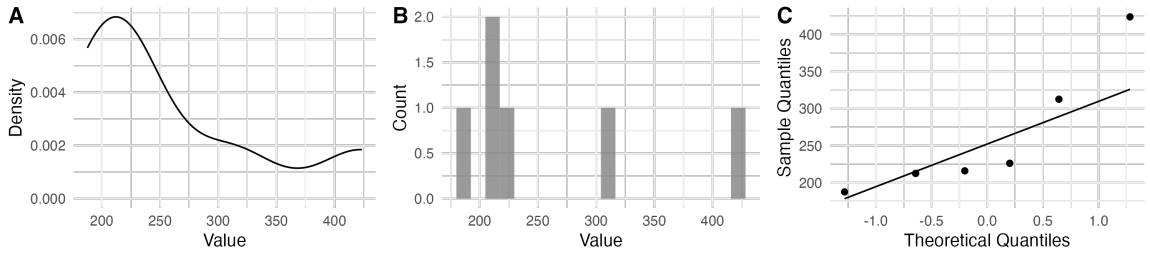

Figure B.3: Joint plot displaying the distribution and normality of fertiliser mass (kg ha^{-1}). **(A)** Density plot showing the probability density function. **(B)** Histogram to illustrate the frequency distribution across value bins. **(C)** Q-Q plot comparing sample quantiles against theoretical quantiles to assess normality.

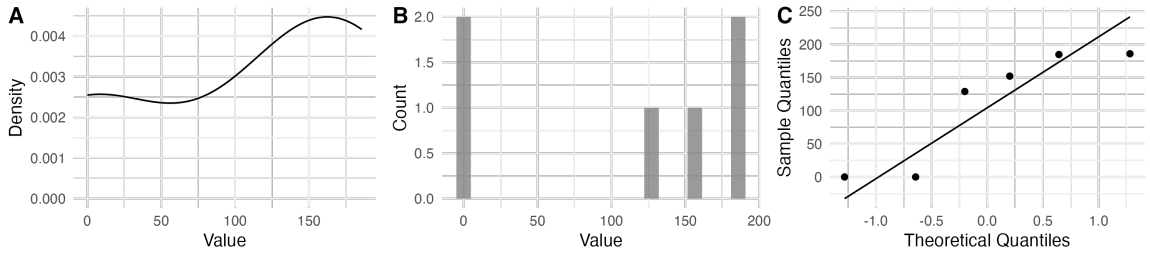

Figure B.4: Joint plot displaying the distribution and normality of Nitrogen fertiliser mass (kg ha^{-1}). **(A)** Density plot showing the probability density function. **(B)** Histogram to illustrate the frequency distribution across value bins. **(C)** Q-Q plot comparing sample quantiles against theoretical quantiles to assess normality.

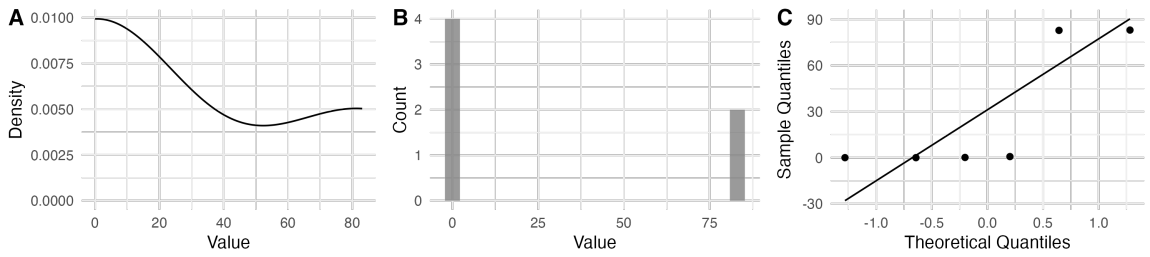

Figure B.5: Joint plot displaying the distribution and normality of Phosphorus fertiliser mass (kg ha^{-1}). **(A)** Density plot showing the probability density function. **(B)** Histogram to illustrate the frequency distribution across value bins. **(C)** Q-Q plot comparing sample quantiles against theoretical quantiles to assess normality.

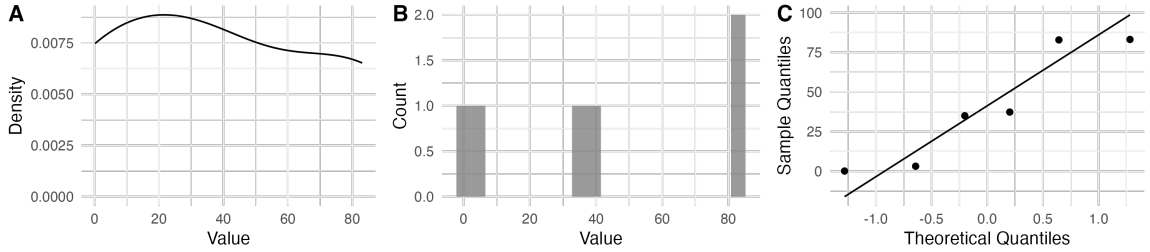

Figure B.6: Joint plot displaying the distribution and normality of Potassium fertiliser mass (kg ha^{-1}). **(A)** Density plot showing the probability density function. **(B)** Histogram to illustrate the frequency distribution across value bins. **(C)** Q-Q plot comparing sample quantiles against theoretical quantiles to assess normality.

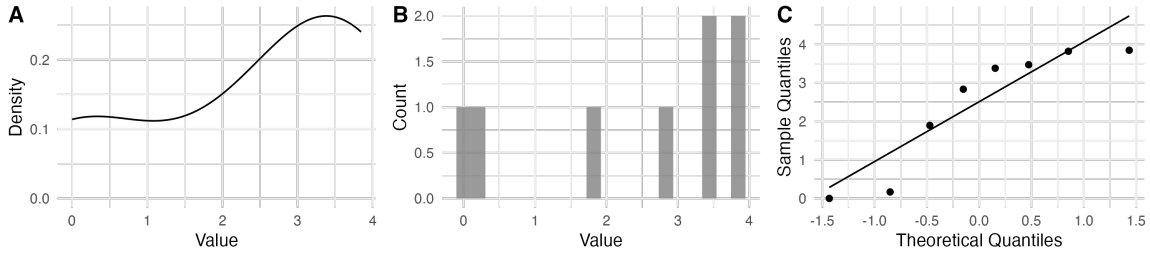

Figure B.7: Joint plot displaying the distribution and normality of pesticides mass (kg ha^{-1}). **(A)** Density plot showing the probability density function. **(B)** Histogram to illustrate the frequency distribution across value bins. **(C)** Q-Q plot comparing sample quantiles against theoretical quantiles to assess normality.

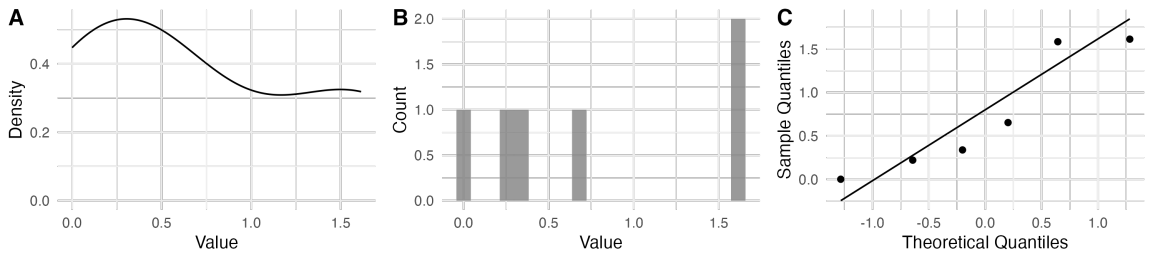

Figure B.8: Joint plot displaying the distribution and normality of fungicide mass (kg ha^{-1}). **(A)** Density plot showing the probability density function. **(B)** Histogram to illustrate the frequency distribution across value bins. **(C)** Q-Q plot comparing sample quantiles against theoretical quantiles to assess normality.

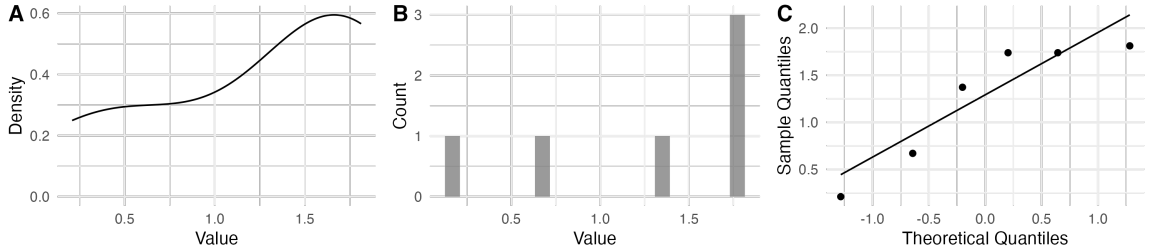

Figure B.9: Joint plot displaying the distribution and normality of herbicide mass (kg ha^{-1}). **(A)** Density plot showing the probability density function. **(B)** Histogram to illustrate the frequency distribution across value bins. **(C)** Q-Q plot comparing sample quantiles against theoretical quantiles to assess normality.

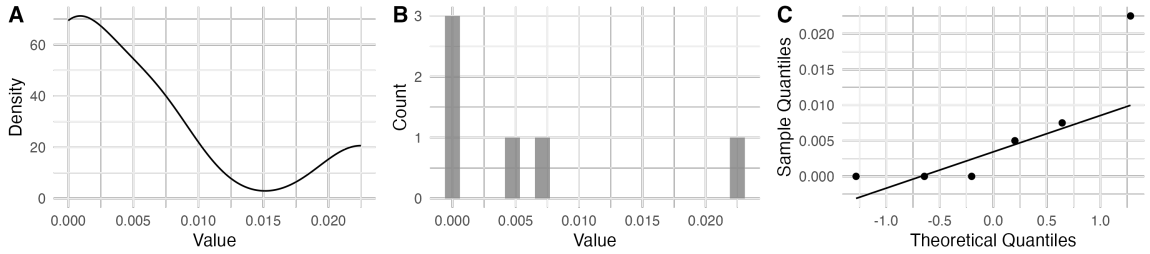

Figure B.10: Joint plot displaying the distribution and normality of insecticide mass (kg ha^{-1}). **(A)** Density plot showing the probability density function. **(B)** Histogram to illustrate the frequency distribution across value bins. **(C)** Q-Q plot comparing sample quantiles against theoretical quantiles to assess normality.

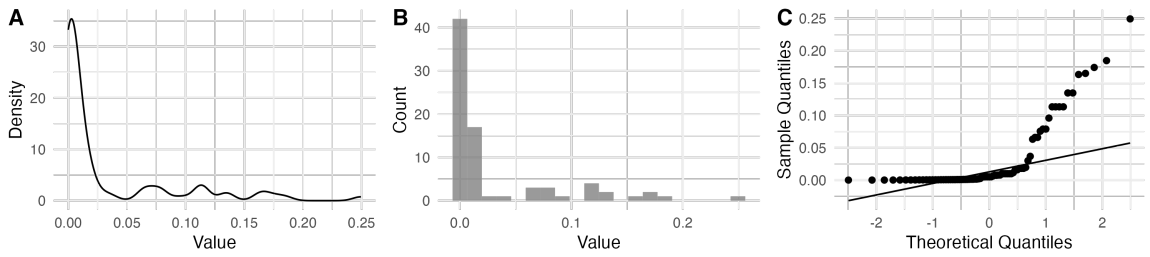

Figure B.11: Joint plot displaying the distribution and normality of Ecotoxicity PLI. **(A)** Density plot showing the probability density function. **(B)** Histogram to illustrate the frequency distribution across value bins. **(C)** Q-Q plot comparing sample quantiles against theoretical quantiles to assess normality.

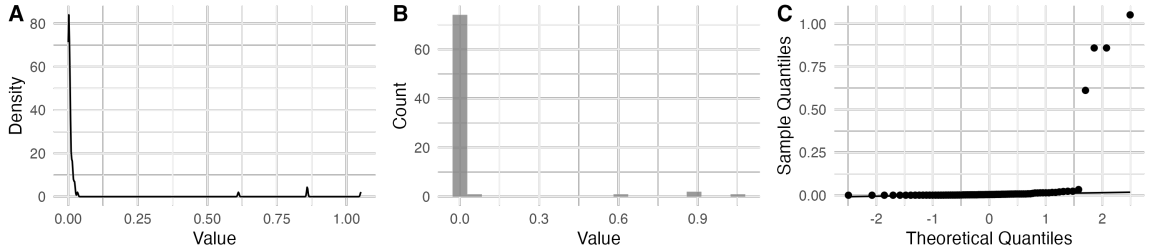

Figure B.12: Joint plot displaying the distribution and normality of Environmental Fate PLI. **(A)** Density plot showing the probability density function. **(B)** Histogram to illustrate the frequency distribution across value bins. **(C)** Q-Q plot comparing sample quantiles against theoretical quantiles to assess normality.

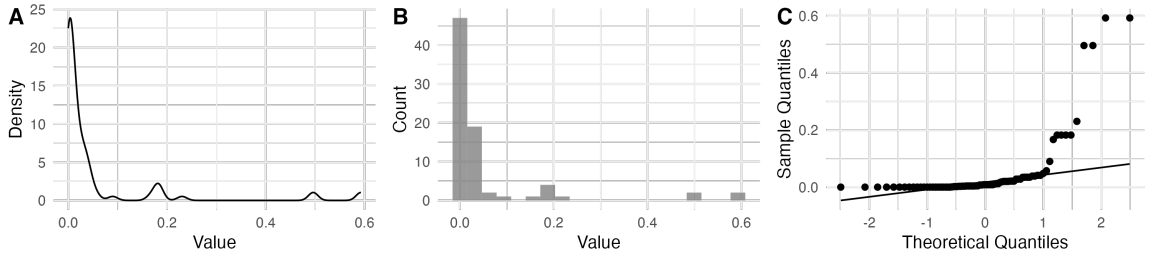

Figure B.13: Joint plot displaying the distribution and normality of Human Health PLI. **(A)** Density plot showing the probability density function. **(B)** Histogram to illustrate the frequency distribution across value bins. **(C)** Q-Q plot comparing sample quantiles against theoretical quantiles to assess normality.

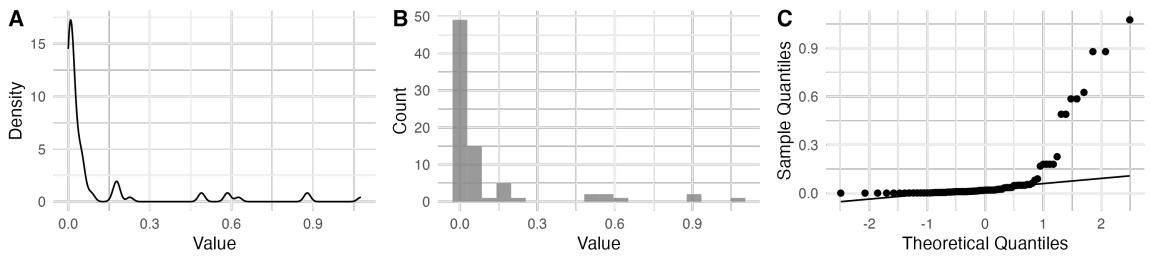

Figure B.14: Joint plot displaying the distribution and normality of Total PLI. **(A)** Density plot showing the probability density function. **(B)** Histogram to illustrate the frequency distribution across value bins. **(C)** Q-Q plot comparing sample quantiles against theoretical quantiles to assess normality.

B.4 Model diagnostics

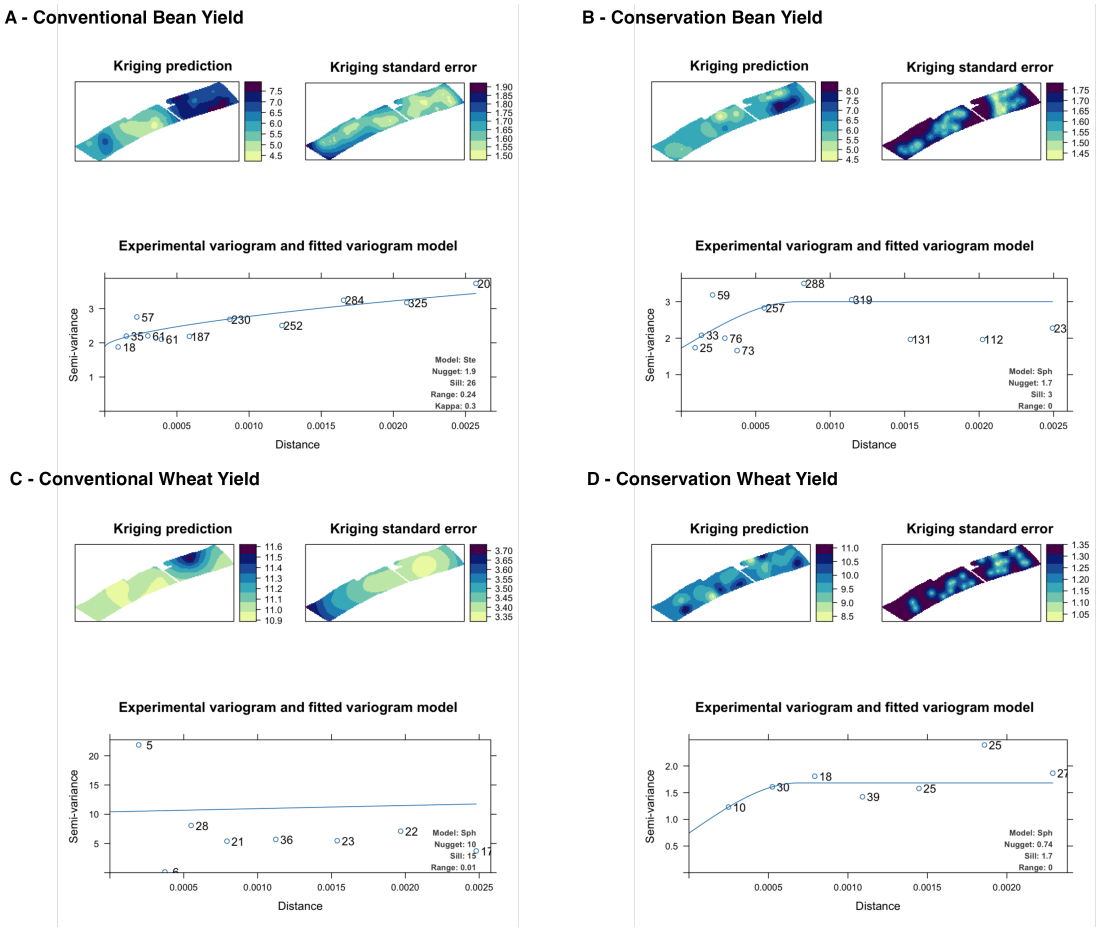

Figure B.15: Plot of crop yield interpolation variograms. **A** - Ordinary kriging statistical plot for the interpolated spring bean yield in the conventional treatment throughout the experiment site. **B** - Ordinary kriging statistical plot for the interpolated spring bean yield in the conservation treatment throughout the experiment site. **C** - Ordinary kriging statistical plot for the interpolated winter wheat yield in the conventional treatment throughout the experiment site. **D** - Ordinary kriging statistical plot for the interpolated winter wheat yield in the conservation treatment throughout the experiment site. The kriging prediction is featured in the top left of the individual plots, the kriging spatial standard error is shown in the top right corner, and the experimental variogram for the prediction model is shown in the centre of the plot. The model parameters used for each model prediction are featured within the variogram plot.

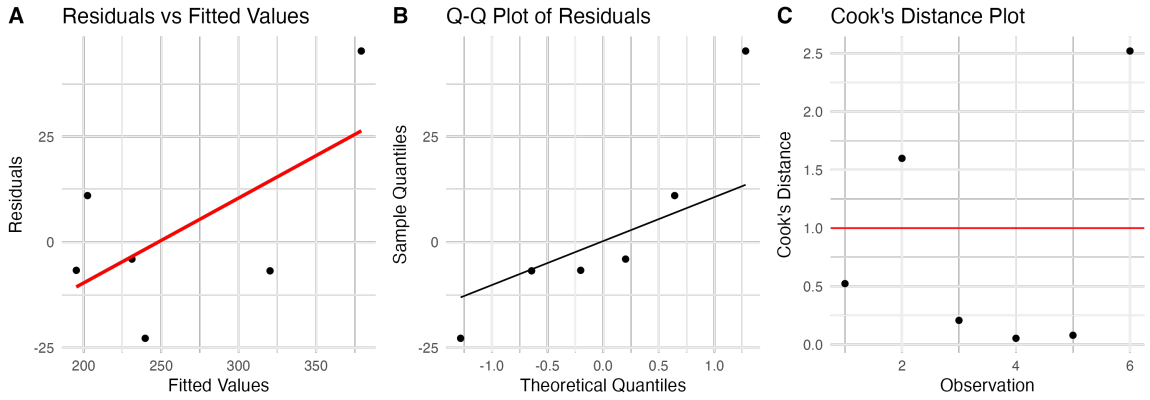

Figure B.16: Diagnostic plots for the generalised linear mixed model assessing fertiliser mass (kg ha^{-1}). **A:** Residuals vs. Fitted Values. **B:** Q-Q plot. **C:** Cook's distance plot.

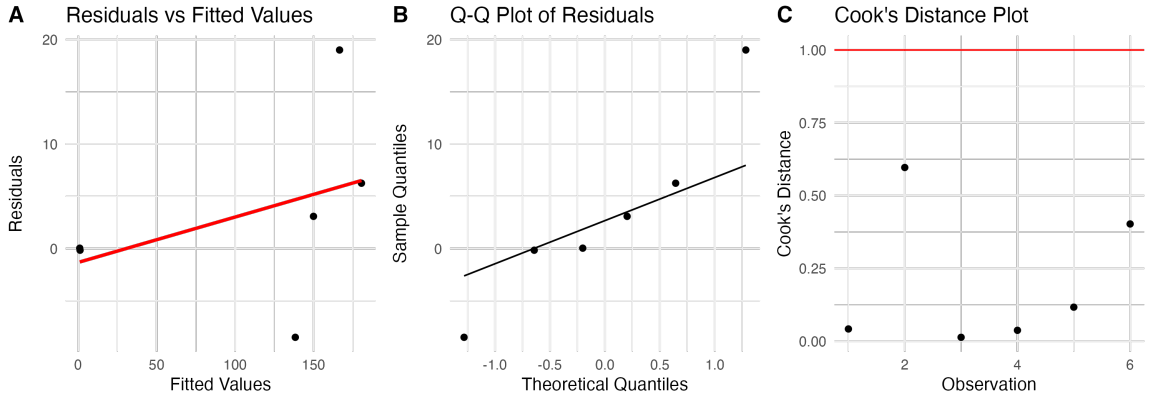

Figure B.17: Diagnostic plots for the generalised linear mixed model assessing nitrogen fertiliser mass (kg ha^{-1}). **A:** Residuals vs. Fitted Values. **B:** Q-Q plot. **C:** Cook's distance plot.

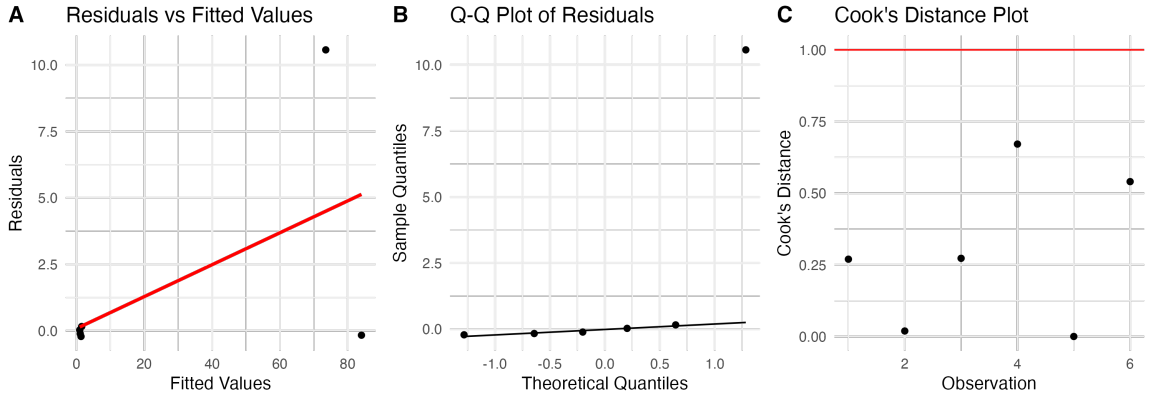

Figure B.18: Diagnostic plots for the generalised linear mixed model assessing Phosphorus fertiliser mass (kg ha^{-1}). **A:** Residuals vs. Fitted Values. **B:** Q-Q plot. **C:** Cook's distance plot.

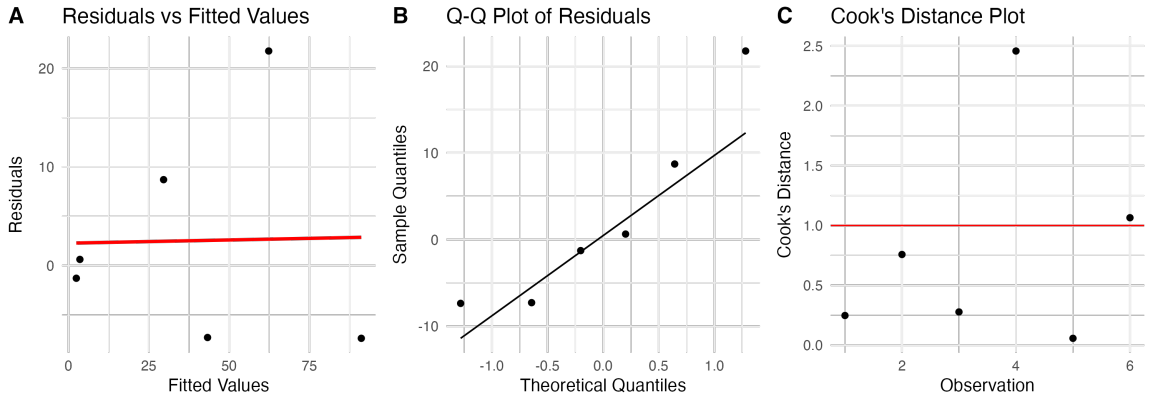

Figure B.19: Diagnostic plots for the generalised linear mixed model assessing Potassium fertiliser mass (kg ha^{-1}). **A:** Residuals vs. Fitted Values. **B:** Q-Q plot. **C:** Cook's distance plot.

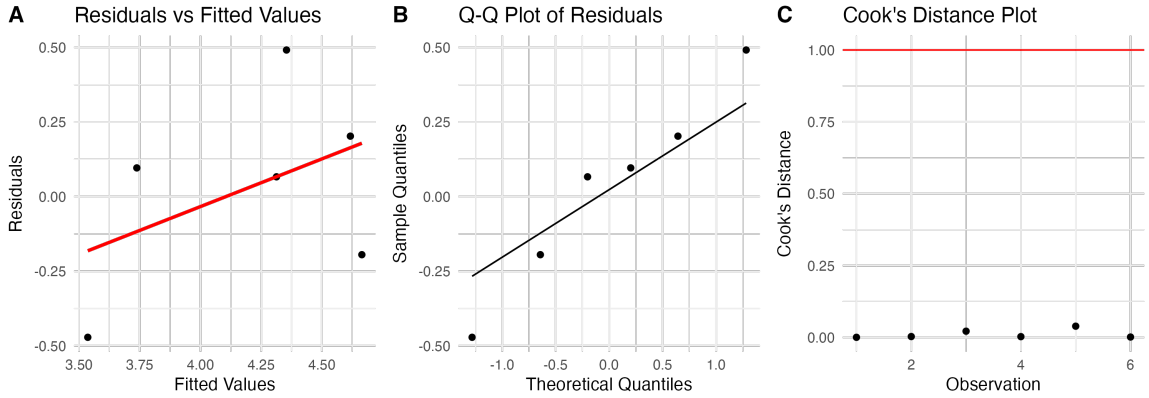

Figure B.20: Diagnostic plots for the generalised linear mixed model assessing total pesticide mass (kg ha^{-1}). **A:** Residuals vs. Fitted Values. **B:** Q-Q plot. **C:** Cook's distance plot.

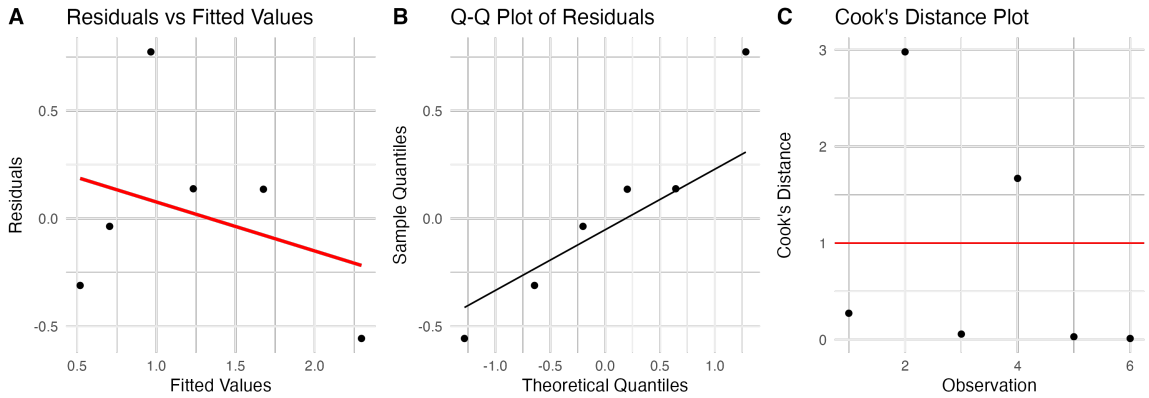

Figure B.21: Diagnostic plots for the generalised linear mixed model assessing total herbicide mass (kg ha^{-1}). **A:** Residuals vs. Fitted Values. **B:** Q-Q plot. **C:** Cook's distance plot.

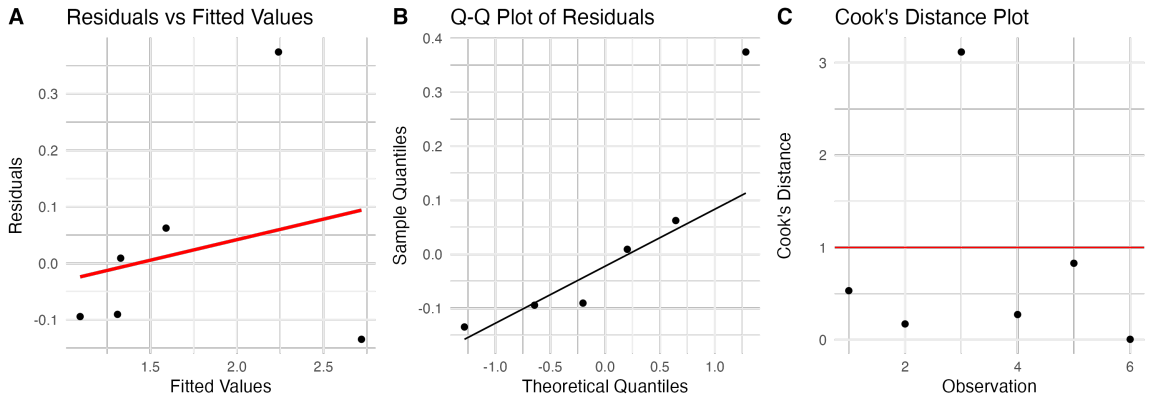

Figure B.22: Diagnostic plots for the generalised linear mixed model assessing total fungicide mass (kg ha^{-1}). **A:** Residuals vs. Fitted Values. **B:** Q-Q plot. **C:** Cook's distance plot.

Appendix C

Soil Greenhouse Gas Emissions Data and Code

C.1 Code availability

The code to produce the data analysis in this chapter can be viewed and cloned from the following Git repositories:

Soil Greenhouse Gas Flux Code:
`https://github.com/jwollins/ghg_flux`

C.2 Data availability

The data to produce this chapter will be made available on request from the author. Please contact:

jcollins@harper-adams.ac.uk

C.3 Data Distributions

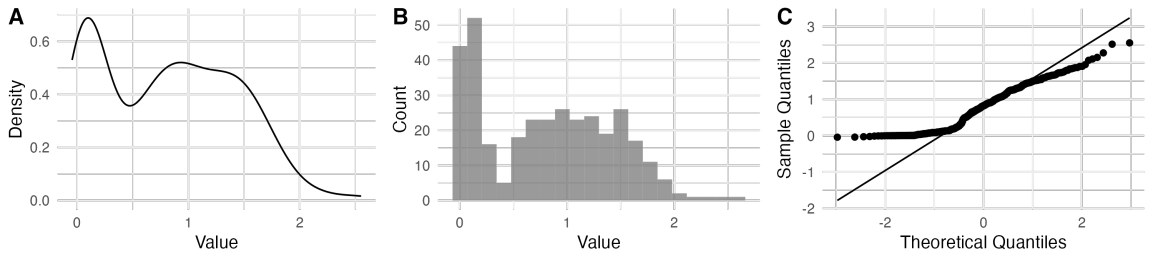

Figure C.1: Joint plot displaying the distribution and normality of the soil CO_2 emissions. **(A)** Density plot showing the probability density function for each group. **(B)** Histogram with jittered bars to illustrate the frequency distribution across value bins. **(C)** Q-Q plot comparing sample quantiles against theoretical quantiles to assess normality

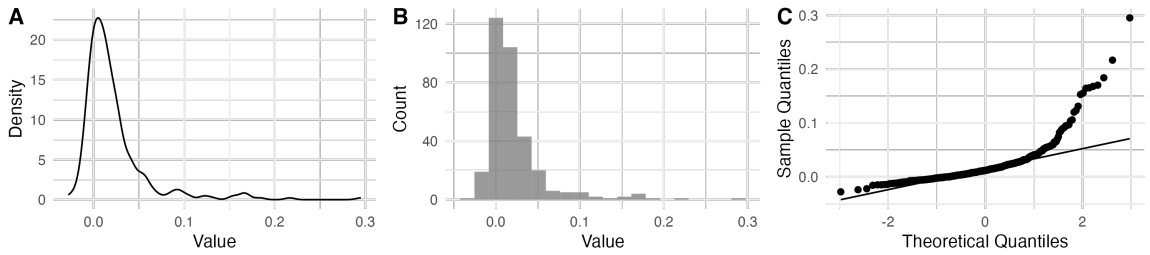

Figure C.2: Joint plot displaying the distribution and normality of the soil N_2O emissions. **(A)** Density plot showing the probability density function for each group. **(B)** Histogram with jittered bars to illustrate the frequency distribution across value bins. **(C)** Q-Q plot comparing sample quantiles against theoretical quantiles to assess normality

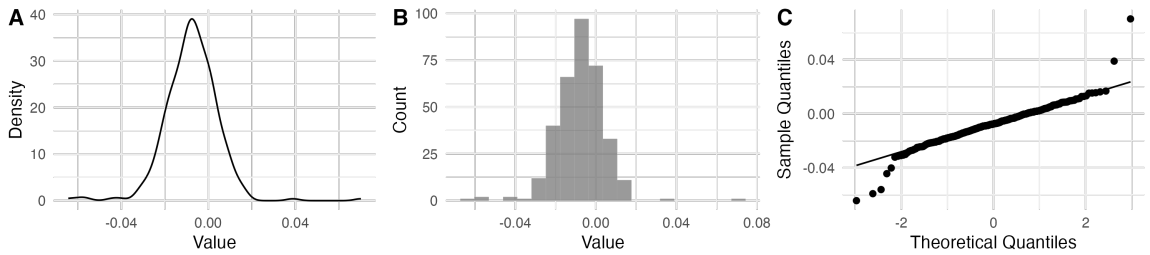

Figure C.3: Joint plot displaying the distribution and normality of the soil CH_4 emissions. **(A)** Density plot showing the probability density function for each group. **(B)** Histogram with jittered bars to illustrate the frequency distribution across value bins. **(C)** Q-Q plot comparing sample quantiles against theoretical quantiles to assess normality

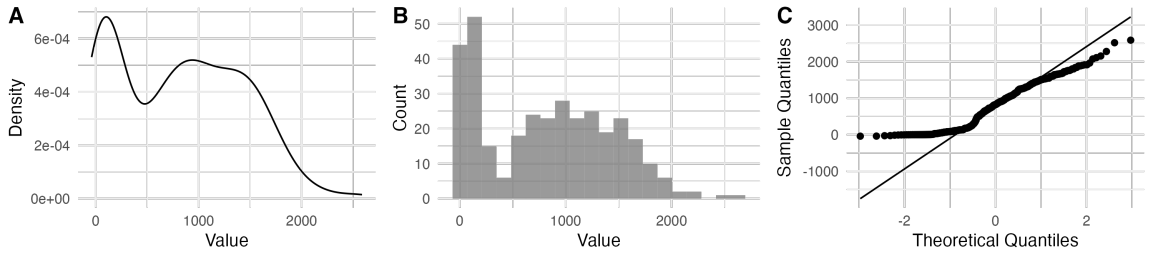

Figure C.4: Joint plot displaying the distribution and normality of the soil GHG flux Global Warming Potential. **(A)** Density plot showing the probability density function for each group. **(B)** Histogram with jittered bars to illustrate the frequency distribution across value bins. **(C)** Q-Q plot comparing sample quantiles against theoretical quantiles to assess normality

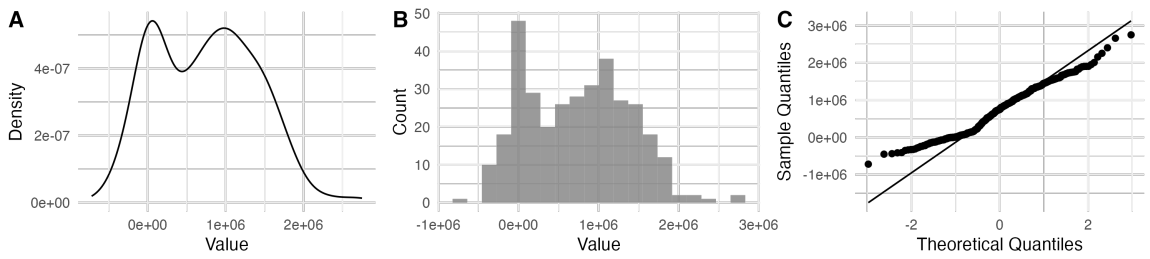

Figure C.5: Joint plot displaying the distribution and normality of the soil GHG flux yield-scaled Global Warming Potential. **(A)** Density plot showing the probability density function for each group. **(B)** Histogram with jittered bars to illustrate the frequency distribution across value bins. **(C)** Q-Q plot comparing sample quantiles against theoretical quantiles to assess normality

C.4 Model diagnostics

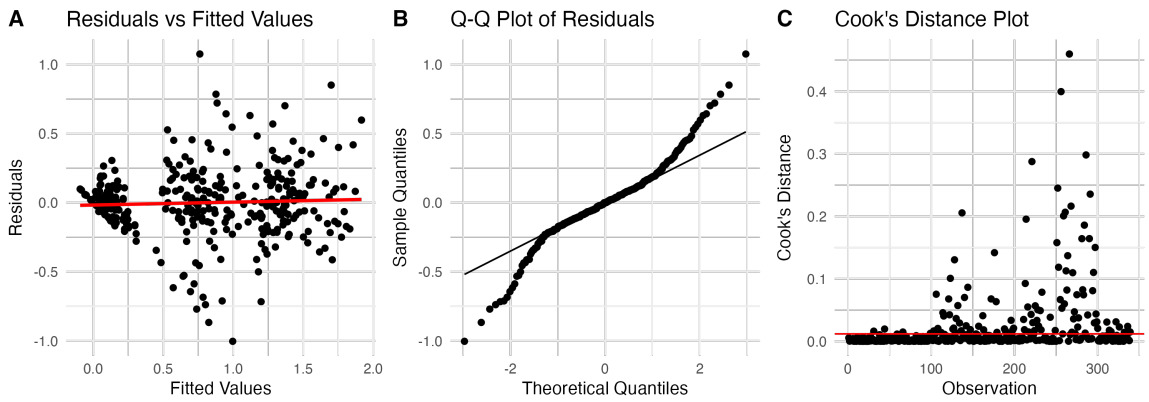

Figure C.6: Diagnostic plots for the generalised linear mixed model assessing soil CO_2 flux. **A:** Residuals vs. Fitted Values. **B:** Q-Q plot. **C:** Cook's distance plot.

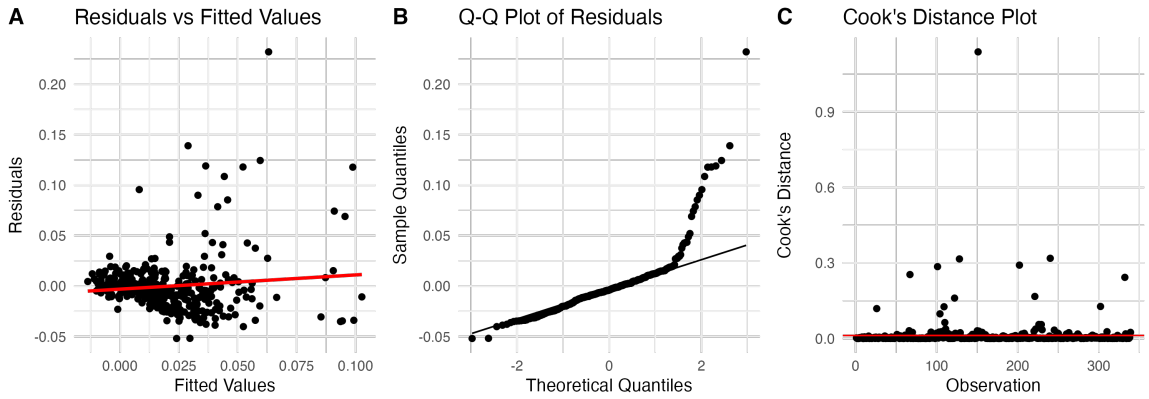

Figure C.7: Diagnostic plots for the generalised linear mixed model assessing soil N_2O flux. **A:** Residuals vs. Fitted Values. **B:** Q-Q plot. **C:** Cook's distance plot.

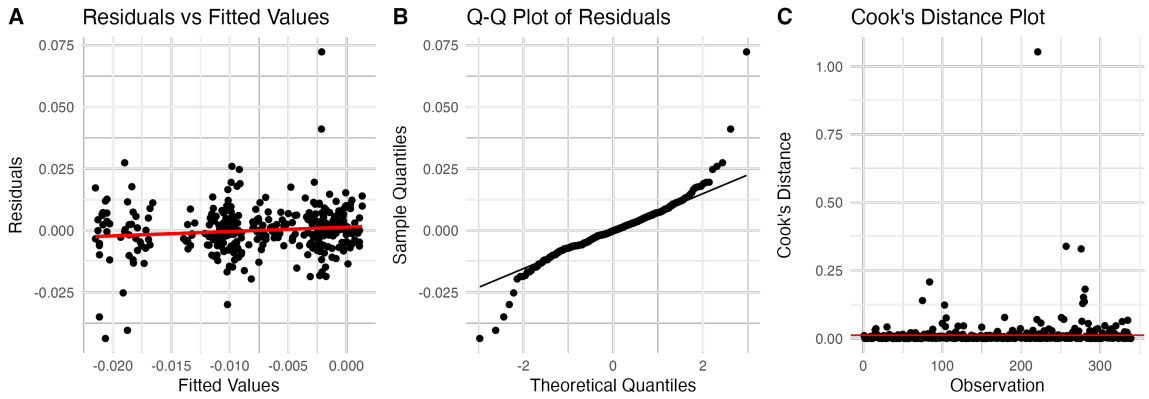

Figure C.8: Diagnostic plots for the generalised linear mixed model assessing soil CH_4 flux. **A:** Residuals vs. Fitted Values. **B:** Q-Q plot. **C:** Cook's distance plot.

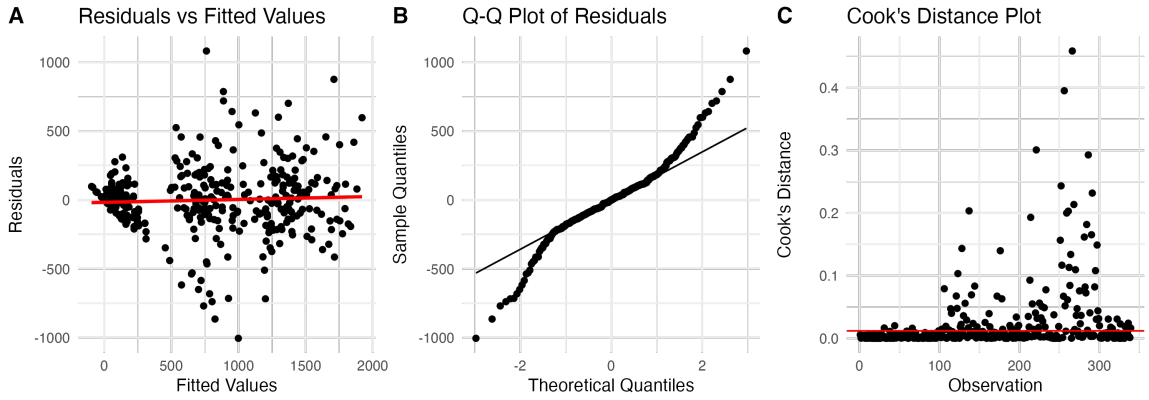

Figure C.9: Diagnostic plots for the generalised linear mixed model assessing soil GHG flux Global Warming Potential. **A:** Residuals vs. Fitted Values. **B:** Q-Q plot. **C:** Cook's distance plot.

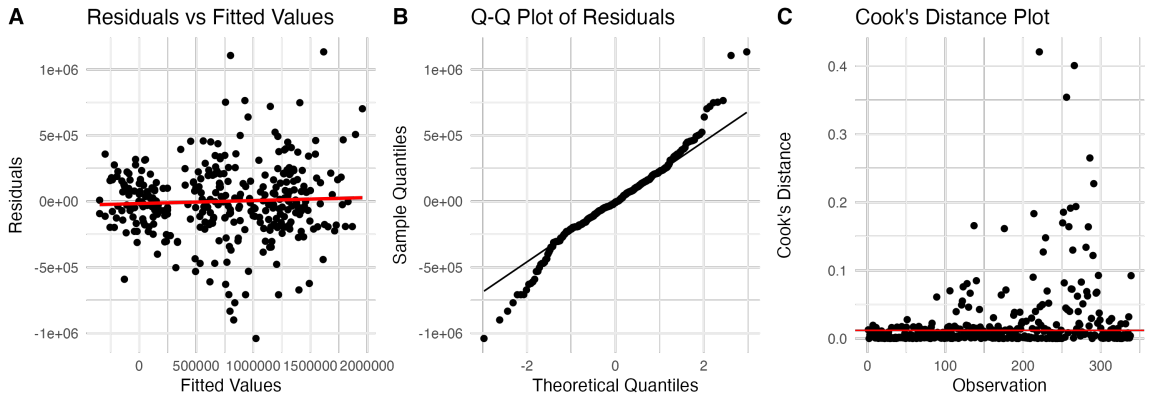

Figure C.10: Diagnostic plots for the generalised linear mixed model assessing soil GHG flux yield-scale Global Warming Potential. **A:** Residuals vs. Fitted Values. **B:** Q-Q plot. **C:** Cook's distance plot.

Appendix D

Economics Data and Code

D.1 Code availability

The code to produce the data analysis in this chapter can be viewed and cloned from the following Git repositories:

Economics Code:
`https://github.com/jwollins/economics`

D.2 Data availability

The data to produce this chapter will be made available on request from the author. Please contact:

jcollins@harper-adams.ac.uk

D.3 Data Distributions

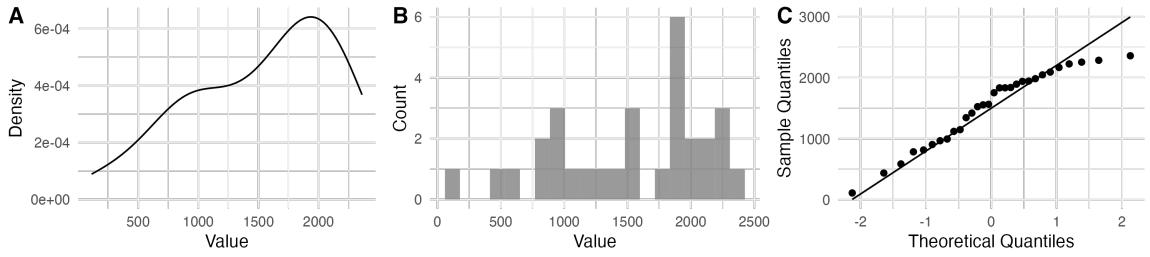

Figure D.1: Joint plot displaying the distribution and normality of the total revenue (£ ha^{-1}). **(A)** Density plot showing the probability density function for each group. **(B)** Histogram with jittered bars to illustrate the frequency distribution across value bins. **(C)** Q-Q plot comparing sample quantiles against theoretical quantiles to assess normality

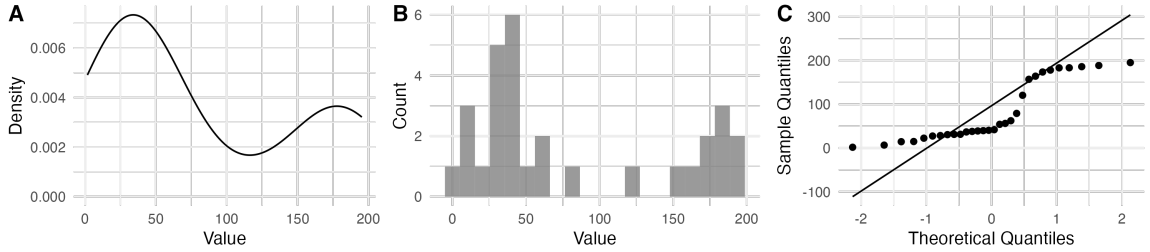

Figure D.2: Joint plot displaying the distribution and normality of the operational expenditure (£ ha^{-1}). **(A)** Density plot showing the probability density function for each group. **(B)** Histogram with jittered bars to illustrate the frequency distribution across value bins. **(C)** Q-Q plot comparing sample quantiles against theoretical quantiles to assess normality

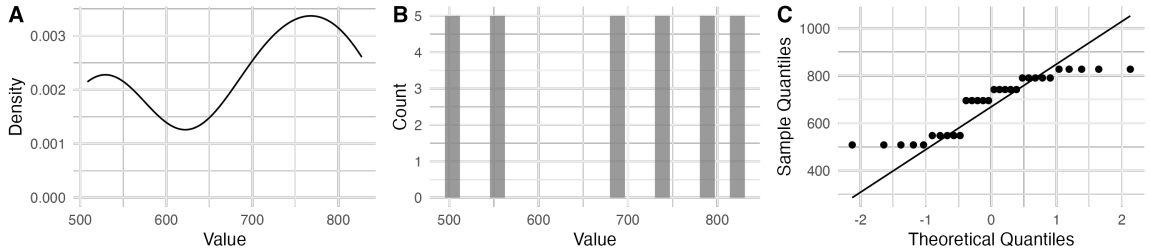

Figure D.3: Joint plot displaying the distribution and normality of the application expenditure (£ ha^{-1}). **(A)** Density plot showing the probability density function for each group. **(B)** Histogram with jittered bars to illustrate the frequency distribution across value bins. **(C)** Q-Q plot comparing sample quantiles against theoretical quantiles to assess normality

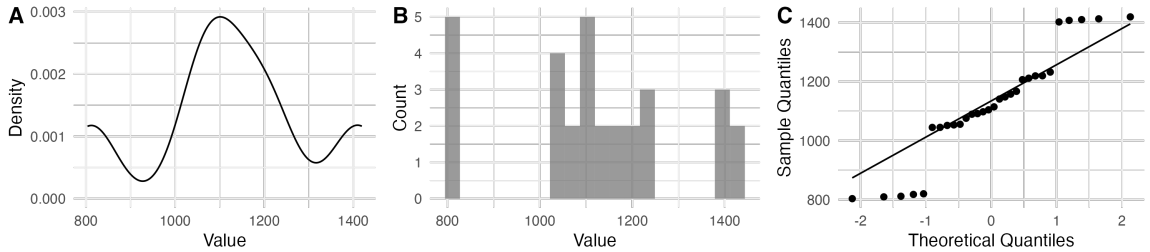

Figure D.4: Joint plot displaying the distribution and normality of the total expenditure (£ ha^{-1}). **(A)** Density plot showing the probability density function for each group. **(B)** Histogram with jittered bars to illustrate the frequency distribution across value bins. **(C)** Q-Q plot comparing sample quantiles against theoretical quantiles to assess normality

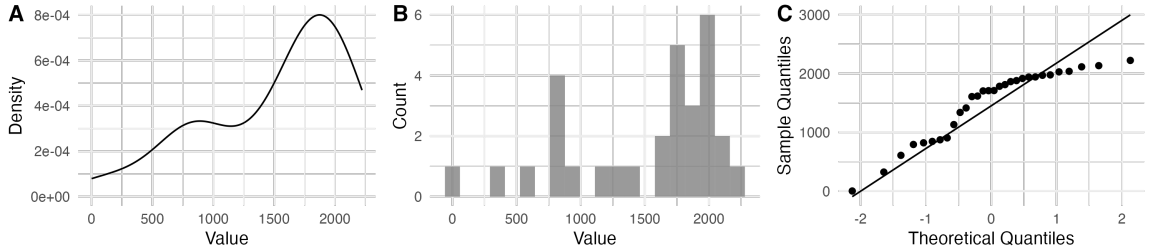

Figure D.5: Joint plot displaying the distribution and normality of the gross margin (£ ha^{-1}). **(A)** Density plot showing the probability density function for each group. **(B)** Histogram with jittered bars to illustrate the frequency distribution across value bins. **(C)** Q-Q plot comparing sample quantiles against theoretical quantiles to assess normality

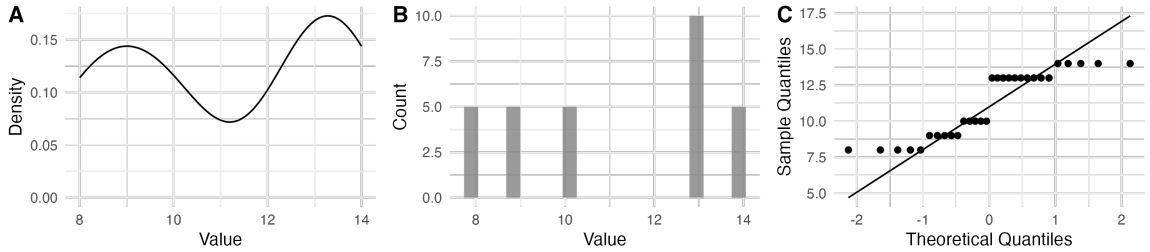

Figure D.6: Joint plot displaying the distribution and normality of the number of machinery operational passes ha^{-1}. **(A)** Density plot showing the probability density function for each group. **(B)** Histogram with jittered bars to illustrate the frequency distribution across value bins. **(C)** Q-Q plot comparing sample quantiles against theoretical quantiles to assess normality

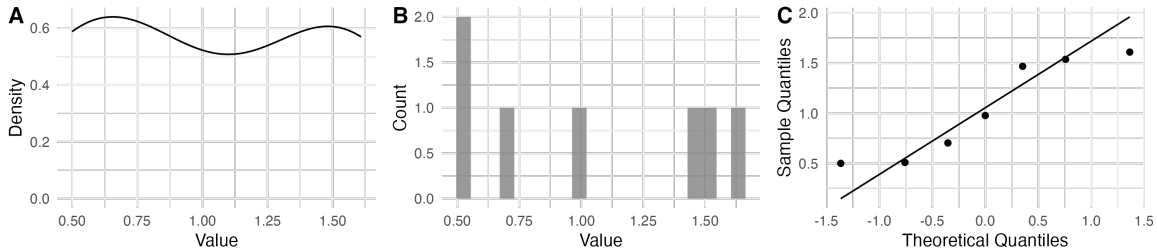

Figure D.7: Joint plot displaying the distribution and normality of the theoretical machinery operational time required (hours ha^{-1}). **(A)** Density plot showing the probability density function for each group. **(B)** Histogram with jittered bars to illustrate the frequency distribution across value bins. **(C)** Q-Q plot comparing sample quantiles against theoretical quantiles to assess normality

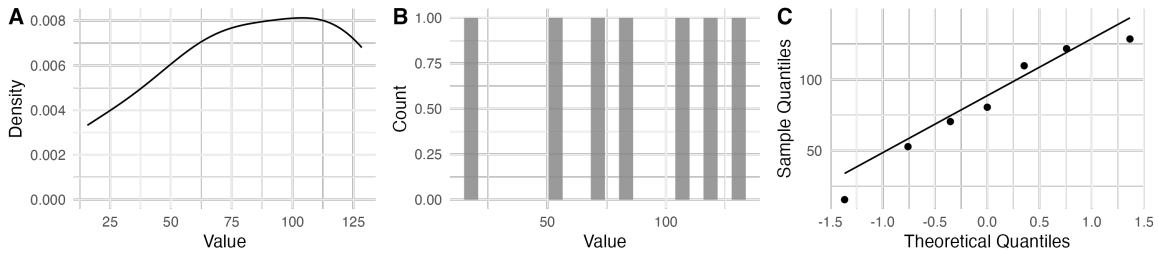

Figure D.8: Joint plot displaying the distribution and normality of the theoretical diesel consumption (l ha^{-1}). **(A)** Density plot showing the probability density function for each group. **(B)** Histogram with jittered bars to illustrate the frequency distribution across value bins. **(C)** Q-Q plot comparing sample quantiles against theoretical quantiles to assess normality

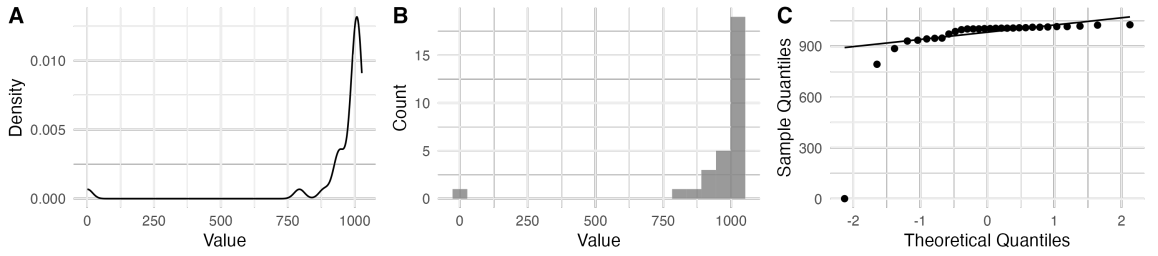

Figure D.9: Joint plot displaying the distribution and normality of the net profit margin (%). **(A)** Density plot showing the probability density function for each group. **(B)** Histogram with jittered bars to illustrate the frequency distribution across value bins. **(C)** Q-Q plot comparing sample quantiles against theoretical quantiles to assess normality

D.4 Model diagnostics

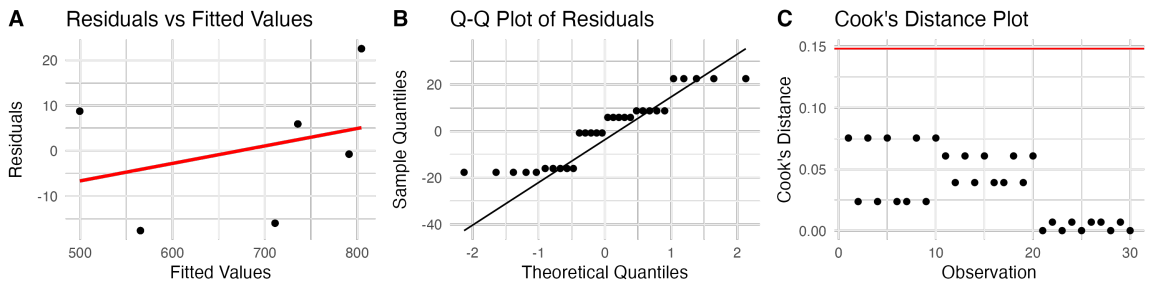

Figure D.10: Diagnostic plots for the model assessing crop application expenditure (£ ha^{-1}). **A:** Residuals vs. Fitted Values. **B:** Q-Q plot. **C:** Cook's distance plot.

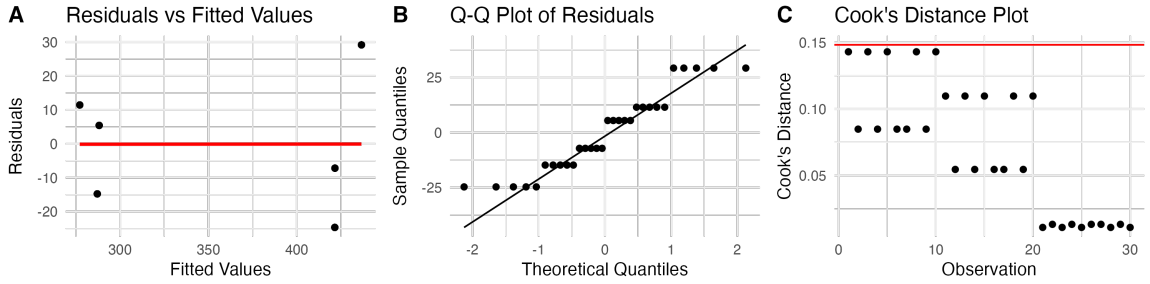

Figure D.11: Diagnostic plots for the model assessing machinery operation expenditure (£ ha^{-1}). **A:** Residuals vs. Fitted Values. **B:** Q-Q plot. **C:** Cook's distance plot.

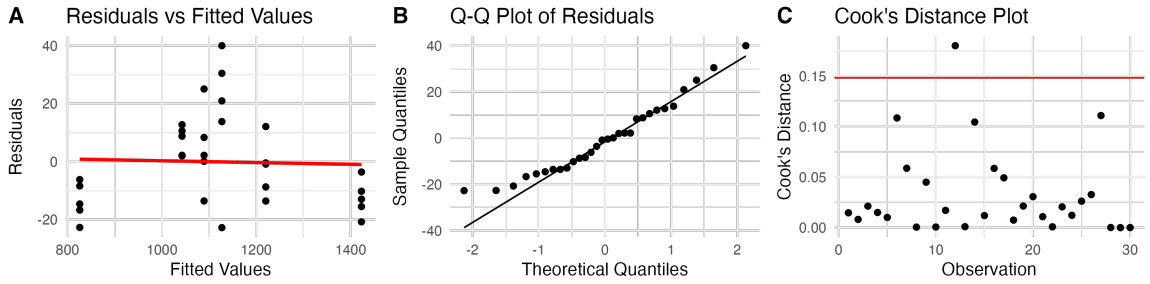

Figure D.12: Diagnostic plots for the model assessing total expenditure (£ ha^{-1}). **A:** Residuals vs. Fitted Values. **B:** Q-Q plot. **C:** Cook's distance plot.

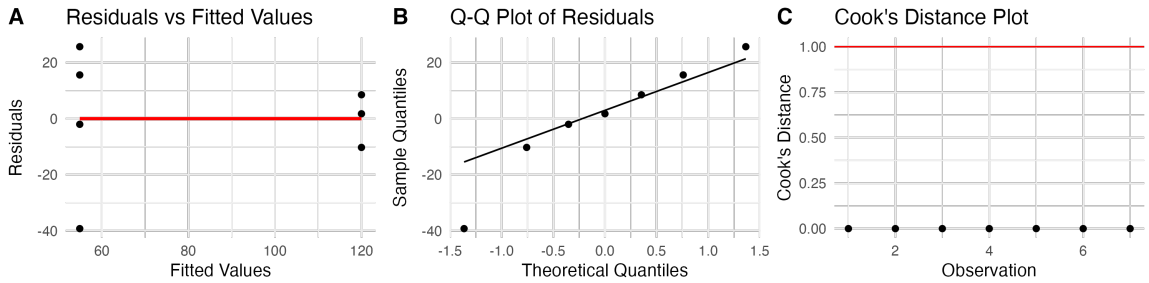

Figure D.13: Diagnostic plots for the model assessing theoretical diesel consumption (l ha^{-1}). **A:** Residuals vs. Fitted Values. **B:** Q-Q plot. **C:** Cook's distance plot.

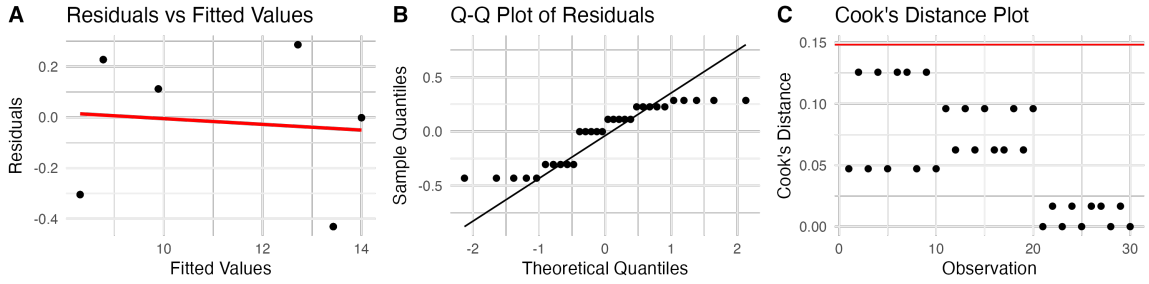

Figure D.14: Diagnostic plots for the model assessing the quantity of machinery passes (n ha^{-1}). **A:** Residuals vs. Fitted Values. **B:** Q-Q plot. **C:** Cook's distance plot.

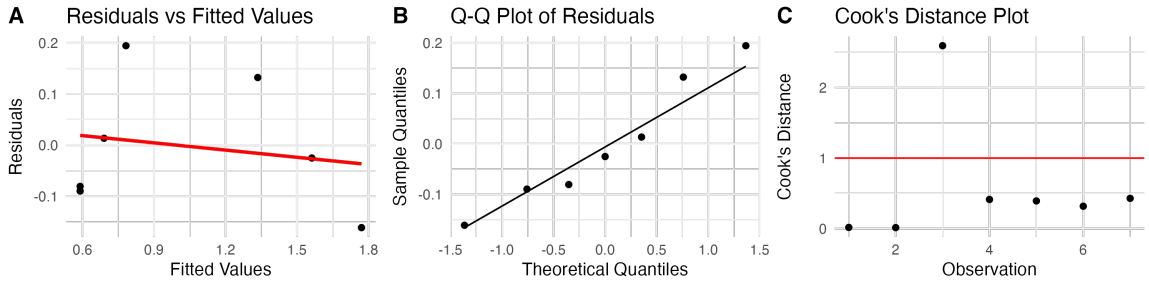

Figure D.15: Diagnostic plots for the model assessing the quantity of machinery time require (hrs ha^{-1}). **A:** Residuals vs. Fitted Values. **B:** Q-Q plot. **C:** Cook's distance plot.

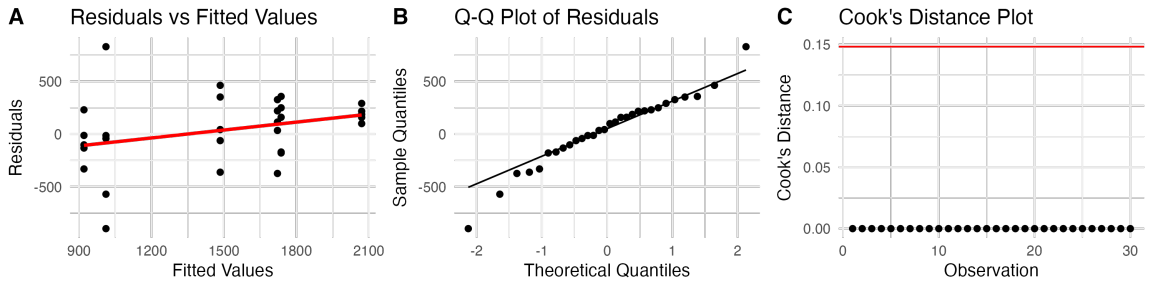

Figure D.16: Diagnostic plots for the model assessing the total revenue (£ ha^{-1}). **A:** Residuals vs. Fitted Values. **B:** Q-Q plot. **C:** Cook's distance plot.

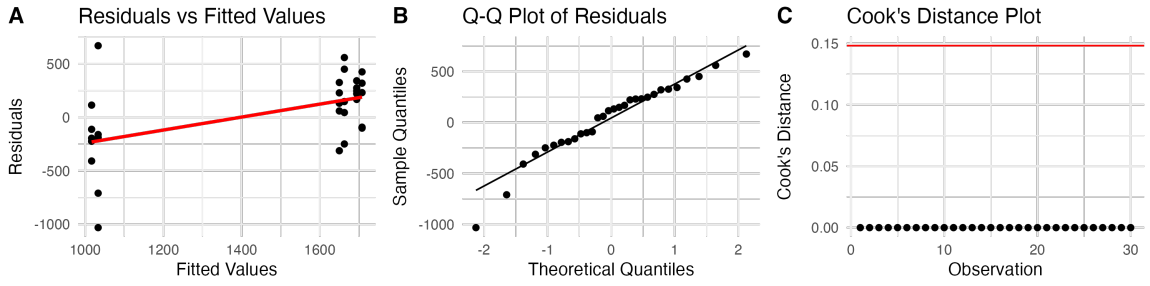

Figure D.17: Diagnostic plots for the model assessing the gross margin (£ ha^{-1}). **A:** Residuals vs. Fitted Values. **B:** Q-Q plot. **C:** Cook's distance plot.

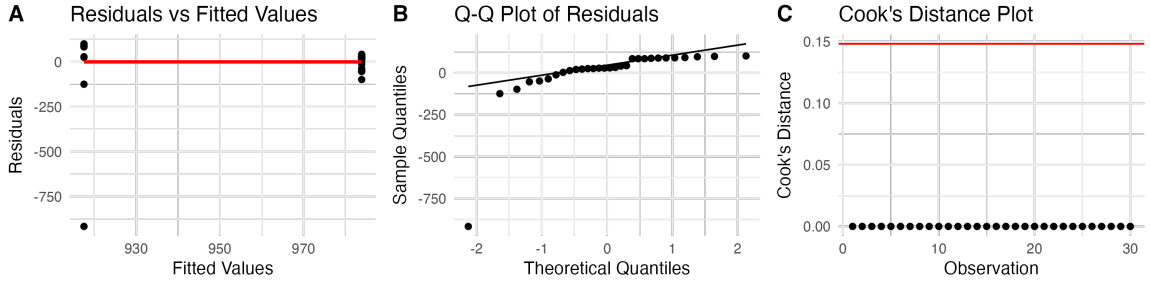

Figure D.18: Diagnostic plots for the model assessing the net profit margin (£ ha^{-1}). **A:** Residuals vs. Fitted Values. **B:** Q-Q plot. **C:** Cook's distance plot.

Bibliography

Abdalla, K., Chivenge, P., Ciais, P., and Chaplot, V. (2016). No-tillage lessens soil CO2 emissions the most under arid and sandy soil conditions: Results from a meta-analysis. *Biogeosciences*, 13(12):3619–3633.

Agrii (2021). Transitioning to No-Till on heavy ground. https://www.agrii.co.uk/news-and-media/news/transitioning-to-no-till-on-heavy-ground/.

AHDB (2017). Nutrient Management Guide RB209. Technical Report May, Agriculture and Horticulture Development Board.

AHDB (2022). Farmbench results: Past, present and future. https://ahdb.org.uk/news/farmbench-results-past-present-and-future.

AHDB (2023a). Grain storage guide. Technical report, Agriculture and Horticulture Development Board.

AHDB (2023b). Section 4 Arable crops Nutrient Management Guide (RB209). Technical report, Agriculture and Horticulture Development Board.

AHDB (2024). Direct drilling on arable land. https://ahdb.org.uk/knowledge-library/direct-drilling-on-arable-land.

AHDB (2025). Fuel prices. https://ahdb.org.uk/fuel-prices.

AHDB Cereals & Oilseeds (2018). Barley Growth Guide 2018. *Agriculture and Horticulture Development Board*.

AHDB Cereals & Oilseeds (2021). Farmbench - Top of the crops. https://ahdb.org.uk/news/top-of-the-crops.

Alakukku, L., Ristolainen, A., and Salo, T. (2009). Grain yield and nutrient balance of spring cereals in different tillage systems. *Proc. 18th ISTRO Conf.*, pages 1–7.

Alesso, C. A., Cipriotti, P. A., Bollero, G. A., and Martin, N. F. (2019). Experimental designs and estimation methods for on-farm research: A simulation study of corn yields at field scale. *Agronomy Journal*, 111(6):2724–2735.

Allen, M., O.P. Dube, W. Solecki, F. Aragón-Durand, W. Cramer, S. Humphreys, M. Kainuma, J. Kala, N. Mahowald, Y. Mulugetta, R. Perez, M. Wairiu, and K. Zickfeld (2022). Framing and Context. In *Global Warming of 1.5° C. An IPCC Special Report on the Impacts of Global Warming of 1.5° C above Pre-Industrial Levels and Related Global*

Greenhouse Gas Emission Pathways, in the Context of Strengthening the Global Response to the Threat of Climate Change., pages 49–92. Cambridge University Press.

Allison, R. (2023). Direct-drilling: Main findings from major five-year trial. *Farmers Weekly*.

Allmaras, R. R. and Dowdy, R. H. (1985). Conservation tillage systems and their adoption in the United States. *Soil and Tillage Research*, 5(2):197–222.

Alskaf, K., Sparkes, D. L., Mooney, S. J., Sjögersten, S., and Wilson, P. (2020). The uptake of different tillage practices in England. *Soil Use and Management*, 36(1):27–44.

Amorim, F. R. D., Guimarães, C. C., Afonso, P., and Tobias, M. S. G. (2024). Forecasting Cost Risks of Corn and Soybean Crops through Monte Carlo Simulation. *Applied Sciences*, 14(17):8030.

Andersson, J., Giller, K., Sumberg, J., and Thompson, J. (2014). Comment on "Evaluating conservation agriculture for small-scale farmers in Sub-Saharan Africa and South Asia" [Agric. Ecosyst. Environ. 187 (2014) 1–10]. *Agriculture, Ecosystems & Environment*, 196:21–23.

Aulakh, M. S., Walters, D. T., Doran, J. W., Francis, D. D., and Mosier, A. R. (1991). Crop Residue Type and Placement Effects on Denitrification and Mineralization. *Soil Science Society of America Journal*, 55(4):1020–1025.

Avery, B. (2006). Soil Classification in the Soil Survey of England and Wales. *Journal of Soil Science*, 24:324–338.

Baayen, R. H., Davidson, D. J., and Bates, D. M. (2008). Mixed-effects modeling with crossed random effects for subjects and items. *Journal of Memory and Language*, 59(4):390–412.

Badagliacca, G., Laudicina, V. A., Amato, G., Badalucco, L., Frenda, A. S., Giambalvo, D., Ingraffia, R., Plaia, A., and Ruisi, P. (2021). Long-term effects of contrasting tillage systems on soil C and N pools and on main microbial groups differ by crop sequence. *Soil and Tillage Research*, 211:104995.

Baeumer, K. (1970). First experiences with direct drilling in Germany. *Netherlands Journal of Agricultural Science*, 18(4):283–292.

Bajwa, A. A. (2014). Sustainable weed management in conservation agriculture. *Crop Protection*, 65:105–113.

Baker, J., Saxton, K., Ritchie, W., Chamen, T., Reicosky, D., Ribeiro, F., Justice, S., and Hobbs, P. (2006). No-tillage Seeding in Conservation Agriculture. *No-Tillage Seeding in Conservation Agriculture: Second Edition*.

Baldivieso-Freitas, P., Blanco-Moreno, J. M., Gutiérrez-López, M., Peigné, J., Pérez-Ferrer, A., Trigo-Aza, D., and Sans, F. X. (2018). Earthworm abundance response to conservation agriculture practices in organic arable farming under Mediterranean climate. *Pedobiologia*, 66:58–64.

Basch, G., Friedrich, T., Kassam, A., and Gonzalez-Sanchez, E. (2015). Conservation Agriculture in Europe. In Farooq, M. and Siddique, K. H. M., editors, *Conservation Agriculture*, pages 357–389. Springer International Publishing, Cham.

Bates, D., Mächler, M., Bolker, B., and Walker, S. (2015). Fitting Linear Mixed-Effects Models Using lme4. *Journal of Statistical Software*, 67(1):1–48.

Beare, M. H., Coleman, D. C., Pohlad, B. R., and Wright, D. H. (1993). Residue Placement and Fungicide Effects on Fungal Communities in Conventional and No-Tillage Soils. *Soil Science Society of America Journal*, 57(2):392–399.

Beare, M. H., Hendrix, P. F., Cabrera, M. L., and Coleman, D. C. (1994). Aggregate-Protected and Unprotected Organic Matter Pools in Conventional- and No-Tillage Soils. *Soil Science Society of America Journal*, 58(3):787–795.

Bedano, J. C., Cantú, M. P., and Doucet, M. E. (2006). Soil springtails (Hexapoda: Collembola), symphylans and pauropods (Arthropoda: Myriapoda) under different management systems in agroecosystems of the subhumid Pampa (Argentina). *European Journal of Soil Biology*, 42(2):107–119.

BEIS (2023). Final UK greenhouse gas emissions national statistics: 1990 to 2021. https://www.gov.uk/government/statistics/final-uk-greenhouse-gas-emissions-national-statistics-1990-to-2021.

Bennett, A. J., Bending, G. D., Chandler, D., Hilton, S., and Mills, P. (2012). Meeting the demand for crop production: The challenge of yield decline in crops grown in short rotations. *Biological Reviews*, 87(1):52–71.

Berry, P., Cook, S., Ellis, S., Gladders, P., and Roques, S. (2015). Oil Seed Rape Guide. *AHDB Cereals & Oilseeds*, 2.

Betts, R. A., Falloon, P. D., Goldewijk, K. K., and Ramankutty, N. (2007). Biogeophysical effects of land use on climate: Model simulations of radiative forcing and large-scale temperature change. *Agricultural and Forest Meteorology*, 142(2-4):216–233.

Bieganowski, A. and Ryżak, M. (2011). Soil Texture: Measurement Methods. In Gliński, J., Horabik, J., and Lipiec, J., editors, *Encyclopedia of Agrophysics*, pages 791–794. Springer Netherlands, Dordrecht.

Blake, G. (1965). Bulk Density. In *Methods of Soil Analysis: Part 1 Physical and Mineralogical Properties, Including Statistics of Measurement and Sampling*, pages 374–390. American Society of Agronomy, Inc.

Blanco-Canqui, H. and Lal, R. (2007). Soil structure and organic carbon relationships following 10 years of wheat straw management in no-till. *Soil and Tillage Research*, 95(1-2):240–254.

Blanco-Canqui, H. and Lal, R. (2009). Crop residue removal impacts on soil productivity and environmental quality. *Critical Reviews in Plant Sciences*, 28(3):139–163.

Blanco-Canqui, H. and Ruis, S. J. (2018). No-tillage and soil physical environment. *Geoderma*, 326(February):164–200.

Blanco-Canqui, H. and Ruis, S. J. (2020). Cover crop impacts on soil physical properties: A review. *Soil Science Society of America Journal*, 84(5):1527–1576.

Breiman, L. (2001). Random Forests. *Machine Learning*, 45(1):5–32.

Breiman, L., Cutler, A., Liaw, A., and Wiener, M. (2024). randomForest: Breiman and Cutlers Random Forests for Classification and Regression.

Brown, J. L., Stobart, R., Hallett, P. D., Morris, N. L., George, T. S., Newton, A. C., Valentine, T. A., and McKenzie, B. M. (2021). Variable impacts of reduced and zero tillage on soil carbon storage across 4–10 years of UK field experiments. *Journal of Soils and Sediments*, 21(2):890–904.

Burton, V. J., Jones, A. G., Robinson, L. D., Eggleton, P., and Purvis, A. (2024). Earthworm Watch: Insights into urban earthworm communities in the UK using citizen science. *European Journal of Soil Biology*, 121:103622.

Byerlee, D., Harrington, L., and Winkelmann, D. L. (1982). Farming Systems Research: Issues in Research Strategy and Technology Design. *American Journal of Agricultural Economics*, 64(5):897–904.

Cannell, R. Q. (1985). Reduced tillage in north-west Europe—A review. *Soil and Tillage Research*, 5(2):129–177.

Cannell, R. Q., Christian, D. G., and Henderson, F. K. G. (1986). A study of mole drainage with simplified cultivation for autumn-sown crops on a clay soil. 4. A comparison of direct drilling and mouldboard ploughing on drained and undrained land on root and shoot growth, nutrient uptake and yield. *Soil and Tillage Research*, 7(3):251–272.

Cannell, R. Q. and Hawes, J. D. (1994). Trends in tillage practices in relation to sustainable crop production with special reference to temperate climates. *Soil and Tillage Research*, 30(2-4):245–282.

Cárceles Rodríguez, B., Durán-Zuazo, V. H., Soriano Rodríguez, M., García-Tejero, I. F., Gálvez Ruiz, B., and Cuadros Tavira, S. (2022). Conservation Agriculture as a Sustainable System for Soil Health: A Review. *Soil Systems*, 6(4):87.

Cardinale, B. J., Duffy, J. E., Gonzalez, A., Hooper, D. U., Perrings, C., Venail, P., Narwani, A., Mace, G. M., Tilman, D., Wardle, D. A., Kinzig, A. P., Daily, G. C., Loreau, M., Grace, J. B., Larigauderie, A., Srivastava, D. S., and Naeem, S. (2012). Biodiversity loss and its impact on humanity. *Nature*, 486(7401):59–67.

Çelik, İ., Günal, H., Acar, M., Acir, N., Bereket Barut, Z., and Budak, M. (2019). Strategic tillage may sustain the benefits of long-term no-till in a Vertisol under Mediterranean climate. *Soil and Tillage Research*, 185:17–28.

Champely, S., Ekstrom, C., Dalgaard, P., Gill, J., Weibelzahl, S., Anandkumar, A., Ford, C., Volcic, R., and Rosario, H. D. (2020). Pwr: Basic Functions for Power Analysis.

Chen, H., Li, X., Hu, F., and Shi, W. (2013). Soil nitrous oxide emissions following crop residue addition: A meta-analysis. *Global Change Biology*, 19(10):2956–2964.

Chernov, T. I. and Zhelezova, A. D. (2020). The Dynamics of Soil Microbial Communities on Different Timescales: A Review. *Eurasian Soil Science*, 53(5):643–652.

Cho, J. B., Guinness, J., Kharel, T., Maresma, Á., Czymmek, K. J., van Aardt, J., and Ketterings, Q. M. (2021). Proposed method for statistical analysis of on-farm single strip treatment trials. *Agronomy*, 11(10).

Choudhary, M. A. (1979). *Interrelationships between Performance of Direct Drilled Seeds, Soil Micro-Environment and Drilling Equipment : A Thesis Presented in Partial Fulfilment of the Requirements for the Degree of Doctor of Philosophy at Massey University*. PhD thesis, Massey University.

Christel, A., Maron, P.-A., and Ranjard, L. (2021). Impact of farming systems on soil ecological quality: A meta-analysis. *Environmental Chemistry Letters*, 19(6):4603–4625.

Clark, P. (2022). Cost of farm inputs soars 34% in a year. *Farmers Weekly*.

Clarke, A. (2015). Building a case for no-till crop establishment. *Farmers Weekly*.

Clough, T. J., Rochette, P., Thomas, S. M., Pihlatie, M., Christiansen, J. R., and Thorman, R. E. (2020). Global Research Alliance N2O chamber methodology guidelines: Design considerations. *Journal of Environmental Quality*, 49(5):1081–1091.

Cohen, J. (2013). *Statistical Power Analysis for the Behavioral Sciences*. Routledge, New York, 2 edition.

Collier, S. M., Ruark, M. D., Oates, L. G., Jokela, W. E., and Dell, C. J. (2014). Measurement of greenhouse gas flux from agricultural soils using static chambers. *Journal of Visualized Experiments*, (90):52110.

Collins, H., Paul, E., Paustian, K., and Elliott, E. T. (1997). Characterization of Soil Organic Carbon Relative to Its Stability and Turnover. In *Soil Organic Matter in Temperate Agroecosystems*, pages 51–72. CRC Press, Boca Raton.

Colomb, V., Amar, S., Basset-Mens, C., Gac, A., Gaillard, G., Koch, P., Mousset, J., Salou, T., Tailleur, A., and van der Werf, H. (2014). AGRIBALYSE®, the French LCI Database for agricultural products: High quality data for producers and environmental labelling. *OCL - Oleagineux Corps Gras Lipides*, 22:D104.

Cook, R. D. (1977). Detection of Influential Observation in Linear Regression. *Technometrics*, 19(1):15–18.

Cooper, H. M., Bennett, E., Blake, J., Blyth, E., Boorman, D., Cooper, E., Evans, J., Fry, M., Jenkins, A., Morrison, R., Rylett, D., Stanley, S., Szczykulska, M., Trill, E., Antoniou, V., Askquith-Ellis, A., Ball, L., Brooks, M., Clarke, M. A., Cowan, N., Cumming, A., Farrand, P., Hitt, O., Lord, W., Scarlett, P., Swain, O., Thornton, J., Warwick, A., and Winterbourn, B. (2021). COSMOS-UK: National soil moisture and hydrometeorology data for environmental science research. *Earth System Science Data*, 13(4):1737–1757.

Cooper, R. J., Hama-Aziz, Z. Q., Hiscock, K. M., Lovett, A. A., Vrain, E., Dugdale, S. J., Sünnenberg, G., Dockerty, T., Hovesen, P., and Noble, L. (2020). Conservation tillage and soil health: Lessons from a 5-year UK farm trial (2013–2018). *Soil and Tillage Research*, 202:104648.

Corbeels, M., Sakyi, RK., Kühne, R., and Whitbread, A. (2014). Meta-analysis of crop responses to conservation agriculture in sub-Saharan Africa. *Rapport CIRAD*, 1(12).

Corbeil, R. R. and Searle, S. R. (1976). Restricted Maximum Likelihood (REML) Estimation of Variance Components in the Mixed Model. *Technometrics*, 18(1):31–38.

Cornaggia, J. (2013). Does risk management matter? Evidence from the U.S. agricultural industry. *Journal of Financial Economics*, 109(2):419–440.

Corwin, D. L. and Lesch, S. M. (2003). Application of Soil Electrical Conductivity to Precision Agriculture. *Agronomy Journal*, 95(3):455.

Cosentino, V. R., Figueiro Aureggui, S. A., and Taboada, M. A. (2013). Hierarchy of factors driving N2O emissions in non-tilled soils under different crops. *European Journal of Soil Science*, 64(5):550–557.

Curry, J. and Momen, F. (1988). The arthropod fauna of grassland on reclaimed cutaway peat in central Ireland. *Pedobiologia*, 32(1-2):99–109.

Cusser, S., Bahlai, C., Swinton, S. M., Robertson, G. P., and Haddad, N. M. (2020). Long-term research avoids spurious and misleading trends in sustainability attributes of no-till. *Global Change Biology*, 26(6):3715–3725.

Dang, Y. P., Balzer, A., Crawford, M., Rincon-Florez, V., Liu, H., Melland, A. R., Antille, D., Kodur, S., Bell, M. J., Whish, J. P. M., Lai, Y., Seymour, N., Carvalhais, L. C., and Schenk, P. (2018). Strategic tillage in conservation agricultural systems of north-eastern Australia: Why, where, when and how? *Environmental Science and Pollution Research*, 25(2):1000–1015.

Darnhofer, I., Gibbon, D., and Dedieu, B. (2012). Farming Systems Research: An approach to inquiry. In Darnhofer, I., Gibbon, D., and Dedieu, B., editors, *Farming Systems Research into the 21st Century: The New Dynamic*, pages 3–31. Springer Netherlands, Dordrecht.

Das, T. K., Ghosh, S., Das, A., Sen, S., Datta, D., Ghosh, S., Raj, R., Behera, B., Roy, A., Vyas, A., and Rana, D. (2021). Conservation agriculture impacts on productivity, resource-use efficiency and environmental sustainability: A holistic review. *Indian Journal of Agronomy*, 66:111–127.

Davis, R. and Sutton, S. (1978). A comparative study of changes in biomass of isopods inhabiting dune grassland. *Sci Proc R Dublin Soc A*, 6:223–233.

DEFRA (2019). Summary of the state of the environment: Soil. https://www.gov.uk/government/publications/state-of-the-environment/summary-state-of-the-environment-soil.

DEFRA (2022). Official Statistics Agri-climate report 2022. Technical report, Department for Environment, Food & Rural Affairs, London.

DEFRA (2024). SOH1: No-till farming. https://www.gov.uk/find-funding-for-land-or-farms/soh1-no-till-farming.

Dendooven, L., Gutiérrez-Oliva, V. F., Patiño-Zúñiga, L., Ramírez-Villanueva, D. A., Verhulst, N., Luna-Guido, M., Marsch, R., Montes-Molina, J., Gutiérrez-Miceli, F. A., Vásquez-Murrieta, S., and Govaerts, B. (2012a). Greenhouse gas emissions under conservation agriculture compared to traditional cultivation of maize in the central highlands of Mexico. *Science of the Total Environment*, 431:237–244.

Dendooven, L., Patiño-Zúñiga, L., Verhulst, N., Luna-Guido, M., Marsch, R., and Govaerts, B. (2012b). Global warming potential of agricultural systems with contrasting tillage and residue management in the central highlands of Mexico. *Agriculture, Ecosystems and Environment*, 152:50–58.

Denier, J., Faucon, M.-P., Dulaurent, A.-M., Guidet, J., Kervroëdan, L., Lamerre, J., and Houben, D. (2022). Earthworm communities and microbial metabolic activity and diversity under conventional, feed and biogas cropping systems as affected by tillage practices. *Applied Soil Ecology*, 169:104232.

Derpsch, R. (1998). Historical review of no-tillage cultivation of crops. *The 1st JIRCAS Seminar on Soybean Research. No-tillage Cultivation and Future Research Needs. March 5-6, 1998*, 1(13):1–18.

Derpsch, R., Franzluebbers, A. J., Duiker, S. W., Reicosky, D. C., Koeller, K., Friedrich, T., Sturny, W. G., Sá, J. C., and Weiss, K. (2014). Why do we need to standardize no-tillage research? *Soil and Tillage Research*, 137(April):16–22.

Derpsch, R. and Friedrich, T. (2009). Global Overview of Conservation Agriculture Adoption . *IV World Congress on Conservation Agriculture*, pages 1–14.

Derrouch, D., Chauvel, B., Felten, E., and Dessaint, F. (2020). Weed Management in the Transition to Conservation Agriculture: Farmers' Response. *Agronomy*, 10(6):843.

DICKEY-john (2024). GAC 2700-UGMA. https://dickey-john.com/products/moisture-testers/benchtop/gac-2700-ugma/.

Dodge, Y. (2008). Analysis of Residuals. In *The Concise Encyclopedia of Statistics*, pages 5–9. Springer, New York, NY.

Doerge, T. A. and Gardner, D. L. (2015). On-Farm Testing Using the Adjacent Strip Comparison Method. In *Proceedings Ofthe Fourth International Conference on Precision Agriculture.*, pages 603–609.

Doetterl, S., Van Oost, K., and Six, J. (2012). Towards constraining the magnitude of global agricultural sediment and soil organic carbon fluxes. *Earth Surface Processes and Landforms*, 37(6):642–655.

Dong, F., Dodson, L., Nemec Boehm, R., Douglass, C., Ranville, M., and Olver, R. (2024). The relative importance of herbicide use for conservation tillage adoption by U.S. corn and soybean producers. *PloS One*, 19(11):e0311960.

Doran, J. W. (1987). Microbial biomass and mineralizable nitrogen distributions in no-tillage and plowed soils. *Biology and Fertility of Soils*, 5(1):68–75.

Doran, J. W. (2002). Soil health and global sustainability: Translating science into practice. *Agriculture, Ecosystems & Environment*, 88(2):119–127.

Dordas, C. (2015). Nutrient Management Perspectives in Conservation Agriculture. In Farooq, M. and Siddique, K. H. M., editors, *Conservation Agriculture*, pages 79–107. Springer International Publishing, Cham.

Douglas, M. R. and Tooker, J. F. (2012). Slug (Mollusca: Agriolimacidae, Arionidae) Ecology and Management in No-Till Field Crops, With an Emphasis on the mid-Atlantic Region. *Journal of Integrated Pest Management*, 3(1):C1–C9.

Dragović, N. and Vulević, T. (2021). Soil Degradation Processes, Causes, and Assessment Approaches. In *Life on Land*, pages 928–939. Springer, Cham.

Drinkwater, L. E., Friedman, D., and Buck, L. (2016). *Systems Research for Agriculture - Innovative Solutions to Complex Challenges*. Sustainable Agriculture Research and Education (SARE) program.

Du, X., Jian, J., Du, C., and Stewart, R. D. (2022). Conservation management decreases surface runoff and soil erosion. *International Soil and Water Conservation Research*, 10(2):188–196.

Dulaurent, A.-M., Houben, D., Honvault, N., Faucon, M.-P., and Chauvat, M. (2023). Beneficial effects of conservation agriculture on earthworm and Collembola communities in Northern France. *Plant and Soil*.

Dusenbury, M. P., Engel, R. E., Miller, P. R., Lemke, R. L., and Wallander, R. (2008). Nitrous Oxide Emissions from a Northern Great Plains Soil as Influenced by Nitrogen Management and Cropping Systems. *Journal of Environmental Quality*, 37(2):542–550.

Earl, R. and Spoor, G. (1994). Direct drilling of oilseed rape through cereal straw residues: Testing and development of two drills. Technical Report Project Report OS10, The Home-Grown Cereals Authority (HGCA).

Ehlers, W. and Claupein, W. (1994). Approaches Toward Conservation Tillage in Germany. In *Conservation Tillage in Temperate Agroecosystems*. CRC Press.

Eijkelkamp Soil & Water (2019). Sample ring kits. Technical report, Eijkelkamp Soil & Water.

Eijkelkamp Soil & Water (2024). Penetrologger with GPS - standard set. https://www.royaleijkelkamp.com/products/field-measuring-equipment/resistance-to-penetration/electronic-with-datalogger/penetrologger-with-gps-standard-set/.

Enesi, R., Dyck, M., Thilakarathna, M., Strelkov, S., and Gorim, L. (2024). Calibrated SoilOptix ® estimates of soil pH and exchangeable cations in three agricultural fields in western Canada – implications for managing spatially variable soil acidity. *Heliyon*, 10:e37106.

European Commission (2008). Regulation No 1272/2008 of the European Parliament and of the Council of 16 December 2008 on classification, labelling and packaging of substances and mixtures. Technical report, European Commission.

Fageria, N. K., Filho, M. B., Moreira, A., and Guimarães, C. M. (2009). Foliar Fertilization of Crop Plants. *Journal of Plant Nutrition*, 32(6):1044–1064.

FAO (1982). World Soil Charter. Technical report, Food and Agriculture Organization.

FAO (2001). The economics of conservation agriculture. Technical report, Food and Agriculture Organization.

FAO (2014). The 3 Principles of Conservation Agriculture. FAO Infographics, Food and Agriculture Organization.

FAO (2017). *Soil Organic Carbon: The Hidden Potential*. Food and Agriculture Organization of the United Nations, Rome, Italy.

FAO (2019a). Soil Erosion: The greatest challenge for sustainable soil management. Technical report, Food and Agriculture Organization, Rome, Italy.

FAO (2019b). Standard operating handling and preparation of soil samples for chemical and physical analyses. *ood and Agriculture Organization of the United Nations, Global Soil Laboratory Network GLOSOLAN*, 2:1–11.

FAO (2019c). Standard operating procedure for soil total carbon. *Food and Agriculture Organization of the United Nations, Global Soil Laboratory Network GLOSOLAN*.

FAO and ITPS (2015). Status of the World's Soil Resources (SWSR) – Main Report. Technical report, Food and Agriculture Organization & Intergovernmental Technical Panel on Soils (ITPS).

Farooq, M. and Siddique, K. H. (2015). Conservation agriculture: Concepts, brief history, and impacts on agricultural systems. In *Conservation Agriculture*, pages 3–17. Springer International Publishing.

Faulkner, E. H. (1987). *Plowman's Folly and A Second Look*. Island Press.

Fernando, M. and Shrestha, A. (2023). The Potential of Cover Crops for Weed Management: A Sole Tool or Component of an Integrated Weed Management System? *Plants*, 12(4):752.

Flower, K. C., Ward, P. R., Micin, S. F., and Cordingley, N. (2021). Crop rotation can be used to manipulate residue levels under no-tillage in a rainfed Mediterranean-type environment. *Soil and Tillage Research*, 212:105062.

Flower, K. C., Ward, P. R., Passaris, N., and Cordingley, N. (2022). Uneven crop residue distribution influences soil chemical composition and crop yield under long-term no-tillage. *Soil and Tillage Research*, 223:105498.

Foley, J. A., Ramankutty, N., Brauman, K. A., Cassidy, E. S., Gerber, J. S., Johnston, M., Mueller, N. D., O'Connell, C., Ray, D. K., West, P. C., Balzer, C., Bennett, E. M., Carpenter, S. R., Hill, J., Monfreda, C., Polasky, S., Rockström, J., Sheehan, J., Siebert, S., Tilman, D., and Zaks, D. P. M. (2011). Solutions for a cultivated planet. *Nature*, 478(7369):337–342.

Follett, R. F. (2001). Soil management concepts and carbon sequestration zin cropland soils. *Soil and Tillage Research*, 61(1-2):77–92.

Francaviglia, R., Almagro, M., and Vicente-Vicente, J. L. (2023). Conservation Agriculture and Soil Organic Carbon: Principles, Processes, Practices and Policy Options. *Soil Systems*, 7(1):17.

Franks, C. and Goings, K. (1997). Above-Ground Biomass (Plant) Determinations. *U.S. Department of Agriculture (USDA) National Reserach Conservation Service (NRCS).*

Fryrear, D. W. and Skidmore, E. L. (1985). Methods for Controlling Wind Erosion. In *Soil Erosion Research Methods*, pages 265–294. Soil and Water Conservation Society and Lucie Press, 2 edition.

Fusaro, S., Gavinelli, F., Lazzarini, F., and Paoletti, M. G. (2018). Soil Biological Quality Index based on earthworms (QBS-e). A new way to use earthworms as bioindicators in agroecosystems. *Ecological Indicators*, 93:1276–1292.

Gadermaier, F., Berner, A., Fliebach, A., Friedel, J. K., and Mäder, P. (2012). Impact of reduced tillage on soil organic carbon and nutrient budgets under organic farming. *Renewable Agriculture and Food Systems*, 27(1):68–80.

Garcia-Ruiz, R. and Baggs, E. M. (2007). N2O emission from soil following combined application of fertiliser-N and ground weed residues. *Plant and Soil*, 299(1-2):263–274.

Gardi, C., Montanarella, L., Arrouays, D., Bispo, A., Lemanceau, P., Jolivet, C., Mulder, C., Ranjard, L., Römbke, J., Rutgers, M., and Menta, C. (2009). Soil biodiversity monitoring in Europe: Ongoing activities and challenges. *European Journal of Soil Science*, 60(5):807–819.

Garmin (2022). Improving GPS, Distance, and Speed Accuracy of an Outdoor Handheld or GLO 2. https://support.garmin.com/en-GB/?faq=ZYN0dmiaBM3acpi5JceDA9.

Gillbard, E. (2024). How foliar nutrition can kickstart crops and cut costs. *Farmers Weekly.*

Giller, K. E., Andersson, J. A., Corbeels, M., Kirkegaard, J., Mortensen, D., Erenstein, O., and Vanlauwe, B. (2015). Beyond conservation agriculture. *Frontiers in Plant Science*, 6(OCTOBER):870.

Giller, K. E., Beare, M. H., Lavelle, P., Izac, A. M. N., and Swift, M. J. (1997). Agricultural intensification, soil biodiversity and agroecosystem function. *Applied Soil Ecology*, 6(1):3–16.

Giller, K. E., Hijbeek, R., Andersson, J. A., and Sumberg, J. (2021). Regenerative Agriculture: An agronomic perspective. *Outlook on Agriculture*, 50(1):13–25.

Giller, K. E., Witter, E., Corbeels, M., and Tittonell, P. (2009). Conservation agriculture and smallholder farming in Africa: The heretics' view. *Field Crops Research*, 114(1):23–34.

Gomes, J., Bayer, C., de Souza Costa, F., de Cássia Piccolo, M., Zanatta, J. A., Vieira, F. C. B., and Six, J. (2009). Soil nitrous oxide emissions in long-term cover crops-based rotations under subtropical climate. *Soil and Tillage Research*, 106(1):36–44.

Gómez-Rey, M. X., Couto-Vázquez, A., and González-Prieto, S. J. (2012). Nitrogen transformation rates and nutrient availability under conventional plough and conservation tillage. *Soil and Tillage Research*, 124:144–152.

Goulding, K. W. T. (2016). Soil acidification and the importance of liming agricultural soils with particular reference to the United Kingdom. *Soil Use and Management*, 32(3):390–399.

Govaerts, B., Verhulst, N., Castellanos-Navarrete, A., Sayre, K. D., Dixon, J., and Dendooven, L. (2009). Conservation agriculture and soil carbon sequestration: Between myth and farmer reality. *Critical Reviews in Plant Sciences*, 28(3):97–122.

Graves, A. R., Morris, J., Deeks, L. K., Rickson, R. J., Kibblewhite, M. G., Harris, J. A., Farewell, T. S., and Truckle, I. (2015). The total costs of soil degradation in England and Wales. *Ecological Economics*, 119:399–413.

Griffin, T. W., Florax, R. J., and Lowenberg-DeBoer, J. (2006). Field-Scale Experimental Designs and Spatial Econometric Methods for Precision Farming : Strip-Trial Designs for Rice Production Decision Making. In *Southern Agricultural Economics Association Annual Meetings*, Orlando, Florida.

Grisso, R., Alley, M., Holshouser, D., and Thomason, W. (2009). Precision farming tools: Soil electrical conductivity. *Virginia Cooperative Extension*, 442(508):1–6.

Guidoboni, M. V., Duparque, A., Boissy, J., Mouny, J. C., Auberger, J., and van der Werf, H. M. (2023). Conservation agriculture reduces climate change impact of a popcorn and wheat crop rotation. *PLoS ONE*, 18(5 May).

Haddaway, N. R., Hedlund, K., Jackson, L. E., Kätterer, T., Lugato, E., Thomsen, I. K., Jørgensen, H. B., and Isberg, P. E. (2017). *How Does Tillage Intensity Affect Soil Organic Carbon? A Systematic Review*, volume 6. BioMed Central.

HALDRUP (2024). Lab machine - thresher LT-21. https://en.haldrup.net/haldrup-products/haldrup-lab-machines/haldrup-lt-21/.

Hallett, S. H., Sakrabani, R., Keay, C. A., and Hannam, J. A. (2017). Developments in land information systems: Examples demonstrating land resource management capabilities and options. *Soil Use and Management*, 33(4):514–529.

Hanna, M. (2016). Estimating the Field Capacity of Farm Machines. Technical Report File A3-24, U.S. Department of Agriculture (USDA).

Harmer (2024). Case Study From Start To Finish How SoilOptix Works.

Harrington, L. W. (2008). A brief history of conservation agriculture in Latin America. *South Asia and Sub-Saharan Africa Conservation Agriculture Newsletter PACA*.

Harwood, R. R. (1983). *International Overview of Regenerative Agriculture*. Rodale Research Center.

Hawkesford, M. J. (2014). Reducing the reliance on nitrogen fertilizer for wheat production. *Journal of Cereal Science*, 59(3):276–283.

Heil, K. and Schmidhalter, U. (2012). Characterisation of soil texture variability using the apparent soil electrical conductivity at a highly variable site. *Computers & Geosciences*, 39:98–110.

Hendrix, P. F., Parmelee, R. W., Crossley Jr., D. A., Coleman, D. C., Odum, E. P., and Groffman, P. M. (1986). Detritus Food Webs in Conventional and No-tillage Agroecosystems. *BioScience*, 36(6):374–380.

Henneron, L., Bernard, L., Hedde, M., Pelosi, C., Villenave, C., Chenu, C., Bertrand, M., Girardin, C., and Blanchart, E. (2015). Fourteen years of evidence for positive effects of conservation agriculture and organic farming on soil life. *Agronomy for Sustainable Development*, 35(1):169–181.

Hergoualc'h, K., Akiyama, H., Bernoux, M., Chirinda, N., Agustin del Prado, A., Åsa Kasimir, A., James Douglas MacDonald, J., Ogle, SM., Regina, K., and Weerden, TJ. (2019). N2O Emissions From Managed Soils, and Co2 Emissions From Lime and Urea Application. *2019 Refinement to the 2006 IPCC Guidelines for National Greenhouse Gas Inventories*, pages 1–48.

Hernanz, J. L., Peixoto, H., Cerisola, C., and Saâ Nchez-Giroâ, V. (2000). An empirical model to predict soil bulk density profiles in field conditions using penetration resistance, moisture content and soil depth. *Journal of Terramechanics*, 37(4):167–184.

Hiemstra, P. H., Pebesma, E. J., Twenhöfel, C. J., and Heuvelink, G. B. (2009). Real-time automatic interpolation of ambient gamma dose rates from the Dutch radioactivity monitoring network. *Computers & Geosciences*, 35(8):1711–1721.

HM Government (2023). Powering Up Britain – The Net Zero Growth Plan. Technical report, Department for Energy Security & Net Zero.

Howlett, S. A. (2012). Terrestrial slug problems: Classical biological control and beyond. *CAB Reviews: Perspectives in Agriculture, Veterinary Science, Nutrition and Natural Resources*, 7(051):10.

Hu, N., Chen, Q., and Zhu, L. (2019). The responses of soil N2O emissions to residue returning systems: A meta-analysis. *Sustainability (Switzerland)*, 11(3):1–17.

Hull, R., Tatnell, L. V., Cook, S. K., Beffa, R., and Moss, S. R. (2014). Current status of herbicide-resistant weeds in the UK. *Aspects of Applied Biology*, 27(Crop Production in Southern Britain: Precision Decisions for Profitable Cropping).

Impey, L. (2022a). Regen ag: Why farmers need to give the system time to deliver. *Farmers Weekly*.

Impey, L. (2022b). Regenerative Agriculture: How to start reducing crop inputs. *Farmers Weekly*.

IPCC (2013). Climate Change 2013: The Physical Science Basis. *Climate Contribution of Working Group 1 to the Fifth Assessment Report of the Intergovernmental Panel on Climate Change. Cambridge University*.

IPCC (2023). *Climate Change 2022 – Impacts, Adaptation and Vulnerability - Sixth Assessment Report of the Intergovernmental Panel on Climate Change*. Cambridge University Press.

ISO/IEC (2019). 17025 - General requirements for the competence of testing and calibration laboratories. https://www.iso.org/publication/PUB100424.html.

IUCN (1980). World Conservation Strategy - Living Resource Conservation for Sustainable Development. Technical report, International Union for Conservation of Nature.

Jeffery, S. and Verheijen, F. G. (2020). A New soil health policy paradigm: Pay for practice not performance! *Environmental Science and Policy*, 112(March):371–373.

Ji, W., Adamchuk, V., Chen, S., Mat Su, A. S., Ismail, A., Gan, Q., Shi, Z., and Biswas, A. (2019). Simultaneous measurement of multiple soil properties through proximal sensor data fusion: A case study. *Geoderma*, 341.

Jin, H., Shuvo Bakar, K., Henderson, B. L., Bramley, R. G., and Gobbett, D. L. (2021). An efficient geostatistical analysis tool for on-farm experiments targeted at localised treatment. *Biosystems Engineering*, 205:121–136.

John Deere (2024). 750A (3.0 Meter). https://www.deere.co.uk/en-gb/products-solutions/drills/750a-no-till-drill-3-0-meter.

Karathanasis, A. D. and Wells, K. L. (1990). Conservation Tillage Effects on the Potassium Status of Some Kentucky Soils. *Soil Science Society of America Journal*, 54(3):800–806.

Kassam, A., Derpsch, R., and Friedrich, T. (2014a). Global achievements in soil and water conservation: The case of Conservation Agriculture. *International Soil and Water Conservation Research*, 2(1):5–13.

Kassam, A., Friedrich, T., and Derpsch, R. (2019). Global spread of Conservation Agriculture. *International Journal of Environmental Studies*, 76(1):29–51.

Kassam, A., Friedrich, T., and Derpsch, R. (2022). Successful Experiences and Lessons from Conservation Agriculture Worldwide. *Agronomy*, 12(4):769.

Kassam, A., Friedrich, T., Shaxson, F., Bartz, H., Mello, I., Kienzle, J., and Pretty, J. (2014b). The spread of Conservation Agriculture: Policy and institutional support for adoption and uptake. *Field Actions Science Reports. The journal of field actions*, 7(Vol. 7):0–12.

Kassam, A., Friedrich, T., Shaxson, F., and Pretty, J. (2009). The spread of Conservation Agriculture: Justification, sustainability and uptake. *International Journal of Agricultural Sustainability*, 7(4):292–320.

Kladivko, E. J. (2001). Tillage systems and soil ecology. *Soil and Tillage Research*, 61(1):61–76.

Knapp, S. and van der Heijden, M. G. (2018). A global meta-analysis of yield stability in organic and conservation agriculture. *Nature Communications*, 9(1):1–9.

Knowler, D. and Bradshaw, B. (2007). Farmers' adoption of conservation agriculture: A review and synthesis of recent research. *Food Policy*, 32(1):25–48.

Kok, M., Sarjant, S., Verweij, S., Vaessen, S. F. C., and Ros, G. H. (2024). On-site soil analysis: A novel approach combining NIR spectroscopy, remote sensing and deep learning. *Geoderma*, 446:116903.

Korkmaz, S., Goksuluk, D., and Zararsiz, G. (2014). MVN: An R Package for Assessing Multivariate Normality. *The R Journal*, 6:151–162.

Kraamwinkel, C. T., Beaulieu, A., Dias, T., and Howison, R. A. (2021). Planetary limits to soil degradation. *Communications Earth & Environment*, 2(1):1–4.

Kucharik, C. J., Brye, K. R., Norman, J. M., Foley, J. A., Gower, S. T., and Bundy, L. G. (2001). Measurements and modeling of carbon and nitrogen cycling in agroecosystems of southern wisconsin: Potential for SOC sequestration during the next 50 years. *Ecosystems*, 4(3):237–258.

Kudsk, P., Jørgensen, L. N., and Ørum, J. E. (2018). Pesticide Load—A new Danish pesticide risk indicator with multiple applications. *Land Use Policy*, 70:384–393.

Kuhn, M., Benesty, M., Weston, S., Williams, A., Keefer, C., Engelhardt, A., Cooper, T., Mayer, Z., Kenkel, B., Team, R. C., Benesty, M., Lescarbeau, R., Ziem, A., Scrucca, L., Tang, Y., Candan, C., and Hunt, T. (2023). Caret: Classification and Regression Training.

Kumara, T. M., Kandpal, A., and Pal, S. (2020). A meta-analysis of economic and environmental benefits of conservation agriculture in South Asia. *Journal of Environmental Management*, 269(January):110773.

Kumi, F., Obour, P. B., Arthur, E., Moore, S. E., Asare, P. A., Asiedu, J., Angnuureng, D. B., Atiah, K., Amoah, K. K., Amponsah, S. K., Dorvlo, S. Y., Banafo, S., and Adu, M. O. (2023). Quantifying root-induced soil strength, measured as soil penetration resistance, from different crop plants and soil types. *Soil and Tillage Research*, 233.

Kuznetsova, A., Brockhoff, P. B., and Christensen, R. H. B. (2017). {lmerTest} Package: Tests in Linear Mixed Effects Models. *Journal of Statistical Software*, 82(13).

Kyveryga, P. M. (2019). On-farm research: Experimental approaches, analytical frameworks, case studies, and impact. *Agronomy Journal*, 111(6):2633–2635.

Kyveryga, P. M., Mueller, T. A., and Mueller, D. S. (2018). On-farm replicated strip trials. In *Precision Agriculture Basics*, pages 189–207. wiley.

Lagerlöf, J. and Scheller, U. (1989). Abundance and activity of Pauropoda and Symphyla (Myriapoda) in four cropping systems. *Pedobiologia*, 33(5):315–321.

Lal, R. (2005). World crop residues production and implications of its use as a biofuel. *Environment International*, 31(4):575–584.

Lal, R. (2015). Restoring Soil Quality to Mitigate Soil Degradation. *Sustainability*, 7(5):5875–5895.

Lalani, B., Dorward, P., and Holloway, G. (2017). Farm-level Economic Analysis - Is Conservation Agriculture Helping the Poor? *Ecological Economics*, 141:144–153.

Landers, J. N., de Freitas, P. L., de Oliveira, M. C., da Silva Neto, S. P., Ralisch, R., and Kueneman, E. A. (2021). Next Steps for Conservation Agriculture. *Agronomy*, 11(12):2496.

Lawrence, M. A., Obour, A. K., Holman, J. D., Simon, L. M., Haag, L. A., and Roozeboom, K. L. (2023). Assessing the Influence of Strategic Tillage on Crop Yields and Soil Properties in Dryland No-Tillage Systems. *Kansas Agricultural Experiment Station Research Reports*, 9(6).

Lehman, R. M., Acosta-Martinez, V., Buyer, J. S., Cambardella, C. A., Collins, H. P., Ducey, T. F., Halvorson, J. J., Jin, V. L., Johnson, J. M. F., Kremer, R. J., Lundgren, J. G., Manter, D. K., Maul, J. E., Smith, J. L., and Stott, D. E. (2015a). Soil biology for resilient, healthy soil. *Journal of Soil and Water Conservation*.

Lehman, R. M., Cambardella, C. A., Stott, D. E., Acosta-Martinez, V., Manter, D. K., Buyer, J. S., Maul, J. E., Smith, J. L., Collins, H. P., Halvorson, J. J., Kremer, R. J., Lundgren, J. G., Ducey, T. F., Jin, V. L., and Karlen, D. L. (2015b). Understanding and Enhancing Soil Biological Health: The Solution for Reversing Soil Degradation. *Sustainability*, 7(1):988–1027.

Lenth, R. V. (2023). Emmeans: Estimated Marginal Means, aka Least-Squares Means.

Lewis, K., Rainford, J., Tzilivakis, J., and Garthwaite, D. (2021). Application of the Danish pesticide load indicator to arable agriculture in the United Kingdom. *Journal of Environmental Quality*, 50(5):1110–1122.

Lewis, K. A., Tzilivakis, J., Warner, D. J., and Green, A. (2016). An international database for pesticide risk assessments and management. *Human and Ecological Risk Assessment: An International Journal*, 22(4):1050–1064.

Li, C., Frolking, S., and Butterbach-Bahl, K. (2005). Carbon Sequestration in Arable Soils is Likely to Increase Nitrous Oxide Emissions, Offsetting Reductions in Climate Radiative Forcing. *Climatic Change*, 72(3):321–338.

Li, H. W., Gao, H. W., Wu, H. D., Li, W. Y., Wang, X. Y., and He, J. (2007). Effects of 15 years of conservation tillage on soil structure and productivity of wheat cultivation in northern China. *Australian Journal of Soil Research*, 45(5):344–350.

Li, Y., Chang, S. X., Tian, L., and Zhang, Q. (2018). Conservation agriculture practices increase soil microbial biomass carbon and nitrogen in agricultural soils: A global meta-analysis. *Soil Biology and Biochemistry*, 121(October 2017):50–58.

Li, Y., Li, Z., Cui, S., and Zhang, Q. (2020a). Trade-off between soil pH, bulk density and other soil physical properties under global no-tillage agriculture. *Geoderma*, 361:114099.

Li, Y., Song, D., Liang, S., Dang, P., Qin, X., Liao, Y., and Siddique, K. H. M. (2020b). Effect of no-tillage on soil bacterial and fungal community diversity: A meta-analysis. *Soil and Tillage Research*, 204:104721.

Limousin, G. and Tessier, D. (2007). Effects of no-tillage on chemical gradients and topsoil acidification. *Soil and Tillage Research*, 92(1):167–174.

Lindstrom, M., Lobb, D., and Schumacher, T. (2001). Tillage Erosion: An Overview. *Annals of Dryland Research*, 40:345–358.

Lindwall, CW. and Sonntag, B. (2010). *Landscape Transformed: The History of Conservation Tillage and Direct Seeding, Knowledge Impact in Society.*, volume 148. University of Saskatchewan, Saskatoon, Saskatch-ewan S7 N 5B8, Canada.

Llewellyn, R., D'Emden, F., and Gobbett, D. (2009). Adoption of no-till and conservation farming practices in Australian grain growing regions: Current status and trends. Preliminary report for SA No-till Farmers Association and CAAANZ. Technical report, Grains Research and Development Corporation, Kingston.

Llewellyn, R. and Ouzman, J. (2019). Conservation agriculture in Australia: 30 years on. In *Australian Agriculture in 2020: From Conservation to Automation*, pages 21–31. Agronomy Australia and Graham Centre for Agricultural Innovation, Charles Sturt University: Wagga Wagga.

Logsdon, S. D. and Karlen, D. L. (2004). Bulk density as a soil quality indicator during conversion to no-tillage. *Soil and Tillage Research*, 78(2):143–149.

Lorenzetti, L. A. and Fiorini, A. (2024). Conservation Agriculture Impacts on Economic Profitability and Environmental Performance of Agroecosystems. *Environmental Management*, 73(3):532–545.

Lu, X. (2020). A meta-analysis of the effects of crop residue return on crop yields and water use efficiency. *PLoS ONE*, 15(4):1–18.

Lv, L., Gao, Z., Liao, K., Zhu, Q., and Zhu, J. (2023). Impact of conservation tillage on the distribution of soil nutrients with depth. *Soil and Tillage Research*, 225:105527.

Madarász, B., Járási, É. Z., Jakab, G., Szalai, Z., and Ladányi, M. (2025). Economic comparison of conventional and conservation tillage in a long-term experiment: Is it worth shifting? *International Soil and Water Conservation Research*.

Madejón, P., Fernández-Boy, E., Morales-Salmerón, L., Navarro-Fernández, C. M., Madejón, E., and Domínguez, M. T. (2023). Could conservation tillage increase the resistance to drought in Mediterranean faba bean crops? *Agriculture, Ecosystems & Environment*, 349:108449.

Mahal, N. K., Osterholz, W. R., Miguez, F. E., Poffenbarger, H. J., Sawyer, J. E., Olk, D. C., Archontoulis, S. V., and Castellano, M. J. (2019). Nitrogen fertilizer suppresses mineralization of soil organic matter in maize agroecosystems. *Frontiers in Ecology and Evolution*, 7(MAR).

Mahmood, H. S., Hoogmoed, W. B., and Van Henten, E. J. (2013). Proximal Gamma-Ray Spectroscopy to Predict Soil Properties Using Windows and Full-Spectrum Analysis Methods. *Sensors*, 13(12):16263–16280.

Manno, M. (1996). Herbicides. *Human Toxicology*, pages 551–560.

Marden, J. I. (2004). Positions and QQ Plots. *Statistical Science*, 19(4):606–614.

Maywald, N. J., Francioli, D., Mang, M., and Ludewig, U. (2023). Role of Mineral Nitrogen Nutrition in Fungal Plant Diseases of Cereal Crops. *Critical Reviews in Plant Sciences*, 42(3):93–123.

McNairn, H. E. and Mitchell, B. (1992). Locus of control and farmer orientation: Effects on conservation adoption. *Journal of Agricultural and Environmental Ethics*, 5(1):87–101.

Mei, K., Wang, Z., Huang, H., Zhang, C., Shang, X., Dahlgren, R. A., Zhang, M., and Xia, F. (2018). Stimulation of N2O emission by conservation tillage management in agricultural lands: A meta-analysis. *Soil and Tillage Research*, 182(March):86–93.

Met Office (2023). UK climate averages - Shawbury (Shropshire). https://www.metoffice.gov.uk/research/climate/maps-and-data/uk-climate-averages/gcqh76ug7.

Met Office (2024). Record-breaking rainfall for some this September. https://www.metoffice.gov.uk/about-us/news-and-media/media-centre/weather-and-climate-news/2024/record-breaking-rainfall-for-some-this-september.

Met Office (2025). Weather and Climate summaries. https://www.metoffice.gov.uk/research/climate/maps-and-data/summaries/index.

Meteostat (2024). Shawbury | Weather History & Climate. https://meteostat.net/en/station/03414?t=2022-01-01/2024-12-31.

Michler, J. D., Baylis, K., Arends-Kuenning, M., and Mazvimavi, K. (2019). Conservation agriculture and climate resilience. *Journal of Environmental Economics and Management*, 93:148–169.

Moeys, J., Shangguan, W., Petzold, R., Minasny, B., Rosca, B., Jelinski, N., Zelazny, W., Souza, R. M. S., Safanelli, J. L., and ten Caten, A. (2024). Soiltexture: Functions for Soil Texture Plot, Classification and Transformation.

Mondal, S., Chakraborty, D., Das, T. K., Shrivastava, M., Mishra, A. K., Bandyopadhyay, K. K., Aggarwal, P., and Chaudhari, S. K. (2019). Conservation agriculture had a strong impact on the sub-surface soil strength and root growth in wheat after a 7-year transition period. *Soil and Tillage Research*, 195:104385.

Montgomery, D. R. (2021). 11 - Soil health and the revolutionary potential of Conservation Agriculture. In Kassam, A. and Kassam, L., editors, *Rethinking Food and Agriculture*, Woodhead Publishing Series in Food Science, Technology and Nutrition, pages 219–229. Woodhead Publishing.

Montzka, S. A., Dlugokencky, E. J., and Butler, J. H. (2011). Non-CO 2 greenhouse gases and climate change. *Nature*, 476(7358):43–50.

Morris, N. L., Miller, P. C., Orson, J. H., and Froud-Williams, R. J. (2010). The adoption of non-inversion tillage systems in the United Kingdom and the agronomic impact on soil, crops and the environment-A review. *Soil and Tillage Research*, 108(1-2):1–15.

Morrison Jr., J. E., Gerik, T. J., Chichester, F. W., Martin, J. R., and Chandler, J. M. (1990). A No-Tillage Farming System for Clay Soils. *Journal of Production Agriculture*, 3(2):219–227.

Mowbray, E. (2020). Retrofit openers offer drill customisation on a budget - Farmers Weekly. *Farmers Weekly*.

Mowbray, E. and Clarke, A. (2019). Groundswell 2019: 12 no-till drills side-by-side. *Farmers Weekly*.

Mueller, D. H., Klemme, R. M., and Daniel, T. C. (1985). Short- and long-term cost comparisons of conventional and conservation tillage systems in corn production. *Journal of Soil and Water Conservation*, 40(5):466–470.

Muhammad, I., Wang, J., Sainju, U. M., Zhang, S., Zhao, F., and Khan, A. (2021). Cover cropping enhances soil microbial biomass and affects microbial community structure: A *meta*-analysis. *Geoderma*, 381:114696.

Mukherjee, S., Sarkar, D., Mandal, B., Kanthal, S., Ghosh, S., Sahu, B., Singh, P., Dey, A., Jaison, M., Dutta, J., Dash, B., and Saha, N. (2024). Conservation agriculture influences soil nitrogen availability in the lower Indo-Gangetic Plains. *Plant and Soil*.

Mulvaney, R. L., Khan, S. A., and Ellsworth, T. R. (2009). Synthetic Nitrogen Fertilizers Deplete Soil Nitrogen: A Global Dilemma for Sustainable Cereal Production. *Journal of Environmental Quality*, 38(6):2295–2314.

Muralikrishna, I. V. and Manickam, V. (2017). Chapter Fourteen - Air Pollution Control Technologies. In Muralikrishna, I. V. and Manickam, V., editors, *Environmental Management*, pages 337–397. Butterworth-Heinemann.

Mutsaers, H. (1997). *Field Guide for On-Farm Experimentation*, volume 1 of *1*. Technical Centre for Agricultural and Rural Cooperation, Ibadan, Nigeria,.

NAAC (2022). National Association of Agricultural Contractors - Contracting Prices Survey 2022. Technical Report 3, National Association of Agricultural Contractors.

Nalewaja, J. D. (2003). Weeds and Conservation Agriculture. In García-Torres, L., Benites, J., Martínez-Vilela, A., and Holgado-Cabrera, A., editors, *Conservation Agriculture: Environment, Farmers Experiences, Innovations, Socio-economy, Policy*, pages 201–210. Springer Netherlands, Dordrecht.

Natural England (2008). TIN037 - Soil texture. *Natural England Technical Information Note*, 1(1).

Nazarko, O. M., Van Acker, R. C., and Entz, M. H. (2005). Strategies and tactics for herbicide use reduction in field crops in Canada: A review. *Canadian Journal of Plant Science*, 85(2):457–479.

Newton, P., Civita, N., Frankel-Goldwater, L., Bartel, K., and Johns, C. (2020). What Is Regenerative Agriculture? A Review of Scholar and Practitioner Definitions Based on Processes and Outcomes. *Frontiers in Sustainable Food Systems*, 4.

NFU (2023). 'Net zero' agriculture. https://www.nfuonline.com/archive?treeid=114805.

Ng, V. K. and Cribbie, R. A. (2017). Using the Gamma Generalized Linear Model for Modeling Continuous, Skewed and Heteroscedastic Outcomes in Psychology. *Current Psychology*, 36(2):225–235.

Nikolić, N., Loddo, D., and Masin, R. (2021). Effect of Crop Residues on Weed Emergence. *Agronomy*, 11(1):163.

NRM (2021a). Advice Sheet 28: Agri-Nutrient Saver Service – Mehlich III. Technical Report 28, NRM - Cawood Scientific.

NRM (2021b). Advice Sheet 30: Textural Classification at NRM. Technical report, NRM - Cawood Scientific.

Nyengere, J., Okamoto, Y., Funakawa, S., and Shinjo, H. (2023). Analysis of spatial heterogeneity of soil physicochemical properties in northern Malawi. *Geoderma Regional*, 35:e00733.

Office for National Statistics (2025). CPIH ANNUAL RATE. https://www.ons.gov.uk/economy/inflationandpriceindices/timeseries/l55o/mm23.

O'Hara, R. B. and Kotze, D. J. (2010). Do not log-transform count data. *Methods in Ecology and Evolution*, 1(2):118–122.

Oksanen, J., Simpson, G. L., Blanchet, F. G., Kindt, R., Legendre, P., Minchin, P. R., O'Hara, R. B., Solymos, P., Stevens, M. H. H., Szoecs, E., Wagner, H., Barbour, M., Bedward, M., Bolker, B., Borcard, D., Carvalho, G., Chirico, M., De Caceres, M., Durand, S., Evangelista, H. B. A., FitzJohn, R., Friendly, M., Furneaux, B., Hannigan, G., Hill, M. O., Lahti, L., McGlinn, D., Ouellette, M.-H., Ribeiro Cunha, E., Smith, T., Stier, A., Ter Braak, C. J. F., Weedon, J., and Borman, T. (2024). Vegan: Community Ecology Package.

Oliveira, E. M., Wittwer, R., Hartmann, M., Keller, T., Buchmann, N., and van der Heijden, M. G. (2024). Effects of conventional, organic and conservation agriculture on soil physical properties, root growth and microbial habitats in a long-term field experiment. *Geoderma*, 447.

Oliver, M. (2017). Is French-made Novag disc drill king of cover crop drilling? - Farmers Weekly. *Farmers Weekly*.

Olsen, S. R. (1954). *Estimation of Available Phosphorus in Soils by Extraction with Sodium Bicarbonate*. U.S. Department of Agriculture.

O'Neill, M., Lanigan, G. J., Forristal, P. D., and Osborne, B. A. (2021). Greenhouse Gas Emissions and Crop Yields From Winter Oilseed Rape Cropping Systems are Unaffected by Management Practices. *Frontiers in Environmental Science*, 9.

Oyeogbe, A. (2021). Nitrogen Management in Conservation Agriculture. In *Nitrogen in Agriculture - Physiological, Agricultural and Ecological Aspects*. IntechOpen.

Page, K. L., Dang, Y. P., and Dalal, R. C. (2020). The Ability of Conservation Agriculture to Conserve Soil Organic Carbon and the Subsequent Impact on Soil Physical, Chemical, and Biological Properties and Yield. *Frontiers in Sustainable Food Systems*, 4:31.

Palm, C., Blanco-Canqui, H., DeClerck, F., Gatere, L., and Grace, P. (2014). Conservation agriculture and ecosystem services: An overview. *Agriculture, Ecosystems and Environment*, 187:87–105.

Pannell, D. J., Llewellyn, R. S., and Corbeels, M. (2014). The farm-level economics of conservation agriculture for resource-poor farmers. *Agriculture, Ecosystems and Environment*, 187:52–64.

Panten, K., Bramley, R. G., Lark, R. M., and Bishop, T. F. (2010). Enhancing the value of field experimentation through whole-of-block designs. *Precision Agriculture*, 11(2):198–213.

Paoletti, M. G., Sommaggio, D., and Fusaro, S. (2013). Proposta di Indice di Qualità Biologica del Suolo (QBS-e) basato sui Lombrichi e applicato agli Agroecosistemi. *Biologia Ambientale*, 27(2):25–43.

Parihar, C. M., Jat, S. L., Singh, A. K., Kumar, B., Rathore, N. S., Jat, M. L., Saharawat, Y. S., and Kuri, B. R. (2018). Energy auditing of long-term conservation agriculture based irrigated intensive maize systems in semi-arid tropics of India. *Energy*, 142:289–302.

Parisi, V., Menta, C., Gardi, C., Jacomini, C., and Mozzanica, E. (2005). Microarthropod communities as a tool to assess soil quality and biodiversity: A new approach in Italy. *Agriculture, Ecosystems and Environment*, 105(1-2):323–333.

Pätzold, Leenen, M., and Heggemann, T.W. (2020). Proximal Mobile Gamma Spectrometry as Tool for Precision Farming and Field Experimentation. *Soil Systems*, 4(2):31.

Paustian, K., Andrén, O., Janzen, H. H., Lal, R., Smith, P., Tian, G., Tiessen, H., Van Noordwijk, M., and Woomer, P. L. (1997). Agricultural soils as a sink. *Soil Use and Management*, 13:230–244.

Pebesma, E., Bivand, R., Racine, E., Sumner, M., Cook, I., Keitt, T., Lovelace, R., Wickham, H., Ooms, J., Müller, K., Pedersen, T. L., Baston, D., and Dunnington, D. (2024). Sf: Simple Features for R.

Pebesma, E. J. (2004). Multivariable geostatistics in S: The gstat package. *Computers & Geosciences*, 30(7):683–691.

Pelosi, C., Bertrand, M., and Roger-Estrade, J. (2009). Earthworm community in conventional, organic and direct seeding with living mulch cropping systems. *Agronomy for Sustainable Development*, 29(2):287–295.

PGRO (2024). Choice and use of seed. https://www.pgro.org/choice-and-use-of-seed1/.

Phillips, S. H. (1984). Introduction. In *No-Tillage Agriculture*, pages 1–10. Springer US, Boston, MA.

Pidgeon, J. D. and Soane, B. D. (1977). Effects of tillage and direct drilling on soil properties during the growing season in a long-term barley mono-culture system. *The Journal of Agricultural Science*, 88(2):431–442.

Piepho, H. P., Richter, C., Spilke, J., Hartung, K., Kunick, A., and Thöle, H. (2011). Statistical aspects of on-farm experimentation. *Crop and Pasture Science*, 62(9):721–735.

Pietola, L. M. (2005). Root growth dynamics of spring cereals with discontinuation of mouldboard ploughing. *Soil & Tillage Research*, 80(1-2):103–114.

Pittelkow, Linquist, B. A., Lundy, M. E., Liang, X., van Groenigen, K. J., Lee, J., van Gestel, N., Six, J., Venterea, R. T., and van Kessel, C. (2015). When does no-till yield more? A global meta-analysis. *Field Crops Research*, 183:156–168.

Pittelkow, C., Liang, X., Bruce A. Linquist, Groenigen, L. J. V., Lee, J., Lundy, M. E., Van Gestel, N., Six, J., Rodney T Venterea, and Van Kessel, C. (2015). Productivity limits and potentials of the principles of conservation agriculture. *Nature*, 517(7534):365–368.

Planet Labs PBC (2024). Planet Application Program Interface: In Space for Life on Earth.

Ponce, M. F., Gutiérrez-Díaz, J., Flores-Macías, A., González-Ortega, E., Mendoza, A. P., Sánchez, L. M. R., Novotny, I., and Espíndola, I. P. M. (2022). Direct and indirect greenhouse gas emissions under conventional, organic, and conservation agriculture. *Agriculture, Ecosystems and Environment*, 340.

Postma-Blaauw, M. B., de Goede, R. G. M., Bloem, J., Faber, J. H., and Brussaard, L. (2010). Soil biota community structure and abundance under agricultural intensification and extensification. *Ecology*, 91(2):460–473.

Potter, C. (2009). Agricultural Stewardship, Climate Change and the Public Goods Debate. In *What Is Land For?* Routledge.

Powell, M. J. (2009). The BOBYQA Algorithm for Bound Constrained Optimization without Derivatives. Technical Report DAMTP 2009/NA06, Centre for Mathematical Sciences, University of Cambridge, UK.

Prather, M. J., Holmes, C. D., and Hsu, J. (2012). Reactive greenhouse gas scenarios: Systematic exploration of uncertainties and the role of atmospheric chemistry. *Geophysical Research Letters*, 39(9).

Pretty, J. (2008). Agricultural sustainability: Concepts, principles and evidence. *Philosophical Transactions of the Royal Society B: Biological Sciences*, 363(1491):447–465.

Pribyl, D. W. (2010). A critical review of the conventional SOC to SOM conversion factor. *Geoderma*, 156(3-4):75–83.

Pringle, M. J., Cook, S. E., and McBratney, A. B. (2004a). Field-scale experiments for site-specific crop management. Part I: Design considerations. *Precision Agriculture*, 5(6):617–624.

Pringle, M. J., Cook, S. E., and McBratney, A. B. (2004b). Field-scale experiments for site-specific crop management. Part II: A Geostatistical Analysis. *Precision Agriculture*, 5(6):617–624.

Prosekov, A. Y. and Ivanova, S. A. (2018). Food security: The challenge of the present. *Geoforum*, 91:73–77.

Pumpanen, J., Kolari, P., Ilvesniemi, H., Minkkinen, K., Vesala, T., Niinistö, S., Lohila, A., Larmola, T., Morero, M., Pihlatie, M., Janssens, I., Yuste, J. C., Grünzweig, J. M., Reth, S., Subke, J. A., Savage, K., Kutsch, W., Østreng, G., Ziegler, W., Anthoni, P., Lindroth, A., and Hari, P. (2004). Comparison of different chamber techniques for measuring soil CO 2 efflux. *Agricultural and Forest Meteorology*, 123(3-4):159–176.

QGIS Association (2024). QGIS Geographic Information System.

R Core Team (2023). R: A language and environment for statistical computing. R Foundation for Statistical Computing.

Reay, D. S., Davidson, E. A., Smith, K. A., Smith, P., Melillo, J. M., Dentener, F., and Crutzen, P. J. (2012). Global agriculture and nitrous oxide emissions. *Nature Climate Change*, 2(6):410–416.

Rees, R. M., Baddeley, J. A., Bhogal, A., Ball, B. C., Chadwick, D. R., Macleod, M., Lilly, A., Pappa, V. A., Thorman, R. E., Watson, C. A., and Williams, J. R. (2013). Nitrous oxide mitigation in UK agriculture. *Soil Science and Plant Nutrition*, 59(1):3–15.

Reeves, D. (1997). The role of soil organic matter in maintaining soil quality in continuous cropping systems. *Soil and Tillage Research*, 43:131–167.

Reinhardt, N. and Herrmann, L. (2019). Gamma-ray spectrometry as versatile tool in soil science: A critical review. *Journal of Plant Nutrition and Soil Science*, 182(1):9–27.

Ren, X., Zou, W., Jiao, J., Stewart, R., and Jian, J. (2023). Soil properties affect crop yield changes under conservation agriculture: A systematic analysis. *European Journal of Soil Science*, 74(5):e13413.

Rhodes, C. J. (2017). The Imperative for Regenerative Agriculture. *Science Progress*, 100(1):80–129.

Rhymes, J., Chadwick, D. R., Williams, A. P., Harris, I. M., Lark, R. M., and Jones, D. L. (2023). Evaluating the accuracy and usefulness of commercially-available proximal soil mapping services for grassland nutrient management planning and soil health monitoring. *Precision Agriculture*, 24(3):898–920.

Richard, G., Boiffin, J., and Duval, Y. (1995). Direct drilling of sugar beet (*Beta vulgaris* L.) into a cover crop: Effects on soil physical conditions and crop establishment. *Soil and Tillage Research*, 34(3):169–185.

Riemens, M., Sønderskov, M., Moonen, A.-C., Storkey, J., and Kudsk, P. (2022). An Integrated Weed Management framework: A pan-European perspective. *European Journal of Agronomy*, 133:126443.

Riemens, M., Van Der Weide, R., Bleeker, P., and Lotz, L. (2007). Effect of stale seedbed preparations and subsequent weed control in lettuce (cv. Iceboll) on weed densities. *Weed Research*, 47(2):149–156.

Riley, H., Børresen, T., Ekeberg, E., and Rydberg, T. (2017). Trends in Reduced Tillage Research and Practice in Scandinavia. In *Conservation Tillage in Temperate Agroecosystems*, pages 23–45. CRC Press, Boca Raton, 1 edition.

Rochette, P. (2008). No-till only increases N2O emissions in poorly-aerated soils. *Soil and Tillage Research*, 101(1-2):97–100.

Rochette, P., Angers, DA., Chantigny, M., and Bertrand, N. (2008). Nitrous Oxide Emissions Respond Differently to No-Till in a Loam and a Heavy Clay Soil. *Soil Science Society of America Journal*, 72(5):1363–1369.

Rockström, J., Kaumbutho, P., Mwalley, J., Nzabi, A. W., Temesgen, M., Mawenya, L., Barron, J., Mutua, J., and Damgaard-Larsen, S. (2009). Conservation farming strategies in East and Southern Africa: Yields and rain water productivity from on-farm action research. *Soil and Tillage Research*, 103(1):23–32.

Roques, S. E., Kindred, D. R., Berry, P., and Helliwell, J. (2022). Successful approaches for on-farm experimentation. *Field Crops Research*, 287.

Rose, M. T., Cavagnaro, T. R., Scanlan, C. A., Rose, T. J., Vancov, T., Kimber, S., Kennedy, I. R., Kookana, R. S., and Van Zwieten, L. (2016). Impact of Herbicides on Soil Biology and Function. In Sparks, D. L., editor, *Advances in Agronomy*, volume 136 of *Advances in Agronomy*, pages 133–220. Academic Press.

Ruan, H., Ahuja, L. R., Green, T. R., and Benjamin, J. G. (2001). Residue Cover and Surface-Sealing Effects on Infiltration. *Soil Science Society of America Journal*, 65(3):853–861.

Sainju, U. M. (2016). A global meta-analysis on the impact of management practices on net global warming potential and greenhouse gas intensity from cropland soils. *PLoS ONE*, 11(2).

Sainju, U. M., Barsotti, J. L., and Wang, J. (2014). Net Global Warming Potential and Greenhouse Gas Intensity Affected by Cropping Sequence and Nitrogen Fertilization. *Soil Science Society of America Journal*, 78(1):248–261.

Schiere, J., Groenland, R., Vlug, A., and Keulen (2004). System thinking in agriculture: An overview. *Emerging challenges for farming systems: lessons from Australian and Dutch agriculture.*

Schmidinger, J., Barkov, V., Tavakoli, H., Correa, J., Ostermann, M., Atzmueller, M., Gebbers, R., and Vogel, S. (2024). Which and how many soil sensors are ideal to predict key soil properties: A case study with seven sensors. *Geoderma*, 450:117017.

Schofield, R. K. (1944). Plowman's Folly. *Nature*, 153(3883):391.

Scholes, R., Montanarella, L., Brainich, A., Barger, N., ten Brink, B., Cantele, M., Erasmus, B., Fisher, J., Gardner, T., Holland, T. G., Kohler, F., Kotiaho, J. S., Maltitz, G. V., Nangendo, G., Pandit, R., Parrotta, J., Potts, M. D., Prince, S., Sankaran, M., and Willemen, L. (2018). Summary for policymakers of the assessment report on land degradation and restoration of the Intergovernmental Science- Policy Platform on Biodiversity and Ecosystem Services. *Intergovernmental Science-Policy Platform on Biodiversity and Ecosystem Services (IPBES)*, pages 1–44.

Schreefel, L., Schulte, R. P. O., de Boer, I. J. M., Schrijver, A. P., and van Zanten, H. H. E. (2020). Regenerative agriculture – the soil is the base. *Global Food Security*, 26:100404.

Shakoor, A., Shahbaz, M., Farooq, T. H., Sahar, N. E., Shahzad, S. M., Altaf, M. M., and Ashraf, M. (2021). A global meta-analysis of greenhouse gases emission and crop yield under no-tillage as compared to conventional tillage. *Science of the Total Environment*, 750:142299.

Shannon, C. E. (1948). A Mathematical Theory of Communication. *Bell System Technical Journal*, 27(3):379–423.

Shelton, R. E., Jacobsen, K. L., and McCulley, R. L. (2017). Cover Crops and Fertilization Alter Nitrogen Loss in Organic and Conventional Conservation Agriculture Systems. *Frontiers in Plant Science*, 8:2260.

Signor, D. and Cerri, C. E. P. (2013). Emissões de óxido nitroso em solos agrícolas: Uma revisão. *Pesquisa Agropecuaria Tropical*, 43(3):322–338.

Singh, V., Barman, K., Singh, R., and Sharma, A. (2015). Weed Management in Conservation Agriculture Systems. In Farooq, M. and Siddique, K. H. M., editors, *Conservation Agriculture*, pages 39–77. Springer International Publishing, Cham.

Sithole, N. J. and Magwaza, L. S. (2019). Long-term changes of soil chemical characteristics and maize yield in no-till conservation agriculture in a semi-arid environment of South Africa. *Soil and Tillage Research*, 194:104317.

Skiba, U., McTaggart, I. P., Smith, K. A., Hargreaves, K. J., and Fowler, D. (1996). Estimates of nitrous oxide emissions from soil in the UK. *Energy Conversion and Management*, 37(6-8):1303–1308.

Smil, V. (1999). Crop Residues: Agriculture's Largest Harvest. *BioScience*, 49(4):299–308.

Soane, B. D., Ball, B. C., Arvidsson, J., Basch, G., Moreno, F., and Roger-Estrade, J. (2012). No-till in northern, western and south-western Europe: A review of problems and opportunities for crop production and the environment. *Soil and Tillage Research*, 118:66–87.

Soto Gómez, D., Fernández Calviño, D., Koefoed Brandt, K., Waeyenberge, L., Zornoza, R., and Martínez Martínez, S. (2020). Handbook - Protocols for sampling, general soil characterization and soil biodiversity analysis. Technical report, SoildiverAgro.

Speratti, A., Turmel, M.-S., Calegari, C., Araujo-Junior, Violic, A., Wall, P., and Govaerts, B. (2015). Conservation agriculture in latin America. In *Conservation Agriculture*, volume 70, pages 391–415. Springer.

Stefanova, K. T., Brown, J., Grose, A., Cao, Z., Chen, K., Gibberd, M., and Rakshit, S. (2023). Statistical analysis of comparative experiments based on large strip on-farm trials. *Field Crops Research*, 297:108945.

Stengel, P., Douglas, J. T., Guérif, J., Goss, M. J., Monnier, G., and Cannell, R. Q. (1984). Factors influencing the variation of some properties of soils in relation to their suitability for direct drilling. *Soil and Tillage Research*, 4(1):35–53.

Su, Y., Gabrielle, B., and Makowski, D. (2021). A global dataset for crop production under conventional tillage and no tillage systems. *Scientific Data*, 8(1):33.

Swanton, C. J. and Weise, S. F. (1991). Integrated Weed Management: The Rationale and Approach. *Weed Technology*, 5(3):657–663.

Swire, J. (2017). New mintill and direct drill coulter points from Dutch Openers added to Spaldings tillage tools range. *News from AA Farmer*.

Sylvester-Bradley, R., Berry, P., Blake, J., Kindred, D., Spink, J., Bingham, I., McVittie, J., and Foulkes, J. (2015). Wheat Growth Guide. Technical report, Agriculture and Horticulture Development Board.

Syngenta (2024). Sustainable System sees profit increase and climate change cut. Technical report, Syngenta, Basel, Switzerland.

Syngenta Group (2025). What is regenerative agriculture? https://www.syngentagroup.com/regenerative-agriculture.

Taubner, H., Roth, B., and Tippkötter, R. (2009). Determination of soil texture: Comparison of the sedimentation method and the laser-diffraction analysis. *Journal of Plant Nutrition and Soil Science*, 172(2):161–171.

Tellez-Rio, A., García-Marco, S., Navas, M., López-Solanilla, E., Tenorio, J. L., and Vallejo, A. (2015). N2O and CH4 emissions from a fallow-wheat rotation with low N input in conservation and conventional tillage under a Mediterranean agroecosystem. *Science of the Total Environment*, 508:85–94.

Teng, J., Hou, R., Dungait, J. A., Zhou, G., Kuzyakov, Y., Zhang, J., Tian, J., Cui, Z., Zhang, F., and Delgado-Baquerizo, M. (2024). Conservation agriculture improves soil health and sustains crop yields after long-term warming. *Nature communications*, 15(1):8785.

Thierfelder, C. and Wall, P. C. (2010). Investigating Conservation Agriculture (CA) Systems in Zambia and Zimbabwe to Mitigate Future Effects of Climate Change. *Journal of Crop Improvement*, 24(2):113–121.

Todisco, F., Vergni, L., Vinci, A., and Torri, D. (2022). Infiltration and bulk density dynamics with simulated rainfall sequences. *CATENA*, 218:106542.

Townsend, T. J., Ramsden, S. J., and Wilson, P. (2016). How do we cultivate in England? Tillage practices in crop production systems. *Soil Use and Management*, 32(1):106–117.

Townsend, T. J., Sparkes, D. L., Ramsden, S. J., Glithero, N. J., and Wilson, P. (2018). Wheat straw availability for bioenergy in England. *Energy Policy*, 122:349–357.

Triplett, G. B. and Dick, W. A. (2008). No-tillage crop production: A revolution in agriculture! *Agronomy Journal*, 100(3 SUPPL.):153–165.

Turmel, M. S., Speratti, A., Baudron, F., Verhulst, N., and Govaerts, B. (2015). Crop residue management and soil health: A systems analysis. *Agricultural Systems*, 134:6–16.

United Nations (2019). World Population Prospects 2019: Highlights. https://population.un.org/wpp/.

USEPA (2012). Summary Report : Greenhouse Gas Emissions : 1990 - 2030. Technical Report EPA 430-S-12-002, Office of Atmospheric Programs Climate Change Division U.S. Environmental Protection Agency, 1200 Pennsylvania Avenue, NW Washington, DC 20460.

USEPA (2015). KABAM Version 1.0 User's Guide and Technical Documentation - Appendix F -Description of Equations Used to Calculate the BCF, BAF, BMF, and BSAF Values. https://www.epa.gov/pesticide-science-and-assessing-pesticide-risks/kabam-version-10-users-guide-and-technical-3.

USEPA (2016). SCI-GROW Description. https://archive.epa.gov/epa/pesticide-science-and-assessing-pesticide-risks/sci-grow-description.html.

Valujeva, K., Pilecka-Ulcugaceva, J., Skiste, O., Liepa, S., Lagzdins, A., and Grinfelde, I. (2022). Soil tillage and agricultural crops affect greenhouse gas emissions from Cambic Calcisol in a temperate climate. *Acta Agriculturae Scandinavica Section B: Soil and Plant Science*, 72(1):835–846.

Van den Putte, A., Govers, G., Diels, J., Gillijns, K., and Demuzere, M. (2010). Assessing the effect of soil tillage on crop growth: A meta-regression analysis on European crop yields under conservation agriculture. *European Journal of Agronomy*, 33(3):231–241.

Van Der Weerden, T. J., Kelliher, F. M., and De Klein, C. A. (2012). Influence of pore size distribution and soil water content on nitrous oxide emissions. *Soil Research*, 50(2):125–135.

van Kessel, C., Venterea, R., Six, J., Adviento-Borbe, M. A., Linquist, B., and van Groenigen, K. J. (2013). Climate, duration, and N placement determine N2O emissions in reduced tillage systems: A meta-analysis. *Global Change Biology*, 19(1):33–44.

Van Leeuwen, J., Sandén, T., Lair, G., Bloem, J., Hemerik, L., Ragnarsdottir, K., Gísladóttir, G., Newton, J., and Ruiter, P. (2015). An ecosystem approach to assess soil quality in organically and conventionally managed farms in Iceland and Austria. *SOIL*, 2015:83–101.

Van Oost, K., Cerdan, O., and Quine, T. A. (2009). Accelerated sediment fluxes by water and tillage erosion on European agricultural land. *Earth Surface Processes and Landforms*, 34(12):1625–1634.

Van Oost, K., Govers, G., de Alba, S., and Quine, T. A. (2006). Tillage erosion: A review of controlling factors and implications for soil quality. *Progress in Physical Geography*, 30(4):443–466.

Vankeerberghen, A. and Stassart, P. M. (2016). The transition to conservation agriculture: An insularization process towards sustainability. *International Journal of Agricultural Sustainability*, 14(4):392–407.

Varah, A., Ahodo, K., Childs, D. Z., Comont, D., Crook, L., Freckleton, R. P., Goodsell, R., Hicks, H. L., Hull, R., Neve, P., and Norris, K. (2024). Acting pre-emptively reduces the long-term costs of managing herbicide resistance. *Scientific Reports*, 14(1):6201.

Vasques, G. M., Rodrigues, H. M., Coelho, M. R., Baca, J. F. M., Dart, R. O., Oliveira, R. P., Teixeira, W. G., and Ceddia, M. B. (2020). Field Proximal Soil Sensor Fusion for Improving High-Resolution Soil Property Maps. *Soil Systems*, 4(3):52.

Venter, Z. S., Jacobs, K., and Hawkins, H.-J. (2016). The impact of crop rotation on soil microbial diversity: A meta-analysis. *Pedobiologia*, 59(4):215–223.

Ver Hoef, J. M. and Boveng, P. L. (2007). Quasi-Poisson Vs. Negative Binomial Regression: How Should We Model Overdispersed Count Data? *Ecology*, 88(11):2766–2772.

Vera, I., Wicke, B., Lamers, P., Cowie, A., Repo, A., Heukels, B., Zumpf, C., Styles, D., Parish, E., Cherubini, F., Berndes, G., Jager, H., Schiesari, L., Junginger, M., Brandão, M., Bentsen, N. S., Daioglou, V., Harris, Z., and van der Hilst, F. (2022). Land use for bioenergy: Synergies and trade-offs between sustainable development goals. *Renewable and Sustainable Energy Reviews*, 161:112409.

Vigani, M., Urquhart, J., Black, J. E., Berry, R., Dwyer, J., and Rose, D. C. (2021). Post-Brexit Policies for a Resilient Arable Farming Sector in England. *EuroChoices*, 20(1):55–61.

Viscarra Rossel, R. A., Adamchuk, V. I., Sudduth, K. A., McKenzie, N. J., and Lobsey, C. (2011). Chapter Five - Proximal Soil Sensing: An Effective Approach for Soil Measurements in Space and Time. In Sparks, D. L., editor, *Advances in Agronomy*, volume 113 of *Advances in Agronomy*, pages 243–291. Academic Press.

Vu, V. Q., Friendly, M., and Tavadyan, A. (2024). Ggbiplot: A Grammar of Graphics Implementation of Biplots.

Wacker, T. S., Jensen, L. S., and Thorup-Kristensen, K. (2022). Conservation agriculture affects soil organic matter distribution, microbial metabolic capacity and nitrogen turnover under Danish field conditions. *Soil and Tillage Research*, 224:105508.

Wackernagel, H. (2003). Ordinary Kriging. In Wackernagel, H., editor, *Multivariate Geostatistics: An Introduction with Applications*, pages 79–88. Springer, Berlin, Heidelberg.

Wang, C., Amon, B., Schulz, K., and Mehdi, B. (2021). Factors that influence nitrous oxide emissions from agricultural soils as well as their representation in simulation models: A review. *Agronomy*, 11(4).

Wang, H., Wang, S., Yu, Q., Zhang, Y., Wang, R., Li, J., and Wang, X. (2020). No tillage increases soil organic carbon storage and decreases carbon dioxide emission in the crop residue-returned farming system. *Journal of Environmental Management*, 261:110261.

Wang, X. B., Cai, D. X., Hoogmoed, W. B., Oenema, O., and Perdok, U. D. (2006). Potential Effect of Conservation Tillage on Sustainable Land Use: A Review of Global Long-Term Studies. *Pedosphere*, 16(5):587–595.

Waydelin, C. W. (1995). Practical experience with reduced tillage farming. In *Proceedings of the EC-Workshop-II-, Silsoe*, pages 15–17.

Wehrle, R. and Pätzold, S. (2024). Site-Independent Mapping of Clay Content in Vineyard Soils via Mobile Proximal Gamma-Ray Spectrometry and Machine Learning Calibrations. *Sensors*, 24(14):4528.

West, T. O. and Post, W. M. (2002). Soil Organic Carbon Sequestration Rates by Tillage and Crop Rotation. *Soil Science Society of America Journal*, 66(6):1930–1946.

White, C. (2020). Why Regenerative Agriculture? *The American Journal of Economics and Sociology*, 79(3):799–812.

Wickham, H. (2016). *Ggplot2: Elegant Graphics for Data Analysis*. Springer-Verlag, New York.

Wilson, G. F., Lal, R., and Okigbo, B. N. (1982). Effects of cover crops on soil structure and on yield of subsequent arable crops grown under strip tillage on an eroded alfisol. *Soil and Tillage Research*, 2(3):233–250.

Wood, D. (2023). The Six Principles of Regenerative Farming: Why are they important? - AgriCaptureCO2.

Woolfolk, C. W., Raun, W. R., Johnson, G. V., Thomason, W. E., Mullen, R. W., Wynn, K. J., and Freeman, K. W. (2002). Influence of Late-Season Foliar Nitrogen Applications on Yield and Grain Nitrogen in Winter Wheat. *Agronomy Journal*, 94(3):429–434.

Xie, H., Huang, Y., Chen, Q., Zhang, Y., and Wu, Q. (2019). Prospects for Agricultural Sustainable Intensification: A Review of Research. *Land*, 8(11):157.

Yates, F. (1954). The Analysis of Experiments Containing Different Crop Rotations. *Biometrics*, 10(3):324–346.

Yvan, C., Stéphane, S., Stéphane, C., Pierre, B., Guy, R., and Hubert, B. (2012). Role of earthworms in regenerating soil structure after compaction in reduced tillage systems. *Soil Biology and Biochemistry*, 55:93–103.

Zadoks, J. C., Chang, T. T., and Konzak, C. F. (1974). A decimal code for the growth stages of cereals. *Weed Research*, 14(6):415–421.

Zeileis, A and Grothendieck, G (2005). Zoo: S3 Infrastructure for Regular and Irregular Time Series. *Journal of Statistical Software*, 14(6):1–27.

Zentner, R. P., Tessier, S., Peru, M., Dyck, F. B., and Campbell, C. A. (1991). Economics of tillage systems for spring wheat production in southwestern Saskatchewan (Canada). *Soil and Tillage Research*, 21(3):225–242.

Zhang, W. J., Wang, X. J., Xu, M. G., Huang, S. M., Liu, H., and Peng, C. (2010). Soil organic carbon dynamics under long-term fertilizations in arable land of northern China. *Biogeosciences*, 7:409–425.

Zhang, Y., Hou, W., Chi, M., Sun, Y., An, J., Yu, N., and Zou, H. (2020). Simulating the effects of soil temperature and soil moisture on CO2 and CH4 emissions in rice straw-enriched paddy soil. *Catena*, 194.

Zhang, Z. S., Cao, C. G., Guo, L. J., and Li, C. F. (2016). Emissions of CH4 and CO2 from paddy fields as affected by tillage practices and crop residues in central China. *Paddy and Water Environment*, 14(1):85–92.

Zhao, J., Yang, Y., Zhang, K., Jeong, J., Zeng, Z., and Zang, H. (2020). Does crop rotation yield more in China? A meta-analysis. *Field Crops Research*, 245(September 2019):107659.

Zuur, A. F. and Ieno, E. N. (2016). A protocol for conducting and presenting results of regression-type analyses. *Methods in Ecology and Evolution*, 7(6):636–645.